1-1-2013

A novel role of lipid rafts in regulating CD44-dependent breast cancer cell migration.

Irina S. Babina
Royal College of Surgeons in Ireland

A novel role of lipid rafts in regulating CD44-dependent breast cancer cell migration

RCSI

Irina S Babina B.Sc. (Hons.)

Royal College of Surgeons in Ireland
Department of Surgery
RCSI Education and Research Centre
Beaumont Hospital, Dublin 9, Ireland

Supervisor: Dr. Ann M Hopkins
Head of Department: Prof. Arnold DK Hill

April 2013

I declare that this thesis, which I submit to RCSI for examination in consideration of the award of a higher degree PhD is my own personal effort. Where any of the content presented is the result of input or data from a related collaborative research programme this is duly acknowledged in the text such that it is possible to ascertain how much of the work is my own. I have not already obtained a degree in RCSI or elsewhere on the basis of this work. Furthermore, I took reasonable care to ensure that the work is original, and, to the best of my knowledge, does not breach copyright law, and has not been taken from other sources except where such work has been cited and acknowledged within the text.

Signed IRINA BABINA 

RCSI Student Number 09110330

Date 08 MAY 2013

In loving memory of my grandparents, Mikhail and Olga.

В любящей памяти моих бабушки и дедушки, Михаила и Ольги.

Table of Contents

Abstract

The majority of breast cancer-related deaths result from metastasis, a process in which tumour cells must dynamically regulate their adhesive and migratory properties. CD44 is a cell-matrix adhesion protein which regulates cell migration. Alterations in its expression have been linked to tumour progression, yet its contribution to breast cancer metastasis remains incompletely understood. A pool of CD44 localises in cholesterol-enriched regions of the cell membrane known as lipid rafts. The aim of this thesis was to interrogate the relationship between lipid rafts and CD44 localisation / function during breast cancer cell migration. We first compared the raft affiliation status of CD44 and its binding partners in a panel of breast cancer cell lines. Raft affiliation of CD44 increased during migration of non-invasive breast cancer cells, but was significantly reduced during migration of highly-invasive cells. CD44 binding partners were detected exclusively in non-raft fractions. To investigate whether CD44 re-localisation outside lipid rafts was sufficient to drive cancer cell migration, we introduced point-mutations into two CD44 palmitoylation sites which target it to lipid rafts. CD44 raft affiliation was significantly reduced in cells transiently transfected with palmitoylation-impaired mutants, which conferred a motile and invasive phenotype compared to control cells. This phenotype was reversible upon termination of selection. Additionally a panel of CD44 non-synonymous human SNPs was identified that could recapitulate our mutagenesis model *in vivo*. Global manipulation of palmitoylation with novel enzyme inhibitors revealed a pattern whereby increased CD44 palmitoylation translated into increased lipid raft affiliation and decreased breast cancer cell migration. Accordingly, mining of published gene array datasets revealed a novel correlation between pro-palmitoylated states and improved breast cancer patient survival. Furthermore, increased levels of palmitoylated CD44 in primary breast cancer patient cultures showed a direct correlation with non-aggressive cancer phenotypes, and an inverse correlation with a putative progenitor/stem cell phenotype in a cell line model. Collectively, our results support a novel mechanism whereby sub-membranous localisation of CD44 outside lipid rafts is sufficient to promote migration in invasive breast cancer cells, and could act as a biomarker of breast cancer aggressiveness. We suggest that pharmacological sequestration of CD44 within lipid rafts represents a novel strategy to reduce breast cancer cell migration and potentially metastasis.

Acknowledgements

This work would not have been possible without the invariable support and encouragement of my supervisor, Dr. Ann Hopkins. I thank you for the inspiration you have given me every day, for all your help, wisdom and enthusiasm.

I would also like to thank Dr. Simona Donatello not only for developing the culture models I used extensively in this project, but also for the constant support and valuable advice over the course of this research project. Your help and expertise were integral in the progress of this work. Likewise, thanks to Prof. Ivan Nabi and Dr. Maria Fairbank for their important advice and assistance. Also thanks to Prof. Arnold Hill for welcoming me in this department and advice over the years.

A big thank you to Elaine, Gozie, Khairun Izlinda, Rachel and all my friends for the support, encouragement and friendship, especially over the last few months of my PhD.

Thanks to my fiancé Alex for supporting and encouraging me every single day, cheering me up every time I was down, as well as updating me on Manchester United scores of all the games I had to miss over these years. You made this journey considerably easier and smoother, so thank you for everything!

Of course, I want to thank my family, especially my mum Nina, for the encouragement and patience over the years. Huge thanks to Cathy, Peter and Stephanie Johnson for their immeasurable positivity, enthusiasm and support every day during this project. Tea and hot water bottles were particularly appreciated!

Finally, thanks to the lab staff for their assistance, and the Health Research Board of Ireland (RP/2008/49 to AMH) and Breast Cancer Ireland for funding this exciting project.

Abbreviations

APT	Acyl thioesterase
BCA	Bicinchoninic acid
BMP	Bone Morphogenetic Protein
BSA	Bovine serim albumin
DCIS	Ductal carcinoma in situ
DHHC	Aspartate-histidine-histidine-cysteine
DMEM	Dulbecco's Modified Eagle's Medium
DN	Double-negative
DP	Double-positive
ECM	Extra-cellular matrix
EGF	Epidermal growth factor
EMT	epithelial-mesenchymal transition
ER	Oestrogen receptor
ERM	Ezrin-radixin-moesin
FAK	Focal adhesion kinase
HA	Hyaluronic acid
HAM	Hydroxylamine
HBSS	Hank's balanced salts solution
HER	Human epidermal growth factor receptor
HMEC	Human mammary epithelial cell
IDC	Invasive ductal carcinoma
ILC	Invasive lobular carcinoma
IT-LC	Invasive tubulo-lobular carcinoma
MET	mesenchymal-epithelial transition
MMP	Matrix metalloproneinase
NEM	N-ethylmaleimide
PAT	Palmitoyl acyltransterase
PI3K	Phosphoinositide 3-kinase
PKC	Protein kinase C
PR	Progesterone receptor
PTHrP	Parathyroid hormone-related protein
SFK	Src family of kinases
SNP	Single nucleotide polymorphism
TEB	Terminal end bud
Tf R	Transferrin receptor
uPAR	Urokinase receptor

Chapter 1

General Introduction

1.1 Introduction

1.1.1 Human mammary gland development

The mammary gland is designed for production of milk proteins and fat to feed the offspring. It is a complex secretory organ that consists of a number of cell types (**Fig. 1.1**). The mature mammary gland consists of alveoli that join up to form lobules, containing milk-secreting cells. Each lobule narrows into a lactiferous (milk) duct, which opens into the nipple. The milk ducts within the gland are composed of epithelial cells and are embedded in a fat pad composed of adipocytes. Vascular endothelial cells make up the blood vessel network, while the supporting stroma is composed of fibroblasts and various immune cells. In the mammary gland there are two main types of epithelium: luminal and basal (Watson and Khaled, 2008). The former generates ducts and alveoli, while the latter is composed of myoepithelial cells. These epithelia form a bi-layered structure within the fatty stroma (**Fig. 1.1**). During the lifetime, the breast undergoes distinct changes in shape, size and function in response to various stages of breast development (Turashvili *et al.*, 2005). The major stages of the mammary gland development are embryonic, pubertal and adult, and have been studied extensively in mouse models (Russo and Russo, 2004).

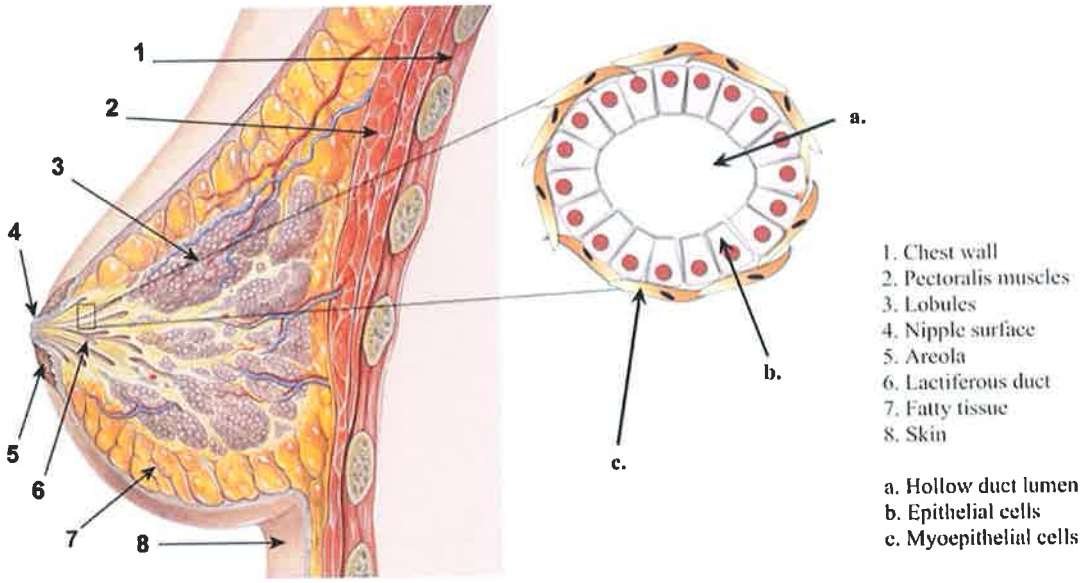

Figure 1.1 Structure of the mammary gland. Schematic representation of the mammary gland within the breast, with a vertical section of a lactiferous duct, lined with epithelial cells forming a hollow lumen and surrounded by myoepithelial cells. Image obtained from http://en.wikipedia.org/wiki/File:Breast_anatomy_normal_scheme.png.

The embryonic stage of breast development is similar in males and females, and begins with invagination of ectoderm to form buds (**Fig. 1.2**) in response to parathyroid hormone-related protein (PTHrP) (Watson and Khaled, 2008). In conjunction with bone morphogenetic protein-4 (BMP4), PTHrP stimulates outgrowth and elongation of buds (Hens *et al.*, 2007). This interaction additionally serves as a signal to the mammary mesenchyme to induce proliferation and differentiation of the epithelium (Hens *et al.*, 2007; Hens and Wysolmerski, 2005). This complicated process is tightly regulated by numerous hormones and growth factors.

Before puberty, growth of the mammary tree is allometric (proportional to the general body growth). The tips of the ducts begin to form terminal end buds (TEBs, **Fig. 1.2**), which protrude into the mammary stroma and elongate the ducts (Hinck and Silberstein, 2005). TEBs are comprised of an outer layer of cap cells, and a bulk of cells at the tips of the ducts. When serum levels of oestrogen increase during puberty, proliferation within TEBs causes ductal elongation, while the surrounding fat and extra-cellular matrix (ECM) are believed to aid tubular formation, either physically or as a provider of secreted factors (Couldrey *et al.*, 2002). In addition to elongation, clefts in TEBs give rise to splitting of ducts and forming of branches. At this stage, apoptosis can be detected in the body cells of TEBs, suggesting formation of ductal lumens (Humphreys *et al.*, 1996). Branching morphogenesis is regulated by numerous epithelial and stromal factors, including hormones, growth factors, matrix metalloproteinases (MMPs), ECM and immune cells (Sternlicht *et al.*, 2006).

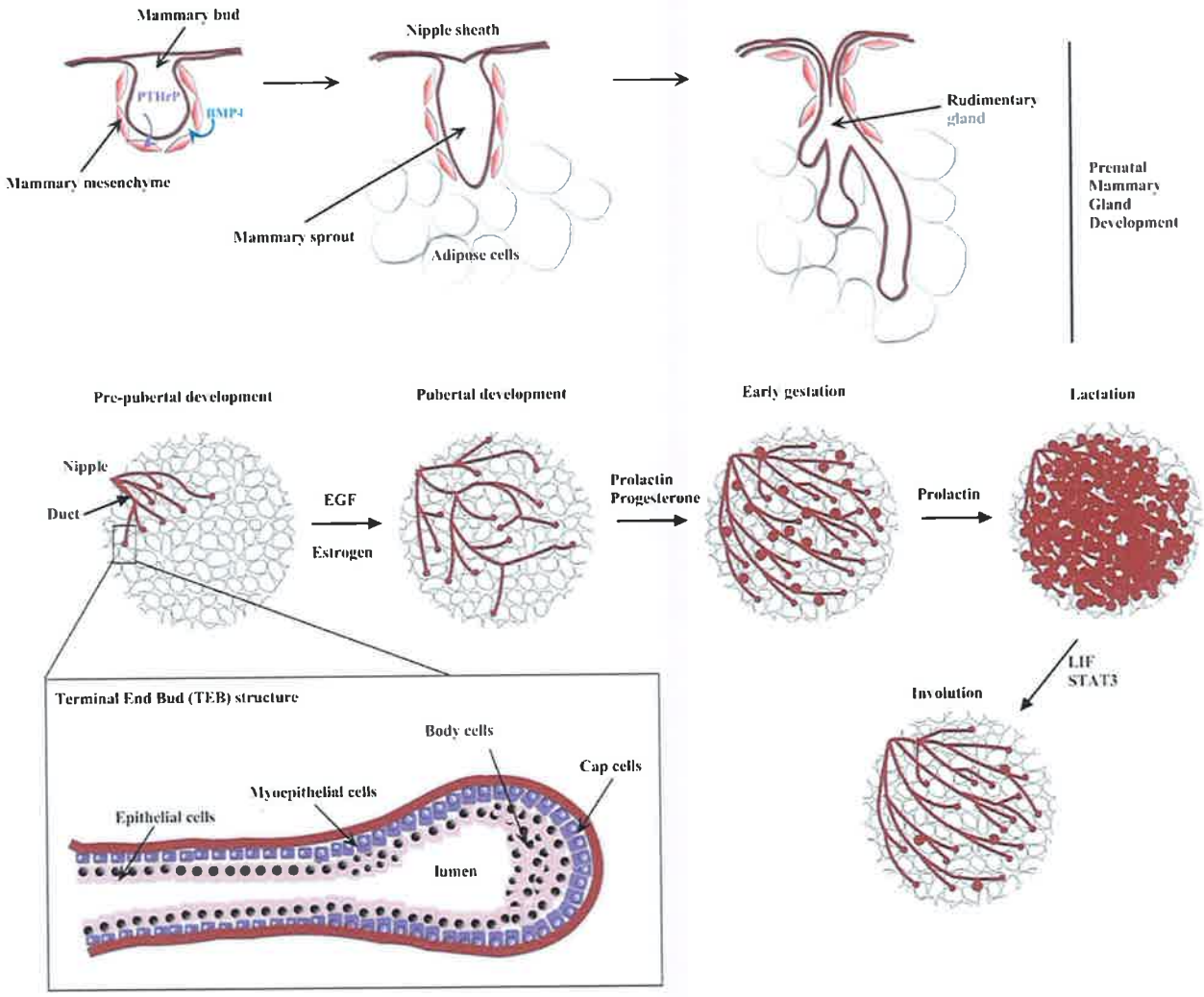

Figure 1.2 Schematic representation of mammary gland development. Stages shown are during prenatal development (top) and pubertal and pregnancy stages (bottom). Inset is the schematic structure of the terminal end bud (TEB).

Further development of the mammary gland takes place during pregnancy in preparation for lactation (**Fig. 1.3**). During lactation, specialised cells for production and secretion of milk are created. Progesterone induces extensive branching and alveolar formation on ductal ends, and in combination with prolactin, promotes differentiation of alveoli to milk-secreting cells (Watson and Khaled, 2008). The mammary gland returns to its non-milk-secreting state through the process of involution. Cessation of milk removal induces apoptosis and the shedding of detached cells into alveolar lumens. This process, in turn, activates matrix metalloproteinases that begin to break down the ECM around each alveolus, resulting in alveolar collapse (**Figs. 1.2 and 1.3**). Re-differentiation of the adipocytes via plasmin and MMP3 activation completes the remodelling (Watson, 2006).

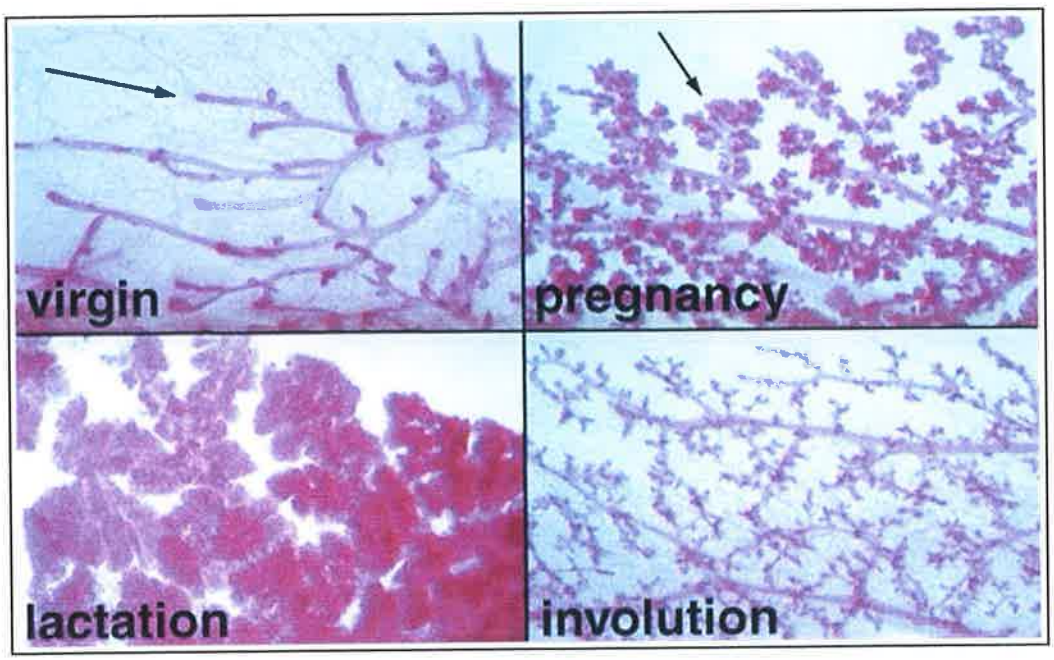

Fig. 1.3 Mammary development in mouse. Morphological differences in the mouse mammary gland over various stages of development and pregnancy. Arrows indicate TEB structures in the virgin mouse and their differentiation during pregnancy. Image contributed by L. Hennighausen, Bethesda, and obtained from

http://mammary.nih.gov/reviews/development/Development001/index.html.

1.1.2 Breast cancer overview

Normal mammary gland development involves numerous processes, including cell proliferation, migration and break-down of the ECM. These processes are tightly-regulated by soluble factors, such as hormones and growth factors, as well as ECM and stromal interactions. Thus it is unsurprising that dysregulation of any of those processes could result in a pathophysiological outcome. Specifically, emerging evidence supports the similarities between developmental processes and the pathophysiology of breast cancer, the most frequently-diagnosed female cancer in the world (DeSantis *et al.*, 2011). In Ireland, over 2500 new cases are diagnosed each year (Irish Cancer Society, 2009). Despite improvements in prophylactic screening programs and better treatments, approximately 620 Irish women die every year from breast cancer-related causes (Irish Health Service Executive, 2012). In order to improve current treatments and minimise the side effects for patients, a better understanding of the molecular processes underlying breast cancer initiation and progression is thus required.

It is generally accepted that breast cancer is not a single disease, but rather a combination of disorders harbouring various genetic and molecular variations and resulting in different clinical outcomes (Vargo-Gogola and Rosen, 2007). In fact, it has been referred to as "an organ" due to changes in functional and molecular associations of tumour cells with the surrounding tissue (Bissell and Radisky, 2001). An assortment of risk factors has been identified, such as genetic predisposition, diet, obesity and environment. During physiological changes within the mammary gland (for instance, pregnancy or involution), the breast cells are more susceptible to these factors, as well as circulating hormones, levels of which rise during such processes.

Nonetheless, events that are responsible for the initial formation of individual tumours remain uncertain. Intrinsic factors, such as genetic

mutations and genomic instability, predispose individuals towards breast cancer formation. Germ-line mutations in *BRCA1* and *BRCA2* genes are widely accepted as instigators of familial breast cancer (Vollebergh *et al.*, 2012). These genes additionally increase the risk of developing other cancer types, such as prostate and pancreatic cancer (Levy-Lahad and Friedman, 2007), or indeed ovarian cancer (Vollebergh *et al.*, 2012). Moreover, breast cancers frequently harbour mutations in *TP53* and *PI3KCA* genes, both of which are associated with aggressive tumour phenotype (Vollebergh *et al.*, 2012). Chromosomal rearrangements lead to corruption of genome integrity and increase the risk of development of breast malignancies (Wiechec, 2011). Detailed profiling of these mutations and genomic alterations in patient breast cancers could aid characterisation of potential predictive and prognostic factors, aimed at the development of more tailored treatments. Extrinsic factors, such as tissue damage or wound healing, could cause alterations in epithelial tissues such as movement and proliferation of epithelial sheets. In a physiological setting, these events are temporary and can be reversed. However, under constitutive repair conditions, the ECM could come under attack from upregulated MMPs and immune cells, and promote abnormal proliferation (Bissell and Hines, 2011). Interaction of genetically-unstable cells with the surrounding micro-environment could in turn induce production of cytokines that will lead to cell proliferation and more abnormal interactions with the micro-environment (Korkaya *et al.*, 2011).

An additional unclear aspect of breast cancer disease is tumour heterogeneity. Two main hypotheses were proposed to explain this phenomenon (**Fig. 1.4**). The first suggests that all cells within a tumour initially have an equal potential of becoming tumourigenic. In this model, spontaneous mutations occur within normal mammary cell population in response to outside signals or treatments, thus driving tumourigenesis and increasing heterogeneity of the tumour population. More recently, however, the second model of tumour-initiating cells, or cancer "stem" cells, has been proposed. It puts

forward the theory that breast cells are heterogeneous to begin with, and therefore have differing potentials for tumourigenesis (Reya *et al.*, 2001). This theory is intriguing, as with every pregnancy the normal mammary gland undergoes cycles of proliferation, differentiation and involution, which are believed to be sustained with the aid of mammary epithelial stem cells. In fact, women who are pregnant at an early age are less likely to develop hormone-sensitive breast cancer (MacMahon *et al.*, 1970). In this context, cancer stem cells stimulate tumour growth and differentiation of non-tumourigenic cells, mimicking, in effect, normal tissue development (Molyneux *et al.*, 2007). Consequently, it has been suggested that failure to eradicate these populations of cancer stem cells using conventional breast cancer therapies underlies the reason for breast cancer relapse. Therefore, a more targeted approach to eradicating tumour-initiating cancer stem cells could improve the prognosis of breast cancer patients, especially those with advanced disease.

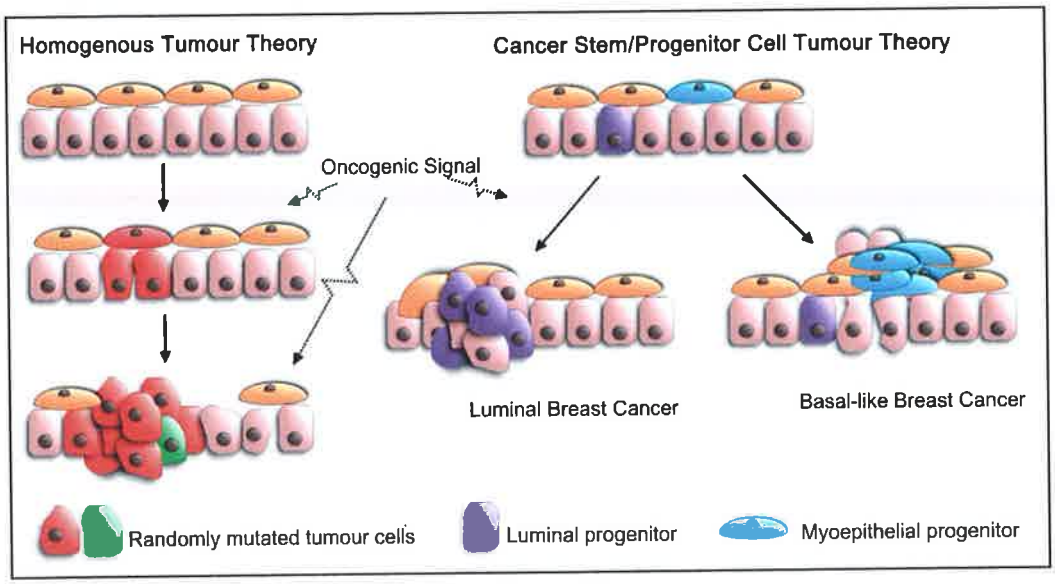

Figure 1.4 Theories about breast cancer heterogeneity. A schematic representation of the homogenous tumour origin (left), which with prolonged oncogenesis sustains several random mutations; and the cancer stem cell theory, where mammary stem/progenitor cells drive differentiation and proliferation of normal epithelial or myoepithelial cells (right).

Notwithstanding these exciting theories, many controversies exist over the putative origins of breast cancer stem cells. Some evidence suggests that breast cancer stem cells are formed by EMT, since cells that underwent EMT have been demonstrated to have similar behaviour and characteristics to normal and neoplastic cells (Mani *et al.*, 2008). Additionally, the induction of EMT in normal mammary epithelial cell lines can reportedly produce cell populations with stem cell characteristics (Morel *et al.*, 2008). The alternative theory proposes that cancer stem cells are a result of de-regulated normal stem cell self-renewal and differentiation. The strongest evidence for this theory arises from noted similarities between normal and cancer stem cells (Dontu *et al.*, 2003). Furthermore, the long lifespan of normal stem cells increases their susceptibility to eventual mutations or oncogenic transformation (Ponti *et al.*, 2005; Velasco-Velazquez *et al.*, 2012). Findings in Max Wicha's laboratory have suggested that breast cancer stem cells originate from basal mammary stem/progenitor cells based on the surface protein expression profiles of the two cell types (Al-Hajj *et al.*, 2003). These two theories about the origin of cancer stem cells are not mutually-exclusive. In fact, recent evidence suggests that normal and malignant breast cancer stem cells exist in inter-convertible states of EMT and MET (mesenchymal-epithelial transition) under the regulation or micro-RNAs (Liu *et al.*, 2012). In this context, different states of breast cancer stem cells and their various differentiation states could give rise to breast cancer heterogeneity and different tumour subtypes.

1.1.3 Breast cancer classification.

1.1.3.1 Clinical subtypes

In a clinical setting, breast tumours are classified according to their pathological features, such as stage of tumour progression, grade and

expression-specific biomarkers such as oestrogen receptor (ER), progesterone receptor (PR) and human epidermal growth factor receptor-2 (HER-2).

According to one classification, tumour progression is categorised by tumour, node and metastasis features, or TNM. Tumour status (T) defines the size of the tumour, node status (N) indicates if the tumour has spread to the lymph nodes and metastasis (M) is indicative of the presence of metastatic spread in other organs. Breast cancers are then classified based on the numerical severity of each of these features. Combined together, they determine the stage of breast cancer, assigned by The American Joint Committee on Cancer (AJCC) staging system as Stages I-IV.

The histological grade of breast cancer is determined microscopically by a pathologist, in accordance with internationally-accepted systems evaluating acinar formation, nuclear size and mitotic activity (Elston and Ellis, 2002). Numerical grading is on a scale of 1 to 3, with 1 assigned to tumours with a well-differentiated normal-like phenotype, while 3 is given to aggressive, poorly-differentiated breast cancers.

Evaluation of steroid and hormone receptor status is another determinant in breast cancer classification. ER and PR play crucial roles in mammary gland development, inducing differentiation of luminal epithelium and lobular-alveolar structures, respectively. Both receptors are typically co-expressed in malignant breast cells (Conneely *et al.*, 2003) and are important prognostic factors. Generally, expression of both these steroid receptors in breast tumours is associated with better patient prognosis and responsiveness to endocrine therapies (Bardou *et al.*, 2003). In 1988, revolutionary progress for breast cancer treatment was made, when Slamon and Clarke described a key role for HER-2 in breast cancer (Slamon and Clark, 1988). They showed that *HER-2* gene amplification led to overexpression of the HER-2 protein product, which in turn promoted proliferation and angiogenesis. Breast tumours that overexpress HER-2 are highly aggressive and generally have poor prognosis,

thus it is currently used as an additional prognostic marker for breast cancer. This discovery led to the development of therapeutic agents targeting HER-2 (such as Trastuzumab and Lapatinib), or members of its protein family, in attempts to suppress the highly metastatic events associated with HER-2 overexpression (Murphy and Morris, 2012).

1.1.3.2. Molecular subtypes of breast cancer

Whilst classic grading and staging systems have been instrumental in the diagnosis and treatment of breast cancers, in recent years large-scale gene expression profiling of tumours has revolutionised our understanding of breast cancer heterogeneity. As a result of such studies, breast cancer is now increasingly classified according to differences in the molecular signature of breast tumour cells.

The original gene expression profiling analyses to study breast cancer molecular diversity were undertaken by Perou and colleagues (Perou *et al.*, 2000) and Sorlie *et al.* (Sorlie *et al.*, 2001), who demonstrated that ER-negative and ER-positive breast cancers were molecularly very distinct. Hierarchical gene clustering analysis revealed four distinct molecular subtypes of breast cancer, namely luminal, HER-2-enriched, basal-like and normal -like (Perou *et al.*, 2000). Subsequent analysis of a larger cohort showed that the ER-positive group could be sub-divided into luminal A and luminal B subtypes, based on increased expression of markers such as ER α gene, GATA binding protein 3, X-box binding protein 1, trefoil factor 3, hepatocyte nuclear factor 3 α, and estrogen-regulated LIV-1. The ER-negative group included normal cells, HER-2-enriched and basal-like tumours (Sorlie *et al.*, 2001). Further validation studies outlined a more detailed classification of breast cancer tumours (Sotiriou *et al.*, 2003), as summarised in **Table 1.1**.

Luminal A

The luminal A breast cancer subtype is characterised by expression of genes activated by the ER transcription factor, typically expressed in the

Table 1.1 Molecular subtypes of breast cancer, determined by microarray gene expression profiling. Compiled using (Eroles *et al.*, 2012; Reis-Filho and Pusztai, 2011)

Molecular Subtype	Histological grade	Proliferation cluster	ER/PR/HER-2	Additional Markers	Benefit from chemotherapy	Patient outcome
Luminal A	**1 / 2**: 70-87% **3**: 13-10%	Low	**ER:** + **PR:** + **HER-2:** -	Ki67: low GATA3, FOXA1, ESR1, KRT8, KRT18, CCDN1, LIV1	Low	Excellent
Luminal B	**1 / 2**: 38-59% **3**: 41-62%	High	**ER:** +/- **PR:** +/- **HER-2:** -/+	Ki67: high GATA3, FOXA1, ESR1, KRT8, KRT18, SQLE, LAPTM4B	Intermediate	Intermediate/Poor
HER-enriched	**1 / 2**: 11-45% **3**: 55-89%	High	**ER:** - **PR:** - **HER-2:** +	Ki67: high GRB7	Intermediate	Poor
Basal-like	**1 / 2**: 7-12% **3**: 88-93%	High	**ER:** - **PR:** - **HER-2:** -	Ki67: high KRT5, KRT17, CDH3, ID4, FABP4, LAMC2	High	Poor
Normal breast-like	**1 / 2**: 37-80% **3**: 20-63%	Low/ intermediate	**ER:** -/+ **PR:** -/+ **HER-2:** -	Ki67: low/intermediate PTN, CD36, FABP4	Low	Intermediate
Claudin-low	**1 / 2**: 23-62% **3**: 38-77%	Intermediate/ High	**ER:** - **PR:** - **HER-2:** -	Ki67: intermediate CD44, SNAI3	Intermediate	Intermediate

Luminal B

In comparison to Luminal A tumours, Luminal B breast cancers have a more aggressive phenotype, higher histological grade and worse prognosis. Bone metastasis is still a prevalent site of distant metastasis, but it also has a high rate of recurrence in the liver (Kennecke *et al.*, 2010). This subtype is also characterised by increased expression of proliferation genes, including HER-1 and HER-2. Luminal B tumours are not as responsive to tamoxifen and aromatase inhibitors as Luminal A tumours, but respond better to neoadjuvant chemotherapy. As treatment for this type of cancer is challenging, some clinical trials are currently in progress of testing small inhibitory molecules of PI3K/Akt/mTOR (Eroles *et al.*, 2012).

HER-2-enriched

This breast cancer subtype is characterised by amplification of the *HER-2* gene and corresponding overexpression of the HER-2 protein product, which translates into a highly-proliferative and aggressive tumour phenotype. Although this subtype is characterised by poor prognosis, development of anti-HER-2 therapies has dramatically improved survival of patients with this type of breast cancer.

Basal-like

This highly-aggressive breast tumour type expresses genes that are present in normal myoepithelial cells (such as cytokeratins -5 and -17, P-cadherin, HER-1 and CD44). They also harbour mutations in p53 and BRCA1 genes, which at least partially account for their aggressiveness. Metastatic relapse of these tumours is very destructive, and predominantly localises to visceral organs (Kennecke *et al.*, 2010). Basal-like tumours lack expression of ER, PR and HER-2, and thus are treated as other triple-negative breast cancers (Eroles *et al.*, 2012).

Normal breast-like

These tumours are very poorly characterised. Their gene expression is similar to adipose tissue, which is why they represent an intermediate prognosis between luminal and basal-like subtypes. These tumours are also triple-negative and do not respond to neoadjuvant chemotherapy. Because of the rarity of this subtype, it has not been studied extensively (Eroles *et al.*, 2012).

Claudin-low

Claudin-low tumours have been characterised as a separate subtype relatively recently (Herschkowitz *et al.*, 2007). Their main distinction is decreased expression of genes involved in intercellular adhesion. These include claudins -3, -4 and -7, occludin, cingulin and E-cadherin. This sub-type was originally grouped with basal-like tumours, thus they share a characteristic gene expression profile. However, in contrast to the basal-like subtype, claudin-low tumours overexpress a set of 40 genes involved in the immune response (Parker *et al.*, 2009). In parallel, these tumours overexpress a subset of genes linked to EMT and mesenchymal differentiation, and clinically correlate with high-grade metaplastic infiltrating tumours (Prat *et al.*, 2010). This subtype is predominantly triple-negative, but some tumours express ER and PR. Long-term prognosis with claudin-low tumours is very poor and response to neoadjuvant therapy is insufficient, falling between basal and luminal tumours (Eroles *et al.*, 2012).

1.1.4. Initiation of breast cancer metastatic cascade.

While the described characterisation of primary breast tumours based on their molecular characteristics has provided a valuable diagnostic tool for oncologists as well as greatly improving mechanistic understanding of the disease, the molecular mechanisms underlying metastatic spread (the major cause of breast cancer-related deaths) remain elusive.

An important feature that separates metastatic cells from normal mammary cells is de-regulated epithelial cell polarity. In normal epithelium, the signals sent from the surrounding environment aid in polarisation and differentiation of apical and basal surfaces. Intercellular contact is maintained by tight, gap and adherens junctions, and attachment to the ECM on the basal surface is mediated by adhesion proteins, such as integrins and CD44, in conjunction with growth factor receptors (Bissell and Radisky, 2001; Cavallaro and Christofori, 2004). In contrast, in intercellular or/and ECM interactions are altered in breast tumours, thus activating migratory and invasive capabilities of cancer cells, mediating invasion into the surrounding ECM and stroma with subsequent intravasation into the blood vessels (Valastyan and Weinberg, 2011).

Most types of basal tumours invade the ECM and stroma as multi-cellular units through a process termed "collective invasion" (reviewed in (Spano *et al.*, 2012)). During collective invasion or migration, cancer cells retain their intercellular junctions and migrate as sheets, tubes or clusters. Alternatively, single tumour cells can invade via integrin-independent "ameboid invasion" or integrin-dependent "mesenchymal invasion" programmes (Friedl and Wolf, 2003; Spano *et al.*, 2012). The latter involves loss of epithelial polarity and a switch to mesenchymal morphology through EMT, which ultimately translates into increased invasiveness. Rare metaplastic tumours and claudin-low subtypes of breast cancer have EMT attributes, and this area of research is currently of major scientific interest.

As already discussed, recent studies have established a link between cells undergoing EMT and the acquisition of stem cell properties (Mani *et al.*, 2008; Morel *et al.*, 2008). The latter are characterised by expression of particular cell surface markers. In breast tumours, a population of cells with high CD44 and low CD24 expression display EMT features (May *et al.*, 2011) and express an "invasiveness" gene signature of 186 genes associated with poor patient outcome (Liu *et al.*, 2007). The CD44+/CD24- molecular signature is now widely accepted

as an identifier of breast cancer stem cells, but the functional role of CD44 in breast cancer stem cells and breast cancer progression remains unclear.

CD44 is an adhesion molecule that can interact with numerous components of the ECM, such as hyaluronan, collagen and laminin. During tumourigenesis, tumour cells secrete oncogenic cytokines and proteases, to break down the basement membrane, grow and migrate out. Changes in the ECM impact the surrounding epithelial cells and stroma, thereby facilitating epithelial cell transformation, hyperplasia and local invasion (Lu *et al.*, 2012). CD44 has been shown to assist in this process by activating MMP proteins and degrading the ECM component hyaluronan (discussed below). Additionally, CD44 expression is elevated in triple-negative mammary tumours and is associated with poor patient outcome (Olsson *et al.*, 2011). Yet, in some cancers, CD44 is paradoxically described as a tumour suppressor (Gao *et al.*, 1997; Horak *et al.*, 2008). Some studies attribute this discrepancy to cell type-dependence and differential CD44 subcellular localisation patterns (Louderbough and Schroeder, 2011; Neame *et al.*, 1995). Consequently, in this thesis we addressed the functional role of CD44 in breast cancer cell migration via regulation of its subcellular localisation.

1.1.5. CD44 and breast cancer

In normal mammary duct epithelium, CD44 has been described to localise within the myoepithelial layer, as well as in the ductal epithelium (Friedrichs *et al.*, 1995; Kaufmann *et al.*, 1995). At a cellular level, CD44 functions in three major categories: as growth factor co-receptor, ECM receptor and actin cytoskeletal organiser (Ponta *et al.*, 2003). Of particular relevance to breast cancer, CD44 can function as a co-receptor for members of the HER and Met receptor tyrosine kinase families. For example, its interactions with HER proteins have been shown to promote HER receptor kinase activation and increased tumour migration in tamoxifen-resistant breast cancer models (Coleman *et al.*, 2009). Additionally, the CD44 isoform containing variant exon 6 (CD44v6) has

proven crucial for c-Met activation by its ligand hepatocyte growth factor, as well as for transduction of c-Met oncogenic signals (Elnagar *et al.*, 2011).

Additionally, CD44 is a major receptor for the ECM component hyaluronan (hyaluronic acid, HA) (Herrera-Gayol and Jothy, 1999). A number of mechanisms have been proposed to regulate their interactions. For instance, co-association of CD44 with matrix metalloproteinase 9 (MMP-9) has been shown to promote tumour invasion via HA degradation (Orian-Rousseau *et al.*, 2002). HA has also been shown to trigger membrane-type 1 MMP-dependent CD44 cleavage, thereby promoting tumour cell migration (Ponta *et al.*, 2003). However, since HA is such a large molecule (up to 1.8MDa), its functional effects are heavily dependent on the size of its fragments. Exogenous large molecular weight HA stimulates CD44 clustering, which is disrupted by smaller fragments of HA (Ostapkowicz *et al.*, 2006). Functionally, small HA oligosaccharides have been shown to induce CD44 cleavage, thereby promoting tumour cell migration and increasing adhesion (Diaz *et al.*, 2005; Ostapkowicz *et al.*, 2006). On the other hand, high molecular weight HA has also been demonstrated to exert inhibitory effects on tumour growth (Neame *et al.*, 1995), CD44-mediated angiogenesis and tumour cell migration (Naor *et al.*, 2008; Ostapkowicz *et al.*, 2006).

Finally, CD44 can mediate cell adhesion and migration via dynamic organisation of the actin cytoskeleton. CD44 directly interacts with cytoskeletal linker proteins, such as ERM (ezrin-radixin-moesin) proteins, which in turn organise actin filaments (Thorne *et al.*, 2004). ERM proteins, which in their resting state are de-phosphorylated and in a closed conformation in the cytoplasm, translocate to the cell membrane and bind to the CD44 cytoplasmic tail upon phosphorylation by protein kinase C (PKC) (Lopez *et al.*, 2005). This interaction enables CD44-linked rearrangement of the actin cytoskeleton, which in turn activates downstream effector molecules such as Ras and ERK, facilitating of cell migration (Ponta *et al.*, 2003). However, dysregulation of CD44-based motility may result in pathophysiological modifications associated with cancer

dissemination and metastasis (reviewed in (Naor *et al.*, 2008)). CD44 is frequently found localised in lipid rafts, specialised areas of the plasma membrane that are enriched in sphingolipids and cholesterol. The functional significance of this association is, however, still unclear and remains contradictory. In this thesis we address this association of CD44 with lipid rafts in the context of breast cancer cell migration.

1.1.6. Lipid rafts and their physiological role

Lipid rafts are sub-domains of the cell membrane that are highly enriched in cholesterol and glycosphingolipids (Le Moyec *et al.*, 1992; Nohara *et al.*, 1998). Detailed analysis of these micro-domains has revealed that they cluster together key proteins involved in the regulation of crucial cellular processes; many of which are altered in cancer cells (de Laurentiis *et al.*, 2007; Pike, 2003). Furthermore, lipid rafts are readily modified by diet and nutrition (Schley *et al.*, 2007; Yaqoob, 2009), and numerous studies have shown that fatty acid supplementation sensitises human mammary tumour cells to the cytotoxic effects of a number of anti-cancer agents both *in vitro* and *in vivo* (Colas *et al.*, 2006; Germain *et al.*, 1998; Menendez *et al.*, 2005).

Lipid rafts are often viewed as signalling platforms or organisation centres for a variety of physiological processes including membrane trafficking, cell polarisation and signal transduction. In polarised epithelial cells the trafficking machinery is also highly polarised, targeting plasma membrane proteins to separate apical and basolateral domains (Mellman and Nelson, 2008). Lipid rafts have been proposed to play a decisive role in vesicle formation and distribution for apical trafficking of newly-synthesised proteins (Schuck and Simons, 2004). Basolateral protein sorting, in turn, is believed to be largely mediated by clathrin-coated vesicles (Deborde *et al.*, 2008; Folsch *et al.*, 2009). Lipid raft-mediated trafficking of lipids and proteins consequently facilitates dynamic regulation of cellular signalling cascades. Numerous tyrosine kinases and other proteins such as integrins and catenins carry out their functions through lipid rafts (Patra, 2008).

Modified signal transduction following lipid raft disruption has been reported in the case of several signalling pathways involving Erk (Furuchi and Anderson, 1998), HER-1 (Ringerike *et al.*, 2002; Schley *et al.*, 2007), insulin receptor (Parpal *et al.*, 2001) and the PDGF receptor (McGuire *et al.*, 1993). Finally, lipid rafts have been described to be actively involved in endocytosis (reviewed in (Lajoie and Nabi, 2010)), promoting internalisation of receptors and signalling molecules.

1.1.7. Role of lipid rafts in breast cancer metastasis

As described above, lipid rafts mediate many important physiological cellular processes, thus much interest has accompanied the notion that tumour cells might utilise lipid rafts for pathophysiological events. Lipid rafts regulate numerous stages in breast cancer initiation, growth and metabolism (reviewed in (Babina *et al.*, 2011)). Their regulation of cell migration and invasion, however, are of particular interest for this thesis, as loss of adhesion, formation of invadopodia and cell migration are essential for the metastatic spread of breast cancer.

Kinases play a significant role in regulating cell adhesion, cell cycle progression and cell migration. The Src family of kinases (SFK) amalgamates and regulates signal transduction from many receptor tyrosine kinases, including IGF-1R, HER-1 and HER-2 (Belsches-Jablonski *et al.*, 2001; Parsons and Parsons, 2004) to multiple downstream targets including PI3-kinase, Ras and focal adhesion kinase (Parsons and Parsons, 2004). Src activation has been specifically linked to lipid rafts in breast cancer cells (Hitosugi *et al.*, 2007). In one publication, conventional inhibitors of Src only significantly inhibited adhesion and cell cycle progression of MCF-7 breast cancer cells when coupled to a lipid raft-targeting domain (Hitosugi *et al.*, 2007). This suggests that selective targeting of raft-affiliated SFK may offer a more potent therapy than conventional SFK inhibitors such as dasatinib or saracatinib. Src has also been shown to phosphorylate the raft marker flotillin-2 in an EGF-dependent manner, resulting in

Src translocation from the cell membrane into endosomes and the enhancement of cell spreading (Neumann-Giesen *et al.*, 2007). Conversely, the finding that knockdown of flotillin-2 reduces cell spreading further highlights the potential regulatory influence of lipid rafts on cell adhesion and actin dynamics (Neumann-Giesen *et al.*, 2007).

Lipid rafts and caveolin-1 have also been shown to be crucial for the formation of invadopodia, membrane protrusions that penetrate the surrounding matrix through a combination of matrix remodelling and physical force (Buccione *et al.*, 2009). Invadopodia cluster together many proteins involved in actin cytoskeleton organisation, signalling, cell-ECM adhesion and membrane remodelling (Gimona *et al.*, 2008). It has been reported that lipid rafts are concentrated at the leading edge of invadopodia in a panel of breast cancer cell lines, and that disruption of lipid rafts suppresses invadopodia formation (Yamaguchi *et al.*, 2009). Invasive potential has also been linked with the raft-affiliated proteins caveolin-1 and membrane type 1 matrix metalloproteinase (MMP14) in both breast (Annabi *et al.*, 2001) and prostate cancer cells (Wang *et al.*, 2009). Accordingly, a reduction in matrix degradation activity of MMP14 has been reported in MDA-MB-231 cells following disruption of lipid rafts by cholesterol depletion or after knockdown of caveolin-1 in MMP14-overexpressiong MDA-MB-231 cells (Yamaguchi *et al.*, 2009). Taken together, these results demonstrate that lipid rafts are important for invadopodia function in breast cancer cells.

MMP14 is not the only lipid raft-affiliated proteinase implicated in breast cancer progression. Aberrant expressions of MMP2 and MMP9, which also localize in rafts during cancer cell migration (Patra, 2008), have been associated with high-grade breast cancer (Mira *et al.*, 2004). Downregulation of MMP2 and MMP9 has been shown to decrease tumour cell invasion (Patra, 2008). Similarly, the serine protease urokinase-type plasminogen activator (uPA) and its receptor (uPAR), which have been linked to breast cancer progression and metastasis (Patra, 2008; Sahores *et al.*, 2008), localise to lipid rafts during cancer cell

migration (Sahores *et al.*, 2008). A recent study investigating the importance of lipid rafts in regulating uPAR and MMP9 functionality in breast cancer has demonstrated that cholesterol depletion reduces co-localisation of uPAR and MMP9 with lipid rafts and significantly decreases their total protein and mRNA levels (Raghu *et al.*, 2010). Lipid raft disruption in the same breast cancer cells also reduced the levels of active Src, FAK, Akt and ERK and promoted uPAR co-localisation with lysosomal markers, which was reversed after cholesterol was re-introduced (Raghu *et al.*, 2010). This is in agreement with previous observations that suggested differences in MMP9-driven breast cancer cell migration according to its sub-cellular localisation in rafts or outside them (Mira *et al.*, 2004). These results propose that lipid raft integrity is critical for breast cancer cell migration and invasion mediated by matrix degradation proteins.

Taken altogether, several key molecules frequently implicated in breast cancer cell migration and invasion are regulated by lipid rafts via sequestration, endocytosis or termination of protein interactions. CD44, by virtue of post-translational lipid modifications (which will be extensively addressed later in this thesis) is frequently targeted to lipid rafts. However, its affiliation with lipid rafts has been shown to have both pro- and anti- tumourigenic properties. Therefore, the focus of this thesis is in elucidating the role of lipid rafts in regulating CD44 during breast cancer cell migration, which may offer a novel therapeutic approach to targeting breast cancer metastatic spread.

1.3 Aims of this thesis

The overall aim of this study was to elucidate the molecular and functional relationships between CD44 and lipid rafts in a variety of breast cancer models. The specific aims are listed below.

1. The first aim was to establish a correlation between CD44 localisation in lipid rafts and the invasive potential of a panel of breast cancer cell lines. The cell lines used for this study were grouped into non-invasive, weakly-invasive and highly-invasive.

2. CD44 is believed to be affiliated with lipid rafts via palmitoylation of cysteines in its transmembrane domain. Thus the second aim was to artificially modulate CD44 palmitoylation sites in an attempt to decrease lipid raft affiliation of CD44, and test our hypothesis that this would increase cell migration and invasion.

3. The final aim of this thesis was to translate the results obtained using cell line models into a clinically-relevant setting via assessment of CD44 raft affiliation and palmitoylation status in primary cultures derives from human breast tumours and putative stem/progenitor populations of a non-tumourigenic cell line.

Chapter 2

Materials and Methods

2.1 Cell Culture

2.1.1 Cell lines

The cell lines examined varied in their invasive capabilities, and were grouped into non-invasive/normal-like (HMEC and MCF-10a), weakly-invasive (MCF-7 and BT-474) and highly-invasive (MDA-MB-231, Hs578T-P and Hs578T-I8).

2.1.1.1 HMEC and MCF-10a

Normal primary human mammary epithelial cells (HMEC) were obtained from Lonza and the MCF-10a cell line was purchased from ATCC. HMEC cells were cultured in Mammary Epithelial Growth Medium (MEGM; Lonza), prepared according to the manufacturer's guidelines with the addition of the following pre-prepared supplements (insulin, hydrocortisone, recombinant human Epidermal Growth Factor (EGF), gentamicin sulphate amphotericin-B and bovine pituitary extract (BPE)) in addition to 100U/mL penicillin and 100µg/mL streptomycin. MCF-10a cells were grown in Dulbecco's Modified Eagle's Medium (DMEM)-F12, supplemented with 0.5µg/mL hydrocortisone, 0.1µg/mL cholera toxin, 10µg/mL insulin, 20ng/mL EGF, 100U/mL penicillin, 100µg/mL streptomycin and 5% horse serum. A list of media components and purchasing details are listed in Appendices I and IV. Cells were cultured in a humidified incubator at 37°C and 5% CO_2.

Cells were subcultured by washing with 5 mL of sterile PBS, followed by incubation in 4mL of 0.05% trypsin-EDTA (per T-75 flask) for approximately 10 minutes. Trypsin was subsequently inactivated by addition of 6 mL of complete medium for MCF-10a cells, and 4 mL of soybean trypsin inhibitor (1:1 volume with trypsin) for HMEC cell line. Cells were subsequently pelleted by centrifugation at 209g for 3 minutes. After re-suspension of the cell pellet in complete media, cells were used at the indicated densities for assays, or split 1:3 for cell line maintenance.

2.1.1.2 BT-474 and MCF-7

The human breast cancer cell line MCF-7 was obtained from ATCC and the BT-474 cell line was a kind gift from Dr. Darran O'Connor (UCD Conway Institute, Ireland). BT-474 cells were cultured in RPMI medium supplemented with 2mM L-glutamine, 100U/mL penicillin, 100µg/mL streptomycin and 10% foetal bovine serum (FBS). MCF-7 cells were cultured in DMEM, with the same additives as used for BT-474 medium, with addition of 1% non-essential amino acids. Cells were cultured in a humidified incubator at 37°C and 5% CO_2; and subcultured as indicated above, with the exception of using a split ratio of 1:4 for cell line maintenance.

2.1.1.3 MDA-MB-231, Hs578T and Hs578Ts(i)$_8$

The human breast cancer cell line MDA-MB-231 was obtained from ATCC. Hs578T and its more invasive sub-clone Hs578Ts(i)$_8$ (Hughes *et al.*, 2008) were donated by Dr. Susan McDonnell (UCD Conway Institute, Ireland). These cell lines were cultured in DMEM supplemented with 2mM L-glutamine, 100U/mL penicillin, 100µg/mL streptomycin and 10% FBS. Hs578T cell lines additionally required 0.1U/mL bovine insulin. Cells were cultured in a humidified incubator at 37°C and 5% CO_2.

MDA-MB-231 cells stably knocked down for caveolin-1 were a kind donation from Prof. I.R. Nabi (University of British Columbia, Vancouver). These had been transfected with a blasticidine-resistant pSHAG-1vector containing shRNA against caveolin-1 as described (Kojic *et al.*, 2007). These shCav-1 MDA-MB-231 cells were cultured in normal MDA-MB-231 medium, with the addition of 5µg/mL blasticidine, and sub-cultured similar to wild-type MDA-MB-231.

To sub-culture MDA-MB-231 and Hs578T cell lines, T-75 flasks were washed with 3 mL of sterile PBS, and incubated in 2 mL of 0.05% trypsin-EDTA for 2-5 minutes. Trypsin was inactivated by addition of 4mL of complete media, and cells were collected in by centrifugation at 209g for 3 minutes. Cells were then resuspended in complete media and used for assays as indicated or at a split ratio of 1:5 for routine maintenance.

2.1.2 Primary cell culture

Mammary tumour primary cell cultures were generated from mastectomies or lumpectomies obtained with full consent and prior ethical approval from symptomatic patients undergoing breast cancer surgery in Beaumont Hospital. The process of culture generation has previously been outlined (Donatello *et al.*, 2011). Primary cell cultures were grown in the same manner as HMEC. Cells used in this study were revived from previously-generated laboratory stocks of low passage number (no higher than 3).

For sub-culturing the primary cell cultures, cells were firstly washed with 3 mL of sterile PBS, and incubated in 2 mL of 0.05% trypsin-EDTA (per T-25 flask) until detachment (assessed by light microscopy). Trypsin was inactivated upon incubation with trypsin inhibitor. Cells were subsequently collected by centrifugation at 209g for 3 minutes. After re-suspension in MEGM medium, cells were used for assays as indicated or split in a 1:2 ratio in T-25 flasks.

2.1.3 Cell transfection

2.1.3.1 siRNA transfections

Small interfering RNA (siRNA) SmartPools against flotillin-1 and caveolin-1, as well as a universal negative control siRNA, were purchased from Dharmacon. Cells were seeded at low densities, as per manufacturer's instructions, in either 6- or 24-well plates, depending on the assay, and allowed to adhere overnight. Cells were then transfected for 72h with 25nM of each siRNA, using Dharmafect-1 transfection reagent, as described in the manufacturer's guidelines. Cells were subsequently used for different assays, as specified.

2.1.3.2 Plasmid DNA transfection

MDA-MB-231 and MCF-10a cells were seeded overnight at densities indicated in Table 2.1. Cells were transfected with pOTB7 plasmid DNA at various concentrations (Table 2.1) using jetPRIME transfection reagent, as per manufacturer's instructions. Briefly, appropriate concentrations of DNA were diluted to the required volumes with jetPRIME buffer, mixed with the transfection

reagent, and incubated at room temperature for 10 minutes. DNA-containing transfection mix was then added to the cells, and the medium was changed to the selective medium 4-5 hours later. The latter was composed of complete MDA-MB-231 or MCF-10a culture medium, with the addition of 300 and 500 µg/mL of chloramphenicol, respectively. Cells were analysed 48 hours post-transfection, unless specified otherwise.

Table 2.1 DNA cell transfection using jetPRIME transfection reagent

MDA-MB-231						
Culture vessel	**No. cells seeded**	**Volume of seeding medium (ml)**	**Volume of jetPRIME buffer (µl)**	**Amount of DNA (µg)**	**Volume of jetPRIME reagent (µl)**	**Volume of selecting medium**
24-well	$6x10^4$	0.5	50	0.5	1	1
6-well	$1.5x10^5$	2	200	2	4	4
10cm	$1x10^6$	10	500	10	20	10
MCF-10a						
24-well	$8x10^4$	0.5	50	0.5	1	1
6-well	$2.5x10^5$	2	200	2	4	4
10cm	$2x10^6$	10	500	10	20	12

2.1.4 Cryopreservation of cell cultures

Cells stocks were prepared by re-suspending cells in freezing medium following trypsinisation. For primary cultures and HMEC, cells were frozen in MEGM medium supplemented with 10% FBS and 5% DMSO, at approximately $2x10^5$ cells per cryo-vial. For all other cell lines the freezing medium was composed of complete medium with addition of 5% DMSO, at $5x10^5$-$1x10^6$ cells per cryo-vial. Cell cryo-vials were then placed into NALGENE® Cryo 1°C freezing container (to achieve -1°C/min cooling rate), and chilled in a -80°C

freezer overnight. Vials were then transferred into liquid nitrogen for long-term storage.

2.2 Protein Biochemistry

2.2.1 Cell Lysis

Cells were first incubated with room temperature -PBS at for 10 minutes at 4°C, followed by two washes in ice-cold PBS (7-10 minutes each, at 4°C), and lysed in different buffers, depending on the experiment.

Whole cell lysate preparation

After washing, cells were scraped in ice-cold lysis buffer containing 100mM KCl, 3mM NaCl, 3.5mM $MgCl_2$, 10mM HEPES, and supplemented with 1% Triton X-100, 1:100 protease inhibitor cocktail and 1:100 phosphatase inhibitor cocktails II and III (all obtained from Sigma-Aldrich). Cells were then homogenised 20 times using a tight-fitting Dounce tissue homogeniser, and centrifuged at 1500g at 4°C for 10 minutes to remove debris.

Lysate preparation for detergent-based lipid raft extraction

Following the PBS washes, cells (2x10cm dish per condition) were scraped in calcium- and magnesium-containing Hank's Balanced Salts Solution (HBSS), supplemented with 1% membrane-grade Triton X-100 (Roche) and 1:100 protease inhibitor cocktail (1mL per dish). Lysates were firstly homogenised with 20 strokes of a tight-fitting Dounce homogeniser, following by 20x trituration through a 26-gauge needle and end-over-end rotation at 4°C for 30 minutes. The resulting lysates were used to extract lipid rafts (see section 2.3).

Lysate preparation for detergent-free lipid raft extraction

Cells were lysed in 500mM sodium carbonate, pH 11.0, supplemented with 1:100 protease inhibitor cocktail. 2x10cm dishes were used per condition, and 1mL of lysis buffer was used per dish. The lysates were dounced 20 times,

triturated 20 times through a 26-gauge needle, and rotated end-over-end for 20 minutes at 4°C. These lysates were then used to isolate lipid rafts on a sucrose gradient (see section 2.3).

2.2.2 Protein quantification

Protein concentrations were calculated using a bicinchoninic acid (BCA) assay. A standard curve was generated with each set of samples by serial dilution of 5mg/mL bovine serum albumin (BSA) in PBS. A blank, containing PBS alone, was subtracted from all the readings. 10µl of each standard (in triplicate) and 10µl of each unknown sample were added to wells of a 96-well plate. BCA reagents A and B were mixed 1:50 and 100µl of the solution was added to each well. The plates were then incubated in the dark at 37°C until a purple colour developed. Absorbance was then read at 540nm with a PerkinElmer Victor X3 plate reader. Linear regression analysis of the standard curve was used to calculate the protein concentrations of each sample.

2.2.3 Immunoprecipitation

All steps were carried out at 4°C. Protein G sepharose (40-50µl/sample) was rinsed 3 times with PBS to remove the preserving buffer and used to pre-clear lysates of equal protein concentrations by end-over-end rotation for 1 hour. The beads were collected by centrifugation at 1000g for 1 minute. The supernatants were subsequently rotated overnight with 3-5µg of CD44 antibody per sample. Immuno-complexes were captured with 40-50µl of protein G sepharose per sample for 3 hours on an end-over-end rotator, and collected via centrifugation at 1000g for 1 minute. The complex-containing beads were then washed 3 times with cold lysis buffer and resuspended in 2X reducing Laemmli sample buffer (containing 40mM dithiothreitol). The CD44-containing complexes were then released by boiling at 100°C for 5 minutes for further analysis by SDS-polyacrylamide gel electrophoresis (PAGE) and immunoblotting.

2.2.4 Acyl-Biotin Exchange Assay

This assay was used to directly measure amounts of palmitoylated CD44 relative to the total CD44 content. For that, CD44 protein was immunoprecipitated from the lysates as described above, using 5μg of precipitating antibody. Antibody-protein complexes were collected by 3-hour rotation at 4°C with 50μl of protein G sepharose, in the presence of 50mM N-ethylmaleimide (NEM), to covalently block sulfhydryl groups (**Fig. 2.1**). Collected complexes were subsequently divided into two fractions, for treatment with and without 1M hydroxylamine (HAM) at room temperature for 1 hour (pH 7.40) to cleave free palmitate groups. Subsequently, samples were incubated with 1μM EZ-link biotin-N-(6-(biotinamido)hexyl)-3'-(2'-pyridyldithio)-propionamide (Biotin-BMCC) at pH 6.20 for 30 minutes at room temperature, to label the reactive cysteine residues. Labelled CD44 was released from the beads via 5 minute incubation at 100°C in 2X reducing Laemelli sample buffer (containing 5mM dithiothreitol), and subjected to SDS-PAGE and immunoblotting. Same blots were used for detection of firstly, palmitoylated CD44 and secondly, total CD44 (see section 2.2.7).

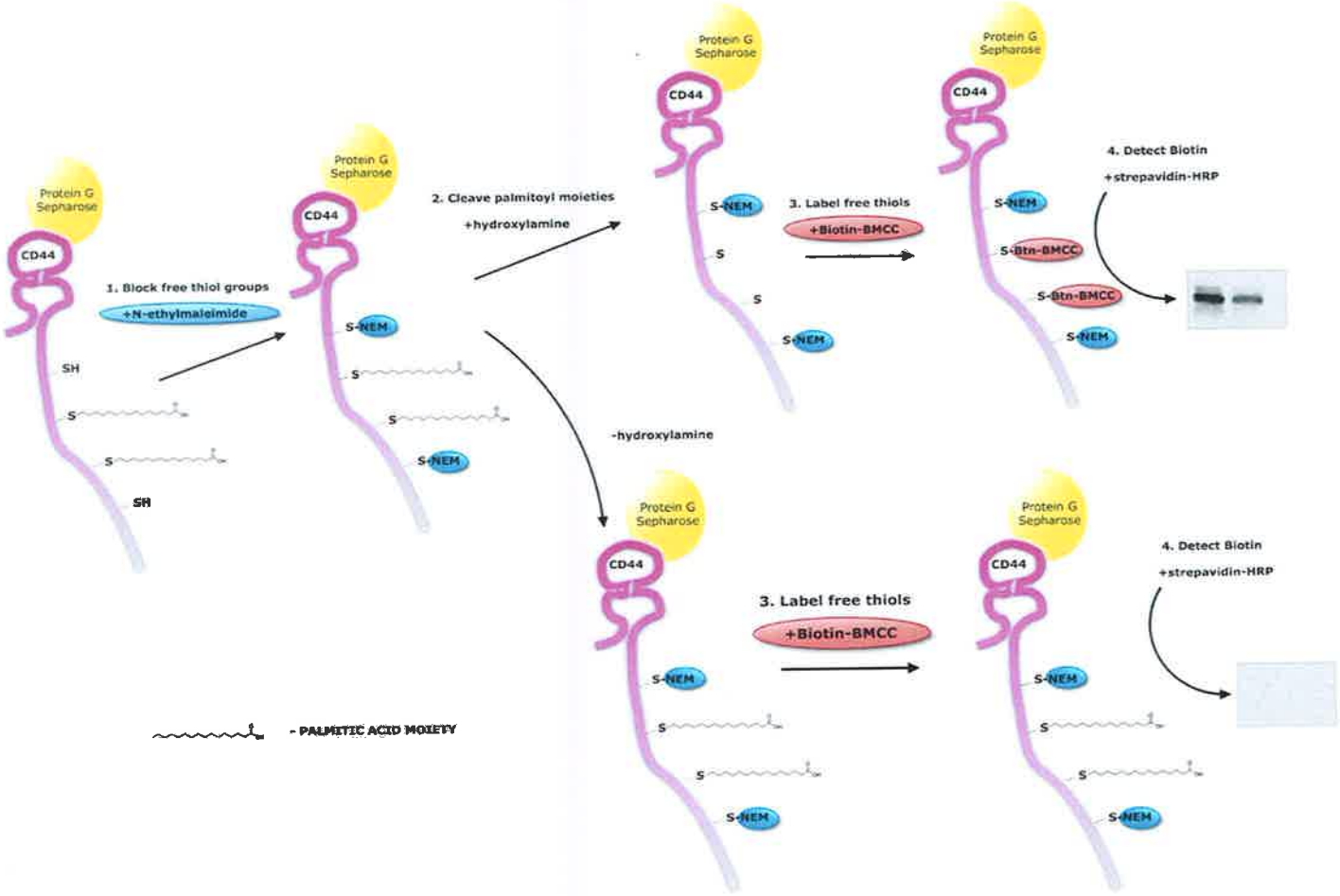

Figure 2.1 Schematic representation of the acyl-biotin exchange chemistry.

2.2.5 Sample preparation

The required sample protein concentrations were mixed with 4X reducing Laemlli sample buffer (80mM dithiothreitol) to yield a final concentration of 1X sample buffer. The samples were then boiled for 5 minutes at 100°C, briefly centrifuged and cooled to room temperature before being subjected to SDS-PAGE.

2.2.6 SDS-PAGE

Predominantly, 10% gels were prepared for protein analysis, but 8-9% gels were also utilized to analyse larger proteins and immonoprecipitated proteins, to allow better separation of bands. The desired protein quantities were loaded and run at a constant current of 40mA per gel in Tris-Glycine running buffer. The full recipes for buffers and gel preparations are listed in Appendix II.

2.2.7 Immunoblotting

Following SDS-PAGE, proteins were transferred onto nitrocellulose membranes by wet transfer at 100V for 1 hour at room temperature. Transfer buffer (Appendix II) was always prepared fresh and kept at 4°C until required. For proteins >150kDa, 0.05% SDS was added to the transfer buffer, and/or gels were transferred overnight at 30V / 4°C. Membranes were incubated for 1 hour (or 3 hours, for biotin detection) at room temperature in blocking buffer (typically 5% skim milk in TBS-Tween, or 5% BSA in TBS-Tween for biotin detection). Membranes were subsequently incubated in primary antibody, diluted in appropriate blocking buffer, at 4°C on a roller shaker. After washing, the membranes were incubated in respective secondary antibody for 1 hour at room temperature. Biotin-BMCC-labelled CD44 was detected upon incubation with streptavidin-HRP, followed by antibody incubation, to visualise total CD44 on the same membrane. Blots were developed by exposure to X-ray film using enhanced chemi-luminescent reagents.

The same membranes were re-probed (up to a maximum of 2 times) for expression of different molecular weight proteins following incubation in stripping buffer supplemented with 2-β-mercaptoethanol for 20 minutes at 60°C. The membranes were then extensively washed in TBS-Tween, and the immunoblotting

procedure was repeated from the blocking step onward. Proteins of similar molecular weight (±10 kDa) were always examined on different gels, as stripping method could introduce false results.

2.3 Lipid raft isolation and analysis

2.3.1 Preparation of sucrose gradients for lipid raft extraction

Fully confluent cells on 10cm dishes (2 dishes per condition) were either serum-starved for 2 hours or extensively scratch-wounded (10 horizontal and 10 vertical scratches made with p200 sterile pipette tip attached to gentle suction) and then allowed to migrate for 2 hours in serum-free medium (unless specified otherwise). These conditions were referred to as "non-migrating" and "migrating", respectively (see **Fig. 2.2** for overview). Cell lysates were obtained as described in section 2.2.1.

For discontinuous 5-45% sucrose gradients, sucrose solutions of 5, 20, 30 and 90% w/v were prepared. Sucrose was dissolved in HBSS containing calcium, magnesium and 10mM HEPES (for detergent extractions), or in 250mM sodium carbonate prepared in HBSS (for detergent-free extractions). All subsequent steps were carried out at 4°C. 2mL of each lysate was mixed with 2mL of 90% sucrose. The resulting 4mL were loaded at the bottom of a 12mL Beckman ultracentrifuge tube, and sequentially overlain with 2.6mL each of 30% and 20% sucrose, followed by 5% sucrose until ~3mm from the top of the tube. Using a pre-chilled SW41 rotor, the gradients were centrifuged at ~260,000g for 19 hours at 4°C in a Beckman Optima L-100K ultracentrifuge. Sequential 1mL fractions were manually collected starting from the top of each tube; and the pellet at the bottom was solubilised in 500µl of 0.2% SDS/PBS.

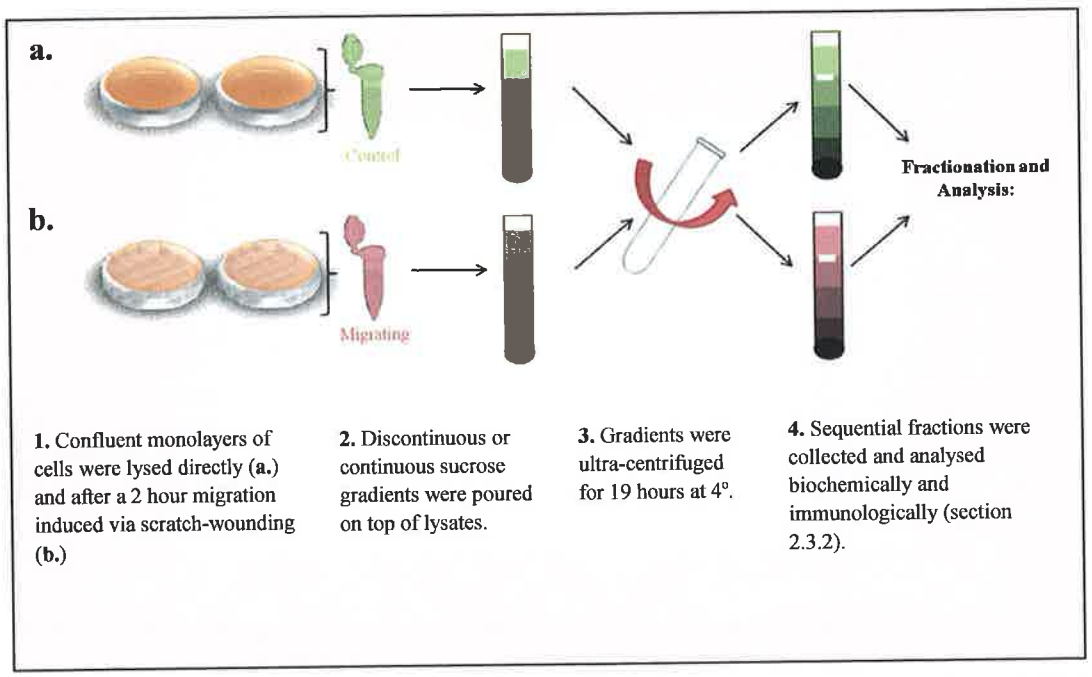

Figure 2.2. Schematic representation of lipid raft isolation procedure. Cells were first lysed and used to underlay continuous or discontinuous sucrose gradients. These were subjected to ultracentrifugation for 19 hours at 4°C, and equal volume fractions were collected for analysis.

2.3.2 Analysis of the sucrose gradient fractions

2.3.2.1 Sucrose density

Sucrose density of each fraction (3µl) was estimated using a hand-held refractometer, and plotted to confirm a linear increase in sucrose density with increasing fraction number.

2.3.2.2 Alkaline phosphatase activity

Alkaline phosphatase is an enzyme found highly enriched in lipid rafts. Its activity was assessed as a biochemical indication of lipid raft presence in fractions collected. 20µl of each fraction (or 20µl of PBS blank) was added to triplicate wells of a 96-well plate. *p*-nitrophenyl phosphate substrate solution was prepared by dissolving Sigma-Aldrich *p*-nitrophenyl phosphate tablets in appropriate volumes of dH_2O. Subsequently, 150µl added to each well. Plates were incubated at 37°C until a yellow colour developed (approximately 1 hour), whereupon absorbance was

measured at 405nm on a PerkinElmer Victor X3 plate reader. Values were normalised to the averaged blank and plotted against fraction number to visualise peaks of alkaline phosphatase activity.

2.3.2.3 Immuno-dot blot

To crudely identify lipid raft versus non-raft fractions, immuno-dot blotting was used to detect expression of the raft and non-raft protein markers flotillin-1 and transferrin receptor (respectively). 2µl of each fraction was spotted onto a nitrocellulose membrane. After air-drying, membranes were blocked in 5% skim milk in TBS-Tween for 1 hour at room temperature and subsequently processed similarly to full immuno-blots (section 2.2.7).

2.3.3 Triton X-100 insolubility assays

Cells were grown to confluence in 6-well plates. Wells were scratch-wounded (5 horizontal and 5 vertical scratches made with a sterile p200 pipette tip attached to gentle suction) and allowed to migrate for 2 hours in serum-free medium ("migrating" condition), or left stationary in serum-free medium for 2 hours ("non-migrating" condition). For various treatments and mutants, confluent non-migrating cells were used, unless otherwise specified. The detergent-soluble pool (enriched in non-raft cellular components) was obtained by harvesting the supernatant of cells rotated for 30 min at 4°C in 400µl ice-cold lysis buffer containing 1% Triton X-100 and protease and phosphatase inhibitor cocktails. The detergent-insoluble pool (enriched in lipid rafts) was subsequently collected via scraping in 200µl of lysis buffer. Protein concentrations were determined by BCA assay (section 2.2.2), and samples of equivalent protein concentration were then analysed by SDS-PAGE and immunoblotting.

2.4 Immunofluorescence

In order to directly visualise cellular protein distribution in cells and estimate its co-localisation with others, 13mm round coverslips were sterilised in 100% ethanol and placed in wells of 24-well plates. Cells were grown to confluence and fixed in ice-cold ethanol for 20 minutes at -20°C. After washing the cells 3 times

with PBS, coverslips were blocked overnight in 5% goat serum, diluted in PBS. Primary antibody and secondary antibodies (diluted in 5% normal goat serum) were incubated for 1 hour at room temperature in a humidity chamber. Nuclei were counterstained with 0.5μg/mL 4',6-diamidino-2-phenylindole (DAPI, diluted in PBS) for 10 minutes at room temperature. Each step was followed by three washes in PBS. Coverslips were mounted in PBS:glycerol:p-phenylenediaminehydrochloride (1:1:0.01 v/v/v), sealed with clear nail varnish and stored at -20° until visualised on a Zeiss LSM 710-meta confocal microscope.

2.5 Generation of CD44 palmitoylation mutants

2.5.1 CD44 wild-type plasmid culture

A bacterial agar stab culture containing pOTB7 plasmid encoding chloramphenicol resistance cassette and the standard isoform of full-length human CD44 was purchased from imaGenes, SourceBioscience LifeSciences, and is illustrated in **Figure 2.3**. The culture was aseptically spread onto Luria-Bertani (LB) agar plates (section 2.5.3) containing 200μg/mL chloramphenicol selection reagent. The plates were incubated overnight at 37° upside-down, and single colonies were aseptically transferred into 20mL tubes containing 5mL LB broth supplemented with 200μg/mL chloramphenicol. The cultures were propagated with vigorous shaking (~300rpm) at 37° overnight. For large-scale plasmid extraction, 50mL of chloramphenicol-positive LB broth was inoculated with 1mL bacterial culture and incubated overnight at 37°C.

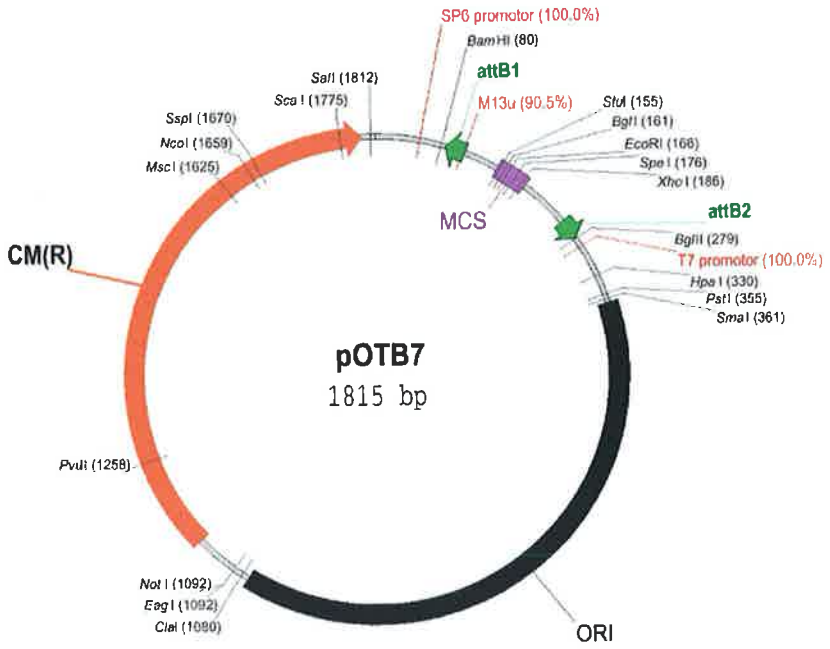

Figure 1.3 Map of the pOTB7. This double-stranded DNA plasmid encodes the human CD44 gene and carries resistance to chloramphenicol antibiotic. (SourceBioscience website; http://www.lifesciences.sourcebioscience.com/genomecube/vector.aspx?v=pOTB7).

2.5.2 Plasmid extraction

Initially, plasmids were extracted using a Qiagen QIAprep Mini-prep kit, until sequencing results confirmed the presence of the desired gene sequence. For that, 5mL bacterial cultures were firstly centrifuged at 6500 x g for 3 minutes at room temperature to collect the cells. The extraction procedure was carried out as per manufacturer's instructions. The key steps are illustrated in **Figure 2.4**. DNA elution buffer volume was optimised to be 70µl using the wild-type plasmid, which was used for all Mini-prep extractions.

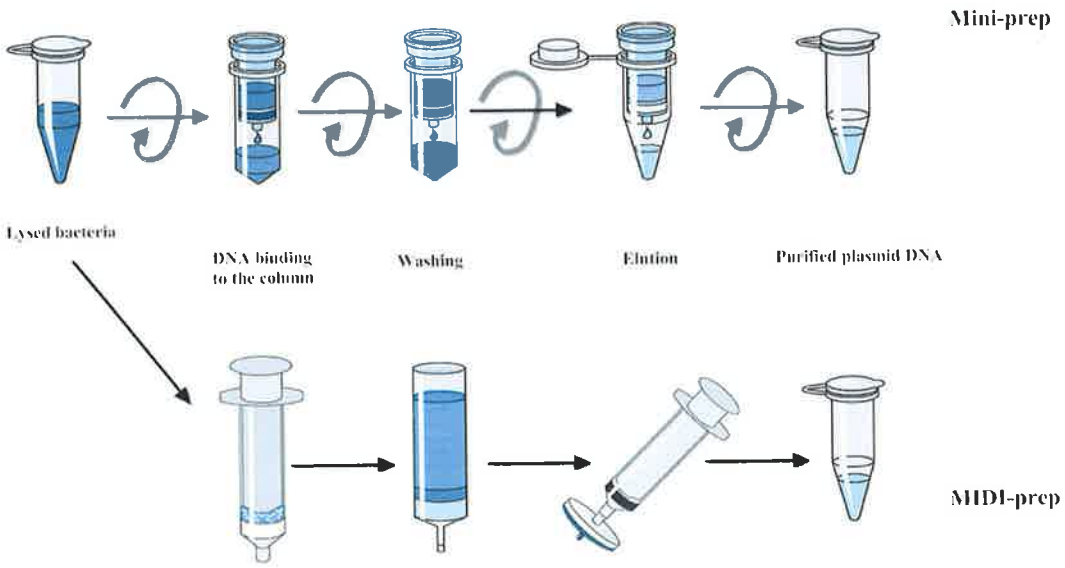

Figure 2.4 Plasmid extraction flow chart. Schematic summarises plasmid DNA extractions using mini-prep kit (above) and MIDI-prep kit (below). The figure is modified from QIAgen DNA purification handbooks, available from http://www.qiagen.com/literature.

After sequence confirmation, Qiagen HiSpeed Plasmid Midi Purification kit was used to extract larger quantities of DNA. 50mL cultures were centrifuged at 6000 x g for 15 minutes at room temperature. The extraction procedure was followed as outlined in the manufacturer's guidelines (summarised in **Figure 2.4**). The eluate was re-eluted 3 times instead of 2, to maximize the yield. DNA stocks were frozen in 20µl aliquots and stored at -20°.

2.5.3 DNA quantification

Eluted DNA was quantified spectrophotometrically at 260nm, using a ThermoScientific Nanodrop spectrophotometer. The machine was first calibrated to a blank (the appropriate elution buffer), then 1µl sample was spotted onto the reader and measured once. The quality of DNA was determined from the measured ratio of the absorbance at 260 and 280nm ($A_{260/280}$). If $A_{260/280}$ ratio of DNA was over 1.8, it was not used for cell transfection.

2.5.4 Site-directed mutagenesis

The CD44 wild-type plasmid was used as a template for single mutations (C286A and C286S) introduced in the palmitoylation sites. The C286A mutation-containing plasmids were in turn used as templates for introducing a point mutation in the second palmitoylation site of CD44 (C286A,295S [SA] and C286A,295A [AA]). Point mutations were introduced using Strategene QuikChange Site-Directed Mutagenesis kit, according the manufacturer's instructions. Mutagenesis primers used were obtained from Eurofins MWG Operon, and contained sequences summarised in Table 2.2.

Upon successful isolation of single mutant bacterial colonies, they were propagated for plasmid extraction (see section 2.5.3). All mutations were confirmed by sequencing (Source Bioscience) and alignment, using BLAST online software (2010 version).

Table 2.2 Oligonucleotide primers used for site-directed mutagenesis

Name	Oligonucleotide (5' to 3')
C286A Forward	GCT TTG ATT CTT GCA GTT GCC ATT GCA GTC AAC AGT CG
C286A Reverse	CGA CTG TTG ACT GCA ATG GCA ACT GCA AGA ATC AAA GC
C286S Forward	GCT TTG ATT CTT GCA GTT TCC ATT GCA GTC AAC AGT CG
C286S Reverse	CGA CTG TTG ACT GCA ATG GAA ACT GCA AGA ATC AAA GC
C295A Forward	CAG TCG AAG AAG GGC TGG GCA GAA GAA AAA GC
C295A Reverse	GCT TTT TCT TCT GCC CAG CCC TTC TTC GAC

2.5.5 Bacterial culture

2.5.5.1 LB broth preparation

LB broth was purchased from Sigma-Aldrich, with an extra 5g NaCl added per litre of broth. All the ingredients (see Appendix II for full list) were dissolved fully in water and sterilised by autoclaving. After cooling the broth to ~40°, appropriate selective antibiotics were aseptically added. The complete broth was stored at 4° for up to 1 week.

2.5.5.2 Preparation of LB agar plates

Sterile bacterial Petri dishes were used for agar plate preparation. For LB agar, agar was added to non-sterile LB broth and allowed to melt fully at 80°C, before being sterilised by autoclaving. Once cooled to ~60°C, the agar was aseptically supplemented with the appropriate selective antibiotics, in front of a Bunsen burner. For mutagenesis control bacteria the agar was additionally supplemented with X-gal and IPTG (both Sigma-Aldrich), as per Stratagene

mutagenesis protocol. Complete agar (25ml/dish) was then poured aseptically into the Petri dishes. Solidified plates were stored upside down at 4°C and warmed to room temperature before use.

2.5.5.3 Bacterial stock preparation

Bacteria were cultured in 5mL of LB broth as for the Mini-prep plasmid extraction protocol. 200µl of overnight cultures were then aseptically mixed 1:1 (v/v) with sterile glycerol and stored at -80°C. To recover the cultures, a small portion of ice from a frozen stock (kept on ice) was placed in the appropriate growth medium with a sterile inoculating loop. The stock tube was then quickly replaced at 80°C.

2.6 Cell treatments

2.6.1 Hyaluronic acid (HA) to stimulate CD44

Sterile HA powder (235kDa) was obtained from Lifecore Biomedical (Chaska, MN). A sterile tube was first weighed to record the initial mass, and re-weighed after sterile addition of HA powder. The weight difference was taken as mass of HA, and it was then dissolved in serum-free medium or PBS at room temperature for 1 hour to make up the final stock concentration of 5mg/ml. HA solutions were prepared fresh before each experiment. For immobilisation of HA, the stock solution was prepared and serially diluted in PBS. 500µl/well was allowed to bind overnight at 4°C in empty 24-well plates, for subsequent high density seeding of cells. For all other experiments HA stock and its dilutions were prepared directly in serum-free medium. Excess HA solutions were disposed of immediately after experiments.

2.6.2 Chemical modulation of palmitoylation status

Palmitic acid, Compounds III and V (palmitoyl transferase (PAT) inhibitors) and Palmostatin B (acyl thioesterase-1 (APT-1) inhibitor) were all dissolved in DMSO. Stocks were prepared in the same manner as HA, using sterile DMSO, at the final concentration of 100mM. Stock solutions were stored at -20° in 5µl aliquots. Specified working dilutions were prepared using appropriate culture medium.

2.7 Functional assays

2.7.1 Proliferation assay

3-(4,5-Dimethylthiazol-2-yl)-2,5-diphenyltetrazolium bromide (MTT) powder was dissolved in PBS to make up a stock of 5mg/ml. It was then filter-sterilised and stored in the dark at 4°C for up to 2 weeks.

In order to estimate proliferation rates of breast cancer cells, cells were seeded in 200µl of medium in 96 well plates and allowed to adhere overnight. 5,000 and 7,000 cells per well respectively were seeded for MDA-MB-231 and MCF-10a cells. Each condition was seeded at least in triplicate in 4 plates. One plate was measured the day after seeding, as a reference point (Day 0), and the others were treated as specified for individual experiments. Five hours before the desired time point, 20µl of MTT reagent was added directly to the medium of each well, and incubated in the dark at 37°C for 5 hours. The MTT medium was aspirated, crystals were dissolved in 200µl/well DMSO, and after a further 5 minute incubation, absorbance was measured at 540nm on a PerkinElmer Victor X3 plate reader. Averages from triplicates were normalised to the readings on Day 0, and plotted as linear plots to visualise rates of proliferation.

2.7.2 Scratch-wound migration assay

In order to measure migration potential of cells, they were seeded in 24-well plates at densities of approximately 50,000 cells/well and grown in complete medium until fully confluent. Cells were then wounded by a single scratch in the centre of the well using a p200 pipette tip, rinsed with PBS to remove any loose cells/remaining medium and allowed to migrate in serum-free medium for a number of hours in a humidified incubator at 37°C / 5% CO_2. Wounds were photographed immediately after wounding (Time=0) using a phase contrast microscope linked to a charge-coupled device camera (Olympus) and that precise location was then photographed every two hours for a duration of 6-8 hours. Wounds were measured at 6 reference points per wound using Scion Image software. The percentage wound closure was calculated relative to the Time=0 for each condition and plotted using SigmaPlot.

2.7.3 Invasion assay

Invasion capabilities of cells were measured using BD Biocoat invasion chambers (BD Biosciences) as per manufacturer's protocols. Briefly, 8μm pore invasion chambers coated with growth factor-reduced Matrigel were re-hydrated with complete medium (0.5 mL in each well and chamber) in a 24-well plate for 2 hours at 37°C and 5% CO_2. Cell suspensions at $5x10^4$cells/mL were prepared in serum-free medium, and after removal of rehydrating medium, 0.5 mL of those suspensions added per invasion chamber. 0.75 mL of complete serum-containing medium was used as a chemoattractant in the bottom well. Plates were incubated for either 6 or 22 hours at 37°C and 5% CO_2, whereupon medium was removed and each chamber scrubbed twice with a cotton bud soaked in PBS (to remove non-invaded cells). The chambers were then fixed in 100% methanol and stained with haemotoxylin (Sigma-Aldrich) for 2 minutes at room temperature. Each chamber was rinsed twice in ddH_2O and allowed to air-dry. The invasion membranes were removed with a scalpel and mounted on glass slides with 1:1 glycerol:PBS (v/v). Invaded cells were counted in five 20X fields or ten 40X fields using bright field microscopy.

2.7.4 Mammosphere formation assay

Mammosphere assay is based on a property of stem/progenitor cells to survive in serum-free suspension. Therefore this assay was used to examine stem/progenitor potential of mammary (cancer) cells. After trypsinisation, 10,000 cells were seeded in ultra-low adherence plates (Costar) in serum-free medium. Mammospheres were allowed to form for 7 days, when they were counted using a phase contrast microscope. The number of mammospheres formed was expressed relative to the original number of cells seeded. In some cases, the mammospheres were collected by centrifugation and lysed to analyse protein expression.

2.7.5 Colony formation assay

Colony formation assay was used to assess the ability of cells to form a colony from a single cell. After trypsinisation into a single-cell suspension, 200 cells

were seeded in 6-well plates in 3 mL of complete medium. Colonies were allowed to form for 10 days at 37°C and 5% CO_2, in a humidified incubator. Cells were then washed with PBS 3 times at room temperature and fixed in ice-cold100% methanol for 10 minutes at -20°C. Colonies were subsequently washed with PBS 3 times, and stained in 0.05% crystal violet (w/v in anhydrous acetic acid/methanol) at room temperature for 15 minutes. The staining solution was aspirated, and wells were washed with water until excess purple stain was removed. Plates were allowed to air-dry, and all colonies were quantified manually. Total colony number was then expressed relative to the original number of cells seeded to calculate colony formation efficiency.

2.8 Image analysis

Western blot films were scanned and band intensities were measured using ImageJ software. Any background signal was eliminated using "Subtract Background" plug-in of the software, followed by measurement of "integrated density" of each band. Co-localisation of confocal images was estimated by ImageJ software using "ColocoliseRGB" and "Area calculator" plug-ins.

2.9 Statistical analysis

Data were expressed as mean ± SEM of 3 or more independent experiments (number indicated in figure legends). In cases where less than 3 experiments were analysed, data were presented as mean ± standard deviation. Raw values were used for statistical analysis from a minimum of three independent experiments, and averages subsequently expressed as percent of internal control. *P* values were calculated using equal variance two-tailed Student's t-tests. For migration assays 2-way ANOVA tests were performed across all the time points using GraphPad Prism software. Results were considered significant if $p<0.05$.

Chapter 3

Correlation of CD44 lipid raft localisation with invasive potential in breast cancer cells

3.1 Introduction

Cell migration is one of the key early events in cancer metastasis (Yilmaz and Christofori, 2010). This process involves dynamic regulation of adhesion via proteins including CD44, an adhesion molecule frequently associated with aggressive tumours. CD44 is known to be localised to specialised cell membrane domains known as lipid rafts, yet functional significance of this association remains controversial. Thus the main focus of this chapter was in investigating a relationship between CD44 sub-localisation in lipid rafts and invasive potential of breast cancer cell lines.

3.1.1 Lipid rafts: membrane micro-domains

The main lipid components of the cell membrane are glycerophospholipids and sphingolipids, which maintain a liquid state at physiological temperatures (Brown and London, 1998). However there are regions in the cell membrane enriched in cholesterol and sphingolipids, creating a rigid state in the lipid bilayer. These micro-environments are called lipid rafts (Simons and Ikonen, 1997). Rafts are resistant to solubilisation in non-ionic detergents such as Triton X-100 (Brown and London, 1998), which enables their isolation along with any proteins associated with them.

Lipid rafts vary in nature due to the types of lipids and amounts of cholesterol present. One example of this is a lipid raft sub-population originally identified morphologically as flask-shaped invaginations of the plasma membrane, termed caveolae (Yamada, 1955). Subsequent characterisation of these domains revealed their enrichment in proteins of the caveolin family (Rothberg *et al.*, 1992). Localisation of caveolin proteins at the cell membrane together with high concentrations of cholesterol results in the characteristic curvature of caveolar membranes. Various classes of lipid rafts are associated with different proteins of diverse functions. **Table 3.1** summarises the variations in protein content of lipid rafts and caveolae, as their lipid compositions are broadly similar (reviewed in (Babina *et al.*, 2011)).

Table 3.1 Lipid and protein contents of caveolae and non-caveolar lipid rafts.

	Lipids	Protein Markers	Receptor Proteins	Signalling Proteins	References
Non-caveolar lipid rafts	Cholesterol Glycosphingolipid Sphingomyelin Ganglioside GM1 Ganglioside GM3	Flotillin-1, -2	Fas EGFR HER-2 IGF-1R CD44 ER	Ras Src Erk2 Shc	(de Laurentiis *et al.*, 2007; Nohara *et al.*, 1998; Patra, 2008)
Caveolae	Cholesterol Glycosphingolipid Sphingomyelin Ganglioside GM1	Caveolin-1, -2 and -3	Fas EGFR HER-2 IGF-1R CD44 ER uPAR MMP-1, -2, -9	Ras Src eNOS PI3 kinase Phospho-lipase C	

3.1.2 Protein markers of lipid rafts

Non-caveolar lipid rafts are associated with enrichment in flotillin-1 and flotillin-2, members of the reggie family of proteins (**Fig. 3.1A**). Flotillins undergo dynamic lipid modifications in order to permit their partitioning to rafts. For example, acylation of flotillin-1 is essential for its localisation to lipid rafts (Morrow *et al.*, 2002), while two hydrophobic stretches also contribute to its raft affiliation (Liu *et al.*, 2005). On the other hand, flotillin-2 is targeted to lipid rafts via both myristoylation and palmitoylation. Flotillins were originally thought to be localised in caveolae (Bickel *et al.*, 1997), however later studies demonstrated the opposite (Neumann-Giesen *et al.*, 2004; Stuermer *et al.*, 2004). Much remains to be determined about the functionality of flotillins in lipid rafts, in particular, the significance of their highly conserved N-terminal domain (Babuke and Tikkanen, 2007; Tavernarakis *et al.*, 1999).

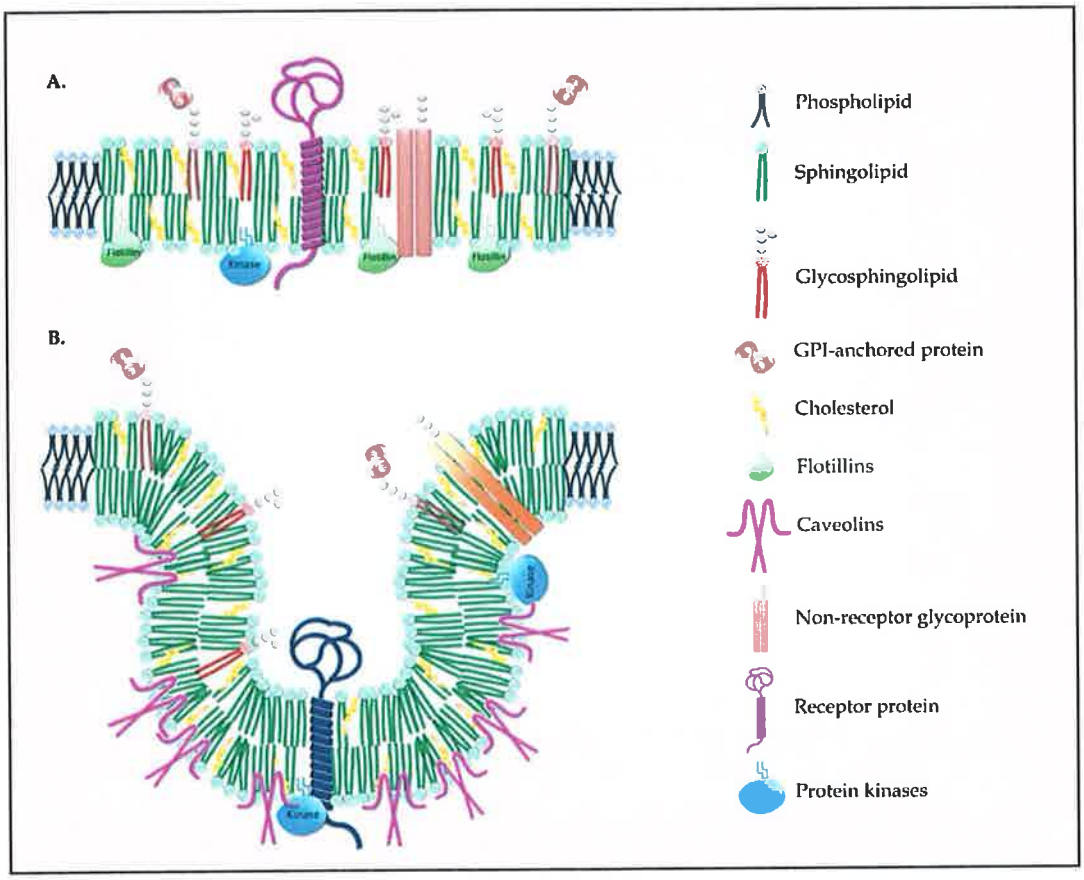

Figure 3.1 Lipid and protein components of (A.) non-caveolar lipid rafts and (B.) caveolae.

In addition to glycosphingolipids (Tran *et al.*, 1987) and increased cholesterol content relative to the bulk plasma membrane (Rothberg *et al.*, 1990), caveolae are enriched in caveolins, a family of 21-24 kDa integral membrane proteins. There are three known caveolins: caveolin-1 (Rothberg *et al.*, 1992), caveolin-2 (Okamoto *et al.*, 1998) and caveolin-3 (Tang *et al.*, 1996). Caveolins form "omega" invaginations in the membrane via cytoplasmic localisation of both their N- and C-termini (**Fig. 3.1B**). Aside from palmitoylation, the ability of caveolins to bind sphingolipids (Fra *et al.*, 1995) and cholesterol (Murata *et al.*, 1995) can also account for their high affinity for caveolar lipid rafts. Caveolins -1 and -2 are abundantly expressed in most cell types, including adipocytes, fibroblasts, endothelial and epithelial cells (Fan *et al.*, 1983; Galbiati *et al.*, 2001). However, expression of caveolin-3 is restricted to muscle (Rubin *et al.*, 2007). The N-terminal region of caveolin-1 contains a scaffolding domain, enabling its interactions with various signalling molecules, highlighting the potential importance of caveolin-1 for integrating the signalling functions of caveolar lipid rafts (Everson and Smart, 2006).

3.1.3 CD44 protein overview

CD44 is an adhesive transmembrane glycoprotein encoded by a single highly-conserved gene on human chromosome 11 (Goodfellow *et al.*, 1982). Multiple CD44 expressional variations occur at the transcription stage, due to alternative splicing of at least nine variant exons of the stem structure of the protein (**Fig. 3.2**) (Borland *et al.*, 1998). The N-terminal domain, the transmembrane region and the cytoplasmic tail of CD44 are highly conserved in various species. The N-terminal domain is vital for interactions with various components of the extracellular matrix (ECM), primarily with hyaluronic acid (HA); while the cytoplasmic tail region is important for interactions of CD44 with the actin cytoskeleton via cytoplasmic linker proteins including members of the ezrin-radixin-moesin (ERM) family, annexin II, and merlin (Bourguignon, 2001).

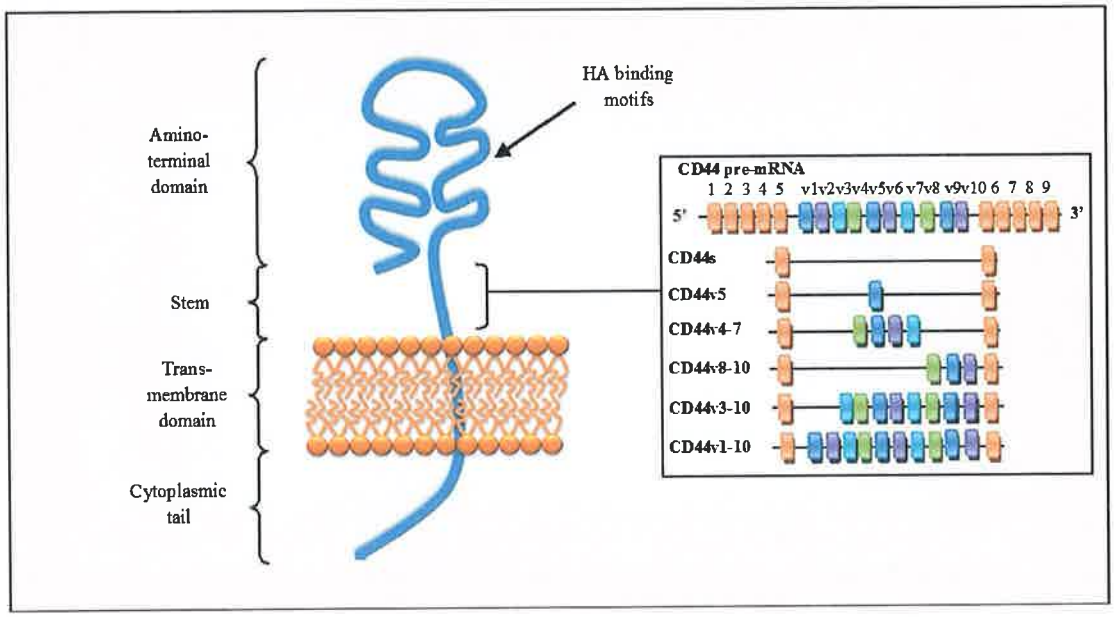

Figure 3.2 Structure of CD44 and its variant isoforms. CD44 comprises an amino-terminal domain responsible for HA binding and other ECM interactions; a stem which can be alternatively spliced to give variant CD44 forms (see inset); a trans-membrane domain containing palmitoylation residues for targeting to lipid rafts, and a cytoplasmic tail containing docking sites for cytoplasmic partner proteins.

3.1.4 Lipid rafts, CD44 and breast cancer

Most breast cancers arise from epithelial cells within the mammary gland, but the resulting tumours are highly heterogeneous and therefore accurate clinical prediction of patient outcome is difficult. Specifically, it is challenging to predict which tumours will progress to aggressive phenotypes as breast cancer biomarkers exclusive to aggressive tumours are still lacking (Gotte and Yip, 2006). This is because the molecular processes involved in tumour cell progression and invasion are still incompletely understood. However, since interactions between the actin cytoskeleton and the cell membrane regulate cancer cell motility, their potential involvement in progression towards tumour metastasis is undeniable (Jiang *et al.*, 1994; Lauffenburger and Horwitz, 1996).

Many studies have been directed at establishing molecular targets on breast cancer cells that would correlate with malignant behaviour such as enhanced proliferation, survival or cell migration. CD44 is one such molecule which has received a lot of attention. Due to its acylation, CD44 is often localised in lipid rafts, but it is unclear how this localisation affects breast cancer cell migration.

CD44 acts as the major receptor for HA (Herrera-Gayol and Jothy, 1999); but it can also act as a co-receptor for growth factors (Bourguignon *et al.*, 1997; Orian-Rousseau *et al.*, 2002) and organise the cellular actin cytoskeleton through cytoplasmic linker proteins (Ponta *et al.*, 2003). CD44 was shown to be associated with MMP9 in the cell membrane of breast tumour cells, promoting tumour cell migration and invasion (Bourguignon *et al.*, 1998). Therefore it is possible that this matrix-degrading association takes place in the lipid rafts of breast cancer cells, where both CD44 and MMP9 localize. Interaction of CD44 with matrix-binding HA also stimulates a variety of events leading to tumour progression, including Rho kinase activation, Ras signalling and others (reviewed in (Bourguignon, 2008)). Although the exact mechanisms of these events are yet to be clarified, one proposed method involves CD44 interaction with ankyrin within lipid rafts, leading to endothelial cell adhesion and progression (Singleton and Bourguignon, 2004). Another matrix glucosaminoglycan, osteopontin, can also activate CD44 to promote

cell survival and increased endothelial adhesion by recruiting Src and integrins into the lipid rafts (Lee *et al.*, 2008).

The influence of CD44 on cancer progression also extends to other growth factor signalling pathways, as it has been previously demonstrated that a growth factor receptor c-Met cannot be activated by its ligand alone but requires CD44 co-expression (van der Voort *et al.*, 1999). c-Met, which has been shown to localise in lipid rafts and whose signalling is sensitive to cholesterol depletion (Coleman *et al.*, 2009), is frequently dysregulated in metastatic breast cancer (Elnagar *et al.*, 2011; Gastaldi *et al.*, 2010). It can thus be hypothesised that lipid rafts are required for successful transduction of growth factor- mediated oncogenic signal through formation of a functional CD44 complex with its targets. Yet much remains to be investigated about the role of rafts in controlling CD44-based migratory events.

Our preliminary data led us to hypothesise that, during breast cancer cell migration, CD44 must move out of lipid rafts in order to interact with its actin-binding partner ezrin. Therefore investigating the affiliation of CD44 with lipid rafts could offer insight into breast cancer cell migratory mechanisms and suggest novel therapeutic targets.

3.2 Aims

Based on our general hypothesis that CD44-based breast cancer cell migration requires translocation of CD44 out of lipid rafts to interact with ezrin, the overall aim of this chapter was to determine the relationship between lipid raft affiliation of CD44 and the invasive potential of a panel of breast cancer cell lines. This was approached via the following specific objectives:

1. to compare expression of CD44 and ezrin inside versus outside of lipid rafts in a panel of breast cancer cell lines of varying invasiveness;
2. to assess CD44 and ezrin localisation in lipid rafts during CD44-specific cell migration, stimulated with HA;
3. to explore involvement of distinct types of lipid rafts in regulation of CD44 localisation and breast cancer cell migration.

3.3 Results

3.3.1 Expression of CD44 in a panel of breast cancer cells in detergent-positive or detergent-free conditions

We first sought to determine CD44 expression and localisation relative to lipid rafts in a panel of breast cancer cell lines with variable invasive capabilities. The models chosen for non-invasive breast cancer were HMEC primary cultures and the MCF-10a cell line. Weakly-invasive cell line models were MCF-7 and BT-474 cells; and highly-invasive cancer cells were represented by the MDA-MB-231, Hs578T and Hs578Ts(i)$_8$ breast cancer cell lines (Lacroix *et al.*, 2004). **Figure 3.4** shows an overview of CD44 expression across these cell lines. Cells were lysed in buffers containing either Triton X-100 (detergent-positive) or sodium carbonate (detergent-free) and probed for CD44, ezrin, flotillin-1 and actin (loading control). Although detergent-positive isolations gave higher protein yields, the expression pattern of all proteins were broadly comparable for both methods.

CD44 was detected in most cell lines analysed, but was low to undetectable in the weakly-invasive cells (**Fig. 3.4**). The MCF-7 cell line had only a minuscule amount of CD44 detected at ~130kDa, whereas BT-474 had no detectable CD44. The non-invasive cell lines expressed a range of bands for CD44. Normal mammary cells (HMEC) showed ~100kDa and 160kDa CD44 bands, and MCF-10a demonstrated predominantly a ~130kDa band, although the standard, ~90kDa form (CD44s) was also detected in smaller amounts. Both Hs578T cell lines exhibited a range of CD44 bands, ranging from CD44s at 90kDa to forms >250kDa. MDA-MB-231 cells expressed predominantly CD44s. When lysates were tested after scratch-wounded cells had been allowed to migrate for 2 hours in serum-free medium, CD44 expression was mostly unchanged with the exception of a small increase in HMEC and MCF-7 cell lines.

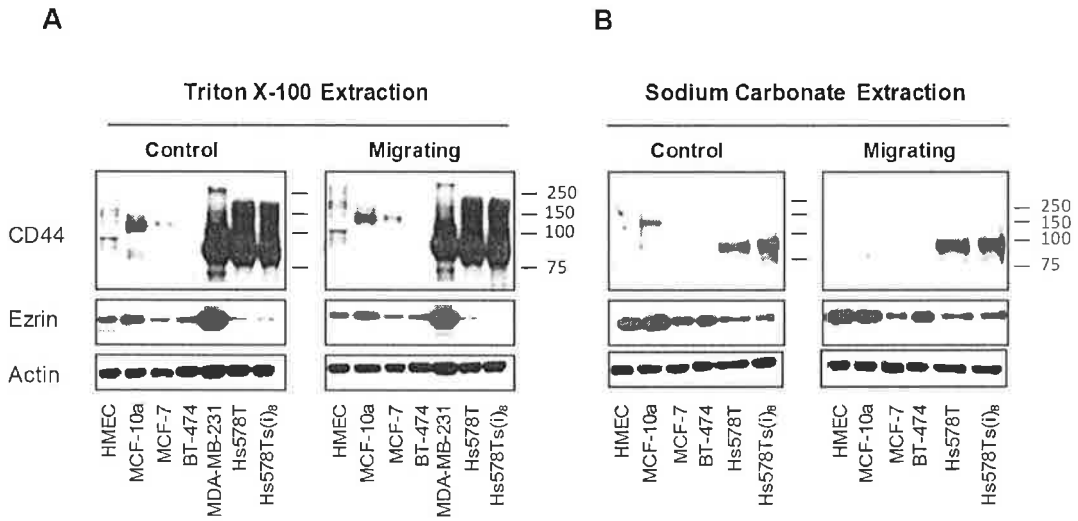

Figure 3.4 Total expression of CD44 and ezrin in a panel of breast cancer cell lines. Total cell lysates were prepared from confluent non-migrating versus migrating cells using detergent-positive or –negative buffers, separated by SDS-PAGE and analysed by western blot for CD44, ezrin or actin expression. Non-invasive cell lines HMEC and MCF-10a demonstrated expression of CD44 bands at approx. 120, 140, 160 and 200 kDa, with the standard form at 90kDa faintly detectable in MCF-10a. The weakly-invasive cell line MCF-7 showed low amounts of CD44 at 130 kDa, and no CD44 was detected in BT-474 cells. The highly-invasive breast cancer cell lines demonstrated strongest expression of CD44, with MDA-MB-231 having predominantly the standard 90kDa band, and both Hs578T cell lines with expression of a panel of CD44 bands from 90-250 kDa. Highest ezrin expression was observed in MDA-MB-231 cells, while Hs578T cell lines showed negligible levels. The remaining cells demonstrated similar amounts of ezrin compared to each other. The two lysis methods differed in the yield of protein obtained, but overall protein expression patterns were comparable.

The two lysis methods differed in their ability to extract ezrin. Under detergent-free extraction conditions, the cell lines expressing the highest amounts of ezrin were those with the least-invasive phenotype, HMEC and MCF-10a. MCF-7, BT-474 and Hs578T cells all had very similar levels of the protein. After stimulation of migration, ezrin levels in all of the cell lines remained relatively unchanged compared to the control.

3.3.2 Comparison of detergent-positive and detergent-free lipid raft extraction.

In order to examine the changes in CD44 and ezrin cellular sub-localisation relative to lipid rafts in migrating cancer cells, lipid rafts were extracted under detergent-positive (1% Triton X-100) and detergent-free (500mM sodium carbonate) conditions using a sucrose density gradient approach. Both methods isolate membrane regions enriched in cholesterol, but each approach may yield a slightly variant population of lipid rafts (Pike, 2004). In order to eliminate the possibility of artifacts arising from the use of cold Triton X-100, both detergent-positive and detergent-free methods were initially used for each cell line.

Fractions collected from each gradient were firstly assessed for activity of the lipid raft-associated enzyme alkaline phosphatase (Milhiet *et al.*, 2002) (**Fig. 3.5A.**). Increased activity was observed in fractions 4-7 (suggestive of lipid raft enrichment in these fractions), although the activity peak for detergent-free extraction was wider than that using the detergent-positive method. The other fractions showed very low alkaline phosphatase activity in comparison. Secondly, the protein concentration of each fraction was calculated by BCA assay (**Fig. 3.5B.**). In both extraction methods, protein concentrations increased towards the bottom of the gradient (fractions 8-11), with top fractions (1-6) and the pellet (fraction 12) having very low protein concentrations. The Triton X-100 extraction method yielded higher protein concentrations compared to the detergent-free approach. Thirdly, sucrose density was measured using a refractometer (**Fig. 3.5C.**) to verify the integrity of the gradients post- centrifugation. In both isolation approaches, sucrose density increased in a linear manner from approximately 10% in the top fraction to approximately 45% in the last fractions. Cloudy bands visibly enriched in lipid particles were usually

observed at fractions of 20-25% sucrose density, coinciding with the alkaline phosphatase activity peak and suggesting lipid raft enrichment in those fractions. Finally, to confirm the presence of lipid rafts in specific fractions, dot blots were performed to detect the lipid raft marker flotillin-1. Both extraction methods demonstrated flotillin-1 enrichment in the fractions of peak alkaline phosphatase activity (**Fig. 3.5D.**). In the detergent-extraction method, flotillin-1 peaked in fractions 4 and 5; while in the detergent-free method flotillin-1 was found to be enriched in fractions 5 and 6.

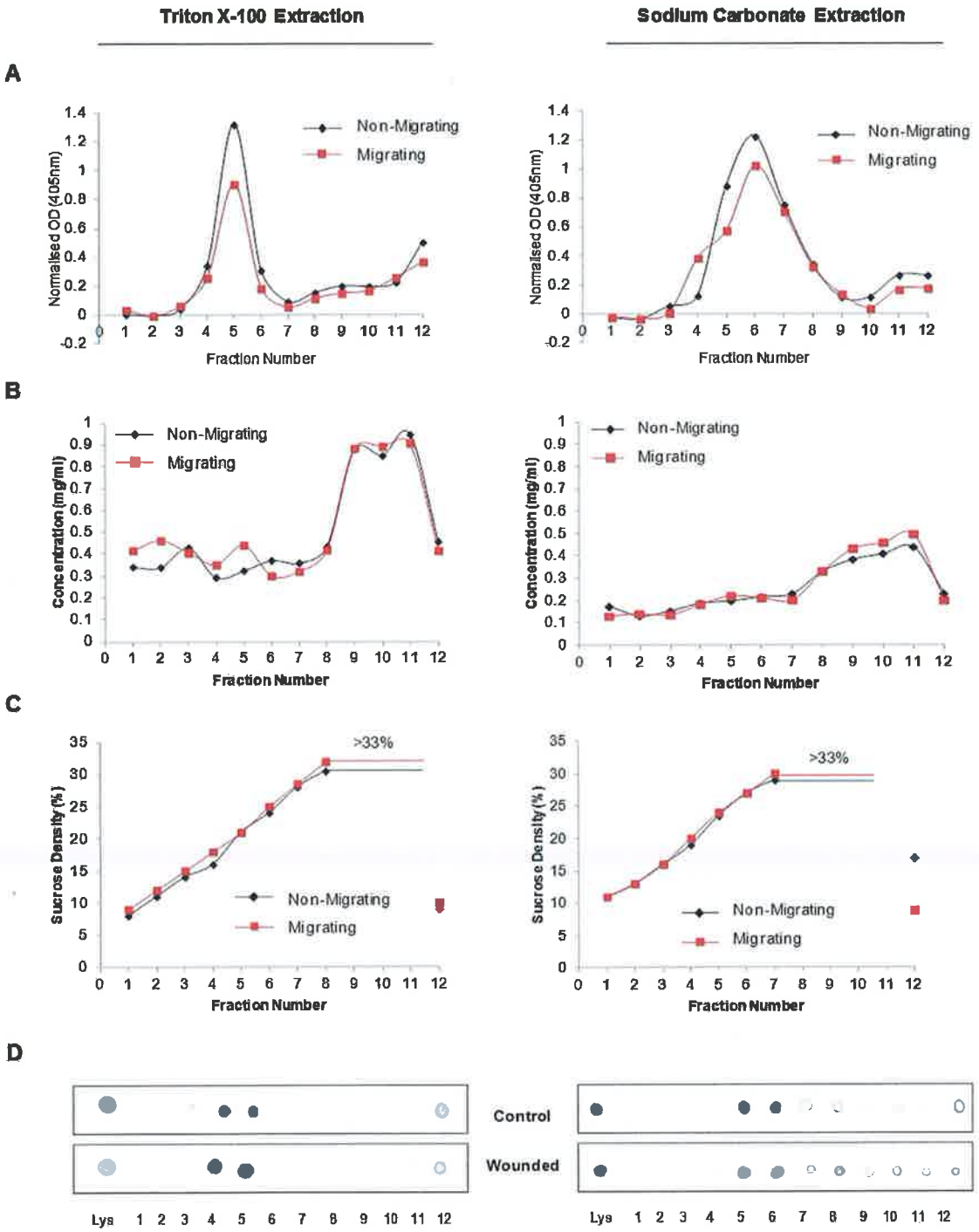
Triton X-100 Extraction
Sodium Carbonate Extraction
A
Normalised OD (405nm)
Non-Migrating
Migrating
Fraction Number
B
Concentration (mg/ml)
Non-Migrating
Migrating
Fraction Number
C
Sucrose Density (%)
>33%
Non-Migrating
Migrating
Fraction Number
D
Control
Wounded
Lys 1 2 3 4 5 6 7 8 9 10 11 12

Figure 3.5 Comparison of Triton X-100 and sodium carbonate methods of lipid raft extraction. Non-migrating and migrating (2hr) MDA-MB-231 cells lysed with either detergent-positive or detergent-free buffers were subjected to lipid raft extractions on sucrose gradients. The 12 collected fractions were subsequently analysed biochemically, measuring **(A.)** activity of a lipid raft enzyme alkaline phosphatase; **(B.)** protein concentration using BCA assay and **(C.)** sucrose density using a refractometer. **(D.)** In addition, immuno-dot blots were performed to analyse relative expression of a lipid raft marker flotillin-1 in the collected fractions. Representative results of at least 3 experiments for each type of lipid raft extraction are shown.

3.3.3 Lipid raft localisation of CD44 in a panel of breast cancer cell lines.

Having established that detergent-positive lipid raft preparations provided higher protein content and better discrimination between raft and non-raft compartments, only results from this method will be shown hereafter. Sucrose gradient fractions that were enriched in flotillin-1 are referred to as "raft" fractions, and fractions towards the bottom of the gradients that lacked flotillin-1 expression but expressed the non-raft marker transferrin receptor are called "non-raft". Blots presented here are from representative lipid raft extractions, while the quantitations represent results from three independent experiments (unless stated otherwise).

Non-invasive cell lines

Figure 3.6A. shows the distribution of CD44 in lipid raft and non-raft fractions in non-invasive HMEC and MCF-10a cells. CD44 was low to undetectable in non-migrating HMEC cells, and was recovered only in transferrin receptor-enriched non-raft fractions. Expression of CD44 in MCF-10a cells (**Fig. 3.6B**) was significantly higher than that in HMEC, with a 130-160kDa isoform of CD44 being recovered exclusively from the flotillin-enriched lipid raft fractions. Non-raft fractions also contained CD44, but only the standard 90kDa isoform. CD44 recovery in lipid raft fractions was increased after migration was induced.

The relative quantities of CD44, flotillin-1 and transferrin receptor were estimated by densitometric analysis of western blot films pooled from 3 independent experiments. A relative ratio of lipid raft-affiliated CD44 (normalised against flotillin-1 expression) to non-raft-CD44 (normalised against transferrin receptor expression) was calculated and used as an objective quantitative measure of CD44 affiliation with lipid rafts (**Fig. 3.6, right panel**). Since no CD44 was detected in the lipid raft fractions of HMEC cells, the CD44 raft/non-raft affiliation ratio was zero. However there was a significant increase in this ratio in MCF-10a cells, indicating increased partitioning of CD44 to lipid rafts during migration.

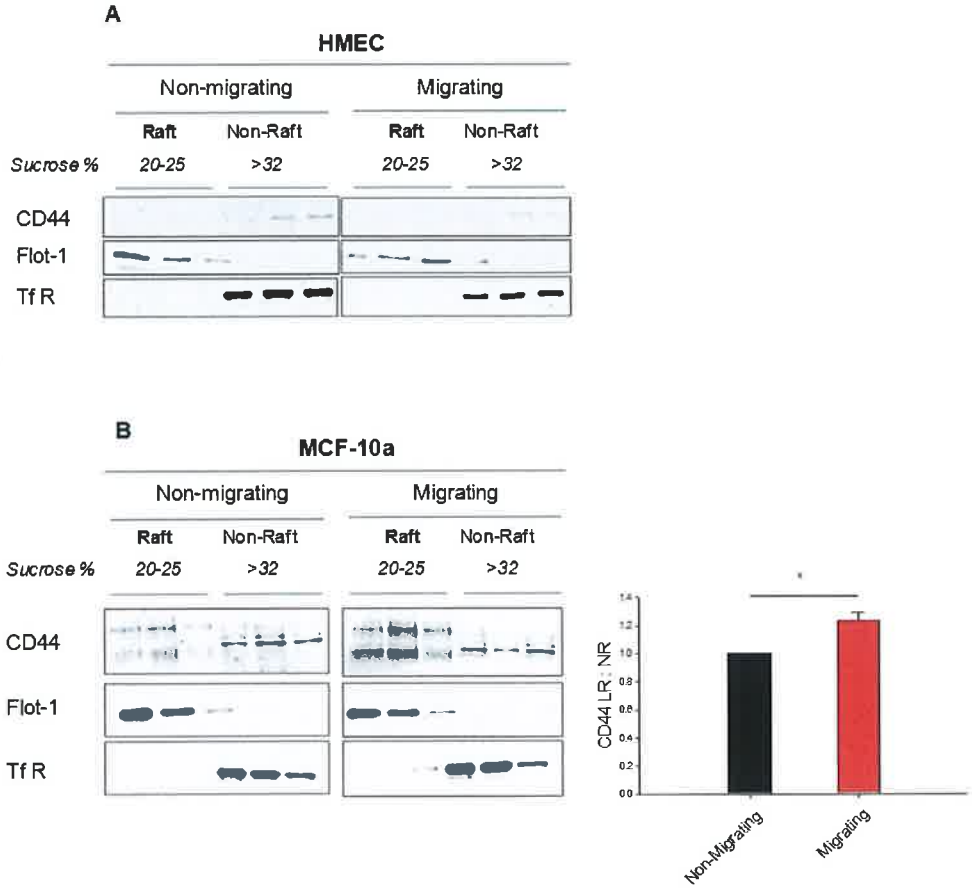

Figure 3.6 CD44 affiliation with lipid raft domains is increased during migration of non-invasive cells. Expression of CD44, raft marker flotillin-1 (Flot-1) and non-raft marker transferrin receptor (Tf R) were measured by western blot in lipid raft and non-raft fractions of HMEC and MCF-10a cells under non-migrating and migrating (2hr) conditions. While unable to detect CD44 in lipid rafts of HMEC cells **(A.)**, CD44 was predominantly localised to lipid rafts of MCF-10a cells **(B.)**. In migrating MCF-10a cells CD44 recovery from raft fractions had increased. Densitometry was used to calculate the relative expression of CD44 inside and outside of rafts, normalised to expression of the respective protein markers Flot-1 and Tf R. An increase in this ratio in MCF-10a cells (CD44 LR:NR, graph) was indicative of an increase in CD44 raft affiliation. *Error bars=SEM; *p<0.05, by unpaired 2-tailed Student's t-test; n=3 experiments.*

Weakly-invasive cell lines

The models for weakly-invasive breast cancer cells were the MCF-7 and BT-474 cell lines. CD44 expression in MCF-7 cells was detected only in non-raft fractions under control and migrating conditions (**Fig. 3.7A.**). Like MCF-7, CD44 was exclusively detected in non-raft fractions of BT-474 cells (**Fig. 3.7B**). Thus the CD44 lipid raft/non-raft ratio for these cells was zero under both non-migrating and migrating conditions.

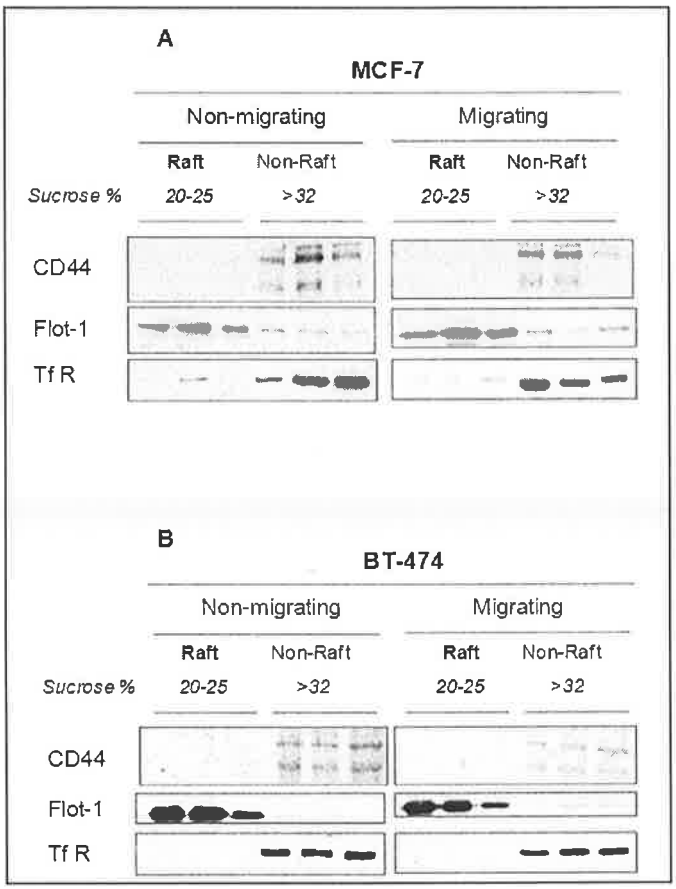

Figure 3.7 CD44 could not be recovered from lipid rafts of weakly-invasive breast cancer cell lines. Expression of CD44, flotillin-1 and transferrin receptor was measured in lipid raft and non-raft fractions of non-migrating and migrating MCF-7 **(A.)** and BT-474 **(B.)** cell lines. CD44 was exclusively recovered from non-raft fractions in both cell lines.

Highly-invasive cell lines

As previously noted, total CD44 levels were substantially higher in highly-invasive cell lines compared to the others (**Fig. 3.4**). Analysis of its partitioning to raft versus non-raft domains of MDA-MB-231 cells (**Fig. 3.8A)** demonstrated a visible enrichment of CD44 in lipid rafts in non-migrating cells. However after 2 hours of migration, CD44 was predominantly detected outside lipid raft domains. This was further demonstrated by a statistically significant decrease in the CD44 raft affiliation ratio under migrating conditions (**Fig. 3.8A, right panel**).

In Hs578T parental cells CD44 was found to be expressed mostly outside rafts, but some protein was also detected in raft fractions (**Fig. 3.8B**). As with MDA-MB-231 cells, the distribution of CD44 was altered after migration was induced. Specifically, a decrease in lipid raft-affiliated CD44 was parallelled by increased CD44 recovery outside lipid rafts in migrating cells. This putative translocation of CD44 outside rafts was also illustrated by a decrease in the CD44 lipid raft affiliation ratio (**Fig. 3.8B, right panel**).

The more invasive isogenic variant Hs578Ts(i)$_8$ cells showed a CD44 raft affiliation profile similar to its parental cell line Hs578T, in which the majority of CD44 was recovered from non-raft domains (**Fig. 3.8C**). A small but consistent pool of raft-affiliated CD44 was reduced after 2 hours of migration, and paralleled by increased CD44 recovery outside lipid rafts. Calculation of the CD44 raft affiliation ratio confirmed a decrease (though not statistically significant) in CD44 affiliation with lipid rafts in migrating Hs578Ts(i)$_8$ cells (**Fig. 3.8C, right panel**).

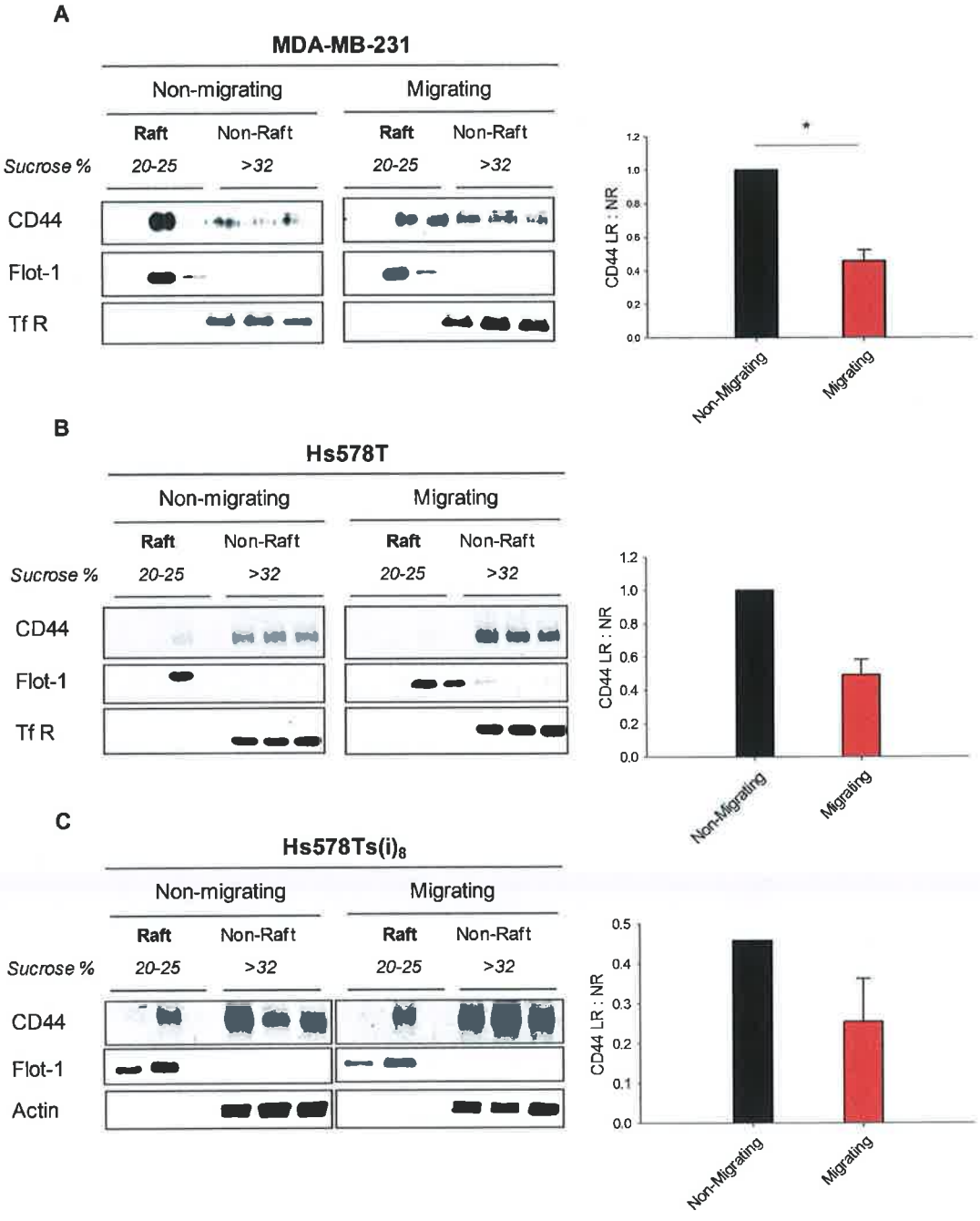
A
MDA-MB-231
Non-migrating
Migrating
Raft
Non-Raft
Raft
Non-Raft
Sucrose %
20-25
>32
20-25
>32
CD44
Flot-1
Tf R
CD44 LR : NR
1.2
1.0
0.8
0.6
0.4
0.2
0.0
*
Non-Migrating
Migrating
B
Hs578T
Non-migrating
Migrating
Raft
Non-Raft
Raft
Non-Raft
Sucrose %
20-25
>32
20-25
>32
CD44
Flot-1
Tf R
CD44 LR : NR
1.2
1.0
0.8
0.6
0.4
0.2
0.0
Non-Migrating
Migrating
C
Hs578Ts(i)8
Non-migrating
Migrating
Raft
Non-Raft
Raft
Non-Raft
Sucrose %
20-25
>32
20-25
>32
CD44
Flot-1
Actin
CD44 LR : NR
0.5
0.4
0.3
0.2
0.1
0.0
Non-Migrating
Migrating

Figure 3.8 CD44 affiliation with lipid rafts was reduced upon migration of highly-invasive cell lines. Lipid rafts of non-migrating and migrating (2hr) MDA-MB-231 **(A.)**, Hs578T **(B.)** and Hs578Ts(i)$_8$ **(C.)** cell lines were analysed for expression of CD44 and the raft /non-raft markers flotillin-1 (Flot-1) and transferrin receptor (Tf R), respectively. Across all three cell lines CD44 expression was predominantly concentrated in non-raft fractions in non-migrating cells. In all migrating cells, CD44 recovery from lipid raft domains was reduced, in parallel with increased CD44 recovery in non-raft domains. Calculation of the CD44 raft affiliation ratio revealed a significant reduction in CD44 association with lipid rafts in migrating MDA-MB-231 cells **(A.,** *Error bars=SEM; *p<0.05 by unpaired 2-tailed Student's t-test; n=3 experiments).* Similar trends of a reduction in CD44 affiliation with lipid rafts during cell migration were observed in the isogenic cell lines Hs578T **(B.)** and Hs578Ts(i)$_8$ **(C.)** (*Error bars=STDEV; n=2 experiments).*

The impact of cell migration on CD44 localisation relative to lipid rafts was additionally assessed using immofluorescence and confocal microscopy. Non-migrating and migrating MDA-MB-231 cells were double-labelled for CD44 (green) and the lipid raft marker flotillin-1 (red, **Fig. 3.9A**). Yellow areas of co-localisation were reduced under migrating conditions, as confirmed by pixel overlap quantification using ImageJ software (**Fig. 3.9B**). Furthermore, CD44 co-localisation with the non-raft marker transferrin receptor was also analysed in MDA-MB-231 cells under migrating versus non-migrating conditions. As evident from **Figure 3.9C**, CD44 strongly co-localised with transferrin receptor after 2 hours of cell migration. Quantification of their co-localisation confirmed the morphological trends, with a statistically significant increase in co-localisation of transferrin receptor and CD44 after 2 hours of MDA-MB-231 cell migration. (**Fig. 3.9D**).

A.

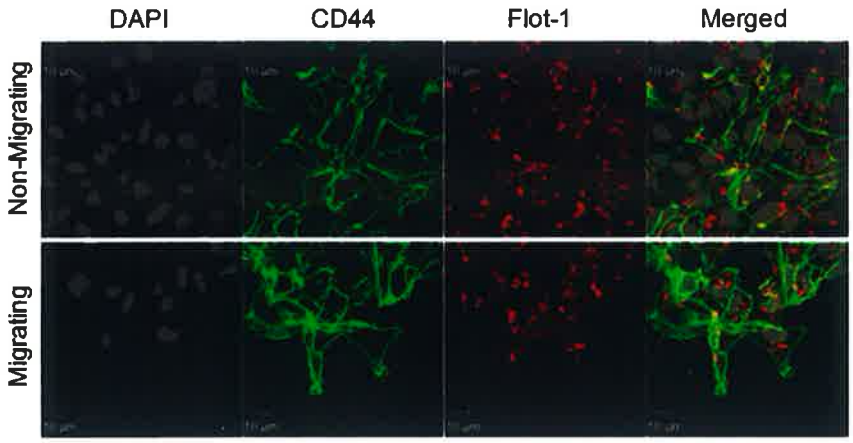
DAPI
CD44
Flot-1
Merged
Non-Migrating
Migrating

B.

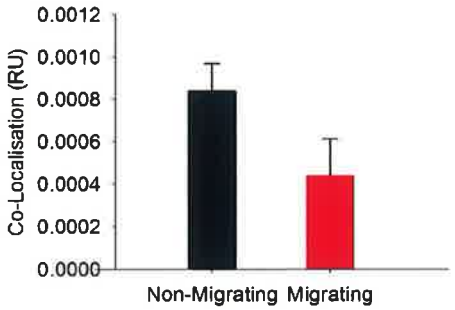
0.0012
0.0010
0.0008
0.0006
0.0004
0.0002
0.0000
Co-Localisation (RU)
Non-Migrating
Migrating

C.

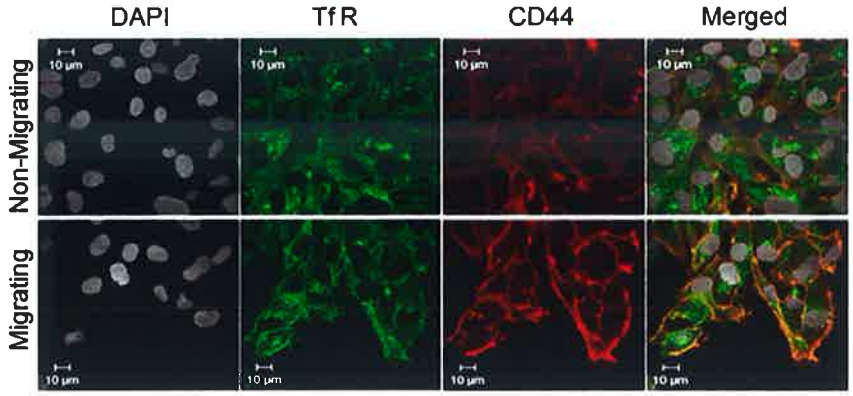
DAPI
TfR
CD44
Merged
Non-Migrating
Migrating
10 µm

D.

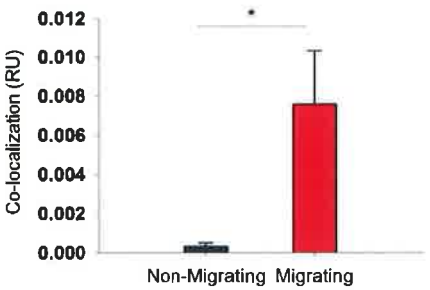
0.012
0.010
0.008
0.006
0.004
0.002
0.000
Co-localization (RU)
*
Non-Migrating
Migrating

Figure 3.9 Immunofluorescent analysis of CD44 co-localisation with raft and non-raft markers during MDA-MB-231 cell migration. **(A.)** Non-migrating and migrating (2hr) MDA-MB-231 cells were stained for expression of CD44 (green) and the lipid raft marker flotillin-1 (Flot-1, red). Nuclei were counter-stained with DAPI (grey). Co-localisation of CD44 with Flot-1 was reduced in migrating MDA-MB-231 cells, which was confirmed numerically after quantification of co-localisation using ImageJ software **(B.,** *Error bars=STDEV, n=2)*. **(C.)** MDA-MB-231 cells under the same conditions were analysed for co-localisation of CD44 with a non-raft marker, transferrin receptor. Co-localisation was visibly increased during cell migration, as confirmed by a significant numerical increase in relative co-localisation in migrating MDA-MB-231 cells **(D.,** *Error bars=SEM; *p<0.05 by unpaired 2-tailed Student's t-test; n=3 experiments)*.

In addition to examining alterations in CD44 sub-cellular localisation during breast cancer cell migration, we also inspected if total levels of CD44 and its binding partners fluctuated over a migration time course. Analysis of MDA-MB-231 cells after 30 min, 2 and 4 hours of migration revealed no temporal changes in expression of CD44, ERM proteins and their active, phosphorylated state, pERM (**Fig. 3.10**). This further supported the concept of CD44 subcellular re-distribution, rather than overall changes in its expression, in breast cancer cell migration.

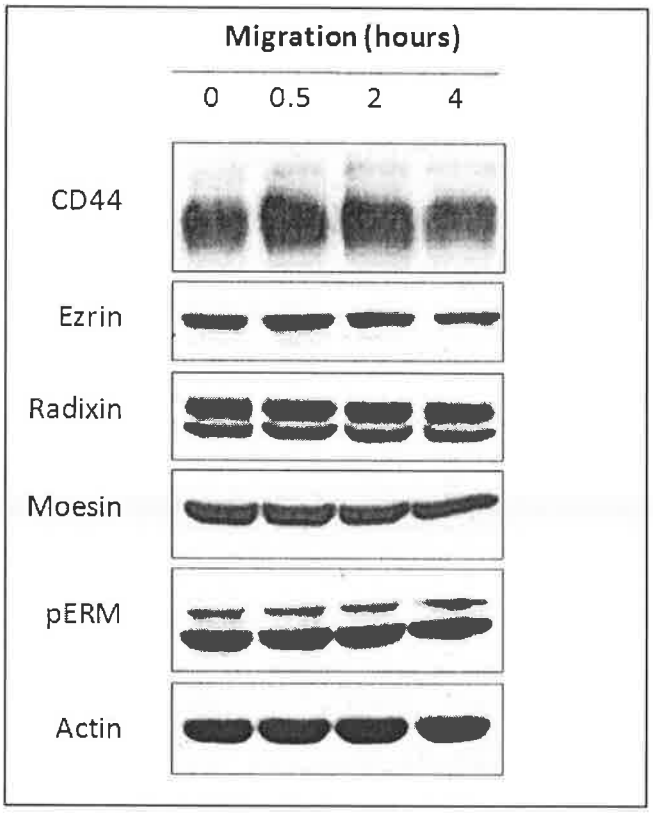

Figure 3.10 Expression of CD44 and its binding partners over a migration time course. MDA-MB-231 cells were analysed for expression of CD44, ezrin, radixin, moesin and active (phospho)-ERM after 30 min, 2- or 4-hour migration in serum-free medium. No changes in total protein expression were observed over time.

3.3.4 Ezrin partitioning in non-migrating and migrating breast cancer cell lines.

Having hypothesised that CD44-ezrin interactions take place outside lipid rafts, ezrin expression was next compared in raft versus non-raft fractions of migrating or non-migrating cells. In most of the cell lines analysed, ezrin was recovered exclusively from non-raft domains (**Fig. 3.11**). Stimulation of migration did not alter the sub-membranous distribution of ezrin in any cell line. These results support the likelihood that CD44 is most likely to encounter ezrin outside lipid raft domains.

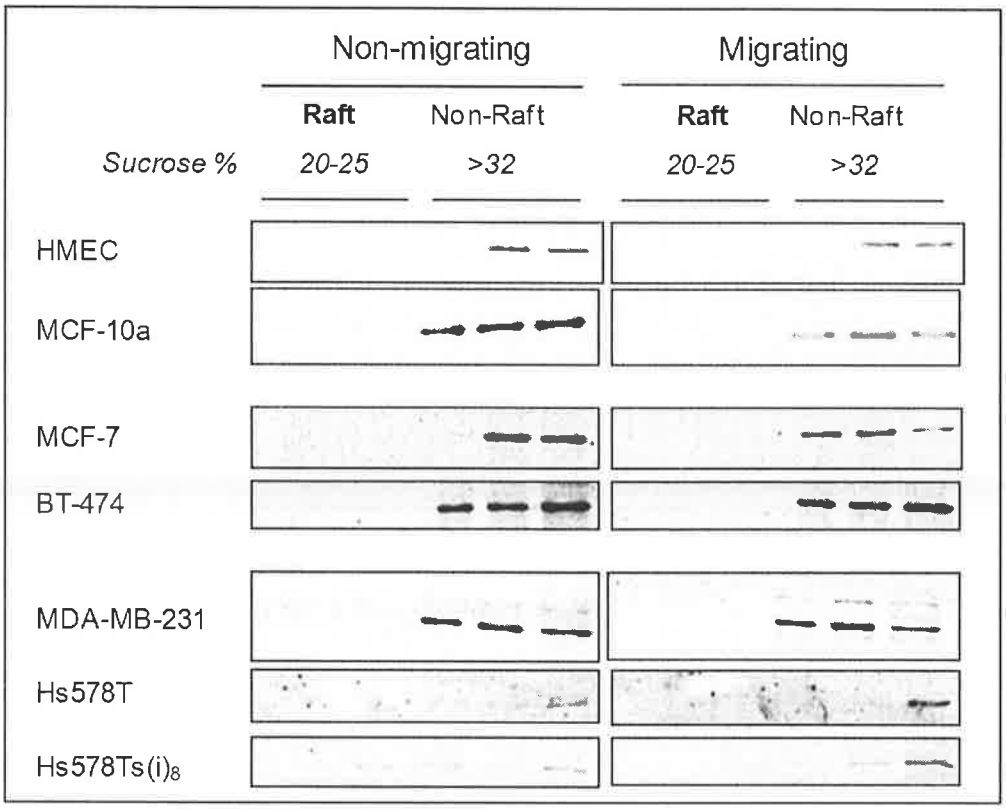

Figure 3.11 Ezrin partitioning in a panel of breast cancer cell lines. Lipid raft and non-raft domains of several breast cell lines under non-migrating and migrating conditions were analysed for ezrin expression. Ezrin was recovered exclusively from non-raft domains across all the cell lines, with no differences in migrating compared to non-migrating cells. Hs578T cell lines demonstrated low levels of ezrin relative to the other cell lines. Blots are representative of at least two independent experiments for each cell line.

3.3.5 Comparison of CD44 cellular distribution and various binding partners in non-migrating and migrating MCF-10a and MDA-MB-231 cell lines

Having established that CD44 localisation in lipid rafts is increased in migrating (non-invasive) MCF-10a cells but decreased in migrating (highly-invasive) MDA-MB-231 cells, we compared the localisation and expression of CD44 and its binding partners in these cell lines. Firstly, we examined CD44 distribution under basal conditions using immunofluorescence. In histologically-normal MCF-10a cells CD44 was entirely localised to cell membranes in non-migrating cells (**Fig. 3.12A**), with no staining detected in the cytoplasm. In highly-invasive MDA-MB-231 cells CD44 staining was also predominantly observed in the cell membrane of non-migrating cells (**Fig. 3.12B**), with a minor component of cytoplasmic and vesicular staining (**Fig. 3.12B, arrows**). Furthermore, expression of the CD44 binding partners radixin, moesin, merlin and annexin II was examined in raft and non-raft domains of these cell lines. Similar to ezrin, all putative binding partners were recovered from non-raft fractions only (**Fig. 3.12C, D**) under both, migratory or non-migratory conditions.

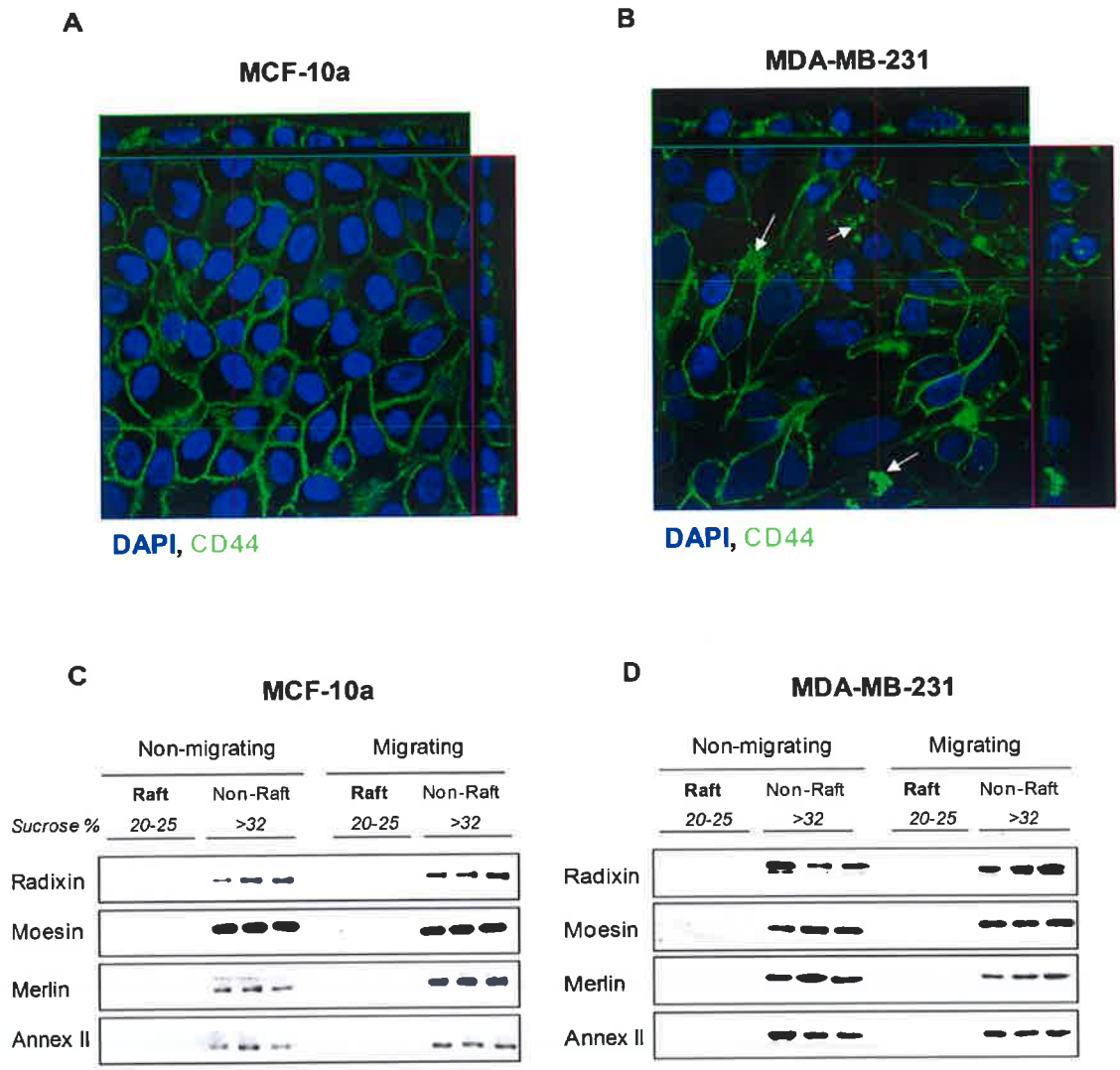

Figure 3.12 CD44 cellular distribution varied in MCF-10a versus MDA-MB-231 cells. **(A.)** Confluent MCF-10a cells were immunofluorescently labelled for CD44 (green) and the nuclei (DAPI; blue). CD44 was entirely localised to cell membranes. **(B.)** Confluent MDA-MB-231 cells were labelled in the same manner. In addition to being localised to cell membranes, CD44 was observed in the cytoplasm and in vesicular structures of MDA-MB-231 cells (arrows). **(C.)** Expression of CD44 binding partners radixin, moesin, merlin and annexin II was examined in rafts and non-raft domains of non-migrating and migrating MCF-10a cells. All of these proteins were recovered from non-raft domains only, with no differences during migratory or non-migratory conditions. **(D.)** Similar trends were observed in MDA-MB-231 cells.

3.3.6 CD44 and ezrin localisation during CD44-specific cell migration.

Having demonstrated that CD44 raft affiliation was decreased in migrating MDA-MB-231 cells, we sought to investigate if CD44 raft affiliation would be altered upon specific stimulation of CD44 with HA. In order to induce CD44-dependent migration, we chose medium-weight HA (~235kDa) which had previously been shown to potentiate migration and invasion of MCF-7 cells (Hill *et al.*, 2006). Scratch-wound migration assays were utilised to choose an appropriate HA concentration, and highly-invasive MDA-MB-231 cells were chosen as the model because they expressed high levels of ezrin and demonstrated a significant decrease in CD44 raft affiliation in migrating cells. We investigated the effects of a range of HA concentrations on MDA-MB-231 cell migration using two methods: 1) immobilising HA in the wells prior to seeding cells or 2) adding solubilised HA to cells after wounding. **Figure 3.13A** shows a significant increase in MDA-MB-231 wound closure on 5mg/ml of immobilised HA, relative to control conditions or lower concentrations of ligand. Treatment with soluble HA also recapitulated a concentration-dependent increase in wound closure in response to HA; with maximal effects observed at 5mg/ml **(Fig. 3.13B)**. This method and 5mg/ml HA was used for all subsequent experiments to stimulate CD44-dependent migration in breast cancer cells.

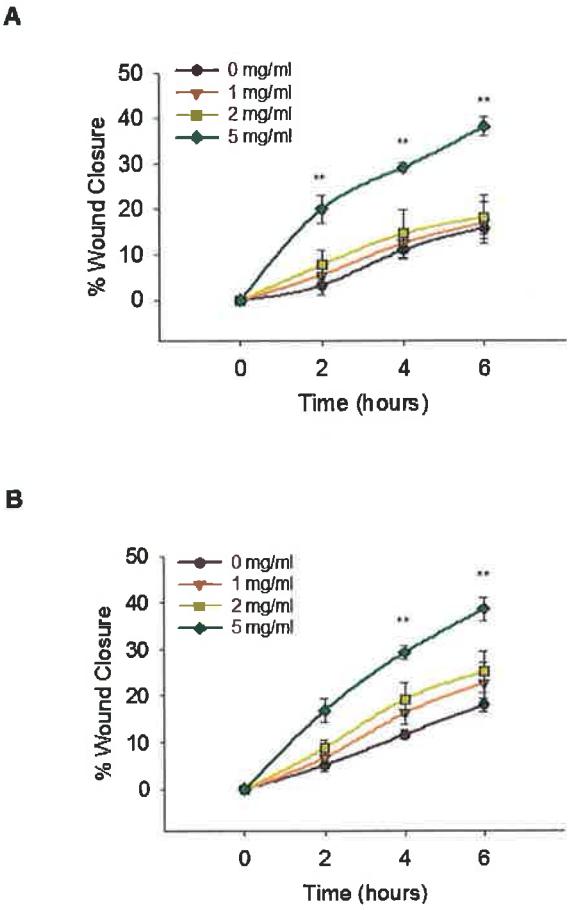

Figure 3.13 HA increased MDA-MB-231 cell migration. Scratch-wound migration assays were utilised to choose a concentration of HA capable of stimulating cell migration. **(A.)** HA concentrations of 1, 2 and 5 mg/ml were immobilised in 24-well plates prior to cell seeding, and the migration of scratch-wounded confluent monolayers estimated every two hours for 6 hours. HA at 5mg/ml significantly increased MDA-MB-231 cell migration relative to the HA-negative control. **(B.)** HA solutions of the same concentrations were prepared in serum-free medium and added to scratch-wounded cells during a migration timecourse of 6 hours. As with immobilised HA, 5mg/ml soluble HA significantly increased cell migration compared to that in untreated cells. *Error bars=SEM; *p<0.05, **p<0.001 by 2-way ANOVA; n=3 experiments.*

We progressed to investigate the partitioning of CD44 and ezrin to lipid rafts in MDA-MB-231 cells during CD44-specific migration induced by HA. Cells were scratch-wounded and allowed to migrate in serum-free medium in the presence or absence of 5mg/ml HA. Total expression of CD44 in migrating or non-migrating cells was not significantly altered by HA treatment (**Fig. 3.14A**). Lipid rafts were subsequently isolated from all four types of lysates and analysed as described previously.

In non-migrating MDA-MB-231 cells, HA treatment did not significantly alter CD44 distribution relative to the untreated cells (**Fig. 3.14B**). Under this condition, CD44 was mostly recovered from the raft fractions, with lesser amounts present in non-raft domains. In contrast, MDA-MB-231 cells migrating in the presence or absence of HA demonstrated a shift towards preferential CD44 recovery in non-raft domains. Ezrin was found to be expressed solely in non-raft fractions. As before, flotillin-1 and transferrin receptor marked lipid raft and non-raft fractions respectively. CD44 affiliation ratios for these conditions are summarised in **Fig. 3.14C**. There was no significant change in CD44 localisation in lipid rafts upon HA treatment of non-migrating cells. However, in cells migrating in the presence of HA, CD44 recovery shifted outside lipid raft domains, mirroring effects observed during non-specific MDA-MB-231 cell migration (**Figs 3.8A and 3.14C**). These results indicate that during cell migration in the presence and absence of its ligand HA, CD44 likely translocates outside lipid rafts.

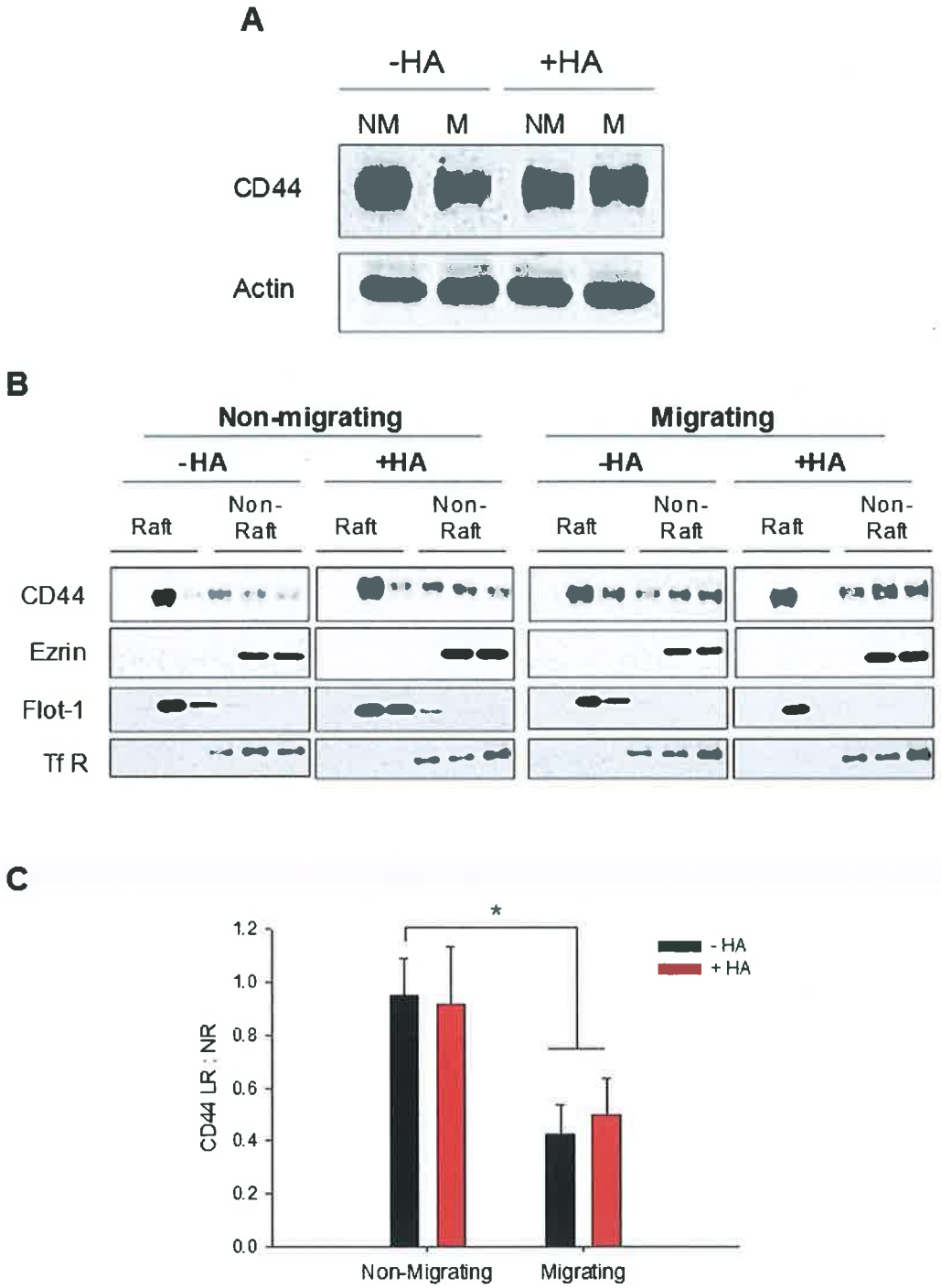
A
-HA
+HA
NM
M
NM
M
CD44
Actin
B
Non-migrating
Migrating
-HA
+HA
-HA
+HA
Raft
Non-Raft
Raft
Non-Raft
Raft
Non-Raft
Raft
Non-Raft
CD44
Ezrin
Flot-1
Tf R
C
*
- HA
+ HA
CD44 LR : NR
1.2
1.0
0.8
0.6
0.4
0.2
0.0
Non-Migrating
Migrating

Figure 3.14 HA did not exert effects on CD44 raft affiliation during migration of MDA-MB-231 cells. (A.) Whole cell lysates of non-migrating (NM) and 2hr-migrating (M) cells in the presence and absence of 5mg/ml HA were examined for expression of CD44. Its expression did not alter across these conditions. Actin was used as a loading control. **(B.)** Lipid rafts were isolated and western blotted for the presence of CD44 and ezrin. Under non-migrating conditions HA treatment did not alter CD44 distribution, with the majority of CD44 concentrated in lipid rafts and lower levels present outside rafts. After stimulation of migration in both HA- and HA+ conditions, CD44 levels in lipid raft fractions were reduced in parallel with increased recovery in non-raft fractions. Total ezrin was recovered only in non-raft domains of both migrating and non-migrating cells irrespective of HA treatment. Flotillin-1 (Flot-1) and transferrin receptor (Tf R) marked raft and non-raft domains respectively. **(C.)** Calculation of the CD44 raft affiliation ratio revealed a significant decrease in CD44 affiliation with lipid rafts during migration of MDA-MB-231 cells in the presence or absence of HA. *Error bars=SEM; *p<0.05 by unpaired 2-tailed Student's t-test; n=3 experiments.*

3.3.7 Sub-types of lipid rafts involved in cell migration.

Having shown that CD44 localisation in lipid rafts is decreased in highly-invasive cell lines, we sought to identify the type of rafts involved in this process. Caveolin-1 and flotillin-1 mark two different populations of rafts, but biochemical separation on sucrose gradients cannot distinguish between them. Thus we used wild type MDA-MB-231 cells and those stably knocked down for caveolin-1 to examine if CD44 localisation during cell migration would be altered in caveolae-reduced cells. Firstly, partial caveolin-1 knockdown of ~50% was confirmed in whole cell lysates (**Fig. 3.15A**). Subsequently, lipid rafts from non-migrating and migrating cells of both cell types were analysed. Flotillin-1 and caveolin-1 were enriched in the same fractions, confirming the presence of lipid rafts; while transferrin receptor marked the non-raft fractions (**Fig. 3.15B**). Quantification of CD44 expression in raft versus non-raft fractions revealed an increase in CD44 recovery outside lipid rafts in migrating wild-type MDA-MB-231 cells (**Fig. 3.15B**), consistent with our previous findings. Likewise, increased levels of CD44 were recovered outside lipid rafts following the induction of migration in caveolin-1 knockdown cells. The CD44 raft affiliation ratio was calculated for these cells as previously described, and expressed relative to that in non-migrating wild-type cells **(Fig. 3.15C**). This revealed insignificant changes in lipid raft-affiliated CD44 after caveolin-1 knockdown in non-migrating and migrating cells relative to the non-migrating and migrating wild-type, respectively. These observations indicated that caveolae do not exert a regulatory influence upon CD44 translocation to non-raft fractions during cell migration, thus suggesting that CD44 is predominantly regulated by flotillin-1-positive rafts. This limited effect of caveolin-1 knockdown on CD44 localisation, however, could also be explained by insufficient knockdown efficiency with shRNA (~50%). Thus, more efficient siRNA approach was used to determine functional effects of caveolin-1 knockdown on MDA-MB-231 cell migration.

A.

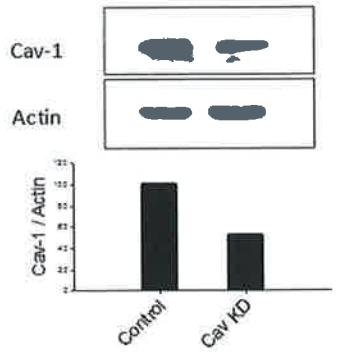
Cav-1
Actin
Cav-1 / Actin
Control
Cav KD

B

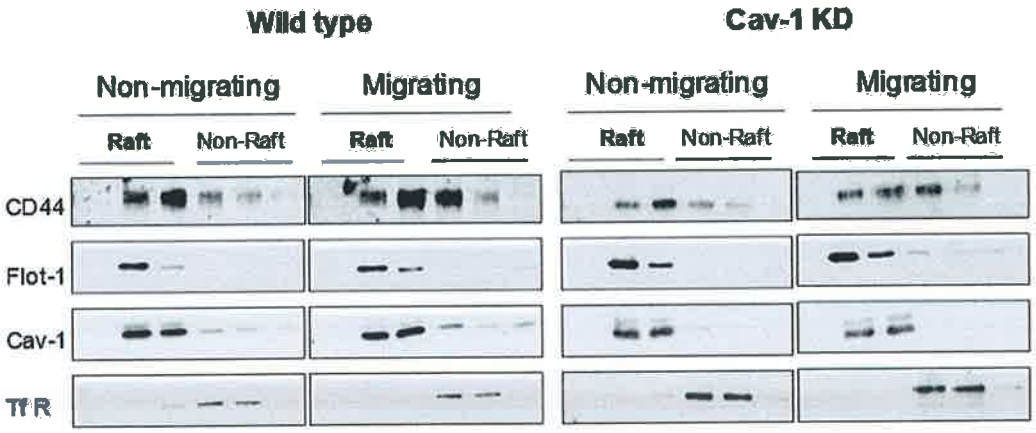
Wild type
Cav-1 KD
Non-migrating
Migrating
Non-migrating
Migrating
Raft
Non-Raft
Raft
Non-Raft
Raft
Non-Raft
Raft
Non-Raft
CD44
Flot-1
Cav-1
TfR

C

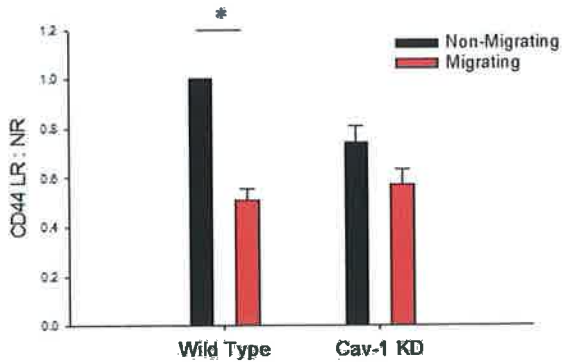
*
Non-Migrating
Migrating
CD44 LR : NR
1.2
1.0
0.8
0.6
0.4
0.2
0.0
Wild Type
Cav-1 KD

Figure 3.15 Stable caveolin-1 knockdown did not affect CD44 localisation in migrating MDA-MB-231 cells. (A.) Caveolin-1 knockdown (Cav-1 KD) in MDA-MB-231 cells was confirmed in whole cell lysates to be approximately 50%. **(B.)** Lipid rafts were extracted from wild type and Cav-1 KD MDA-MB-231 cells under non-migrating or 2hr-migrating conditions. Partitioning of CD44 to raft or non-raft compartments was determined by Western blot analysis in conjunction with the lipid raft markers flotillin-1 and caveolin-1 and the non-raft marker transferrin receptor. CD44 recovery from non-raft domains of migrating relative to non-migrating wild type cells was increased, as expected. CD44 expression in rafts of Cav-1 KD cells was visibly reduced compared to the wild type cells. **(C.)** The CD44 raft affiliation ratio in migrating wild type cells, expressed as a percentage of that in non-migrating wild type cells, was significantly reduced. CD44 raft affiliation was not significantly altered in non-migrating or migrating Cav-1 KD cells relative to non-migrating and migrating wild type, respectively. *Error bars=SEM;* * $p<0.05$ *by unpaired Student's t-test; n=3 experiments.*

In order to test functional importance of flotillin-1-positive rafts, and given the limitations of the shRNA approach, flotillin-1 and caveolin-1 were transiently silenced separately in MDA-MB-231 cells using siRNA technology. Overall expression of either protein was successfully reduced by >90% 72 hours post-transfection, with caveolin-1 expression also reduced upon flotillin-1 knockdown **(Fig. 3.16A)**. Migration analysis of these knockdown cells demonstrated no change in cell migration patterns relative to that in cells transfected with the negative control siRNA **(Fig. 3.16B)**. This suggested functional compensation between these types of rafts in regulating proteins involved in cell migration, especially in light of the reduced expression of caveolin-1 upon flotillin-1 knockdown. Thus we performed a combined knockdown of caveolin-1 and flotillin-1 in MDA-MB-231 cells to search for an impact on cell migration. Western blot analysis demonstrated successful knockdown of both proteins together, relative to the untransfected and negative siRNA controls (**Fig. 3.17C**). Coincident knockdown of these proteins significantly impaired cell migration compared to control and negative siRNA-transfected cells (**Fig. 3.17D**). These data highlight the overall importance of functional lipid rafts in efficient breast cancer cell migration, whether through regulating the localisation of CD44 alone or more likely it and additional molecules involved in the migratory response.

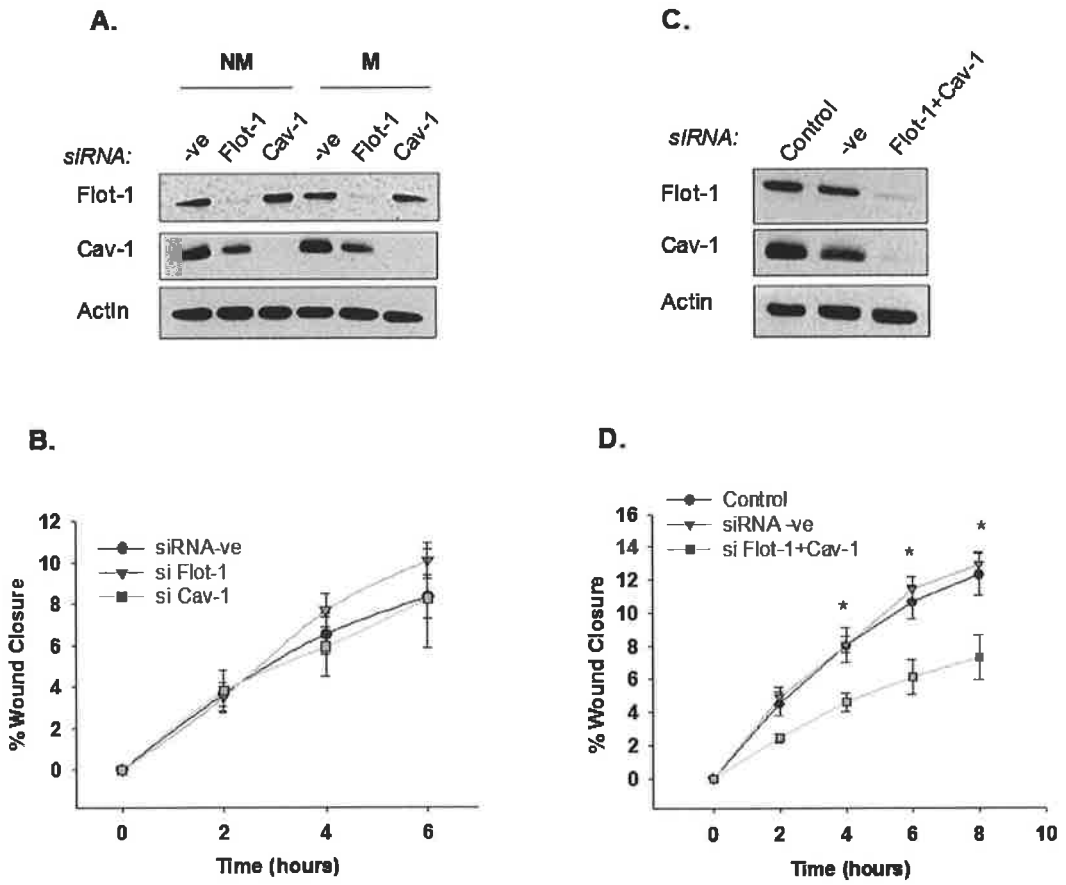

Figure 3.16 Dual flotillin-1 and caveolin-1 knockdown reduced MDA-MB-231 cell migration. (A.) Flotillin-1 (Flot-1) and caveolin-1 (Cav-1) were transiently knocked down by siRNA (25nM), relative to a universal negative control siRNA (si –ve). Their protein expression levels were reduced by ~90% at 72 hours post-transfection. **(B.)** In scratch-wound migration assays, Flot-1 and Cav-1 knockdown cells showed no significant changes in migration relative to those transfected with the negative control siRNA. **(C.)** Efficiency of simultaneous knockdown of Flot-1 and Cav-1 72 hours post-transfection with 25nM of each siRNA was assessed by western blot, demonstrating successful downregulation of both proteins together. **(D.)** Analysis of cell migration of double-knockdown cells revealed significant impairments in migration relative to that in untransfected control and negative siRNA-transfected cells. *Error bars=SEM; *p<0.05 by 2-way ANOVA; n=3 experiments.*

To summarise, in this chapter we began addressing the hypothesis that CD44-ezrin interactions involved in cell migration occur outside lipid rafts. Firstly, we attempted to correlate the raft affiliation of CD44 with migration of a panel of non-invasive, weakly and highly invasive cell lines. CD44 affiliation with lipid rafts was found to increase during migration of non-invasive cells, and to decrease during migration of highly-invasive cell lines. Similar results were observed in migrating cells in the presence or absence of a CD44 ligand, HA. Our hypothesis was further strengthened by exclusive recovery of ezrin and several other CD44 binding partners outside lipid raft domains of MDA-MB-231 cells. We questioned whether a specific sup-population of lipid rafts could be involved in this sub-membranous regulation of CD44 during cell migration, and established that both flotillin- and caveolin-positive rafts are likely to play a regulatory role in successful breast cancer cell migration. Some of the novel data from this chapter were recently published (Donatello & Babina *et al.*, 2012)

3.4 Discussion

Cell migration out of the primary tumour is one of the earliest events in the metastatic spread of breast cancer, and requires coordinated activation of numerous cell adhesion signalling cascades (Yilmaz and Christofori, 2010). CD44 is an important adhesion molecule with a variety of tissue-dependent functions. Many studies have investigated the contribution of individual CD44 isoforms to cancer progression (Borland *et al.*, 1998; Herrera-Gayol and Jothy, 1999; Negi *et al.*, 2012; Weidle *et al.*, 2011), but we focused our attention on the relationship of CD44 with lipid rafts during breast cancer cell migration. Lipid rafts are organisation centres for many important molecules that play a role in cell migration, including receptor tyrosine kinases, integrins, catenins, growth factor receptors and adhesion molecules (Patra, 2008). Thus in this chapter we investigated affiliation of CD44 and its binding partner, ezrin, with lipid rafts during cell migration in a panel of breast cancer cell lines of varying invasiveness. Additionally, we examined if a particular type of lipid rafts is involved in regulation of CD44 during breast cancer cell migration.

We found that breast cancer cell lines of different invasive potential expressed a mixture of CD44 molecules of different molecular weights and at various levels. The non-invasive cell lines mostly expressed isoforms of CD44 whose molecular weights correlate with those of CD44 variants 3-8. It has been previously reported that CD44v3 expression correlates with histological grade of malignancy in breast carcinomas (Kalish *et al.*, 1999), potentially due to its ability to act as an acceptor for heparin sulphate, and subsequently, heparin sulphate-binding growth factors (Bennett *et al.*, 1995). In addition, a more widely studied variant, v6, has also been reported to play an important role in tumour progression in colon, pancreas, prostate, ovarian and breast cancers (Gunthert, 1996; Heider *et al.*, 2004). Therefore it was somewhat unexpected to detect these CD44 forms in normal-like cells with no metastatic potential. More recently, however, Olsson and colleagues have correlated a panel of CD44 isoforms with breast cancer subtypes, revealing that high expression of variant CD44 isoforms associated with well-differentiated, non-aggressive tumour clinicopathological parameters (namely positive steroid receptor status, low proliferation and luminal A subtype) (Olsson *et al.*, 2011). These findings

thus concurred with our observations of higher molecular weight bands of CD44 in non-invasive cell lines. Conversely, high expression of the standard CD44 isoform (CD44s) has been shown to correlate with basal subtype and strong HER-2 staining, indicators of aggressive, undifferentiated cells (Olsson *et al.*, 2011). Additionally, expression of CD44s has been directly linked to breast cancer migration and invasion (Afify *et al.*, 2009), and antibody-based functional antagonism of CD44s has been shown to significantly inhibit cell motility (Herrera-Gayol and Jothy, 1999). Our findings were in agreement with those results, as the highly-invasive cell lines we tested expressed predominantly the standard CD44 isoform, unlike the weakly- and non-invasive cell lines, which abundantly expressed variant CD44 isoforms. Furthermore this suggests that changes in CD44 protein expression levels alone are unlikely to be of singular importance in cancer progression; and illustrates the potential importance of evaluating a role for altered CD44 subcellular localisation in cancer progression events like cell migration.

Like CD44, the expression of its binding partner ezrin was highest in highly-invasive MDA-MB-231 cells compared to the other cell lines. This is in agreement with previous publications that link high ezrin expression to breast cancer progression (Curto and McClatchey, 2004; Meng *et al.*, 2010). In contrast, the other highly-invasive cell line we tested, Hs578T, showed barely detectable levels of ezrin. However previous findings in our laboratory showed very low ezrin gene expression in the Hs578T cells (E. McSherry, personal communication). This may suggest that in these cells CD44 mediates cell migration via an ezrin-independent pathway, such as CD44-mediated upregulation of collagen-degrading enzymes and their activity in Hs578T cells (Montgomery *et al.*, 2012).

As lipid rafts have been described to be crucial for oncogenic stimulation of numerous molecules in breast cancer (reviewed by (Babina *et al.*, 2011)), we sought to compare CD44 localisation within lipid raft domains of non-migrating and migrating cancer cells. Different methods exist to isolate various populations of lipid rafts, but most are based on the concept of isolating cholesterol-enriched parts of the membrane by ultra-centrifugation on density gradients. With the two methods we adopted, the Triton X-100 method yields lipid rafts enriched in sphingomyelin and

glycosphingolipids (Brown and Rose, 1992); compared to the sodium carbonate (detergent-free) method which yields lipid rafts more enriched in glycerosphingolipids (Song *et al.*, 1996). These methods would yield slightly different populations of lipid rafts (Pike, 2009), but since little information exists on the exact types of rafts CD44 is targeted to, we isolated lipid rafts from all the cell lines tested using both methods. In addition, our approach would eliminate the possibility of introducing potential artifacts that could arise from the use of cold non-ionic detergents, which has been suggested by some (Nothdurfter, 2007).

In analysing the quality of the gradients we noted some differences between the two methodological approaches. Firstly, the activity peak for the lipid raft marker enzyme alkaline phosphatase was spread over a maximum of 3 fractions (numbers 4-6) in the case of Triton X-100 gradients, with highly enriched activity recorded in a single fraction (#5). Conversely, in the case of sodium carbonate extractions, the enzyme activity peak was spread over 4 or 5 fractions (#4-8), peaking in fraction number 6. This shift in alkaline phosphatase activity is indicative of more diffuse lipid rafts isolated in the sodium carbonate preparation. There could even be a possibility of contamination of lipid raft fractions by non-raft membrane domains (Nothdurfter, 2007; Pike, 2003). Secondly, the protein concentration following the Triton X-100 isolation procedure was much higher compared to that of detergent-free extraction method. Finally, comparison of flotillin-1 expression revealed results predicted by alkaline phosphatase assays. In Triton X-100 preparations, the lipid raft marker flotillin-1 was enriched in fractions 4 and 5, which correlates with previous findings (Simons and Sampaio, 2011). In the detergent-free extractions, however, there were hints of flotillin-1 in sucrose-dense fractions of the sodium carbonate preparations, which indicated presence of potential impurities using this lipid raft extraction method compared to the detergent approach. Nonetheless, both experimental approaches had broadly similar outcomes, also demonstrating gradient profiles with protein concentrations which increased in step with sucrose density and fraction number.

In order to objectively compare relative amounts of CD44 inside and outside of rafts across multiple experimental gradients, we devised a numerical ratio of lipid

raft-affiliated CD44 versus non-raft CD44 (Donatello & Babina *et al.*, 2012). This was calculated by expressing CD44 recovered from raft fractions (normalised to flotillin-1 expression) relative to non-raft CD44 (normalised to transferrin receptor expression), which we termed the CD44 "raft affiliation ratio". Consequently we sought to establish a correlation between CD44 localisation in lipid rafts and the invasive potential of breast cancer cells, as this has not yet been reported. A decrease in the raft affiliation ratio in migrating relative to non-migrating cells would support our theory of CD44 relocalisation outside of rafts during migration. In practice, this ratio was hard to estimate due to the absence of CD44 in the raft fractions of some cell lines (HMEC, MCF-7 and BT-474). In fact, CD44 expression has been shown to be virtually undetectable in MCF-7 and BT-474 lysates (Murohashi *et al.*, 2010; Ostapkowicz *et al.*, 2006). For BT-474 cells the primary migratory mechanism could potentially involve HER-2 downstream signalling events that could lead to loss of E-cadherin function and subsequent migration and invasion (Hiraguri *et al.*, 1998). MCF-7 cells have been reported to migrate and invade via IGF receptors, as well as TGF-β receptors (Walsh and Damjanovski, 2011). Nevertheless, we were able to recover raft-bound CD44 from a normal-like cell line (MCF-10a) and from all of the invasive cell lines.

During migration of normal-like MCF-10a cells, CD44 recovery in lipid rafts was found to be significantly higher than that in non-migrating cells, as depicted by an increase in CD44 raft affiliation ratio. It is tempting to speculate that non-malignant polarised cells sequester proteins like CD44 inside lipid raft affiliation in order to limit cell migration. Accordingly, heavier CD44 isoforms have been shown to be present in lipid rafts along with CD44s and annexin II in a non-tumorigenic breast epithelial cell line, EpH4 (Oliferenko *et al.*, 1999). Annexin II has been implicated in interactions with the actin network (Thiel *et al.*, 1992). As both MCF-10a and EpH4 are polarised cell lines, we first speculated that CD44 may also engage annexin II in MCF-10a cells, potentially competing with ezrin for binding to CD44. However, in our hands annexin II was recovered only from non-raft fractions of MCF-10a cells, indicating a more complex regulation of CD44 in these normal-like cells.

Although protein expression of CD44 was increased in our highly-invasive cells (in agreement with clinical links between CD44 overexpression and invasive breast carcinoma as well as increased cancer cell survival (Diaz *et al.*, 2005; Olsson *et al.*, 2011), we were interested in the sub-membranous localisation of CD44 in migrating highly-invasive cell lines compared to non-tumourigenic cells. Conversely to MCF-10a cells, we demonstrated a decrease in the CD44 raft affiliation ratio after stimulation of migration in the highly-invasive cell lines MDA-MB-231 and Hs578T, suggesting translocation of CD44 out of rafts during cell migration of highly-invasive breast cancer cells. There are no specific reports of a link between CD44 raft localisation and breast cancer cell migration, yet localisation of CD44 outside lipid rafts in human glioblastoma cells resulted in metalloproteinase-mediated CD44 shedding and tumour cell migration (Murai *et al.*, 2004). This was further confirmed after membrane cholesterol modulation with methyl-β-cyclodextrin, filipin and simvastatin (Murai *et al.*, 2011). Nonetheless, CD44 localisation within lipid rafts has conversely been described to promote cell survival in gastric adenocarcinoma and colorectal cancer (Lee *et al.*, 2008). Additionally, pro-proliferative effects of CD44 affiliation with lipid rafts have been demonstrated in aortic endothelial cells through interactions with ankyrin (Singleton and Bourguignon, 2004). Our data showed an increase of CD44 affiliation with rafts during migration of normal-like cells, and a decrease of CD44 raft affiliation during migration of invasive breast cancer cells. This suggested that CD44 localisation outside lipid rafts is associated with breast cancer cell migration. Given the involvement of the CD44 cytoskeletal binding partners ezrin (Elliott *et al.*, 2005) and ankyrin (Singleton and Bourguignon, 2004) in cancer progression, and merlin in tumour suppression (Morrison *et al.*, 2007), we speculate that interaction of CD44 with a particular cytosolic partner, as well as changes in the extracellular environment, may differentially regulate cancer cell migration. These interactions could be regulated by lipid raft domains via recruitment of specific effector proteins or enzymes to stimulate appropriate downstream signalling.

We next sought to investigate if CD44 localisation patterns relative to lipid rafts would be altered by direct stimulation with its principal ligand HA. Enrichment

in matrix levels of HA have been described in many types of tumours (Knudson *et al.*, 1989), and HA concentrations have been shown to be elevated in malignant tumour tissue compared to the corresponding normal or benign tissue in cancer patients (Toole and Hascall, 2002). In fact, in some tumour types HA is used as a predictive marker of malignancy (Toole and Hascall, 2002). Specifically in breast cancer patients, HA levels were found to be increased in the sera (Delpech *et al.*, 1990). We first identified a concentration of HA that exerted functional effects on MDA-MB-231 cell migration (5mg/ml; which was within physiological ranges and not toxic (Forrester and Wilkinson, 1981)). After two hours of HA-stimulated migration, CD44 affiliation with lipid rafts decreased relative to non-migrating cells to a level also observed in cells that had received a non-specific migratory stimulus (scratch-wounding). This indicated that CD44 translocation outside lipid rafts during breast cancer cell migration is independent of ligand stimulation. CD44-HA binding can differ significantly depending on cell type (Tzircotis *et al.*, 2005). In addition, their interaction was described to have signalling effects after as early as 10 minutes, which then stabilised after 15 minutes (Bourguignon *et al.*, 2010). In addition, the size of HA molecules directly impacts downstream effects (reviewed in (Ponta *et al.*, 2003)). In our system we could not predict the size of HA upon solubilisation, which could account for the lack of effect of HA treatment alone on CD44 localisation in non-migrating cells. Overall, however, our hypothesis was supported by confirmation of reduced CD44 affiliation with lipid rafts during cancer cell migration, either in the presence or absence of HA.

Having established a relationship between CD44 and lipid rafts in breast cancer cell migration, we sought to investigate if a particular sub-population of lipid raft was involved. Two key populations of lipid rafts have been described, caveolin-1- and flotillin-1-positive rafts (reviewed in (Babina *et al.*, 2011; Rimmerman *et al.*, 2011)). From immunofluorescence studies carried out previously in our lab, it was observed that CD44 predominantly co-localised with flotillin-1-positive rafts (Donatello & Babina *et al.*, 2012). In MDA-MB-231 cells stably knocked down for caveolin-1 we noted a trend towards decreased raft-affiliated CD44 compared to the wild type control, suggesting that a pool of CD44 localises to caveolae. Yet after

stimulation of migration, raft-affiliated CD44 in caveolin-1-knockdown cells further decreased to a level almost identical to that of control MDA-MB-231 cells. An insignificant decrease in CD44 raft affiliation even in the reduced presence of caveolin-1 suggests that the pool of CD44 affiliated with caveolin-1-positive rafts is not directly involved in cell migration. However, knockdown efficiency of stable caveolin-1 knockdown cells was very poor and could account for the reduced effects seen in these cells. In fact, uptake and degradation of HA by CD44, which can eventually promote cancer progression, has been reported to occur independently of clathrin, caveolae or pinocytotic uptake pathways (Knudson *et al.*, 2002). Knockdown of flotillin-1 in MDA-MB-231 cells has been shown to impair cell proliferation and colony formation ability and to decrease tumour volume and weight (Lin *et al.*, 2011). However our findings did not show a significant functional effect on cell migration upon inhibition of either flotillin-1 or caveolin-1 alone. Potentially each compensates for the other to preserve key cellular functions, such as migration. This could even be due to a potential crosstalk between these two proteins, as we witnessed a reduction in total caveolin expression in response to flotillin-1 knockdown. This has also been previously documented in intestinal epithelial cells, where flotillin-1 downregulation decreased caveolin-1 expression via lysosomal degradation (Galbiati *et al.*, 1998). This possibility was further strengthened by significant inhibition of MDA-MB-231 cell migration upon double knockdown of caveolin-1 and flotillin-1. This result supported our hypothesis that organised lipid raft machinery is required for functional cell migration.

Overall, these results, which were recently published (Donatello & Babina *et al.*, 2012) suggest a novel mechanism whereby CD44 affiliation with lipid rafts could regulate breast cancer cell migration. Investigations into mechanisms of lipid raft affiliation of CD44 could therefore be of value in regulating breast cancer cell migration, a key precursor to metastasis. Thus the next step was to decrease CD44 affiliation with lipid rafts in an attempt to increase breast cancer cell migration.

Chapter 4

Modulation of CD44 palmitoylation status and its effects on CD44 raft localisation and breast cancer cell migration.

4.1 Introduction

Cell migration is one of the key early events in the multi-step process of metastasis and requires activation of numerous cell adhesion and cell signalling cascades. One such cascade involves CD44, a cell adhesion transmembrane glycoprotein with a variety of tissue-dependent functions around the body (Platt and Szoka, 2008). Unsurprisingly, CD44 has been shown to be involved in progression of a variety of cancers (Ostapkowicz *et al.*, 2006), and its aberrant expression has been associated with aggressive histological features, particularly in breast cancer (Diaz *et al.*, 2005). CD44 is frequently found in lipid rafts, but little is known about the functional effects of this association.

4.1.1 Protein targeting to lipid rafts

CD44, along with many other proteins involved in regulation of cell migration, is known to be targeted to lipid rafts. Perhaps the best-characterised system of protein association with lipid rafts is via post-translational modification with GPI anchors. The GPI anchor itself is a conserved oligosaccharide core that is covalently linked to a lipid moiety embedded in the outer leaflet of the cell membrane through acyl or alkyl chains (Levental *et al.*, 2010a). These anchors are added to soluble polypeptides in the lumen of the endoplasmic reticulum (ER), thereby acquiring detergent resistance and promoting membrane raft affiliation (Brown and Rose, 1992). Partitioning of GPI-anchored proteins into lipid rafts has been proposed as a mechanism to allow sorting of these proteins to the apical surface of polarised epithelial cells (Fiedler *et al.*, 1993).

Another way in which proteins are targeted to lipid rafts is through addition of prenyl groups in the process of prenylation. Two types of prenyl groups, C_{15} farnesyl and C_{20} geranylgeranyl, are known to be added on to C-terminal cysteine-rich domains of cytoplasmic proteins by prenyl transferases (Casey and Seabra, 1996), with subsequent other modifications (methylation, proteolysis or palmitoylation) (Glomset *et al.*, 1990); (Zhang and Casey, 1996). Although prenylated proteins reportedly affiliate preferentially with lipid rafts (Parmryd *et al.*, 2003; Prior and Hancock, 2001), it is thought that the prenyl groups interact with lipid raft-affiliated proteins

rather than being directly integrated into the membrane domains (Magee and Seabra, 2003).

Another lipid post-translational modification, palmitoylation, is dynamically regulated by enzymes (Kang *et al.*, 2008); (Wan *et al.*, 2007), and thus offers an active mechanism to influence protein affiliation with lipid rafts in physiological and pathophysiological settings. Palmitoylation is the addition of palmitic acid moieties to integral and peripheral membrane proteins through esterification (Bhatnagar and Gordon, 1997). However, the relevant enzymes are still poorly characterised. Membrane-associated palmitoyl acyltransferase (PAT) is the most studied palmitoylation enzyme (Planey and Zacharias, 2009), while the palmitoyl thioesterase family has been implicated in the removal of palmitate groups (Camp and Hofmann, 1995). Close proximity of protein cysteine residues to the membrane is thought to facilitate palmitoylation by PAT, whereas membrane-distal residues are more likely to be prenylated or N-myristoylated (Bijlmakers and Marsh, 2003). PAT activity has been linked to lipid rafts (Dunphy *et al.*, 2001), with palmitoylated proteins found either at the cell membrane or on intracellular membranes (Lobo *et al.*, 2002; Roth *et al.*, 2002). Palmitoylated proteins are naturally more hydrophobic, which increases their affinity for highly-hydrophobic lipid rafts. There are countless examples of proteins targeted to lipid rafts through palmitoylation, including Src family kinases, endothelial nitric oxide synthase and various transmembrane receptors (Ghosh *et al.*, 1998; Gong *et al.*, 2003). Lipid raft structural marker proteins such as flotillins are also known to be palmitoylated. CD44 also contains two palmitoylation sites, which have been demonstrated to target this molecule to lipid rafts (Thankamony and Knudson, 2006). However the functional role of CD44 affiliation with lipid rafts still remains controversial, and in this chapter we address this topic by artificially modulating CD44 palmitoylation.

4.1.2 Functions of the CD44 cytoplasmic domain

CD44 consists of extracellular, transmembrane and cytoplasmic domains. Its cytoplasmic tail, which is highly conserved among species, is required for numerous CD44-mediated structural and signalling events. The CD44 cytoplasmic tail has been

shown to be necessary for effective HA binding (Perschl *et al.*, 1995). However upon domain replacement with an equivalent domain from different proteins, HA binding efficiency and adhesion properties were not impaired (Lesley *et al.*, 2000; Perschl *et al.*, 1995). HA internalisation and degradation have been implicated in cancer progression (Bourguignon, 2001), however it could also have important physiological functions. For instance, HA accumulation results in skin and corneal lesions upon CD44 downregulation in basal keratinocytes (Kaya *et al.*, 1999); suggesting that CD44/HA interactions are important for barrier integrity. Likewise, HA aggregations have been observed in lung inflammation and patients with myxoid dermafibroma (Calikoglu *et al.*, 2003; Teder *et al.*, 2002; Wang *et al.*, 2002). Although in the processes regulating HA-CD44 interactions have been extensively studied, the processes regulating CD44-HA internalisation remain poorly understood. One report has classified it as clathrin-, pinocytosis- and caveolae-inpedendent, resulting in delivery to the lysosomes and CD44 recycling (Tammi *et al.*, 2001). This suggests that the CD44 cytoplasmic tail contains information that prevents its entry into coated vesicles, which could be cell type-dependent. A dihydrophobic motif, Leu331+Val332, has been implicated in successful delivery of CD44 to the lateral cell membrane in epithelial cells (Sheikh and Isacke, 1996). However much remains to be understood about CD44 intracellular trafficking in the presence and absence of ligand stimulation.

As CD44-dependent cell migration requires interactions with the cellular actin cytoskeleton, the cytoplasmic tail plays an important role in binding cytoplasmic actin-linking proteins. The ERM family of proteins binds to CD44 at a polybasic stretch of amino acids termed the FERM domain (^{292}RRRCGQKKK^{300}) (Mori *et al.*, 2008). A protein structurally similar to ERMs, merlin (neurofibromin 2), also binds the same domain (Mori *et al.*, 2008), but is thought to have different functions. Whereas ERM-CD44 interactions are believed to promote tumour cell migration and adhesion (Martin *et al.*, 2003), CD44 association with merlin is considered to be growth- and migration-inhibitory (Morrison *et al.*, 2007). ERMs and merlin are controlled by phosphorylation, but while ERM is activated by

phosphorylation (most likely PKC-dependent (Legg *et al.*, 2002); merlin binds to CD44 after dephosphorylation (Morrison *et al.*, 2001).

4.1.3 Post-translational modifications of the CD44 cytoplasmic domain and its relevance to lipid raft affiliation

Additionally, several residues on the CD44 cytoplasmic tail undergo post-translational modifications, such as phosphorylation and palmitoylation (**Fig. 4.1**).

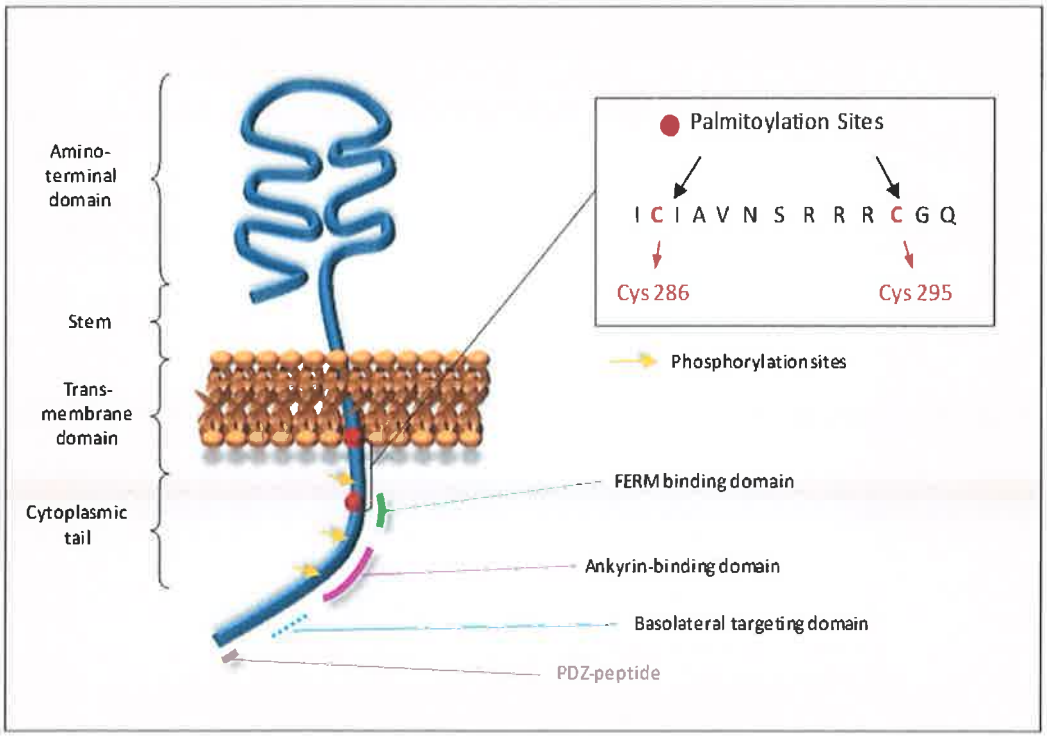

Figure 4.1 Overview of the CD44 cytoplasmic tail. The CD44 cytoplasmic tail contains 2 palmitoylation sites, Cys286 and Cys295 (red, inset), an ERM-binding domain (FERM), an ankyrin-binding domain, a basolateral targeting sequence and a hypothetical PDZ-peptide. Yellow arrows indicate serine residues that have been shown to be phosphorylated.

Several kinases may be involved in the phosphorylation of CD44. Ser316, which is highly conserved among species (Thorne *et al.*, 2004), is located in a predicted protein kinase A consensus site which was demonstrated to be unphosphorylated in non-migrating cells (Neame and Isacke, 1992). However this site becomes phosphorylated following activation of protein kinase C (PKC), an event reportedly crucial in activating chemotaxis in response to phorbol ester gradients (Tzircotis *et al.*, 2006). Interestingly however, mutations in this site did not affect random breast cancer cell motility or chemotaxis towards non-specific chemo-attractants (Tzircotis *et al.*, 2006). Additionally, CD44 has been shown to be constitutively phosphorylated on Ser325 in resting breast cancer cells *in vitro* (Neame and Isacke, 1992). Although the functional role of phosphorylation at this site remains unclear, introducing mutations at this site proved important in successful HA-mediated cell migration (Peck and Isacke, 1998). In osteoclasts, engagement of CD44 with HA resulted in rapid de-phosphorylation of Ser325 residue (Pivetta *et al.*, 2011). Furthermore, this site has been shown to be dynamically regulated by PKC, which in turn stimulated CD44-ezrin interactions and subsequent directional cell motility (Legg *et al.*, 2002).

The latter observations are particularly interesting, as Ser291 is located between two CD44 palmitoylation sites, Cys286 and Cys295. Reversible addition of palmitoyl moieties to CD44 has been described in lymphoma cells (Bourguignon *et al.*, 1991), and is thought to enhance CD44 association with ankyrin to promote tumour cell migration (Zhu and Bourguignon, 2000). Because addition of palmitoyl moieties increases the hydrophobicity of proteins, it has been proposed that palmitoylation of CD44 enables its partitioning into lipid rafts. Accordingly, mutations in both Cys residues of the CD44 cytoplasmic tail notably reduced CD44 partitioning into lipid raft domains in COS-7 and Flp-293 cells (Thankamony and Knudson, 2006). Functionally this translated into impaired CD44-mediated HA internalisation in those cell types (Thankamony and Knudson, 2006). Nonetheless, CD44 expression and partitioning into lipid rafts is largely cell type-dependent (Neame *et al.*, 1995), and this has not been extensively studied in breast cancer cells. Thus in the present chapter we concentrated on elucidating the functional relevance

of CD44 palmitoylation on breast cancer cell migration via its affiliation with lipid rafts.

4.2 Aims

In the previous chapter we showed that CD44 raft affiliation decreased during migration of highly-invasive breast cancer cells (Donatello & Babina *et al.*, 2012). Thus we sought to directly manipulate the raft affiliation of CD44 via site-directed mutagenesis of its palmitoylation sites to test its impact on cell motility. Hence the objectives of this chapter were as follows:

1. to generate CD44 palmitoylation mutants for transfection into human breast cell lines;

2. to examine if expression of palmitoylation-impaired CD44 in breast cancer cells influences its affiliation with lipid rafts;

3. to assess the functional effects of CD44 palmitoylation mutants in non-invasive and invasive cells;

4. to perform data-mining for SNPs around the CD44 palmitoylation site that could recapitulate the mutagenesis model in a physiological setting.

4.3 Results

4.3.1 Successful generation of palmitoylation-impaired CD44 mutants and their overexpression in breast cancer cells.

In the previous chapter we established a novel link between reductions in CD44 affiliation with lipid rafts and migration of highly-invasive breast cancer cells. Consequently, we sought to investigate if forcing CD44 outside lipid rafts would directly promote breast cancer cell migration. There are two known CD44 palmitoylation sites responsible for targeting CD44 to lipid rafts, Cys286 and Cys295. Using site-directed mutagenesis, point mutations were successfully introduced into one (C286A or C286S) or both (C286A, C295A and C286S, C295A) sites in human CD44. **Figure 4.2A** shows an overview of the desired CD44 sequence alterations encoded in the pOTB7 plasmid carrying a chloramphenicol resistance cassette. Mutations were sequenced and aligned to confirm the protein sequence of the region of interest (**Fig. 4.2B**). In order to determine a concentration of chloramphenicol which would be toxic to untransfected cells not expressing the chloramphenicol resistance cassette, MTT proliferation assays were performed in MDA-MB-231 cells (**Fig. 4.2C**). All concentrations tested reduced cell proliferation compared to controls, and 300μg/ml chloramphenicol was chosen as the optimal starting concentration for negative selection.

Accordingly, MDA-MB-231 cells were transiently transfected with the CD44 single and double mutants and whole lysates harvested after 48 hours. All transfected cells showed higher CD44 expression compared to non-transfected control cells (**Fig. 4.3A**). The intensity of CD44 bands was quantified, normalised to actin expression, and expressed as a percentage of that in control cells (**Fig. 4.3B**). Overall, transient transfection of MDA-MB-231 cells with wild-type (WT) CD44 and its palmitoylation mutants resulted in ≥50% higher CD44 expression.

A.

CD44 mutants		Trans-membrane domain	FERM domain	Ankyrin domain	
CD44WT	270	WLIILASLLALALILAVCIAV	NSRRRCGQKKKLV	INSGNGAVEDRKPSGL	319
C286A		----------A---	-----C-------	----------	
C286S		----------S---	-----C-------	----------	
SA		----------S---	-----A-------	----------	
AA		----------A---	-----A-------	----------	

B.

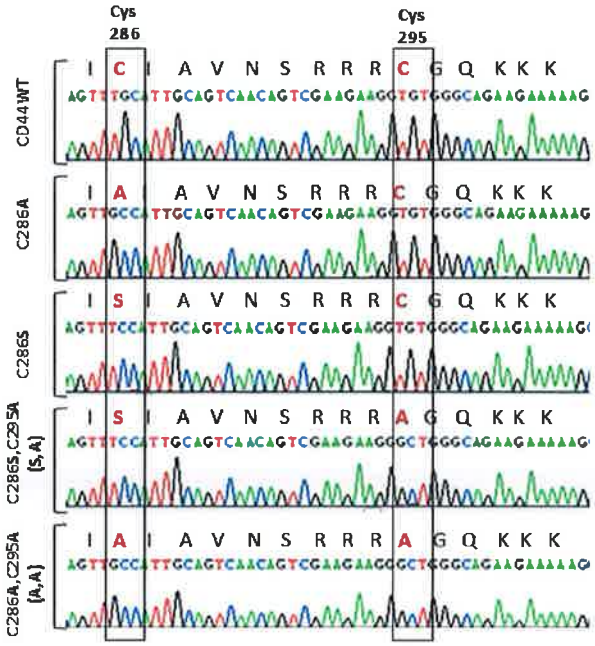

C.

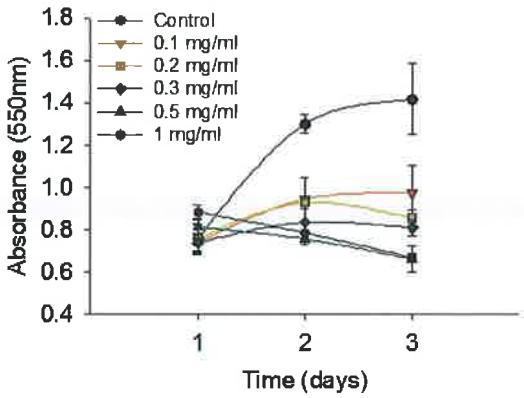

Figure 4.2. CD44 palmitoylation mutants overview. (A.) Single (Cys286Ala, Cys286Ser) or double (Cys286S, Cys295Ala [SA], Cys286Ala, Cys295Ala [AA]) CD44 palmitoylation mutants were generated and mutations confirmed by **(B.)** sequencing and BLAST alignment. **(C.)** MTT proliferation assays were performed in MDA-MB-231 cells using a range of chloramphenicol concentrations to determine a lethal concentration to select for CD44 mutants after transfection. 500µg/ml and 1mg/ml proved to be lethal to MDA-MB-231 cells. *Error bars=STDEV, n=2 experiments.*

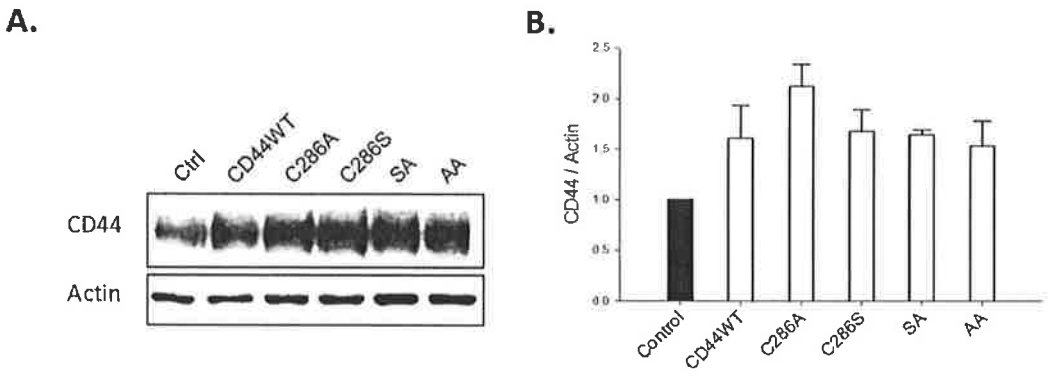

Figure 4.3 Successful overexpression of WT-CD44 and palmitoylation-impaired constructs in MDA-MB-231 cells. MDA-MB-231 cells were transfected for 48 hours with CD44 (WT or palmitoylation-mutant) DNA using jetPRIME transfection reagent, and mutant-expressing cells selected with chloramphenicol for 48 hours. **(A.)** CD44 expression was determined using western blot in whole cell lysates. **(B.)** CD44 band intensity was quantified and expressed relative to that of actin, then that in transfected cells was normalised to non-transfected control MDA-MB-231 cells. CD44 expression was increased by ~40-50% in all transfected cells. *Error bars=STDEV, n=2 experiments.*

4.3.2 Overexpression of CD44 palmitoylation mutants decreased CD44 affiliation with rafts.

MDA-MB-231 cells were transfected with full-length human CD44 and a range of palmitoylation-impaired mutants using jetPRIME transfection reagent, and grown in the presence of chloramphenicol for 2 days to select for mutant-expressing cells. As wild-type CD44 and its palmitoylation mutants are of the same molecular weight (and the mutants were untagged), we could not blot specifically for each mutant. Consequently, since palmitoylation-impaired CD44 should localise outside lipid rafts, full-scale lipid raft extractions were performed to analyse the raft versus non-raft distribution of CD44 in mutant cells. Compared to control and CD44 wild-type-expressing cells, raft-affiliated CD44 was decreased in cells expressing either single or double mutants (**Fig. 4.4A**). Quantification of the raft affiliation ratio of CD44 confirmed statistically significant reductions in CD44 affiliation with lipid rafts in single and double CD44 palmitoylation mutants when compared to either untransformed control MDA-MB-231 cells or those overexpressing wild-type CD44 (**Fig. 4.4B**).

Due to requirement for large quantities of starting material to perform full-scale lipid raft extractions, Triton X-100 insolubility assays were used as a surrogate for gradient raft extractions to estimate relative amounts of CD44 in detergent-insoluble (lipid raft-enriched) and detergent–soluble (non-raft-enriched) pools. To confirm the validity of this approach, detergent-soluble and -insoluble fractions were tested for the presence of flotillin-1 and transferrin receptor (**Fig. 4.4C**). As expected, Triton X-100-insoluble fractions were strongly enriched in flotillin-1 (mirroring lipid raft compartments), while detergent-soluble fractions had greatly increased expression of transferrin receptor (mirroring non-raft compartments). MDA-MB-231 cells transfected with wild-type CD44 had a similar CD44 solubility/insolubility profile compared to control cells. In contrast, cells transfected with CD44 palmitoylation mutants showed decreased CD44 recovery in detergent-insoluble pools and a corresponding increase in that recovered from detergent-soluble pools (**Fig. 4.4C**). These results were quantified to calculate a ratio of CD44 affiliation with detergent-insoluble fractions ("CD44 Insoluble:Soluble"; **Fig. 4.4D**). Compared

to control and CD44WT-overexpressing cells, CD44 single and double palmitoylation mutants had significantly lower affiliations with detergent-insoluble fractions ($p<0.05$ for all), suggesting a decrease in CD44 raft affiliation. Since these findings mirrored our results from large-scale isopycnic sucrose gradient lipid raft extractions, the simpler detergent-extraction approach was chosen for subsequent experiments.

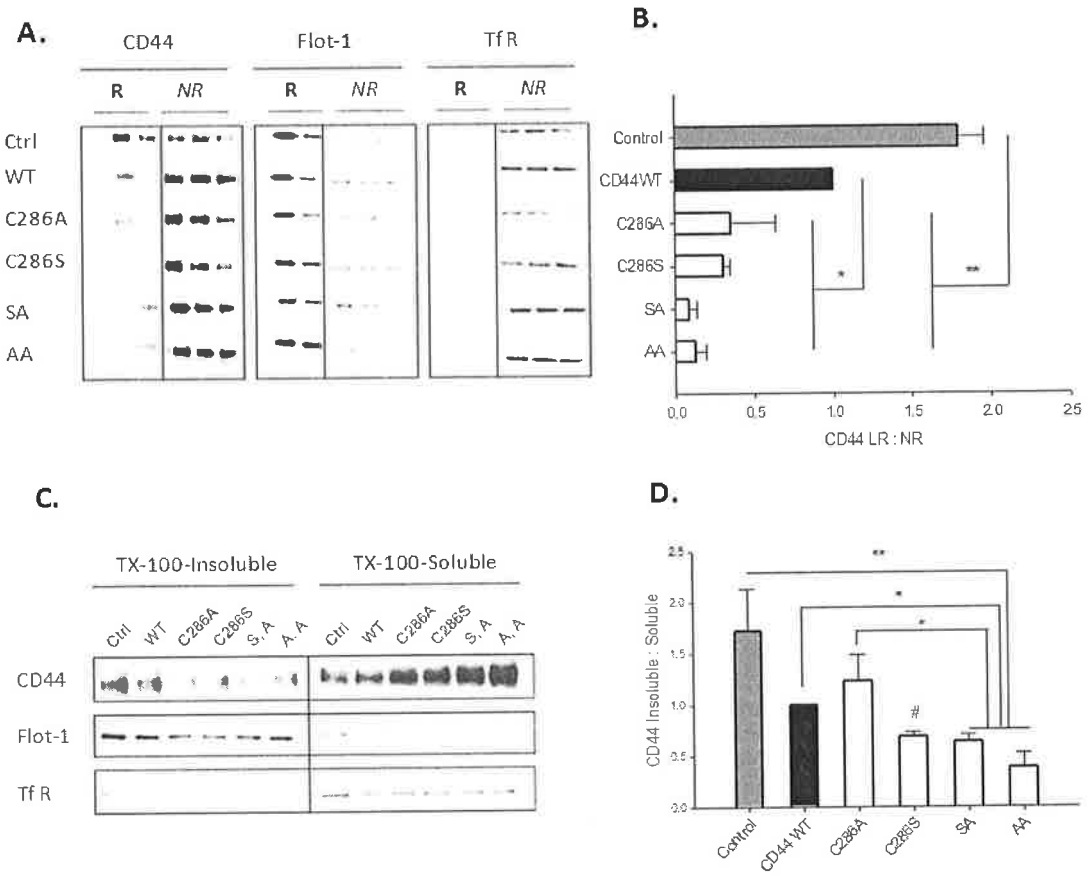

Figure 4.4. CD44 palmitoylation-impaired constructs have reduced affiliation with lipid rafts. MDA-MB-231 cells were transfected with full-length CD44 (CD44WT) or CD44 single-site (C286A, C286S) and double-site (SA, AA) palmitoylation-impaired mutants for 48 hours. **(A.)** Triton X-100-insoluble and –soluble fractions were isolated and confirmed to be enriched respectively in lipid raft (Flot-1) or non-raft (Tf R) components. CD44 recovery from lipid raft-enriched fractions was reduced in cells overexpressing mutant CD44 and paralleled by increased recovery of CD44 in non-raft fractions. **(B.)** Calculation of the affiliation ratio of CD44 with detergent-insoluble versus –soluble fractions confirmed reductions in the detergent-insoluble pool of CD44 from cells expressing the mutant constructs relative to controls. **(C.)** Full-scale lipid raft extractions confirmed reductions in raft-affiliated CD44 in cells expressing the mutant constructs relative to controls. **(D.)** Calculation of the LR/NR ratio for multiple experiments confirmed statistically significant reductions in raft affiliation of CD44 upon expression of the CD44 palmitoylation-impaired mutants. *Error bars=SEM, n=3 experiments; #p<0.05 (C286S vs Control); *p<0.05; **p<0.01, all by upaired 2-tailed Student's t-test.*

To confirm that these changes reflected reductions in CD44 palmitoylation, biotin-BMCC assays were performed on non-migrating cells overexpressing representative single and double palmitoylation mutants (**Fig. 4.5 A-B**). Free palmitate groups were cleaved from CD44 immunoprecipitates using HAM, whereupon reactive cysteine residues were labelled with biotin-BMCC and detected by streptavidin immunoblotting. Biotin-labelled (palmitoylated) CD44 was reduced in cells expressing single and double palmitoylation mutants, compared with wild-type and control cells. Negative control samples untreated with HAM had no detectable biotin-BMCC-CD44 complexes, and control IgG-precipitated lanes completely lacked CD44 (as expected). Band quantitation of palmitoylated relative to total CD44 in HAM-treated samples confirmed significant reductions in palmitoylated CD44 in MDA-MB-231 cells overexpressing single and double CD44 palmitoylation mutants (**Fig. 4.5B**). Additionally, CD44 sub-cellular distribution in MDA-MB-231 cells transfected with CD44WT and select single (C286A) and double (AA) mutants was analysed using immunofluorescence confocal microscopy (**Fig. 4.5C**). Compared to control MDA-MB-231 cells, all transfected cells demonstrated increased cytoplasmic and vesicular staining of CD44 (green).

A.

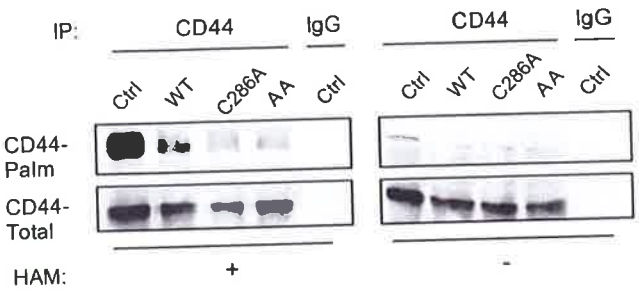
IP:
CD44
IgG
CD44
IgG
Ctrl
WT
C286A
AA
Ctrl
Ctrl
WT
C286A
AA
Ctrl
CD44-Palm
CD44-Total
HAM:
+
-

B.

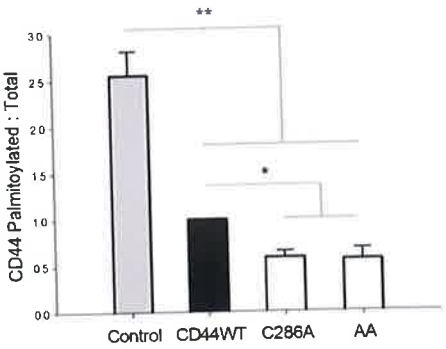
**
*
CD44 Palmitoylated : Total
30
25
20
15
10
0.5
0.0
Control
CD44WT
C286A
AA

C.

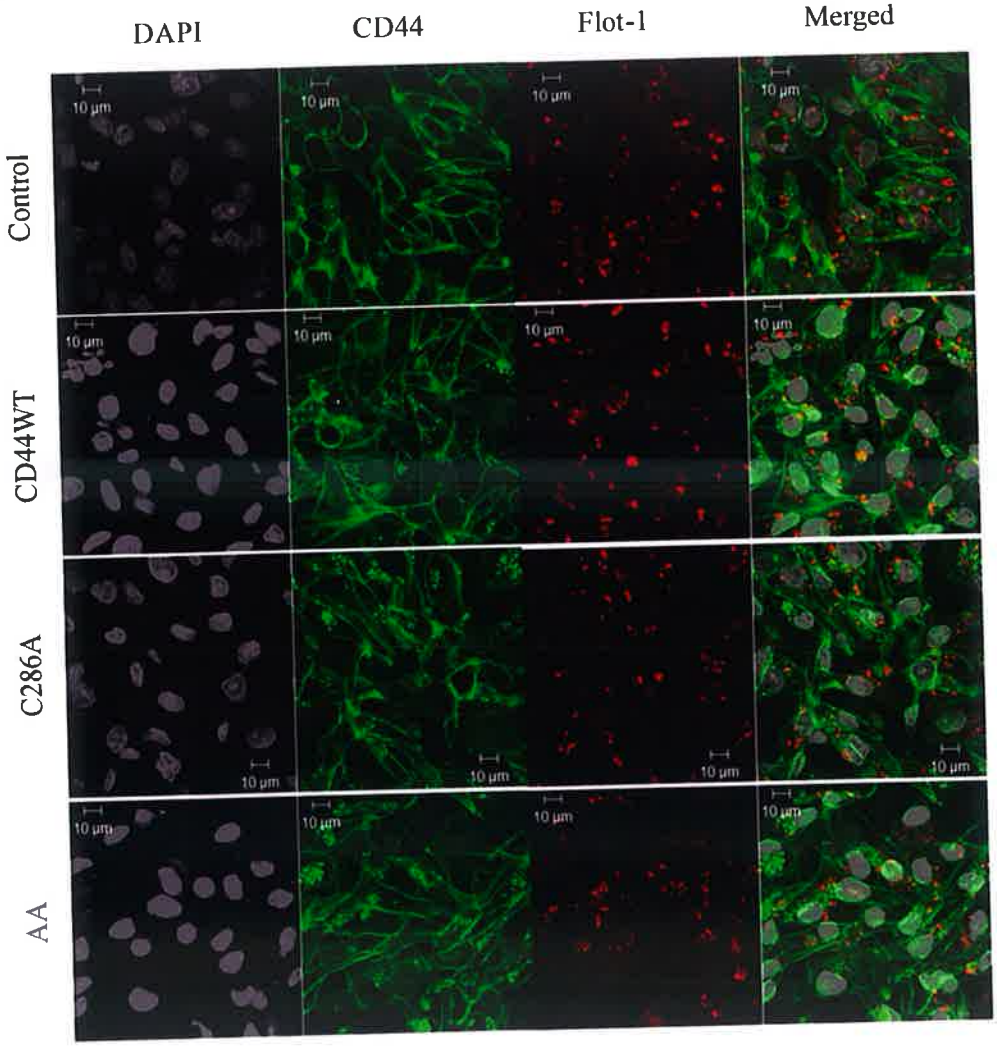
DAPI
CD44
Flot-1
Merged
Control
CD44WT
C286A
AA
10 µm

Figure 4.5 CD44 palmitoylation and localisation with flotillin-1 were reduced in mutant-expressing cells. (A.) Biotin-BMCC assays were used to measure palmitoylated CD44 (CD44-Palm) in cells expressing representative single and double palmitoylation mutants, and compared to total CD44 levels (CD44-Total). Isotype-matched IgG was used as a negative control for CD44 immunoprecipitations, and omission of HAM reagent was a BMCC negative control. CD44-Palm was reduced in cells over-expressing CD44 palmitoylation-impaired mutant constructs. **(B.)** Densitometric quantification of multiple experiments confirmed significant reductions in CD44-Palm relative to CD44-Total in mutant cells. *Error bars=SEM, n=3 experiments; *p<0.05 by unpaired 2-tailed Student's t-test.* **(C.)** CD44 cellular distribution upon transfection with CD44WT and select single (C286A) and double (AA) mutants was compared with that in control MDA-MB-231 cells. Whereas CD44 in control cells largely localised in the cell membrane, with occasional cytoplasmic staining, all transfected cells had cytoplasmic CD44 staining, as well as increased vesicular staining. In addition, there were fewer co-localisation areas of CD44 (green) with lipid raft marker flotillin-1 (red). Pictures are representative of 2 independent experiments.

4.3.3 Cancer cells overexpressing CD44 palmitoylation mutants have an altered phenotype.

To test whether forced exclusion of CD44 from lipid rafts directly promoted cell migration, a series of scratch-wound migration assays was performed in MDA-MB-231 cells transiently transfected with the CD44 palmitoylation-impaired mutants (**Fig. 4.6**). Overexpression of CD44WT or CD44 single-site palmitoylation mutants approximately doubled wound closure compared to control conditions. Transfection with CD44 double-site palmitoylation mutants resulted in four-fold better wound closure than that in control MDA-MB-231 cells (**Fig. 4.6A**), and double that of wild type and single CD44 mutant-overexpressing cells. In addition to migration, invasion characteristics of the transfected cells in classic Boyden chamber assays were also examined (**Fig. 4.6B**). While cells overexpressing CD44 palmitoylation-impaired mutants showed increased invasion at 6 and 22 hours, in this model the figures were not statistically different from enhanced invasion levels induced upon over-expression of CD44WT alone (**Fig. 4.6B**). However this supports our hypothesis as we also observed decreased CD44 raft affiliation in WT-overexpressing cells. Taken as a whole, our data are consistent with a model whereby decreased palmitoylation of CD44, which forces CD44 outside lipid rafts, increases breast cancer cell migration capabilities.

A.

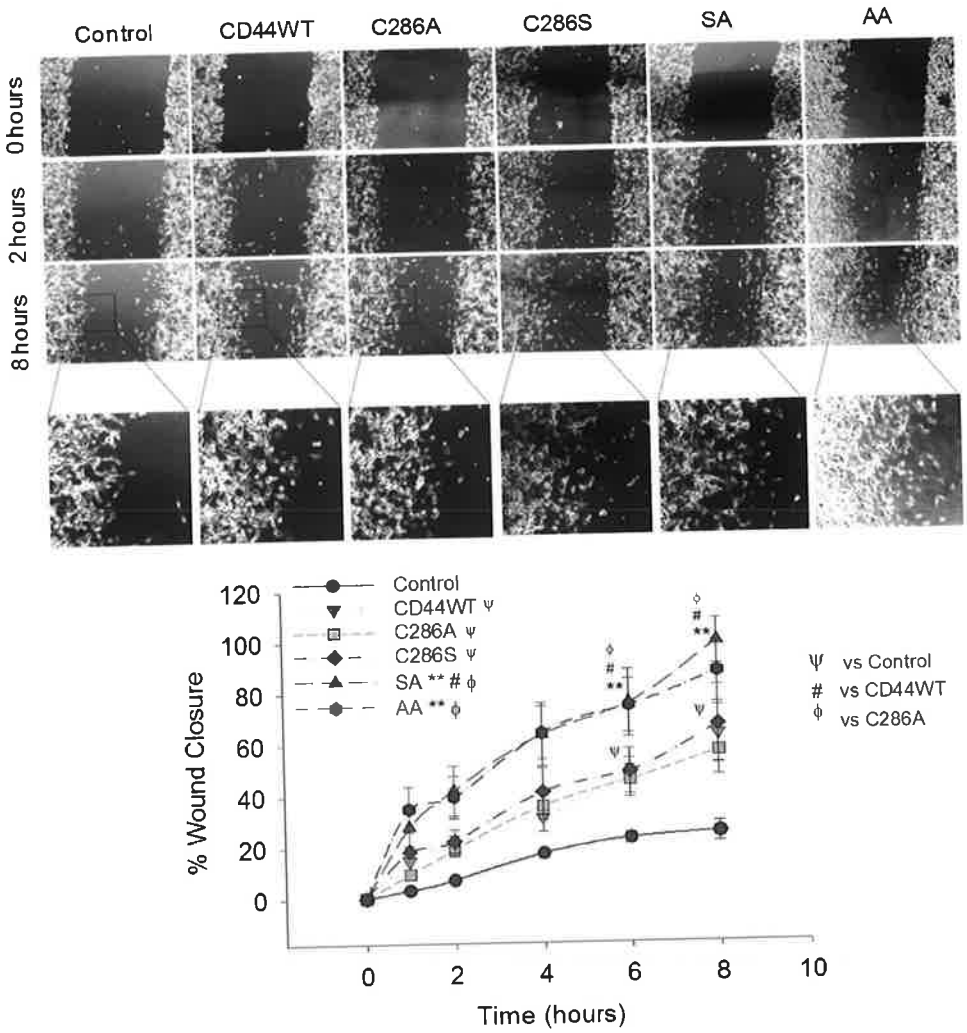
Control
CD44WT
C286A
C286S
SA
AA
0hours
2hours
8hours
% Wound Closure
Time (hours)
Control
CD44WT ψ
C286A ψ
C286S ψ
SA ** # ϕ
AA ** ϕ
ψ vs Control
vs CD44WT
ϕ vs C286A

B.

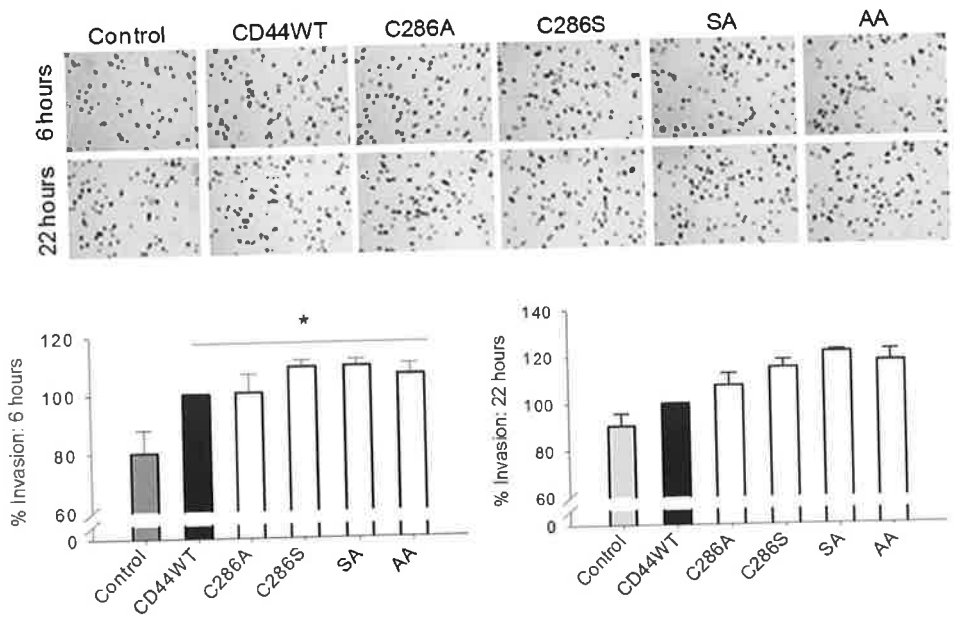
Control
CD44WT
C286A
C286S
SA
AA
6hours
22hours
% Invasion: 6 hours
% Invasion: 22 hours

Figure 4.6 Reduced CD44 affiliation with lipid rafts correlates with increased cell migration and invasion. (A.) Phase contrast micrographs of scratch-wound migration assays performed in MDA-MB-231 cells transfected for 48h with CD44-WT or CD44 single-site (C286A, C286S) or double-site (SA, AA) palmitoylation-impaired mutants. Cell migration was significantly enhanced in mutant-expressing cells compared to control cells, as indicated in the graphical representation of multiple experiments. *Error bars=SEM, n=3 experiments;* ψ# φ *$p<0.05$; **$p<0.01$ vs control, 2-way ANOVA.* **(B.)** Transwell invasion assays of MDA-MB-231 cells transfected for 48h with CD44WT, single-site (C286A, C286S) or double-site (SA, AA) palmitoylation-impaired mutant constructs. Invasion was quantitated at 6 and 22 hours. *Error bars=SEM from n=3 experiments (6 hours) or SD from n=2 experiments (22 hours); *$p<0.05$, by unpaired 2-tailed Student's t-test.*

4.3.4 Transfection with CD44 mutants decreased CD44 affiliation with rafts in MCF-10a cells.

In the previous chapter we demonstrated that MCF-10a cells, in contrast to invasive MDA-MB-231 or Hs578T cells, had an increased CD44 raft affiliation ratio after stimulation of migration. Thus we next sought to test whether forced exclusion of CD44 from lipid rafts in non-invasive breast cells was sufficient to induce a migratory phenotype. MCF-10a cells were transfected with palmitoylation-impaired CD44 DNA constructs, and Triton X-100 insolubility assays performed to compare the relative expression of CD44, flotillin-1 and transferrin receptor (**Fig. 4.7A**). Cells transfected with CD44 single palmitoylation mutants showed decreased CD44 recovery in Triton X-100-insoluble pools compared to controls, while detergent-insoluble CD44 in cells transfected with CD44 double palmitoylation mutants was almost abolished. This decrease was paralleled by increased CD44 recovery in detergent-soluble pools. The presence of a variant CD44 form in Triton X-100-soluble fractions of control and CD44WT-overexpressing cells is noteworthy, since it disappears in MCF-10a cells transfected with single, and, in particular, double CD44 palmitoylation mutants. The detergent insolubility ratio was calculated as for MDA-MB-231, considering only the 90kD standard form of CD44 (**Fig. 4.7B**). This ratio was significantly decreased in cells expressing double-site CD44 palmitoylation mutants compared to wild-type and untransfected MCF-10a cells.

In order to confirm that the decrease in raft affiliation reflected reductions in CD44 palmitoylation, biotin-BMCC assays were performed on non-migrating MCF-10a cells overexpressing representative single and double mutants (**Fig. 4.7C**). Palmitoylated CD44 was successfully reduced in cells overexpressing the palmitoylation-impaired mutant forms of CD44. Negative controls (lacking HAM treatment) showed no palmitoylated CD44, and the IgG isotype control immunoprecipitation had negligible total CD44. Palmitoylated CD44 bands were expressed relative to total CD44, and there was a significant reduction in palmitoylated CD44 in cells overexpressing the CD44 double-palmitoylation mutant (**Fig. 4.7D**).

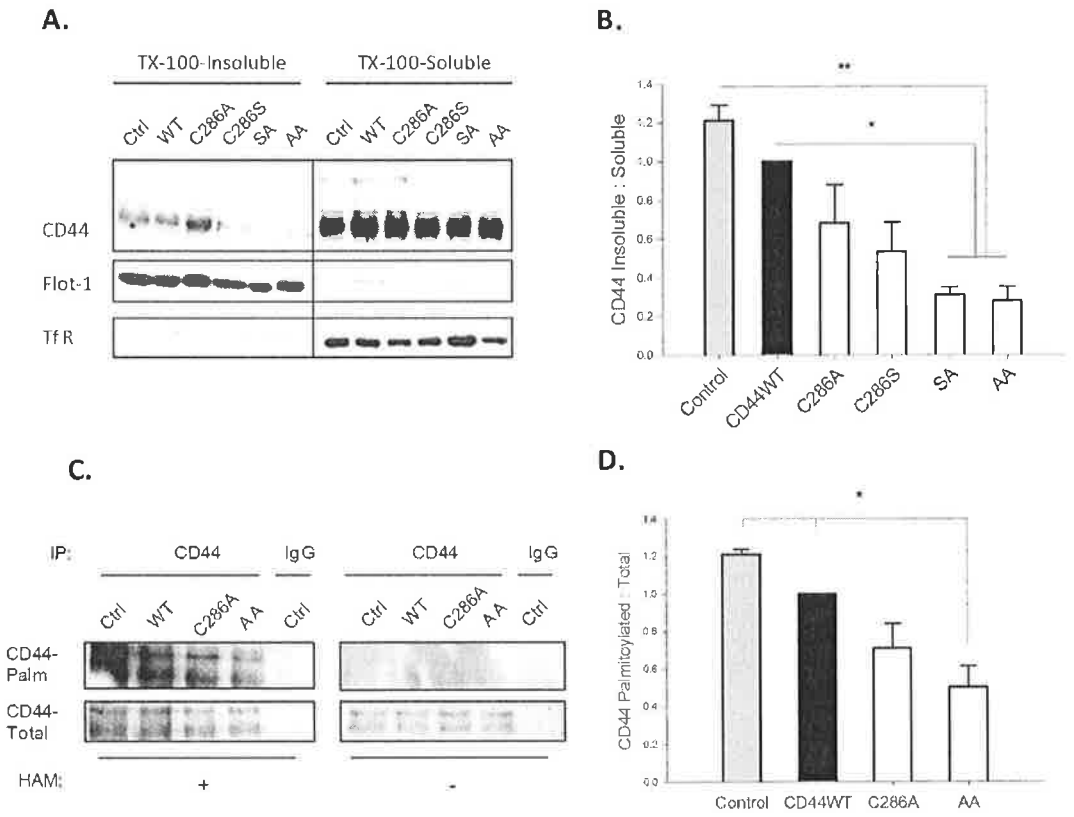

Figure 4.7 Expression of CD44 palmitoylation-impaired CD44 reduced CD44 raft affiliation in MCF-10a cells. MCF-10a cells were transfected for 48 hours with full-length CD44 (CD44WT), and single-site (C286A, C286S) or double-site (SA, AA) palmitoylation-impaired mutants. **(A.)** Triton X-100-insoluble and –soluble fractions were isolated, and confirmed to be enriched in respectively lipid raft (Flot-1) and non-raft (Tf R) marker proteins. Overexpression of mutant CD44 reduced CD44 recovery from raft-containing fractions compared to that in untransfected controls and CD44WT-expressing cells. **(B.)** The calculated ratios of CD44 affiliation with detergent-insoluble fractions reflected significant reductions in CD44 raft affiliation in mutant cells compared to untransfected control cells, and furthermore in CD44 double-site mutants compared to CD44WT. **(C.)** CD44 palmitoylation was assessed by BMCC assay in CD44 immunoprecipitates of control, CD44WT- and CD44 mutant-expressing cells. Palmitoylated CD44 was detected with streptavidin (CD44-Palm), and total CD44 using CD44 antibody (CD44-Total). No CD44 was recovered in immunoprecipitates of isotype-matched

IgG control lanes, and no palmitoylated CD44 was detected in HAM- control conditions. In the HAM+ condition, palmitoylated CD44 was reduced in mutant-expressing cells. **(D.)** Quantification of palmitoylated CD44 (as a ratio of total CD44) revealed significant reductions in cells over-expressing the double-site CD44 palmitoylation-impaired mutant (AA) relative to control or CD44WT-expressing cells. *Error bars=SEM; n=3 experiments; *p<0.05; **p<0.01 by unpaired 2-tailed Student's test.*

4.3.5 MCF-10a cells overexpressing CD44 mutants have an altered phenotype.

Having shown that migration was increased in MDA-MB-231 cells overexpressing CD44 palmitoylation-impaired mutants, we wanted to test whether decreased CD44 palmitoylation would also affect CD44 raft localisation and migration in non-tumourigenic MCF-10a cells. Forcing CD44 outside lipid rafts in MCF-10a cells (via overexpression of CD44 palmitoylation-impaired mutants) resulted in a drastic change in cell morphology (**Fig. 4.8**). Compared to control non-transfected MCF-10a cells, overexpression of either CD44WT or CD44 palmitoylation-impaired mutants disrupted the tight colony formation characteristic of these cells, inducing cell scattering and a phenotypic appearance reminiscent of epithelial-mechenchymal transition (EMT). These effects were rescued upon termination of selection for the CD44 palmitoylation-impaired mutants. In support of the speculation about EMT, we noted reduced protein expression of the epithelial marker EpCAM (epithelial cell adhesion molecule) and enhanced expression of the mesenchymal marker vimentin in cells expressing CD44WT or CD44 palmitoylation-impaired mutants (relative to control cells; **Fig. 4.9**).

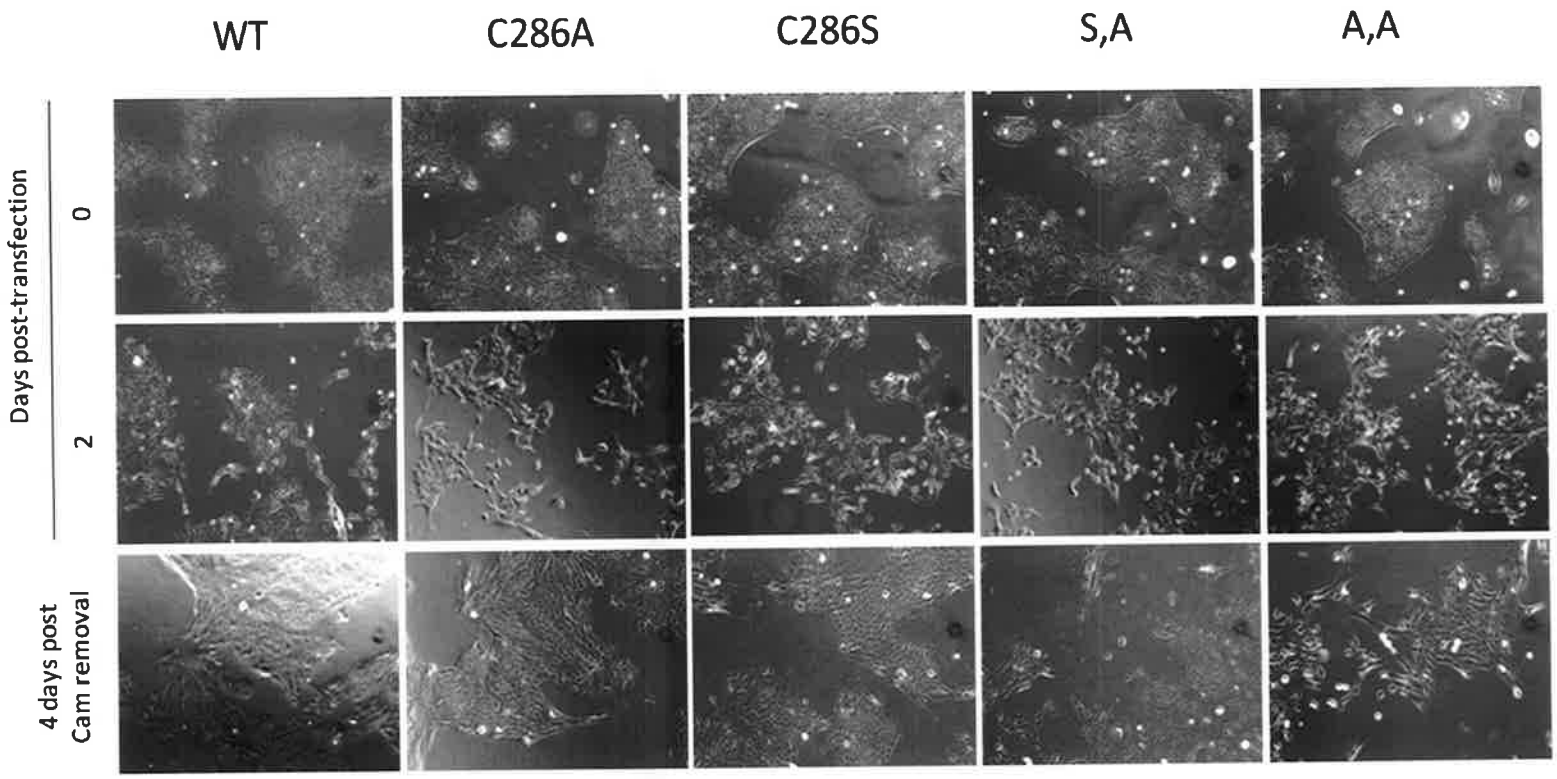

Figure 4.8. Morphological changes in MCF-10a cells following CD44 overexpression. Phase contrast micrographs were taken prior to MCF-10a cell transfection with CD44 DNA (Day 0), and then 2 days post-transfection. Chloramphenicol selection was subsequently terminated, and cells were photographed 4 days after removal of chloramphenicol. Pictures are representative of at least 3 independent experiments.

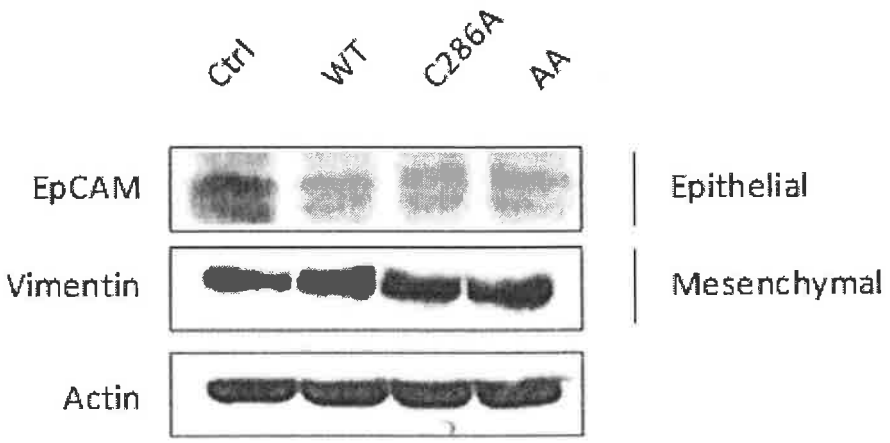

Figure 4.9 Over-expression of CD44 or its palmitoylation-impaired mutants induces altered expression of EMT markers. MCF-10a cells were transfected for 48h with CD44WT, single-site (C286A) or double-site (AA) palmitoylation-impaired mutant constructs. Immunoblotting revealed a decrease in the epithelial marker EpCAM and an increase in the mesenchymal marker vimentin, suggesting an EMT-like switch in cells over-expressing CD44WT or its palmitoylation mutants.

Functional assessment of MCF-10a cells overexpressing WT-CD44 and its palmitoylation mutants further supported the development of an altered cell phenotype. Specifically, MCF-10a cells over-expressing CD44WT or CD44 single mutants showed increased cell migration after 4 hours relative to control cells (**Fig. 4.10A**). Enhanced migration was most obvious in cells overexpressing double-site CD44 palmitoylation mutants, being observed as early as 2 hours post-wounding and maintained over 8 hours. Although differences between CD44 single and double mutants were not statistically significant, category-based grouping was observed, similar to our observations in MDA-MB-231 cells.

Additionally, the invasion capabilities of MCF-10a cells were examined after 22 hours of invasion (**Fig. 4.10B**). Compared to control cells, cells overexpressing CD44WT showed ~17% greater invasion (**Fig. 4.10B**). An increase in invasion capacity (~35%) was also observed in cells expressing double CD44-palmitoylation mutants compared to controls. A small increase in invasion (20-25%) was also recorded in cells over-expressing CD44WT or the single-site CD44 palmitoylation-impaired mutants. Overall, these results demonstrate for the first time that modifying the affiliation of CD44 with lipid rafts is capable of transforming normal-like MCF-10a cells into a more motile and invasive phenotype.

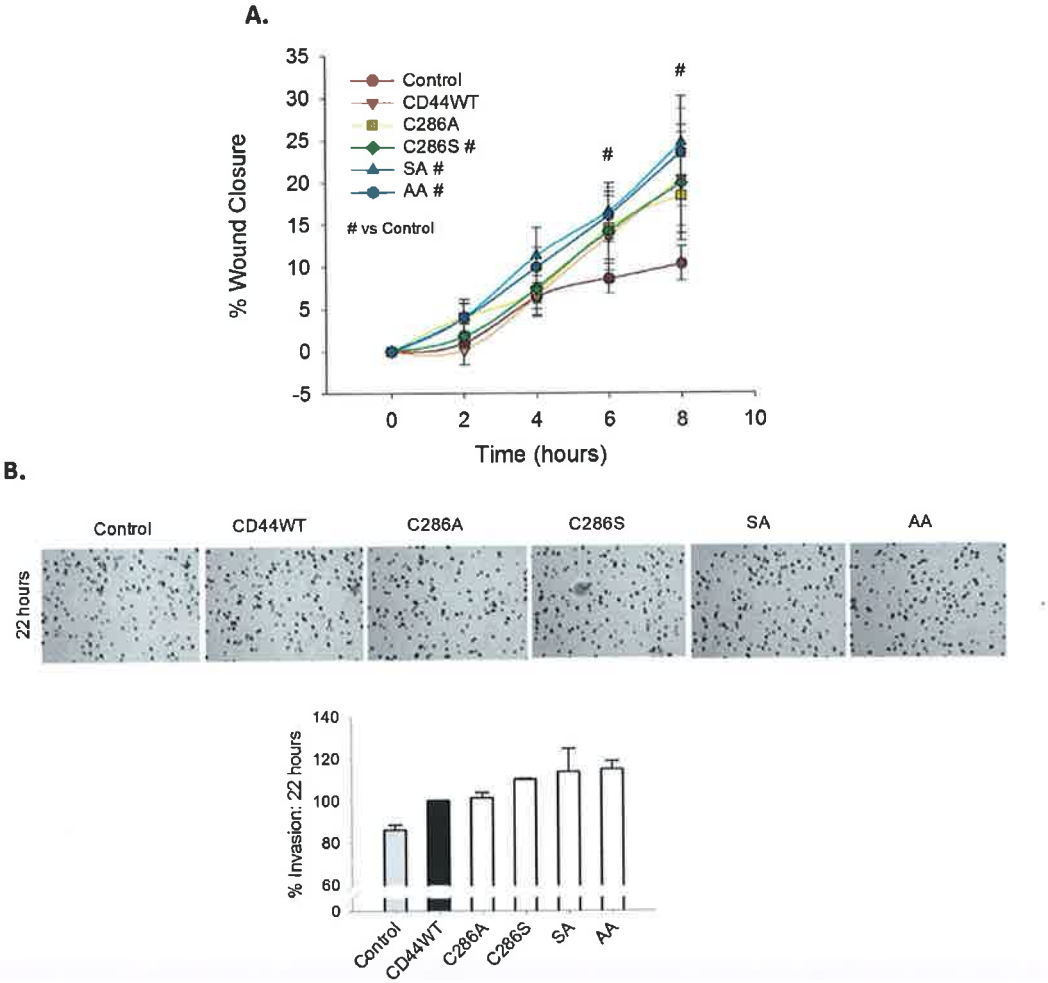

Figure 4.10 CD44 palmitoylation impairement increased migration of MCF-10a cell line. (A.) Scratch-wound assays revealed significant enhancements in the migratory capacity of MCF-10a cells transfected for 48 hours with CD44 palmitoylation-impaired mutants, relative to control cells. *Error bars=SEM, n=3 experiments; #p<0.05 vs control, 2-way ANOVA.* **(B.)** Transwell invasion assays of MCF-10a cells transfected for 48h with CD44WT, single-site (C286A, C286S) or double-site (SA, AA) palmitoylation-impaired mutant constructs. Invasion was quantitated at 22 hours, and all transfected cells observed to have higher invasion capabilities compared to controls. *Error bars=STDEV, n=2 experiments.*

4.3.6 Acquired phenotypes are reversible

To confirm that the observed phenotypic changes in MCF-10a cells reflected specific interference with CD44 raft affiliation, we undertook recovery experiments in which chloramphenicol selection was terminated after 48 hours and cells were passaged twice in normal medium before being subjected to Triton X-100 solubilisation assays or scratch-wound migration assays (**Fig. 4.11**). Mutant de-selection induced an increase in CD44 recovery from detergent-insoluble fractions, which had previously been decreased in mutant-transfected MCF-10a cells (**Fig. 4.12A**). Furthermore, the high molecular weight CD44 isoform which had been lost upon overexpression of palmitoylation-impaired CD44 (**Fig. 4.7**), was restored in detergent-soluble fractions. Calculation of the CD44 detergent-insoluble affiliation ratios in de-selected cells confirmed the reversibility of reductions in CD44 affiliation shown previously in transfected cells, to levels not statistically different to untransfected controls (**Fig. 4.12B**). This was functionally supported by the normalisation of migratory properties in de-selected cells, mirroring instead wound closure patterns in control cells (**Fig. 4.12C**) and losing the migratory advantage formerly associated with mutant expression (**Fig. 4.8**). Visually, the scattered EMT-like colony appearance of the mutant-overexpressing MCF-10a cells returned to the original tight colony organisation of control cells upon de-selection of mutant expression (**Fig. 4.8, lower panel**). Collectively, our results indicate that reducing the lipid raft affiliation of CD44 by interfering with its palmitoylation was sufficient to transform normal-like MCF-10a cells into a more motile phenotype than that of the parent cells.

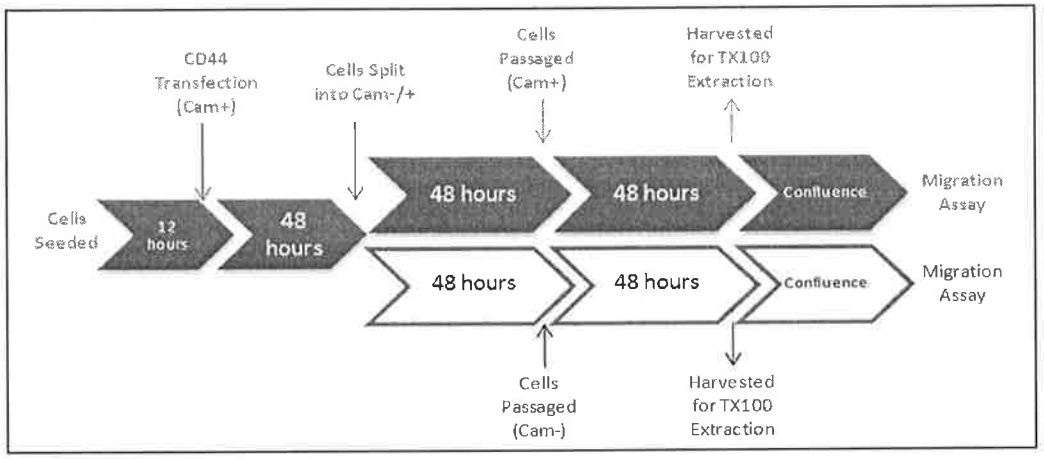

Figure 4.11. Schematic representation of phenotype restoration experiments. The time course indicates the flow of events from the moment of seeding untransformed cells for transfection, through to analysis of longer culture in presence and absence of the selective antibiotic chloramphenicol (Cam).

Reversibility of the phenotype was supported by parallel investigations in MDA-MB-231 cells. While in mutant-transfected MDA-MB-231 cells the CD44 raft affiliation ratio was significantly reduced relative to control (**Fig. 4.4**), de-selected cells acquired a profile of CD44 partitioning not statistically different from that of control cells (**Fig. 4.12D**). Normalisation of the CD44 affiliation ratio between de-selected mutants and control cells confirmed the biochemical reversibility of the process (**Fig. 4.12E**). Functionally, scratch wound migration assays also confirmed that de-selected CD44 palmitoylation mutants lost the migratory advantage (**Fig. 4.12F**) that had been previously linked to mutant expression.

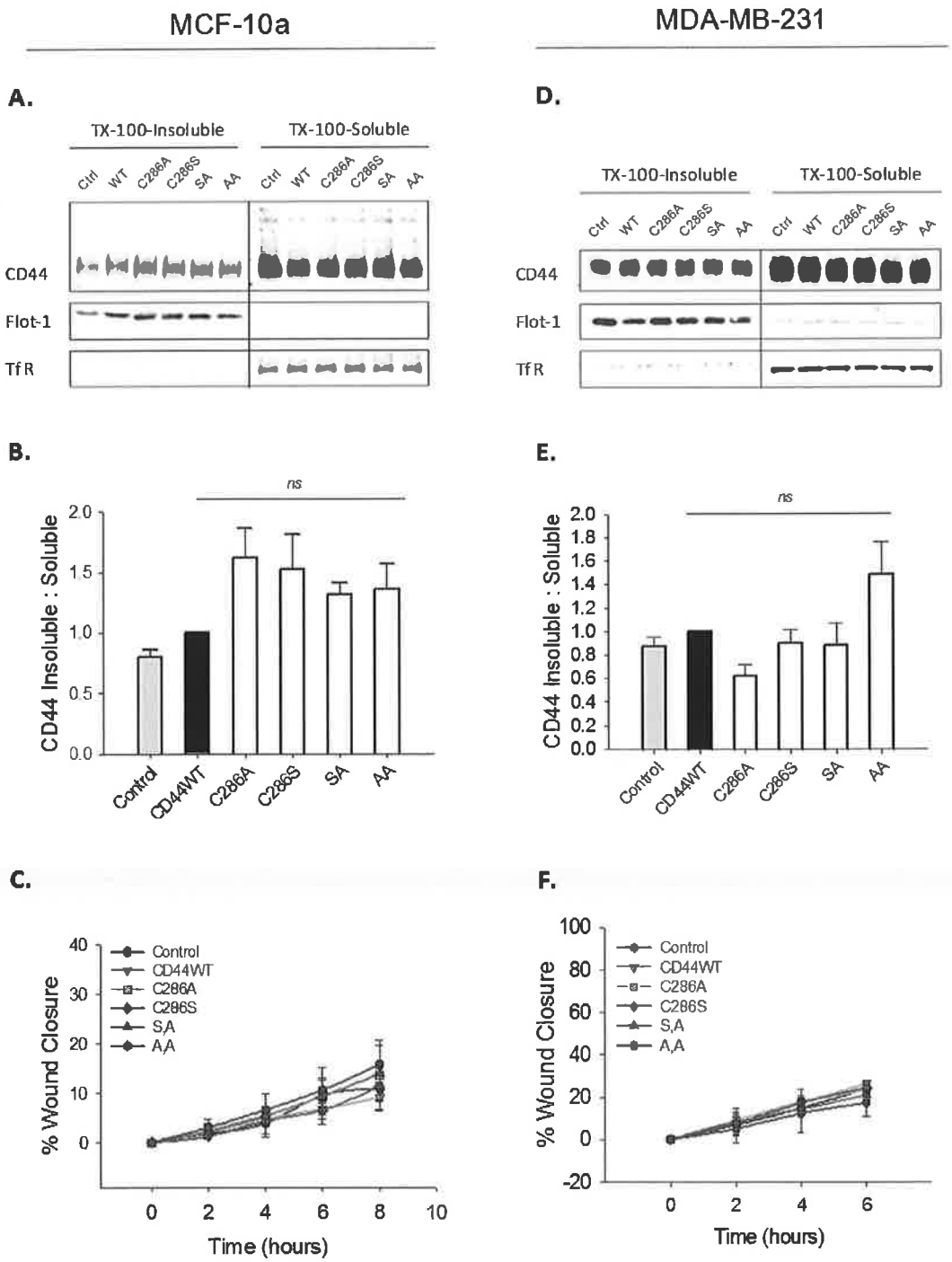
MCF-10a
MDA-MB-231
A.
TX-100-Insoluble
TX-100-Soluble
Ctrl
WT
C286A
C286S
SA
AA
CD44
Flot-1
TfR
D.
B.
E.
ns
CD44 Insoluble : Soluble
Control
CD44WT
C286A
C286S
SA
AA
C.
F.
% Wound Closure
Time (hours)
Control
CD44WT
C286A
C286S
S,A
A,A

Figure 4.12 Biochemical and functional phenotypes in cells overexpressing CD44 palmitoylation-impaired mutants are reversible. Following 48h expression of CD44WT or palmitoylation-impaired single (C268A, C286S) or double (SA, AA) mutants in MDA-MB-231 and MCF-10A cells, cells were subcultured and the selection reagent removed for a further 48hr. **(A.)** After termination of CD44WT or mutant selection in MCF-10A cells, CD44 recovery from Triton X-100-insoluble fractions was restored to match that of control cells. **(B.)** Lack of statistically-significant differences *(ns, not significant, unpaired 2-tailed Student's t-test)* between the raft affiliation ratios of CD44 in control MCF-10A cells versus those in which mutant selection had been terminated confirmed restoration of a normal biochemical phenotype. **(C.)** Scratch-wound assays confirmed that cell migration returned to control levels in MCF-10A cells following termination of expression of CD44WT or palmitoylation-impaired mutants *(by 2-way ANOVA)*. **(D.)** After termination of CD44WT or mutant selection in MDA-MB-231 cells, CD44 recovery from Triton X-100-insoluble fractions was restored to match that of control cells *(ns, not significant, 2-tailed Student's t-test)*. **(E.)** Scratch-wound assays confirmed that cell migration returned to control levels in MDA-MB-231 cells following termination of selection for expression of CD44WT or palmitoylation-impaired mutants *(2-way ANOVA). Error bars=SEM, n=3 experiments.*

4.3.7 Potential recapitulation of CD44 palmitoylation defects *in vivo*.

Having presented novel evidence that *in vitro* modulation of CD44 palmitoylation status reversibly modifies cancer cell motility, we sought to examine whether any published single nucleotide polymorphisms (SNPs) might *in vivo* reflect the CD44 palmitoylation defects modelled in our site-directed mutagenesis strategy. Using the NCBI dbSNP database, we searched specifically for any reported SNPs around the CD44 palmitoylation region. **Figure 4.13** summarises published non-synonymous SNPs in the CD44 transmembrane (TM) region and its proximal domains. Since the hydrophobicity of membrane proteins critically influences its potential incorporation into lipid rafts (Simons and Sampaio, 2011), we concentrated on amino acid changes that would affect hydrophobicity of the CD44 membrane-proximal regions. One SNP in the TM domain (rs61755294) is responsible for an alanine to proline switch, which would reduce hydrophobicity (Kyte and Doolittle, 1982). Other non-synonymous SNPs have been reported adjacent to the Cys295 palmitoylation site, in a highly-charged arginine-rich, ERM-binding (Thorne *et al.*, 2004) domain. Both amino acid changes in this instance favour the hydrophobic amino acids glutamine and threonine. Finally, two SNPs at the tail-ends of the CD44 FERM and ankyrin-binding domains are responsible for hydrophilic substitutions of valine to methionine and leucine to proline (respectively). Such shifts in CD44 lipophilic properties could potentially alter the partitioning of CD44 within raft versus non-raft regions of the cell membrane, accordingly influencing the likelihood of encountering specific binding partners which are required for cell migration.

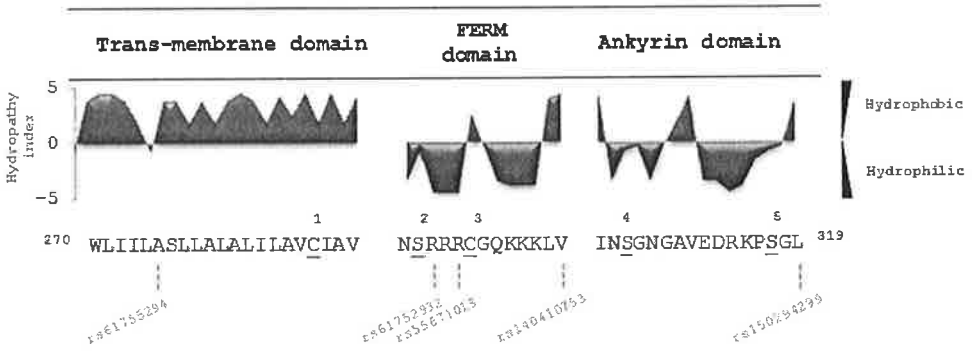

No.	Position	Residue	Modification
1	286	Cysteine	Palmitoylation
2	291	Serine	Phosphorylation, by PKC
3	295	Cysteine	Palmitoylation
4	305	Serine	Phosphorylation
5	316	Serine	Phosphorylation

dbSNP rs#	Chr. position	AA position	Contig AA	Missense AA	Hydrophobicity
rs61755294	35243218	276	Ala (A)	Pro (P)	↓
rs61752932	35243273	292	Arg (R)	Gln (Q)	↑
rs55671018	35243279	294	Arg (R)	Thr (T)	↑
rs140410753	35250722	302	Val (V)	Met (M)	↓
rs150294299	35250747	318	Leu (L)	Pro (P)	↓

Figure 4.13 SNP and amino acid characterisation that could alter CD44 palmitoylation and its lipid raft localisation. The CD44 transmembrane and proximal regions were analysed for previously-reported non-synonymous SNPs that might affect protein hydrophobicity and thus the likelihood of its incorporation into rafts. Post-translational modifications of identified residues are underlined, and the nature of the modification outlined in the table underneath. Residues reported to contain SNPs resulting in non-synonymous amino acid substitution are outlined in the bottom table, along with the relevant increase or decrease in CD44 hydrophobicity. This could in turn influence CD44 partitioning into highly-hydrophobic lipid raft domains.

Taken together, our results suggest that forcing CD44 outside lipid rafts promotes migratory and invasive breast cancer cell phenotypes and can even transform normal-like breast epithelial cells to become motile and invasive. The reversibility of these effects upon termination of selection for mutant CD44 supports the dependence of these effects upon CD44. Overall, this demonstrates a novel and exciting mechanism whereby containment of CD44 within lipid rafts may attenuate breast cancer cell migration, and could be explored as a potential strategy to diminish cancer cell dissemination.

4.4 Discussion

Breast cancer cell migration is one of the earliest molecular events in the metastatic spread of tumours. Identifying breast tumour markers that can predict metastatic potential or act as therapeutic targets is a focus of numerous studies. CD44 has been the subject of extensive investigation because of its expressional correlation with invasive breast carcinomas (Sheridan *et al.*, 2006) and aggressive basal-like clinicopathological parameters (Klingbeil *et al.*, 2010). Many studies have addressed the contribution of individual CD44 splice isoforms to breast cancer progression (Olsson *et al.*, 2011), however we focused on the role of the standard CD44 isoform in breast cancer cell migration. CD44 resides in lipid rafts (Ilangumaran and Hoessli, 1998; Ostapkowicz *et al.*, 2006; Tarone *et al.*, 1984), which are organisation centres for many molecules that play key roles in cell migration and whose altered functional behaviour has been implicated in many diseases including breast cancer (reviewed in (Babina *et al.*, 2011)). In the previous chapter we demonstrated reduced raft affiliation of CD44 during stimulated migration of MDA-MB-231 or Hs578T invasive breast cells. In the present chapter we further dissected the relationship between CD44 affiliation with lipid rafts and the migratory potential of breast cancer cells. Specifically, we mechanistically addressed the contribution of CD44 palmitoylation to its localisation in lipid rafts, and the subsequent regulation of breast cancer cell migration.

It has been previously shown that dual acylation of two cysteine residues (Cys286 and Cys295) in the transmembrane region of CD44 is required for its association with lipid rafts in fibroblasts and embryonic kidney epithelial cells (Thankamony and Knudson, 2006). We used transient overexpression of CD44 palmitoylation-impaired mutants in MDA-MB-231 cells as a tool to decrease CD44 affiliation with lipid rafts. Triton X-100 insolubility assays were used as a simplistic model for lipid raft extractions, as detergent-insoluble fractions have been shown to be enriched in lipid rafts (Murai *et al.*, 2011; Simons and Ikonen, 1997). Both our Triton X-100

insolubility assays and full-scale lipid raft extractions reflected the same results, namely that overexpression of CD44 palmitoylation-impaired mutants reduced CD44 affiliation with detergent-insoluble or lipid raft subcellular fractions. However both methods also revealed that CD44WT-overexpressing cells too had decreased CD44 raft affiliation compared to controls. This was paralleled by a decrease in palmitoylated CD44. We thus speculate that CD44WT may be dynamically removed from lipid rafts by its targeting to compartments such as early endosomes, given the coincident increase in expression of the early endosomal marker transferrin receptor, compared to that in control cells.

Functional analysis of cells with reduced CD44-raft affiliation revealed enhanced cell migration compared to that in control MDA-MB-231 cells. Single and double CD44 palmitoylation mutants had migratory enhancements of two- and four-fold respectively, compared to controls, indicating that CD44 localisation outside lipid rafts results in a more motile cancer cell phenotype. The fact that CD44WT overexpression alone also doubled cell migration could potentially be accounted for by the proportionally lower levels of palmitoylated relative to total CD44 in the over-expressing condition. Additionally, our results demonstrated a similar subcellular distribution of CD44 in both CD44WT- and mutant-transfected cells. Similarly, individual mutation of the same acylation sites 286 and 295 in hybridoma did not alter CD44 partitioning into raft domains compared to CD44WT cells (Lee *et al.*, 2008). Our CD44WT results are also in agreement with previous reports where CD44 overexpression alone increased cell migration and invasion (Roetger *et al.*, 1998) and furthermore, was associated with increased risk of metastasis in patients (Diaz *et al.*, 2005). Because CD44 affiliation with lipid rafts is cell-type dependent (Neame *et al.*, 1995), and because there have been no reports of specific targeting of CD44 palmitoylation in breast cancer, our findings are novel in highlighting that modification of CD44 palmitoylation status and consequently its affiliation with lipid rafts are involved in regulating CD44 functions during breast cancer cell migration.

Having previously shown an increase in CD44 raft affiliation ratio during migration of non-tumourigenic MCF-10a cells, we sought to investigate if forcing CD44 outside lipid rafts would be sufficient to make their phenotype more motile and invasive. Morphological changes between control and CD44-overexpressing cells were quickly apparent, with palmitoylation-impaired mutants gaining an EMT-like appearance and altering their expression levels of epithelial and mesenchymal markers within 48 hours. Cells overexpressing CD44WT also acquired the morphological features of EMT, but over a longer time-course. This latter observation was consistent with a recent study showing a decrease in epithelial markers and an increase in mesenchymal markers upon CD44 activation (Brown *et al.*, 2011). Importantly, our morphological observations of EMT were paralleled by enhanced migration in MCF-10a cells (in a manner mimicking functional changes in MDA-MB-231 cells). This is in agreement with findings that CD44 is important in EMT and breast cancer progression (Brown *et al.*, 2011). Our observed effects related specifically to CD44 mutant expression was confirmed upon loss of acquired morphological and functional changes after termination of mutant selection for CD44. Interestingly, it has been shown that for EMT to occur in MCF-10a cells, the high molecular weight CD44 isoform (which we observed in lipid rafts of normal-like MCF-10a cells) must switch to the standard form of CD44 (Brown *et al.*, 2011). It has not yet been determined whether this transition should happen inside or outside lipid rafts; however we noted reduced expression of high molecular weight CD44 in CD44 palmitoylation-impaired mutants. Taken together, it is intriguing to speculate that, at the early stages of cancer progression, the standard form of CD44 becomes prevalent and localises outside lipid raft domains to bind pro-oncogenic binding partners and stimulate cancer cell migration. One possible mechanism could involve upregulation of NFκB and AP-1 transcription factors, as they have been shown to influence expression of standard CD44 in breast cancer cells (Smith and Cai, 2012).

In light of functional enhancements in cancer cell migration by point-mutations in cysteine residues that control CD44 palmitoylation and raft

trafficking, we searched for polymorphisms in the vicinity of CD44 palmitoylation sites that might predict aggressive or metastatic behaviour in human cancers. In general, polymorphisms in the *CD44* gene have not been broadly studied. The only predictive polymorphisms in *CD44* reported to date are concentrated around the HA-binding domain, and the relationship with cancer progression has not yet been investigated. Nonetheless, Arg46 was previously shown to be crucial for HA binding (Acconcia *et al.*, 2004), with a heterozygous SNP in that site reducing the availability of the HA-binding consensus sequence (Adams *et al.*, 2000). SNPs in intron 1 (Aigner *et al.*, 1997) and exon 2 of *CD44* (Annabi *et al.*, 2001) were recently identified in breast cancer patients. However these would need to be tested on larger populations to draw strong correlations with breast cancer prediction and prevention. Jiang *et al.* have determined that a *CD44* rs13347 C>T polymorphism has a significant predictive and prognostic value for breast cancer patients in Chinese populations (Aroui *et al.*, 2009). The relevance to our model is that non-synonymous SNPs resulting in amino-acid changes around the palmitoylation sites of CD44 (summarised in **Fig. 4.13**) could affect its hydrophobicity (Coleman *et al.*, 2009), potentially altering its lipid raft localisation and therefore access to (or affinity for) cytosolic partners or enzymes. This model is graphically represented in **Fig. 4.14**. We speculate that increased localisation of CD44 in lipid rafts, either via its enhanced palmitoylation or by an increase in its hydrophobicity (through mechanisms such as the aforementioned SNPs) may mask the ERM-binding site. However when CD44 is de-palmitoylated or its hydrophobicity is reduced, its re-localisation outside rafts could expose the ERM-binding site. This would in turn recruit additional effector molecules to allow pro-migratory interactions between CD44 and ERM proteins, which, as described in the previous chapter, we recovered exclusively from non-raft domains. An example of such effector molecules could be membrane-associated kinases, which de-phosphorylate serine 291 and phosphorylate serine 325 on CD44, a process previously described to be involved in dynamic associations of ERM and CD44 (Legg *et*

al., 2002). Alternatively, CD44 palmitoylation and localisation in lipid rafts may be subject to regulation by palmitoylation enzymes, which have previously been described to directly affect localisation and function of other important palmitoylated proteins such as Ras (Gormer *et al.*, 2012) and to play a role in disease progression (Resh, 2012).

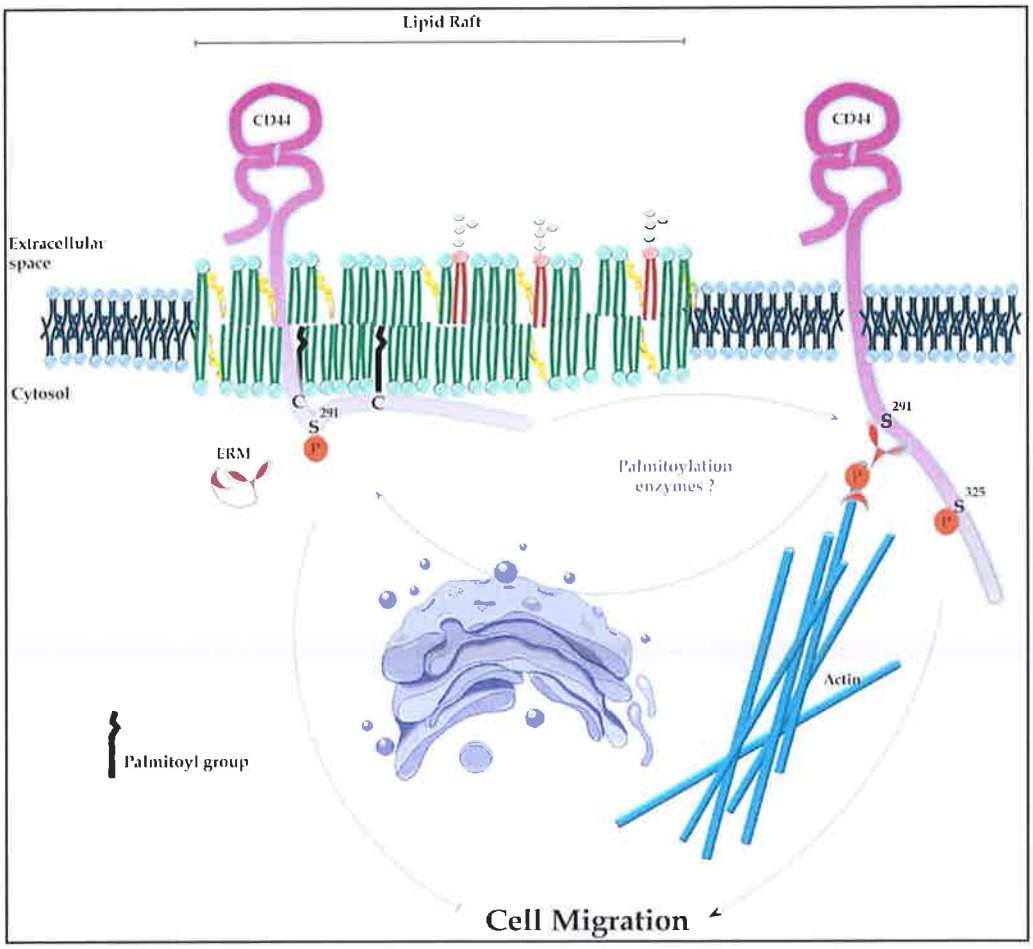

Figure 4.14. Schematic representation of the proposed model of regulation of breast cancer cell migration via CD44 localisation in lipid rafts. When CD44 is affiliated with lipid rafts via palmitoylation of its cysteine residues, it is sequestered from binding its cytoplasmic binding partners and thus migration is restrained. However when CD44 translocates outside lipid rafts in its de-palmitoylated state, its cytoplasmic tail is free to bind its cytoskeletal partners such as ERMs, subsequently facilitating cell migration.

Collectively, our observations are consistent with a novel role for CD44 palmitoylation and its subsequent trafficking to lipid rafts as a mechanism to influence breast cancer cell migration. We propose that lipid rafts regulate the availability of CD44 for interactions with binding partners or other effector proteins during breast cancer cell migration. Further investigations into the regulation of CD44 palmitoylation could explain its role in mammary cancers and prove therapeutically useful in preventing breast cancer metastatic spread.

Chapter 5

Potential clinical implications of CD44 palmitoylation and raft localisation in breast cancer.

5.1 Introduction

5.1.1 Enzymes involved in regulation of palmitoylation.

In the previous chapter we showed that mutagenesis of CD44 palmitoylation sites reduced its affiliation with lipid rafts and promoted a pro-migratory phenotype in breast cells. Based on these data, it is intriguing to speculate that CD44 palmitoylation could provide a novel pharmacological target to attenuate CD44-based motility in breast cancer cells. Palmitoylation is a dynamic and reversible post-translational modification of a wide range of proteins. Addition of a palmitic acid (PA) moiety is believed to affect proteins in two main ways. Firstly, it could increase protein hydrophobicity and thus its affinity for hydrophobic lipid raft domains. This has been associated with functional modification of GTPase proteins, endothelial nitric oxide synthase (eNOS) and postsynaptic density protein-95 (PSD-95) (Greaves and Chamberlain, 2007). In G-coupled receptors, palmitoylation could alter protein conformation at the carboxy-terminal domain, thereby affecting subsequent signalling events (Adams *et al.*, 2011; Anavi-Goffer *et al.*, 2007).

Palmitoylation-regulating enzymes are still poorly characterised, and have been mainly researched using model organisms (Lobo *et al.*, 2002). However this approach has allowed identification of a family of proteins with a conserved aspartate-histidine-histidine-cysteine (DHHC) cysteine-rich domain, which is considered to be an active site of palmitoyl acyltransferases (PAT) (Mitchell *et al.*, 2006). PAT enzymes are thought to catalyse the thioester linkage of PA to proteins. Currently, 25 DHHC genes have been identified in humans, compared to seven in yeast (Rocks *et al.*, 2010). Human DHHC PATs were shown to be localised in various cellular compartments in a tissue-dependent manner (Rocks *et al.*, 2010). For instance, DHHC2 and DHHC9 are reportedly expressed in ER/Golgi, DHHC1 and DHHC6-in ER and DHHC7 and DHHC8 in the Golgi. However a membrane-bound localisation for some PATs has also been described, namely DHHC5, DHHC20 and DHHC21

(Rocks *et al.*, 2010). A variety of localisation profiles potentially aids the protein sorting function of PAT enzymes. Apart from the DHHC motif being crucial for the palmitoyl transferase activity, the substrate specificity of these enzymes remains largely unknown. For instance, hyper-variable domains of Ras proteins require palmitoylation for membrane association (Choy *et al.*, 1999). It has been shown that these domains are palmitoylated in different ways to ensure specific localisation of Ras isoforms to distinct cellular compartments (Laude and Prior, 2008). Therefore much remains to be understood about specific actions of various DHHC PAT enzymes.

As palmitoylation is a dynamic and reversible process, de-palmitoylation events which remove the palmitate group from palmitoylated proteins are also catalysed by enzymes. As with PAT enzymes, de-palmitoylating thioeserases remain to be fully characterised, and maybe even discovered. Nonetheless, acyl protein thioesterase-1 (APT-1) and palmitoyl-protein thiosterase-1 (PPT1) have been shown to de-palmitoylate proteins *in vitro* (Zeidman *et al.*, 2009). The latter, however, is believed to act predominantly on proteins destined for degradation, as it was found to be a lysosomal enzyme (Verkruyse and Hofmann, 1996). On the other hand, APT-1 has been described to localise mainly in the cytoplasm (Duncan and Gilman, 1998), and its substrates include proteins such as Ras (Xu *et al.*, 2012) and eNOS (Yeh *et al.*, 1999). A homolog of APT-1, named APT-2, has been identified and shown to have thioesterase qualities. However, it has been found mainly in the lysosome, and has substrate specificity for palmitoyl-CoA instead of proteins (Soyombo and Hofmann, 1997).

5.1.2 Methods of studying palmitoylation enzymes

In order to identify protein palmitoylation sites, site-directed mutagenesis of candidate domains is predominantly used. However investigating specific enzymes involved in the palmitoylation of specific proteins is more complex. Given the relatively recent identification of a large

number of human DHHC PAT enzymes, antibodies against them are usually generic, targeting the conserved domains of the proteins. As DHHC enzymes get increasingly better characterised, genetic manipulation of individual PAT enzymes is emerging as a specific tool for studying the enzymes. However, so far, pre-designed siRNAs against human PATs have not always proven to be efficient or potent (Tian *et al.*, 2010). Until recently, generic, non-specific pharmacological palmitoylation inhibitors were also used as tools to study palmitoylation. One of these is a palmitate analogue, 2-bromopalmitate (2-BP), which has been widely used for palmitoylation inhibition of proteins such as Rho family members and Ras (Webb *et al.*, 2000). More recently, non-lipid small molecule inhibitors of PAT enzymes have been identified (Ducker *et al.*, 2006); with five chemotypes displaying anti-PAT activity (**Fig. 5.1**). Compounds I-IV are reportedly specific for PATs that act on farnesylated proteins, while compound V inhibits a class of PATs that recognises myristoylated proteins (Ducker *et al.*, 2006). Therefore such inhibitors, which (unlike 2-BP) inhibit specific classes of PAT proteins, can be utilised as tools to narrow down the contribution of individual PAT classes to specific protein palmitoylation events.

On the opposite end of the scale is the goal of pharmacologically targeting de-palmitoylation events. Dekker and colleagues have developed a small molecule inhibitor of APT-1, called Palmostatin B, which demonstrated specific activity against APT-1 and disrupted the normal localisation of H-Ras (Dekker *et al.*, 2010), N- and K-Ras (Xu *et al.*, 2012). To date, this is the only inhibitor molecule targeted against thioesterase activity. Thus the functional effects and molecular events associated with inhibition of thioesterase enzymes in different cell types remain to be characterised.

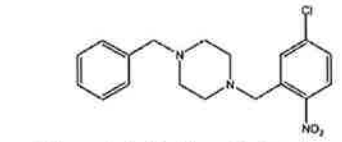

Compound I

1-Benzyl-4-(5-chloro-2-nitro-benzyl)-piperazine

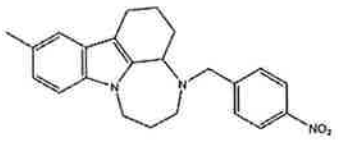

Compound II

11-Methyl-4-(4-nitro-benzyl)-1,2,3,3a,4,5,6,7-octahydro-[1,4]diazepino[3,2,1-*jk*]carbazole

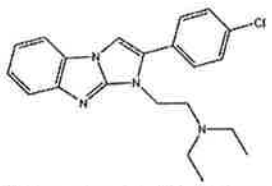

Compound III

{2-[2-(4-Chloro-phenyl)-1,3a,8-triaza-cyclopenta[*a*]inden-1-yl]-ethyl}-diethyl-amine

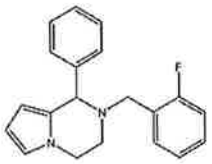

Compound IV

2-(2-Fluoro-benzyl)-1-phenyl-1,2,3,4-tetrahydro-pyrrolo[1,2-*a*]pyrazine

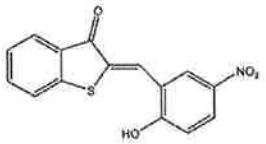

Compound V

2-(2-Hydroxy-5-nitro-benzylidene)-benzo[*b*]thiophen-3-one

Figure 5.1. Structures and chemical names of the small molecule PAT inhibitors. Inhibitor names that were used in this thesis are displayed on the right. Chemical structures were adapted from (Ducker *et al.*, 2006).

5.1.3. Human mammary stem cells

In a normal physiological setting, luminal epithelial and myoepithelial cells are formed from mammary progenitor cells located on the basal side of mammary ducts. A basement membrane separates the epithelial layers from the fatty stromal surroundings (Richert *et al.*, 2000). Mammary gland development and the role of stem cells in this process have been mainly studied in murine models, and have provided comprehensive models applicable to humans (Booth *et al.*, 2008). Epithelial and myoepithelial cells can be distinguished by expression of cell type-specific cytoskeletal markers. Luminal epithelial cells are characterised by expression of cytokeratins -8, -18 and -19, while α-smooth muscle actin (SMA) and cytokeratin-14 are associated with basal myoepithelial cells (Smalley *et al.*, 1998). Both of these cell types arise from progenitor cell populations, which have a pre-differentiated, limited self-renewal potential (Smith and Boulanger, 2002). In contrast, stem cells are thought to have unlimited self-renewal and differentiating potential.

Human breast surface markers include MUC-1 (luminal epithelium), ESA (epithelium) and CALLA (basal/myoepithelial marker) (Molyneux *et al.*, 2007). However definitive breast progenitor cell markers remain controversial, with several different combinations being described to date. Luminal and myoepithelial cell populations have been flow cytometrically isolated using EMA and CALLA, respectively (O'Hare *et al.*, 1991); while other studies have used the same markers to assess progenitor properties of mammary cells (Clayton *et al.*, 2004). The latter study identified cells that were double-negative (DN) or double-positive (DP) for these markers, which could generate colonies containing both luminal and myoepithelial cells. However DN cells formed predominantly luminal colonies. Donatello *et al.* have recently adopted a similar approach, where progenitor populations were isolated from breast primary cells and cell lines using EpCAM (epithelial) and CALLA (myoepithelial) markers (Donatello *et al.*, 2011). This led to the characterisation of four main populations, in which an increase in DN cells was

associated with high grade tumours, HER-2 positivity or ER-negativity in primary cultures, as well as a more invasive phenotype in cell lines.

Studying stem cells in humans is challenging due to the paucity of *in vivo* models. Cleared fat pad transplantation assays, where stem cell populations are able to re-populate the mouse fat pad, are to date considered the "gold standard" for stem cell studies (Smalley *et al.*, 2012). *In vitro*, the ability of cells to grow in suspension and form mammospheres has been best linked to enrichment in stem cells (Charafe-Jauffret *et al.*, 2009). This technique is based on the ability of cells to resist anoikis in serum-free conditions, and has been instrumental in implicating developmental pathways such as Hedgehog and Notch in self-renewal and differentiation of mammary stem cells (Dontu *et al.*, 2004; Liu *et al.*, 2006). Specifically, stimulation of Notch or Hedgehog pathways has been shown to promote mammosphere formation by mammary cells. Furthermore, Notch signalling affected proliferation and branching morphogenesis when mammospheres were placed in differentiating cultures (Dontu *et al.*, 2004). However, this technique has functional limitations, and a link between this system and *in vivo* functional transplantation results has yet to be shown (Smalley *et al.*, 2012).

5.1.4. Breast cancer stem cells

Cancer stem cells were originally described in leukaemia, when a population of cells demonstrated self-renewal abilities (Bonnet and Dick, 1997). These cells had a $CD34^+/CD38^-$ stem cell marker signature. Subsequent studies have identified cells with similar "stem" behaviour in solid tumours such as brain, colon, pancreas and breast (Dontu *et al.*, 2003). In 2003, Al-Hajj and colleagues discovered a population of highly tumourigenic breast cancer cells in patient breast primary tumours, bearing an $EpCAM^+/CD44^+/CD24^-$ surface protein signature (Al-Hajj *et al.*, 2003). Subsequently, gene expression profiling of putative stem cell populations in normal and breast tumours characterised stem cells as $CD44^+/CD24^-/PROCR^+/CALLA^-$ (Shipitsin *et al.*,

2007). Additional markers of cancer stem cells include $CD49f^{+}$, $MUC1^{-}$, $ALDH1^{+}$ and $CD133^{+}$ (Korkaya *et al.*, 2011). However to this day there is no standardised definition of a marker signature that unequivocally denotes cancer stem cells. Nor is there a uniform term that defines a cancer stem cell. For the sake of clarity, these cancer cell populations will be referred to as stem/progenitor cell populations in this thesis. It is interesting to note that expression of CD44 in conjunction with lack of CD24 has been most frequently used to define cancer stem/progenitor cells throughout the literature. However there is no information on the role of CD44 in these putative tumour-initiating cells, or indeed the functional relevance of its palmitoylation status or affiliation with lipid raft domains. Our laboratory has previously isolated populations of $CALLA^{+}/EpCAM^{+}$ (double-positive, DP), $CALLA^{-}/EpCAM^{-}$ (double-negative, DN), $CALLA^{-}/EpCAM^{+}$ (EpCAM) and $CALLA^{+}/EpCAM^{-}$ (CALLA) cell populations across a panel of breast primary cultures and cell lines (Donatello *et al.*, 2011). The DN and DP populations displayed phenotypical and functional similarities of stem/progenitor cells. In this chapter, we therefore sought to investigate the contribution of CD44 palmitoylation and raft localisation to this putative progenitor phenotype, alongside functional studies in patient primary cultures derived from breast tumours of varying aggressiveness.

5.2 Aims

In the previous chapter we established a novel correlation between CD44 palmitoylation status and the migration potential of breast cells (Babina *et al.*, manuscript submitted). Thus we hypothesise that CD44 palmitoylation may represent a novel pharmacological target to reduce cancer cell motility, an important functional behaviour associated with tumour progression. Furthermore, since CD44 positivity is considered a major marker of cancer stem cells (putative tumour-initiating cells thought to play a role in tumour resistance to chemotherapy (Smalley *et al.*, 2012), in the present chapter we therefore set out to investigate the following:

1. To determine the potential of pharmacological palmitoylating and de-palmitoylating enzyme inhibitors to modulate CD44 raft localisation and palmitoylation;

2. To investigate potential correlations between palmitoylation-regulating enzymes, breast cancer cell migration and breast cancer patient survival;

3. To assess CD44 localisation in lipid rafts and palmitoylation in putative progenitor populations and primary breast cancer cell lines and correlate it with functional differences of those cells.

5.3 Results

5.3.1 Global inhibition of palmitoylation enzymes affects CD44 raft localisation

Having shown in the previous chapter that *in vitro* modulation of CD44 palmitoylation status directly alters cell migration, we sought to examine the reverse - whether migration itself might drive alterations in CD44 palmitoylation status. Direct measurement of palmitoylated versus total CD44 revealed statistically significant reductions in levels of palmitoylated CD44 over a migration time-course (**Fig. 5.2**).

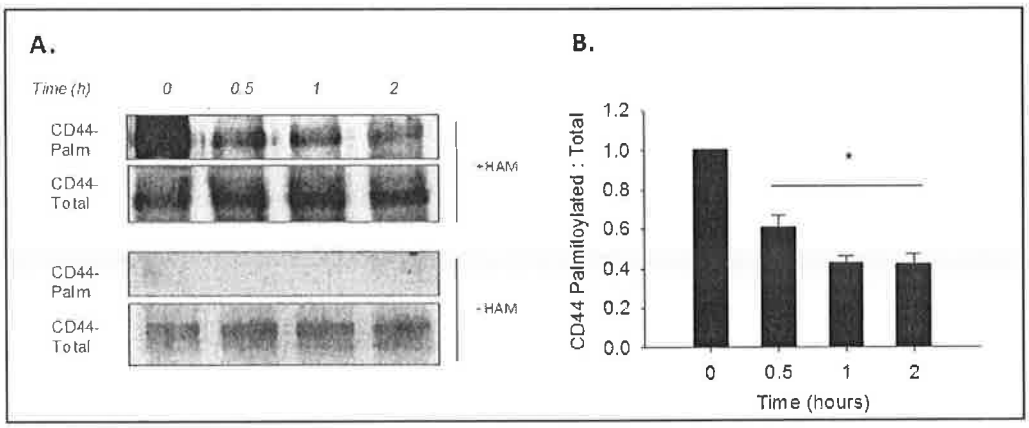

Figure 5.2. CD44 palmitoylation is decreased over time during MDA-MB-231 migration. A. Confluent MDA-MB-231 cells were scratch-wounded and allowed to migrate in serum-free medium for the indicated time-points. CD44 immunprecipitates from each time point were probed for palmitoylated CD44 by BMCC assay. Palmitoylated CD44 was detected using streptavidin (CD44-Palm), and total CD44 using a CD44 primary antibody (CD44-Total). The absence of HAM treatment was a negative control for palmitoylated CD44. CD44-Palm levels decreased over the migration timecourse. **B.** Quantification of CD44-Palm as a ratio of CD44-Total revealed significant time-dependent reductions during migration. *Error bars=SEM, n=3 experiments, *p<0.05, by 2-tailed unpaired Student's t-test.*

This suggested that increases in CD44 palmitoylation over the course of migration might reflect temporally-increased activity / expression of palmitoylating enzymes, or indeed temporally-decreased activity / expression of de-palmitoylating enzymes. However our ability to test this was hampered by a lack of commercially-available assays to measure activity of specific palmitoylating/de-palmitoylating enzymes, or even antibodies to perform expressional analysis for the same enzymes. Therefore we asked a broader question, whether global changes in expression of palmitoylating or de-palmitoylating enzymes might predict disease progression parameters in cancer patients.

Using an online survival analysis tool of published Affymetrix micro-array data sets in breast cancer patients (Gyorffy *et al.*, 2010), we first assessed expression of the DHHC family of pro-palmitoylation palmitoyl acyltransferase (PAT) enzymes. As 23 members of this family have been identified to date (Linder and Deschenes, 2007), a panel of the known genes was tested. As shown in Kaplan-Meier plots in **Fig. 5.3A**, statistically-significant correlations were observed between recurrence-free survival and high gene expression of DHHC3 (probe 218077_s_at), DHHC6 (probe 218249_at), DHHC7 (probe 218606_at), DHHC8 (probe 222274_at). In contrast, high gene expression of DHHC13 (probe 222274_at) and DHHC14 (probe 219247_s_at) was associated with reduced recurrence-free survival in the same patients.

The same survival analysis tool was also used to assess the impact of expressional changes in the de-palmitoylating enzymes APT-1 (probe 203007_x_at) and APT-2 (probe 215566_x_at). High expression of the de-palmitoylating thioesterase enzyme APT-1 significantly correlated with poorer breast cancer recurrence-free survival (**Fig. 5.3B**). Conversely, high expression of APT-2 had a more beneficial outcome, correlating with better recurrence-free survival of the same patients.

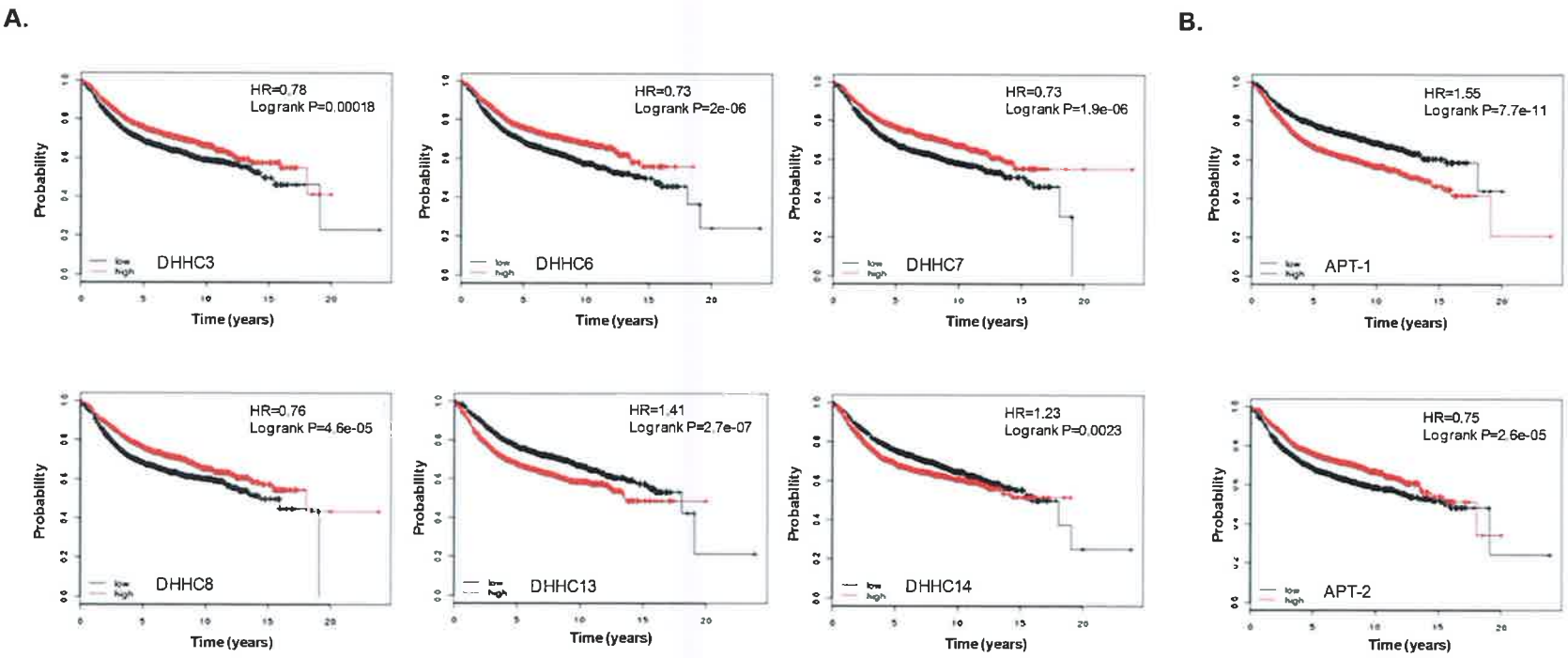

Figure 5.3. Better recurrence-free survival broadly correlates with high expression of palmitoylating enzymes. Recurrence-free survival plots of breast cancer patients were generated from previously-published gene expression data sets. **(A.)** High expression (red lines) of PAT enzymes DHHC3, 6, 7 and 8 correlated with better recurrence-free survival, while high expression (red lines) of DHHC13 and 14 correlated with poorer survival. **(B.)** High expression (red) of the de-palmitoylating enzyme APT-1 was strongly correlated with poor breast cancer patient survival. In contrast, high expression (red) of its homologue, APT-2, correlated with better recurrence-free survival. Kaplan-Meier analysis was performed using gene expression information on 2,627 breast cancer patients, with graphs, hazard risk (HR) and logrank *p* values generated by the online software.

These observations of statistically-relevant relationships between patient survival and expression of palmitoylation-regulating enzymes led us to question whether pharmacological interference with enzyme activity could alter CD44 localisation relative to lipid rafts, and, in turn, cell migration. As tools we used chemical PAT inhibitors with reported substrate specificity (Ducker *et al.*, 2006), and in parallel targeted the de-palmitoylation activity of APT-1 for downregulation with Palmostatin B. Taking the opposite pharmacological approach, we also used exogenous addition of palmitic acid (PA) as a tool to non-specifically promote protein palmitoylation. Under all these conditions, immunofluorescence/confocal microscopy was used to compare potential co-localisation between CD44 and the lipid raft marker flotillin-1 in non-migrating and migrating MDA-MB-231 cells (**Fig. 5.4**).

In contrast to our expectations, pre-treatment with PA or the PAT inhibitor compounds III and V (100μM / 1h) increased CD44 co-localisation with flotillin-1 in non-migrating cells, compared to the DMSO control. Conversely, CD44/flotillin-1 co-localisation was reduced in cells pre-treated with Palmostatin B compared to DMSO and other treatments. These results were the opposite of what we anticipated, with each treatment group exhibiting contrasting effects. After 2 hours of migration the co-localisation of both proteins in PA and inhibitors III and V-pre-treated cells remained higher than that of DMSO-treated cells, and remained similar in Palmostatin B-treated cells. Interestingly, treatment with PAT inhibitors, and to a lesser extent PA, appeared to enhance the membranous localisation of flotillin-1 in both non-migrating and migrating cells. Pixel overlap quantification of the green and red channels revealed a statistically significant increase in CD44 localisation with flotillin-1 in compounds III- and V-pre-treated conditions versus DMSO controls in non-migrating cells (**Fig. 5.4, graph**). Additionally, pre-treatment with PAT inhibitors III and V resulted in significant co-localisation of CD44 and flotillin-1 during MDA-MB-231 cell migration compared to the DMSO control and Palmostatin B-treated cells.

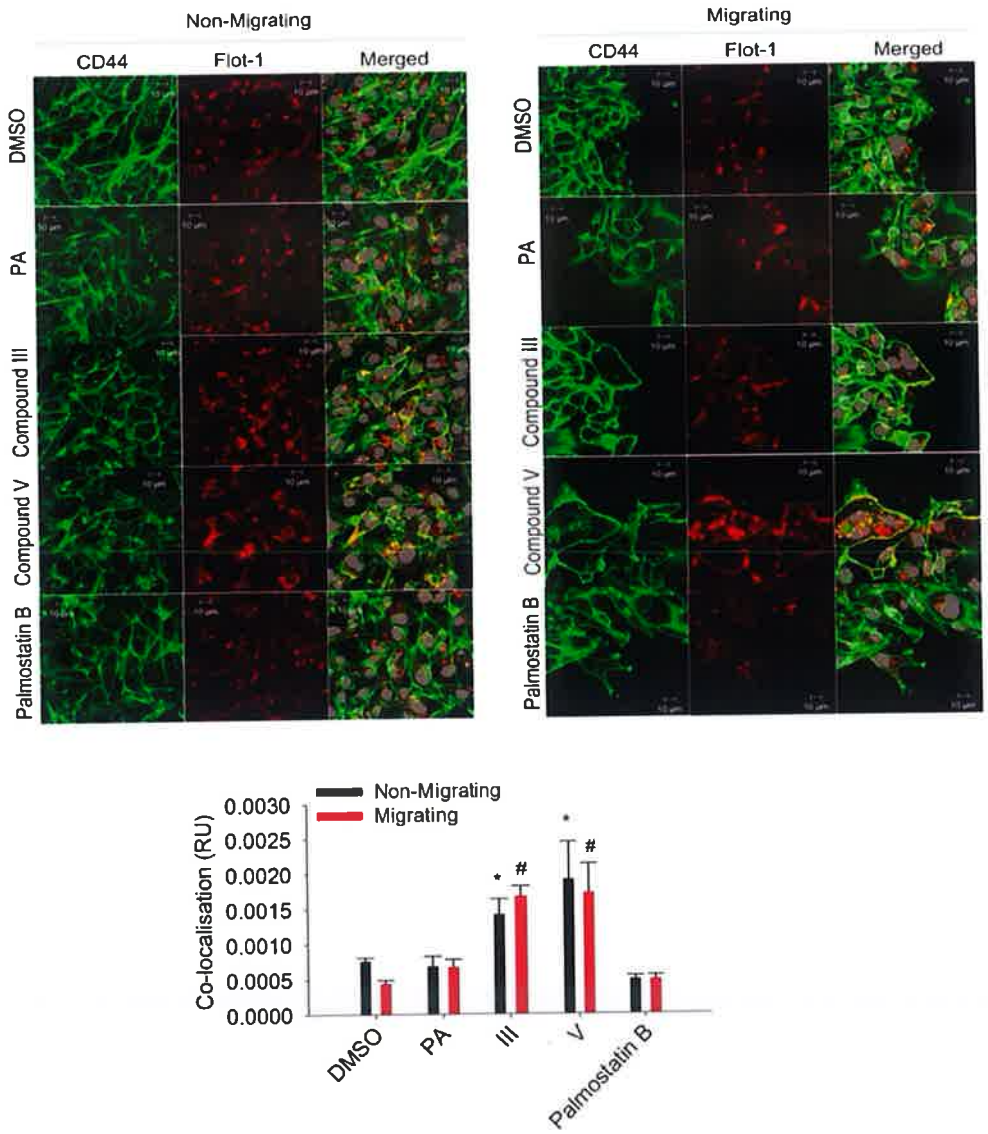

Figure 5.4 Inhibition of PAT enzymes increases CD44 co-localisation with flotillin-1. Non-migrating and migrating (2hr) MDA-MB-231 cells, pre-treated with PA, PAT inhibitors compounds III and V or APT-1 inhibitor Palmostatin B (all 100μM), were stained for CD44 (green) and flotillin-1 (Flot-1, red). Nuclei were stained with DAPI and are shown in grey. Pre-treatment with both PAT inhibitors resulted in increased co-localisation of CD44 and Flot-1 in both conditions relative to DMSO control, while Palmostatin B pre-treated cells had similar co-localisation levels as migrating DMSO control conditions. *$p<0.05$ *vs non-migrating DMSO;* $^{\#}p<0.05$ *vs migrating DMSO, all by 2-tailed unpaired Student's t-test.*

CD44 localisation in lipid raft domains during the migration of MDA-MB-231 cells pre-treated with PAT inhibitors or PA was further analysed by Triton X-100 insolubility preparations. Migrating MDA-MB-231 cells pre-treated for 1 hour with DMSO, PA, compound III or compound V (100μM) were tested for CD44 affiliation with detergent-insoluble (raft-enriched) and detergent-soluble (non-raft) pools. Mirroring the unexpected immunofluorescence results, PAT inhibitor V unexpectedly induced an increase in CD44 affiliation with raft-containing domains compared to all other conditions, as determined by western blot analysis and quantitatively confirmed by calculation of the Triton X-100-insoluble/-soluble affiliation ratio (**Fig. 5.5A**).

In order to examine if this change in localisation reflected alterations in CD44 palmitoylation status, we measured palmitoylated CD44 using an acyl-biotin exchange approach. Samples not treated with HAM (HAM-) and IgG immunoprecipitations (IP: IgG) were used as internal controls. Compared to the DMSO control, MDA-MB-231 cells pre-treated with PAT inhibitors (100μM / 1 hour) had increased levels of palmitoylated CD44 (CD44-Palm). (**Fig. 5.5B**). Quantification of CD44-Palm relative to total CD44 revealed statistically significant increases in CD44 palmitoylation following treatment with inhibitors III or V (**Fig. 5.5B, graph**).

Having observed intriguing results using palmitoylation enzyme inhibitors, we next analysed whether de-palmitoylating enzyme inhibition had the opposite effects on cell migration and CD44 raft affiliation. To this end, migrating MDA-MB-231 cells were pre-treated for 1 hour with different concentrations of the APT-1 inhibitor Palmostatin B and analysed in the same manner. Exposure to 25, 50 or 100μM Palmostatin B unexpectedly evoked a reduced affiliation of CD44 with lipid raft-containing domains (**Fig. 5.5C**). Calculation of CD44 affiliation with raft-enriched domains confirmed a significant decrease in CD44 association with lipid raft domains under these conditions. To test whether this decrease was associated with reduced CD44

palmitoylation, the acyl-biotin exchange assay was used to compare biotin-labelled, palmitoylated CD44 (CD44-Palm) to total CD44. A decrease in palmitoylated CD44 was observed in MDA-MB-231 cells pre-treated with Palmostatin B, compared to the DMSO control (**Fig. 5.5D**). When palmitoylated CD44 was expressed as a ratio of total CD44 relative to the DMSO control, significant reductions in palmitoylated CD44 were confirmed in migrating MDA-MB-231 cells pre-treated with 50 or 100μM Palmostatin B (**Fig. 5.5D, graph**). Taken together, our results indicate that palmitoylation and de-palmitoylation enzymes regulate the palmitoylation status of CD44 and its affiliation with lipid rafts in a complex manner.

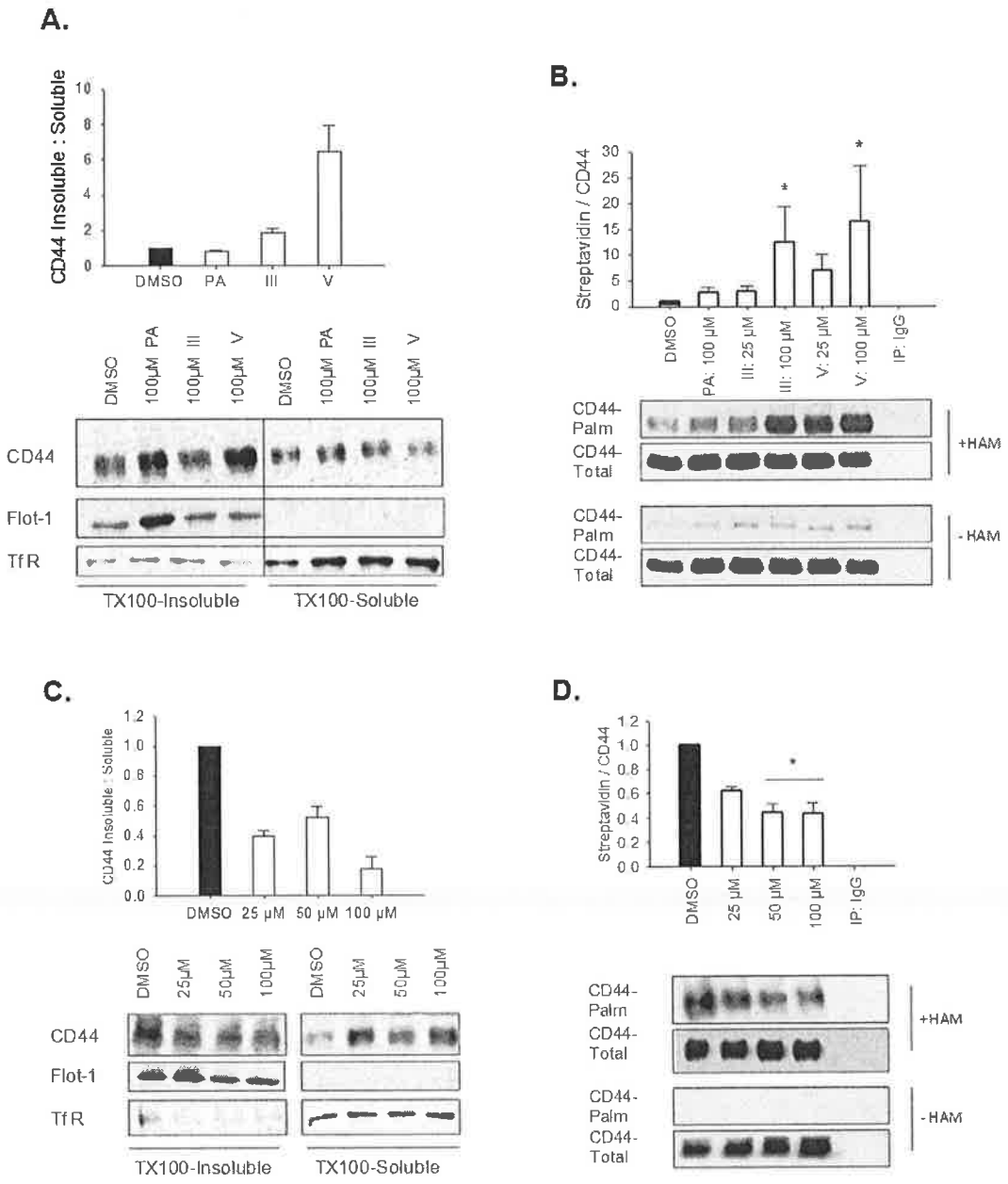
A.
CD44 Insoluble : Soluble
DMSO
PA
III
V
DMSO
100µM PA
100µM III
100µM V
CD44
Flot-1
TfR
TX100-Insoluble
TX100-Soluble
B.
Streptavidin / CD44
DMSO
PA: 100 µM
III: 25 µM
III: 100 µM
V: 25 µM
V: 100 µM
IP: IgG
CD44-Palm
CD44-Total
+HAM
-HAM
C.
CD44 Insoluble : Soluble
DMSO
25 µM
50 µM
100 µM
CD44
Flot-1
TfR
TX100-Insoluble
TX100-Soluble
D.
Streptavidin / CD44
DMSO
25 µM
50 µM
100 µM
IP: IgG
CD44-Palm
CD44-Total
+HAM
-HAM

Figure 5.5 Effects of palmitoylation and de-palmitoylation inhibitors on CD44 palmitoylation and raft localisation. MDA-MB-231 cells pre-treated with the indicated concentrations of PA, PAT inhibitors (III and V) and an APT-1 inhibitor (Palmostatin B) were stimulated to migrate for 2 hours and then subjected to Triton X-100 insolubility preparations and acyl-biotin exchange assays. (**A.**) Detergent-insoluble and –soluble pools were analysed for the presence of CD44 relative to lipid raft and non-raft markers flotillin-1 (Flot-1) and transferrin receptor (Tf R) respectively. CD44 affiliation with the lipid raft-enriched detergent-insoluble pool was increased in compound V-treated cells relative to DMSO control cells. This was confirmed by calculation of the numerical Insoluble:Soluble ratio, expressed relative to the DMSO control (*Error bars=STDEV; n=2 experiments*). (**B.**) Palmitoylated CD44 (CD44-Palm) was measured in migrating (2hr) MDA-MB-231 cells and found to increase in cells treated with the PAT inhibitors III or V. Calculation of CD44-Palm relative to CD44-Total (expressed relative to the DMSO condition) demonstrated a significant increase in palmitoylated CD44 relative to DMSO control upon PAT inhibition (*Error bars=SEM; *p<0.05 by unpaired 2-tailed Student's t-test; n=3 experiments*). (**C.**) Triton X-100 insolubility assays in MDA-MB-231 cells pre-treated with the indicated concentrations of Palmostatin B revealed a decreased association of CD44 with the putative raft-enriched pool, paralleled by an increased recovery of CD44 from non-raft-enriched domains. Calculation of the CD44 Insoluble:Soluble ratio confirmed decreased association of CD44 with raft domains in Palmostatin-treated cells (*Error bars=STDEV, n=2 experiments*). (**D.**) Palmostatin B-treated cells also demonstrated decreased levels of palmitoylated CD44, normalised against total CD44, and expressed relative to the DMSO control. Numerically, 50μM and 100μM Palmostatin B significantly reduced levels of palmitoylated CD44 in MDA-MB-231 cells (*Error bars=SEM, *p<0.05 by unpaired 2-tailed Student's t-test; n=3 experiments*).

5.3.2 Functional effects of chemical palmitoylation and de-palmitoylation inhibition

Having shown that PAT and APT-1 inhibitors regulate CD44 palmitoylation status and its affiliation with lipid rafts, we next investigated whether this translated into a functional impact on breast cancer cell migration. MDA-MB-231 cells pre-treated for 1 hour with PA or PAT inhibitors III and V (100μM) were scratch-wounded and wound closure was measured over 8 hours (**Fig. 5.6A**). PA induced a small but statistically–insignificant reduction in cell migration relative to DMSO control-treated cells. PAT inhibitor III significantly inhibited wound closure after 8 hours of migration relative to the DMSO control, whilst PAT inhibitor V completely abolished cell migration at all time points. These effects were consistent with the noted enhancements in palmitoylated, raft-affiliated CD44 in PAT inhibitor-treated cells. Effects of inhibiting the de-palmitoylating enzyme APT-1 were also investigated, using MDA-MB-231 cells pre-treated for 1 hour with Palmostatin B (25, 50 and 100μM) prior to scratch-wound migration assays. All concentrations significantly increased cell migration compared to the DMSO control (**Fig. 5.6B**), which was again consistent with Palmostatin-induced reductions in the palmitoylation and lipid raft affiliation of CD44.

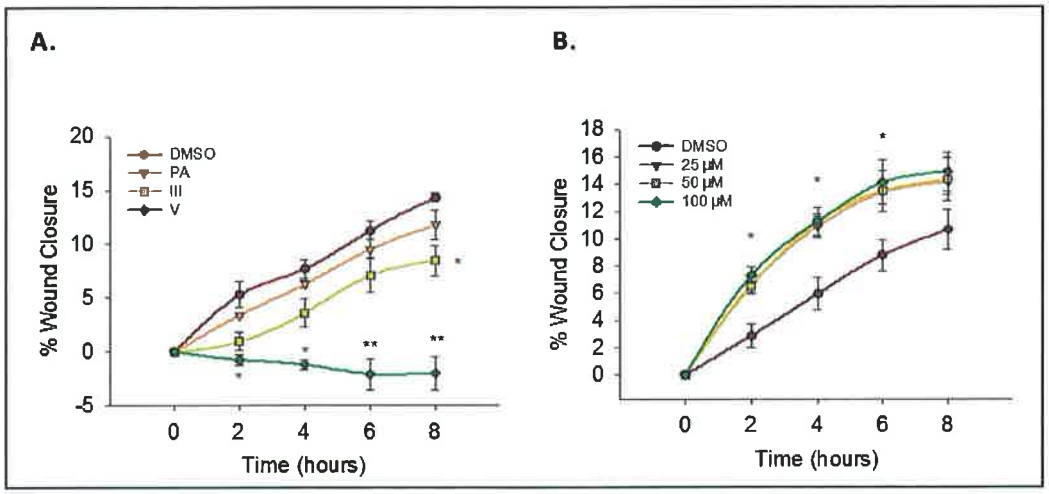

Figure 5.6 Inhibition of PAT enzymes and APT-1 have opposing effects on MDA-MB-231 cell migration. (**A.**) Confluent MDA-MB-231 cells were pre-treated for 1 hour with PA or PAT inhibitors III and V (100µM), and subjected to scratch-wound migration assays. PAT inhibitor III reduced migration relative to the DMSO control after 8 hours, while compound V abolished cell migration. (**B.**) MDA-MB-231 cells were pre-treated for 1 hour with the indicated concentrations of the APT-1 inhibitor Palmostatin B, and subjected to migration assays. All concentrations of Palmostatin B increased cell migration after as early as 2 hours, although not in a concentration-dependent manner. *Error bars=SEM; *p<0.05; **p<0.01 by 2-way ANOVA; n=3 experiments.*

In order to estimate longer-term functional effects of the chemical inhibitors, we also examined the effects of pharmacological PAT and APT-1 inhibition on breast cancer cell proliferation. MCF-10a and MDA-MB-231 cells were grown in the presence of PA, compounds III and V or Palmostatin B (50 and 100μM). Proliferation was measured daily for 3 days and expressed as optical density relative to that of cells prior to treatment application (Day 0). In MDA-MB-231 cells, 100μM PA reduced proliferation relative to the DMSO control after 2 days (**Fig. 5.7A**). Both PAT inhibitors also significantly reduced proliferation in a concentration-dependent manner (**Fig. 5.7B, C**). In contrast, Palmostatin B did not affect the proliferation of MDA-MB-231 cells (**Fig. 5.7D**). In MCF-10a cells, PA treatment did not alter cell proliferation compared to the DMSO control (**Fig. 5.7E**). Treatment with PAT inhibitor III (100μM) significantly reduced the number of viable cells after 2 days, relative to DMSO control conditions (**Fig. 5.7F**). PAT inhibitor V significantly reduced MCF-10a proliferation compared to controls, in a concentration-dependent manner (**Fig. 5.7G**). Palmostatin B treatment significantly reduced cell proliferation relative to controls, but only at the higher concentration of 100μM (**Fig. 5.7H**).

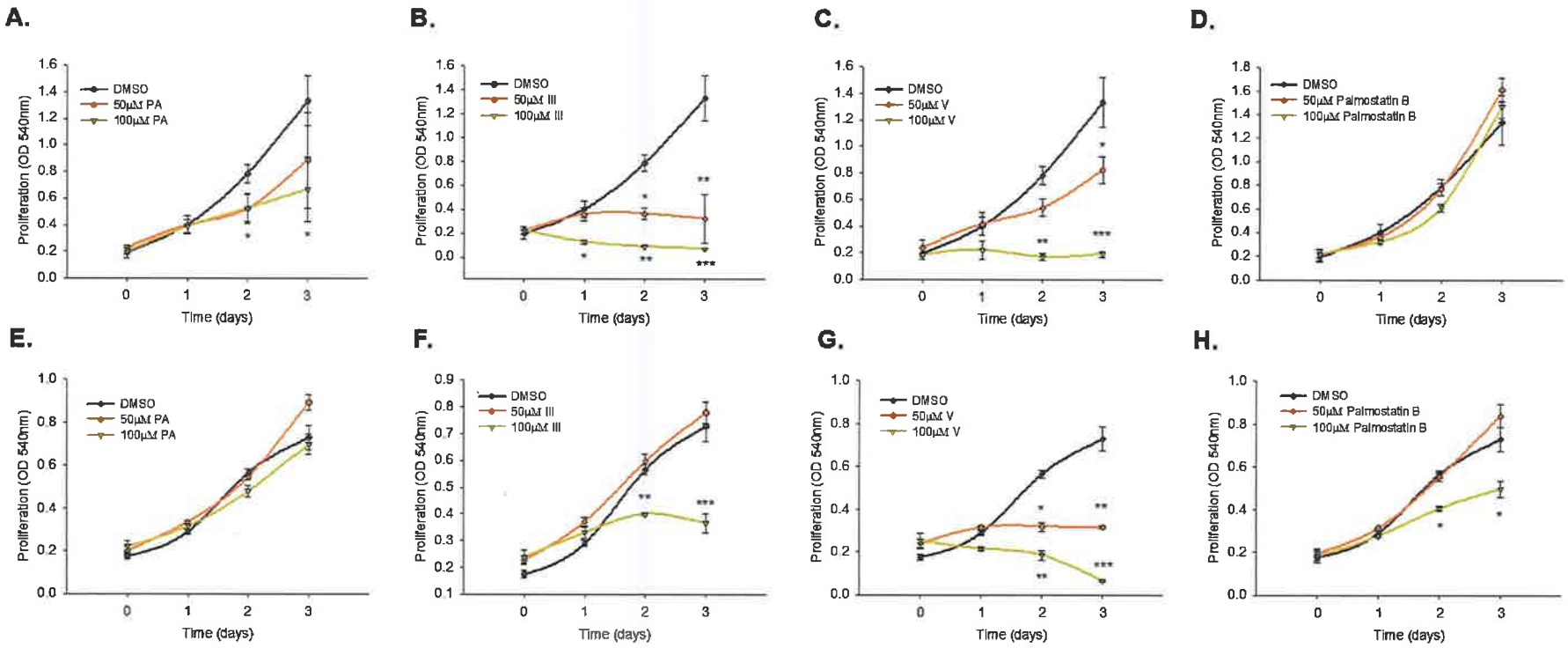

Figure 5.7 Effects of PAT and APT-1 inhibitors on proliferation of MDA-MB-231 and MCF-10a cells. MDA-MB-231 (**A-D**) and MCF-10a cells (**E-F**) were grown in the presence of 50μM and 100μM of the indicated treatments for 3 days, whereupon MTT assays were used to estimate the long-term effects of chemical interference with palmitoylation on proliferation. All values were

normalised to Day 0 before the treatment was applied. (**A.**) Palmitic acid (PA) at 100μM decreased MDA-MB-231 proliferation relative to DMSO; (**B,C.**) PAT inhibitors III and V reduced proliferation in concentration-dependent manner, while (**D.**) APT-1 inhibitor Palmostatin B did not have any long-term effect on proliferation of MDA-MB-231 cells. (**E.**) In MCF-10a cells, PA did not affect proliferation, (**F.**) only 100μM of PAT inhibitor III reduced proliferation of these cells, (**G.**) PAT inhibitor V demonstrated concentration-depended proliferation inhibition, while (**H.**) 100μM of Palmostatin B exerted anti-proliferative effects in MCF-10a cells. *Error bars=SEM, *p<0.05; **p<0.01; ***p<0.001 by 2-way ANOVA; n=3 experiments.*

Furthermore, we assessed colony formation efficiency of MCF-10a and MDA-MB-231 cells grown in the presence of PA, compounds III and V or Palmostatin B (50μM). MDA-MB-231 cells did not form colonies as readily as MCF-10a cells (**Fig. 5.8A**), potentially due to their propensity to act as individual mesenchymal-like cells. In both cell lines PAT inhibition resulted in almost complete abolition of colony formation. Colonies were manually counted and expressed relative to the original number seeded in order to calculate colony-forming efficiency. MDA-MB-231 cells treated with PA formed fewer colonies compared to the DMSO controls (**Fig. 5.8B**). However, PAT inhibitors virtually abrogated the colony-forming ability of MDA-MB-231 cells. Palmostatin B did not have a notable effect on colony formation in these cells. PAT inhibitors and Palmostatin B also reduced colony-forming ability in MCF-10a cells (**Fig. 5.8C**).

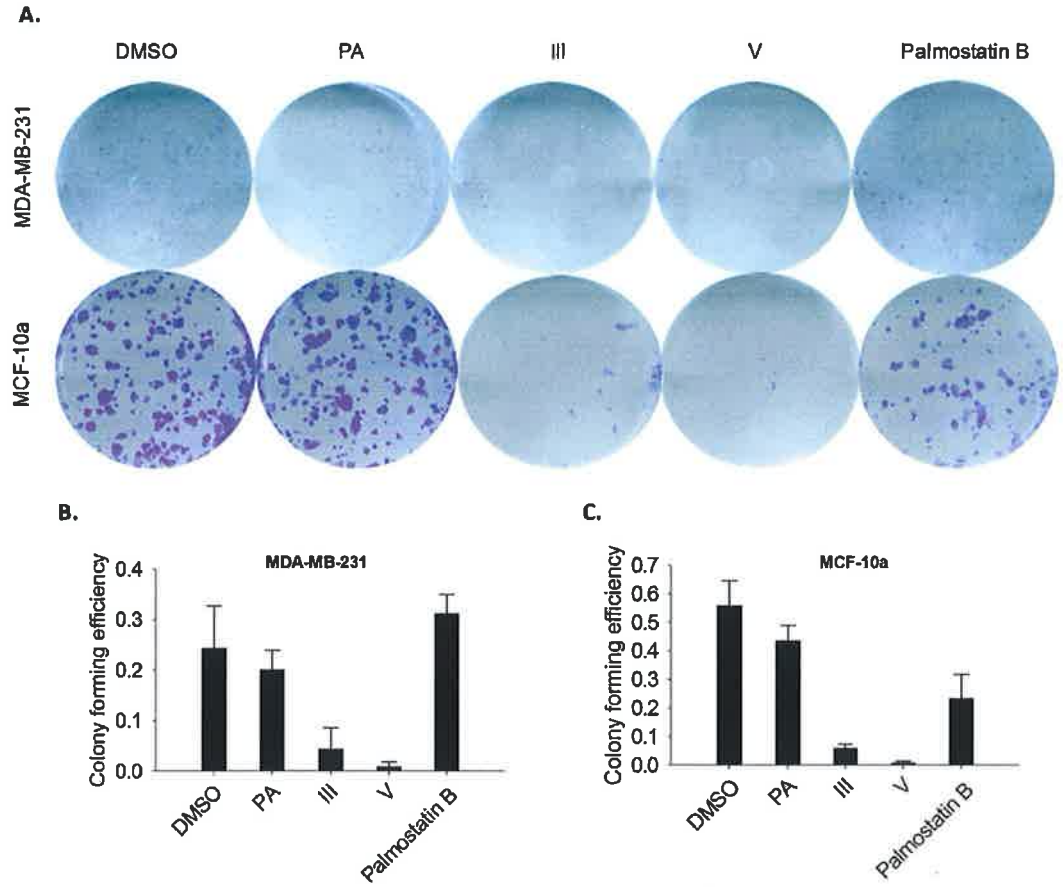

Figure 5.8 Effects of PAT and APT-1 inhibitors on colony-forming abilities of MDA-MB-231 and MCF-10a cells. MDA-MB-231 or MCF-10a cells in a single-cell suspension of 200 cells were seeded in 6 well plates and grown in the presence of the indicated treatments (100μM) for 7 days to form colonies. (**A.**) Colonies were stained with crystal violet, and representative wells of both cell lines photographed. Manually-counted colonies were then expressed relative to the original number of cells seeded to calculate colony forming efficiency of MDA-MB-231 (**B.**) and MCF-10a (**C.**) cells. In both cell lines, PAT inhibitors III and V completely abolished colony formation, while the APT-1 inhibitor Palmostatin B had no effect on colony formation in MDA-MB-231 cells and only slightly reduced colony numbers in MCF-10a cells. *Error bars=STDEV, n=2 experiments.*

Finally, we examined the potential of palmitoylation-modulating enzyme inhibitors to influence MDA-MB-231 survival in suspension and mammosphere formation, which is considered a model for enrichment in early progenitor/stem cells (Charafe-Jauffret *et al.*, 2009). Cells were seeded in ultra-low adherence plates and allowed to grow in serum-free medium in the presence of PA, PAT inhibitors III and V or Palmostatin B (100μM). After 7 days, mammospheres were counted using phase-contrast microscopy (**Fig. 5.9**). MDA-MB-231 cells formed low numbers of mammospheres in the presence of DMSO and PA, however PAT and APT-1 inhibition with compounds III / V or Palmostatin B (respectively) prevented mammosphere formation. Collectively, the above results indicate that palmitoylation-regulating enzymes are important for colony formation and anchorage-independent growth in breast cells.

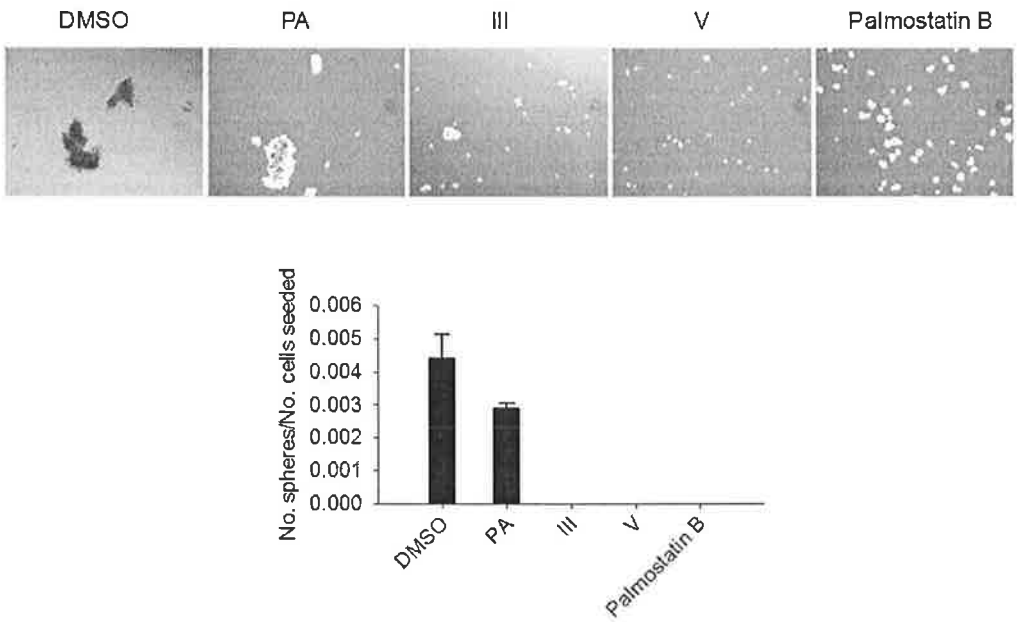

Figure 5.9 PAT or APT-1 inhibition abolish mammosphere-forming ability of MDA-MB-231 cells. $1x10^4$ cells were seeded in serum-free medium containing DMSO or 100μM of each indicated treatment and allowed to grow in ultra-low attachment plates for 7 days. Mammospheres were photographed, manually counted and expressed relative to the original number of cells seeded. While PA reduced the low levels of mammosphere formation by MDA-MB-231 cells, PAT and APT-1 inhibitors completely abolished mammosphere-forming efficiency of this cell line. *Error bars=STDEV; n=2 experiments.*

5.3.3 CD44 affiliation with lipid rafts varies across primary cell lines and progenitor populations.

So far this thesis has shown that gene expression of palmitoylation-regulating enzymes correlates with breast cancer patient survival; and their inhibition exerts regulatory effects on CD44 and its lipid raft affiliation, and in turn modulates cancer cell migration and growth. Therefore we next attempted to translate these results into a more patient-relevant context, by investigating CD44 palmitoylation and raft affiliation status in primary cultures isolated from breast cancer patients and in progenitor cell populations suspected to play a key role in driving cancer initiation. Primary cultures from patients with invasive lobular carcinoma (ILC), invasive tubulo-lobular carcinoma (IT-LC), ductal carcinoma *in situ* (DCIS) and invasive ductal carcinoma (IDC) displayed variable morphologies (**Fig. 5.10A**). Before reaching confluence, all had heterogeneously-sized mixtures cells. Upon reaching confluence, cells from DCIS cultures organised into colonies of cells resembling luminal epithelial structures, surrounded by flattened, myoepithelial-like cells. IDC cultures contained predominantly flattened protrusive cells. ILC and IT-LC cultures at confluence were composed of largely disorganised populations of cells.

In addition to primary cultures, we also cultured putative progenitor populations previously isolated from the non-tumourigenic MCF-10a cell line. MCF-10a cells were sorted into $CALLA^+/EpCAM^+$ (double-positive, DP), $CALLA^-/EpCAM^-$ (double-negative, DN), $CALLA^-/EpCAM^+$ (EpCAM) and $CALLA^+/EpCAM^-$ (CALLA) cell populations, as described previously (Donatello *et al.*, 2011). Similar to the patient primary cultures, these populations had distinct morphologies (**Fig. 5.10B**). The EpCAM population was characterised by tightly-adherent cells of similar size. CALLA cells were more loosely organised and flattened or elongated. DP cells represented a mixture of small, tightly-adherent and larger elongated cells, while the DN population was characterised by very small, tightly-adherent cells.

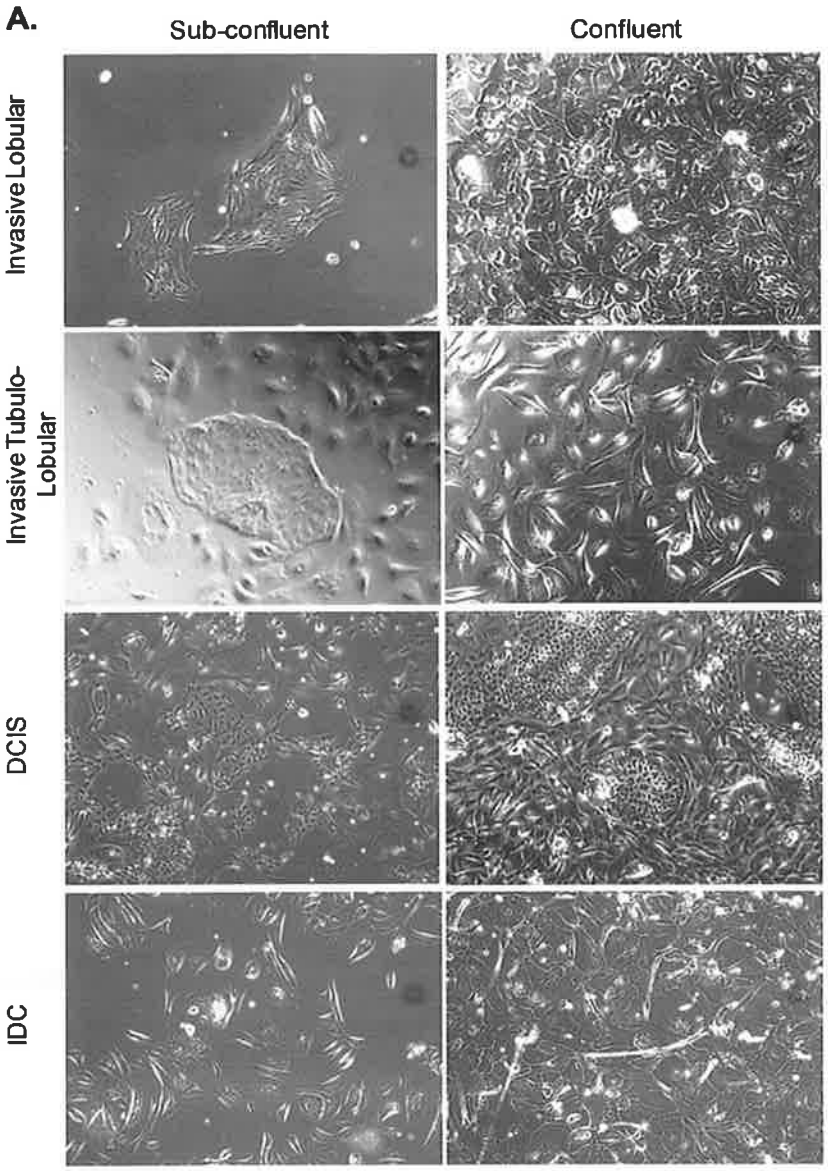
A.
Sub-confluent
Confluent
Invasive Lobular
Invasive Tubulo-Lobular
DCIS
IDC

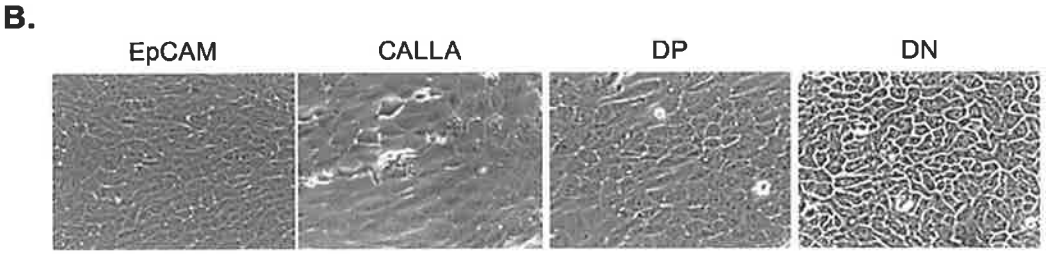
B.
EpCAM
CALLA
DP
DN

Figure 5.10 Morphologies of primary breast cell lines and MCF-10a progenitor populations. Phase contrast micrographs of (**A.**) breast primary cell cultures from patients with invasive lobular carcinoma (ILC), invasive tubulo-lobular carcinoma (IT-LC), ductal carcinoma *in situ* (DCIS) and invasive ductal carcinoma (IDC) at sub-confluent and confluent stages. All cell primary cell lines contained a heterogenous mixture of cells, presumed to reflect a mixed luminal epithelial - myoepithelial lineage. (**B.**) Phase contrast micrographs of $EpCAM^{+}$, $CALLA^{+}$, double-positive (DP) and double-negative (DN) sub-populations of MCF-10a cells revealed variable morphologies. EpCAM sub-populations were composed of tightly-adherent, highly-polarised cells, while CALLA sub-populations were more loosely packed and elongated. DP sub-populations demonstrated a mixture of both phenotypes, while DP sub-populations were very small and tightly packed together. Magnification: 10X.

Having observed distinct morphological differences in primary cultures derived from tumours of different prognosis, we sought to establish whether CD44 lipid raft affiliation would differ in these cells. Firstly, CD44 co-localisation with the lipid raft marker flotillin-1 was estimated using immunofluorescence confocal microscopy. CD44 predominantly co-localised with flotillin-1 in DCIS primary cells (**Fig. 5.11A**). It is also interesting to note that in DCIS cells flotillin-1 mainly localised to the cell membrane, while in other primary cultures it was predominantly cytoplasmic or perinuclear. Similar results were observed during migration of these cells, with little co-localisation of the two proteins in ILC, IT-LC or IDC cultures compared to those from DCIS cultures. However, CD44-flotillin-1 localisation somewhat decreased in DCIS migrating cells relative to the non-migrating condition. It was previously noted that DCIS and IT-LC cells displayed areas of highly adherent colonies, surrounded by larger, loosely organised cells (**Fig. 5.10**). It was thus intriguing to compare CD44-flotillin-1 co-localisation in these two populations. As shown in **Figure 5.11B**, tightly-adherent cells had increased co-localisation between CD44 and flotillin-1 (filled arrows) relative to the surrounding larger cells (double-ended arrows) in both, DCIS and IT-LC cell lines. The larger cells showed suggestive evidence of cytoplasmic and vesicular localisation of CD44 and flotillin-1 compared to the smaller adherent cells, which predominantly expressed both proteins in the cell membrane.

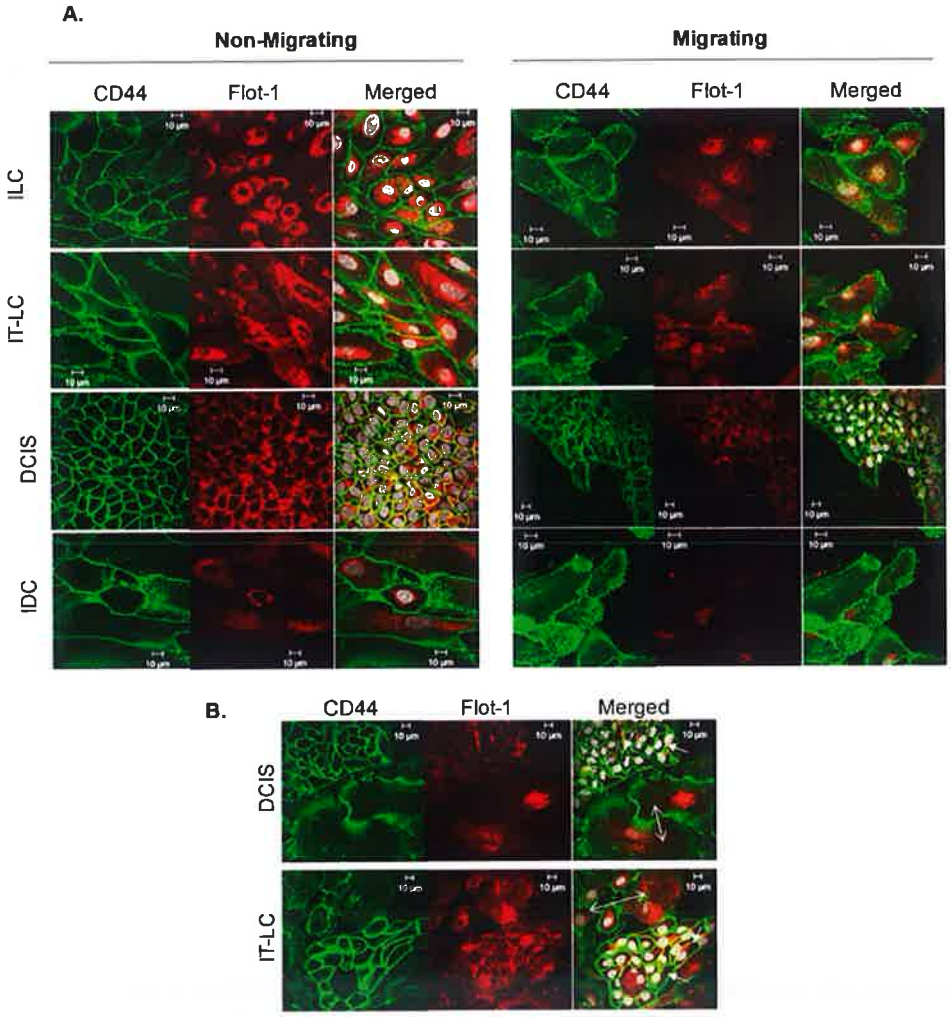

Figure 5.11 Immunofluorescent analysis of CD44 and flotillin-1 co-localisation in breast primary cultures. **(A.)** Non-migrating and migrating (2hr) breast primary cell lines were stained for CD44 (green) and flotillin-1 (Flot-1, red). Nuclei were stained with DAPI and are shown in grey. Ductal carcinoma *in situ* (DCIS) primary cells demonstrated the highest co-localisation of the two proteins compared to invasive tubulo-lobular carcinoma (IT-LC), invasive lobular (ILC) and invasive ductal (IDC) carcinomas in both, non-migrating and migrating conditions. **(B.)** DCIS and IT-LC displayed areas of luminal-like cells, with strong CD44-Flot-1 co-localisation (filled arrows), surrounded by cells resembling myoepithelial cells (double-ended arrows), which had little or no co-localisation. Pictures are representative of at least 2 independent experiments, with multiple fields analysed per experiment.

MCF-10a sub-populations of cells were also analysed for co-localisation between CD44 and the lipid raft marker flotillin-1. Despite a similar membranous distribution of CD44 across all sub-populations, flotillin-1 was mainly found in the membrane and vesicle-like structures of EpCAM and CALLA cells, while it was vesicular in DP cells and predominantly cytoplasmic in DN cells (**Fig. 5.12A**). EpCAM and CALLA sub-populations had high CD44/ flotillin-1 co-localisation under non-migrating conditions. After 2 hours of migration, EpCAM and CALLA sub-populations partially retained CD44 co-localisation with flotillin-1 at cell-cell junctions and in vesicles (respectively). DP and DN sub-populations, however, displayed very few yellow areas of CD44/ flotillin-1 co-localisation compared to that in EpCAM and CALLA sub-populations, and there was enhanced localisation of CD44 at the leading edge of the membrane (arrows). Given the variations in staining of flotillin-1 across primary cell lines and progenitor populations, we also examined whether its expression could correlate with patient outcome parameters in commercially-available datasets. Using the online Kaplan-Meier breast cancer survival tool (Gyorffy *et al.*, 2010), a significant correlation between high flotillin-1 (probe 208749_x_at) gene expression and better recurrence-free survival was revealed (**Fig. 5.12B**).

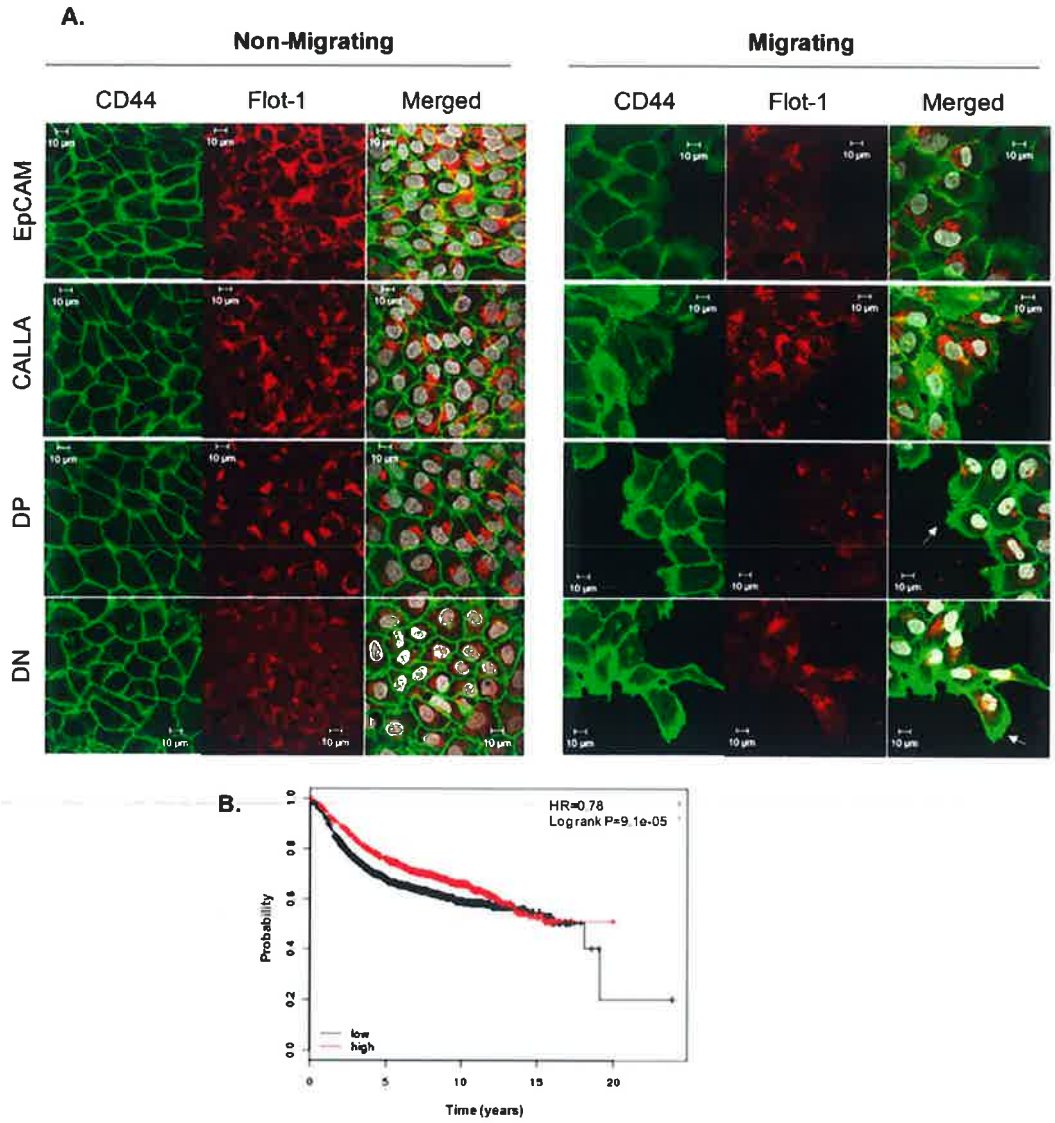

Figure 5.12 Immunofluorescent analysis of CD44 and flotillin-1 co-localisation in MCF-10a progenitor populations. (A.) Non-migrating and migrating (2hr) EpCAM$^+$, CALLA$^+$, double-positive (DP) and double-negative (DN) progenitor populations from the MCF-10a cell line were immunostained for CD44 (green) and flotillin-1 (Flot-1, red). Nuclei were stained with DAPI and are shown in grey. All cells demonstrated similar CD44/Flot-1 co-localisation patterns under both migratory and non-migratory conditions. However, the staining pattern for Flot-1 in DN sub-populations differed from that in other MCF-10a sub-populations, as it was diffusely distributed throughout the cytoplasm, unlike the vesiclular/membraneous distribution in

other sub-populations. Images are representative of 2 experiments. (**B.**) Online breast cancer survival analysis tool revealed a strong correlation of high Flot-1 gene expression (red) with good recurrence-free survival of breast cancer patients.

To biochemically support our immunofluorescence observations, we performed Triton X-100 insolubility isolations of lipid raft- and non-raft-enriched domains from non-migrating and migrating primary cell cultures and MCF-10a sub-populations. In the primary breast cancer cultures CD44 was recovered from both lipid raft and non-raft fractions of non-migrating and migrating cells (**Fig. 5.13**). After 2 hours of stimulated migration CD44 recovery from the non-raft domains of migrating cells was reduced. Calculation of numerical ratio of CD44 affiliation with raft-enriched domains revealed an increase in raft CD44 in migrating DCIS and IT-LC cells (**Fig. 5.13, graph**). Primary cells from IDC and ILC tumours demonstrated similar levels of CD44 raft affiliation under non-migrating and migrating conditions.

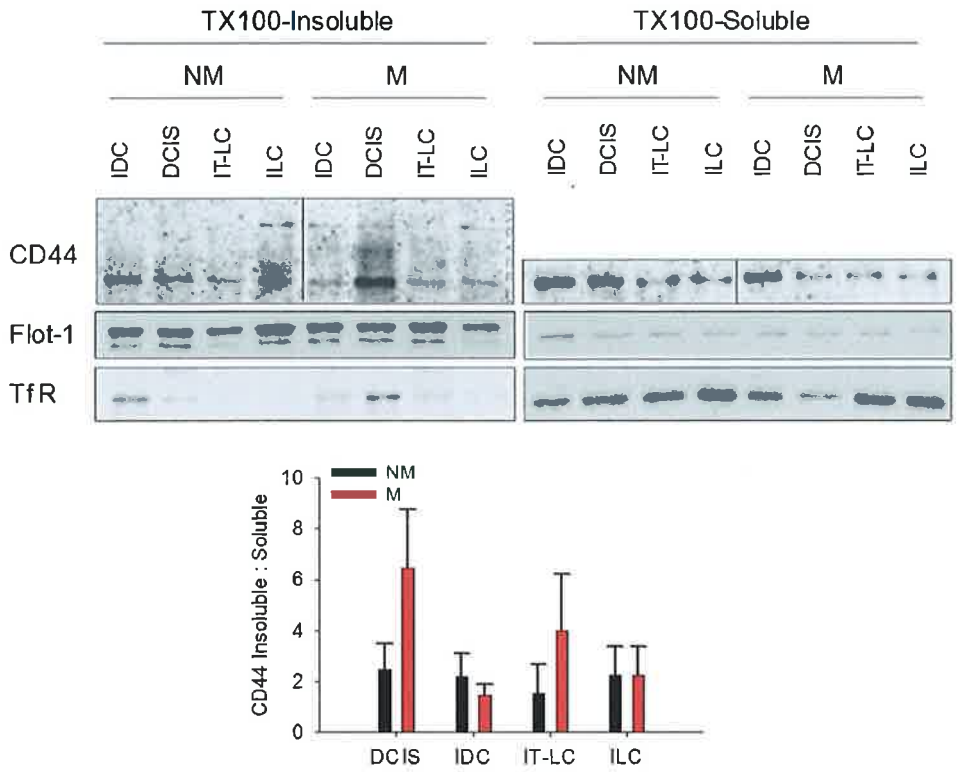

Figure 5.13 CD44 localisation in lipid raft domains varied across breast primary cell cultures. Non-migrating and migrating (2hr) primary cell cultures were subjected to Triton X-100 insolubility assays. Detergent-insoluble (raft-enriched) pools were marked by increased flotillin-1 (Flot-1) expression, while non-raft domains were represented by expression of transferrin receptor (Tf R). CD44 recovery in raft-enriched pools was increased during migration of ductal carcinoma *in situ* (DCIS) cells in relation to non-migrating cells. An additional high molecular weight band for CD44 was also recovered in raft-enriched pools. In other cell types there was no notable change in CD44 affiliation with lipid raft domains under migrating conditions relative to non-migrating conditions. However CD44 recovery from non-raft domains slightly decreased during migration of all primary cells except the invasive ductal carcinoma (IDC) culture. Calculation of the CD44 Insoluble:Soluble ratio revealed an trend towards an increased ratio in migrating DCIS cells, but no statistically significant changes throughout. *Error bars=STDEV; n=2 experiments.*

Similarly to primary cultures, MCF-10a cell sub-populations displayed both standard and variant CD44 expression in the lipid raft-containing domains, and only standard CD44 (CD44s) expression in non-raft domains (**Fig. 5.14**). There was an increase in CD44 affiliation with non-raft domains in non-migrating CALLA sub-populations compared to the other sub-populations. Under migratory conditions, CD44 recovery was increased in the lipid raft pools of all sub-populations except DP. Calculation of the CD44 insoluble:soluble ratio suggested a trend towards increased CD44 affiliation with raft-enriched domains in migrating EPCAM, CALLA and DN sub-populations (**Fig. 5.14, graph**).

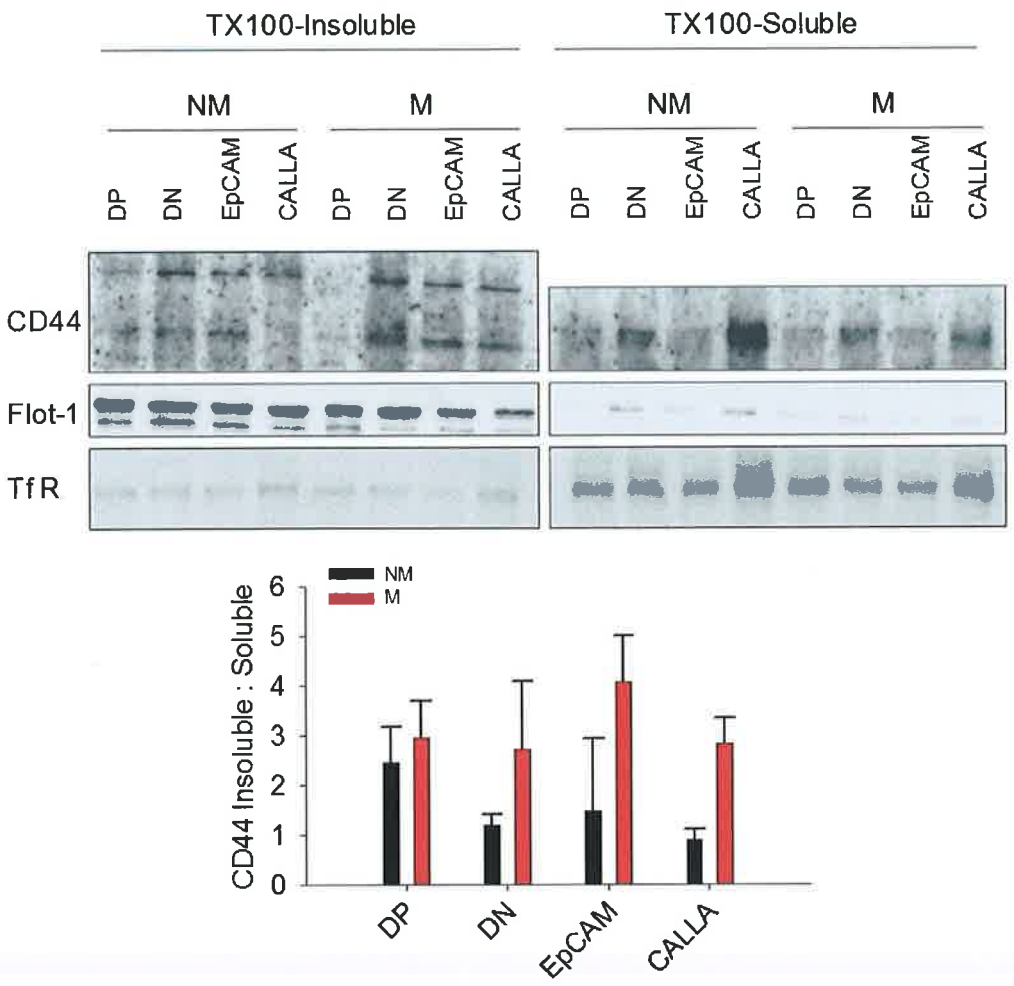

Figure 5.14 CD44 localisation in lipid raft domains is increased during migration of MCF-10a populations. Non-migrating and migrating (2hr) $EpCAM^+$, $CALLA^+$, double-positive (DP) and double-negative (DN) populations of MCF-10a cells were subjected to Triton X-100 insolubility assays. Detergent-insoluble pools were marked by increased flotillin-1 (Flot-1) expression, while non-raft domains were represented by expression of transferrin receptor (Tf R). There was increased CD44 affiliation with raft-containing domains of all cell lines tested under migrating conditions, paralleled by reductions in CD44 affiliation with non-raft domains. Calculation of the CD44 Insoluble:Soluble ratio revealed small increases in CD44 raft affiliation across all cell types. *Error bars=STDEV; n=2 experiments.*

In order to inspect if differences in CD44 raft affiliation observed in primary cultures were due to differing levels of CD44 palmitoylation, we measured palmitoylated CD44 in lysates from representative cultures using the acyl-biotin exchange approach. Non-tumour (NT), DCIS and IDC (grades 2 and 3) whole cell extracts were examined for levels of palmitoylated CD44 using the acyl-biotin exchange assay as before (**Fig. 5.15A**). HAM-untreated lysates served as internal negative controls. The highest palmitoylated CD44 content was observed in NT lysates (lanes 1, 4), with DCIS and IDC displaying similar levels of palmitoylated CD44, but much lower compared to NT samples. This was further confirmed by calculating relative palmitoylated CD44 levels from densitometrically-analysed blots (**Fig. 5.15A, graph**). These values were subsequently pooled into NT, DCIS, IDC Grade 2 and IDC Grade 3 groups, and expressed relative to NT levels of palmitoylated CD44 (**Fig. 5.15B**). DCIS and both grades of IDC displayed markedly lower levels of palmitoylated CD44 compared to NT samples.

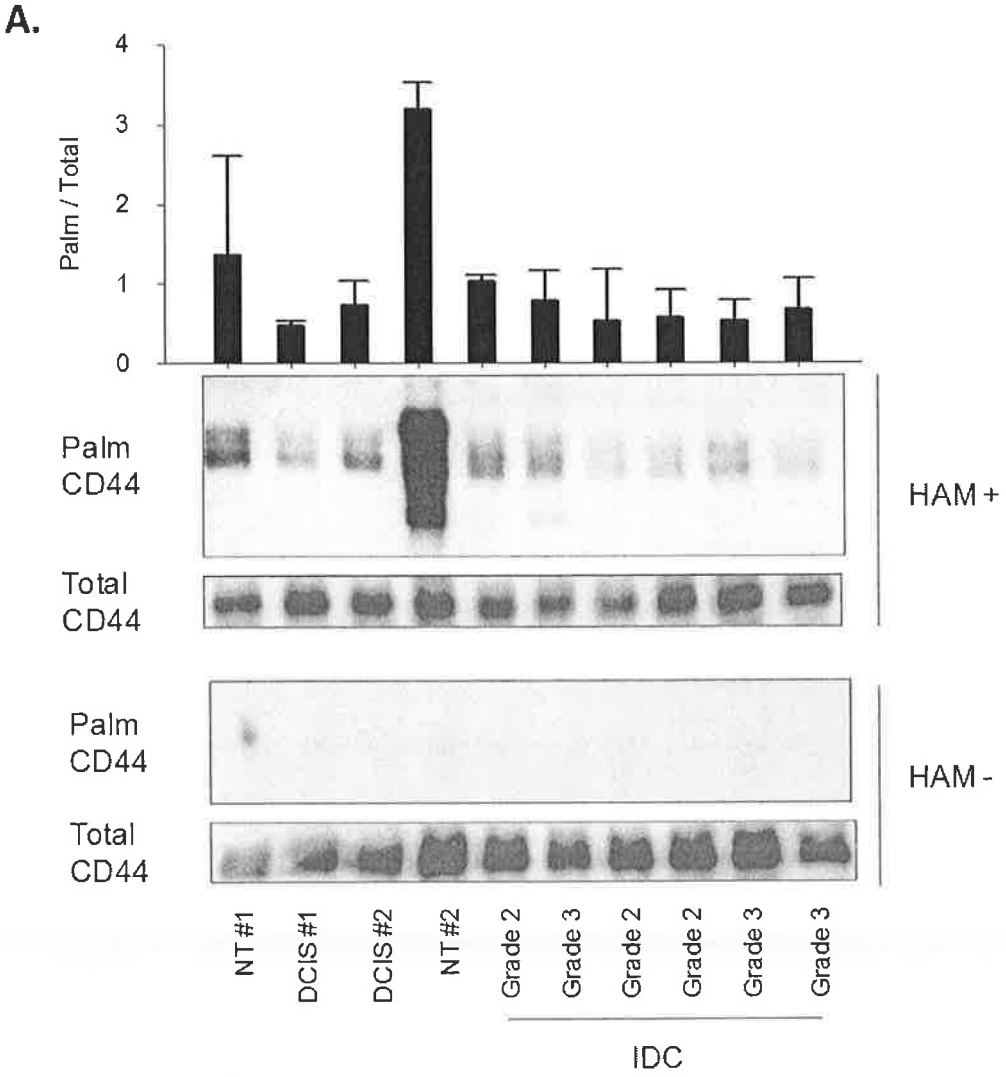
A.
Palm / Total
4
3
2
1
0
Palm CD44
Total CD44
HAM +
Palm CD44
Total CD44
HAM -
NT #1
DCIS #1
DCIS #2
NT #2
Grade 2
Grade 3
Grade 2
Grade 2
Grade 3
Grade 3
IDC

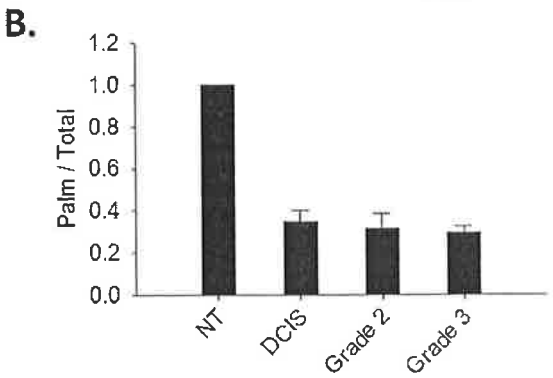
B.
Palm / Total
1.2
1.0
0.8
0.6
0.4
0.2
0.0
NT
DCIS
Grade 2
Grade 3

Figure 5.15 Decreased palmitoylation of CD44 is associated with a tumourigenic phenotype. Whole cell lysates of primary cultures from two non-tumour (NT), two ductal carcinomas *in situ* (DCIS) and six invasive ductal carcinomas (IDC) of tumour grade 2 and 3 (three of each) were subjected to acyl-biotin exchange assays to compare palmitoylated CD44 levels. (**A.**) Most palmitoylated CD44 (CD44-Palm) was recovered from NT cultures, while all patient breast cancer cultures displayed comparatively little CD44-Palm. Palmitoylated CD44 levels densitometrically normalised to total CD44 (CD44-Total) further demonstrated increased levels of CD44-Palm in NT samples. *Error bars=STDEV of duplicates in one experiment.* (**B.**) Numerical values for CD44-Palm were pooled among samples and expressed relative to NT samples, revealing a decrease in CD44 palmitoylation in breast cancer samples compared to NT samples. *Error bars=STDEV; NT: n=2 samples, DCIS: n=2 samples, IDC grades 2 and 3: n=3 each.*

5.3.4 Correlation between CD44 raft affiliation/palmitoylation and functional properties of primary cultures and progenitor cell populations.

Having established differences in CD44 palmitoylation status and raft localisation across the breast cancer translational models, we finally sought to correlate them with functional properties of the different culture types. Firstly, we sought to investigate if primary breast cancer cultures and MCF-10a progenitor populations varied in their migratory capacities, via scratch-wound migration assays. Representative IDC and ILC primary cells demonstrated the highest migratory potential compared to DCIS and IT-LC cells (**Fig. 5.16A**), with approximately 15% wound closure by 8 hours. DCIS cells exhibited approximately 10% wound closure by 8 hours, while IT-LC proved to have the slowest migration pattern, with only <5% wound closure by 8 hours. DP and DN putative progenitor sub-populations derived from the MCF-10a cell line demonstrated a higher rate of migration (according to the slope of the graphs) compared to the slow linear increase in EpCAM and CALLA sub-populations (**Fig. 5.16B**). After 8 hours, the migration of DN cells was significantly greater than that of the EpCAM sub-population.

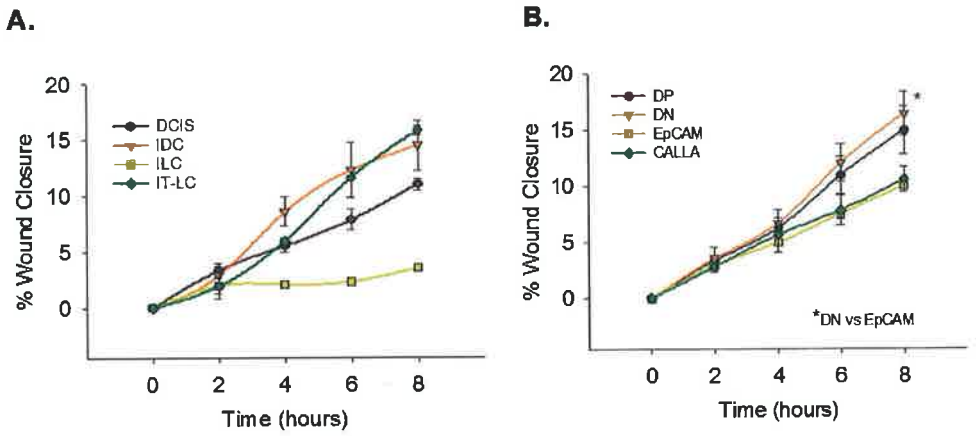

Figure 5.16 Migration differences among primary breast cell cultures and MCF-10a progenitor populations. Confluent monolayers of all cells were subjected to scratch-wound migration assays over 8 hours. (**A.**) Breast primary cell cultures demonstrated various migratory abilities, with invasive tubulo-lobular carcinoma (IT-LC) showing slowest migration, with ductal carcinoma *in situ* (DCIS) in the middle and invasive lobular (ILC) and invasive ductal (IDC) carcinomas having the most efficient migration (*Error bars=STDEV, n=2 experiments*). (**B.**) Putative progenitor populations from MCF10A cells also demonstrated differences in migratory characteristics, with double-negative (DN) and double-positive (DP) sub-populations demonstrating faster migration than EpCAM and CALLA sub-populations. *Error bars=SEM, *p<0.05, relative to EpCAM by 2-way ANOVA; n=3 experiments.*

Additionally, we explored the capacity of the above cells to form colonies from a single cell, in order to relate this to CD44 raft/extra-raft affiliation. While the colony-forming efficiency of primary cultures was very low, MCF-10a sub-populations successfully formed many colonies after 7 days (**Fig. 5.17A**). CALLA and DN populations formed notably more colonies than EpCAM and DP cells, although they were smaller in size. Quantification of colony-forming efficiency further supported these observations (**Fig. 5.17B**). In addition to colony-forming assays, we estimated the stem/progenitor potential of the selected cell cultures using non-adherent mammosphere-forming assays. While ILC and IT-LC cell lines failed to form mammospheres, candidate DCIS and IDC cultures successfully grew in suspension (**Fig. 5.17C**). Cells derived from IDC tumours formed more colonies than those from DCIS tumours. Surprisingly, although numerous mammospheres were formed, MCF-10a sub-populations largely adhered to the plate surface (**Fig. 5.17C**). The EpCAM sub-population predominantly grew in suspension, with occasional attachments to the plate surface. Furthermore, those cells that adhered formed polarised circular structures resembling mammary ducts (**Fig. 5.17, inset EpCAM**). Conversely, CALLA, DP and DN populations formed predominantly adherent colonies on the plate surface. Interestingly, however, while DP cells formed round adherent colonies, CALLA and DN colonies were large, diffusely-spread and more loosely organised. All mammospheres were counted and expressed relative to the original cell number seeded (**Fig. 5.17D**). In addition to mammospheres, all adhered colonies of MCF-10a sub-populations were also enumerated. Although still low, cells from IDC cultures exhibited the best mammosphere-forming efficiency compared to other primary cultures. This was in fact quantitatively similar to the mammosphere-forming efficiency of the MCF-10a EpCAM cell sub-population. Despite CALLA and DN populations having the lowest mammosphere-forming efficiency from the four MCF-10a sub-populations, those had the highest count of adherent colonies. Taken together, this illustrates that even within one cell line exist sub-populations of cells with differential functional properties.

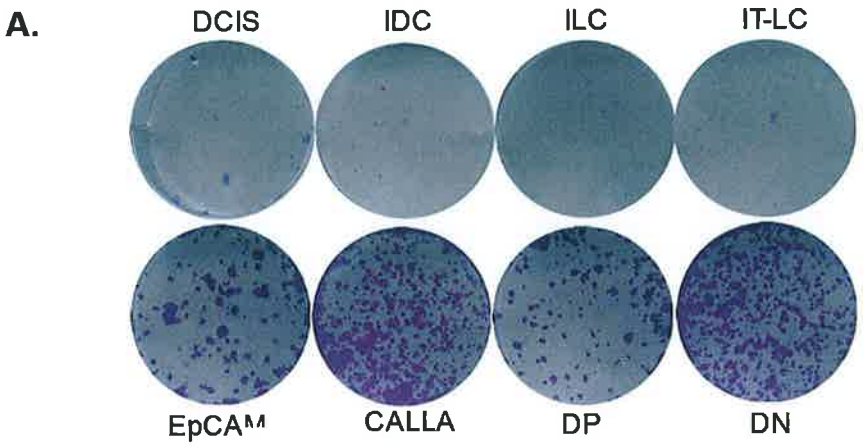
A.
DCIS
IDC
ILC
IT-LC
EpCAM
CALLA
DP
DN

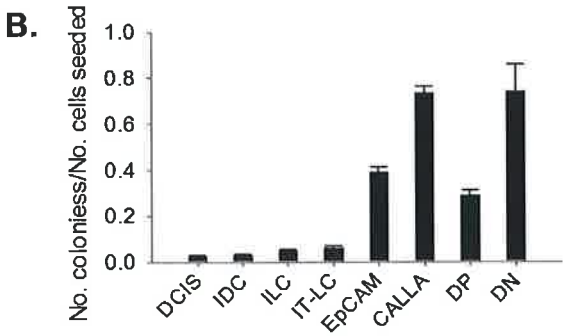
B.
No. colonies/No. cells seeded
1.0
0.8
0.6
0.4
0.2
0.0
DCIS
IDC
ILC
IT-LC
EpCAM
CALLA
DP
DN

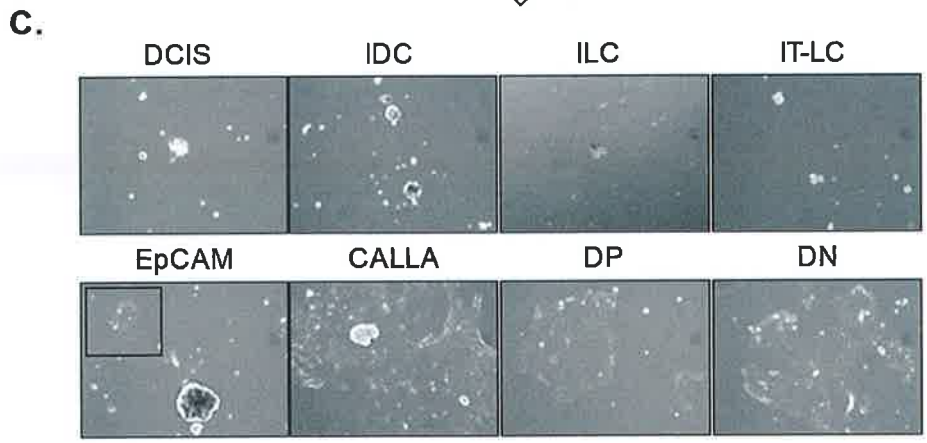
C.
DCIS
IDC
ILC
IT-LC
EpCAM
CALLA
DP
DN

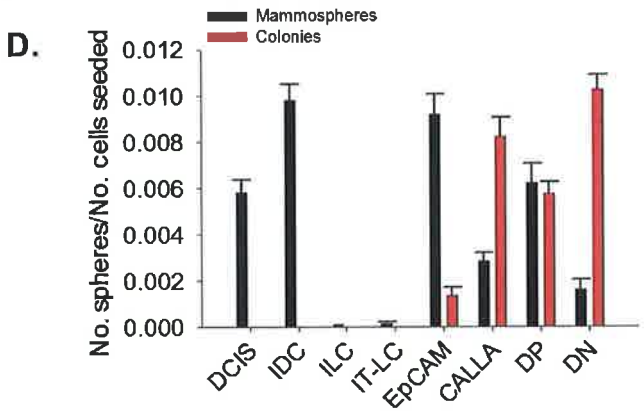
D.
Mammospheres
Colonies
No. spheres/No. cells seeded
0.012
0.010
0.008
0.006
0.004
0.002
0.000
DCIS
IDC
ILC
IT-LC
EpCAM
CALLA
DP
DN

Figure 5.17 Colony- and mammosphere-forming abilities of primary breast cell cultures and MCF-10a sub-populations. (**A.**) 200 of the indicated cell types in single-cell suspension format were seeded in 6 well plates and grown for 7 days to form clonogenic colonies. (**A.**) Cells were then stained with crystal violet, and representative wells of both cell lines were photographed using phase contrast microscopy. While primary cultures formed very few colonies, MCF-10a sub-populations formed numerous colonies, with CALLA and double-negative (DN) populations producing notably more colonies. (**B.**) This was further confirmed by manually-counted colonies expressed relative to the original number seeded (colony-forming efficiency). (**C.**) $1x10^4$ cells were seeded in ultra-low attachment plates and checked 7 days later for mammosphere formation. Mammospheres were photographed, manually counted and (**D.**) expressed relative to the original number of cells seeded (mammosphere-forming efficiency). Primary cultures from a representative ductal carcinoma *in situ* (DCIS) specimen produced fewer mammospheres than that from an invasive ductal carcinoma (IDC) specimen, while the other two primary cultures formed negligible numbers in comparison. MCF-10a sub-populations, in addition to mammospheres (black bars) formed adherent colonies (red bars). EpCAM populations formed the most mammospheres in comparison to other cellular sub-populations, followed by double-positive cells (DP), with CALLA and double-negative cells (DN) forming the least mammospheres. However, the latter formed the most adherent colonies, in comparison to EpCAM, which produced very few. *Error bars=STDEV; n=2 experiments.*

Collectively, results outlined in this chapter suggest a novel clinical relevance for the regulation of palmitoylation and lipid raft affiliation of CD44 in breast cancer, either via expressional changes in palmitoylation enzymes or via their modulation of CD44 palmitoylation status. Additionally, diverse CD44 palmitoylation profiles in patient breast cancer cells and putative progenitor populations highlight an exciting potential avenue for targeting CD44-based breast cancer cell migration prior to metastatic spread of the disease.

5.4 Discussion

The functionality of numerous proteins involved in breast cancer cell migration is modulated by post-translational modification with palmitate groups. This process is believed to be catalysed by PAT proteins. De-palmitoylating events are thought to be regulated by thioesterase enzymes, of which APT-1 is best characterised. Dynamic palmitoylation and de-palmitoylation of a variety of proteins (such as Rho and Ras) involved in breast cancer and other diseases has been recently reviewed (Resh, 2012). Our findings outlined in the previous chapter suggested a potential role for CD44 palmitoylation in breast cancer. However no reports to date have addressed how CD44 is palmitoylated in breast cancer cells, or the functional implications of its palmitoylation. Consequently, in the present chapter we investigated the potential of pharmacologically targeting palmitoylation-regulating enzymes to modify CD44 palmitoylation, raft localisation and migration of breast cancer cells. Furthermore, we have begun to investigate the clinical relevance of CD44 palmitoylation and its affiliation with lipid rafts using patient-derived primary cultures and putative progenitor sub-populations of MCF-10a cells.

Numerous PAT enzymes have been identified in humans, which begs the question why so many PATs are required in one organism. In yeast, each PAT has been demonstrated to act on a particular substrate (Putilina *et al.*, 1999). In humans, these enzymes are predominantly expressed in ER/Golgi, except DHHC5, -20 and -21 which are strongly expressed at the cell membrane (Ohno *et al.*, 2006). In this study we noted that high gene expression of a panel of PAT enzymes (DHHC3, 6, 7, and 8) correlated significantly with improved breast cancer recurrence-free survival. An intriguing contrast is that increased expression of DHHC13 and 14 was associated with decreased survival. Interestingly, the former localise to the Golgi while the latter are found in the ER (Ohno *et al.*, 2006). Provided gene expression was proportional to protein expression, and because trafficking from the ER is slower than that from the

Golgi, proteins that undergo palmitoylation in the ER could have a longer half-life, thus contributing to increased tumourigenesis. These different outcomes with PAT enzymes once again highlight the complexity of intracellular regulation of protein function, and require thorough studies.

De-palmitoylating activity is controlled by thioesterase enzymes. We also correlated the gene expression of two thioesterases (APT-1 and APT-2) with breast cancer recurrence-free survival, and again obtained opposing outcomes. While increased expression of APT-1 was associated with poor patient survival, increased expression of its homologue APT-2 correlated with better recurrence-free survival. These conflicting outcomes could again be accounted for by different cellular localisations of the two proteins. Unlike APT-1, which is mainly found in the cyloplasm (Duncan and Gilman, 1998), APT-2 is believed to be a lysosomal protein (Soyombo and Hofmann, 1997). It has been established that Ras proteins, which are frequently implicated in breast cancer (Stamatakos *et al.*, 2010), are de-palmitoylated by APT-1 (Rusch *et al.*, 2011). Thus hyper-activity of APT-1 enzyme would likely decrease the levels of palmitoylated Ras; thereby increasing its trafficking to and from the Golgi to be re-palmitoyated, and consequently facilitating its oncogenic signalling. Overall however, these survival studies on gene expression of palmitoylating and de-palmitoylating enzymes point to a complex relationship between global palmitoylation patterns and cancer progression. Nonetheless the balance of evidence seems to suggest that a pro-palmitoylation state is pro-survival; supporting our hypothesis of an inverse correlation between CD44 palmitoylation / raft affiliation and cell migratory potential.

Given our novel finding that stimulated migration of breast cancer cells decreased CD44 palmitoylation over time, we hypothesised that CD44 was being directly regulated by the clinically-relevant palmitoylation and de-palmitoylation enzymes mentioned above. Thus we adopted recently-characterised inhibitors of PAT activity to investigate the effects of PAT inhibition on CD44 raft localisation and palmitoylation. Specifically, we

targeted two major classes of PATs with compounds III and V, which demonstrated specific inhibitory effects against PATs catalysing farnesylated and myristoylated proteins respectively (Ducker *et al.*, 2006). Although there are no reports suggesting that CD44 is lipidated by additional fatty acids, such as myristate, farnesyl or geranylgeranyl, the Cys286 residue of CD44 fits the description of a farnesylated motif, being located in a putative farnesylation site containing a "CAAX" domain (Cysteine, 2 aliphatic amino acids and a variable amino acid X) (Hancock *et al.*, 1989). On the CD44 molecule this corresponds to "^{286}Cys-Ile-Ala-Val^{289}" (see Fig. 4.2), the last amino acids of the transmembrane domain. Thus we speculated that inhibition of either class of PAT enzymes would result in decreased palmitoylation of CD44. However both inhibitors paradoxically increased CD44 palmitoylation, its co-localisation with the lipid raft marker flotillin-1 and its affiliation with lipid raft domains. The extent of these effects was similar for both inhibitors, with compound V proving marginally more potent than compound III. This is in agreement with a previous study that showed compound V having a similar de-palmitoylating efficiency to a broad non-specific inhibitor 2-BP and much higher than that of compound III (Jennings *et al.*, 2009).

To date, modulation of palmitoylation has been shown to affect proteins like eNOS, Ras and PSD-95 (Baekkeskov and Kanaani, 2009), but it has not been extensively studied in receptor proteins or breast cancer specifically. We observed an increase in levels of membrane-bound flotillin-1 upon broad inhibition of palmitoylating activity. This was surprising given an established role of palmitoylation in flotillin-1 translocation to the plasma membrane (reviewed by (Babina *et al.*, 2011)). However the inhibitors we used mainly targeted PAT enzymes located in the ER/Golgi, and flotillin-1 has been shown to be trafficked to the cell membrane in a Golgi-independent manner (Morrow *et al.*, 2002). Furthermore, a recent study identified DHHC5 as an enzyme that palmitoylates a homologue of flotillin-1, flotillin-2 (Li *et al.*, 2012). As both flotillin proteins share a conserved homology domain (Morrow and Parton,

2005) which is responsible for their membrane association (Morrow *et al.*, 2002), flotillin-1 could also be a substrate for the action of DHHC5 PAT enzyme. Finally, because DHHC5 is one of three PAT enzymes localised to the cell membrane (Ohno *et al.*, 2006), it could explain the increased membrane localisation of flotillin-1 when broad palmitoylation in the Golgi/ER was inhibited, subsequently increasing co-localisation with CD44.

The PAT inhibitors also induced longer-term effects, since proliferation over 3 days and colony forming ability after 7 days were reduced in MDA-MB-231 and MCF-10a cell lines. Because of the similar de-palmitoylation activity of compound V and 2-BP (Jennings *et al.*, 2009), they could potentially exert similar effects in cells. In MDA-MB-231 cells it has been reported that 2-BP induces cytochrome C release and increases apoptosis (Hardy *et al.*, 2003), which would account for the anti-proliferative properties of PAT inhibitor V. Furthermore, the same study demonstrated growth-inhibitory effects of saturated PA at 100μM, which is in agreement with our PA effects outlined in this chapter. Importantly, PA did not modify proliferation in normal-like MCF-10a cells, which highlights PA as a potential anti-tumourigenic agent that could be supplied via nutritional supplementation.

Despite expectations, we established that inhibition of palmitoylating enzymes in fact *increased* the palmitoylation of CD44, likely via complex feedback mechanisms which remain elusive. Consequently, we sought to investigate if inhibition of a *de*-palmitoylating enzyme (APT-1, with Palmostatin B) would increase CD44 palmitoylation and its raft localisation. In MDA-MB-231 cells Palmostatin B in fact *decreased* CD44 co-localisation with flotillin-1 and its affiliation with lipid raft domains. This may suggest that CD44 is not a direct substrate for APT-1 de-palmitoylation, and that antagonism of APT-1 function triggers a reflex activation of palmitoylation enzymes that target CD44. Thus APT-1 activity may have an inverse relationship with CD44 palmitoylation (and raft affiliation), similar to the manner in which inhibition of PAT enzymes paradoxically upregulated CD44

palmitoylation and its raft affiliation (instead of the predicted downregulation secondary to inhibition of pro-palmitoylation enzymes). APT-1 is an established de-palmitoylating enzyme of Ras proteins (Dekker *et al.*, 2010), however its inhibition results in reduced localisation of Ras in the cell membrane (Xu *et al.*, 2012). This has been associated with entropy-driven diffusion of palmitoylated Ras throughout the cell (Rocks *et al.*, 2010). Availability of palmitoylated Ras in endomembranes could enable oncogenic, pro-migratory activity of Ras proteins (Reeves *et al.*, 2010), which might explain our observed increase in MDA-MB-231 cell migration upon treatment with Palmostatin B. Accordingly, activated Ras has been shown to stimulate CD44 mRNA production and activation of MAPK signalling in HeLa cervical cancer cells (Cheng *et al.*, 2006), ultimately leading to tumourigenesis. The effects we describe using broadly-specific enzyme inhibitors, are certain to impact many palmitoylated protein targets in addition to just CD44. However, regardless of the paradoxical effects of specific enzyme inhibitors on CD44 palmitoylation, it is important to point out that reduced migration in our system was always accompanied by a decrease in CD44 palmitoylation. This supports our hypothesis of a direct relationship between decreased CD44 palmitoylation (and decreased raft localisation) and the promotion of cell migration.

CD44 is frequently used as a marker for cancer progenitor cells, along with low expression of surface CD24 (Dontu *et al.*, 2003). Increasing evidence suggests that most cancers arise from a single cell with stem-like properties (Korkaya *et al.*, 2011). Cancer progenitor cells are believed to be responsible for the initiation of breast tumour growth and tumour resistance to chemotherapy (Smalley *et al.*, 2012). Since we were able to modulate CD44 palmitoylation status with inhibitors of palmitoylation and de-palmitoylation, we set out to determine if MDA-MB-231 cells with increased/decreased CD44 palmitoylation levels had progenitor properties, using mammosphere-forming assays. While MDA-MB-231 cells formed viable mammospheres, a global reduction in palmitoylation via inhibition of palmitoylating enzymes

completely abolished that ability. Global reductions in de-palmitoylation via the APT-1 inhibitor Palmostatin B also demonstrated inhibitory effects toward mammosphere formation, although cells retained the ability to form small clusters of 5-10 cells. Finally, treatment with exogenous palmitic acid itself reduced the number of mammospheres formed relative to control conditions, but some cells were still able to proliferate in suspension. Of course, none of these agents are specific to CD44 alone, but would affect palmitoylation of many proteins in a cell. However a plausible explanation for the decrease in progenitor cells secondary to interference with palmitoylation or de-palmitoylation is that these broad inhibitors also target key proteins involved in cell self-renewal, such as Wnt and Hedgehog. Activation of these proteins has been previously demonstrated to increase mammosphere-forming capacity of breast cells (Liu *et al.*, 2006). Both of these proteins are extensively acylated (Buglino and Resh, 2012), and site-directed mutagenesis of their acylation sites has been shown to abolish signal transduction and secretion of these proteins, blocking oncogenesis (reviewed in (Resh, 2012)). In support of our PA results, supplementation of MDA-MB-231 growth medium with polyphenolic acids has been shown to significantly reduce mammosphere formation and to upregulate PTEN expression, thereby reducing Wnt signalling (Montales *et al.*, 2012). This once again highlights the potential importance of fatty acids in inhibition of oncogenic signalling.

Having presented novel evidence that interfering with global protein palmitoylation affects cell fate and progenitor capabilities, we questioned whether CD44 raft affiliation and palmitoylation itself can distinguish between MCF-10a putative progenitor sub-populations or predict the aggressiveness of tumours from breast cancer patients. We have previously isolated four sub-populations of cells from the non-tumourigenic MCF-10a cell line (Donatello *et al.*, 2011), based on single or double positivity / negativity for the epithelial and myoepithelial markers EpCAM and CALLA (respectively). Similar populations extracted from the primary cultures of reduction mammoplasties

have been characterised as candidates for alveolar and ductal progenitors *in vivo* (Stingl *et al.*, 1998). We utilized the pre-isolated DP, DN, EpCAM and CALLA populations, as well as breast primary cultures generated from patient lumpectomy/mastectomy samples (Donatello *et al.*, 2011) as tools to evaluate the importance of CD44 raft affiliation in a clinical setting. Despite being used as one of the key identifiers of tumour-initiating cells, to date nothing has been published regarding CD44 sub-cellular localisation and function in these cells. Of the primary cultures tested, DCIS cells demonstrated the most striking co-localisation of CD44 with the raft marker flotillin-1 compared to the representative invasive primary cultures. Furthermore, in primary cultures, areas of epithelial cells displayed strong CD44/flotillin-1 co-localisation, while surrounded by larger, myoepithelial-like cells that had little or no CD44/flotillin-1 overlap. This could indicate that co-localisation of these proteins is associated with a more differentiated, luminal phenotype. Indeed, flotillins have been demonstrated to regulate levels of oncogenic HER-2 and its downstream signalling in SKBR3 breast cancer cells (Pust *et al.*, 2012).

Our observations in patient primary cultures were further supported by findings in progenitor populations isolated from non-tumourigenic MCF-10a cells. While CD44/flotillin-1 localisation was similar across various populations, undifferentiated DN cells displayed diffused cytoplasmic staining patterns for flotillin-1, similar to that in primary cultures from invasive breast carcinomas. While the functions of flotillins are not comprehensively clear, they have been implicated in T cell activation, insulin signalling, protein recruitment and many other processes (reviewed in (Zhao *et al.*, 2011)). In breast cancer, flotillin-2 gene expression has recently been correlated with disease-free survival in a cohort of 194 patients, while flotillin-1 gene expression did not yield significant correlations with patient outcome (Pust *et al.*, 2012). However using an online Kaplan-Meier breast cancer survival tool of over 2600 patients (Gyorffy *et al.*, 2010), we established a correlation between increased flotillin-1 gene expression and better recurrence-free

survival of breast cancer patients. Provided the protein expression of flotillin-1 is proportional to that at gene level, enhanced flotillin-1 expression may suggest increased levels of rafts, and in turn a relative increase in the proportion of CD44 affiliated with rafts. It would be exciting to explore flotillin-1 gene expression in CD44-positive tumours, as loss of flotillin-1 and subsequent release of CD44 from rafts could accordingly be associated with tumourigenesis.

We then questioned whether our hypothesis could be applicable in a clinical setting, by comparing CD44 palmitoylation status in a panel of non-tumour, DCIS and IDC patient primary cultures. We observed high levels of palmitoylated CD44 in non-tumour samples, while DCIS and IDC tumours expressed comparatively little palmitoylated CD44. These findings support the hypothesis that increased palmitoylation of CD44, and consequently its affiliation with lipid rafts, correlates with non-tumourigenic behaviour of mammary cells. We detected no palmitoylation differences between DCIS and IDC cultures or between different grades of IDC, which is encouraging in light of reports that genetic changes predisposing to tumourigenicity do not substantially differ between DCIS and IDC tumours (Kuukasjarvi *et al.*, 1997; Moelans *et al.*, 2011). Although the numbers we tested were small, our results collectively demonstrate for the first time a novel potential role for CD44 palmitoylation and consequent modification of raft affiliation in breast tumourigenesis *ex vivo*.

Finally we sought to correlate any functional differences between patient primary cultures or MCF-10a sub-populations with CD44 localisation status relative to lipid rafts. DN and DP progenitor cells, representing undifferentiated and multipotent sub-populations (Stingl *et al.*, 2001), demonstrated the highest migration capacity relative to terminally-differentiated EpCAM and CALLA sub-populations. As the normal balance between these cell types is tightly regulated in non-tumour cells, a shift in DN and DP populations in either direction could potentially result in de-regulation

of cellular machinery that controls functional behaviours relevant to cancer progression (including cell migration). Our laboratory has previously demonstrated that an imbalance in DN/DP progenitor populations correlates with high-grade, ER-negative and HER-2 positive tumours (Donatello *et al.*, 2011). Interestingly, in our hands the low level migration of DCIS primary cells mimicked that of EpCAM and CALLA sub-populations, while IDC cells mirrored the enhanced migratory potential of DN and DP sub-populations. This lends further support to the progenitor imbalance hypothesis.

In contrast to cell migration, the colony-forming abilities of DN and DP cells differed. Whereas DN cells behaved like the myoepithelial CALLA sub-population, producing many small colonies, EpCAM formed fewer but larger colonies and DP cells yielded a mixture of both. CALLA expression is thought to discriminate basal from luminal epithelial sub-populations and to reflect the aggressive claudin-low cancer subtype (Keller *et al.*, 2012), whereas the DN population is thought to be undifferentiated (Stingl *et al.*, 2001). This could in part explain the high colony-forming efficiency associated with these two sub-populations. In contrast, EpCAM expression in DP and EpCAM cells could be responsible for a more controlled, moderate clonogenic growth, especially since $EpCAM^+$ cells have been described to give rise to luminal lineages and to form bigger colonies (Villadsen *et al.*, 2007). Additionally, Keller *et al.* demonstrated that the sparse EpCAM clonogenic breast cancer colonies were enriched in luminal markers cytokeratin -8 and -18, while extensive colonies of CALLA cells stained exclusively for the myoepithelial marker cytokeratin -14 (Keller *et al.*, 2012). This functional grouping of CALLA/DN and EpCAM/DP was also maintained when the progenitor capacity of these cells was estimated. In agreement with our findings, it has been demonstrated previously that $EpCAM^+$ cells preferentially grew in suspension, while myoepithelial $CALLA^+$ cells formed adherent colonies (Keller *et al.*, 2012). Strikingly, CALLA, DN and (to a lesser extent) DP cells adhered to the surface of ultra-low adherence plates. Very few mammospheres from EpCAM sub-populations adhered, but

true to their luminal nature were able to form structures reminiscent of ducts in 3D cultures of normal cells (Debnath *et al.*, 2003). Remarkably, numerical assessment of mammospheres versus adherent colonies revealed an approximate 90:10 ratio for EpCAM, 20:80 for CALLA, 50:50 for multipotent DP and 10:90 for undifferentiated DN cells. Collectively, these findings suggest that different progenitor properties within sub-populations of even non-tumourigenic cells could potentially give rise to a range of undifferentiated tumours (CALLA, DN) and differentiated ductal carcinomas (EpCAM, DP). Speculatively, these populations could secrete their own extracellular matrix, enabling their attachment to a non-adherent substrate. In fact, bone marrow-derived human mesenchymal stem cells have been demonstrated to adhere to a non-adherent substrate by synthesizing their own ECM components laminin, fibronectin and collagen type I and IV (Kollmer *et al.*, 2012). Importantly, the same study demonstrated an increase in surface expression of CD44 by these cells. This implies that CD44 is functionally important for maintenance of stem/progenitor populations. Taken together, our results are consistent with a model whereby CD44 palmitoylation status correlates with a specific lineage of progenitor cells, and can be summarised as follows:

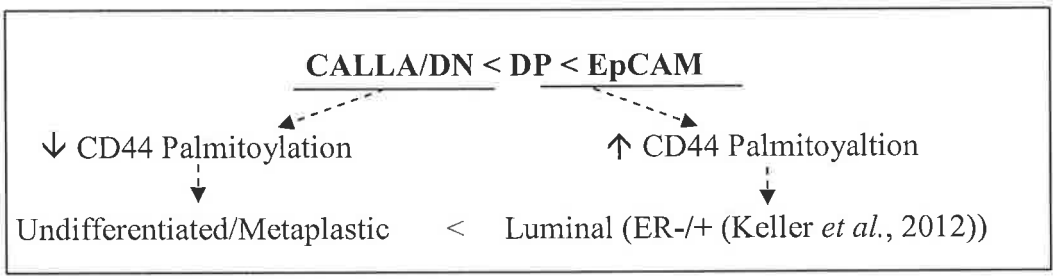

Further insights into the mechanisms of CD44 palmitoylation and its lipid raft affiliation may provide valuable knowledge of breast cancer progression, progenitor-driven or otherwise. Based on our findings, we hypothesise that containment of CD44 within lipid raft domains can reduce, or halt, breast cancer cell migration, and may be of potential therapeutic value.

Chapter 6

General Discussion

6.1 General discussion

Breast cancer is the most frequently diagnosed cancer worldwide and is the leading cause of cancer-related deaths in women (Jemal *et al.*, 2011). In Ireland, it is second most common female cancer after skin cancer, with over 2500 women diagnosed each year (Irish Cancer Society, 2009). Although breast cancer death rates have been declining world-wide since the early 1990s due to nationwide breast cancer screening programs and improvements in treatments (DeSantis *et al.*, 2011), in Ireland an average of 620 women still die from the disease each year (Irish Health Service Executive, 2012).

The majority of breast cancer-related deaths occur due to spreading of the primary tumour cells to distant sites via a series of molecular events termed metastasis. Migration and invasion of tumour cells is one of the critical parameters in dissemination of tumour cells in the early stages of metastasis. Migrating cells undergo numerous molecular and cellular changes in response to changes in the micro-environment, chemokines and growth factors to facilitate metastatic spread (Yilmaz and Christofori, 2010). Yet despite extensive research, much remains to be understood about how cells utilize their migrating machinery to escape the primary tumour and migrate to distant sites. Dynamic regulation of the adhesive properties of cancer cells is crucial in tumour cell migration, thus the study how adhesion molecules are regulated will broaden our understanding of the early events involved in metastasis.

CD44 is an adhesion molecule widely expressed in a variety of tissues. Despite its aberrant expression being implicated in the dissemination of numerous cancers, its upregulation is not always associated with unfavourable outcome and has in fact been demonstrated to have protective effects in some neoplasms (Naor *et al.*, 2002). This illustrates that expressional changes alone are unlikely to resolve contradictions in our current understanding of how CD44 contributes to cancer progression. CD44 is known to be localised to cholesterol- and sphingolipid-enriched regions in the plasma membrane, termed lipid rafts (Ilangumaran *et al.*, 1999). Rafts play a critical regulatory

role in many cellular processes involved in breast cancer (reviewed in (Babina *et al.*, 2011)). Although some doubts over the *in vivo* existence of lipid rafts still persist, these mainly arose due to limitations in the methods used to study these domains. However methodologies for studying these domains are constantly evolving (Simons and Gerl, 2010), and in fact results obtained from studying membrane compositions of various tumours clearly reveal variable lipid contents that correlate with patient prognosis (Chajes *et al.*, 1995; Lanson *et al.*, 1990). Additional *in vivo* evidence for the existence of lipid rafts has been provided using atomic force microscopy of breast tumours (Orsini *et al.*, 2012) and Förster resonance energy transfer (FRET) analysis in porcine brain (Petruzielo *et al.*, 2013). In our studies we reduced the possibility of artifacts by utilising two different methods of lipid raft extraction, the standard isolation in cold non-ionic Triton-X100 detergent (Brown and Rose, 1992) and one under detergent-free conditions (Smart *et al.*, 1995).

Based on early findings in our laboratory (Donatello, 2009), we hypothesised that CD44 localises outside lipid rafts during breast cancer cell migration in order to interact with its cytoskeletal binding partners. Therefore the overall aim of this thesis was to investigate the involvement of lipid rafts in regulating CD44-dependent breast cancer cell migration. To address this, we used *in vitro* models of breast cancer, including breast cancer cell lines of varying invasiveness, patient-derived primary cultures isolated from lumpectomies/mastectomies and finally progenitor populations isolated from the non-tumourigenic cell line MCF-10a. The resulting novel findings have been published (Donatello & Babina *et al.*, 2012) and also submitted for publication (Babina *et al.*, 2013, submitted).

We first set out to investigate a relationship between CD44 localisation in lipid rafts and the invasive potential of a panel of breast cancer cell lines. Contradictory reports exist about the functional outcomes of raft-affiliated CD44. While it has been shown that lipid rafts recruit CD44, Src and integrins to promote cell survival of gastric and colorectal cancers (Lee *et al.*, 2008),

CD44 ligation and its consequent accumulation in rafts actually stimulates apoptosis in acute myeloid leukemia models (Qian *et al.*, 2012). Furthermore, CD44 localisation outside lipid rafts in glioblastoma cells makes it susceptible to metalloproteinase-mediated shedding and subsequent tumour cell migration (Murai *et al.*, 2011). These varying functional effects of CD44 raft localisation could be attributed to cell type dependence, as CD44 interactions with lipid rafts change in different tissues (Neame *et al.*, 1995). Our findings showed that an increase in CD44 raft affiliation is associated with the migration of non-tumourigenic breast cancer cells, while a decrease in its raft affiliation was characteristic of migration in highly invasive cell lines. In support of our hypothesis that a panel of CD44 binding partners was recovered exclusively from non-raft fractions.

This putative translocation of CD44 outside lipid raft domains in breast cancer cells could be aided by variable membrane compositions of cells. Lipid rafts are highly enriched in sphingolipids and cholesterol, while the bulk of the plasma membrane is composed predominantly of phospholipids. Membrane compositions of breast cancer cells vary dramatically. Previous studies of membrane lipid content from breast cancer biopsies revealed that low levels of poly-unsaturated fatty acids, which disrupt lipid rafts (Schley *et al.*, 2007), were associated with a frequent occurrence of metastasis (Lanson *et al.*, 1990). Similar results were obtained in *in vitro* models of breast cancer (Le Moyec *et al.*, 1992). Additionally, an increase in lipids composing lipid rafts has been correlated with a differentiated state, whereas a decrease in these lipids was associated with an undifferentiated state in colonic cell lines (Reynier *et al.*, 1991). Yet the mechanisms whereby membrane lipid composition in breast cancer might be differentially modified from that of normal mammary cells remain elusive.

One way in which CD44 could be targeted outside lipid rafts in breast cancer, but retained in non-tumourigenic mammary cells, is by dynamic modulation of CD44 palmitoylation status. It is believed that CD44 is targeted

to lipid rafts via addition of a palmitoyl moiety to its cysteine residues in the transmembrane and proximal domains (Thankamony and Knudson, 2006). Therefore our next aim was to determine the role of CD44 palmitoylation status in regulating its affiliation with lipid rafts and subsequently influencing breast cancer cell migration. Palmitoylation is a dynamic post-translational modification whereby addition of a fatty acid (palmitate) to transmembrane and proximal cysteine residues of proteins increases their hydrophobicity. This in turn enhances their affinity for highly-hydrophobic lipid rafts (Levental *et al.*, 2010b). Due to the rapid dynamics of this process, palmitoylation has been extensively studied in Ras proteins, which are swiftly lipidated and trafficked between cell membrane and ER/Golgi (Choy *et al.*, 1999). However palmitoylation has not been studied extensively in transmembrane proteins such as CD44.

To date, the most effective targeted approach to study palmitoylation has been via site-directed mutagenesis of predicted protein palmitoylation sites. In adopting this method for our study, we showed that mutation of CD44 palmitoylation sites significantly reduced its raft affiliation in both highly-invasive and non-tumourigenic cell lines, similar to previous observations in kidney epithelial cells (Thankamony and Knudson, 2006). We utilised scratch-wound migration assays as tools to study breast cancer cell migration in palmitoylation-impaired cells, as wound healing events reportedly recapitulate the activation of pathways engaged during normal cell migration (Fenteany *et al.*, 2000). In fact, tumours have been previously described as "wounds that do not heal" (Dvorak, 1986). In agreement with our hypothesis, our findings revealed increased migration of breast cancer cells upon reduction of CD44 palmitoylation via expression of palmitoylation-impaired mutants of CD44. In fact translocation of CD44 outside lipid rafts via decreased palmitoylation was sufficient to mimic epithelial-to-mesenchymal transition (EMT) and to promote migration in non-tumorigenic breast cancer cells. EMT is frequently characterised by disruption of intercellular contact, loss and re-modelling of

cell-cell and cell-matrix adhesions and enhanced motility, all of which assists tumour dissemination (Guarino *et al.*, 2007; Tiwari *et al.*, 2012). Intriguingly, impairment of CD44 palmitoylation in non-tumourigenic cells induced the disappearance of a putative CD44 variant isoform. In a recent study, functional analysis of CD44 alternative splicing during EMT revealed a switch from a variant CD44 isoform to the standard CD44 isoform across a panel of non-tumourigenic epithelial breast cancer cell lines (Brown *et al.*, 2011). Importantly, the overall expression levels of CD44 did not change during EMT in these experiments, as with our findings. Furthermore, expression of the standard CD44 isoform has been strongly associated with a mesenchymal phenotype and recurrent high-grade breast cancer (Brown *et al.*, 2011; Olsson *et al.*, 2011). Although we cannot conclusively confirm that the higher molecular weight CD44 band in our studies was a variant isoform, the molecular weights are consistent with those demonstrated in a study by Brown and colleagues (Brown *et al.*, 2011). Given the important role assigned to EMT in malignant transformation, we speculate that CD44 de-palmitoylation and translocation outside lipid rafts could play a role in the initiating events of that process.

In an attempt to translate results from our CD44 de-palmitoylation and raft translocation mutagenesis experiments into a more physiological setting, we investigated potential ways in which CD44 could be modulated *in vivo*. A number of non-synonymous single-nucleotide polymorphisms (SNPs) were identified that could affect the chemical properties of the CD44 molecule in ways predicted to alter its association with lipid rafts. However no information has yet been published on the correlation of these SNPs with disease. We feel certain that future studies investigating CD44 conserved domain polymorphisms in large populations of breast cancer patients will provide enlightening insights. In the meantime, we also approached CD44 physical de-palmitoylation from a different angle, via global targeting of palmitoylation and de-palmitoylation enzymes. Targeting protein palmitoylation has only

recently emerged as a strategy of potential therapeutic value, being the only lipid modification of proteins that is reversible and highly dynamic (Resh, 1999). Many proteins involved in breast cancer are palmitoylated, including Ras proteins, Src family members and Wnt proteins (Hernandez *et al.*, 2012). Yet little is known about palmitoylation of transmembrane proteins. In this study we have presented novel evidence that CD44 palmitoylation status is indirectly regulated by palmitoylating and de-palmitoylating enzymes. Although in our model we could not monitor enzyme kinetics, we demonstrated a direct link between activity of these enzymes and palmitoylation status of CD44. Using this approach further strengthened our hypothesis, since decreasing CD44 palmitoylation increased breast cancer cell migration and vice versa. Moreover, high gene expression of pro-palmitoylating enzymes correlated with improved recurrence-free survival in a breast cancer patient population, which supports the potential *in vivo* relevance of our studies in targeting CD44 palmitoylation as a strategy to reduce breast cancer cell migration.

Having firmly established a correlation between reductions in CD44 palmitoylation and its raft affiliation and increased breast cancer cell migration, as a final aim we sought to investigate if palmitoylation of CD44 and its raft localisation could be relevant in mammary stem/progenitor populations and breast cancer patient primary cultures. High CD44 surface expression is one of the defining characteristics of stem/progenitor cells (Korkaya *et al.*, 2011), yet its significance is unknown. Broadly, breast cancers have been classified into luminal- and basal-type tumours, based on their gene expression profiles, as described previously (Perou *et al.*, 2000; Sorlie *et al.*, 2001). It has been theorised that luminal type breast cancer forms from luminal progenitors, whereas basal-like lineages arise from basal or myoepithelial progenitors (Polyak, 2007). Our previous work demonstrated that an imbalance in putative progenitor populations, marked by either co-expression or coincident absence of both EpCAM (luminal) and CALLA (myoepithelial) markers, reflects breast

cancer tumour progression (Donatello *et al.*, 2011). In these same populations, this thesis uncovered a decrease in CD44 palmitoylation and raft affiliation in $EpCAM^-CALLA^-$ (DN) progenitors and $EpCAM^-CALLA^+$ populations, both of which correlate with aggressive undifferentiated/metaplastic tumours (Keller *et al.*, 2012; Stingl *et al.*, 2001). In contrast, $EpCAM^+CALLA^+$ (DP) progenitors and $EpCAM^+CALLA^-$ populations had higher CD44 raft affiliation and palmitoylation compared to the other cell types, and these have been shown to correlate with the less aggressive luminal types of breast cancer (Donatello *et al.*, 2011; Keller *et al.*, 2012). Our findings are in agreement with previous hypotheses that myoepithelial tumours lack CALLA expression and may arise from luminal progenitors (Keller *et al.*, 2010; Lim *et al.*, 2009; Proia *et al.*, 2011). These four populations additionally had important functional distinctions, which correlated with CD44 palmitoylation status. Our previous cell line work demonstrated that CD44 localisation inside rafts is affiliated with non-invasive (luminal-like) cells, while CD44 outside lipid rafts correlated with the highly-invasive (basal-like) tumour cells. Furthermore, forcing CD44 outside lipid rafts in non-tumourigenic, luminal-type cells was sufficient to induce the functional appearance of EMT. Given the various populations within the luminal MCF-10a cells, it is intriguing to speculate that CD44 de-palmitoylation and translocation outside rafts could be a factor aiding transformation of luminal breast cells into more myoepithelial, $CALLA^+$ populations, potentially via enrichment in DN progenitors. Our study suggests novel insight into the role of CD44 in stem/progenitor cells and breast cancer progression.

Finally, to begin testing the clinical relevance of CD44 palmitoylation, we examined CD44 palmitoylation status different stages of ductal carcinoma, the most prevalent type of breast cancer (DeSantis *et al.*, 2011). In a selection of representative patient-derived primary breast cultures, we demonstrated that increased palmitoylation of CD44 was associated with non-tumour primary cultures, while those from DCIS and IDC of grades 2 and 3 had reduced levels

of palmitoylated CD44. These findings reflected our results obtained in breast cancer cell lines. Although the sample size used in this study was small, it provided an important initial indicator of relevance of CD44 palmitoylation in breast cancer patients. Furthermore, in accordance with the results discussed previously, it is intriguing to speculate that this could act as a potential biomarker of tumourigenic progression.

In this study overall we demonstrated a novel role of lipid rafts in regulating CD44-mediated breast cancer cell migration, whereby CD44 de-palmitoylation causes its translocation outside lipid rafts and promotes a migratory phenotype. However it remains an unanswered question what causes CD44 to move outside rafts. Lifestyle is a known risk factor for breast cancer initiation and progression (Jemal *et al.*, 2011). Diet and obesity have been linked to breast cancer progression, and certainly influence overall mortality in breast cancer survivors (Thomson, 2012; Vucenik and Stains, 2012). The biological mechanisms underlying this relationship, however, are not well understood. So far the key signalling pathway implicated in linking these factors is the PI3K/Akt cascade (Vucenik and Stains, 2012), which has been implicated in upstream activation of CD44, cytoskeletal protein accumulation and the formation of leading edge protrusions, as demonstrated in a panel of cell lines (Golub and Caroni, 2005). Circulating free fatty acids associated with obesity-promoting diets could strongly influence CD44 localisation within lipid rafts by modifying the lipid content of cell membranes. Additionally, dietary supplementation with poly-unsaturated fatty acids has been shown to disrupt lipid rafts and to affect receptor-mediated cell signalling (Schley *et al.*, 2007). Furthermore, dietary intake of long chain fatty acids results in their incorporation into the cell membrane and increases lipid raft domains, which has been associated with inhibition of mammary carcinogenesis (Stoll, 2002). Obese mammary adipose tissue also creates a chronic inflammatory micro-environment that is beneficial for EMT, migration and invasion (Gilbert and Slingerland, 2013). In turn, consumption of saturated dietary palmitic acid

reduces levels of endogenous cholesterol and aggregation of immune cells, and is correlated with improved immune function (Oguntibeju *et al.*, 2009). Indeed findings outlined in this thesis have demonstrated an anti-proliferative role for palmitic acid selectively in tumour cells, without affecting normal cells. Collectively, these findings suggest an intriguing role for dietary fatty acids in modulating cell membranes in breast cancers, and consequentially the potential sub-membranous localisation of CD44 inside or outside of lipid rafts.

Another question that remains to be answered is what would contain CD44 *inside* lipid rafts, where according to our hypothesis it would exert an inhibitory tone on cell migration. Currently there are no specific molecular or chemical approaches that would induce constitutive palmitoylation of CD44. We have previously attempted to increase CD44 palmitoylation by using broad de-palmitoylation inhibitors, which resulted in reduced breast cancer cell migration (Donatello & Babina *et al.*, 2012). In the current study, our use of pharmacological modifiers of palmitoylation enzymes resulted in increased CD44 palmitoylation and inhibition of breast cancer cell migration. The main caveat of using generic inhibitors is, of course, their lack of specificity. Thus the reductions in cell migration which we observed could be due to collective modulation of the palmitoylation status of numerous proteins. Nonetheless, using various models, we demonstrated that a decrease in palmitoylated CD44 strongly correlated with tumourigenic cells in patient samples, relative to non-tumour sections, as well as increased breast cancer cell migration. Therefore this study has overall offered novel insights into the regulation of CD44-dependent breast cancer cell migration and how manipulation of its palmitoylation status may be of future prognostic and therapeutic value.

6.2 Future directions

Work outlined in this thesis, linking decreased CD44 raft affiliation and palmitoylation with breast cancer cell migration, offers new avenues for studying breast cancer progression and role of CD44 in metastasis. Future planned work consists of:

1. Investigating direct CD44 interactions with a panel of binding partners in lipid rafts and non-raft domains during cell migration in various models (breast cancer cell lines, mutant-expressing cells, primary cultures and progenitor populations) in an attempt to elucidate any potential differences in CD44 interactions with the migrating machinery in non-tumourigenic and invasive breast cancers.

2. Interrogating the mechanisms of CD44 trafficking in and outside lipid rafts via immunofluorescent co-localisation and immunoprecipitation studies of CD44 with various effector molecules and transport proteins.

3. Examining CD44 palmitoylation status of a large cohort of primary cultures (matched or non-matched) in order to confirm our preliminary observations of association of decreased CD44 palmitoylation with aggressive clinical prognosis in breast primary cultures.

4. Defining the effects of dietary fatty acids, saturated and unsaturated, on CD44 palmitoylation, raft localisation and breast cancer cell migration.

References

Acconcia, F., Ascenzi, P., Fabozzi, G., Visca, P., and Marino, M. (2004). S-palmitoylation modulates human estrogen receptor-alpha functions. Biochem Biophys Res Commun *316*, 878-883.

Adams, M.N., Christensen, M.E., He, Y., Waterhouse, N.J., and Hooper, J.D. (2011). The role of palmitoylation in signalling, cellular trafficking and plasma membrane localisation of protease-activated receptor-2. PLoS One *6*, e28018.

Adams, T.E., Epa, V.C., Garrett, T.P., and Ward, C.W. (2000). Structure and function of the type 1 insulin-like growth factor receptor. Cell Mol Life Sci *57*, 1050-1093.

Afify, A., Purnell, P., and Nguyen, L. (2009). Role of CD44s and CD44v6 on human breast cancer cell adhesion, migration, and invasion. Exp Mol Pathol *86*, 95-100.

Aigner, S., Sthoeger, Z.M., Fogel, M., Weber, E., Zarn, J., Ruppert, M., Zeller, Y., Vestweber, D., Stahel, R., Sammar, M., *et al.* (1997). CD24, a mucin-type glycoprotein, is a ligand for P-selectin on human tumor cells. Blood *89*, 3385-3395.

Al-Hajj, M., Wicha, M.S., Benito-Hernandez, A., Morrison, S.J., and Clarke, M.F. (2003). Prospective identification of tumorigenic breast cancer cells. Proc Natl Acad Sci U S A *100*, 3983-3988.

Anavi-Goffer, S., Fleischer, D., Hurst, D.P., Lynch, D.L., Barnett-Norris, J., Shi, S., Lewis, D.L., Mukhopadhyay, S., Howlett, A.C., Reggio, P.H., *et al.* (2007). Helix 8 Leu in the CB1 cannabinoid receptor contributes to selective signal transduction mechanisms. J Biol Chem *282*, 25100-25113.

Annabi, B., Lachambre, M., Bousquet-Gagnon, N., Page, M., Gingras, D., and Beliveau, R. (2001). Localisation of membrane-type 1 matrix metalloproteinase in caveolae membrane domains. Biochem J *353*, 547-553.

Aroui, S., Brahim, S., Hamelin, J., De Waard, M., Breard, J., and Kenani, A. (2009). Conjugation of doxorubicin to cell penetrating peptides sensitizes

human breast MDA-MB 231 cancer cells to endogenous TRAIL-induced apoptosis. Apoptosis *14*, 1352-1365.

Babina, I.S., Donatello, S., Nabi, I.R., and Hopkins, A.M. (2011). Lipid Rafts as Master Regulators of Breast Cancer Cell Function. In Breast Cancer - Carcinogenesis, Cell Growth and Signalling Pathways, M.G.a.E. Gunduz, ed. (InTech), pp. 401-428.

Babuke, T., and Tikkanen, R. (2007). Dissecting the molecular function of reggie/flotillin proteins. Eur J Cell Biol *86*, 525-532.

Baekkeskov, S., and Kanaani, J. (2009). Palmitoylation cycles and regulation of protein function (Review). Mol Membr Biol *26*, 42-54.

Bardou, V.J., Arpino, G., Elledge, R.M., Osborne, C.K., and Clark, G.M. (2003). Progesterone receptor status significantly improves outcome prediction over estrogen receptor status alone for adjuvant endocrine therapy in two large breast cancer databases. J Clin Oncol *21*, 1973-1979.

Belsches-Jablonski, A.P., Biscardi, J.S., Peavy, D.R., Tice, D.A., Romney, D.A., and Parsons, S.J. (2001). Src family kinases and HER2 interactions in human breast cancer cell growth and survival. Oncogene *20*, 1465-1475.

Bennett, K.L., Jackson, D.G., Simon, J.C., Tanczos, E., Peach, R., Modrell, B., Stamenkovic, I., Plowman, G., and Aruffo, A. (1995). CD44 isoforms containing exon V3 are responsible for the presentation of heparin-binding growth factor. J Cell Biol *128*, 687-698.

Bhatnagar, R.S., and Gordon, J.I. (1997). Understanding covalent modifications of proteins by lipids: where cell biology and biophysics mingle. Trends Cell Biol *7*, 14-20.

Bickel, P.E., Scherer, P.E., Schnitzer, J.E., Oh, P., Lisanti, M.P., and Lodish, H.F. (1997). Flotillin and epidermal surface antigen define a new family of caveolae-associated integral membrane proteins. J Biol Chem *272*, 13793-13802.

Bijlmakers, M.J., and Marsh, M. (2003). The on-off story of protein palmitoylation. Trends Cell Biol *13*, 32-42.

Bissell, M.J., and Hines, W.C. (2011). Why don't we get more cancer? A proposed role of the microenvironment in restraining cancer progression. Nat Med *17*, 320-329.

Bissell, M.J., and Radisky, D. (2001). Putting tumours in context. Nat Rev Cancer *1*, 46-54.

Bonnet, D., and Dick, J.E. (1997). Human acute myeloid leukemia is organized as a hierarchy that originates from a primitive hematopoietic cell. Nat Med *3*, 730-737.

Booth, B.W., Boulanger, C.A., and Smith, G.H. (2008). Stem cells and the mammary microenvironment. Breast Dis *29*, 57-67.

Borland, G., Ross, J.A., and Guy, K. (1998). Forms and functions of CD44. Immunology *93*, 139-148.

Bourguignon, L.Y. (2001). CD44-mediated oncogenic signaling and cytoskeleton activation during mammary tumor progression. J Mammary Gland Biol Neoplasia *6*, 287-297.

Bourguignon, L.Y. (2008). Hyaluronan-mediated CD44 activation of RhoGTPase signaling and cytoskeleton function promotes tumor progression. Semin Cancer Biol *18*, 251-259.

Bourguignon, L.Y., Kalomiris, E.L., and Lokeshwar, V.B. (1991). Acylation of the lymphoma transmembrane glycoprotein, GP85, may be required for GP85-ankyrin interaction. J Biol Chem *266*, 11761-11765.

Bourguignon, L.Y., Wong, G., Earle, C., Krueger, K., and Spevak, C.C. (2010). Hyaluronan-CD44 interaction promotes c-Src-mediated twist signaling, microRNA-10b expression, and RhoA/RhoC up-regulation, leading to Rho-kinase-associated cytoskeleton activation and breast tumor cell invasion. J Biol Chem *285*, 36721-36735.

Bourguignon, L.Y., Zhu, D., and Zhu, H. (1998). CD44 isoform-cytoskeleton interaction in oncogenic signaling and tumor progression. Front Biosci *3*, d637-649.

Bourguignon, L.Y., Zhu, H., Chu, A., Iida, N., Zhang, L., and Hung, M.C. (1997). Interaction between the adhesion receptor, CD44, and the oncogene

product, p185HER2, promotes human ovarian tumor cell activation. J Biol Chem *272*, 27913-27918.

Brown, D.A., and London, E. (1998). Functions of lipid rafts in biological membranes. Annu Rev Cell Dev Biol *14*, 111-136.

Brown, D.A., and Rose, J.K. (1992). Sorting of GPI-anchored proteins to glycolipid-enriched membrane subdomains during transport to the apical cell surface. Cell *68*, 533-544.

Brown, R.L., Reinke, L.M., Damerow, M.S., Perez, D., Chodosh, L.A., Yang, J., and Cheng, C. (2011). CD44 splice isoform switching in human and mouse epithelium is essential for epithelial-mesenchymal transition and breast cancer progression. J Clin Invest *121*, 1064-1074.

Buccione, R., Caldieri, G., and Ayala, I. (2009). Invadopodia: specialized tumor cell structures for the focal degradation of the extracellular matrix. Cancer Metastasis Rev *28*, 137-149.

Buglino, J.A., and Resh, M.D. (2012). Palmitoylation of Hedgehog proteins. Vitam Horm *88*, 229-252.

Calikoglu, E., Chavaz, P., Saurat, J.H., and Kaya, G. (2003). Decreased CD44 expression and stromal hyaluronate accumulation in myxoid dermatofibroma. Dermatology *207*, 104-106.

Camp, L.A., and Hofmann, S.L. (1995). Assay and isolation of palmitoyl-protein thioesterase from bovine brain using palmitoylated H-Ras as substrate. Methods Enzymol *250*, 336-347.

Casey, P.J., and Seabra, M.C. (1996). Protein prenyltransferases. J Biol Chem *271*, 5289-5292.

Cavallaro, U., and Christofori, G. (2004). Cell adhesion and signalling by cadherins and Ig-CAMs in cancer. Nat Rev Cancer *4*, 118-132.

Chajes, V., Lanson, M., Fetissof, F., Lhuillery, C., and Bougnoux, P. (1995). Membrane fatty acids of breast carcinoma: contribution of host fatty acids and tumor properties. Int J Cancer *63*, 169-175.

Charafe-Jauffret, E., Ginestier, C., and Birnbaum, D. (2009). Breast cancer stem cells: tools and models to rely on. BMC Cancer *9*, 202.

Cheng, C., Yaffe, M.B., and Sharp, P.A. (2006). A positive feedback loop couples Ras activation and CD44 alternative splicing. Genes Dev *20*, 1715-1720.

Choy, E., Chiu, V.K., Silletti, J., Feoktistov, M., Morimoto, T., Michaelson, D., Ivanov, I.E., and Philips, M.R. (1999). Endomembrane trafficking of ras: the CAAX motif targets proteins to the ER and Golgi. Cell *98*, 69-80.

Clayton, H., Titley, I., and Vivanco, M. (2004). Growth and differentiation of progenitor/stem cells derived from the human mammary gland. Exp Cell Res *297*, 444-460.

Colas, S., Maheo, K., Denis, F., Goupille, C., Hoinard, C., Champeroux, P., Tranquart, F., and Bougnoux, P. (2006). Sensitization by dietary docosahexaenoic acid of rat mammary carcinoma to anthracycline: a role for tumor vascularization. Clin Cancer Res *12*, 5879-5886.

Coleman, D.T., Bigelow, R., and Cardelli, J.A. (2009). Inhibition of fatty acid synthase by luteolin post-transcriptionally down-regulates c-Met expression independent of proteosomal/lysosomal degradation. Mol Cancer Ther *8*, 214-224.

Conneely, O.M., Jericevic, B.M., and Lydon, J.P. (2003). Progesterone receptors in mammary gland development and tumorigenesis. J Mammary Gland Biol Neoplasia *8*, 205-214.

Couldrey, C., Moitra, J., Vinson, C., Anver, M., Nagashima, K., and Green, J. (2002). Adipose tissue: a vital *in vivo* role in mammary gland development but not differentiation. Dev Dyn *223*, 459-468.

Curto, M., and McClatchey, A.I. (2004). Ezrin...a metastatic detERMinant? Cancer Cell *5*, 113-114.

de Laurentiis, A., Donovan, L., and Arcaro, A. (2007). Lipid rafts and caveolae in signaling by growth factor receptors. Open Biochem J *1*, 12-32.

Debnath, J., Muthuswamy, S.K., and Brugge, J.S. (2003). Morphogenesis and oncogenesis of MCF-10A mammary epithelial acini grown in three-dimensional basement membrane cultures. Methods *30*, 256-268.

Deborde, S., Perret, E., Gravotta, D., Deora, A., Salvarezza, S., Schreiner, R., and Rodriguez-Boulan, E. (2008). Clathrin is a key regulator of basolateral polarity. Nature *452*, 719-723.

Dekker, F.J., Rocks, O., Vartak, N., Menninger, S., Hedberg, C., Balamurugan, R., Wetzel, S., Renner, S., Gerauer, M., Scholermann, B., *et al.* (2010). Small-molecule inhibition of APT-1 affects Ras localisation and signaling. Nat Chem Biol *6*, 449-456.

Delpech, B., Chevallier, B., Reinhardt, N., Julien, J.P., Duval, C., Maingonnat, C., Bastit, P., and Asselain, B. (1990). Serum hyaluronan (hyaluronic acid) in breast cancer patients. Int J Cancer *46*, 388-390.

DeSantis, C., Siegel, R., Bandi, P., and Jemal, A. (2011). Breast cancer statistics, 2011. CA Cancer J Clin *61*, 409-418.

Diaz, L.K., Zhou, X., Wright, E.T., Cristofanilli, M., Smith, T., Yang, Y., Sneige, N., Sahin, A., and Gilcrease, M.Z. (2005). CD44 expression is associated with increased survival in node-negative invasive breast carcinoma. Clin Cancer Res *11*, 3309-3314.

Donatello, S. (2009). Extrinsic and intrinsic regulation of breast cancer progression - promoting an aggressive phenotype via alterations in cellular populations and subcellular compartments. In Department of Surgery (Dublin Royal College of Surgeons in Ireland).

Donatello, S., Babina, I. S., Hazelwood, L.D., Hill, A.D., Nabi, I.R., and Hopkins, A.M. (2012). Lipid Raft Association Restricts CD44-Ezrin Interaction and Promotion of Breast Cancer Cell Migration. Am J Pathol.

Donatello, S., Hudson, L., Cottell, D.C., Blanco, A., Aurrekoetxea, I., Shelly, M.J., Dervan, P.A., Kell, M.R., Stokes, M., Hill, A.D., *et al.* (2011). An imbalance in progenitor cell populations reflects tumour progression in breast cancer primary culture models. J Exp Clin Cancer Res *30*, 45.

Dontu, G., Al-Hajj, M., Abdallah, W.M., Clarke, M.F., and Wicha, M.S. (2003). Stem cells in normal breast development and breast cancer. Cell Prolif *36 Suppl 1*, 59-72.

Dontu, G., Jackson, K.W., McNicholas, E., Kawamura, M.J., Abdallah, W.M., and Wicha, M.S. (2004). Role of Notch signaling in cell-fate determination of human mammary stem/progenitor cells. Breast Cancer Res *6*, R605-615.

Ducker, C.E., Griffel, L.K., Smith, R.A., Keller, S.N., Zhuang, Y., Xia, Z., Diller, J.D., and Smith, C.D. (2006). Discovery and characterization of inhibitors of human palmitoyl acyltransferases. Mol Cancer Ther *5*, 1647-1659.

Duncan, J.A., and Gilman, A.G. (1998). A cytoplasmic acyl-protein thioesterase that removes palmitate from G protein alpha subunits and p21(RAS). J Biol Chem *273*, 15830-15837.

Dunphy, J.T., Greentree, W.K., and Linder, M.E. (2001). Enrichment of G-protein palmitoyltransferase activity in low density membranes: *in vitro* reconstitution of Galphai to these domains requires palmitoyltransferase activity. J Biol Chem *276*, 43300-43304.

Dvorak, H.F. (1986). Tumors: wounds that do not heal. Similarities between tumor stroma generation and wound healing. N Engl J Med *315*, 1650-1659.

Elliott, B.E., Meens, J.A., SenGupta, S.K., Louvard, D., and Arpin, M. (2005). The membrane cytoskeletal crosslinker ezrin is required for metastasis of breast carcinoma cells. Breast Cancer Res *7*, R365-373.

Elnagar, A.Y., Sylvester, P.W., and El Sayed, K.A. (2011). (-)-Oleocanthal as a c-Met Inhibitor for the Control of Metastatic Breast and Prostate Cancers. Planta Med.

Elston, C.W., and Ellis, I.O. (2002). Pathological prognostic factors in breast cancer. I. The value of histological grade in breast cancer: experience from a large study with long-term follow-up. Histopathology *41*, 154-161.

Eroles, P., Bosch, A., Perez-Fidalgo, J.A., and Lluch, A. (2012). Molecular biology in breast cancer: intrinsic subtypes and signaling pathways. Cancer Treat Rev *38*, 698-707.

Everson, W.V., and Smart, E.J. (2006). Caveolin and its Role in Intracellular Chaperone Complexes (Wiley-VCH Verlag GmbH & Co. KGaA).

Fan, J.Y., Carpentier, J.L., van Obberghen, E., Grunfeld, C., Gorden, P., and Orci, L. (1983). Morphological changes of the 3T3-L1 fibroblast plasma membrane upon differentiation to the adipocyte form. J Cell Sci *61*, 219-230.

Fenteany, G., Janmey, P.A., and Stossel, T.P. (2000). Signaling pathways and cell mechanics involved in wound closure by epithelial cell sheets. Curr Biol *10*, 831-838.

Fiedler, K., Kobayashi, T., Kurzchalia, T.V., and Simons, K. (1993). Glycosphingolipid-enriched, detergent-insoluble complexes in protein sorting in epithelial cells. Biochemistry *32*, 6365-6373.

Folsch, H., Mattila, P.E., and Weisz, O.A. (2009). Taking the scenic route: biosynthetic traffic to the plasma membrane in polarized epithelial cells. Traffic *10*, 972-981.

Forrester, J.V., and Wilkinson, P.C. (1981). Inhibition of leukocyte locomotion by hyaluronic acid. J Cell Sci *48*, 315-331.

Fra, A.M., Masserini, M., Palestini, P., Sonnino, S., and Simons, K. (1995). A photo-reactive derivative of ganglioside GM1 specifically cross-links VIP21-caveolin on the cell surface. FEBS Lett *375*, 11-14.

Friedl, P., and Wolf, K. (2003). Tumour-cell invasion and migration: diversity and escape mechanisms. Nat Rev Cancer *3*, 362-374.

Friedrichs, K., Franke, F., Lisboa, B.W., Kugler, G., Gille, I., Terpe, H.J., Holzel, F., Maass, H., and Gunthert, U. (1995). CD44 isoforms correlate with cellular differentiation but not with prognosis in human breast cancer. Cancer Res *55*, 5424-5433.

Furuchi, T., and Anderson, R.G. (1998). Cholesterol depletion of caveolae causes hyperactivation of extracellular signal-related kinase (ERK). J Biol Chem *273*, 21099-21104.

Galbiati, F., Engelman, J.A., Volonte, D., Zhang, X.L., Minetti, C., Li, M., Hou, H., Jr., Kneitz, B., Edelmann, W., and Lisanti, M.P. (2001). Caveolin-3 null mice show a loss of caveolae, changes in the microdomain distribution of the dystrophin-glycoprotein complex, and t-tubule abnormalities. J Biol Chem *276*, 21425-21433.

Galbiati, F., Volonte, D., Engelman, J.A., Watanabe, G., Burk, R., Pestell, R.G., and Lisanti, M.P. (1998). Targeted downregulation of caveolin-1 is sufficient to drive cell transformation and hyperactivate the p42/44 MAP kinase cascade. EMBO J *17*, 6633-6648.

Gao, A.C., Lou, W., Dong, J.T., and Isaacs, J.T. (1997). CD44 is a metastasis suppressor gene for prostatic cancer located on human chromosome 11p13. Cancer Res *57*, 846-849.

Gastaldi, S., Comoglio, P.M., and Trusolino, L. (2010). The Met oncogene and basal-like breast cancer: another culprit to watch out for? Breast Cancer Res *12*, 208.

Germain, E., Chajes, V., Cognault, S., Lhuillery, C., and Bougnoux, P. (1998). Enhancement of doxorubicin cytotoxicity by polyunsaturated fatty acids in the human breast tumor cell line MDA-MB-231: relationship to lipid peroxidation. Int J Cancer *75*, 578-583.

Ghosh, R.N., Mallet, W.G., Soe, T.T., McGraw, T.E., and Maxfield, F.R. (1998). An endocytosed TGN38 chimeric protein is delivered to the TGN after trafficking through the endocytic recycling compartment in CHO cells. J Cell Biol *142*, 923-936.

Gilbert, C.A., and Slingerland, J.M. (2013). Cytokines, obesity, and cancer: new insights on mechanisms linking obesity to cancer risk and progression. Annu Rev Med *64*, 45-57.

Gimona, M., Buccione, R., Courtneidge, S.A., and Linder, S. (2008). Assembly and biological role of podosomes and invadopodia. Curr Opin Cell Biol *20*, 235-241.

Glomset, J.A., Gelb, M.H., and Farnsworth, C.C. (1990). Prenyl proteins in eukaryotic cells: a new type of membrane anchor. Trends Biochem Sci *15*, 139-142.

Golub, T., and Caroni, P. (2005). PI(4,5)P2-dependent microdomain assemblies capture microtubules to promote and control leading edge motility. J Cell Biol *169*, 151-165.

Gong, M., Wilson, M., Kelly, T., Su, W., Dressman, J., Kincer, J., Matveev, S.V., Guo, L., Guerin, T., Li, X.A., *et al.* (2003). HDL-associated estradiol stimulates endothelial NO synthase and vasodilation in an SR-BI-dependent manner. J Clin Invest *111*, 1579-1587.

Goodfellow, P.N., Banting, G., Wiles, M.V., Tunnacliffe, A., Parkar, M., Solomon, E., Dalchau, R., and Fabre, J.W. (1982). The gene, MIC4, which controls expression of the antigen defined by monoclonal antibody F10.44.2, is on human chromosome 11. Eur J Immunol *12*, 659-663.

Gormer, K., Burger, M., Kruijtzer, J.A., Vetter, I., Vartak, N., Brunsveld, L., Bastiaens, P.I., Liskamp, R.M., Triola, G., and Waldmann, H. (2012). Chemical-biological exploration of the limits of the Ras de- and repalmitoylating machinery. Chembiochem *13*, 1017-1023.

Gotte, M., and Yip, G.W. (2006). Heparanase, hyaluronan, and CD44 in cancers: a breast carcinoma perspective. Cancer Res *66*, 10233-10237.

Greaves, J., and Chamberlain, L.H. (2007). Palmitoylation-dependent protein sorting. J Cell Biol *176*, 249-254.

Guarino, M., Rubino, B., and Ballabio, G. (2007). The role of epithelial-mesenchymal transition in cancer pathology. Pathology *39*, 305-318.

Guarneri, V., and Conte, P. (2009). Metastatic breast cancer: therapeutic options according to molecular subtypes and prior adjuvant therapy. Oncologist *14*, 645-656.

Gunthert, U. (1996). CD44 in malignant disorders. Curr Top Microbiol Immunol *213 (Pt 1)*, 271-285.

Gyorffy, B., Lanczky, A., Eklund, A.C., Denkert, C., Budczies, J., Li, Q., and Szallasi, Z. (2010). An online survival analysis tool to rapidly assess the effect of 22,277 genes on breast cancer prognosis using microarray data of 1,809 patients. Breast Cancer Res Treat *123*, 725-731.

Hancock, J.F., Magee, A.I., Childs, J.E., and Marshall, C.J. (1989). All ras proteins are polyisoprenylated but only some are palmitoylated. Cell *57*, 1167-1177.

Hardy, S., El-Assaad, W., Przybytkowski, E., Joly, E., Prentki, M., and Langelier, Y. (2003). Saturated fatty acid-induced apoptosis in MDA-MB-231 breast cancer cells. A role for cardiolipin. J Biol Chem *278*, 31861-31870.

Heider, K.H., Kuthan, H., Stehle, G., and Munzert, G. (2004). CD44v6: a target for antibody-based cancer therapy. Cancer Immunol Immunother *53*, 567-579.

Hens, J.R., Dann, P., Zhang, J.P., Harris, S., Robinson, G.W., and Wysolmerski, J. (2007). BMP4 and PTHrP interact to stimulate ductal outgrowth during embryonic mammary development and to inhibit hair follicle induction. Development *134*, 1221-1230.

Hens, J.R., and Wysolmerski, J.J. (2005). Key stages of mammary gland development: molecular mechanisms involved in the formation of the embryonic mammary gland. Breast Cancer Res *7*, 220-224.

Hernandez, J.L., Majmudar, J.D., and Martin, B.R. (2012). Profiling and inhibiting reversible palmitoylation. Curr Opin Chem Biol.

Herrera-Gayol, A., and Jothy, S. (1999). Adhesion proteins in the biology of breast cancer: contribution of CD44. Exp Mol Pathol *66*, 149-156.

Herschkowitz, J.I., Simin, K., Weigman, V.J., Mikaelian, I., Usary, J., Hu, Z., Rasmussen, K.E., Jones, L.P., Assefnia, S., Chandrasekharan, S., *et al.* (2007). Identification of conserved gene expression features between murine mammary carcinoma models and human breast tumors. Genome Biol *8*, R76.

Hill, A., McFarlane, S., Mulligan, K., Gillespie, H., Draffin, J.E., Trimble, A., Ouhtit, A., Johnston, P.G., Harkin, D.P., McCormick, D., *et al.* (2006). Cortactin underpins CD44-promoted invasion and adhesion of breast cancer cells to bone marrow endothelial cells. Oncogene *25*, 6079-6091.

Hinck, L., and Silberstein, G.B. (2005). Key stages in mammary gland development: the mammary end bud as a motile organ. Breast Cancer Res *7*, 245-251.

Hiraguri, S., Godfrey, T., Nakamura, H., Graff, J., Collins, C., Shayesteh, L., Doggett, N., Johnson, K., Wheelock, M., Herman, J., *et al.* (1998).

Mechanisms of inactivation of E-cadherin in breast cancer cell lines. Cancer Res *58*, 1972-1977.

Hitosugi, T., Sato, M., Sasaki, K., and Umezawa, Y. (2007). Lipid raft specific knockdown of SRC family kinase activity inhibits cell adhesion and cell cycle progression of breast cancer cells. Cancer Res *67*, 8139-8148.

Horak, C.E., Lee, J.H., Marshall, J.C., Shreeve, S.M., and Steeg, P.S. (2008). The role of metastasis suppressor genes in metastatic dormancy. APMIS *116*, 586-601.

Hughes, L., Malone, C., Chumsri, S., Burger, A.M., and McDonnell, S. (2008). Characterisation of breast cancer cell lines and establishment of a novel isogenic subclone to study migration, invasion and tumourigenicity. Clin Exp Metastasis *25*, 549-557.

Humphreys, R.C., Krajewska, M., Krnacik, S., Jaeger, R., Weiher, H., Krajewski, S., Reed, J.C., and Rosen, J.M. (1996). Apoptosis in the terminal endbud of the murine mammary gland: a mechanism of ductal morphogenesis. Development *122*, 4013-4022.

Ilangumaran, S., Borisch, B., and Hoessli, D.C. (1999). Signal transduction via CD44: role of plasma membrane microdomains. Leuk Lymphoma *35*, 455-469.

Ilangumaran, S., and Hoessli, D.C. (1998). Effects of cholesterol depletion by cyclodextrin on the sphingolipid microdomains of the plasma membrane. Biochem J *335 (Pt 2)*, 433-440.

Jemal, A., Bray, F., Center, M.M., Ferlay, J., Ward, E., and Forman, D. (2011). Global cancer statistics. CA Cancer J Clin *61*, 69-90.

Jennings, B.C., Nadolski, M.J., Ling, Y., Baker, M.B., Harrison, M.L., Deschenes, R.J., and Linder, M.E. (2009). 2-Bromopalmitate and 2-(2-hydroxy-5-nitro-benzylidene)-benzo[b]thiophen-3-one inhibit DHHC-mediated palmitoylation *in vitro*. J Lipid Res *50*, 233-242.

Jiang, W.G., Puntis, M.C., and Hallett, M.B. (1994). Molecular and cellular basis of cancer invasion and metastasis: implications for treatment. Br J Surg *81*, 1576-1590.

Kalish, E.D., Iida, N., Moffat, F.L., and Bourguignon, L.Y. (1999). A new CD44V3-containing isoform is involved in tumor cell growth and migration during human breast carcinoma progression. Front Biosci *4*, A1-8.

Kang, R., Wan, J., Arstikaitis, P., Takahashi, H., Huang, K., Bailey, A.O., Thompson, J.X., Roth, A.F., Drisdel, R.C., Mastro, R., *et al.* (2008). Neural palmitoyl-proteomics reveals dynamic synaptic palmitoylation. Nature *456*, 904-909.

Kaufmann, M., Heider, K.H., Sinn, H.P., von Minckwitz, G., Ponta, H., and Herrlich, P. (1995). CD44 variant exon epitopes in primary breast cancer and length of survival. Lancet *345*, 615-619.

Kaya, G., Rodriguez, I., Jorcano, J.L., Vassalli, P., and Stamenkovic, I. (1999). Cutaneous delayed-type hypersensitivity response is inhibited in transgenic mice with keratinocyte-specific CD44 expression defect. J Invest Dermatol *113*, 137-138.

Keller, P.J., Arendt, L.M., Skibinski, A., Logvinenko, T., Klebba, I., Dong, S., Smith, A.E., Prat, A., Perou, C.M., Gilmore, H., *et al.* (2012). Defining the cellular precursors to human breast cancer. Proc Natl Acad Sci U S A *109*, 2772-2777.

Keller, P.J., Lin, A.F., Arendt, L.M., Klebba, I., Jones, A.D., Rudnick, J.A., DiMeo, T.A., Gilmore, H., Jefferson, D.M., Graham, R.A., *et al.* (2010). Mapping the cellular and molecular heterogeneity of normal and malignant breast tissues and cultured cell lines. Breast Cancer Res *12*, R87.

Kennecke, H., Yerushalmi, R., Woods, R., Cheang, M.C., Voduc, D., Speers, C.H., Nielsen, T.O., and Gelmon, K. (2010). Metastatic behavior of breast cancer subtypes. J Clin Oncol *28*, 3271-3277.

Klingbeil, P., Natrajan, R., Everitt, G., Vatcheva, R., Marchio, C., Palacios, J., Buerger, H., Reis-Filho, J.S., and Isacke, C.M. (2010). CD44 is overexpressed in basal-like breast cancers but is not a driver of 11p13 amplification. Breast Cancer Res Treat *120*, 95-109.

Knudson, W., Biswas, C., Li, X.Q., Nemec, R.E., and Toole, B.P. (1989). The role and regulation of tumour-associated hyaluronan. Ciba Found Symp *143*, 150-159; discussion 159-169, 281-155.

Knudson, W., Chow, G., and Knudson, C.B. (2002). CD44-mediated uptake and degradation of hyaluronan. Matrix Biol *21*, 15-23.

Kojic, L.D., Joshi, B., Lajoie, P., Le, P.U., Cox, M.E., Turbin, D.A., Wiseman, S.M., and Nabi, I.R. (2007). Raft-dependent endocytosis of autocrine motility factor is phosphatidylinositol 3-kinase-dependent in breast carcinoma cells. J Biol Chem *282*, 29305-29313.

Kollmer, M., Keskar, V., Hauk, T.G., Collins, J.M., Russell, B., and Gemeinhart, R.A. (2012). Stem cell-derived extracellular matrix enables survival and multilineage differentiation within superporous hydrogels. Biomacromolecules *13*, 963-973.

Korkaya, H., Liu, S., and Wicha, M.S. (2011). Breast cancer stem cells, cytokine networks, and the tumor microenvironment. J Clin Invest *121*, 3804-3809.

Kuukasjarvi, T., Tanner, M., Pennanen, S., Karhu, R., Kallioniemi, O.P., and Isola, J. (1997). Genetic changes in intraductal breast cancer detected by comparative genomic hybridization. Am J Pathol *150*, 1465-1471.

Kyte, J., and Doolittle, R.F. (1982). A simple method for displaying the hydropathic character of a protein. J Mol Biol *157*, 105-132.

Lajoie, P., and Nabi, I.R. (2010). Lipid rafts, caveolae, and their endocytosis. Int Rev Cell Mol Biol *282*, 135-163.

Lanson, M., Bougnoux, P., Besson, P., Lansac, J., Hubert, B., Couet, C., and Le Floch, O. (1990). N-6 polyunsaturated fatty acids in human breast carcinoma phosphatidylethanolamine and early relapse. Br J Cancer *61*, 776-778.

Laude, A.J., and Prior, I.A. (2008). Palmitoylation and localisation of RAS isoforms are modulated by the hypervariable linker domain. J Cell Sci *121*, 421-427.

Lauffenburger, D.A., and Horwitz, A.F. (1996). Cell migration: a physically integrated molecular process. Cell *84*, 359-369.

Le Moyec, L., Tatoud, R., Eugene, M., Gauville, C., Primot, I., Charlemagne, D., and Calvo, F. (1992). Cell and membrane lipid analysis by proton magnetic resonance spectroscopy in five breast cancer cell lines. Br J Cancer *66*, 623-628.

Lee, J.L., Wang, M.J., Sudhir, P.R., and Chen, J.Y. (2008). CD44 engagement promotes matrix-derived survival through the CD44-SRC-integrin axis in lipid rafts. Mol Cell Biol *28*, 5710-5723.

Legg, J.W., Lewis, C.A., Parsons, M., Ng, T., and Isacke, C.M. (2002). A novel PKC-regulated mechanism controls CD44 ezrin association and directional cell motility. Nat Cell Biol *4*, 399-407.

Lesley, J., English, N., Charles, C., and Hyman, R. (2000). The role of the CD44 cytoplasmic and transmembrane domains in constitutive and inducible hyaluronan binding. Eur J Immunol *30*, 245-253.

Levental, I., Grzybek, M., and Simons, K. (2010a). Greasing their way: lipid modifications determine protein association with membrane rafts. Biochemistry *49*, 6305-6316.

Levental, I., Lingwood, D., Grzybek, M., Coskun, U., and Simons, K. (2010b). Palmitoylation regulates raft affinity for the majority of integral raft proteins. Proc Natl Acad Sci U S A *107*, 22050-22054.

Levy-Lahad, E., and Friedman, E. (2007). Cancer risks among BRCA1 and BRCA2 mutation carriers. Br J Cancer *96*, 11-15.

Li, Y., Martin, B.R., Cravatt, B.F., and Hofmann, S.L. (2012). DHHC5 protein palmitoylates flotillin-2 and is rapidly degraded on induction of neuronal differentiation in cultured cells. J Biol Chem *287*, 523-530.

Lim, E., Vaillant, F., Wu, D., Forrest, N.C., Pal, B., Hart, A.H., Asselin-Labat, M.L., Gyorki, D.E., Ward, T., Partanen, A., *et al.* (2009). Aberrant luminal progenitors as the candidate target population for basal tumor development in BRCA1 mutation carriers. Nat Med *15*, 907-913.

Lin, C., Wu, Z., Lin, X., Yu, C., Shi, T., Zeng, Y., Wang, X., Li, J., and Song, L. (2011). Knockdown of FLOT1 impairs cell proliferation and tumorigenicity in breast cancer through upregulation of FOXO3a. Clin Cancer Res *17*, 3089-3099.

Linder, M.E., and Deschenes, R.J. (2007). Palmitoylation: policing protein stability and traffic. Nat Rev Mol Cell Biol *8*, 74-84.

Liu, J., Deyoung, S.M., Zhang, M., Dold, L.H., and Saltiel, A.R. (2005). The stomatin/prohibitin/flotillin/HflK/C domain of flotillin-1 contains distinct sequences that direct plasma membrane localisation and protein interactions in 3T3-L1 adipocytes. J Biol Chem *280*, 16125-16134.

Liu, R., Wang, X., Chen, G.Y., Dalerba, P., Gurney, A., Hoey, T., Sherlock, G., Lewicki, J., Shedden, K., and Clarke, M.F. (2007). The prognostic role of a gene signature from tumorigenic breast-cancer cells. N Engl J Med *356*, 217-226.

Liu, S., Clouthier, S.G., and Wicha, M.S. (2012). Role of microRNAs in the regulation of breast cancer stem cells. J Mammary Gland Biol Neoplasia *17*, 15-21.

Liu, S., Dontu, G., Mantle, I.D., Patel, S., Ahn, N.S., Jackson, K.W., Suri, P., and Wicha, M.S. (2006). Hedgehog signaling and Bmi-1 regulate self-renewal of normal and malignant human mammary stem cells. Cancer Res *66*, 6063-6071.

Lobo, S., Greentree, W.K., Linder, M.E., and Deschenes, R.J. (2002). Identification of a Ras palmitoyltransferase in Saccharomyces cerevisiae. J Biol Chem *277*, 41268-41273.

Lopez, J.I., Camenisch, T.D., Stevens, M.V., Sands, B.J., McDonald, J., and Schroeder, J.A. (2005). CD44 attenuates metastatic invasion during breast cancer progression. Cancer Res *65*, 6755-6763.

Louderbough, J.M., and Schroeder, J.A. (2011). Understanding the dual nature of CD44 in breast cancer progression. Mol Cancer Res *9*, 1573-1586.

Lu, P., Weaver, V.M., and Werb, Z. (2012). The extracellular matrix: a dynamic niche in cancer progression. J Cell Biol *196*, 395-406.

MacMahon, B., Cole, P., Lin, T.M., Lowe, C.R., Mirra, A.P., Ravnihar, B., Salber, E.J., Valaoras, V.G., and Yuasa, S. (1970). Age at first birth and breast cancer risk. Bull World Health Organ *43*, 209-221.

Magee, A.I., and Seabra, M.C. (2003). Are prenyl groups on proteins sticky fingers or greasy handles? Biochem J *376*, e3-4.

Mani, S.A., Guo, W., Liao, M.J., Eaton, E.N., Ayyanan, A., Zhou, A.Y., Brooks, M., Reinhard, F., Zhang, C.C., Shipitsin, M., *et al.* (2008). The epithelial-mesenchymal transition generates cells with properties of stem cells. Cell *133*, 704-715.

Martin, T.A., Harrison, G., Mansel, R.E., and Jiang, W.G. (2003). The role of the CD44/ezrin complex in cancer metastasis. Crit Rev Oncol Hematol *46*, 165-186.

May, C.D., Sphyris, N., Evans, K.W., Werden, S.J., Guo, W., and Mani, S.A. (2011). Epithelial-mesenchymal transition and cancer stem cells: a dangerously dynamic duo in breast cancer progression. Breast Cancer Res *13*, 202.

McGuire, T.F., Corey, S.J., and Sebti, S.M. (1993). Lovastatin inhibits platelet-derived growth factor (PDGF) stimulation of phosphatidylinositol 3-kinase activity as well as association of p85 subunit to tyrosine-phosphorylated PDGF receptor. J Biol Chem *268*, 22227-22230.

Mellman, I., and Nelson, W.J. (2008). Coordinated protein sorting, targeting and distribution in polarized cells. Nat Rev Mol Cell Biol *9*, 833-845.

Menendez, J.A., Lupu, R., and Colomer, R. (2005). Exogenous supplementation with omega-3 polyunsaturated fatty acid docosahexaenoic acid (DHA; 22:6n-3) synergistically enhances taxane cytotoxicity and downregulates Her-2/neu (c-erbB-2) oncogene expression in human breast cancer cells. Eur J Cancer Prev *14*, 263-270.

Meng, Y., Lu, Z., Yu, S., Zhang, Q., Ma, Y., and Chen, J. (2010). Ezrin promotes invasion and metastasis of pancreatic cancer cells. J Transl Med *8*, 61.

Mira, E., Lacalle, R.A., Buesa, J.M., de Buitrago, G.G., Jimenez-Baranda, S., Gomez-Mouton, C., Martinez, A.C., and Manes, S. (2004). Secreted MMP9

promotes angiogenesis more efficiently than constitutive active MMP9 bound to the tumor cell surface. J Cell Sci *117*, 1847-1857.

Mitchell, D.A., Vasudevan, A., Linder, M.E., and Deschenes, R.J. (2006). Protein palmitoylation by a family of DHHC protein S-acyltransferases. J Lipid Res *47*, 1118-1127.

Moelans, C.B., de Wegers, R.A., Monsuurs, H.N., Maess, A.H., and van Diest, P.J. (2011). Molecular differences between ductal carcinoma in situ and adjacent invasive breast carcinoma: a multiplex ligation-dependent probe amplification study. Cell Oncol (Dordr) *34*, 475-482.

Molyneux, G., Regan, J., and Smalley, M.J. (2007). Mammary stem cells and breast cancer. Cell Mol Life Sci *64*, 3248-3260.

Montales, M.T., Rahal, O.M., Kang, J., Rogers, T.J., Prior, R.L., Wu, X., and Simmen, R.C. (2012). Repression of mammosphere formation of human breast cancer cells by soy isoflavone genistein and blueberry polyphenolic acids suggests diet-mediated targeting of cancer stem-like/progenitor cells. Carcinogenesis *33*, 652-660.

Montgomery, N., Hill, A., McFarlane, S., Neisen, J., O'Grady, A., Conlon, S., Jirstrom, K., Kay, E.W., and Waugh, D.J. (2012). CD44 enhances invasion of basal-like breast cancer cells by upregulating serine protease and collagen-degrading enzymatic expression and activity. Breast Cancer Res *14*, R84.

Morel, A.P., Lievre, M., Thomas, C., Hinkal, G., Ansieau, S., and Puisieux, A. (2008). Generation of breast cancer stem cells through epithelial-mesenchymal transition. PLoS One *3*, e2888.

Mori, T., Kitano, K., Terawaki, S., Maesaki, R., Fukami, Y., and Hakoshima, T. (2008). Structural basis for CD44 recognition by ERM proteins. J Biol Chem *283*, 29602-29612.

Morrison, H., Sherman, L.S., Legg, J., Banine, F., Isacke, C., Haipek, C.A., Gutmann, D.H., Ponta, H., and Herrlich, P. (2001). The NF2 tumor suppressor gene product, merlin, mediates contact inhibition of growth through interactions with CD44. Genes Dev *15*, 968-980.

Morrison, H., Sperka, T., Manent, J., Giovannini, M., Ponta, H., and Herrlich, P. (2007). Merlin/neurofibromatosis type 2 suppresses growth by inhibiting the activation of Ras and Rac. Cancer Res *67*, 520-527.

Morrow, I.C., and Parton, R.G. (2005). Flotillins and the PHB domain protein family: rafts, worms and anaesthetics. Traffic *6*, 725-740.

Morrow, I.C., Rea, S., Martin, S., Prior, I.A., Prohaska, R., Hancock, J.F., James, D.E., and Parton, R.G. (2002). Flotillin-1/reggie-2 traffics to surface raft domains via a novel golgi-independent pathway. Identification of a novel membrane targeting domain and a role for palmitoylation. J Biol Chem *277*, 48834-48841.

Murai, T., Maruyama, Y., Mio, K., Nishiyama, H., Suga, M., and Sato, C. (2011). Low cholesterol triggers membrane microdomain-dependent CD44 shedding and suppresses tumor cell migration. J Biol Chem *286*, 1999-2007.

Murai, T., Miyazaki, Y., Nishinakamura, H., Sugahara, K.N., Miyauchi, T., Sako, Y., Yanagida, T., and Miyasaka, M. (2004). Engagement of CD44 promotes Rac activation and CD44 cleavage during tumor cell migration. J Biol Chem *279*, 4541-4550.

Murata, M., Peranen, J., Schreiner, R., Wieland, F., Kurzchalia, T.V., and Simons, K. (1995). VIP21/caveolin is a cholesterol-binding protein. Proc Natl Acad Sci U S A *92*, 10339-10343.

Murohashi, M., Hinohara, K., Kuroda, M., Isagawa, T., Tsuji, S., Kobayashi, S., Umezawa, K., Tojo, A., Aburatani, H., and Gotoh, N. (2010). Gene set enrichment analysis provides insight into novel signalling pathways in breast cancer stem cells. Br J Cancer *102*, 206-212.

Murphy, C.G., and Morris, P.G. (2012). Recent advances in novel targeted therapies for HER2-positive breast cancer. Anticancer Drugs *23*, 765-776.

Naor, D., Nedvetzki, S., Golan, I., Melnik, L., and Faitelson, Y. (2002). CD44 in cancer. Crit Rev Clin Lab Sci *39*, 527-579.

Naor, D., Wallach-Dayan, S.B., Zahalka, M.A., and Sionov, R.V. (2008). Involvement of CD44, a molecule with a thousand faces, in cancer dissemination. Semin Cancer Biol *18*, 260-267.

Neame, S.J., and Isacke, C.M. (1992). Phosphorylation of CD44 *in vivo* requires both Ser323 and Ser325, but does not regulate membrane localisation or cytoskeletal interaction in epithelial cells. EMBO J *11*, 4733-4738.

Neame, S.J., Uff, C.R., Sheikh, H., Wheatley, S.C., and Isacke, C.M. (1995). CD44 exhibits a cell type dependent interaction with triton X-100 insoluble, lipid rich, plasma membrane domains. J Cell Sci *108 (Pt 9)*, 3127-3135.

Negi, L.M., Talegaonkar, S., Jaggi, M., Ahmad, F.J., Iqbal, Z., and Khar, R.K. (2012). Role of CD44 in tumour progression and strategies for targeting. J Drug Target *20*, 561-573.

Neumann-Giesen, C., Falkenbach, B., Beicht, P., Claasen, S., Luers, G., Stuermer, C.A., Herzog, V., and Tikkanen, R. (2004). Membrane and raft association of reggie-1/flotillin-2: role of myristoylation, palmitoylation and oligomerization and induction of filopodia by overexpression. Biochem J *378*, 509-518.

Neumann-Giesen, C., Fernow, I., Amaddii, M., and Tikkanen, R. (2007). Role of EGF-induced tyrosine phosphorylation of reggie-1/flotillin-2 in cell spreading and signaling to the actin cytoskeleton. J Cell Sci *120*, 395-406.

Nohara, K., Wang, F., and Spiegel, S. (1998). Glycosphingolipid composition of MDA-MB-231 and MCF-7 human breast cancer cell lines. Breast Cancer Res Treat *48*, 149-157.

Nothdurfter (2007). Pitfalls in isolating lipid rafts. Nat Rev Neurosci *8*, 567.

O'Hare, M.J., Ormerod, M.G., Monaghan, P., Lane, E.B., and Gusterson, B.A. (1991). Characterization *in vitro* of luminal and myoepithelial cells isolated from the human mammary gland by cell sorting. Differentiation *46*, 209-221.

Oguntibeju, O.O., Esterhuyse, A.J., and Truter, E.J. (2009). Red palm oil: nutritional, physiological and therapeutic roles in improving human wellbeing and quality of life. Br J Biomed Sci *66*, 216-222.

Ohno, Y., Kihara, A., Sano, T., and Igarashi, Y. (2006). Intracellular localisation and tissue-specific distribution of human and yeast DHHC cysteine-rich domain-containing proteins. Biochim Biophys Acta *1761*, 474-483.

Okamoto, T., Schlegel, A., Scherer, P.E., and Lisanti, M.P. (1998). Caveolins, a family of scaffolding proteins for organizing "preassembled signaling complexes" at the plasma membrane. J Biol Chem *273*, 5419-5422.

Oliferenko, S., Paiha, K., Harder, T., Gerke, V., Schwarzler, C., Schwarz, H., Beug, H., Gunthert, U., and Huber, L.A. (1999). Analysis of CD44-containing lipid rafts: Recruitment of annexin II and stabilization by the actin cytoskeleton. J Cell Biol *146*, 843-854.

Olsson, E., Honeth, G., Bendahl, P.O., Saal, L.H., Gruvberger-Saal, S., Ringner, M., Vallon-Christersson, J., Jonsson, G., Holm, K., Lovgren, K., *et al.* (2011). CD44 isoforms are heterogeneously expressed in breast cancer and correlate with tumor subtypes and cancer stem cell markers. BMC Cancer *11*, 418.

Orian-Rousseau, V., Chen, L., Sleeman, J.P., Herrlich, P., and Ponta, H. (2002). CD44 is required for two consecutive steps in HGF/c-Met signaling. Genes Dev *16*, 3074-3086.

Orian-Rousseau, V., Morrison, H., Matzke, A., Kastilan, T., Pace, G., Herrlich, P., and Ponta, H. (2007). Hepatocyte growth factor-induced Ras activation requires ERM proteins linked to both CD44v6 and F-actin. Mol Biol Cell *18*, 76-83.

Orsini, F., Cremona, A., Arosio, P., Corsetto, P.A., Montorfano, G., Lascialfari, A., and Rizzo, A.M. (2012). Atomic force microscopy imaging of lipid rafts of human breast cancer cells. Biochim Biophys Acta *1818*, 2943-2949.

Ostapkowicz, A., Inai, K., Smith, L., Kreda, S., and Spychala, J. (2006). Lipid rafts remodeling in estrogen receptor-negative breast cancer is reversed by histone deacetylase inhibitor. Mol Cancer Ther *5*, 238-245.

Parker, J.S., Mullins, M., Cheang, M.C., Leung, S., Voduc, D., Vickery, T., Davies, S., Fauron, C., He, X., Hu, Z., *et al.* (2009). Supervised risk predictor of breast cancer based on intrinsic subtypes. J Clin Oncol *27*, 1160-1167.

Parmryd, I., Adler, J., Patel, R., and Magee, A.I. (2003). Imaging metabolism of phosphatidylinositol 4,5-bisphosphate in T-cell GM1-enriched domains containing Ras proteins. Exp Cell Res *285*, 27-38.

Parpal, S., Karlsson, M., Thorn, H., and Stralfors, P. (2001). Cholesterol depletion disrupts caveolae and insulin receptor signaling for metabolic control via insulin receptor substrate-1, but not for mitogen-activated protein kinase control. J Biol Chem *276*, 9670-9678.

Parsons, S.J., and Parsons, J.T. (2004). Src family kinases, key regulators of signal transduction. Oncogene *23*, 7906-7909.

Patra, S.K. (2008). Dissecting lipid raft facilitated cell signaling pathways in cancer. Biochim Biophys Acta *1785*, 182-206.

Peck, D., and Isacke, C.M. (1998). Hyaluronan-dependent cell migration can be blocked by a CD44 cytoplasmic domain peptide containing a phosphoserine at position 325. J Cell Sci *111 (Pt 11)*, 1595-1601.

Perou, C.M., Sorlie, T., Eisen, M.B., van de Rijn, M., Jeffrey, S.S., Rees, C.A., Pollack, J.R., Ross, D.T., Johnsen, H., Akslen, L.A., *et al.* (2000). Molecular portraits of human breast tumours. Nature *406*, 747-752.

Perschl, A., Lesley, J., English, N., Trowbridge, I., and Hyman, R. (1995). Role of CD44 cytoplasmic domain in hyaluronan binding. Eur J Immunol *25*, 495-501.

Petruzielo, R.S., Heberle, F.A., Drazba, P., Katsaras, J., and Feigenson, G.W. (2013). Phase Behavior and Domain Size in Sphingomyelin-Containing Lipid Bilayers. Biochim Biophys Acta.

Pike, L.J. (2003). Lipid rafts: bringing order to chaos. J Lipid Res *44*, 655-667.

Pike, L.J. (2009). The challenge of lipid rafts. J Lipid Res *50 Suppl*, S323-328.

Pivetta, E., Scapolan, M., Wassermann, B., Steffan, A., Colombatti, A., and Spessotto, P. (2011). Blood-derived human osteoclast resorption activity is impaired by Hyaluronan-CD44 engagement via a p38-dependent mechanism. J Cell Physiol *226*, 769-779.

Planey, S.L., and Zacharias, D.A. (2009). Palmitoyl acyltransferases, their substrates, and novel assays to connect them (Review). Mol Membr Biol *26*, 14-31.

Platt, V.M., and Szoka, F.C., Jr. (2008). Anticancer therapeutics: targeting macromolecules and nanocarriers to hyaluronan or CD44, a hyaluronan receptor. Mol Pharm *5*, 474-486.

Polyak, K. (2007). Breast cancer: origins and evolution. J Clin Invest *117*, 3155-3163.

Ponta, H., Sherman, L., and Herrlich, P.A. (2003). CD44: from adhesion molecules to signalling regulators. Nat Rev Mol Cell Biol *4*, 33-45.

Ponti, D., Costa, A., Zaffaroni, N., Pratesi, G., Petrangolini, G., Coradini, D., Pilotti, S., Pierotti, M.A., and Daidone, M.G. (2005). Isolation and *in vitro* propagation of tumorigenic breast cancer cells with stem/progenitor cell properties. Cancer Res *65*, 5506-5511.

Prag, S., Parsons, M., Keppler, M.D., Ameer-Beg, S.M., Barber, P., Hunt, J., Beavil, A.J., Calvert, R., Arpin, M., Vojnovic, B., *et al.* (2007). Activated ezrin promotes cell migration through recruitment of the GEF Dbl to lipid rafts and preferential downstream activation of Cdc42. Mol Biol Cell *18*, 2935-2948.

Prat, A., Parker, J.S., Karginova, O., Fan, C., Livasy, C., Herschkowitz, J.I., He, X., and Perou, C.M. (2010). Phenotypic and molecular characterization of the claudin-low intrinsic subtype of breast cancer. Breast Cancer Res *12*, R68.

Prior, I.A., and Hancock, J.F. (2001). Compartmentalization of Ras proteins. J Cell Sci *114*, 1603-1608.

Proia, T.A., Keller, P.J., Gupta, P.B., Klebba, I., Jones, A.D., Sedic, M., Gilmore, H., Tung, N., Naber, S.P., Schnitt, S., *et al.* (2011). Genetic predisposition directs breast cancer phenotype by dictating progenitor cell fate. Cell Stem Cell *8*, 149-163.

Pust, S., Klokk, T.I., Musa, N., Jenstad, M., Risberg, B., Erikstein, B., Tcatchoff, L., Liestol, K., Danielsen, H.E., van Deurs, B., *et al.* (2012). Flotillins as regulators of ErbB2 levels in breast cancer. Oncogene.

Putilina, T., Wong, P., and Gentleman, S. (1999). The DHHC domain: a new highly conserved cysteine-rich motif. Mol Cell Biochem *195*, 219-226.

Qian, H., Xia, L., Ling, P., Waxman, S., and Jing, Y. (2012). CD44 ligation with A3D8 antibody induces apoptosis in acute myeloid leukemia cells through binding to CD44s and clustering lipid rafts. Cancer Biol Ther *13*, 1276-1283.

Raghu, H., Sodadasu, P.K., Malla, R.R., Gondi, C.S., Estes, N., and Rao, J.S. (2010). Localisation of uPAR and MMP-9 in lipid rafts is critical for migration, invasion and angiogenesis in human breast cancer cells. BMC Cancer *10*, 647.

Reeves, M.E., Baldwin, S.W., Baldwin, M.L., Chen, S.T., Moretz, J.M., Aragon, R.J., Li, X., Strong, D.D., Mohan, S., and Amaar, Y.G. (2010). Ras-association domain family 1C protein promotes breast cancer cell migration and attenuates apoptosis. BMC Cancer *10*, 562.

Reis-Filho, J.S., and Pusztai, L. (2011). Gene expression profiling in breast cancer: classification, prognostication, and prediction. Lancet *378*, 1812-1823.

Resh, M.D. (1999). Fatty acylation of proteins: new insights into membrane targeting of myristoylated and palmitoylated proteins. Biochim Biophys Acta *1451*, 1-16.

Resh, M.D. (2012). Targeting protein lipidation in disease. Trends Mol Med *18*, 206-214.

Reya, T., Morrison, S.J., Clarke, M.F., and Weissman, I.L. (2001). Stem cells, cancer, and cancer stem cells. Nature *414*, 105-111.

Reynier, M., Sari, H., d'Anglebermes, M., Kye, E.A., and Pasero, L. (1991). Differences in lipid characteristics of undifferentiated and enterocytic-differentiated HT29 human colonic cells. Cancer Res *51*, 1270-1277.

Richert, M.M., Schwertfeger, K.L., Ryder, J.W., and Anderson, S.M. (2000). An atlas of mouse mammary gland development. J Mammary Gland Biol Neoplasia *5*, 227-241.

Rimmerman, N., Bradshaw, H.B., Kozela, E., Levy, R., Juknat, A., and Vogel, Z. (2011). Compartmentalization of Endocannabinoids into Lipid Rafts in a Microglial Cell Line, Which Is Devoid of Caveolin-1. Br J Pharmacol.

Ringerike, T., Blystad, F.D., Levy, F.O., Madshus, I.H., and Stang, E. (2002). Cholesterol is important in control of EGF receptor kinase activity but EGF receptors are not concentrated in caveolae. J Cell Sci *115*, 1331-1340.

Rocks, O., Gerauer, M., Vartak, N., Koch, S., Huang, Z.P., Pechlivanis, M., Kuhlmann, J., Brunsveld, L., Chandra, A., Ellinger, B., *et al.* (2010). The palmitoylation machinery is a spatially organizing system for peripheral membrane proteins. Cell *141*, 458-471.

Roetger, A., Merschjann, A., Dittmar, T., Jackisch, C., Barnekow, A., and Brandt, B. (1998). Selection of potentially metastatic subpopulations expressing c-erbB-2 from breast cancer tissue by use of an extravasation model. Am J Pathol *153*, 1797-1806.

Roth, A.F., Feng, Y., Chen, L., and Davis, N.G. (2002). The yeast DHHC cysteine-rich domain protein Akr1p is a palmitoyl transferase. J Cell Biol *159*, 23-28.

Rothberg, K.G., Heuser, J.E., Donzell, W.C., Ying, Y.S., Glenney, J.R., and Anderson, R.G. (1992). Caveolin, a protein component of caveolae membrane coats. Cell *68*, 673-682.

Rothberg, K.G., Ying, Y.S., Kolhouse, J.F., Kamen, B.A., and Anderson, R.G. (1990). The glycophospholipid-linked folate receptor internalizes folate without entering the clathrin-coated pit endocytic pathway. J Cell Biol *110*, 637-649.

Rubin, J., Schwartz, Z., Boyan, B.D., Fan, X., Case, N., Sen, B., Drab, M., Smith, D., Aleman, M., Wong, K.L., *et al.* (2007). Caveolin-1 knockout mice have increased bone size and stiffness. J Bone Miner Res *22*, 1408-1418.

Rusch, M., Zimmermann, T.J., Burger, M., Dekker, F.J., Gormer, K., Triola, G., Brockmeyer, A., Janning, P., Bottcher, T., Sieber, S.A., *et al.* (2011). Identification of acyl protein thioesterases 1 and 2 as the cellular targets of the Ras-signaling modulators palmostatin B and M. Angew Chem Int Ed Engl *50*, 9838-9842.

Russo, J., and Russo, I.H. (2004). Development of the human breast. Maturitas *49*, 2-15.

Sahores, M., Prinetti, A., Chiabrando, G., Blasi, F., and Sonnino, S. (2008). uPA binding increases UPAR localisation to lipid rafts and modifies the receptor microdomain composition. Biochim Biophys Acta *1778*, 250-259.

Schley, P.D., Brindley, D.N., and Field, C.J. (2007). (n-3) PUFA alter raft lipid composition and decrease epidermal growth factor receptor levels in lipid rafts of human breast cancer cells. J Nutr *137*, 548-553.

Schuck, S., and Simons, K. (2004). Polarized sorting in epithelial cells: raft clustering and the biogenesis of the apical membrane. J Cell Sci *117*, 5955-5964.

Sheikh, H., and Isacke, C.M. (1996). A di-hydrophobic Leu-Val motif regulates the basolateral localisation of CD44 in polarized Madin-Darby canine kidney epithelial cells. J Biol Chem *271*, 12185-12190.

Sheridan, C., Kishimoto, H., Fuchs, R.K., Mehrotra, S., Bhat-Nakshatri, P., Turner, C.H., Goulet, R., Jr., Badve, S., and Nakshatri, H. (2006). CD44+/CD24- breast cancer cells exhibit enhanced invasive properties: an early step necessary for metastasis. Breast Cancer Res *8*, R59.

Shipitsin, M., Campbell, L.L., Argani, P., Weremowicz, S., Bloushtain-Qimron, N., Yao, J., Nikolskaya, T., Serebryiskaya, T., Beroukhim, R., Hu, M., *et al.* (2007). Molecular definition of breast tumor heterogeneity. Cancer Cell *11*, 259-273.

Simons, K., and Gerl, M.J. (2010). Revitalizing membrane rafts: new tools and insights. Nat Rev Mol Cell Biol *11*, 688-699.

Simons, K., and Ikonen, E. (1997). Functional rafts in cell membranes. Nature *387*, 569-572.

Simons, K., and Sampaio, J.L. (2011). Membrane organization and lipid rafts. Cold Spring Harb Perspect Biol *3*, a004697.

Singleton, P.A., and Bourguignon, L.Y. (2004). CD44 interaction with ankyrin and IP3 receptor in lipid rafts promotes hyaluronan-mediated Ca2+ signaling leading to nitric oxide production and endothelial cell adhesion and proliferation. Exp Cell Res *295*, 102-118.

Slamon, D.J., and Clark, G.M. (1988). Amplification of c-erbB-2 and aggressive human breast tumors? Science *240*, 1795-1798.

Smalley, M., Piggott, L., and Clarkson, R. (2012). Breast cancer stem cells: Obstacles to therapy. Cancer Lett.

Smalley, M.J., Titley, J., and O'Hare, M.J. (1998). Clonal characterization of mouse mammary luminal epithelial and myoepithelial cells separated by fluorescence-activated cell sorting. *In vitro* Cell Dev Biol Anim *34*, 711-721.

Smart, E.J., Ying, Y.S., Mineo, C., and Anderson, R.G. (1995). A detergent-free method for purifying caveolae membrane from tissue culture cells. Proc Natl Acad Sci U S A *92*, 10104-10108.

Smith, G.H., and Boulanger, C.A. (2002). Mammary stem cell repertoire: new insights in aging epithelial populations. Mech Ageing Dev *123*, 1505-1519.

Smith, S.M., and Cai, L. (2012). Cell Specific CD44 Expression in Breast Cancer Requires the Interaction of AP-1 and NFkappaB with a Novel cis-Element. PLoS One *7*, e50867.

Song, K.S., Li, S., Okamoto, T., Quilliam, L.A., Sargiacomo, M., and Lisanti, M.P. (1996). Co-purification and direct interaction of Ras with caveolin, an integral membrane protein of caveolae microdomains. Detergent-free purification of caveolae microdomains. J Biol Chem *271*, 9690-9697.

Sorlie, T., Perou, C.M., Tibshirani, R., Aas, T., Geisler, S., Johnsen, H., Hastie, T., Eisen, M.B., van de Rijn, M., Jeffrey, S.S., *et al.* (2001). Gene expression patterns of breast carcinomas distinguish tumor subclasses with clinical implications. Proc Natl Acad Sci U S A *98*, 10869-10874.

Sotiriou, C., Neo, S.Y., McShane, L.M., Korn, E.L., Long, P.M., Jazaeri, A., Martiat, P., Fox, S.B., Harris, A.L., and Liu, E.T. (2003). Breast cancer classification and prognosis based on gene expression profiles from a population-based study. Proc Natl Acad Sci U S A *100*, 10393-10398.

Soyombo, A.A., and Hofmann, S.L. (1997). Molecular cloning and expression of palmitoyl-protein thioesterase 2 (PPT2), a homolog of lysosomal palmitoyl-protein thioesterase with a distinct substrate specificity. J Biol Chem *272*, 27456-27463.

Spano, D., Heck, C., De Antonellis, P., Christofori, G., and Zollo, M. (2012). Molecular networks that regulate cancer metastasis. Semin Cancer Biol *22*, 234-249.

Stamatakos, M., Stefanaki, C., Kontzoglou, K., Masouridi, S., Sakorafas, G., and Safioleas, M. (2010). Recapitulation of ras oncogene mutations in breast cancer. Onkologie *33*, 540-544.

Sternlicht, M.D., Kouros-Mehr, H., Lu, P., and Werb, Z. (2006). Hormonal and local control of mammary branching morphogenesis. Differentiation *74*, 365-381.

Stingl, J., Eaves, C.J., Kuusk, U., and Emerman, J.T. (1998). Phenotypic and functional characterization *in vitro* of a multipotent epithelial cell present in the normal adult human breast. Differentiation *63*, 201-213.

Stingl, J., Eaves, C.J., Zandieh, I., and Emerman, J.T. (2001). Characterization of bipotent mammary epithelial progenitor cells in normal adult human breast tissue. Breast Cancer Res Treat *67*, 93-109.

Stoll, B.A. (2002). N-3 fatty acids and lipid peroxidation in breast cancer inhibition. Br J Nutr *87*, 193-198.

Stuermer, C.A., Langhorst, M.F., Wiechers, M.F., Legler, D.F., Von Hanwehr, S.H., Guse, A.H., and Plattner, H. (2004). PrPc capping in T cells promotes its association with the lipid raft proteins reggie-1 and reggie-2 and leads to signal transduction. FASEB J *18*, 1731-1733.

Tammi, R., Rilla, K., Pienimaki, J.P., MacCallum, D.K., Hogg, M., Luukkonen, M., Hascall, V.C., and Tammi, M. (2001). Hyaluronan enters keratinocytes by a novel endocytic route for catabolism. J Biol Chem *276*, 35111-35122.

Tang, Z., Scherer, P.E., Okamoto, T., Song, K., Chu, C., Kohtz, D.S., Nishimoto, I., Lodish, H.F., and Lisanti, M.P. (1996). Molecular cloning of caveolin-3, a novel member of the caveolin gene family expressed predominantly in muscle. J Biol Chem *271*, 2255-2261.

Tarone, G., Ferracini, R., Galetto, G., and Comoglio, P. (1984). A cell surface integral membrane glycoprotein of 85,000 mol wt (gp85) associated with triton X-100-insoluble cell skeleton. J Cell Biol *99*, 512-519.

Tavernarakis, N., Driscoll, M., and Kyrpides, N.C. (1999). The SPFH domain: implicated in regulating targeted protein turnover in stomatins and other membrane-associated proteins. Trends Biochem Sci *24*, 425-427.

Teder, P., Vandivier, R.W., Jiang, D., Liang, J., Cohn, L., Pure, E., Henson, P.M., and Noble, P.W. (2002). Resolution of lung inflammation by CD44. Science *296*, 155-158.

Thankamony, S.P., and Knudson, W. (2006). Acylation of CD44 and its association with lipid rafts are required for receptor and hyaluronan endocytosis. J Biol Chem *281*, 34601-34609.

Thiel, C., Osborn, M., and Gerke, V. (1992). The tight association of the tyrosine kinase substrate annexin II with the submembranous cytoskeleton depends on intact p11- and Ca(2+)-binding sites. J Cell Sci *103 (Pt 3)*, 733-742.

Thomson, C.A. (2012). Diet and breast cancer: understanding risks and benefits. Nutr Clin Pract *27*, 636-650.

Thorne, R.F., Legg, J.W., and Isacke, C.M. (2004). The role of the CD44 transmembrane and cytoplasmic domains in co-ordinating adhesive and signalling events. J Cell Sci *117*, 373-380.

Tian, L., McClafferty, H., Jeffries, O., and Shipston, M.J. (2010). Multiple palmitoyltransferases are required for palmitoylation-dependent regulation of large conductance calcium- and voltage-activated potassium channels. J Biol Chem *285*, 23954-23962.

Tiwari, N., Gheldof, A., Tatari, M., and Christofori, G. (2012). EMT as the ultimate survival mechanism of cancer cells. Semin Cancer Biol *22*, 194-207.

Toole, B.P., and Hascall, V.C. (2002). Hyaluronan and tumor growth. Am J Pathol *161*, 745-747.

Tran, D., Carpentier, J.L., Sawano, F., Gorden, P., and Orci, L. (1987). Ligands internalized through coated or noncoated invaginations follow a common intracellular pathway. Proc Natl Acad Sci U S A *84*, 7957-7961.

Turashvili, G., Bouchal, J., Burkadze, G., and Kolar, Z. (2005). Mammary gland development and cancer. Cesk Patol *41*, 94-101.

Tzircotis, G., Thorne, R.F., and Isacke, C.M. (2005). Chemotaxis towards hyaluronan is dependent on CD44 expression and modulated by cell type variation in CD44-hyaluronan binding. J Cell Sci *118*, 5119-5128.

Tzircotis, G., Thorne, R.F., and Isacke, C.M. (2006). Directional sensing of a phorbol ester gradient requires CD44 and is regulated by CD44 phosphorylation. Oncogene *25*, 7401-7410.

Valastyan, S., and Weinberg, R.A. (2011). Tumor metastasis: molecular insights and evolving paradigms. Cell *147*, 275-292.

van der Voort, R., Taher, T.E., Wielenga, V.J., Spaargaren, M., Prevo, R., Smit, L., David, G., Hartmann, G., Gherardi, E., and Pals, S.T. (1999). Heparan sulfate-modified CD44 promotes hepatocyte growth factor/scatter factor-induced signal transduction through the receptor tyrosine kinase c-Met. J Biol Chem *274*, 6499-6506.

Vargo-Gogola, T., and Rosen, J.M. (2007). Modelling breast cancer: one size does not fit all. Nat Rev Cancer *7*, 659-672.

Velasco-Velazquez, M.A., Homsi, N., De La Fuente, M., and Pestell, R.G. (2012). Breast cancer stem cells. Int J Biochem Cell Biol *44*, 573-577.

Verkruyse, L.A., and Hofmann, S.L. (1996). Lysosomal targeting of palmitoyl-protein thioesterase. J Biol Chem *271*, 15831-15836.

Villadsen, R., Fridriksdottir, A.J., Ronnov-Jessen, L., Gudjonsson, T., Rank, F., LaBarge, M.A., Bissell, M.J., and Petersen, O.W. (2007). Evidence for a stem cell hierarchy in the adult human breast. J Cell Biol *177*, 87-101.

Vollebergh, M.A., Jonkers, J., and Linn, S.C. (2012). Genomic instability in breast and ovarian cancers: translation into clinical predictive biomarkers. Cell Mol Life Sci *69*, 223-245.

Vucenik, I., and Stains, J.P. (2012). Obesity and cancer risk: evidence, mechanisms, and recommendations. Ann N Y Acad Sci *1271*, 37-43.

Walsh, L.A., and Damjanovski, S. (2011). IGF-1 increases invasive potential of MCF 7 breast cancer cells and induces activation of latent TGF-beta1 resulting in epithelial to mesenchymal transition. Cell Commun Signal *9*, 10.

Wan, J., Roth, A.F., Bailey, A.O., and Davis, N.G. (2007). Palmitoylated proteins: purification and identification. Nat Protoc *2*, 1573-1584.

Wang, Q., Teder, P., Judd, N.P., Noble, P.W., and Doerschuk, C.M. (2002). CD44 deficiency leads to enhanced neutrophil migration and lung injury in Escherichia coli pneumonia in mice. Am J Pathol *161*, 2219-2228.

Wang, X., Wilson, M.J., Slaton, J.W., Sinha, A.A., Ewing, S.L., and Pei, D. (2009). Increased aggressiveness of human prostate PC-3 tumor cells expressing cell surface localized membrane type-1 matrix metalloproteinase (MT1-MMP). J Androl *30*, 259-274.

Watson, C.J. (2006). Involution: apoptosis and tissue remodelling that convert the mammary gland from milk factory to a quiescent organ. Breast Cancer Res *8*, 203.

Watson, C.J., and Khaled, W.T. (2008). Mammary development in the embryo and adult: a journey of morphogenesis and commitment. Development *135*, 995-1003.

Webb, Y., Hermida-Matsumoto, L., and Resh, M.D. (2000). Inhibition of protein palmitoylation, raft localisation, and T cell signaling by 2-bromopalmitate and polyunsaturated fatty acids. J Biol Chem *275*, 261-270.

Weidle, U.H., Maisel, D., Klostermann, S., Weiss, E.H., and Schmitt, M. (2011). Differential splicing generates new transmembrane receptor and extracellular matrix-related targets for antibody-based therapy of cancer. Cancer Genomics Proteomics *8*, 211-226.

Wiechec, E. (2011). Implications of genomic instability in the diagnosis and treatment of breast cancer. Expert Rev Mol Diagn *11*, 445-453.

Xu, J., Hedberg, C., Dekker, F.J., Li, Q., Haigis, K.M., Hwang, E., Waldmann, H., and Shannon, K. (2012). Inhibiting the palmitoylation/depalmitoylation

cycle selectively reduces the growth of hematopoietic cells expressing oncogenic Nras. Blood *119*, 1032-1035.

Yamada, E. (1955). The fine structure of the gall bladder epithelium of the mouse. J Biophys Biochem Cytol *1*, 445-458.

Yamaguchi, H., Takeo, Y., Yoshida, S., Kouchi, Z., Nakamura, Y., and Fukami, K. (2009). Lipid rafts and caveolin-1 are required for invadopodia formation and extracellular matrix degradation by human breast cancer cells. Cancer Res *69*, 8594-8602.

Yaqoob, P. (2009). The nutritional significance of lipid rafts. Annu Rev Nutr *29*, 257-282.

Yeh, D.C., Duncan, J.A., Yamashita, S., and Michel, T. (1999). Depalmitoylation of endothelial nitric-oxide synthase by acyl-protein thioesterase 1 is potentiated by Ca(2+)-calmodulin. J Biol Chem *274*, 33148-33154.

Yilmaz, M., and Christofori, G. (2010). Mechanisms of motility in metastasizing cells. Mol Cancer Res *8*, 629-642.

Zeidman, R., Jackson, C.S., and Magee, A.I. (2009). Protein acyl thioesterases (Review). Mol Membr Biol *26*, 32-41.

Zhang, F.L., and Casey, P.J. (1996). Protein prenylation: molecular mechanisms and functional consequences. Annu Rev Biochem *65*, 241-269.

Zhao, F., Zhang, J., Liu, Y.S., Li, L., and He, Y.L. (2011). Research advances on flotillins. Virol J *8*, 479.

Zhu, D., and Bourguignon, L.Y. (2000). Interaction between CD44 and the repeat domain of ankyrin promotes hyaluronic acid-mediated ovarian tumor cell migration. J Cell Physiol *183*, 182-195.

Appendix I

Tissue Culture Solutions

Hydrocortisone – H0888, Sigma-Aldrich

5mg of hydrocortisone was dissolved in 5ml of 100% ethanol and stored at -20°C. 250µl of the stock was added to 500ml of media to yield 500ng/ml final concentration.

Cholera Toxin – C8052, Sigma-Aldrich

1ml of sterile distilled water was injected into the vial to yield 2mg/ml stock. 26.3µl of stock were added to 500ml of media to give final concentration of 100ng/ml. The stock was stored at 4°C.

Insulin – I5500, Sigma-Aldrich

100mg of bovine insulin was first suspended in 20ml of 0.005M HCl, and then 80ml of sterile distilled water was added to yield a final concentration of 1mg/ml. 5ml of the stock was added to a final volume of 500ml. 5ml aliquots of the stock solution were stored at -20°C.

Appendix II

Buffer Recipes

Relax Buffer (for Triton X-100 insolubility analysis)

100mM	KCl
3mM	NaCl
3.5mM	MgCl2
10mM	HEPES

pH to 7.40, stored at 4°C. Immediately before use fresh Triton X-100, protease and phosphatase inhibitors were added.

LB Broth

10g	NaCl
10g	Tryptone
5g	Yeast Extract

Added water to a final volume of 1L, sterilized by autoclaving, stored at 4°C for a week.

LB Agar

20g agar per 1L LB Broth, fully melted at 80°C, sterilized by autoclaving, poured into Petri dished at ~25ml/dish, stored at 4oC, upside down, for up to two weeks.

Tris-HCl/SDS pH 8.80 (for separating gel)

90.83g	Trizma base
300ml	distilled water

pH to 8.80 with conc. HCl

10ml	20% SDS

Made up to a final volume of 500ml with distilled water. Stored at 4°C.

HANKS Buffer (for lipid raft extractions)

Hank's Balanced Salts (H1387, Sigma-Aldrich)
dissolved in 800ml distilled water

10mM	HEPES
0.35g of	$NaHCO_3$

pH to 7.40 and made up to a final volume of 1L. Used within 24 hours

NZY+ Broth

10g	NZ amine
5g	yeast extract
5g	NaCl

Made up to a final volume of 1L with distilled water and sterilized by autoclaving. Immediately before use the following additives were added

12.5ml	1M MgCl2
12.5ml	1M MgSO4
20ml	20% (w/v) sucrose (filter-sterilised)

Tris-HCl/SDS pH 6.80 (for stacking gel)

15.14g	Trizma base
150ml	distilled water

pH to 6.80 with conc. HCl

5ml	20% SDS

Made up to a final volume of 250ml with distilled water. Stored at 4°C.

10% Ammonium Persulphate (APS)

1g of APS dissolved in 10ml of H_2O, aliquoted and stored at -20°C.

Non-Stringent Buffer for Acyl-Biotin Exchange

4.38g	NaCl
0.1g	NaN3
25ml	100X Tris-EDTA

Dissolved in ~450ml distilled water, pH to either 7.20 (for washes and incubations) and 6.20 for Biotin-BMCC washes and incubations. Made up to a final volume of 500ml. Stored at 4°C.

Separating Gels (in ml)

	8%	9%	10%
30% acrylamide/0.8% bisacrylamide	4.00	4.50	5.00
Tris-HCl pH 8.80	3.75	3.75	3.75
Distilled water	7.25	6.75	6.25
10% APS	0.05	0.05	0.05
TEMED	0.01	0.01	0.01

Stacking Gel

30% acrylamide/0.8% bisacrylamide	0.65ml
Tris-HCl pH 6.80	1.25ml
Distilled water	3.05ml
10% APS	0.025ml
TEMED	0.005ml

1X Running Buffer

3.03 g	Trizma base
14.4g	Glycine
5ml	20% SDS

Made up to 1L with distilled water

1X Transfer Buffer

2.5g	Trizma base
11.5g	Glycine
160ml	Methanol

Made up to 800ml of distilled water

10X TBS

80g	NaCl
2g	KCl
30g	Trizma Base

Dissolved in ~800ml of distilled water, pH to 7.40 with conc. HCl. Made up to a final volume of 1L with distilled water, stored at 4°C.

1X TBS-Tween

100ml	10XTBS
900ml	distilled water
1ml	Tween (100%)

Appendix III

Antibodies

Primary Antigen	Source	MW (kDa)	Cat #	Supplier	Working Dilution	
					WB	IF
Actin	Rabbit	42	A2066	Sigma	1:5000	-
Annexin II	Rabbit	40	GTX100046	Genetex	1:2000	1:500
Caveolin-1	Rabbit	23	3238	Cell Signalling	1:1000	1:250
CD44	Mouse	80	DF1485	Santa Cruz	1:500	1:500
CD44	Mouse	80	BBA10	R&D Systems	1:1000	-
CD44	Rabbit	80	3578	Cell Signalling	1:1000	1:200
EpCAM	Mouse	40	2929	Cell Signalling	1:1000	-
Ezrin	Rabbit	80	sc20773	Santa Cruz	-	1:200
Ezrin	Mouse	80	610602	BD Biosciences	1:1000	1:500
Flotillin-1	Rabbit	48	F1180	Sigma	-	1:250
Flotillin-1	Mouse	48	610821	BD Biosciences	1:1000	1:250
Merlin	Rabbit	59	GTX113505	Genetex	1:2000	1:500
Moesin	Rabbit	68	GTX101708	Genetex	1:2000	1:500
p63	Mouse	63	550025	BD Biosciences	1:1000	-
phospho-ERM	Rabbit	85	3141	Cell Signalling	1:1000	1:250
Radixin	Rabbit	69	GTX114219	Genetex	1:2000	1:500
Transferrin Receptor	Mouse	190	136800	Invitrogen	1:2000	1:250
Vimentin	Mouse	57	550513	BD Biosciences	1:1000	-

Primary Antigen	Source	Cat #	Supplier	Working Dilution
Anti-mouse IgG-HRP	rabbit	A9044	Sigma-Aldrich	1:500
Anti-rabbit IgG-HRP	goat	7074	Cell Signalling	1:2000
AlexaFluor anti-mouse 488	goat	A10667	Molecular Probes	1:1000
AlexaFluor anti-mouse 568	goat	A11011	Molecular Probes	1:1000
Streptavidin-HRP	-	SA202	Millipore	1:5000

Appendix IV

Reagents

Reagent	Supplier	Cat #
Cell Culture		
Blasticidin	Invitrogen	R210-01
Bovine insulin	Sigma-Aldrich	I5500
Cholera Toxin	Sigma-Aldrich	C8052
DMEM	Sigma-Aldrich	D6546
DMEM-F12	Sigma-Aldrich	D8437
Foetal Bovine Serum	Lonza	DE14-801F
Horse Serum	Sigma-Aldrich	H1138
Human EGF	Sigma-Aldrich	E4269
Hydrocortisone	Sigma-Aldrich	H0888
L-glutamine	Gibco	25030024
MEGM	Lonza	CC-3150
Penicillin/Streptomycin	Gibco	15140122
Trypsin inhibitor	Sigma-Aldrich	T6414
Trypsin-EDTA	Biosciences	25300-054
Buffers		
Agar	Sigma-Aldrich	A1296
Glycine	Sigma-Aldrich	G7126
Hank's Buffer	Sigma-Aldrich	H1387
HEPES	Sigma-Aldrich	H0887
LB Broth	Sigma-Aldrich	L3022
Methanol	Sigma-Aldrich	24229
NZYM Broth	Sigma-Aldrich	74725
Sucrose	Sigma-Aldrich	S9378
Tris-EDTA	Sigma-Aldrich	T9285
Trizma base	Sigma-Aldrich	T6066
Tween	Sigma-Aldrich	P1379

Protein Assays		
Acrylamide	Sigma-Aldrich	A3699
Ammonium Persulphate	Sigma-Aldrich	A3678
BCA	ThermoScientific	23228
Bovine Serum Albumin	Sigma-Aldrich	A9647
DTT	Sigma-Aldrich	D9163
ECL	PerkinElmer	265-12291
Hydroxylamine	Sigma-Aldrich	467804
N-ethylmameimide	Sigma-Aldrich	E3876
Phosphatase Inhibitor Cocktail III	Sigma-Aldrich	P5726
Phosphatase Inhibitor Cocktail III	Sigma-Aldrich	P0044
Protease Inhibitor Cocktail	Sigma-Aldrich	P2714
Protein G Sepharose	Sigma-Aldrich	P3296
SigmaFAST Tablets	Sigma-Aldrich	N1891
Triton X-100	Sigma-Aldrich	X100
Triton X-100 (for lipid rafts)	Roche	11332481001

Genetic Manipulations		
Chloramphenicol (ethanol-soluble)	Sigma-Aldrich	C0378
Chloramphenicol (water-soluble)	Sigma-Aldrich	C3175
jetPRIME transfection reagent	Source Bioscience	114-07
siRNA against Caveolin-1	Dharmacon	M003467-01
siRNA against Flotillin-1	Dharmacon	M010636-00
Site-Directed Mutagenesis kit	Strategene	200518
Universal negative control siRNA	Santa Cruz	D2409

Specific Reagents		
Compound III	ChemBridge	5790443
Compound V	ChemBridge	5657368
Hyaluronic Acid	LifeCore BioMedical	23552
Palmitic Acid	Sigma-Aldrich	P0500
Palmostatin B	Calbiochem	178501

Oral Presentations and Awards

Babina IS and Hopkins AM., 2010. Rafted CD44: a boat to safety from breast cancer metastasis? *Irish Epithelial Physiology Group Meeting*

Babina IS and Hopkins AM., 2011. "Rafting" to safety from breast cancer metastasis. *Beaumont Hospital Sheppard Prize*

Babina IS and Hopkins AM., 2011. CD44 affiliation with lipid rafts is associated with decreased motility of breast cancer cells. *Irish Association for Cancer Research annual meeting*

Babina IS and Hopkins AM., 2011. Lipid raft affiliation of CD44 is associated with decreased motility of breast cancer cells. *Gordon Research Conference in Mammary Gland Biology.* **Award: Travel Fellowship from the British Association for Cancer Research. Also selected as a discussion leader for the GRC seminar in 2012**

Babina IS and Hopkins AM., 2011. A novel approach to regulating breast cancer cell motility. *Royal Irish Academy of Medicine annual meeting*

Babina IS and Hopkins AM., 2011. Subcellular CD44 localisation as a novel regulator of breast cancer cell motility. *Irish Epithelial Physiology Group Meeting 2011.* **Award: Best presentation in PhD category**

Babina IS and Hopkins AM., 2012. Modulation of CD44 sub-cellular localization decreases breast cancer cell motility. *Irish Association for Cancer Research annual meeting.* **Award: Best proffered paper oral presentation**

Babina IS and Hopkins AM., 2012. *Gordon Research Conference in Mammary Gland Biology.* **Selected as a discussion leader for the GRC seminar in 2013 and as the chair for GRC seminar in 2014.**

Babina IS and Hopkins AM., 2013. Modulation of CD44 sub-cellular localization decreases breast cancer cell motility. *Beaumont Hospital annual research meeting.* **Award: Best oral presentation in the PhD category.**

Babina IS and Hopkins AM., 2013. Palmitoylation of CD44 regulates breast cancer cell migration via alterations in its lipid raft affiliation. *Irish Association for Cancer Research annual meeting*

Babina IS and Hopkins AM., 2013. Palmitoylation of CD44 regulates breast cancer cell migration via alterations in its lipid raft affiliation. *RCSI Annual Research Day.* **Award: First prize in PhD poster presentation.**

Publications and manuscripts

Simona Donatello*, Irina S. Babina*, Lee D. Hazelwood, I. Robert Nabi, Ann M. Hopkins. (2012). Lipid Raft association restricts CD44-ezrin interaction and promotion of breast cancer cell migration. *Am J Pathol. 2012 Dec;181(6):2172-87, PMID 23031255*

*equal contribution

Irina S. Babina, Simona Donatello, Ivan R. Nabi and Ann M. Hopkins (2011). Lipid Rafts as Master Regulators of Breast Cancer Cell Function, *Breast Cancer - Carcinogenesis, Cell Growth and Signalling Pathways*, Mehmet Gunduz and Esra Gunduz (Ed.), ISBN: 978-953-307-714-7, InTech, Available from: http://www.intechopen.com/articles/show/title/lipid-rafts-as-master-regulators-of-breast-cancer-cell-function

Rachel V. Bowie, Simona Donatello, Clíona Lyes, Mark B. Owens, Irina S. Babina, Lance Hudson, Shaun V. Walsh, Diarmuid P. O'Donoghue, Sylvie Amu, Sean P. Barry, Padraic G. Fallon, Ann M. Hopkins (2011). Lipid rafts are disrupted in mildly-inflamed intestinal microenvironments without overt disruption of the epithelial barrier. *Am J Physiol Gastrointest Liver Physiol. 2012 Apr 15;302(8):G781-93, PMID: 22241861*

Submitted:

Irina S Babina, Simona Donatello, Arnold DK Hill, Ann M Hopkins (2013). Modulation of CD44 palmitoylation status regulates breast cancer cell migration via alterations in affiliation with lipid rafts.

Irina S Babina, Ann M Hopkins (2013). Increasing CD44 palmitoylation status by targeting PAT enzymes decreases breast cancer cell migration.

Enhancement of CD44 Palmitoylation Reduces Breast Cancer Cell Migration – A Novel Target for Metastasis?

Irina S. Babina, Ann M. Hopkins[§]

Department of Surgery, Royal College of Surgeons in Ireland, Dublin, Ireland

[§] **Address correspondence to:**

Dr. Ann M. Hopkins,

Department of Surgery,

Royal College of Surgeons in Ireland,

RCSI Education and Research Centre,

Beaumont Hospital,

Dublin 9,

IRELAND.

Tel: +353-1-809-3858; Fax: +353-1-633-5082

Email: annhopkins@rcsi.ie

Running title: CD44 palmitoylation influences cancer cell migration

Keywords: Breast cancer, CD44, cell migration, lipid rafts, palmitoylation.

Abstract

Cell migration is an obligate precursor to cancer metastasis, the major cause of breast cancer-related deaths. The important migratory protein CD44 localises to lipid rafts, cholesterol-enriched membrane microdomains that act as signalling platforms. Reversible addition of palmitoyl moieties (palmitoylation) to CD44 cysteine residues contributes to CD44 raft localisation. We have previously shown that palmitoylation sequesters CD44 within lipid rafts and restricts its contribution to cell migration. In this letter we report for the first time that a global pro-palmitoylation state, namely high gene expression of palmitoylating enzymes or low expression of de-palmitoylating enzymes, correlates with improved breast cancer patient survival. Furthermore we present novel data that CD44 palmitoylation and raft localisation can be increased by inhibitors of enzymes involved in the palmitoylation cascade, which in conjunction reduces breast cancer cell migration. We therefore suggest that pharmacological manipulation of palmitoylating enzymes merits investigation as a novel therapeutic target for breast cancer metastasis.

Introduction

The majority of breast cancer deaths occur due to metastatic spread of tumour cells to distant sites. Breast cancer cell migration is one of the earliest events in the metastatic cascade. The transmembrane glycoprotein CD44 is an established mediator of cell migration and has been implicated in dissemination of many cancers, including breast cancer, yet the underlying mechanisms remain incompletely understood[1]. CD44 frequently localises in lipid rafts, which are specialised plasma membrane areas enriched in cholesterol and sphingolipids[2]. Our previous findings provided the first evidence that translocation of CD44 outside lipid raft domains is associated with breast cancer cell migration[3]. CD44 is thought to affiliate with lipid rafts through post-translational addition of palmitoyl groups to cysteine residues, a process termed palmitoylation. We recently found that mutagenesis of CD44 palmitoylation sites reduced its affiliation with lipid rafts and promoted a pro-migratory phenotype in breast cells (Babina et al, manuscript under review). Based on these data, we speculated that CD44 palmitoylation could provide a novel pharmacological target to attenuate CD44-based motility in breast cancer cells.

Palmitoylation is a dynamic and reversible process catalysed by enzymes. Palmitoylation-regulating enzymes are still poorly characterised, and have been mainly researched using model organisms[4]. This approach has identified a family of proteins with a conserved aspartate-histidine-histidine-cysteine (DHHC) cysteine-rich domain, considered to be an active site of palmitoyl acyltransferases (PAT)[5]. PAT enzymes are thought to catalyse the thioester linkage of palmitate to proteins. Human DHHC PATs have been localised in various cellular compartments in a tissue-dependent manner[6]. Apart from the DHHC motif being crucial for the palmitoyl transferase activity, the substrate specificity of these enzymes remains largely unknown. De-palmitoylation reactions, which remove palmitate groups from palmitoylated proteins, are also catalysed by enzymes. As with PAT enzymes, de-palmitoylating thioeserases remain to be fully characterised. Nonetheless, acyl protein thioesterase-1 (APT-1) has been shown to de-palmitoylate proteins *in vitro*[7]. APT-1 reportedly localises mainly in the cytoplasm[8], and its substrates include proteins such as Ras[9] and eNOS[10]. A homolog of APT-1, named APT-2, has been identified and shown to have thioesterase qualities. However, it has been found mainly in the lysosome, and has substrate specificity for palmitoyl-CoA instead of proteins[11].

Until recently, only generic palmitoylation inhibitors were available as tools to study palmitoylation. One of these, the palmitate analogue 2-bromopalmitate (2-BP), has been widely used to interfere with palmitoylation of proteins such as Rho and Ras family members[12]. More recently, non-lipid small molecule inhibitors of PAT enzymes have been identified[13]. Specifically five chemotypes displaying anti-PAT activity have been described, with Compound III reportedly being specific for PATs that act on farnesylated proteins, while compound V inhibits a class of PATs that recognises myristoylated proteins[13].

In light of our novel findings that CD44 palmitoylation and raft affiliation inversely regulate cell migration[3] (Babina et al, manuscript under review), we hypothesised that CD44 palmitoylation represents a novel pharmacological target to reduce cancer cell motility, an important functional behaviour associated with metastasis. In this letter we first established a clinical relevance for palmitoylation-regulating enzymes in breast cancer, since gene expression datasets revealed a correlation between pro-palmitoylated states and improved breast cancer patient survival. Furthermore, targeted pharmacological modification of palmitoylating enzymes uncovered a strong relationship between CD44 palmitoylation, its raft localisation and consequent restraint of cell migration. Collectively, our data are consistent with a model whereby CD44 palmitoylation could act as a novel target to diminish breast cancer cell migration such as that during the early stages of metastasis.

Materials and Methods

Cell culture– The human breast cancer cell line MDA-MB-231 was obtained from ATCC (LGC Standards, Middlesex, UK). MDA-MB-231 cells were cultured in Dulbecco's Modified Eagles Medium (Sigma-Aldrich, Arklow, Ireland) supplemented with 10% foetal bovine serum, 2mM L-glutamine, 100U/ml penicillin and 100µg/ml streptomycin. Cells were cultured in a humidified incubator at 37°C and 5% CO_2 and confirmed to be mycoplasma-free by quarterly testing.

Antibodies and reagents– For modulation of CD44 palmitoylation, Compounds III and V (PAT inhibitors) were prepared to a concentration of 100mM using sterile DMSO. Specified working dilutions were prepared using appropriate culture medium, and cells were pre-treated for 1 hour before experimentation. Mouse CD44 primary antibody, detecting all isoforms of the protein, was obtained from R&D Systems (Abingdon, UK) and used for western blot analysis. For immunofluorescence and immunoprecipitation, mouse CD44 antibody was purchased from Santa Cruz Biotechnology (Heidelberg, Germany). Mouse flotillin-1 antibody for Western blot analysis was purchased from BD Biosciences (Oxford, UK). Rabbit flotillin-1 antibody (for immunofluorescence analysis) was obtained from Sigma-Aldrich, and mouse transferrin receptor was obtained from Cell Signaling Technologies (Danvers, MA, US). Anti-mouse-HRP secondary antibody was obtained from Sigma-Aldrich, and anti-rabbit-HRP from Cell Signaling Technologies. For the detection of biotin, Streptavidin-HRP was from ThermoScientific (Ballycoolin, Ireland) and Millipore (Cork, Ireland).

Triton X-100 insolubility assay– Cells were grown to confluence in 6-well plates. Detergent-soluble fractions (enriched in non-raft cellular components) were obtained following 30 min incubation at 4°C in lysis buffer (100mM KCl, 3mM NaCl, 3.5mM $MgCl_2$, 10mM HEPES) containing 1% Triton X-100 and protease and phosphatase inhibitor cocktails (Sigma-Aldrich). The detergent-insoluble pool (enriched in lipid rafts) was subsequently collected via scraping the wells in one-half volume of lysis buffer. After determination of protein concentrations using BCA assay, fractions of equivalent protein concentration were analysed by immunoblotting.

Immunoblotting– Equal protein concentrations were loaded onto 10% Tris-HCl gels and subjected to SDS-PAGE. Protein was subsequently transferred onto nitrocellulose by wet transfer at 100V/1h, incubated in blocking buffer (5% skim milk or BSA in TBS-0.1%Tween) for 1 hour and probed with primary antibody overnight at 4°C. After washing, membranes were incubated with HRP-conjugated secondary antibody for 1 hour at room temperature and developed by exposure to X-ray film (Sigma-Aldrich) using enhanced chemi-luminescent reagents (PerkinElmer Life Sciences, Waltham, MA).

Acyl-Biotin Exchange (BMCC assay) – This method was adapted from a previous publication[14]. Briefly, CD44 protein was immunoprecipitated from whole cell lysates via overnight incubation at 4°C with 3µg of mouse anti-human CD44 antibody as described[3]. Antibody-protein complexes were collected by 3-hour rotation at 4°C with 50µg of protein G sepharose (Sigma-Aldrich), in the presence of 50mM N-ethylmaleimide (NEM, Sigma-Aldrich) to covalently block sulfhydryl groups. Collected complexes were subsequently divided into two fractions, for treatment with and without 1M hydroxylamine (HAM, Sigma-Aldrich) at room temperature for 1 hour (pH 7.40) to cleave free palmitate groups. Subsequently, samples were incubated with 1µM EZ-link biotin-N-(6-(biotinamido)hexyl)-3'-(2'-pyridyldithio)-propionamide (Biotin-BMCC, Thermo Scientific) at pH 6.2 for 1 hour at room temperature, to label the reactive cysteine residues. Labelled CD44 was released from the beads via 5 minute incubation at 100°C in 2x reducing Lamelli sample buffer, and subjected to SDS-PAGE and immunoblotting. Biotin-BMCC-labelled CD44 was detected with streptavidin-HRP, followed by antibody incubation, to visualise total CD44.

Scratch wound migration assay– Cells were grown to confluence and scratch-wound assays performed as described[15]. Briefly, cells were wounded by a single scratch in the centre of the well using a sterile p200 pipette tip attached to suction, rinsed with PBS to remove any loose cells/remaining medium and allowed to migrate in serum-free medium in a humidified incubator at 37°C / 5% CO_2. The precise location of the wound was photographed immediately after wounding (Time=0) and subsequently every two hours for 6-8 hours. Wounds were measured using Scion Image software (Scion Corporation Ltd., Frederick, MD, USA), and percentage wound closure calculated relative to Time=0 for each condition and plotted using SigmaPlot.

Image analysis and statistics– Densitometric analysis was performed on western blot films (exposed for equivalent times) using ImageJ software (National Institute of Health). Raw values were used for statistical analysis from a minimum of three independent experiments, and averages subsequently expressed as percent of internal control. *P* values were calculated using equal variance two-tailed unpaired Student's t-tests. For migration assays, 2-way ANOVA tests were performed across all time points using GraphPad Prism software. Results were considered significant if $p<0.05$.

Results

Having established a link between CD44 palmitoylation and its containment in lipid rafts as a mechanism to reduce breast cancer cell migration[3](Babina et al., manuscript under review), we first questioned whether global changes in expression of palmitoylating or depalmitoylating enzymes might predict disease progression parameters in breast cancer patients. Using an online survival analysis tool of published Affymetrix micro-array data sets in breast cancer patients[16], we first assessed the relationship between survival and expression of the DHHC family of pro-palmitoylation PAT enzymes. As 23 members of this family have been identified to date[17], a representative panel of the known genes was tested. As shown in Kaplan-Meier plots in **Fig. 1a**, statistically-significant correlations were observed between better recurrence-free survival and high gene expression of DHHC3 (probe 218077_s_at), DHHC6 (probe 218249_at), DHHC7 (probe 218606_at) or DHHC8 (probe 222274_at). The same survival analysis tool was also used to assess the impact of expressional changes in the de-palmitoylating enzymes APT-1 (probe 203007_x_at) and APT-2 (probe 215566_x_at). Accordingly, low expression of the de-palmitoylating thioesterase enzyme APT-1 significantly correlated with better breast cancer recurrence-free survival (**Fig. 1b**). Conversely, high expression of APT-2 correlated with better recurrence-free survival of the same patients.

These observations of statistically-relevant relationships between patient survival and expression of palmitoylation-regulating enzymes led us to question whether pharmacological interference with enzyme activity could alter CD44 localisation relative to lipid rafts, and, in turn, cell migration. As tools we used two chemical PAT inhibitors (compounds III and V) with reported substrate specificity[13]. Immunofluorescence and confocal microscopy were used to compare spatial co-localisation between CD44 and the lipid raft marker flotillin-1 in non-migrating and migrating highly-invasive MDA-MB-231 breast cancer cells (**Fig. 2**). Under both conditions, pre-treatment with the PAT inhibitors compounds III and V (100μM / 1h) increased CD44 co-localisation with flotillin-1 relative to that in vehicle control-treated cells. Interestingly, treatment with PAT inhibitors appeared to enhance the membranous localisation of flotillin-1 in both non-migrating and migrating cells. Pixel overlap quantification of the green (CD44) and red (flotillin-1) channels revealed a statistically significant increase in CD44 localisation with flotillin-1 in compounds III- and V-pre-treated conditions versus DMSO controls in both migrating or non-migrating cells (**Fig. 2, graph**).

The impact of PAT inhibition on CD44 localisation relative to lipid raft domains was further analysed by biochemical detergent fractionation. Migrating MDA-MB-231 cells pre-treated for 1 hour with compound III or compound V (100μM; versus DMSO vehicle control) were tested for CD44 affiliation with detergent-insoluble (raft-enriched) and detergent-soluble (non-raft) pools (**Fig. 3a**). Compound V induced a significant increase in CD44 affiliation with raft-containing domains compared to all other conditions, as determined by western blot analysis and quantitatively confirmed by calculation of the detergent-insoluble/-soluble affiliation ratio (**Fig. 3a, graph**). This ratio was calculated in a similar manner to the lipid raft affiliation ratio described previously[3]. Briefly, the ratio represents pooled densitometric quantitation of CD44 in lipid raft-enriched domains (normalised to flotillin-1) relative to CD44 in the non-raft pool (normalised to transferrin receptor, TfR). In order to examine if this change in localisation reflected alterations in CD44 palmitoylation status, we measured palmitoylated CD44 using an acyl-biotin exchange approach. Samples not treated with hydroxylamine (HAM-) and IgG immunoprecipitations (IP: IgG) were used as internal controls. Compared to DMSO controls, MDA-MB-231 cells pre-treated with PAT inhibitors (100μM / 1 hour) had increased levels of palmitoylated CD44 (CD44-Palm, **Fig. 3b**). Quantification of CD44-Palm relative to total CD44 revealed statistically significant increases in CD44

palmitoylation following treatment with compounds III or V (**Fig. 3b, graph**). Having shown that PAT inhibitors paradoxically promote CD44 palmitoylation status and its affiliation with lipid rafts, we investigated whether this translated into functional reductions in breast cancer cell migration. MDA-MB-231 cells pre-treated with PAT inhibitors compounds III and V (100μM/1h) were scratch-wounded and cell migration measured over 8 hours (**Fig. 3c**). Compound III significantly inhibited cell migration after 8 hours relative to the DMSO control, whilst compound V completely abolished cell migration at all time points. These effects were consistent with noted enhancements in palmitoylated, raft-affiliated CD44 in PAT inhibitor-treated cells.

Discussion

The functionality of numerous proteins involved in breast cancer cell migration, a key early event in metastasis, is modulated by post-translational addition of palmitate groups. This process is believed to be catalysed by PAT enzymes. De-palmitoylating events are thought to be regulated by thioesterase enzymes, of which APT-1 is best-characterised. Dynamic palmitoylation and de-palmitoylation of a variety of proteins (such as Rho and Ras) involved in breast cancer and other diseases has been recently reviewed[18]. Our recent findings suggested that CD44 palmitoylation, and its consequent sequestration in lipid rafts, negatively regulates breast cancer cell migration (Babina et al., manuscript under review)[3]. However no reports to date have addressed how CD44 is palmitoylated in breast cancer cells, or the functional implications of its palmitoylation. Consequently, in the present report we investigated the potential of pharmacologically targeting palmitoylation-regulating enzymes to modify CD44 palmitoylation and its raft localisation, which we hypothesised would have a direct functional impact on the migration of breast cancer cells.

Numerous pro-palmitoylating PAT enzymes have been identified, and in yeast models each PAT has been demonstrated to act on a particular substrate[19]. In humans, PAT enzymes are predominantly expressed in the endoplasmic reticulum (ER)/Golgi, except DHHC5, -20 and -21 which are strongly expressed at the cell membrane[20]. In this study we noted that high gene expression of a panel of PAT enzymes (DHHC-3, -6, -7, -8) correlated significantly with improved recurrence-free survival of breast cancer patients. An intriguing contrast is that high expression of DHHC13 and 14 was associated with *decreased* survival (data not shown). Interestingly, the former localise to the Golgi while the latter are found in the ER[20]. Opposing survival outcomes according to expression of ER- versus Golgi-localised PAT enzymes highlight a complex regulation of protein functions by post-translational modifications. A paucity of knowledge on the principal substrates for each of those enzymes further complicates the interpretation of functional relationships between enzyme expression and survival. It is also noteworthy that single genes alone are less powerful predictors of survival than gene signatures. Regardless, our findings demonstrate a novel potential importance in investigating the druggability of palmitoylation enzymes for oncological purposes.

Since palmitoylation is a dynamic and reversible process, we also investigated potential relationships between gene expression of the main de-palmitoylating enzymes and breast cancer patient survival. In conjunction with our observed links between pro-palmitoylated states and better survival, low expression of the de-palmitoylating enzyme APT-1 was associated with improved patient survival. Paradoxically, however, high expression of its homologue APT-2 correlated with better recurrence-free survival. While single genes alone have diminishing predictive power in the bioinformatic era, these conflicting survival outcomes could nonetheless be influenced by different cellular localisations of the two proteins. Unlike APT-1, which is mainly found in the cytoplasm[8], APT-2 is believed to be a lysosomal protein[11]. It has been established that Ras proteins, which are frequently implicated in breast cancer[21], are de-palmitoylated by APT-1[22]. Thus high activity of APT-1 would likely decrease levels of palmitoylated Ras; increasing its trafficking to and from the Golgi to be re-palmitoyated, and consequently facilitating its oncogenic signalling. Overall however, these survival studies on gene expression of palmitoylating and de-palmitoylating enzymes point to a complex relationship between global palmitoylation patterns and cancer progression. Despite our simplified consideration of single genes in relation to survival potential, a balance of evidence nonetheless suggests that a pro-palmitoylation state is pro-survival. This supports our *in vitro* results of an inverse correlation between CD44 palmitoylation (with its subsequent sequestration inside lipid rafts) and invasive behaviour in breast cancer cells.

In light of novel findings that palmitoylation of CD44 undergoes temporal reductions during breast cancer cell migration (Babina et al, manuscript under review), we hypothesised that CD44 was being directly regulated by the clinically-relevant palmitoylation and de-palmitoylation enzymes mentioned above. Thus we adopted recently-characterised PAT enzyme inhibitors to investigate the effects of PAT inhibition on CD44 raft localisation and palmitoylation. Compounds III and V reportedly have specific inhibitory activity against PATs catalysing respectively farnesylation and myristoylation events[13]. Although it is unknown whether CD44 is lipidated by fatty acids such as myristate, farnesyl or geranylgeranyl, the Cys286 residue of CD44 fits the description of a farnesylated motif, being located in a putative farnesylation site containing a "CAAX" domain (Cysteine, 2 aliphatic amino acids and a variable amino acid X)[23]. On the CD44 molecule this corresponds to "^{286}Cys-Ile-Ala-Val^{289}", the last amino acids of the transmembrane domain. Thus we speculated that inhibition of either class of PAT enzymes would decrease CD44 palmitoylation. However both inhibitors paradoxically increased CD44 palmitoylation, which predictably was accompanied by increased co-localisation with the raft marker flotillin-1 and increased affiliation with raft-enriched biochemical fractions. The extent of these effects was similar for both inhibitors, with compound V proving marginally more potent than compound III. This could explain why pre-treatment with compound V had a more pronounced effect than compound III on CD44 affiliation with lipid raft pools. This is in agreement with a previous study showing compound V to have de-palmitoylating efficiency similar to that of a broad non-specific inhibitor (2-BP) and much higher than that of compound III[24].

To date, modulation of palmitoylation has been shown to affect proteins like eNOS, Ras and PSD-95[25], but it has not been extensively studied in receptor proteins such as CD44 or in breast cancer specifically. We observed an increase in levels of membrane-bound flotillin-1 upon broad inhibition of palmitoylating activity. This was surprising given an established role of palmitoylation in flotillin-1 translocation to the plasma membrane[2]. However the inhibitors we used mainly targeted PAT enzymes located in the ER/Golgi, and flotillin-1 has been shown to be trafficked to the cell membrane in a Golgi-independent manner[26]. Furthermore, a recent study identified DHHC5 as an enzyme that palmitoylates a homologue of flotillin-1, flotillin-2[27]. As both flotillin proteins share a conserved homology domain[28] which is responsible for their membrane association[26], flotillin-1 could also be a substrate for the action of DHHC5 PAT enzyme. Finally, because DHHC5 is one of three PAT enzymes localised in the cell membrane[20], it could explain the increased membrane localisation of flotillin-1 when broad palmitoylation in the Golgi/ER was inhibited. Despite our expectations, we established that inhibition of palmitoylating enzymes increased the palmitoylation of CD44, likely via complex feedback mechanisms which remain elusive.

Conclusion

The effects we describe using broadly-specific enzyme inhibitors are certain to impact many palmitoylated protein targets in addition to just CD44. However, regardless of the paradoxical effects of specific enzyme inhibitors on CD44 palmitoylation levels, it is important and noteworthy that reduced CD44 palmitoylation was always paralleled by reduced breast cancer cell migration in our *in vitro* studies. This supports our hypothesis of a direct relationship between decreased CD44 palmitoylation, its decreased lipid raft localisation and the promotion of cell migration. Further insights into the mechanisms of CD44 palmitoylation and its lipid raft affiliation may provide valuable knowledge into the cell migratory events associated with metastasis during

breast cancer progression. Furthermore, based on our findings, we speculate that containment of CD44 within lipid raft domains represents a novel druggable target to reduce or halt breast cancer cell migration.

Abbreviations: APT, acyl thioesterase; DHHC, aspartate-histidine-histidine-cysteine; HAM, hydroxylamine; PAT, palmitoyl acyl transferase.

Conflict of interest: Authors declare no conflict of interest.

Acknowledgements: This work was predominantly funded by Health Research Board of Ireland (RP/2008/49 to AMH). We are also grateful to Breast Cancer Ireland for support.

Figure Legends:

Figure 1. A pro-palmitoylated state broadly correlates with better recurrence-free survival of breast cancer patients. Recurrence-free survival plots of breast cancer patients were generated from publicly-available gene expression data sets. (A.) High expression (red lines) of pro-palmitoylating PAT enzymes DHHC3, 6, 7 and 8 correlated with significantly better recurrence-free survival. (B.) Low expression (black) of the de-palmitoylating enzyme APT-1 also significantly correlated with better recurrence-free survival of breast cancer patients. In contrast, high expression (red) of its homologue, APT-2, correlated with better recurrence-free survival. Kaplan-Meier analysis was performed using gene expression information on 2,627 breast cancer patients, with graphs, hazard risk (HR) and logrank p values generated by the online software available at kmplotter.com

Figure 2. Inhibition of PAT enzymes increases CD44 co-localisation with flotillin-1. Non-migrating and migrating (2hr) MDA-MB-231 cells, pre-treated with PAT inhibitor compounds III or V (100μM), were double-immunolabelled for CD44 (green) and flotillin-1 (Flot-1, red). Nuclei were stained with DAPI and are shown in grey. Pre-treatment with both PAT inhibitors significantly increased the co-localisation of CD44 and Flot-1 in migratory or non-migratory conditions relative to the DMSO control, graphically represented by pixel overlap quantitation from 3 independent experiments. *$p<0.05$ vs non-migrating DMSO; #$p<0.05$ vs migrating DMSO, all by 2-tailed unpaired Student's t-test.

Figure 3. Palmitoylation inhibitors increase CD44 palmitoylation and its raft localisation while decreasing cell migration. (A.) MDA-MB-231 cells pre-treated with the indicated concentrations of PAT inhibitors (compounds III and V) were stimulated to migrate for 2 hours and subjected to Triton X-100 insolubility preparations and acyl-biotin exchange assays. Detergent-insoluble and –soluble pools were analysed for the presence of CD44 relative to lipid raft and non-raft markers flotillin-1 (Flot-1) and transferrin receptor (TfR) respectively. CD44 affiliation with the lipid raft-enriched detergent-insoluble pool was significantly increased in compound V-treated cells relative to DMSO control cells, as confirmed by calculation of the numerical Insoluble:Soluble ratio, expressed relative to that in DMSO-treated cells. (B.) Palmitoylated CD44 (CD44-Palm) was measured in migrating (2hr) MDA-MB-231 cells and found to increase following treatment with the PAT inhibitors compounds III or V. Calculation of CD44-Palm relative to CD44-Total (expressed relative to the DMSO condition) demonstrated a significant increase in palmitoylated CD44 relative to DMSO control upon PAT inhibition (A and B: Error bars=SEM; *$p<0.05$ by unpaired 2-tailed Student's t-test; n=3 experiments). (C.) Confluent MDA-MB-231 cells were pre-treated for 1 hour with PAT inhibitors compounds III and V (100μM), and subjected to scratch-wound migration assays. Compound III reduced migration relative to the DMSO control after 8 hours, while compound V abolished cell migration throughout the timecourse. Error bars=SEM; *$p<0.05$; **$p<0.01$ by 2-way ANOVA; n=3 experiments.

References:

[1] Ponta H, Sherman L, Herrlich PA. CD44: from adhesion molecules to signalling regulators. Nat Rev Mol Cell Biol. 2003 Jan;4(1):33-45.

[2] Babina IS, Donatello S, Nabi IR, Hopkins AM. Lipid Rafts as Master Regulators of Breast Cancer Cell Function. In: Gunduz MGaE, ed. *Breast Cancer - Carcinogenesis, Cell Growth and Signalling Pathways*: InTech 2011:401-28.

[3] Donatello S, Babina, I. S., Hazelwood LD, Hill AD, Nabi IR, Hopkins AM. Lipid Raft Association Restricts CD44-Ezrin Interaction and Promotion of Breast Cancer Cell Migration. Am J Pathol. 2012 Sep 29.

[4] Lobo S, Greentree WK, Linder ME, Deschenes RJ. Identification of a Ras palmitoyltransferase in Saccharomyces cerevisiae. J Biol Chem. 2002 Oct 25;277(43):41268-73.

[5] Mitchell DA, Vasudevan A, Linder ME, Deschenes RJ. Protein palmitoylation by a family of DHHC protein S-acyltransferases. J Lipid Res. 2006 Jun;47(6):1118-27.

[6] Rocks O, Gerauer M, Vartak N, Koch S, Huang ZP, Pechlivanis M, et al. The palmitoylation machinery is a spatially organizing system for peripheral membrane proteins. Cell. 2010 Apr 30;141(3):458-71.

[7] Zeidman R, Jackson CS, Magee AI. Protein acyl thioesterases (Review). Mol Membr Biol. 2009 Jan;26(1):32-41.

[8] Duncan JA, Gilman AG. A cytoplasmic acyl-protein thioesterase that removes palmitate from G protein alpha subunits and p21(RAS). J Biol Chem. 1998 Jun 19;273(25):15830-7.

[9] Xu J, Hedberg C, Dekker FJ, Li Q, Haigis KM, Hwang E, et al. Inhibiting the palmitoylation/depalmitoylation cycle selectively reduces the growth of hematopoietic cells expressing oncogenic Nras. Blood. 2012 Jan 26;119(4):1032-5.

[10] Yeh DC, Duncan JA, Yamashita S, Michel T. Depalmitoylation of endothelial nitric-oxide synthase by acyl-protein thioesterase 1 is potentiated by Ca(2+)-calmodulin. J Biol Chem. 1999 Nov 12;274(46):33148-54.

[11] Soyombo AA, Hofmann SL. Molecular cloning and expression of palmitoyl-protein thioesterase 2 (PPT2), a homolog of lysosomal palmitoyl-protein thioesterase with a distinct substrate specificity. J Biol Chem. 1997 Oct 24;272(43):27456-63.

[12] Webb Y, Hermida-Matsumoto L, Resh MD. Inhibition of protein palmitoylation, raft localization, and T cell signaling by 2-bromopalmitate and polyunsaturated fatty acids. J Biol Chem. 2000 Jan 7;275(1):261-70.

[13] Ducker CE, Griffel LK, Smith RA, Keller SN, Zhuang Y, Xia Z, et al. Discovery and characterization of inhibitors of human palmitoyl acyltransferases. Mol Cancer Ther. 2006 Jul;5(7):1647-59.

[14] Fairbank M, Huang K, El-Husseini A, Nabi IR. RING finger palmitoylation of the endoplasmic reticulum Gp78 E3 ubiquitin ligase. FEBS Lett. 2012 Jul 30;586(16):2488-93.

[15] Colas S, Maheo K, Denis F, Goupille C, Hoinard C, Champeroux P, et al. Sensitization by dietary docosahexaenoic acid of rat mammary carcinoma to anthracycline: a role for tumor vascularization. Clin Cancer Res. 2006 Oct 1;12(19):5879-86.

[16] Gyorffy B, Lanczky A, Eklund AC, Denkert C, Budczies J, Li Q, et al. An online survival analysis tool to rapidly assess the effect of 22,277 genes on breast cancer prognosis using microarray data of 1,809 patients. Breast Cancer Res Treat. 2010 Oct;123(3):725-31.

[17] Linder ME, Deschenes RJ. Palmitoylation: policing protein stability and traffic. Nat Rev Mol Cell Biol. 2007 Jan;8(1):74-84.

[18] Resh MD. Targeting protein lipidation in disease. Trends Mol Med. 2012 Apr;18(4):206-14.

[19] Putilina T, Wong P, Gentleman S. The DHHC domain: a new highly conserved cysteine-rich motif. Mol Cell Biochem. 1999 May;195(1-2):219-26.

[20] Ohno Y, Kihara A, Sano T, Igarashi Y. Intracellular localization and tissue-specific distribution of human and yeast DHHC cysteine-rich domain-containing proteins. Biochim Biophys Acta. 2006 Apr;1761(4):474-83.

[21] Stamatakos M, Stefanaki C, Kontzoglou K, Masouridi S, Sakorafas G, Safioleas M. Recapitulation of ras oncogene mutations in breast cancer. Onkologie. 2010;33(10):540-4.

[22] Rusch M, Zimmermann TJ, Burger M, Dekker FJ, Gormer K, Triola G, et al. Identification of acyl protein thioesterases 1 and 2 as the cellular targets of the Ras-signaling modulators palmostatin B and M. Angew Chem Int Ed Engl. 2011 Oct 10;50(42):9838-42.

[23] Hancock JF, Magee AI, Childs JE, Marshall CJ. All ras proteins are polyisoprenylated but only some are palmitoylated. Cell. 1989 Jun 30;57(7):1167-77.

[24] Jennings BC, Nadolski MJ, Ling Y, Baker MB, Harrison ML, Deschenes RJ, et al. 2-Bromopalmitate and 2-(2-hydroxy-5-nitro-benzylidene)-benzo[b]thiophen-3-one inhibit DHHC-mediated palmitoylation in vitro. J Lipid Res. 2009 Feb;50(2):233-42.

[25] Baekkeskov S, Kanaani J. Palmitoylation cycles and regulation of protein function (Review). Mol Membr Biol. 2009 Jan;26(1):42-54.

[26] Morrow IC, Rea S, Martin S, Prior IA, Prohaska R, Hancock JF, et al. Flotillin-1/reggie-2 traffics to surface raft domains via a novel golgi-independent pathway. Identification of a novel membrane targeting domain and a role for palmitoylation. J Biol Chem. 2002 Dec 13;277(50):48834-41.
[27] Li Y, Martin BR, Cravatt BF, Hofmann SL. DHHC5 protein palmitoylates flotillin-2 and is rapidly degraded on induction of neuronal differentiation in cultured cells. J Biol Chem. 2012 Jan 2;287(1):523-30.
[28] Morrow IC, Parton RG. Flotillins and the PHB domain protein family: rafts, worms and anaesthetics. Traffic. 2005 Sep;6(9):725-40.

Figure 1: Babina et al

A.

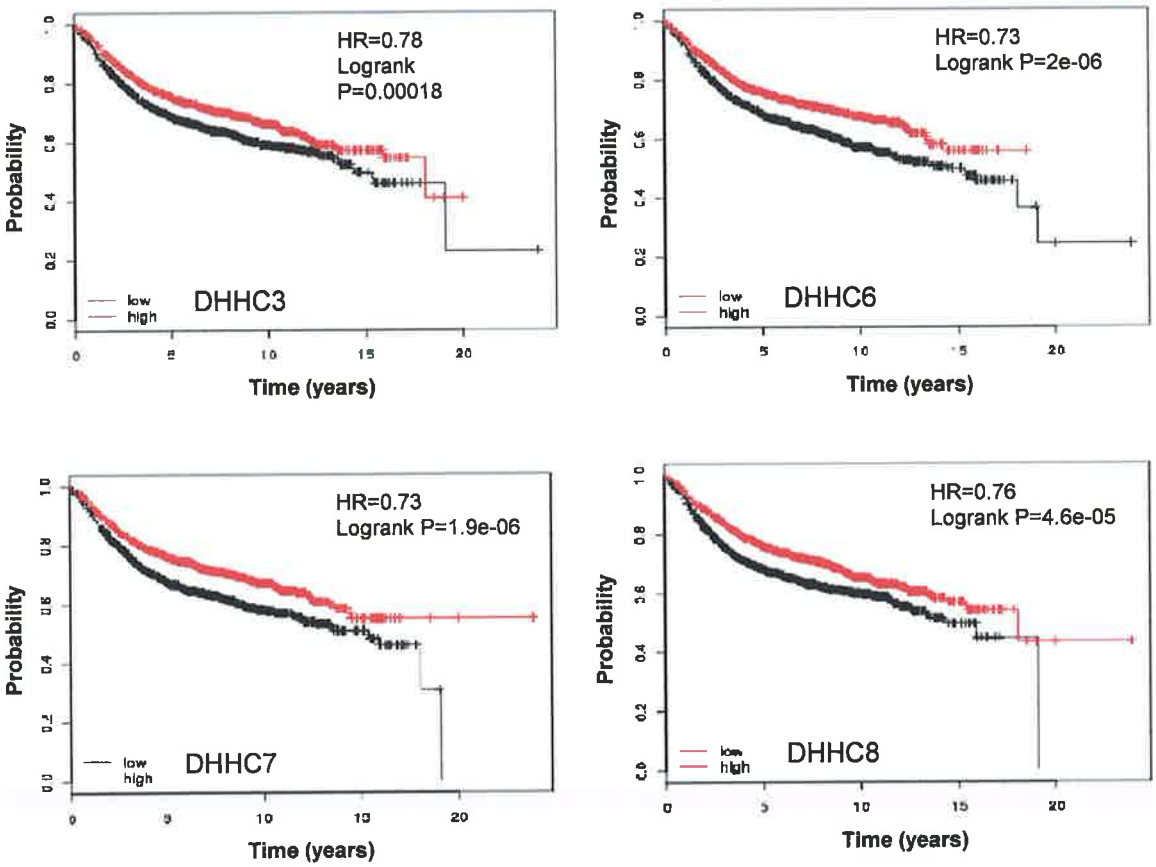

B.

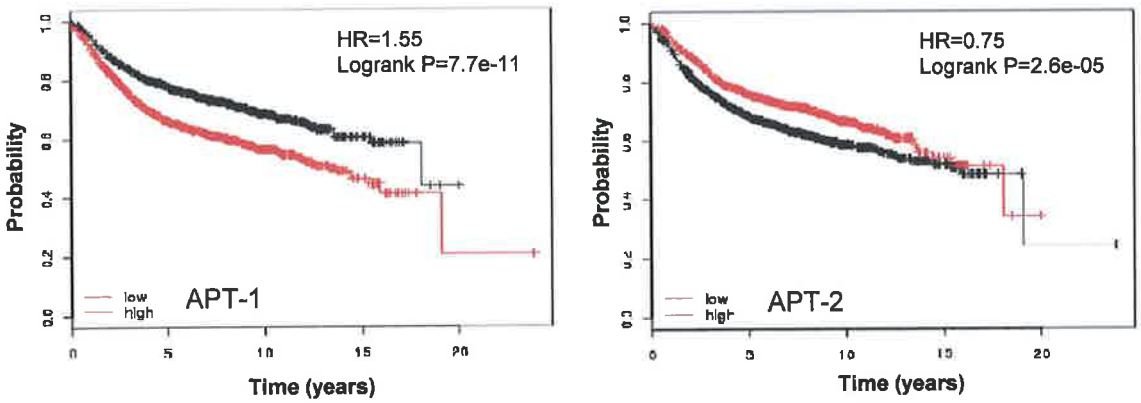

Figure 2: Babina et al

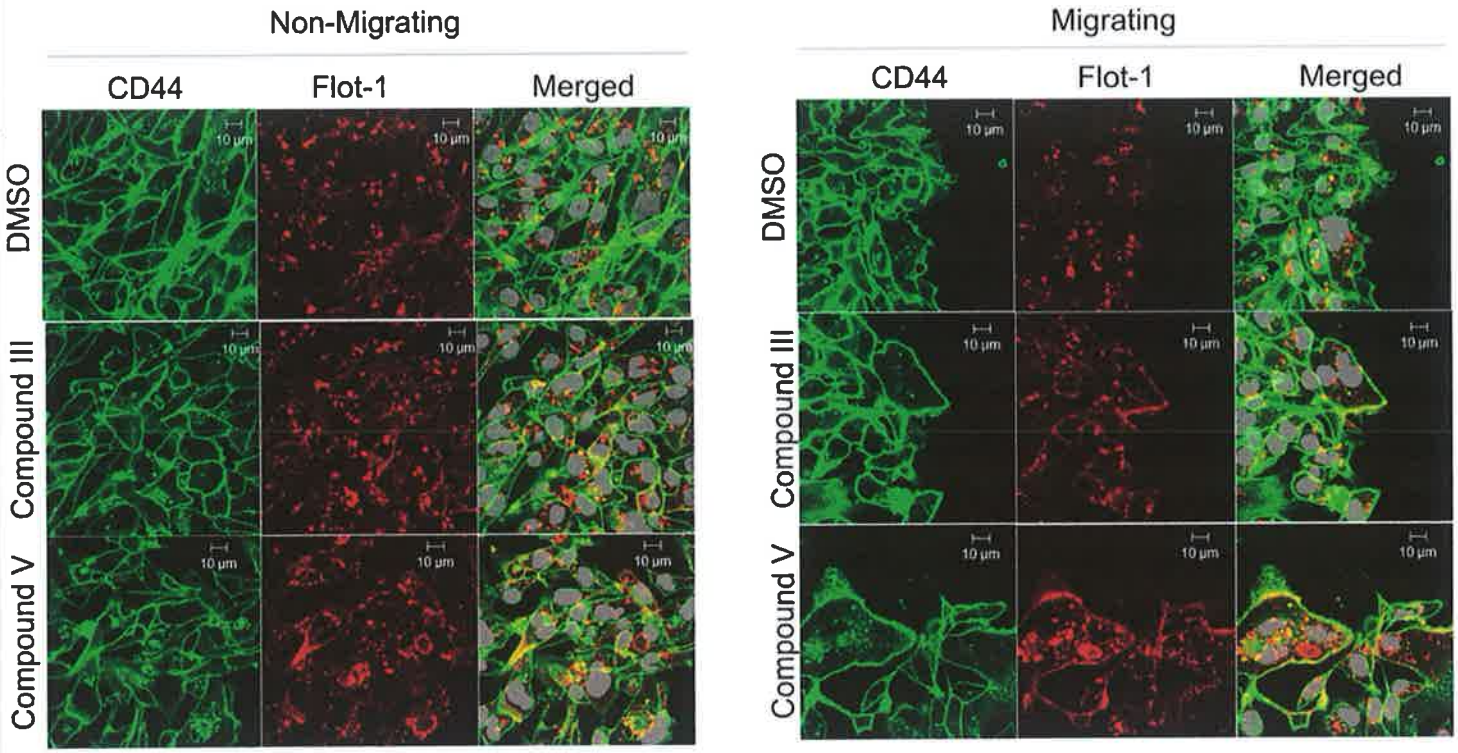

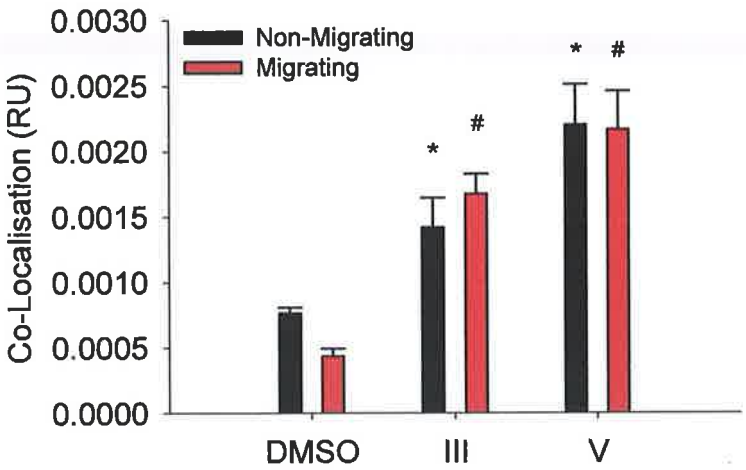

FIGURE 3

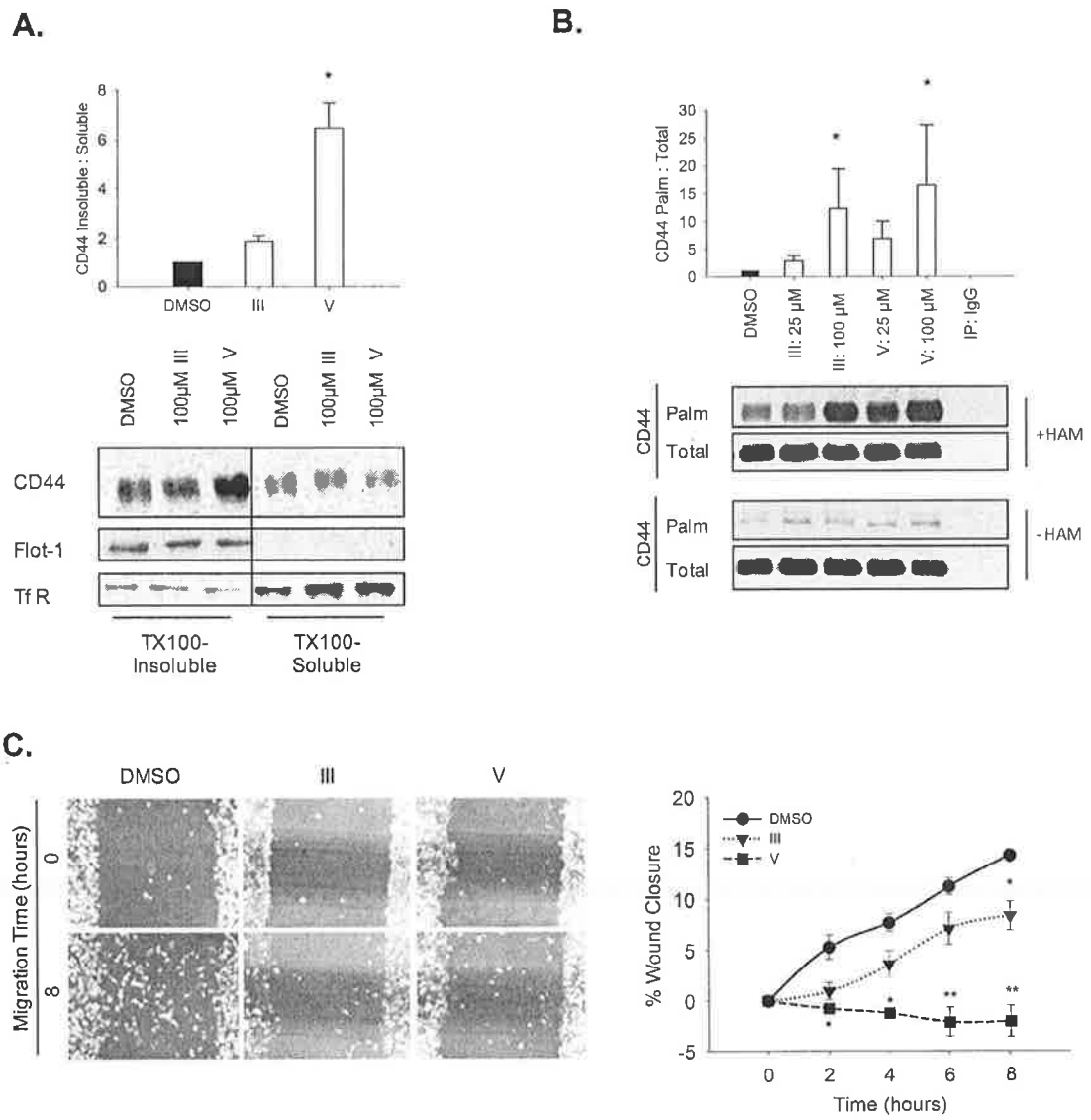
A.
CD44 Insoluble : Soluble
DMSO
III
V
DMSO
100μM III
100μM V
DMSO
100μM III
100μM V
CD44
Flot-1
Tf R
TX100-Insoluble
TX100-Soluble
B.
CD44 Palm : Total
DMSO
III: 25 μM
III: 100 μM
V: 25 μM
V: 100 μM
IP: IgG
CD44
Palm
Total
+HAM
CD44
Palm
Total
-HAM
C.
DMSO
III
V
Migration Time (hours)
0
8
% Wound Closure
DMSO
III
V
Time (hours)

Palmitoylation of CD44 regulates breast cancer cell migration via alterations in its lipid raft affiliation

Irina S. Babina, Simona Donatello, Arnold D.K. Hill, Ann M. Hopkins[§]
Department of Surgery, Royal College of Surgeons in Ireland, Dublin, Ireland

Short title: *CD44 palmitoylation and breast cancer cell motility*

[§] **Address correspondence to:**
Ann M. Hopkins,
Department of Surgery,
Royal College of Surgeons in Ireland,
RCSI Education and Research Centre,
Beaumont Hospital,
Dublin 9,
IRELAND
Tel: +353-1-809-3858
Fax: +353-1-633-5082
Email: annhopkins@rcsi.ie

Keywords: CD44, breast cancer, palmitoylation, lipid rafts, cell migration.

Abbreviations: ECM, extracellular matrix; HA, hyaluronan; APT, acyl protein thioesterase; BMCC, 1-Biotinamido-4-[4'-(maleimidomethyl)cyclohexanecarboxamido]butane; EMT, epithelial-to-mesenchymal transition; ERM, ezrin/radixin/moesin; Flot-1, flotillin-1; HAM, hydroxylamine; LR, lipid raft; NR, non-lipid raft; PAT, protein acyl transferase; TM, trans-membrane; TfR, transferrin receptor.

Article Category: Cancer Cell Biology

Abstract

Most breast cancer-related deaths result from metastasis, a process requiring dynamic regulation of tumour cell adhesive and migratory properties. The adhesion protein CD44, an important regulator of cell migration, is enriched in cholesterol-enriched membrane regions termed lipid rafts. We recently reported that CD44 raft affiliation negatively regulates interactions with its pro-migratory binding partner ezrin. Since raft affiliation is regulated by post-translational modifications including palmitoylation, we sought to define the contribution of CD44 palmitoylation and lipid raft affiliation to cell migration. Firstly we demonstrated that CD44 raft affiliation was increased during migration of non-invasive breast cell lines, but decreased during migration of highly-invasive cells. The latter was paralleled by increased CD44 recovery in non-raft fractions, and exclusive non-raft recovery of its binding partners. Point mutation of CD44 palmitoylation sites reduced CD44 raft affiliation in invasive MDA-MB-231 cells, increased CD44-ezrin co-precipitation and accordingly enhanced cell migration. Expression of palmitoylation-impaired (raft-excluded) CD44 mutants in non-invasive MCF-10a cells was sufficient to reversibly induce the phenotypic appearance of epithelial-to-mesenchymal transition and to increase cell motility. Furthermore the induction of cell migration temporally reduced CD44 palmitoylation in wild-type breast cells, while levels of palmitoylated CD44 were lower in primary cultures from invasive ductal carcinomas relative to non-tumour tissue. In conclusion, our results support a novel mechanism whereby CD44 palmitoylation inversely regulates breast cancer cell migration and may act as a new therapeutic target in breast cancer metastasis.

Brief description of novelty and impact: We provide novel evidence that palmitoylation of the cell migratory protein CD44, by inducing its sequestration in membrane lipid rafts, is sufficient to negatively regulate breast cancer cell migration. Since CD44-dependent cell migration has been implicated in cancer metastasis, the impact of this study is in suggesting CD44 palmitoylation as a novel target to reduce cancer cell dissemination during early metastasis.

Word count (introduction to acknowledgements, inclusive) = 4010

Introduction

Despite improvements in screening and care, breast cancer remains a leading cause of death in women worldwide [1]. Most breast cancer-related deaths arise from tumour metastasis to secondary sites. Cell migration out of the primary tumour is one of the earliest events in the metastatic cascade, and requires coordinated activation of numerous cell adhesion signalling cascades. CD44 is an important cell adhesion molecule with a variety of tissue-dependent functions[2]. It is the major receptor for the extracellular matrix (ECM) component hyaluronan (HA)[3]; can act as a co-receptor for growth factors[4] and can organise the actin cytoskeleton through a range of cytoplasmic linker proteins[5]. CD44 dysregulation has been implicated in progression of a variety of cancers[6], and in particular, associated with aggressive histological features of breast cancer[7].

Palmitoylation of two CD44 cysteine residues at positions 286 and 295 in the transmembrane and juxta-membrane regions confers high affinity for cholesterol- and sphingolipid-enriched regions of the cell membrane, termed lipid rafts[8]. Rafts are dynamic membrane regions which cluster together components of many signalling cascades known to be altered in cancer[9, 10]. The CD44 cytoplasmic tail helps organise the actin cytoskeleton via cytoplasmic actin-binding linker proteins, including members of the ezrin/radixin/moesin (ERM) family, merlin, annexin II and ankyrin. The intrinsic role of actin reorganisation in cellular adhesion and migration underlies why dysregulation of CD44-based signalling has been associated with the pathophysiological manifestations of cancer dissemination and metastasis[7, 11]. However the specific contribution of lipid rafts to the regulation of CD44-dependent adhesion/migration signalling remains incompletely understood. Several reports have linked CD44 lipid raft affiliation to cell survival and oncogenic signalling[12, 13]. It has been suggested that CD44-HA interactions take place in the lipid rafts of breast cancer cells[14], while CD44 interactions with its cytoplasmic binding partner merlin have been shown to inhibit cancer cell growth through ECM-driven signals[15].

Having recently shown that CD44 affiliation with lipid rafts is reduced in migrating breast cancer cells and hypothesised that translocation outside rafts permits cell migration[16] we set out to examine whether dynamic alterations in CD44 palmitoylation could directly drive cell migratory

events by modifying CD44 raft affiliation. We show for the first time that manipulation of CD44 raft affiliation via site-directed mutagenesis of palmitoylation sites influences the migration of invasive breast cancer cells, and is sufficient to induce a motile phenotype and functions in non-invasive cells. Furthermore, we demonstrate temporal reductions in palmitoylated CD44 during stimulated migration of breast cancer cells. Importantly, we provide evidence that reductions in CD44 palmitoylation are paralleled by increased CD44 co-association with its binding partner ezrin. Our findings in cell lines are supported by data from breast primary cell cultures, in which lower palmitoylation and co-localisation of CD44 with raft markers correlates with more aggressive cancers. Our data are consistent with a novel model whereby palmitoylation-induced retention of CD44 within lipid rafts exerts a suppressive effect on breast cancer cell migration; thus we speculate that pharmacological targeting of CD44 palmitoylation may offer a fresh strategy to reduce cancer cell dissemination during the early stages of metastasis.

Materials and Methods

Cell culture and transfection– Human breast cancer cell lines MCF-10a and MDA-MB-231 were obtained from ATCC (LGC Standards, Middlesex, UK). MDA-MB-231 cells were cultured in Dulbecco's Modified Eagles Medium (DMEM) (Sigma-Aldrich, Arklow, Ireland) supplemented with 10% foetal bovine serum (FBS), 2mM L-glutamine, 100U/ml penicillin and 100µg/ml streptomycin. MCF-10a cells were cultured in DMEM-F12 Ham (Sigma-Aldrich) supplemented with 100 U/ml penicillin, 5% horse serum, 0.5µg/ml hydrocortisone, 0.1µg/ml cholera toxin, 10µg/ml insulin and 20ng/ml epidermal growth factor (EGF) (all Sigma-Aldrich). Mammary tumour primary cell cultures were generated as described[17] from mastectomies or lumpectomies obtained with full consent and prior ethical approval (Beaumont Hospital Medical Ethics (Research) Committee) from symptomatic patients undergoing breast cancer surgery in Beaumont Hospital. Primary cultures were grown in Mammary Epithelial Growth Medium (MEGM; Lonza), prepared according to the manufacturer's guidelines. For transient transfections (48h, unless indicated otherwise) of plasmid DNA into the cells, jetPRIME transfection reagent (Source Bioscience, Dublin, Ireland) was used according to the manufacturer's guidelines. Control cells were incubated with DNA-diluting buffer alone. Transfected cells were selected using chloramphenicol (Sigma-Aldrich) dissolved directly in culture medium, at 30µg/ml for MDA-MB-231 and 50µg/ml for MCF-10a, as determined by kill curve proliferation assays (data not shown). All cells were cultured in a humidified incubator at 37°C and 5% CO_2 and confirmed to be mycoplasma-free by quarterly testing.

Antibodies and reagents– Anti-human CD44 primary antibody, detecting all isoforms of the protein, was obtained from R&D Systems (Abingdon, UK) and used for western blot analysis. For immunofluorescence and immunoprecipitation, mouse CD44 antibody was purchased from Santa Cruz Biotechnology (Heidelberg, Germany). Antibodies to detect flotillin-1 and ezrin (mouse) were from BD Biosciences (Oxford, UK). Mouse transferrin receptor antibody and anti-rabbit-HRP were from Cell Signaling Technologies (Danvers, MA, US). Antibodies against radixin, moesin, annexin II and merlin (rabbit) were from GeneTex, Inc. (Irvine, CA, US). Rabbit flotillin-1 antibody (immunofluorescence), anti-actin primary antibody and anti-mouse-

HRP secondary antibody were from Sigma-Aldrich. Streptavidin-HRP was from ThermoScentific (Ballycoolin, Ireland) and Millipore (Cork, Ireland).

Plasmid constructs– A pOTB7 plasmid encoding wild-type human CD44 (imaGenes; Source Bioscience) was grown on LB agar plates with 20μg/ml chloramphenicol and subsequently in LB broth with the same antibiotic concentration. Plasmid extraction was carried out using Qiagen Midi-Prep kits following the manufacturer's protocols (Qiagen, West Sussex, UK). This preparation was used as template genetic material for site-directed mutagenesis of CD44 palmitoylation sites. Single point mutations were obtained using QuikChange Site-Directed Mutagenesis kit (Agilent Technologies Ireland Ltd, Cork, Ireland). Cys286 was mutated to either Serine (C286S) or Alanine (C286A). A double mutation was achieved by using the mutated Cys286 DNA as a template for introducing a mutation at Cys295 to Alanine. The mutagenesis primers were obtained from Eurofins MWG Operon (Ebersberg, Germany) and contained the following sequences:

Table 1. ***Oligonucleotide primers used for site-directed mutagenesis***

Name	Oligonucleotide (5'-3')
C286A Forward	GCT TTG ATT CTT GCA GTT GCC ATT GCA GTC AAC AGT CG
C286A Reverse	CGA CTG TTG ACT GCA ATG GCA ACT GCA AGA ATC AAA GC
C286S Forward	GCT TTG ATT CTT GCA GTT TCC ATT GCA GTC AAC AGT CG
C286S Reverse	CGA CTG TTG ACT GCA ATG GAA ACT GCA AGA ATC AAA GC
C295A Forward	CAG TCG AAG AAG GGC TGG GCA GAA GAA AAA GC
C295A Reverse	GCT TTT TCT TCT GCC CAG CCC TTC TTC GAC TG

All mutations were confirmed by sequencing of the synthesised plasmids (Source Bioscience), and alignment using BLAST software.

Triton X-100 insolubility assay– Cells were grown to confluence in 6-well plates. Detergent-soluble fractions (enriched in non-raft cellular components) were obtained following 30 min incubation at 4°C in lysis buffer (100mM KCl, 3mM NaCl, 3.5mM $MgCl_2$, 10mM HEPES) containing 1% Triton X-100 and protease and phosphatase inhibitor cocktails (Sigma-Aldrich).

The detergent-insoluble pool (enriched in lipid rafts) was subsequently collected via scraping the wells in one-half volume of lysis buffer. After determination of protein concentrations using BCA assay, fractions of equivalent protein concentration were analysed by immunoblotting.

Lipid raft extraction by discontinuous sucrose gradient fractionation– All steps were carried out at 4°C. Cells were lysed in calcium- and magnesium-positive Hank's Balanced Salts Solution (Sigma-Aldrich) supplemented with 1% Triton X-100 (Roche Diagnostics, West Sussex, UK) and a protease inhibitor cocktail (Sigma-Aldrich). Lysates were dounced x20 and triturated x20 using a 26-gauge needle, then mixed in a 1:1 ratio with 90% (w/v) sucrose (dissolved in Hank's Solution. 4 ml was loaded into an ultracentrifuge tube (Roche) and sequentially overlain with equal volumes of 30%, 20% and 5% (w/v) sucrose. Preparations were ultracentrifuged in a Beckman Optima L-100K ultracentrifuge using an SW41Ti rotor (~260,000xg/19 hours/4°C). 1ml fractions were collected from the top and analysed as described[18]. Briefly, sucrose density was estimated using a refractometer. Alkaline phosphatase activity, to identify lipid raft-enriched fractions, was quantitated by incubating 1:10 volumes of fraction:*p*-nitrophenyl phosphate substrate (Sigma-Aldrich) for 30 min, and measuring absorbance at 405nm. Additionally, each fraction was tested for expression of lipid raft and non-raft markers, Flotillin-1 and transferrin receptor (TfR), respectively, using immuno-dot blot.

Immunoblotting– Equal protein concentrations were loaded onto 10% Tris-HCl gels and subjected to SDS-PAGE. Protein was transferred onto a nitrocellulose membrane by wet transfer at 100V/1h, incubated in blocking buffer (5% skim milk or BSA in TBS-0.1%Tween-20) for 1 hour and incubated with primary antibody overnight at 4°C. For dot blots, 2µl of each fraction was loaded directly onto membranes, blocked, and incubated with primary antibody overnight. After washing, membranes were incubated with an appropriate HRP-conjugated secondary antibody for 1 hour at room temperature. Membranes were developed by exposure to X-ray film (Sigma-Aldrich) using enhanced chemi-luminescent reagents (PerkinElmer Life Sciences, Waltham, MA). The same membranes were re-probed for expression of other proteins via stripping the primary antibody complexes with 0.7% 2-β-mercaptoethanol (Sigma-Aldrich) as described[18].

Acyl-Biotin Exchange (BMCC assay) – This method was adapted from a previous publication[19]. Briefly, CD44 protein was immunoprecipitated from lysates via overnight incubation at 4°C with 3 µg of mouse anti-human CD44 antibody as described[20]. Antibody-protein complexes were collected by 3-hour rotation at 4°C with 50µg of protein G-sepharose (Sigma-Aldrich), in the presence of 50mM N-ethylmaleimide (NEM, Sigma-Aldrich), to covalently block sulfhydryl groups. Complexes were subsequently divided into two fractions, for treatment with and without 1M hydroxylamine (HAM, Sigma-Aldrich) at room temperature for 1 hour (pH 7.40) to cleave free palmitate groups. Subsequently, samples were incubated with 1µM EZ-link biotin-N-(6-(biotinamido)hexyl)-3'-(2'-pyridyldithio)-propionamide (Biotin-BMCC, Thermo Scientific) at pH 6.2 for 1 hour at room temperature, to label the reactive cysteine residues. Labelled CD44 was released from the beads via 5 minute incubation at 100°C in 2x reducing Lamelli sample buffer, and subjected to SDS-PAGE and immunoblotting. Biotin-BMCC-labelled CD44 was detected with streptavidin-HRP incubation, followed by antibody incubation, to visualise total CD44.

Scratch wound migration assay– Confluent cells were subjected to scratch-wound assays as described[21]. Briefly, cells were wounded by a single scratch using a sterile p200 pipette tip attached to suction, rinsed with PBS and allowed to migrate in serum-free medium in a humidified incubator at 37°C /5% CO_2. Wells were imaged immediately after wounding (Time=0) and the precise location subsequently photographed every two hours for 6-8 hours. Wounds were measured using Scion Image software (Scion Corporation Ltd., Frederick, MD, USA), and percentage wound closure calculated relative to Time=0 for each condition and plotted using SigmaPlot.

Image analysis and statistics– Densitometric analysis was performed on western blot films (exposed for equivalent times) using ImageJ software (National Institute of Health). Raw values were used for statistical analysis from a minimum of three independent experiments, and averages expressed as percentage of internal control (non-migrating condition for untransfected cells, and CD44WT for transfected cells). *P* values were calculated using equal variance two-tailed Student's t-tests. For migration assays 2-way ANOVA tests were performed across all the time points using GraphPad Prism. Results were considered significant when $p<0.05$.

Results

CD44 raft affiliation varies across differentially-invasive breast cancer cells– We previously reported a decrease in CD44 lipid raft affiliation in migrating MDA-MB-231 and Hs578T cell lines[20]. In the present study we firstly compared the raft affiliation status of CD44 in the non-invasive, normal-like cell line MCF-10a and the highly-invasive cell line, MDA-MB-231. Isopycnic sucrose density gradient fractionation was used to isolate rafts under migrating versus non-migrating conditions, and fractions were analysed for activity of the raft-affiliated enzyme alkaline phosphatase. The enzyme was most active in fractions 4-6 (**Fig.1A**), suggesting enrichment of rafts at sucrose densitites of 20-25%. Immuno-dot blots (**Fig.1B**) confirmed partitioning of the raft marker protein Flotillin-1 to the same fractions, and exclusive detection of the non-raft marker TfR at higher sucrose densities (Fractions 8-12; >30% sucrose). Thereafter, we refer to fractions 4-6 as "lipid raft fractions" and fractions 9-11 as "non-raft fractions".

Western blotting was used to compare the affiliation of CD44 and its binding partners with rafts under non-migrating and migrating conditions. In MCF-10a cells, CD44 recovery in raft fractions was increased in migrating versus non-migrating cells (**Fig.1C**). A high molecular weight CD44 band was also noted in raft fractions. Integrated band densities from n=3 independent experiments were used to calculate a ratio of CD44 affiliation with lipid rafts (described previously[20]). This value (CD44 LR:NR) is CD44 normalised to Flotillin-1 as a loading control for raft fractions, divided by CD44 normalised to TfR as a loading control for non-raft fractions. An increase in the ratio reflects increased CD44 raft affiliation. A significant increase in the ratio was noted in migrating MCF-10a cells (**Fig.1C**, lower panel; $p<0.05$). The CD44 binding partners ezrin, radixin, moesin, merlin and annexin II were detected only in non-raft fractions (**Fig.1C**). In contrast to MCF-10a cells, CD44 recovery in non-raft fractions of MDA-MB-231 was increased after the induction of migration (**Fig.1D**). This was accordingly quantified as a significant decrease in the CD44 raft affiliation ratio (**Fig.1D**, lower panel; $p<0.05$). As with MCF-10a, all of the CD44 binding partners tested were recovered exclusively from non-raft fractions in non-migrating and migrating cells.

CD44 palmitoylation-impaired mutants have reduced raft affiliation– Having observed reduced CD44 raft affiliation in migrating highly-invasive cells, we sought to directly manipulate CD44 raft affiliation to test its impact on cell motility. Site-directed mutagenesis was used to introduce point mutations into one (C286A or C286S) or both (C286A,295A [AA] and C286S,295A [SA]) cysteine residues which control CD44 palmitoylation and incorporation into rafts (**Fig.2A**). MDA-MB-231 cells were transiently transfected with palmitoylation-impaired CD44 constructs, negatively-selected for 48 hours and subjected to sucrose density gradient fractionation. Raft and non-raft fractions were identified by enrichment in respectively Flotillin-1 and TfR (**Fig.2B**). Cells expressing palmitoylation-impaired mutants had less CD44 in lipid raft fractions and correspondingly more recovered from non-raft domains. Compared to either CD44WT-expressing or control cells, the CD44 raft affiliation ratio was significantly reduced in cells expressing single or double palmitoylation mutants (**Fig.2C**, $p<0.05$). Given the requirement for large quantities of material for raft extraction preparations, Triton X-100 insolubility assays were investigated as a surrogate to estimate relative amounts of CD44 in detergent-insoluble (putatively raft-enriched) and detergent–soluble (putatively non-raft-enriched) pools. As expected, Triton X-100-insoluble fractions were enriched in Flotillin-1, while detergent-soluble fractions were enriched in TfR (**Fig.2D**). MDA-MB-231 cells expressing wild-type CD44 had a similar CD44 solubility/insolubility profile compared to control cells. In contrast, cells transfected with CD44 palmitoylation mutants showed decreased CD44 recovery in detergent-insoluble pools and a corresponding increase in recovery from detergent-soluble pools. Calculation of the affiliation ratio of CD44 with detergent-insoluble fractions ("CD44 Insoluble:Soluble"; **Fig.2E**) revealed reductions in cells expressing single or double palmitoylation mutants versus control or CD44WT-overexpressing cells ($p<0.05$ for all). Since these findings mirrored results from sucrose gradient raft extractions, the simpler detergent-extraction approach was subsequently used.

Direct reduction of CD44 palmitoylation promotes a migratory phenotype– To confirm that changes in CD44 raft distribution reflected reductions in its palmitoylation, biotin-BMCC assays were performed on non-migrating cells overexpressing representative single and double

palmitoylation mutants (**Fig.3A-B**). Free palmitate groups were cleaved from CD44 immunoprecipitates using HAM, whereupon reactive cysteines were labelled with biotin-BMCC and detected with streptavidin. Biotin-labelled (palmitoylated) CD44 was less in cells expressing palmitoylation mutants versus wild-type or control cells. Band quantitation of palmitoylated versus total CD44 confirmed significant reductions in palmitoylated CD44 in MDA-MB-231 cells overexpressing single and double mutants (**Fig.3B**). To determine whether forced exclusion of CD44 from rafts directly promoted cell migration, scratch-wound assays were performed in MDA-MB-231 cells transiently transfected with CD44 palmitoylation-impaired mutants (**Fig.3C**). Overexpression of CD44WT or CD44 single-site palmitoylation mutants doubled cell migration compared to controls. Overexpression of CD44 double-site palmitoylation mutants improved cell migration four-fold relative to control cells (**Fig.3C**), or two-fold relative to CD44WT or single mutant cells ($p<0.05$).

We next tested if forced exclusion of CD44 from rafts was sufficient to induce a migratory phenotype in non-invasive breast cells. CD44 palmitoylation-impaired mutants were over-expressed in histologically-normal MCF-10a cells, whereupon Triton X-100 insolubility assays confirmed reduced partitioning to raft fractions (**Fig.4A**). CD44 recovery in detergent-insoluble pools was virtually abolished in cells expressing double-site mutants (**Fig.4B;** $p<0.05$ vs CD44WT; $p<0.01$ vs Control). Biotin-BMCC assays confirmed reductions in palmitoylated CD44 in cells overexpressing CD44 palmitoylation-impaired mutants (**Fig.4C-D**). Relative to control MCF-10a cells, overexpression of either CD44WT or CD44 palmitoylation-impaired mutants disrupted characteristically tight colonies in these cells, inducing cell scattering and an EMT-like appearance (**Fig.4E**) in conjunction with reduced expression of the epithelial marker EpCAM and enhanced expression of the mesenchymal marker vimentin (**Supp. Fig.S1**). This was accompanied by increased cell migration, particularly in cells overexpressing CD44 double-site mutants (**Fig.4F** $p<0.05$ vs Control). Mutant de-selection after 48h followed by two subcultures in normal medium normalised both the CD44 raft affiliation ratio (**Supp. Fig.S2A-D**) and cell migration (**Supp. Fig.S2E-F**) to control levels.

Reduced CD44 palmitoylation facilitates ezrin binding and correlates with invasive phenotype – Since modulation of CD44 palmitoylation reversibly modified cell migration, we questioned the reverse- whether stimulation of cell migration might reduce CD44 palmitoylation to facilitate its extra-raft translocation. CD44 palmitoylation decreased in a statistically-significant manner during a migration time-course (**Fig.5A-B**). This was accompanied by a notable increase in CD44 co-precipitation with its pro-migratory binding partner ezrin at 1-2h (**Fig.5C**). Similarly, CD44/ezrin co-precipitation was increased in migrating cells expressing a CD44 double-site palmitoylation mutant (**Fig.5D**).

Having shown a direct relationship between CD44 palmitoylation status and cell migration, we translated this into a more patient-relevant context by evaluating CD44 palmitoylation and raft affiliation status in representative primary cultures isolated from non-invasive versus invasive human breast tumours. Cultures derived from non-invasive ductal carcinoma *in situ* (DCIS) tumours formed organised colonies of luminal-like epithelial cells surrounded by flattened, myoepithelial-like cells (**Fig.5E**, phase contrast). Cultures derived from invasive ductal carcinoma (IDC) tumours contained predominantly flattened protrusive cells. CD44 co-localised extensively with Flotillin-1 in the cell membranes of DCIS cultures (**Fig.5E**), but there was little spatial overlap of these proteins in IDC cultures. Accordingly, lower levels of palmitoylated CD44 were detected in whole cell extracts from six representative IDC cultures relative to two representative non-tumour (NT) cultures (**Fig.5F**). Collectively, these results suggest a novel clinical relevance for the regulation of palmitoylation and lipid raft affiliation of CD44 in breast cancer cells.

Discussion

Cell migration is an early molecular event in breast cancer metastasis, and identifying tumour markers that correlate with metastatic potential is a focus of numerous studies. Despite expressional correlations of CD44[22, 23] or its splice variants[24] with progression of aggressive breast cancers, specific mechanisms of CD44-dependent cell migration remain controversial. CD44 resides in lipid rafts[6, 25, 26], organisation centres for molecules that play key roles in cell migration and whose altered functional behaviour has been implicated in diseases including breast cancer[9]. We have shown that CD44 localisation in rafts limits associations with its cytoskeletal linker binding partner ezrin[20]. We therefore hypothesized that translocation of CD44 outside rafts to bind to migratory partners (such as ezrin) is a novel regulatory mechanism controlling CD44-dependent cell migration. In the present study we dissected the relationship between CD44 raft affiliation, ezrin association and migratory potential in breast cancer cells.

Having shown reduced CD44 raft affiliation during migration of invasive MDA-MB-231 and Hs578T breast cells[20], here we found that, in the normal-like breast epithelial cell line MCF-10a, CD44 affiliation with lipid rafts was in fact *increased* under migratory conditions. This may suggest that lipid rafts sequester CD44 to limit the migration of normal-like cells. Accordingly, the importance of lipid raft domains in maintaining front-rear polarity during breast cancer cell migration has been highlighted[27]. In contrast to MCF-10a cells, CD44 lipid raft affiliation in the metastatic cell line MDA-MB-231 was almost halved during cell migration. To our knowledge, these are the first reports of a link between CD44 raft localisation and breast cancer cell migration. However, localisation of CD44 outside lipid rafts in human glioblastoma cells has been shown to induce metalloproteinase-mediated CD44 shedding and tumour cell migration[28], which was further confirmed after membrane cholesterol modulation with methyl-β-cyclodextrin, filipin and simvastatin[29]. In contrast, raft affiliation of CD44 has been demonstrated to recruit Src and integrins in gastric and colorectal cancers, promoting cell survival and increasing endothelial adhesion[30]. Our data in breast cells suggest that CD44 localisation outside lipid rafts is associated with a pro-migratory state; furthermore a range of CD44 binding partners was only ever recovered from non-raft domains. Given the reported

involvement of ezrin[31] and ankyrin[32] in cancer progression and merlin in tumour suppression[15], we speculate that the spatial availability of CD44 to interact with specific cytosolic partners may differentially regulate cancer cell migration.

It has been shown that dual acylation of two cysteine residues (Cys286 and Cys295) in the CD44 transmembrane region is required for its raft association in fibroblasts and embryonic kidney cells[33]. We thus used transient overexpression of palmitoylation-impaired mutants as a tool to decrease CD44 affiliation with lipid rafts. Triton X-100 insolubility assays were used as a surrogate for lipid raft extractions, since detergent-insoluble fractions have been shown to be enriched in lipid rafts[29, 34]. Overexpression of CD44 palmitoylation-impaired mutants reduced the affiliation of CD44 with rafts, however CD44WT-overexpressing cells too had decreased CD44 raft affiliation. This may reflect enhanced CD44 trafficking, since we observed a coincident increase in vesicular/cytoplasmic staining of an early endosomal marker in CD44WT cells (data not shown). Nonetheless, despite only using a transient transfection approach, distinct functional differences were observed in MDA-MB-231 cells as a consequence of reduced CD44 raft affiliation. Specifically, migration was higher in cells expressing CD44 palmitoylation mutants relative to controls or CD44WT-expressing cells. It is also noteworthy that higher cell migration in CD44-WT versus control cells was paralleled by lower levels of palmitoylated CD44 in the former. Thus the published links between CD44WT overexpression and cell migration/invasion in breast cancer cell lines[35] and patient samples[7] may also reflect a proportional decrease in CD44 palmitoylation status.

Our data have revealed that forcing CD44 outside lipid rafts with palmitoylation mutants was sufficient to enhance cell migration and induce the appearance of EMT in histologically-normal MCF-10a breast cells. Cells overexpressing CD44WT also acquired the morphological features of EMT, but over a longer time-course. This is consistent with studies showing decreased epithelial markers and increased mesenchymal markers upon CD44 activation[36], and links between CD44, EMT and breast cancer progression[36]. That our observed effects related specifically to CD44 mutant expression was confirmed upon termination of selection.

Interestingly, EMT in MCF-10a cells has been linked to a switch between a high molecular weight CD44 isoform and the standard isoform[36]. It is unknown where this transition should take place; however we noted reduced expression of high molecular weight CD44 in palmitoylation mutant cells. Taken together, this might suggest that, in the early stages of cancer progression, the standard form of CD44 becomes prevalent and localises outside lipid rafts in order to bind its oncogenic binding partners and stimulate cell migration.

Having shown that CD44 palmitoylation inversely regulates cell migration, we sought to examine whether migration itself might alter CD44 palmitoylation. We present novel evidence that CD44 palmitoylation is temporally reduced during breast cancer cell migration. Although the mechanisms for this reduction remain elusive, it is possible that actin rearrangements during migration facilitate altered spatial access of palmitoylating or de-palmitoylating enzymes to targets such as CD44. More importantly, reductions in CD44 palmitoylation were paralleled by enhanced co-association of CD44 with the linker protein ezrin, providing a direct mechanism for cytoskeletal engagement in order to drive cell migration. The potential clinical significance of this is illustrated by the fact that CD44 palmitoylation levels were low in primary cultures from human invasive ductal carcinomas in comparison to non-tumour tissue; and that co-localisation of CD44 with the lipid raft marker Flotillin-1 was also low in invasive specimens. Thus our findings are consistent with a novel model in which CD44 palmitoylation facilitates its sequestration within lipid rafts, restricting its availability to bind to pro-migratory binding partners such as ezrin (**Fig. 6**) and thereby restraining tumourigenic behaviour. We submit that further studies into mechanisms underlying the regulation of CD44 palmitoylation and lipid raft containment may merit evaluation as a novel target to reduce breast cancer metastatic spread.

Acknowledgements

This work was funded by the Health Research Board of Ireland (RP/2008/49, AMH) and Breast Cancer Ireland. We thank Prof. Robert Nabi and Dr. Maria Fairbank (University of British Columbia) for BMCC assay advice.

References

1. Jemal A, Bray F, Center MM, Ferlay J, Ward E, Forman D: Global cancer statistics, CA Cancer J Clin 2011, 61:69-90
2. Platt VM, Szoka FC, Jr.: Anticancer therapeutics: targeting macromolecules and nanocarriers to hyaluronan or CD44, a hyaluronan receptor, Mol Pharm 2008, 5:474-486
3. Herrera-Gayol A, Jothy S: Adhesion proteins in the biology of breast cancer: contribution of CD44, Exp Mol Pathol 1999, 66:149-156
4. Orian-Rousseau V, Chen L, Sleeman JP, Herrlich P, Ponta H: CD44 is required for two consecutive steps in HGF/c-Met signaling, Genes Dev 2002, 16:3074-3086
5. Ponta H, Sherman L, Herrlich PA: CD44: from adhesion molecules to signalling regulators, Nat Rev Mol Cell Biol 2003, 4:33-45
6. Ostapkowicz A, Inai K, Smith L, Kreda S, Spychala J: Lipid rafts remodeling in estrogen receptor-negative breast cancer is reversed by histone deacetylase inhibitor, Mol Cancer Ther 2006, 5:238-245
7. Diaz LK, Zhou X, Wright ET, Cristofanilli M, Smith T, Yang Y, Sneige N, Sahin A, Gilcrease MZ: CD44 expression is associated with increased survival in node-negative invasive breast carcinoma, Clin Cancer Res 2005, 11:3309-3314
8. Neame SJ, Uff CR, Sheikh H, Wheatley SC, Isacke CM: CD44 exhibits a cell type dependent interaction with triton X-100 insoluble, lipid rich, plasma membrane domains, J Cell Sci 1995, 108 (Pt 9):3127-3135
9. Babina IS, Donatello S, Nabi IR, Hopkins AM: Lipid Rafts as Master Regulators of Breast Cancer Cell Function. Edited by Gunduz MGaE. InTech, 2011, p. pp. 401-428
10. Staubach S, Hanisch FG: Lipid rafts: signaling and sorting platforms of cells and their roles in cancer, Expert Rev Proteomics 2011, 8:263-277
11. Naor D, Wallach-Dayan SB, Zahalka MA, Sionov RV: Involvement of CD44, a molecule with a thousand faces, in cancer dissemination, Semin Cancer Biol 2008, 18:260-267
12. Coleman DT, Bigelow R, Cardelli JA: Inhibition of fatty acid synthase by luteolin post-transcriptionally down-regulates c-Met expression independent of proteosomal/lysosomal degradation, Mol Cancer Ther 2009, 8:214-224
13. Elnagar AY, Sylvester PW, El Sayed KA: (-)-Oleocanthal as a c-Met Inhibitor for the Control of Metastatic Breast and Prostate Cancers, Planta Med 2011,
14. Bourguignon LY: Hyaluronan-mediated CD44 activation of RhoGTPase signaling and cytoskeleton function promotes tumor progression, Semin Cancer Biol 2008, 18:251-259
15. Morrison H, Sperka T, Manent J, Giovannini M, Ponta H, Herrlich P: Merlin/neurofibromatosis type 2 suppresses growth by inhibiting the activation of Ras and Rac, Cancer Res 2007, 67:520-527
16. Donatello S, Babina, I. S., Hazelwood LD, Hill AD, Nabi IR, Hopkins AM: Lipid Raft Association Restricts CD44-Ezrin Interaction and Promotion of Breast Cancer Cell Migration, Am J Pathol 2012,
17. Donatello S, Hudson L, Cottell DC, Blanco A, Aurrekoetxea I, Shelly MJ, Dervan PA, Kell MR, Stokes M, Hill AD, Hopkins AM: An imbalance in progenitor cell populations reflects tumour progression in breast cancer primary culture models, J Exp Clin Cancer Res 2011, 30:45

18. Bowie RV, Donatello S, Lyes C, Owens MB, Babina IS, Hudson L, Walsh SV, O'Donoghue DP, Amu S, Barry SP, Fallon PG, Hopkins AM: Lipid rafts are disrupted in mildly inflamed intestinal microenvironments without overt disruption of the epithelial barrier, Am J Physiol Gastrointest Liver Physiol 2012, 302:G781-793
19. Fairbank M, Huang K, El-Husseini A, Nabi IR: RING finger palmitoylation of the endoplasmic reticulum Gp78 E3 ubiquitin ligase, FEBS Lett 2012, 586:2488-2493
20. Hughes L, Malone C, Chumsri S, Burger AM, McDonnell S: Characterisation of breast cancer cell lines and establishment of a novel isogenic subclone to study migration, invasion and tumourigenicity, Clin Exp Metastasis 2008, 25:549-557
21. Colas S, Maheo K, Denis F, Goupille C, Hoinard C, Champeroux P, Tranquart F, Bougnoux P: Sensitization by dietary docosahexaenoic acid of rat mammary carcinoma to anthracycline: a role for tumor vascularization, Clin Cancer Res 2006, 12:5879-5886
22. Sheridan C, Kishimoto H, Fuchs RK, Mehrotra S, Bhat-Nakshatri P, Turner CH, Goulet R, Jr., Badve S, Nakshatri H: CD44+/CD24- breast cancer cells exhibit enhanced invasive properties: an early step necessary for metastasis, Breast Cancer Res 2006, 8:R59
23. Klingbeil P, Natrajan R, Everitt G, Vatcheva R, Marchio C, Palacios J, Buerger H, Reis-Filho JS, Isacke CM: CD44 is overexpressed in basal-like breast cancers but is not a driver of 11p13 amplification, Breast Cancer Res Treat 2010, 120:95-109
24. Olsson E, Honeth G, Bendahl PO, Saal LH, Gruvberger-Saal S, Ringner M, Vallon-Christersson J, Jonsson G, Holm K, Lovgren K, Ferno M, Grabau D, Borg A, Hegardt C: CD44 isoforms are heterogeneously expressed in breast cancer and correlate with tumor subtypes and cancer stem cell markers, BMC Cancer 2011, 11:418
25. Ilangumaran S, Hoessli DC: Effects of cholesterol depletion by cyclodextrin on the sphingolipid microdomains of the plasma membrane, Biochem J 1998, 335 (Pt 2):433-440
26. Tarone G, Ferracini R, Galetto G, Comoglio P: A cell surface integral membrane glycoprotein of 85,000 mol wt (gp85) associated with triton X-100-insoluble cell skeleton, J Cell Biol 1984, 99:512-519
27. Manes S, Mira E, Gomez-Mouton C, Lacalle RA, Keller P, Labrador JP, Martinez AC: Membrane raft microdomains mediate front-rear polarity in migrating cells, EMBO J 1999, 18:6211-6220
28. Murai T, Miyazaki Y, Nishinakamura H, Sugahara KN, Miyauchi T, Sako Y, Yanagida T, Miyasaka M: Engagement of CD44 promotes Rac activation and CD44 cleavage during tumor cell migration, J Biol Chem 2004, 279:4541-4550
29. Murai T, Maruyama Y, Mio K, Nishiyama H, Suga M, Sato C: Low cholesterol triggers membrane microdomain-dependent CD44 shedding and suppresses tumor cell migration, J Biol Chem 2011, 286:1999-2007
30. Lee JL, Wang MJ, Sudhir PR, Chen JY: CD44 engagement promotes matrix-derived survival through the CD44-SRC-integrin axis in lipid rafts, Mol Cell Biol 2008, 28:5710-5723
31. Elliott BE, Meens JA, SenGupta SK, Louvard D, Arpin M: The membrane cytoskeletal crosslinker ezrin is required for metastasis of breast carcinoma cells, Breast Cancer Res 2005, 7:R365-373
32. Singleton PA, Bourguignon LY: CD44 interaction with ankyrin and IP3 receptor in lipid rafts promotes hyaluronan-mediated Ca2+ signaling leading to nitric oxide production and endothelial cell adhesion and proliferation, Exp Cell Res 2004, 295:102-118

33. Thankamony SP, Knudson W: Acylation of CD44 and its association with lipid rafts are required for receptor and hyaluronan endocytosis, J Biol Chem 2006, 281:34601-34609
34. Simons K, Ikonen E: Functional rafts in cell membranes, Nature 1997, 387:569-572
35. Roetger A, Merschjann A, Dittmar T, Jackisch C, Barnekow A, Brandt B: Selection of potentially metastatic subpopulations expressing c-erbB-2 from breast cancer tissue by use of an extravasation model, Am J Pathol 1998, 153:1797-1806
36. Brown RL, Reinke LM, Damerow MS, Perez D, Chodosh LA, Yang J, Cheng C: CD44 splice isoform switching in human and mouse epithelium is essential for epithelial-mesenchymal transition and breast cancer progression, J Clin Invest 2011, 121:1064-1074

Figure legends

FIGURE 1. CD44 affiliation with lipid rafts is reduced during migration of highly-invasive breast cancer cells. Sucrose density gradient fractionation was used to isolate lipid rafts from non-migrating versus migrating MDA-MB-231 cells. **A.** Raft fractions were identified on the basis of peak biochemical activity of the lipid raft-affiliated enzyme alkaline phosphatase. **B.** Enrichment of the marker proteins Flotillin-1 and transferrin receptor (TfR) by immuno-dot blot was further used to define the identity of respectively raft versus non-raft fractions. **C.** The Western blot expression profile of CD44 and its binding partners in MCF-10a normal-like breast cells revealed increased recovery of raft-affiliated CD44 after 2 hours of migration compared to non-migrating controls. This was verified by calculation of the raft affiliation ratio from the quantification of three independent experiments (histogram). The CD44 binding partners tested were exclusively recovered from non-raft fractions. **D.** CD44 recovery from lipid raft fractions of highly-invasive MDA-MB-231 breast cancer cells was reduced in migrating relative to non-migrating conditions; and paralleled by increased CD44 recovery from non-raft fractions in migrating conditions. This was verified by calculation of the raft affiliation ratio from the quantification of three independent experiments (histogram). The CD44 binding partners tested were exclusively recovered from non-raft fractions. *Error bars=SEM, n=3 experiments; *$p<0.05$, Student's t-test.*

FIGURE 2. CD44 palmitoylation-impaired constructs have reduced affiliation with lipid rafts. A. Schematic representation of palmitoylation-impaired CD44 constructs generated by site-directed mutagenesis of human CD44. Single-site mutants were termed C286A and C286S, while double-site mutants (C286S+C295A, C286A+C295A) were termed SA and AA respectively. **B.** MDA-MB-231 cells were transfected with full-length CD44 (CD44WT) or CD44 single-site (C286A, C286S) and double-site (SA, AA) palmitoylation-impaired mutants for 48 hours. Full-scale lipid raft extractions confirmed reductions in raft-affiliated CD44 in cells expressing the mutant constructs relative to controls. **C.** Calculation of the LR:NR ratio for multiple experiments confirmed statistically significant reductions in CD44 raft affiliation upon

expression of the CD44 palmitoylation-impaired mutants. **D.** Triton X-100-insoluble and –soluble fractions were isolated and confirmed to be enriched in respectively lipid raft (Flotillin-1) or non-raft (TfR) markers. CD44 recovery from raft-enriched fractions was reduced in cells overexpressing mutant CD44, and paralleled by increased recovery of CD44 in non-raft fractions. **E.** Calculation of the affiliation ratio of CD44 with detergent-insoluble versus –soluble fractions confirmed reductions in raft-affiliated CD44 from cells expressing mutant constructs relative to controls. *Error bars=SEM, n=3; $^{\#}p<0.05$ (C286S vs Control); *p<0.05; **p<0.01, Student's t-test.*

FIGURE 3. Reduced CD44 palmitoylation is paralleled by increased cell migration. A. Biotin-BMCC assays were used to measure palmitoylated CD44 (CD44-Palm) in cells expressing representative single and double palmitoylation mutants, and compared to total CD44 levels (CD44-Total). Isotype-matched IgG was used as a negative control for CD44 immunoprecipitations, and omission of HAM reagent was a BMCC negative control. CD44-Palm was reduced in cells over-expressing CD44 palmitoylation-impaired mutant constructs. **B.** Densitometric quantification of multiple experiments confirmed significant reductions in CD44-Palm relative to CD44-Total in mutant cells. *Error bars=SEM, n=3; *p<0.05; **p<0.01, Student's t-test.* **C.** Phase contrast micrographs of scratch-wound migration assays performed in MDA-MB-231 cells transfected for 48h with CD44-WT or CD44 single-site (C286A, C286S) or double-site (SA, AA) palmitoylation-impaired mutants. Cell migration was significantly enhanced in mutant-expressing cells compared to control cells, as indicated in the graphical representation of multiple experiments. *Error bars=SEM, n=3; # φ*p<0.05; **p<0.01, 2-way ANOVA.*

FIGURE 4. Reducing CD44 is sufficient to alter normal phenotype in breast cells. MCF-10a cells were transfected for 48 hours with full-length CD44 (CD44WT), and single-site (C286A, C286S) or double-site (SA, AA) palmitoylation-impaired mutants. **A.** Triton X-100-insoluble and –soluble fractions were isolated, and confirmed to be enriched in respectively lipid raft (Flotillin-1) and non-raft (TfR) marker proteins. Overexpression of mutant CD44 reduced CD44

recovery from raft-containing fractions compared to that in untransfected controls and CD44WT-expressing cells. **B.** The calculated ratios of CD44 affiliation with detergent-insoluble fractions reflected significant reductions in CD44 raft affiliation in mutant cells compared to untransfected control cells, and furthermore in CD44 double-site mutants compared to CD44WT. **C.** CD44 palmitoylation was assessed by BMCC assay in CD44 immunoprecipitates of control, CD44WT- and CD44 mutant-expressing cells. Palmitoylated CD44 was detected with streptavidin (CD44-Palm), and total CD44 using CD44 antibody (CD44-Total). No CD44 was immunoprecipitated in the isotype-matched IgG control lanes, and no palmitoylated CD44 was detected in the HAM- control conditions. In the HAM+ condition, palmitoylated CD44 was reduced in mutant-expressing cells. **D.** Quantification of palmitoylated CD44 (as a ratio of total CD44) revealed significant reductions in cells over-expressing a double-site CD44 palmitoylation-impaired mutant (AA) relative to control or CD44WT-expressing cells (*$p<0.05$; **$p<0.01$, *Student's t-test).* **E.** Phase contrast micrographs 48 hours post transfection revealed a change in the morphology of control MCF-10A colonies (Ctrl) following CD44 over-expression, with a protrusive, disseminated EMT-like appearance in all the CD44-overexpressing cells (arrows) which was particularly pronounced in those expressing the CD44 palmitoylation-impaired mutants. **F.** Scratch-wound assays revealed significant enhancements in the migratory capacity of MCF-10A cells expressing CD44 palmitoylation-impaired mutants relative to control cells (*$p<0.05$, *2-way ANOVA). Error bars=SEM, n= 3 experiments.*

FIGURE 5. Decreased CD44 palmitoylation is paralleled by increased co-association with ezrin. A. CD44 immunprecipitates from different MDA-MB-231 migration time points were probed for palmitoylated CD44 by BMCC assay. Palmitoylated CD44 was detected using streptavidin (CD44-Palm), and total CD44 using a CD44 primary antibody (CD44-Total). The absence of HAM treatment was a negative control for palmitoylated CD44. CD44-Palm levels decreased over the migration time course. **B.** Quantification of CD44-Palm as a ratio of CD44-Total revealed significant time-dependent reductions during migration. *Error bars=SEM, n=3 experiments, *$p<0.05$, Student's t-test.* **C.** CD44 was immunoprecipitated from whole cell lysates of MDA-MB-231 cells at the indicated migration points, with IgG as an internal control.

Immunoprecipitates were probed for CD44 and ezrin, with the IgG heavy chain band intensity considered as a loading control. Ezrin-CD44 co-IP was increased after 1 and 2 hours of cell migration compared to non-migrating cells (Time=0). **D.** CD44 was immunoprecipitated from migrating (2 hours) untransfected MDA-MB-231 (Ctrl), WT-, single- and double palmitoylation mutant-expressing cells. The latter cells had a notable increase in CD44-ezrin co-association. IP experiments are representative of 3 independent experiments. **E.** Confluent breast primary cells were stained for CD44 (green) and flotillin-1 (Flotillin-1, red). Nuclei were stained with DAPI and are shown in grey. Ductal carcinoma *in situ* (DCIS) primary cells demonstrated the highest co-localisation of the two proteins compared to invasive ductal (IDC) carcinomas. **F.** Whole cell lysates of primary cultures from two non-tumour (NT), and six IDC of tumour grade 2 and 3 (three of each) were subjected to BMCC assays to compare palmitoylated CD44 levels. Most palmitoylated CD44 (CD44-Palm) was recovered from NT cultures, while all patient IDC cultures displayed comparatively little CD44-Palm. Palmitoylated CD44 levels densitometrically normalised to total CD44 (CD44-Total) further demonstrated increased levels of CD44-Palm in NT samples. *Error bars=STDEV of duplicates in one experiment.*

FIGURE 6. Schematic representation of the proposed model of regulation of breast cancer cell migration via CD44 localisation in lipid rafts. When CD44 is affiliated with lipid rafts via palmitoylation of its cysteine residues, it is sequestered from binding its cytoplasmic binding partners and thus migration is restrained. However when CD44 translocates outside lipid rafts in its de-palmitoylated state, its cytoplasmic tail is free to bind its cytoskeletal partners, subsequently facilitating cell migration.

Supplementary Figure S1. Biochemical and functional phenotypes in cells overexpressing CD44 palmitoylation-impaired mutants are reversible. Following 48h expression of CD44WT or palmitoylation-impaired single (C268A, C286S) or double (SA, AA) mutants in MDA-MB-231 and MCF-10A cells, cells were subcultured and grown without selection reagent for a further 48h. **A.** After termination of CD44WT or mutant selection in MCF-10A cells, CD44 recovery from Triton X-100-insoluble fractions was restored to match that of control cells. **B.**

Lack of statistically-significant differences *(ns, not significant, Student's t-test)* between the raft affiliation ratio of CD44 in control MCF-10A cells, versus those in which mutant selection had been terminated, confirmed restoration of a normal biochemical phenotype. **C.** Scratch-wound assays confirmed that cell migration returned to control levels in MCF-10A cells following termination of expression of CD44WT or palmitoylation-impaired mutants *(2-way ANOVA)*. **D.** After termination of CD44WT or mutant selection in MDA-MB-231 cells, CD44 recovery from Triton X-100-insoluble fractions was restored to match that of control cells *(ns, not significant, Student's t-test)*. **E.** Scratch-wound assays confirmed that cell migration returned to control levels in MDA-MB-231 cells following termination of expression of CD44WT or palmitoylation-impaired mutants *(2-way ANOVA). Error bars=SEM, n=3 experiments.*

Supplementary Figure S2. Over-expression of CD44 or its palmitoylation-impaired mutants induces an EMT-like state. MCF-10a cells were transfected for 48h with CD44WT, single-site (C286A) or double-site (AA) palmitoylation-impaired mutant constructs. Immunoblotting for the epithelial marker EpCAM and the mesenchymal marker vimentin suggested an EMT-like switch in cells over-expressing CD44WT or its palmitoylation mutants.

Figure 1

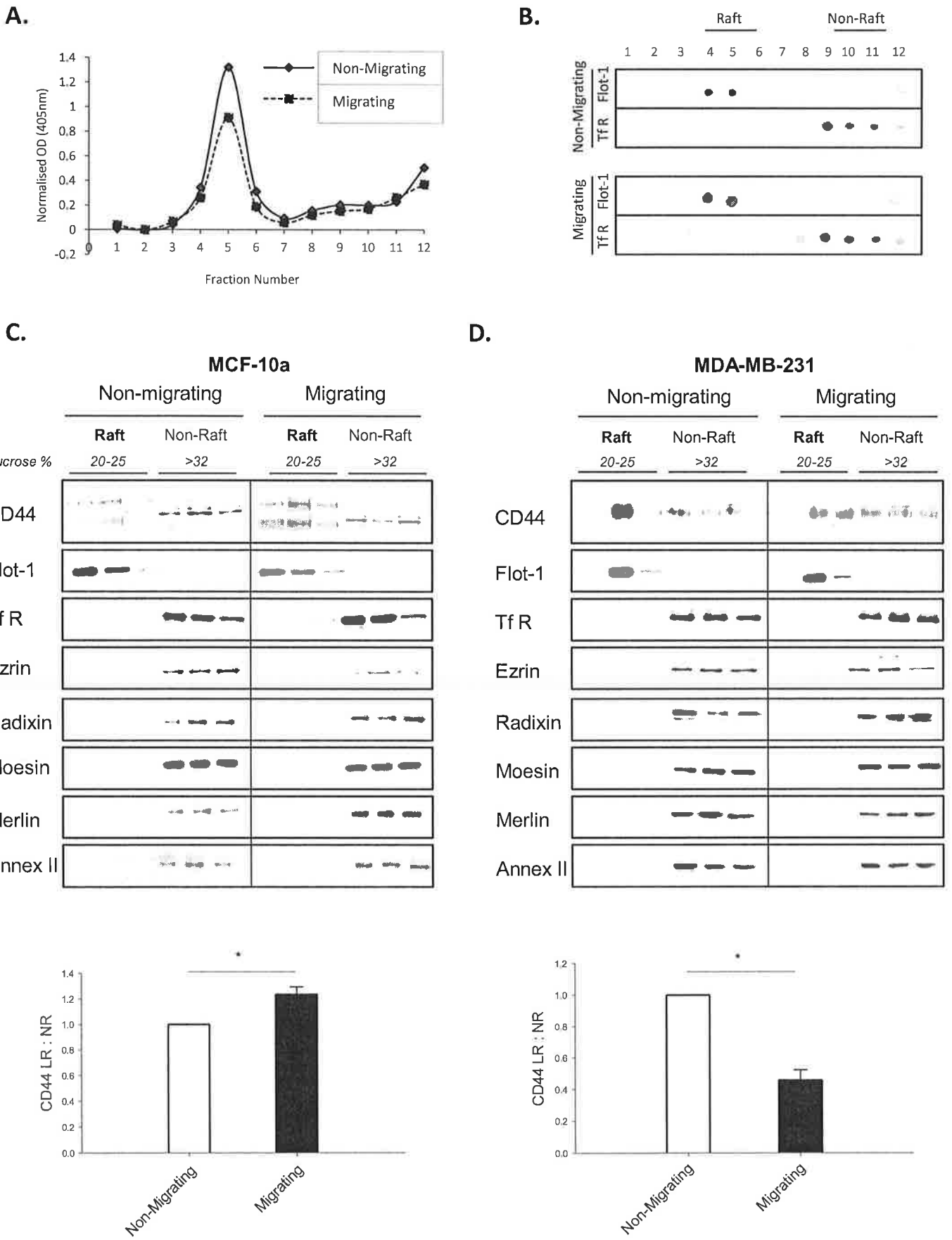
A.
Normalised OD (405nm)
Fraction Number
Non-Migrating
Migrating
B.
Raft
Non-Raft
Non-Migrating
Migrating
Flot-1
Tf R
C.
MCF-10a
Non-migrating
Migrating
Raft
Non-Raft
Sucrose %
20-25
>32
CD44
Flot-1
Tf R
Ezrin
Radixin
Moesin
Merlin
Annex II
CD44 LR : NR
Non-Migrating
Migrating
D.
MDA-MB-231

Figure 2

A.

CD44 mutants		Trans-membrane domain	FERM domain	Ankyrin domain	
CD44WT	270	WLIILASLLALALILAVCIAV	NSRRRCGQKKKLV	INSGNGAVEDRKPSGL	319
C286A		----------A---	-----C-------	----------	
C286S		----------S---	-----C-------	----------	
SA		----------S---	-----A-------	----------	
AA		----------A---	-----A-------	----------	

B.

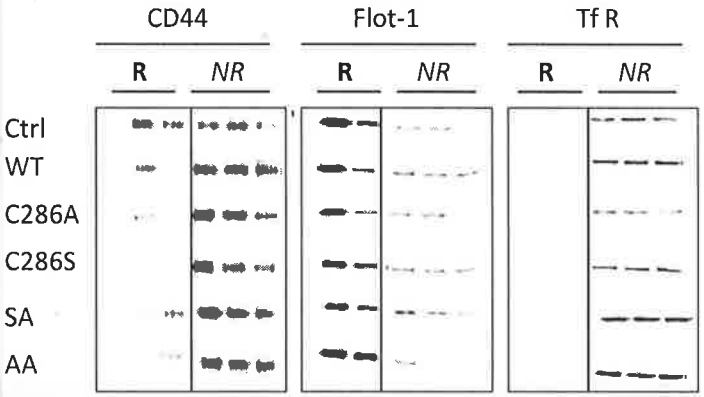

C.

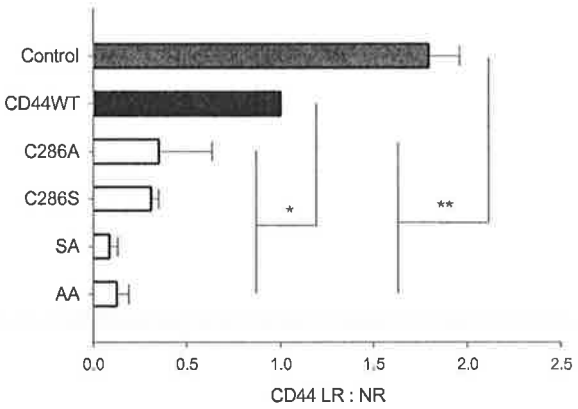

D.

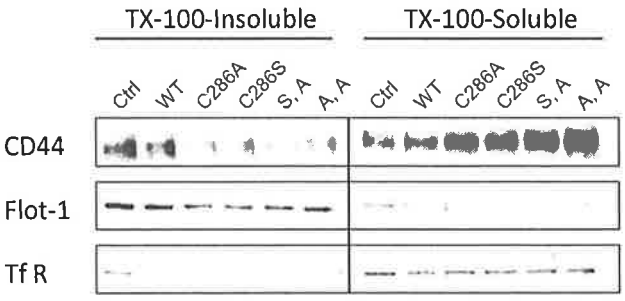

E.

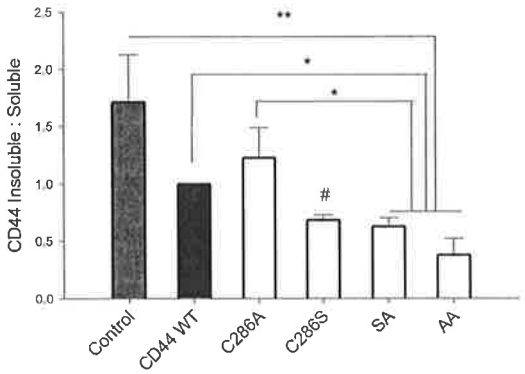

Figure 3

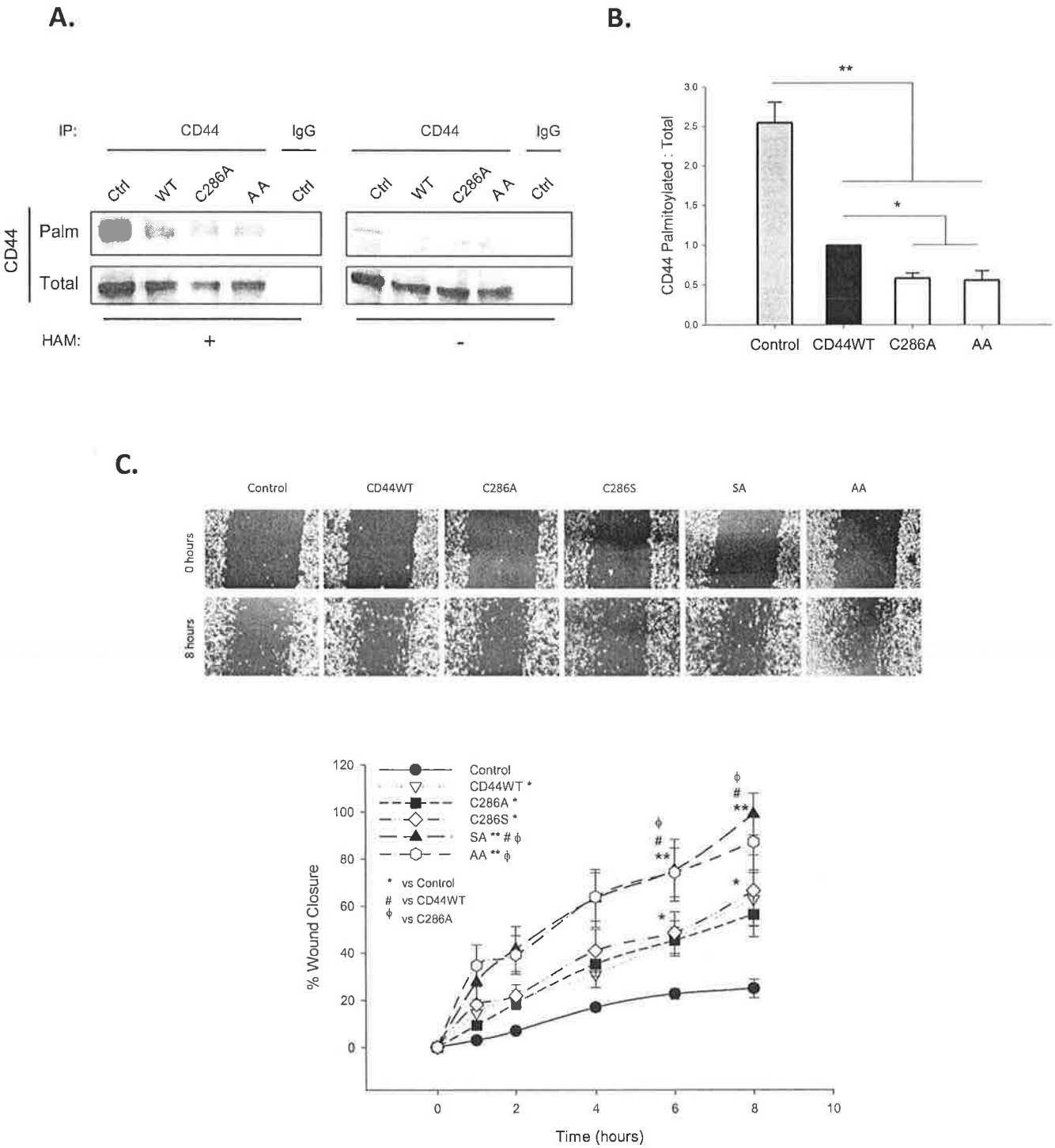
A.
IP:
CD44
IgG
CD44
IgG
Ctrl
WT
C286A
A A
Ctrl
Ctrl
WT
C286A
A A
Ctrl
CD44
Palm
Total
HAM:
+
-
B.
CD44 Palmitoylated : Total
3.0
2.5
2.0
1.5
1.0
0.5
0.0
**
*
Control
CD44WT
C286A
AA
C.
Control
CD44WT
C286A
C286S
SA
AA
0 hours
8 hours
% Wound Closure
120
100
80
60
40
20
0
Control
CD44WT *
C286A *
C286S *
SA ** # ϕ
AA ** ϕ
* vs Control
# vs CD44WT
ϕ vs C286A
0
2
4
6
8
10
Time (hours)

Figure 4

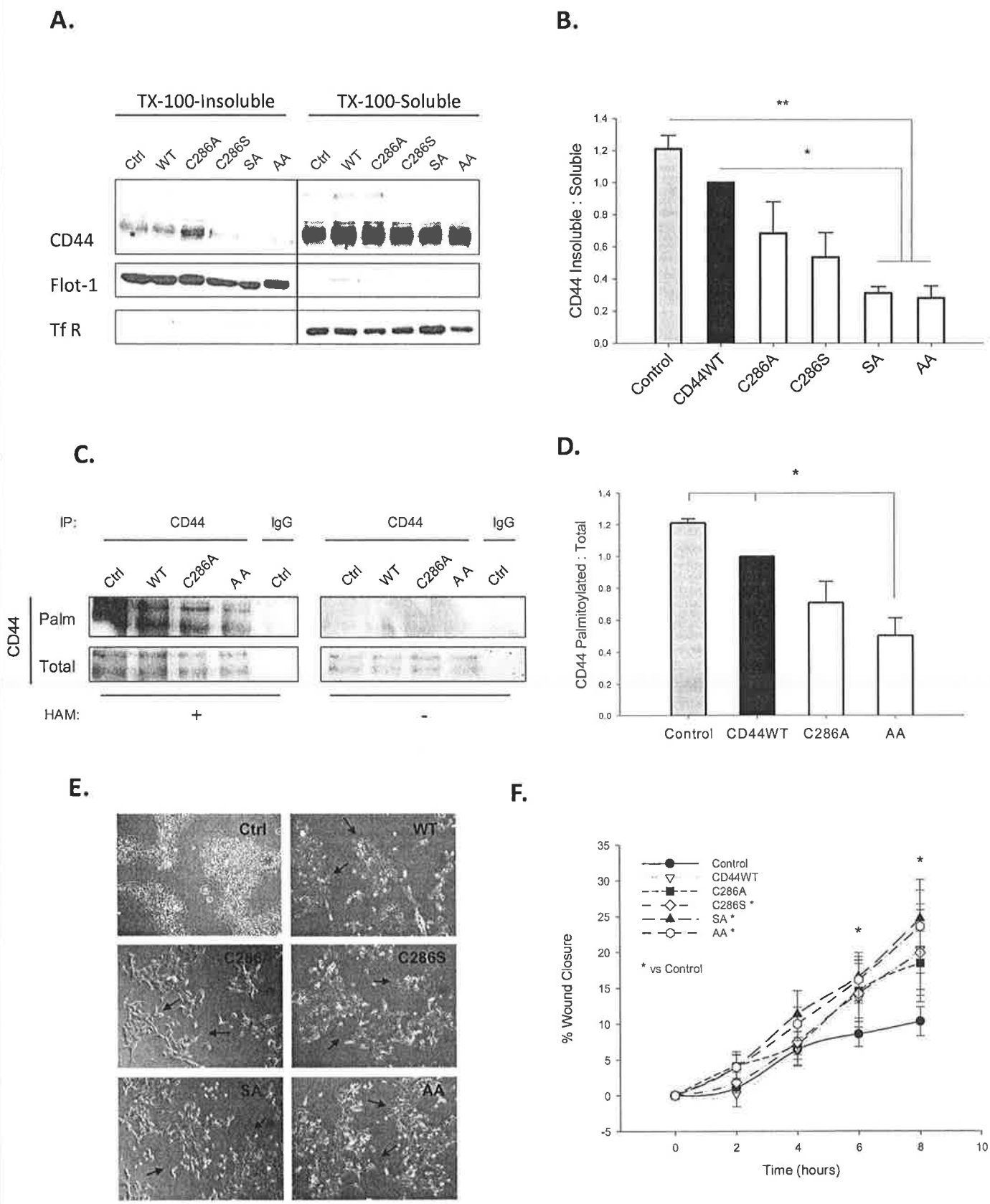
A.
TX-100-Insoluble
TX-100-Soluble
Ctrl
WT
C286A
C286S
SA
AA
CD44
Flot-1
Tf R
B.
CD44 Insoluble : Soluble
Control
CD44WT
C286A
C286S
SA
AA
C.
IP:
CD44
IgG
Palm
Total
HAM:
D.
CD44 Palmitoylated : Total
E.
F.
% Wound Closure
Time (hours)
* vs Control

Figure 5

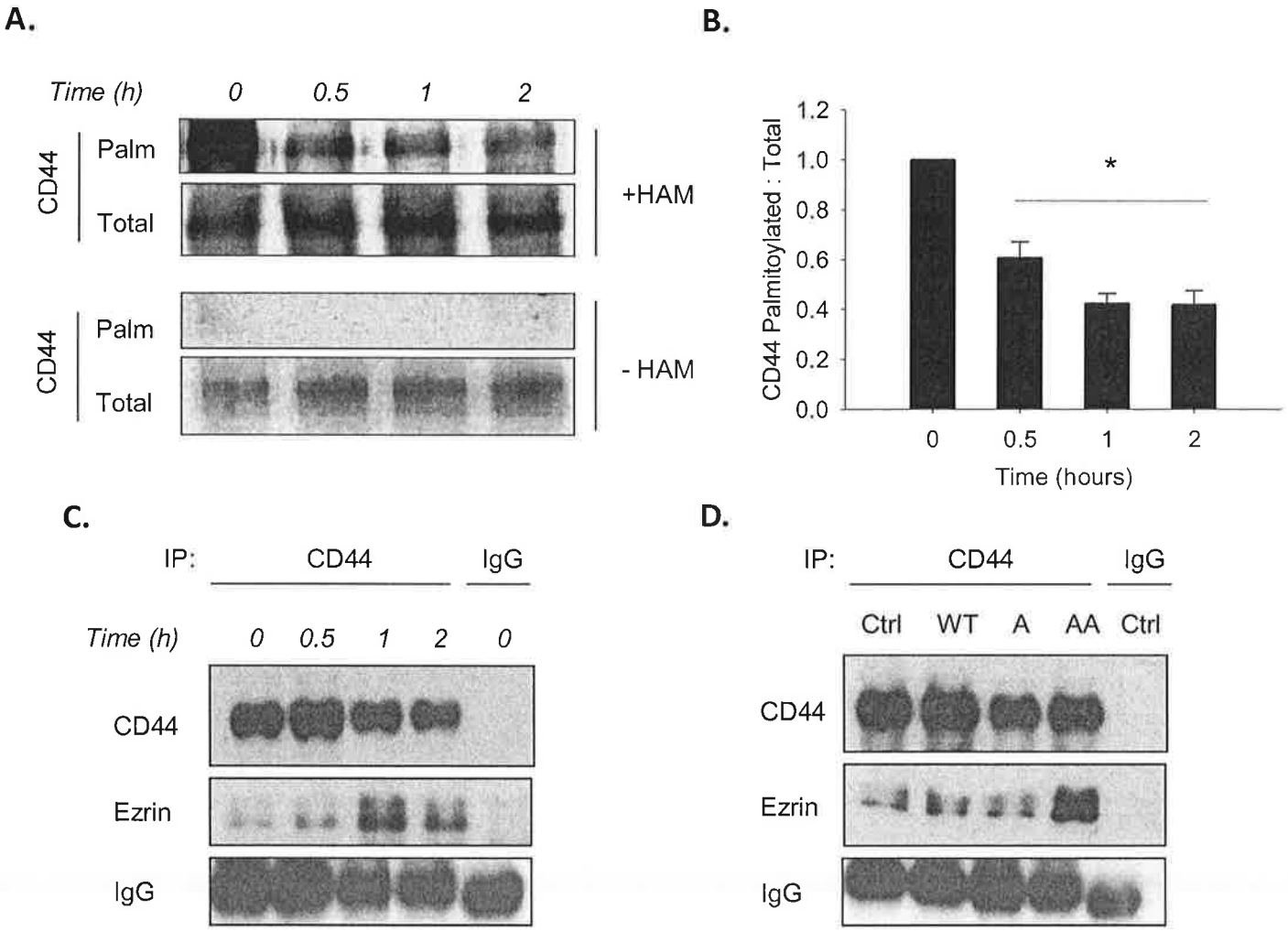
A.
Time (h)
0
0.5
1
2
CD44
Palm
Total
+HAM
CD44
Palm
Total
- HAM
B.
CD44 Palmitoylated : Total
1.2
1.0
0.8
0.6
0.4
0.2
0.0
*
0
0.5
1
2
Time (hours)
C.
IP:
CD44
IgG
Time (h)
0
0.5
1
2
0
CD44
Ezrin
IgG
D.
IP:
CD44
IgG
Ctrl
WT
A
AA
Ctrl
CD44
Ezrin
IgG

E.

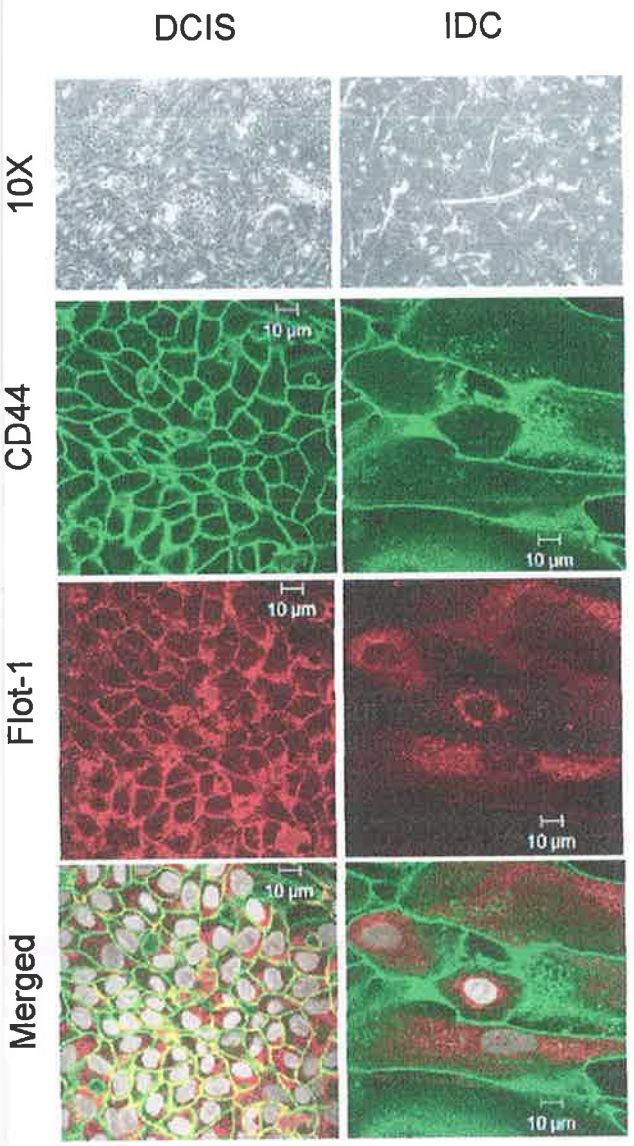
DCIS
IDC
10X
CD44
Flot-1
Merged
10 µm

F.

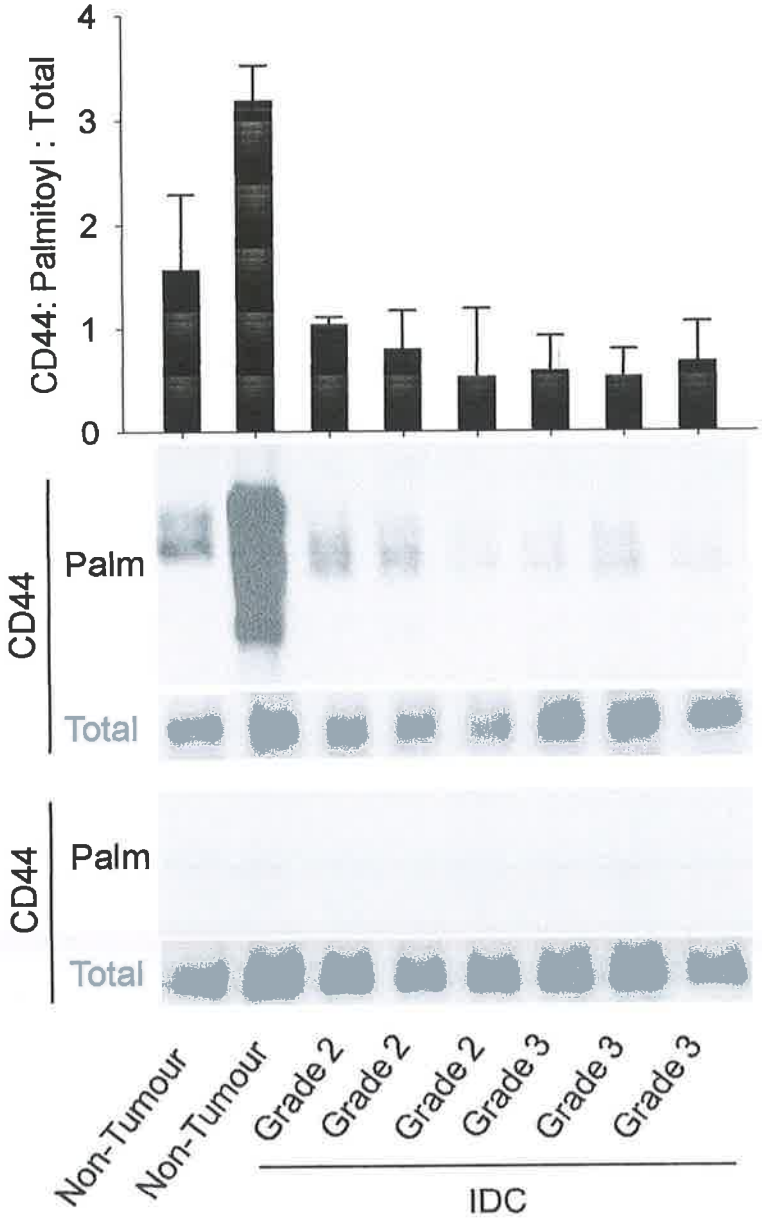
CD44: Palmitoyl : Total
0
1
2
3
4
CD44
Palm
Total
CD44
Palm
Total
Non-Tumour
Non-Tumour
Grade 2
Grade 2
Grade 2
Grade 3
Grade 3
Grade 3
IDC

Figure 6

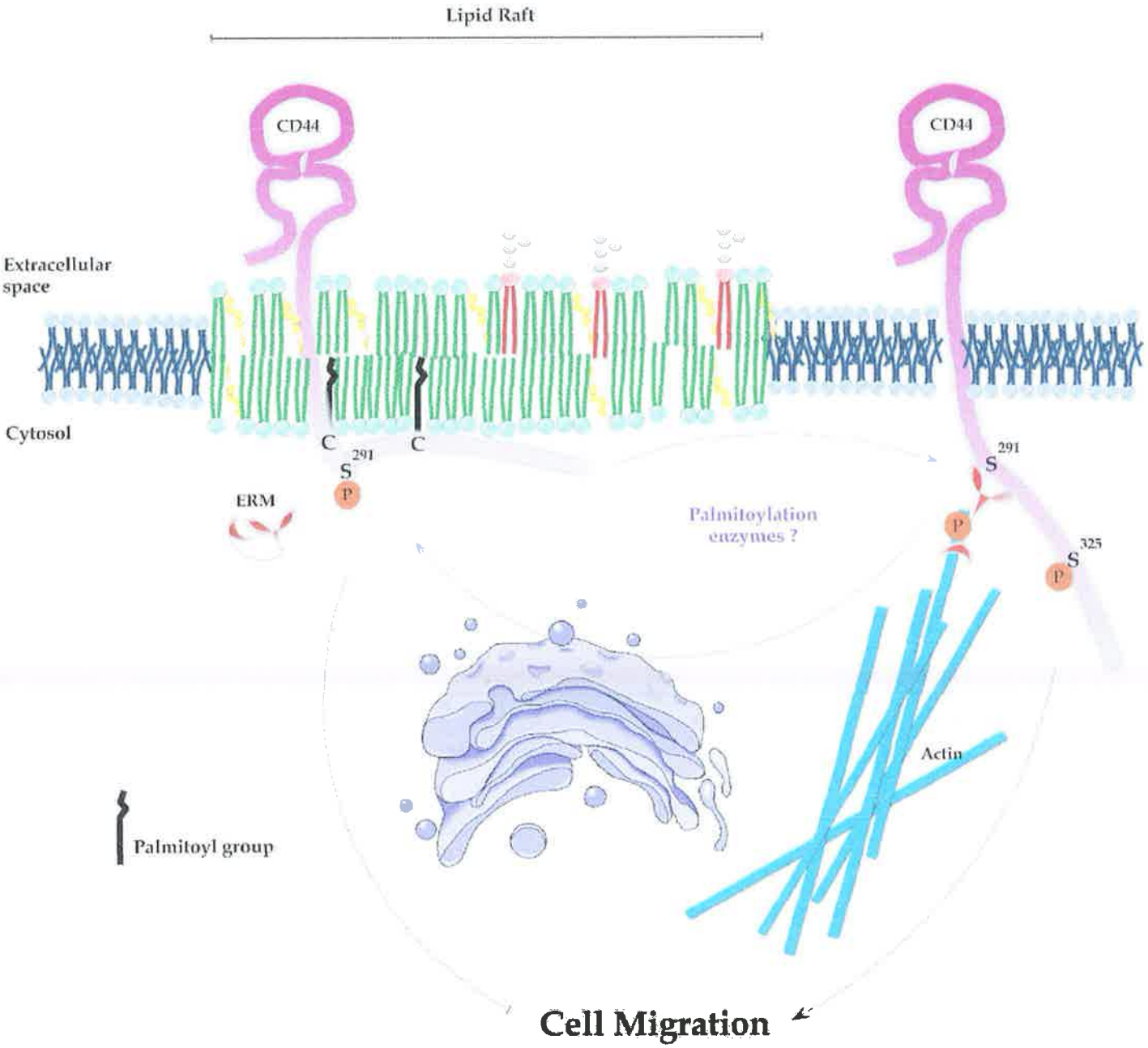
Lipid Raft
CD44
CD44
Extracellular space
Cytosol
C
C
S
291
P
ERM
Palmitoylation enzymes ?
S
291
P
S
325
P
Actin
Palmitoyl group
Cell Migration

Supplementary Figure S1

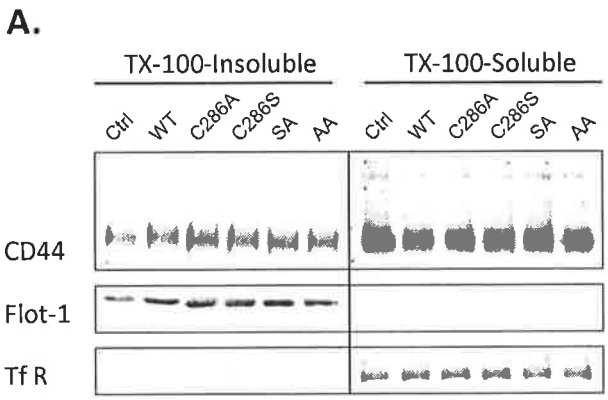

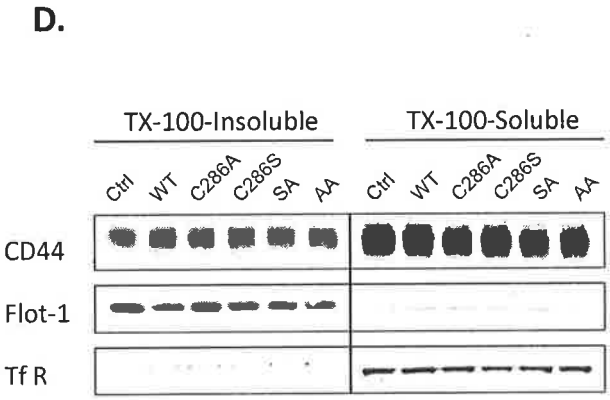

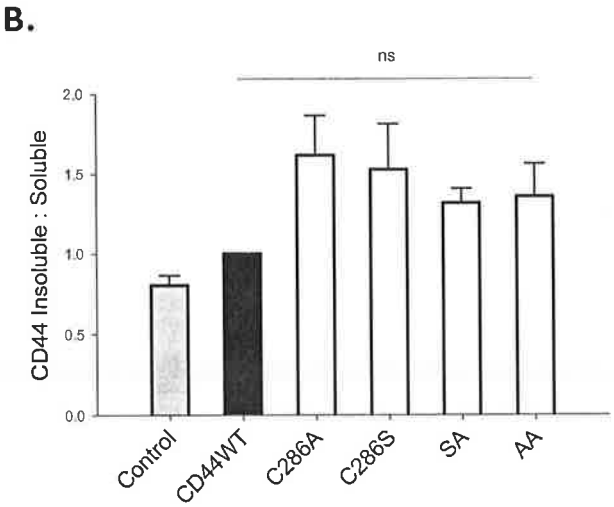

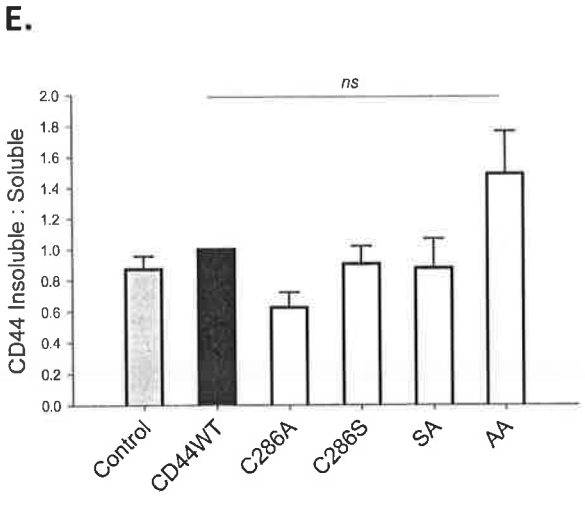

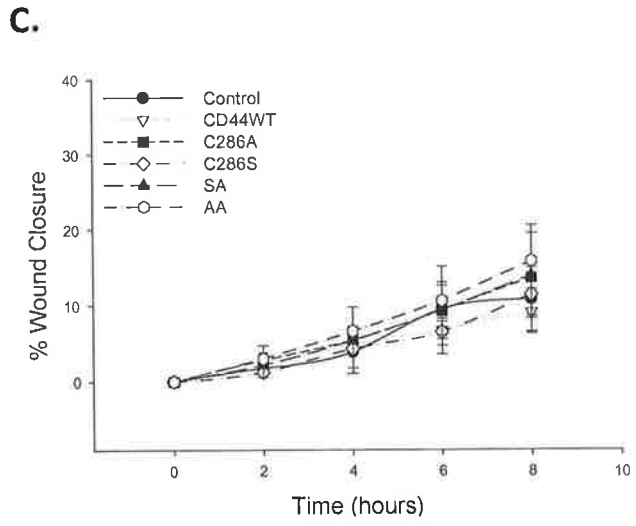

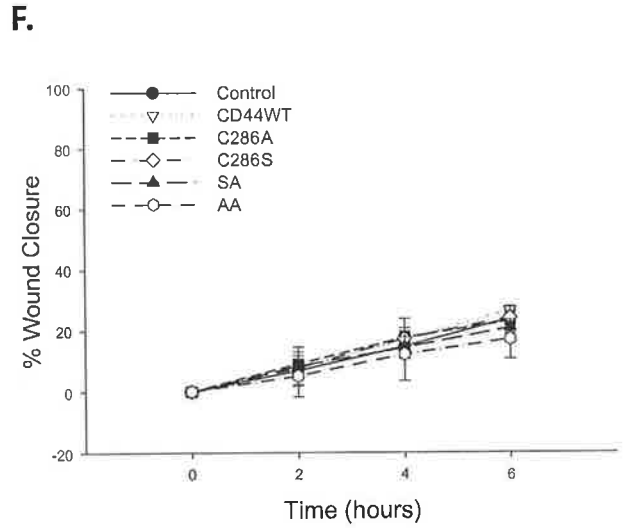

Supplementary Figure S2

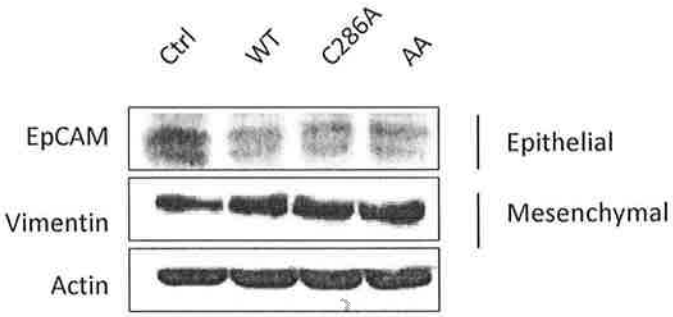

The American Journal of Pathology, Vol. 181, No. 6, December 2012

http://dx.doi.org/10.1016/j.ajpath.2012.08.025

Tumorigenesis and Neoplastic Progression

Lipid Raft Association Restricts CD44-Ezrin Interaction and Promotion of Breast Cancer Cell Migration

Simona Donatello,* Irina S. Babina,* Lee D. Hazelwood,† Arnold D.K. Hill,* Ivan R. Nabi,‡ and Ann M. Hopkins*

From the Department of Surgery, Royal College of Surgeons in Ireland, Dublin, Ireland; the Faculty of Biological Sciences,† the University of Leeds, Leeds, United Kingdom; and the Department of Cellular and Physiological Sciences,‡ Life Sciences Institute, University of British Columbia, Vancouver, British Columbia, Canada*

Cancer cell migration is an early event in metastasis, the main cause of breast cancer-related deaths. Cholesterol-enriched membrane domains called lipid rafts influence the function of many molecules, including the raft-associated protein CD44. We describe a novel mechanism whereby rafts regulate interactions between CD44 and its binding partner ezrin in migrating breast cancer cells. Specifically, in nonmigrating cells, CD44 and ezrin localized to different membranous compartments: CD44 predominantly in rafts, and ezrin in nonraft compartments. After the induction of migration (either nonspecific or CD44-driven), CD44 affiliation with lipid rafts was decreased. This was accompanied by increased coprecipitation of CD44 and active (threonine-phosphorylated) ezrin-radixin-moesin (ERM) proteins in nonraft compartments and increased colocalization of CD44 with the nonraft protein, transferrin receptor. Pharmacological raft disruption using methyl-β-cyclodextrin also increased CD44-ezrin coprecipitation and colocalization, further suggesting that CD44 interacts with ezrin outside rafts during migration. Conversely, promoting CD44 retention inside lipid rafts by pharmacological inhibition of depalmitoylation virtually abolished CD44-ezrin interactions. However, transient single or double knockdown of flotillin-1 or caveolin-1 was not sufficient to increase cell migration over a short time course, suggesting complex crosstalk mechanisms. We propose a new model for CD44-dependent breast cancer cell migration, where CD44 must relocalize outside lipid rafts to drive cell migration. This could have implications for rafts as pharmacological targets to down-regulate cancer cell migration. (Am J Pathol 2012, 181:2172–2187; http://dx.doi.org/10.1016/j.ajpath.2012.08.025)

The membrane protein CD44 is a multifaceted molecule involved in many different cellular processes, including organ development, neuronal axon guidance, immune functions, hematopoiesis, and migration.[1–4] It acts as a receptor for the extracellular matrix component hyaluronic acid (HA)[5,6] and for the secreted extracellular protein osteopontin.[7] CD44 is an important mediator of cellular adhesion and migration due to its active influence on the organization of the actin cytoskeleton. This occurs through direct interactions between CD44 and different actin-binding partners, of which the most common are proteins belonging to the ezrin-moesin-radixin (ERM) family. The ERM proteins form a bridge between CD44 and the actin cytoskeleton, mediating cell morphology changes that are important for cell migration. Ezrin interacts with CD44 and F-actin, respectively, through its conserved N-terminal band four-point-one, ezrin, radixin, moesin domain and C-terminal ERM Association Domain

Supported by Cancer Research Ireland (CRI05HOP/AMH), the Irish Research Council for Science, Engineering & Technology (EMBARK 2005/SD), Health Research Board of Ireland (HRA/2009/49 to A.M.H.), Breast Cancer Ireland, EU-funded Network of Excellence ENFIN (LSHG-CT-2005-518254), and the UK Medical Research Council (L.D.H.). The confocal microscope and ultracentrifuge were funded through the National Biophotonics and Imaging Platform, Ireland, and funded by the Irish Government's Programme for Research in Third Level Institutions, Cycle 4, Ireland's EU Structural Funds Programmes 2007–2013.

Accepted for publication August 13, 2012.

S.D. and I.S.B. contributed equally to this work.

CME Disclosure: The authors of this article and the planning committee members and staff have no financial relationships with commercial interest to disclose.

Supplemental material for this article can be found at *http://ajp.amjpathol.org* or at *http://dx.doi.org/10.1016/j.ajpath.2012.08.025*.

Address reprint requests to Ann M. Hopkins, Ph.D., Department of Surgery, Royal College of Surgeons in Ireland, RCSI Education and Research Centre, Beaumont Hospital, Dublin 9, Ireland. E-mail: annhopkins@rcsi.ie.

domain. In the inactive configuration of ezrin, both domains interact with each other and block the binding sites for CD44 and F-actin. Ezrin activation is mediated by phosphorylation-induced conformational changes,[8] with phosphorylation on threonine-567 being necessary for binding to the F-actin cytoskeleton.[9]

Phosphorylation of CD44 has also been shown to be important for its activation, particularly on serine residues in the C-terminal domain.[8,10] CD44 has been described to be enriched in cholesterol- and sphingomyelin-enriched membrane microdomains termed lipid rafts.[11] Much evidence has suggested the involvement of lipid rafts in regulating different cellular events, including migration.[12] Because some of these cellular events are frequently altered in cancer, it has been hypothesized that lipid rafts play a crucial role in regulating cancer progression.[13] However, although alterations in CD44 expression have been associated with many cancers,[14] how lipid rafts influence the subcellular localization (and thus migratory functions) of CD44 and its contribution toward cancer progression is not well understood.

Whether or not CD44 and its binding partners localize to lipid rafts may in fact regulate several signaling cascades. CD44 is usually directed toward lipid rafts via posttranslational lipid modifications called acylation reactions, the most common of which is palmitoylation. Due to its dynamic and reversible nature, palmitoylation can have important functions in dictating protein fate such as protein trafficking, lateral segregation, and cellular localization. Palmitoylation plays an important role in CD44-HA turnover, with palmitoylated CD44 promoting CD44-HA endocytosis. Accordingly, lipid rafts have been described to play an important role in cellular endocytosis.[15]

Ezrin localization to lipid rafts is controversial[16] and the mechanisms regulating its affiliation with lipid rafts incompletely understood. Ezrin interactions with phosphatidylinositol 4,5-biphosphate (PIP2) may be important for its activation, causing the four-point-one and C-terminal ERM domains to open[17] and permitting ezrin localization at the plasma membrane.[18] Because PIP2 has been described to be enriched in lipid rafts,[19] it is possible that ezrin localizes to lipid rafts through an interaction with PIP2.

In this paper, we set out to investigate the role of lipid rafts in regulating CD44-dependent breast cancer cell migration. Our initial findings revealed that CD44 and ezrin localized to different membrane fractions in nonmigrating cells, biochemically characterized as lipid raft and nonraft domains, respectively. In response to migratory stimuli (either random or CD44-specific), the proportion of raft-affiliated CD44 decreased whereas that of ezrin did not change. Moreover, under migrating compared to nonmigrating conditions, immunofluorescence confocal microscopy revealed increased colocalization of CD44 with the nonraft marker transferrin receptor. Altogether, we present novel evidence that physical interactions between CD44 and ezrin occur in nonraft fractions of migrating cells. In support of our observations, pharmacological disruption of lipid rafts increased CD44-ezrin coprecipitation, whereas enhanced retention of CD44 within rafts abolished CD44-ezrin coprecipitation. Surprisingly, flotillin-1 or caveolin-1 transient knockdown alone did not affect cell migration in these cells, suggesting compensatory mechanisms that make up for the presumed loss of one or other raft compartment. In support of this assumption, coincident knockdown of flotillin-1 and caveolin-1 significantly impaired cell migration. Nonetheless, our data are consistent with a novel regulatory mechanism in which CD44 translocates outside lipid rafts to bind ERM binding partners such as ezrin and drive cell migration. Future exploration of the precise mechanisms regulating this translocation may reveal future targets for interfering with breast cancer cell migration during the early stages of metastasis.

Materials and Methods

Antibodies and Reagents

CD44 antibodies were purchased from Santa Cruz Biotechnology (immunoprecipitations and immunofluorescence; Santa Cruz Biotechnology, Heidelberg, Germany), Abcam and R&D Systems (Western blotting; Abcam, Cambridge, UK, and R&D Systems, Abingdon, UK); ezrin from BD Biosciences (Oxford, UK); phosphothreonine-ERM from Cell Signaling Technology (Danvers, MA), flotillin-1 from BD Biosciences, actin from Sigma-Aldrich (Arklow, Ireland), caveolin-1 from Cell Signaling Technology, radixin and moesin from GeneTex/Source Biosciences (Irvine, CA), transferrin receptor primary and Alexa-Fluor secondary antibodies both from Invitrogen (Bio-Sciences, Dun Laoghaire, Ireland). Triton X-100 (10%) was purchased from Roche (Dublin, Ireland), protein G-sepharose 4B from GE Healthcare (Little Chalfont, UK).

Cell Culture

MDA-MB-231 cells were obtained from the ATCC (Manassas, VA) and cultured in Dulbecco's modified Eagle's medium, 10% fetal bovine serum, 2 mmol/L L-glutamine, 100 U/mL penicillin, and 100 μg/mL streptomycin. MDA-MB-231 cells stably knocked-down for caveolin-1 via a vector containing short-hairpin RNA against caveolin-1 and carrying a resistance cassette for blasticidin (Invitrogen)[20] were cultured similarly but with the addition of 5 ng/μL blasticidin. For some experiments, small-interfering RNA (siRNA) against flotillin-1 or caveolin-1 was used to transiently knock down gene expression for 72 hours before performing migration assays or immunofluorescence analysis. In brief, cells were grown at low density for up to 24 hours on 24-well plates or 13-mm coverslips and transfected with 25 nmol/L siRNA against flotillin-1 or caveolin-1 (Dharmafect SmartPools; Dharmacon, Lafayette, CO) or a universal negative control siRNA (Dharmafect) using Dharmafect-1 reagent as per the manufacturer's instructions (Dharmacon).

Cell Treatments

Methyl-β-cyclodextrin (MβCD, 10 mmol/L; Sigma-Aldrich) was used to disrupt lipid raft physiology by cholesterol depletion as already described.[21–23] MβCD was prepared in serum-free medium and added to confluent 10-cm dishes of cells for 30 minutes before wounding with a sterile pipette tip attached to a vacuum. To convert a proportion of cells into spreading and migrating cells, monolayers were extensively wounded by making nine horizontal and nine vertical scratches per dish using a sterile pipette tip attached to suction. Depalmitoylation inhibitors (DPI) methyl arachidonyl fluorophosphonate (5 μmol/L) and palmityl trifluoromethyl ketone (20 μmol/L) were obtained from Cayman Chemicals (Ann Arbor, MI) and incubated with cells for 30 minutes before wounding. All treated cells were washed once and allowed to migrate in serum-free medium for the indicated times. Confluent cells were wounded and treated for 30 minutes with 5 mg/mL HA where indicated.

Scratch-Wound Migration Assays

Cells were grown to confluence in 24-well plates and scratch wounded once using a sterile pipette tip attached to a vacuum. Cells were then washed once and incubated in the relevant treatments in serum-free medium. Wounds were photographed at specific time points on a phase contrast microscope linked to a charge-coupled device camera (Olympus, Tokyo, Japan), and the wound size at a single reference point measured over time using Cell B software (Olympus).

Immunofluorescence Microscopy

Cells were grown to confluence on sterile coverslips, treated as indicated, and then fixed in 3.7% paraformaldehyde (pH 7.4) for 10 minutes at room temperature, in ice-cold ethanol or 80% methanol/20% acetone for 20 minutes at −20°C. The primary antibody and secondary antibodies (diluted in 5% normal goat serum) were incubated for 1 hour at room temperature. Nuclei were counterstained with DAPI for 10 minutes at room temperature. Each step was followed by three washes in phosphate-buffered saline (PBS). Coverslips were mounted in PBS:glycerol:*o*-phenylenediamine hydrochloride (1:1:0.01 v/v/v) and visualized on a Zeiss LSM 510-meta or 710-meta confocal microscope using 63× oil immersion lenses (Carl Zeiss, Oberkochen, Germany).

Protein Immunoprecipitations

Cells were washed in cold PBS, lysed, and scraped in Relax buffer (100 mmol/L KCl, 3 mmol/L NaCl, 3.5 mmol/L $MgCl_2$, 10 mmol/L HEPES) containing 1% Triton X-100 and protease and phosphatase inhibitor cocktails (Sigma-Aldrich). Lysates were homogenized with a Dounce tissue homogenizer (Sigma-Aldrich) 20 times and centrifuged at 1500 × *g* at 4°C for 5 minutes. Equivalent amounts of total protein per treatment condition (eg, migrating versus nonmigrating cell lysates) were used in matched immunoprecipitation experiments. After a preclear step with protein G–sepharose, 3 μg of mouse anti-human CD44 antibody (or an equivalent concentration of control mouse IgG) was added to each sample and rotated overnight at 4°C. Immunocomplexes were collected by rotation with 50 μL of protein G–sepharose for 3 hours at 4°C. Immunocomplexes were washed three times with lysis buffer, resuspended in 2× Laemmli reducing sample buffer, boiled, and then analyzed by SDS-PAGE and Western blotting.

Lipid Raft Isolation

Two confluent 10-cm dishes per condition were treated as described. Hanks balanced salt solution (HBSS) containing calcium, magnesium, and 10 mmol/L HEPES (Sigma-Aldrich) was used to wash cells before scraping them into 400 μL/dish lysis buffer (HBSS, 1% Triton-X100, protease, and phosphatase inhibitors). Lysates were homogenized with a tissue homogenizer 20× and triturated 20× through a 26-gauge needle. At 4°C, lysates were mixed 1:1 with a 90% (w/v) sucrose solution (in HBSS) and loaded at the bottom of a micro-ultracentrifuge tube. This was then overlain sequentially with solutions of 30%, 20%, and 5% sucrose (w/v) and ultracentrifuged in an RP55S rotor at 281,591 × *g* for 19 hours at 4°C in a Sorvall RC M120EX micro-ultracentrifuge (Kendro Laboratory Products, Asheville, NC). Starting from the top of the tube (fractions of lowest sucrose density), gradients were fractionated manually at 4°C into six equal-volume fractions. For some experiments, continuous sucrose gradients were prepared from 200-cm dishes of confluent cells in larger (12-mL) tubes essentially as described.[24,25] Briefly, cell lysates were prepared in 2.5 mL of HBSS containing 1% Triton X-100 and a protease inhibitor cocktail. At 4°C, 2 mL of lysate was mixed with 2 mL of 60% sucrose and placed at the bottom of an ultracentrifuge tube. A 200-μL "cushion" of 30% sucrose was manually layered on top, whereupon a continuous 30% to 5% gradient was poured using an Auto Densi-Flow density gradient fractionator (Labconco, Kansas City, MO). Gradients were ultracentrifuged at 260,343 × *g*/19 hours at 4°C in a Beckman Optima L-100K ultracentrifuge (Sw41 Ti rotor) and fractionated manually into 12× 1-mL fractions. In each case, a peak of alkaline phosphatase activity and enriched flotillin-1 expression was used to identify lipid raft fractions. Because both peaked at ~20% to 26% sucrose, irrespective of the gradient preparation, the small- and large-gradient preparations were highly comparable even though fraction numbers did not directly correlate. For clarity in Western blot results, sucrose densities of gradient fractions have been presented instead of fraction numbers; and fractions with peak alkaline phosphatase activity have been highlighted with circles.

SDS-PAGE and Western Blot Analysis

Because protein concentrations were nonuniform across gradient fractions, 5 μg of protein per lane (unless otherwise indicated) were separated on fixed-percentage acrylamide gels at 40-mA constant current. To control for

the possibility that equivalent protein loading would induce artifacts not present under equivalent volume loading conditions, electrophoresis of equivalent fraction volumes was also performed in representative blots and confirmed to have a similar outcome (see Supplemental Figure S1 at *http://ajp.ampathol.org*). Proteins were then transferred to nitrocellulose membranes at a constant voltage of 100 V for 1 hour and blocked in 5% nonfat dry milk Tris-buffered saline (TBS)–0.1% Tween-20 for 1 hour at room temperature. Primary (as indicated) and secondary (mouse-, rabbit-, or rat–horseradish peroxidase conjugated; Sigma-Aldrich) antibodies were prepared in 5% nonfat dry milk in TBS containing 0.1% Tween-20 (TBS-T). Primary antibodies were incubated overnight at 4°C, and secondary antibodies for 1 hour at room temperature. Each step was followed by 3× 10-minute washes in TBS-T. Luminescent signals were developed onto Kodak film (Rochester, NY) after incubation with Western Lightning enhanced chemiluminescent reagent (Perkin Elmer, Waltham, MA).

Image Analysis

Densitometric analysis of Western blot films was performed using Image J software (NIH, Bethesda, MD). Pixel colocalization of different color channels in confocal images was analyzed by Image J software using the plugins "ColocalizeRGB" and "Area calculator."

Migration Matrix and Pathway Reconstruction

Immunoprecipitation changes observed within migrating cells relative to nonmigrating cells were used to infer the signaling network using logical reasoning.[26] For example, movement of CD44 from lipid raft to nonraft regions was presumed if a decrease of CD44 in raft fractions accompanied by an increase of CD44 in nonraft fractions was observed. Other network paths were constructed in the same manner with the additional model constraint and assumption that CD44 only binds to ezrin in its phosphorylated state.[9] In all cases, there was an explicit assumption that the total amount of CD44, ezrin, and phospho-ERM remained constant within cells over the time course of individual experiments (confirmed in Supplemental Figure S2 at *http://ajp.ampathol.org*).

Statistical Analysis

Data were expressed as mean ± SEM. Different conditions were compared using unpaired Student's *t*-tests and nonparametric tests. Linear regression analysis in GraphPad Prism v5 (GraphPad Software, La Jolla, CA) was used to test statistical differences between the slopes of scratch wound assays under different treatment conditions.

Results

CD44 and Ezrin Interact at the Migrating Edge in MDA-MB-231 Cells

Although the involvement of CD44 in breast cancer migration has been described in many settings, the regulatory mechanisms are incompletely understood and often conflicting. A likely mechanism is that CD44 interacts with the actin cytoskeleton through ezrin, a member of the ERM family.[27] We used scratch wounding as a tool to induce migration in MDA-MB-231 breast cancer cells to study the role of lipid rafts in regulating CD44 and ezrin interactions. Monolayers of cells were extensively wounded by making nine horizontal and nine vertical scratches per 10-cm dish. The total number of migrating cells per experiment was estimated by surface area calculations to be less than 10%. Because the mechanical stress applied by scratch wounding directly stimulates migration three to five cell diameters back from the wound edge,[28] the depth covered by three to five cells along each side of each wound was used to calculate the estimated total migrating surface. However, it is well known that migrating cells secrete factors that can affect signaling even in cells distal to those that are directly migrating.[29] Because CD44-ezrin interactions are reportedly rapid and transient,[8] MDA-MB-231 cells were allowed to migrate for 30 minutes in serum-free medium following scratch wounding. CD44 immunoprecipitate complexes were separated by SDS-PAGE and analyzed by immunoblotting for the presence of ezrin and CD44. Figure 1A shows that CD44 recovery was marginally increased in migrating cells compared to nonmigrating cells. However, a substantial increase in ezrin recovery was observed in CD44 immunoprecipitates of migrating cells compared to nonmigrating controls, even though CD44 and actin levels in the input lysates were confirmed to be similar between treatment conditions. Furthermore, expression levels of CD44 and ezrin were observed to be stable over a migration time course from 30 minutes to 4 hours (see Supplemental Figure S2 at *http://ajp.ampathol.org*).

To interact with CD44 and the cytoskeleton, ezrin must undergo posttranslational conformational changes induced by phosphorylation on threonine-567. We used an antibody that recognizes the phosphorylation of threonine-567 on ezrin and also the corresponding phosphorylation sites on moesin and radixin, related proteins belonging to the ERM family. Like ezrin, radixin and moesin are also highly expressed in MDA-MB-231 cells and exhibit stable levels over a migration time course (see Supplemental Figure S2 at *http://ajp.ampathol.org*). As shown in Figure 1A, threonine-phosphorylated levels of the ERM proteins (p-ERM) were slightly increased in migrating cells compared to nonmigrating controls, but with little overall change in the ratio of p-ERM to total ezrin under migrating versus nonmigrating conditions. Neither CD44 nor ezrin were detected in lysates immunoprecipitated with a nonspecific control IgG antibody.

Colocalization of CD44 and ezrin under migrating and nonmigrating conditions was also examined by confocal

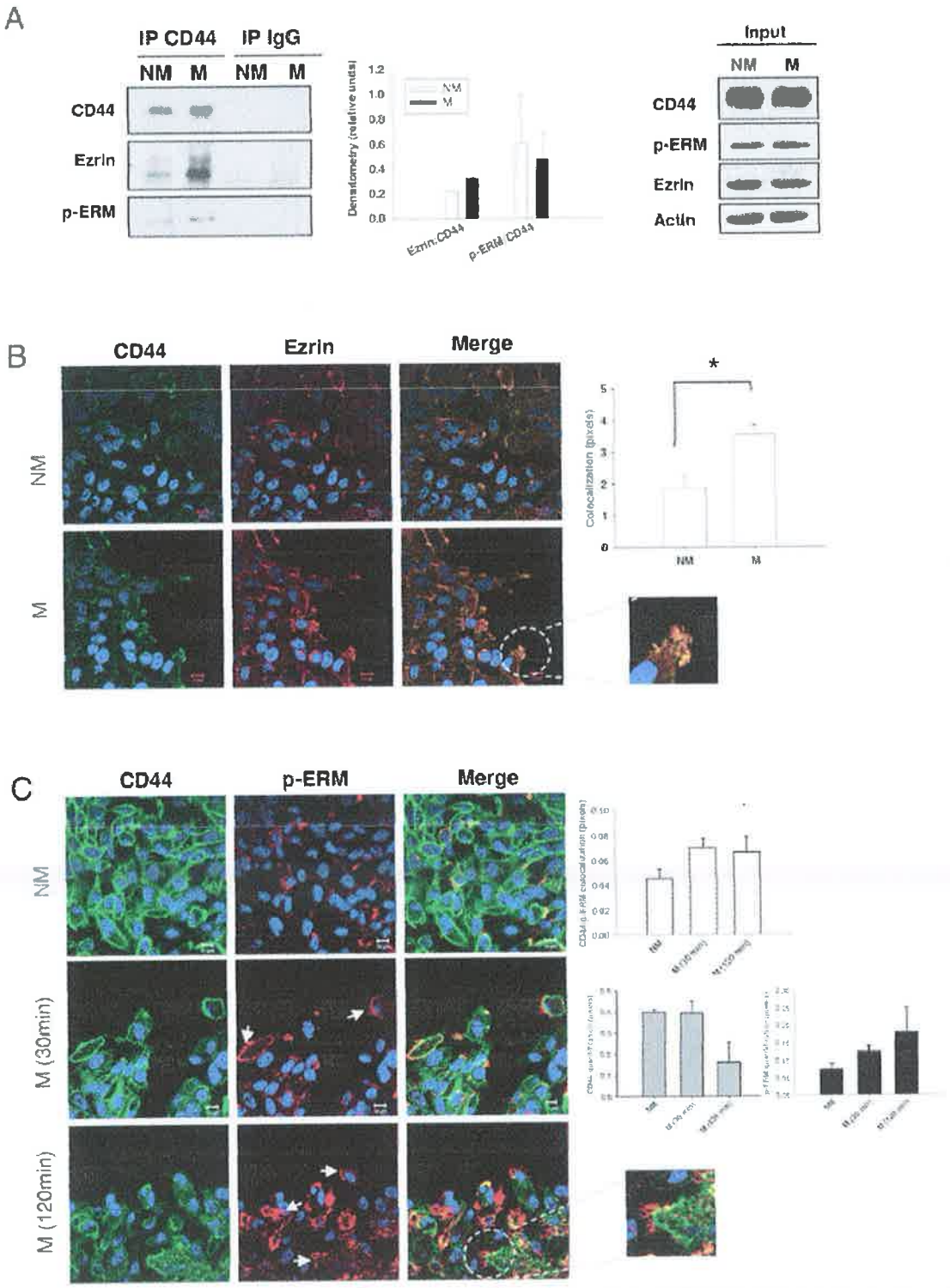

Figure 1. CD44 and ezrin interaction during breast cancer cell migration. As CD44 was immunoprecipitated (IP) from equal amounts of total protein extracted from migrating (M) and nonmigrating (NM) MDA-MB-231 cells (**left panel**). Increased binding between CD44 and ezrin was observed in migrating conditions, but no changes in p-threonine-ERM (p-ERM) binding to CD44 were observed (**middle panel**) (error bars refer to the SEM of three independent experiments with unpaired two-tailed *t*-tests used for statistical analysis). Blots from input lysates (**right panel**) confirm similar expression levels of CD44, p-ERM, ezrin, and actin in both treatment conditions. Immunofluorescence analysis of CD44 and ezrin (B, green and red, respectively) or CD44 and p-ERM (C, green and red, respectively) colocalization (yellow, merge) in nonmigrating (NM) and migrating (M) MDA-MB-231 cells. A significant increase in CD44 and ezrin colocalization was observed in migrating compared to nonmigrating cells (**B**) (**right panel**, $^*P = 0.0108$, unpaired two-tailed *t*-test; error bars represent SEM of two independent experiments), especially at the leading edge of migrating cells (**B**, **enlargement**). **C**, **right panels**: A nonsignificant increase of CD44 and p-ERM colocalization was also observed (white bars). A decrease of total CD44 expression was observed over time (grey bars). Conversely, increased expression and localization of p-ERM in membrane ruffles at the migrating edge was seen over time in cell migration (**C**, **arrows** and **enlargement**) together with a total increase in p-ERM expression (**C**, far **right panel**, at 30 minutes and at 120 minutes black bars). Error bars refer to the SEM of duplicate experiments.

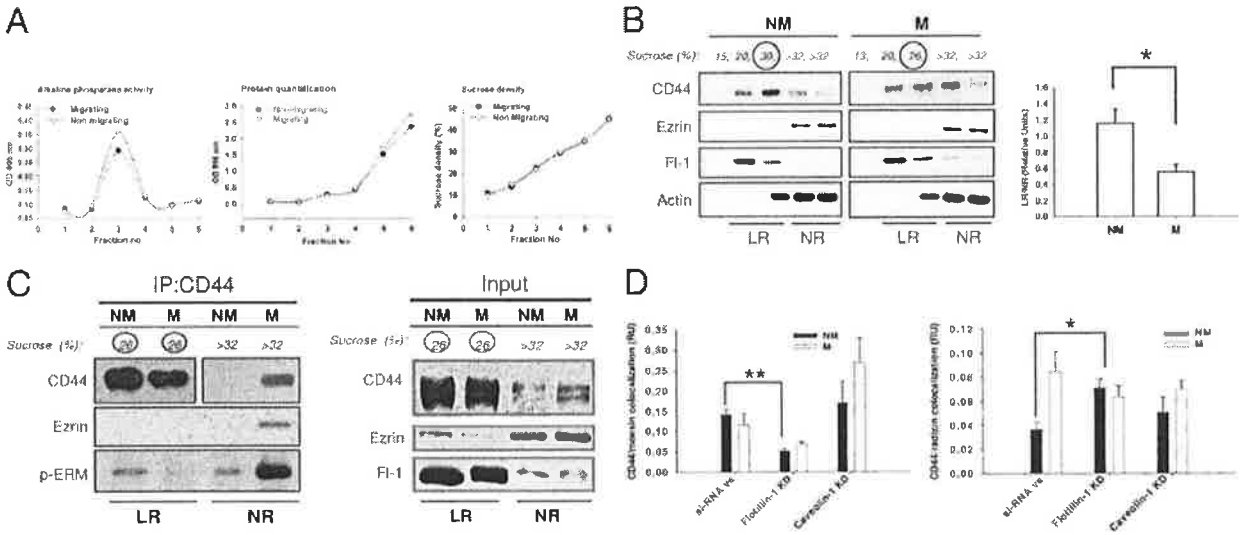

Figure 2. CD44 and ezrin localization to lipid rafts during breast cancer cell migration. **A:** Lipid rafts were isolated from migrating and nonmigrating MDA-MB-231 cells via isopycnic sucrose density gradient fractionation, and successive fractions analyzed for activity of the raft marker enzyme alkaline phosphatase, protein concentration, or sucrose density. OD, optical density. **B:** Equivalent protein concentrations from gradient fractions were separated by SDS-PAGE and analyzed by Western blotting for the expression of CD44, flotillin-1 (Fl-1), ezrin, and actin (**left panel**). The amount of CD44 present in lipid raft versus nonraft fractions was significantly higher (*$P = 0.036$, unpaired two-tailed *t*-test) in nonmigrating compared to migrating cells (**right panel**) (error bar refers to SEM of triplicate experiments). **C:** Equal amounts of total cellular protein from lipid raft and non-lipid raft fractions of migrating and nonmigrating MDA-MB-231 cells were immunoprecipitated for CD44 and probed for CD44, ezrin, and p-threonine-ERM (one replicate) (**left panel**). Due to strong differences in CD44 levels between raft and nonraft fractions, Western blots of two different exposure times are given: short exposure times for lipid raft fractions (26% sucrose) and longer exposure times for nonraft fractions (≥32% sucrose). Blots from input lysates (**right panel**; same exposure time) confirmed much higher expression of CD44 in raft compared to nonraft fractions together with ezrin enrichment in nonraft fractions, irrespective of cell migratory status. CD44 recovery from lipid raft fractions was decreased in migrating cells compared to nonmigrating cells, and CD44-ezrin coprecipitation was observed predominantly in non-lipid raft fractions of migrating cells. **D:** MDA-MB-231 cells were transfected with siRNA against the principal structural components of different lipid raft populations, flotillin-1, or caveolin-1. Migrating versus nonmigrating cells were subsequently analyzed by immunofluorescence confocal microscopy for CD44 colocalization with either moesin (**left panel**) or radixin (**right panel**), which was quantitated with ImageJ software. Flotillin-1 knockdown (KD) significantly decreased the colocalization of CD44 and moesin while significantly increasing the colocalization of CD44 and radixin. Error bars refer to SEM of representative triplicate images. (*$P = 0.0247$, **$P = 0.0027$, unpaired two-tailed *t*-test).

immunofluorescence microscopy (Figure 1B). In migrating cells, the merged image of CD44 and ezrin demonstrated significantly increased colocalization, particularly at the migrating edge (Figure 1B) (differences in pixel overlap, $P < 0.05$). This suggested that changes in CD44 and ezrin localization within specific cellular regions accompanied cell migration. Localization of p-ERM relative to CD44 was also analyzed by confocal microscopy (Figure 1C). p-ERM specifically localized to membrane ruffles, as already described,[10,29] and was highly polarized at the leading edge of migrating cells. p-ERM was the only protein examined that we observed to directly localize in filopodia-like structures at the edge of migrating cells (Figure 1C). At 30 minutes after induction of migration, CD44 and p-ERM localization was strongly identified anterior to such filipodia-like structures (Figure 1C). However no significant alteration in CD44–p-ERM colocalization by ImageJ analysis was detected (Figure 1C). Interestingly, CD44 expression in single planes measured appeared to decrease, whereas that of p-ERM increased over time (Figure 1C).

CD44 and Ezrin Stably Interact in Non-Lipid Raft Regions of Migrating Cells

With evidence that CD44 and ezrin colocalize at the plasma membrane of migrating MDA-MB-231 cells, we next investigated whether they localized to the same biochemical compartments within membranes. Because CD44 has been described to localize to lipid raft domains, we first investigated the distribution of CD44 and ezrin relative to lipid raft membrane compartments. Lipid rafts were isolated from migrating or nonmigrating MDA-MB-231 cells using nondetergent (data not shown) or detergent extraction methods in combination with isopycnic sucrose density gradient fractionation. Both methods yielded similar results. Gradient fractions were analyzed for enzyme activity of the lipid raft marker alkaline phosphatase,[31] protein concentration, and sucrose density, as shown in Figure 2A. Top fractions from both small- and large-gradient preparations were characterized by low alkaline phosphatase activity, a sucrose density of <20%, and negligible protein content (Figure 2A). The exceptionally low protein content of these fractions mostly precluded their inclusion in SDS-PAGE gels. Conversely, middle fractions exhibited high alkaline phosphatase activity, a sucrose density of 20% to 25%, a low but measurable protein concentration, and high expression of the lipid raft marker protein flotillin-1 (Figure 2, A and B). Taken together, this was consistent with the enrichment of lipid rafts in these fractions. By contrast, the bulk of total cellular protein content was enriched in flotillin-low fractions at the bottom of sucrose gradients (sucrose density ≥30%). CD44 was observed to localize

mainly in flotillin-enriched lipid raft fractions (Figure 2B), although it was not exclusively restricted to raft fractions. By contrast, ezrin was detected throughout flotillin-low fractions in a pattern similar to that of the nonraft protein actin (Figure 2B). Interestingly, the relative recovery of CD44 in flotillin-low (nonraft) fractions was increased after the induction of migration. This was further supported by a significant increase in CD44 colocalization with transferrin receptor, a known marker for nonraft domains, at the leading edge of migrating cells (see Supplemental Figure S3 at *http://ajp.amjpathol.org*). Quantification of the relative levels of CD44 in raft fractions (normalized to flotillin-1) versus nonraft fractions (normalized to ezrin) from multiple experiments confirmed a significant decrease in the quantity of raft-affiliated CD44 (Figure 2B) ($P < 0.05$). Similar results were also obtained using the invasive breast cancer cell line Hs578T (see Supplemental Figure S4 at *http://ajp.amjpathol.org*).

We next used a co-immunoprecipitation approach to examine whether CD44-ezrin interactions took place inside or outside of lipid raft domains. Equal concentrations of total cellular protein from lipid raft and nonraft fractions of migrating or nonmigrating cells were immunoprecipitated with CD44 and analyzed for the presence of ezrin and p-ERM (Figure 2C). As expected, CD44 was highly enriched in lipid raft fractions of both migrating and nonmigrating cells. However, CD44 recovery from lipid rafts in migrating cells was less than that in nonmigrating cells, in conjunction with the appearance of a small pool of CD44 in immunoprecipitates from nonraft fractions of migrating cells. Interestingly, ezrin was significantly enriched in CD44 immunoprecipitates recovered from nonraft fractions of migrating cells (Figure 2C). The absence of detectable ezrin bands in the other immunoprecipitate lanes does not exclude CD44-ezrin coprecipitation, but rather illustrates that such interactions take place at exceptionally low levels relative to the coprecipitation of CD44-ezrin in nonraft fractions from migrating cells. Interestingly, this suggests that even a very small pool of CD44 in nonraft fractions of migrating cells is sufficient to account for the bulk of interactions with ezrin. More importantly, it also suggests that CD44 and ezrin interact outside lipid rafts during cell migration. Accordingly, p-ERM showed a dramatic enrichment in nonraft fractions from CD44 immunoprecipitates of migrating cells (Figure 2C). These results further supported the hypothesis that interactions between CD44 and ERM proteins such as ezrin occur outside lipid rafts in migrating cells. However, because radixin and moesin are also expressed in MDA-MB-231 cells (see Supplemental Figure S2 at *http://ajp.amjpathol.org*), it is likely that the p-ERM signal reflects the combined presence of the activated form of each ERM family member, but in proportions that are as yet unknown. To begin interrogating the influence of lipid rafts on potential interactions between CD44 and radixin or moesin, a siRNA approach was used. Flotillin-1 or caveolin-1 (the two main structural proteins in lipid rafts) were separately knocked down in MDA-MB-231 cells, whereupon we checked for colocalization between CD44 and either moesin (Figure 2D, top panel; see also Supplemental Figure S5 at http://ajp.amjpathol.org) or radixin (Figure 2D, bottom panel; see also Supplemental Figure S5 at *http://ajp.amjpathol.org*). Interestingly, flotillin-1 knockdown significantly decreased CD44 and moesin colocalization under nonmigrating conditions relative to a siRNA negative (siRNA-ve) control. Conversely, flotillin-1 knockdown significantly increased CD44 and radixin colocalization under nonmigrating conditions compared to a siRNA negative control. This further supports that both moesin and radixin could contribute to the p-ERM signal coprecipitating with CD44 under nonmigrating conditions (Figure 2C). It is also interesting to note that only flotillin-1 loss significantly affected the colocalization of CD44 with either moesin or radixin, suggesting a lack of involvement of caveolin-positive rafts in the process. However, decreased colocalization of CD44 with moesin was accompanied by decreased expression of the latter in flotillin-1 knockdown cells (see Supplemental Figure S5 at *http://ajp.amjpathol.org*).

CD44 and Ezrin Binding Is Sensitive to Raft Disruption or Altered CD44 Raft Affiliation

To further probe the proposed interaction of CD44 and ezrin outside lipid raft domains in migrating MDA-MB-231 breast cancer cells, we tested the effect of pharmacological disruption of lipid rafts on CD44-ezrin interactions. Confluent cells were treated with the cholesterol-sequestering reagent MβCD (10 mmol/L) to disrupt lipid rafts, and then allowed to migrate in serum-free medium and immunoprecipitated for CD44. CD44 recovery was marginally increased in MβCD-treated cells compared to controls. However, there was a large increase in ezrin recovery in CD44 immunoprecipitates from raft-disrupted (MβCD-treated) cells (Figure 3A). Western blot quantification analysis revealed the increase in ezrin binding to CD44 MβCD-treated cells versus controls was statistically significant (Figure 3A) ($P = 0.0412$). No significant alteration in p-ERM-CD44 coprecipitation was observed between control and MβCD-treated cells when each was normalized to their respective levels of total ezrin detected in CD44 immunoprecipitates (Figure 3A). Furthermore, CD44 levels in the input lysates were confirmed to be similar between treatment conditions (Figure 3A), and neither CD44 nor ezrin were recovered from negative control experiments using nonspecific IgG as the immunoprecipitating antibody.

Because interference with the raft structure affected interactions between CD44 and ezrin, we next tested the effect of raft disruption on cell migration. Confluent MDA-MB-231 cells exposed to MβCD or vehicle were scratch wounded and their migration quantitated over time. However, MβCD-treated cells in fact migrated slower than untreated cells, with the two slopes showing statistically significant differences (Figure 3B, $P = 0.0144$). This potential conflict was explained by immunofluorescence analysis (Figure 3C), in which MβCD-treated cells showed increased CD44 and ezrin colocalization throughout the cell membrane rather than specifically at the migrating edge where the interaction could drive migration (Figure 3C). We hypothesized that the net antimigratory effect of MβCD may

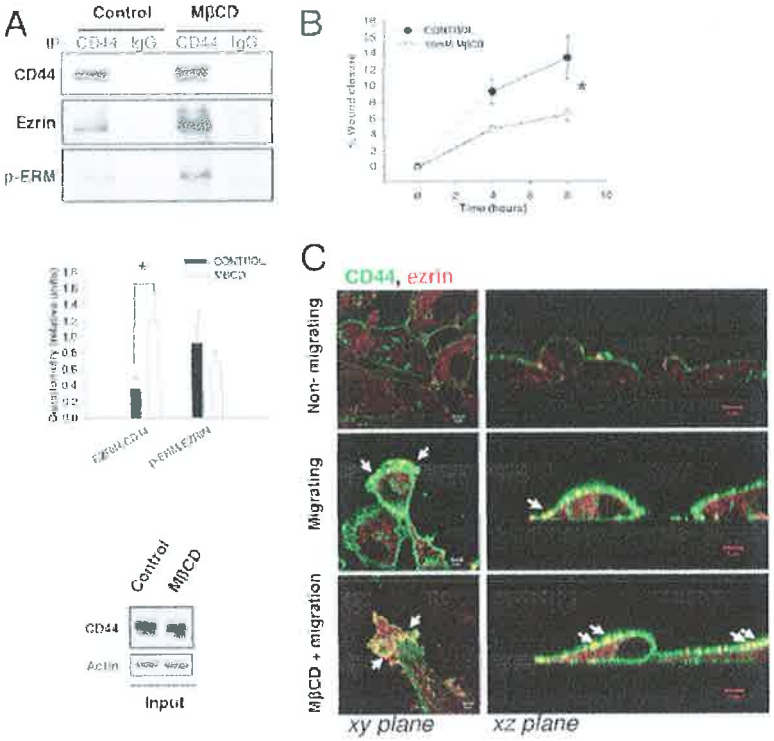

Figure 3. Disruption of lipid rafts alters CD44-ezrin interactions and cell migratory capabilities. **A:** CD44 was immunoprecipitated (IP) from equal amounts of total cellular protein isolated from MDA-MB-231 cells treated with 10 mmol/L MβCD (or vehicle) for 30 minutes in serum-free medium before the induction of cell migration for 30 minutes (**top panel**). Following MβCD treatment, CD44 and ezrin binding was significantly increased compared to that in control untreated cells (**middle panel**). Error bars refer to SEM of three replicate experiments (unpaired two-tailed *t*-test, $P = 0.0112$). Blots from input lysates (**bottom panel**) confirm similar expression levels of CD44 in both treatment conditions. **B:** The effect of MβCD on MDA-MB-231 cell migration was tested by scratch wound assay. Cells treated with 10 mmol/L MβCD for 30 minutes showed significant impairments in cell migration over time. Error bars refer to SEM of $n = 5$ experiments (GraphPad Prism linear regression analysis, $P = 0.0144$). **C:** Immunofluorescence detection of CD44 (green) and ezrin (red) in nonmigrating cells or during cell migration in nontreated cell (control) and in cells treated with 10 mmol/L MβCD for 30 minutes (**left panels**). After MβCD treatment, confocal imaging in the *xz* plane (**right panels**) revealed extensive colocalization of CD44 and ezrin throughout the membranes of cells both at the leading and trailing edges of migrating cell sheets (arrows).

reflect disrupted cellular polarity and impairment of lipid raft–mediated events.

Because the reversible posttranslational addition of palmitoyl lipid groups has been shown to promote CD44 localization within rafts,[24] we next tested whether pharmacological inhibition of depalmitoylation would promote CD44 retention within rafts and consequently decrease CD44-ezrin interactions. MDA-MB-231 cells were co-treated with two DFI, methyl arachidonyl fluorophosphonate and palmityl trifluoromethyl ketone, and allowed to migrate before analyzing recovery of raft-affiliated versus nonraft-affiliated CD44, flotillin-1, and ezrin (Figure 4A, left panel). As before, CD44 mainly localized in lipid raft fractions whereas ezrin was recovered mainly from nonraft fractions. Given the challenges in defining biochemical fractions/compartments, we devised a novel arithmetic ratio of CD44 in raft fractions to CD44 in nonraft fractions to better describe the movement of CD44 from raft to nonraft compartments and vice versa. Because traditional loading controls (such as actin) are unequally distributed throughout sucrose density gradient preparations, we had to choose separate loading controls for raft versus nonraft fractions. Flotillin-1 was chosen as a representative loading control strongly enriched in raft fractions, and ezrin as a marker of flotillin-low nonraft fractions. Thus, by densitometric quantification of blots exposed for identical periods of time, CD44 expression was normalized to flotillin-1 to estimate its abundance in lipid rafts, or to ezrin to estimate its abundance in non-lipid raft fractions. As shown in Figure 4A, DFI treatment induced a statistically significant increase (nearly three-fold; $P < 0.05$) in the proportion of raft-affiliated CD44 (described by the lipid raft/non-lipid raft ratio). DFI treatment did not alter the raft affiliation of CD44 under non-migrating conditions, further supporting the possibility that CD44 translocation outside lipid rafts is activated only during cell migration.

Having achieved increased retention of CD44 within lipid rafts on DFI treatment, we next tested whether binding interactions between CD44 and ezrin would consequently be reduced. MDA-MB-231 cells were treated with or without DFI for 30 minutes before induction of migration (Figure 4B). As a positive control for increased CD44 and ezrin binding, some cells were treated for 30 minutes with 10 mmol/L MβCD before the induction of migration. Following wound induction, cells were allowed to migrate in serum-free medium for 30 minutes and immunoprecipitated for CD44. As already shown (Figure 1A), CD44 and ezrin coprecipitation was increased in migrating cells, whereas disruption of lipid rafts due to MβCD (Figure 3A) significantly increased this binding ($P = 0.029$). Interestingly, DFI treatment, which increased CD44 retention in lipid rafts, virtually abolished the coprecipitation of CD44 and ezrin (Figure 4B). Densitometric quantification of CD44 and ezrin binding, normalized to CD44 expression, is shown in Figure 4B. This was also paralleled by a statistically significant decrease in migration after DFI treatment (Figure 4C) ($P = 0.0162$).

CD44 Localizes Outside Rafts after Induction of CD44-Specific Migration by Hyaluronic Acid

Although scratch wound–induced cell migration was capable of indirectly activating CD44-ezrin interactions, we also used HA as a stimulus to directly activate CD44-

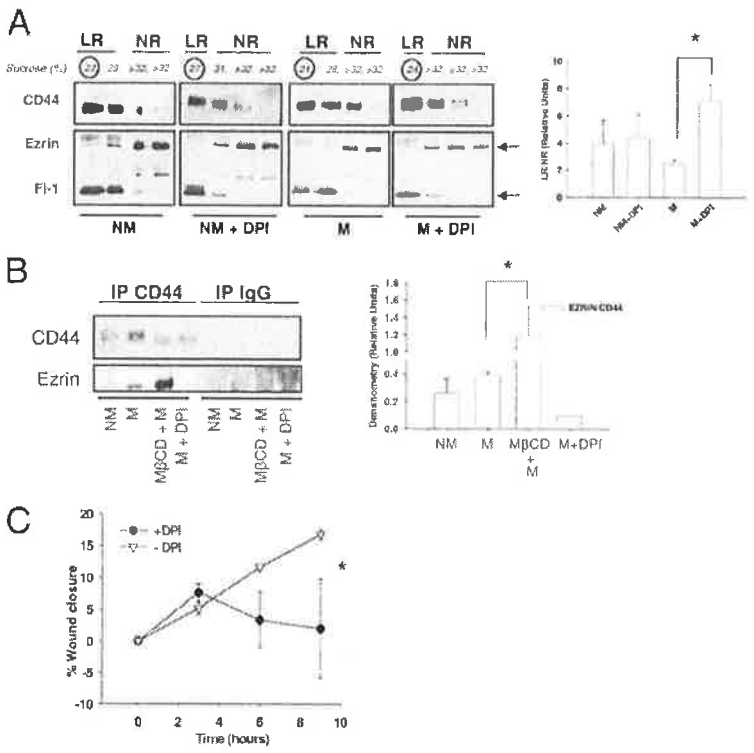

Figure 4. Forced CD44 affiliation with lipid rafts disrupts CD44 and ezrin binding and cell migratory abilities. **A:** MDA-MB-231 cells were treated with depalmitoylation inhibitors (DPI; 5 μmol/L methyl arachidonyl fluorophosphonate and 20 μmol/L palmityl trifluoromethyl ketone) or vehicle for 30 minutes, and either induced to migrate or left stationary for 30 minutes in serum-free medium. Cells were extracted for lipid raft isolation with 1% Triton X-100 and analyzed by SDS-PAGE and Western blotting for expression of CD44, flotillin-1 (Fl-1), and ezrin (**left panel**). CD44 within lipid raft fractions was normalized to flotillin-1 expression whereas non-raft CD44 was normalized to ezrin expression, and the relative amount of CD44 in lipid rafts was given by the LR/NR ratio (**right panel**). A significant increase in CD44 localization to lipid rafts in migrating cells was observed after DPI treatment, whereas no changes in ezrin localization were observed after DPI treatment. Error bars refer to SEM of duplicate experiments (unpaired two-tailed *t*-test, $^*P = 0.0331$. **B:** Ezrin and CD44 binding was analyzed in nonmigrating (NM) or migrating (M) MDA-MB-231 cells treated for 30 minutes with 10 mmol/L MβCD or a combination of the DPIs 5 μmol/L methyl arachidonyl fluorophosphonate and 20 μmol/L palmityl trifluoromethyl ketone (DPI) in serum-free medium. After treatment, cells were immunoprecipitated (IP) for CD44 and probed for ezrin (**left panel**). Band quantification is also presented (**right panel**). Compared to control conditions, MβCD treatment significantly increased CD44-ezrin coprecipitation, whereas DPI greatly decreased CD44-ezrin coprecipitation. Error bars refer to SEM of triplicate experiments ($^*P = 0.028$, unpaired two-tailed *t*-test). **C:** The effect of DPI treatment on MDA-MB-231 cell migration was tested by scratch wound assay. Cells were pretreated with a combination of 5 μmol/L methyl arachidonyl fluorophosphonate and 20 μmol/L palmityl trifluoromethyl ketone (DPI) or vehicle for 30 minutes and then scratch wounded. Wound closure was measured over time up to 9 hours. Error bars refer to SEM of duplicate experiments, with multiple replicates per experiment. DPI treatment significantly slowed wound closure compared to control conditions (GraphPad Prism linear regression analysis, $^*P = 0.0162$). LR, lipid raft; NR, non-lipid raft.

dependent migration.[33,34] The concentration of HA (5 mg/mL) was chosen on the basis of its ability to promote cell migration in scratch-wounded MDA-MB-231 cells (Figure 5A). Because we had previously observed reduced CD44 recovery from lipid rafts after nonspecific induction of migration, we hypothesized that CD44-specific migration via HA would induce a similar effect. Confluent MDA-MB-231 cells were scratch wounded or left stationary and treated with HA for 30 minutes before isolation of raft and nonraft fractions (Figure 5B). HA treatment in migrating cells significantly increased the recovery of CD44 outside lipid raft fractions, compared to the nonmigrating HA-untreated condition (Figure 5B). However, no significant variations were observed between nonmigrating and migrating conditions in the presence of HA treatment. No changes in ezrin, actin, and flotillin-1 raft affiliation were observed among the different conditions. These results support the possibility that CD44 is released from lipid rafts during CD44-mediated cancer cell migration.[32,35]

Interference with Caveolin-1 or Flotillin-1 Alone Is Not Sufficient to Alter Cell Migration

Because HA–CD44 binding has been described to be involved in the recycling of CD44[36] and since their binding has been described to happen in lipid rafts, we have begun to investigate the types of lipid rafts involved in this process. However, although flotillin-1 and caveolin-1 mark two different types of lipid rafts, biochemical separation via sucrose density gradient fractionation cannot easily distinguish between them. In fact, caveolin-1 and flotillin-1 were enriched in similar fractions in both migrating and nonmigrating MDA-MB-231 cells (Figure 6A). We, therefore, used immunofluorescence studies to ask whether spatial differences in the localization of either raft marker could shed light on the potential contribution of each raft family to migration in MDA-MB-231 cells. Migrating and nonmigrating cells were double stained for caveolin-1 or flotillin-1, and examined by confocal microscopy at the basal and suprabasal aspects of the cells (Figure 6B). Subtle differences in the basal and suprabasal localization patterns of flotillin-1 and caveolin-1 were observed. For clarity, we define basal pole as the lowest point along the vertical (xz) axis, right at the point of attachment to the matrix. This was also the point at which we could clearly see projections (filopodia, lamellipodia) in the flattened cells at the leading edge of migrating cells. The aspect was a higher point along the xz axis above the basal pole. We made this distinction to point out that the proteins of interest differentially localize in different planes of the cells.

Specifically, flotillin-1 at the suprabasal aspect of the cells was predominantly enriched in the cell membrane, and its expression levels or distribution did not vary significantly between nonmigrating and migrating cells (Figure 6B). By contrast, caveolin-1 expression appeared to increase at the suprabasal aspect of migrating relative to nonmigrating cells, and its localization was submembranous in addition to membranous. At the basal pole of MDA-MB-231 cells (the surface at which the cells dynamically attach to and detach from the substratum during migration), there was a strong enrichment of flotillin-1 in the plasma membrane of pseudopodial projections in

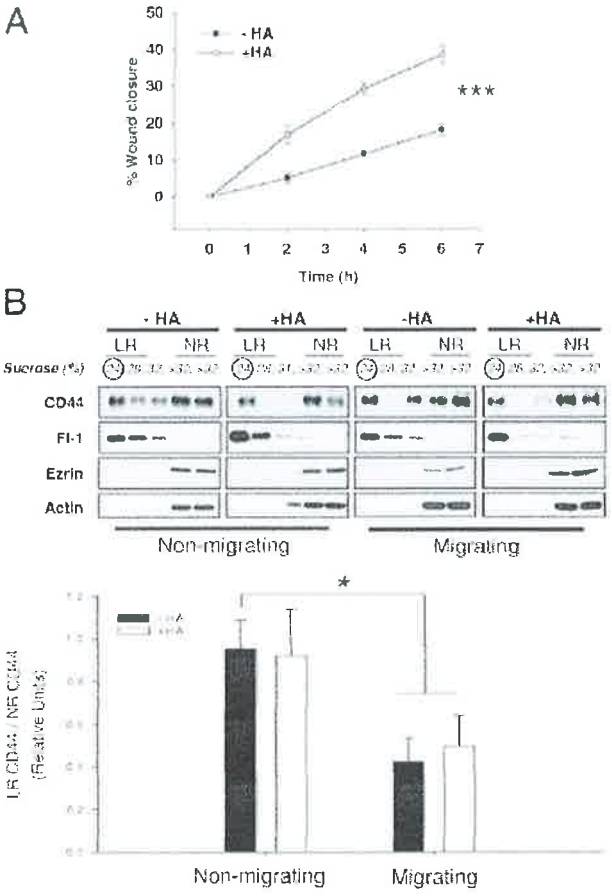

Figure 5. HA-stimulated migration in MDA-MB-231 cells is associated with reductions in raft-affiliated CD44. **A:** After wounding, MDA-MB-231 cells were stimulated with 5 mg/mL HA (+HA) or serum-free medium alone (−HA) and allowed to migrate for up to 8 hours. Wound closure was measured over time. HA treatment promoted wound closure approximately twofold more than control conditions, and linear regression analysis confirmed a statistical difference between the two curves. Error bars refer to SEM of triplicate experiments. (***$P = 0.005$, GraphPad Prism linear regression analysis). **B:** MDA-MB-231 cells were stimulated with 5 mg/mL HA or with vehicle alone, and scratch wounded (migrating, M) or left stationary (nonmigrating, NM). Cells were separated into lipid raft and nonraft fractions by ultracentrifugation on sucrose gradients and each fraction analyzed by SDS-PAGE for CD44, ezrin, flotillin-1 (Fl-1), and actin expression (**top panel**). **Bottom panel:** CD44 localization to lipid raft (LR) versus non-lipid raft (NR) fractions in the different conditions, expressed as LR/NR ratio. Error bars refer to the SEM of three experiments. There was a statistically significant reduction in CD44 recovery from rafts under HA-treated or -untreated migrating conditions compared to HA-untreated nonmigrating conditions. *$P = 0.031$ nonmigrating versus migrating for HA−; $P = 0.014$ nonmigrating versus migrating for HA+, unpaired two-tailed *t*-test.

migrating cells. Distribution of caveolin-1 at the basal pole did not vary dramatically between migrating and nonmigrating cells, and was again submembranous in addition to membranous under both conditions. Overall, there was limited colocalization between flotillin-1 and caveolin-1 at either the suprabasal or basal cellular aspects, and no significant changes in colocalization were observed during migration (confirmed by pixel overlap quantification of multiple experiments; data not shown).

These data support the possibility that flotillin-enriched lipid rafts and caveolin-enriched lipid rafts define different subtypes of rafts that could be involved in different cellular processes. Accordingly, in our hands, these raft populations had different subcellular distributions and different patterns of re-localization in MβCD-treated cells compared to controls (Figure 7). Specifically, MβCD treatment promoted the enrichment of flotillin-1 but not caveolin-1 staining at the leading edge of migrating cells.

To begin testing the relative involvement of flotillin-1 and caveolin-1 in driving breast cancer cell migration, we also transiently knocked-down the expression of each protein using siRNA technology. After 72 hours, protein expression of either flotillin-1 or caveolin-1 was successfully reduced by >90% (Figure 8A). Immunofluorescence confocal micrographs of flotillin-1 and caveolin-1 further confirmed efficient knockdown of flotillin-1 and caveolin-1 (Figure 8B, left and right panels, respectively). Surprisingly, analysis of scratch-wound assays revealed that loss of caveolin-1 or flotillin-1 alone was not sufficient to alter cell migration relative to that in cells transfected with negative control siRNA (Figure 8C). This likely reflects complexity issues relating to raft crosstalk and also raft-mediated regulation of other proteins involved in migration (besides just CD44). This was supported by double-knockdown experiments for flotillin-1 and caveolin-1 (Figure 8D), in which the overall migratory machinery appears to have been affected. Accordingly, scratch-wound assays revealed that double-knockdown cells migrated significantly less than control or siRNA-ve cells (Figure 8E, $P = 0.0125$ control versus knockdown; $P = 0.0092$ siRNA-ve versus knockdown, linear regression by GraphPad Prism).

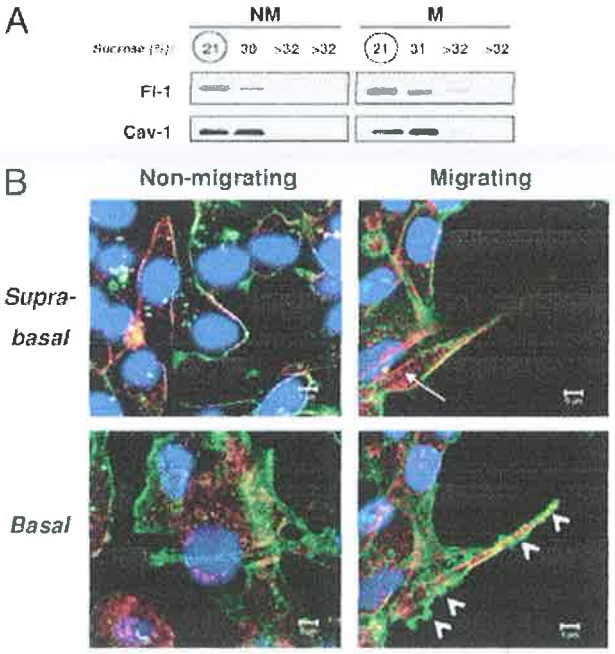

Figure 6. Flotillin-positive lipid rafts and caveolin-positive lipid rafts have different subcellular localizations. **A:** Lipid rafts were isolated from migrating (M) or nonmigrating (NM) MDA-MB-231 cells and immunoblotted for flotillin-1 (Fl-1) and caveolin-1 (Cav-1). Both flotillin-1 and caveolin-1 localized in the same fractions harvested from sucrose density gradients. **B:** MDA-MB-231 cells were analyzed by immunofluorescence confocal microscopy for flotillin-1 (green) and caveolin-1 (red) colocalization at either the suprabasal or basal aspects of the cells. Flotillin-1 was strongly enriched in protrusive structures at the basal aspect of migrating cells. Three confocal micrographs containing three to five cells each were analyzed.

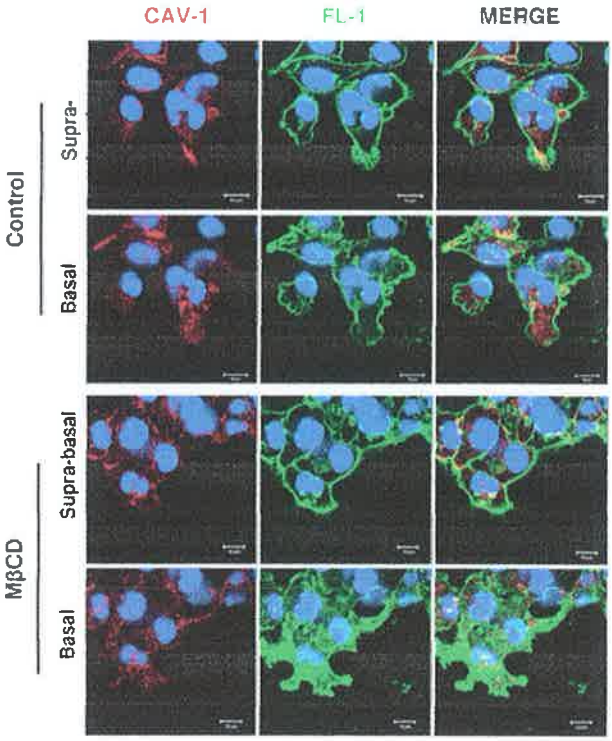

Figure 7. MβCD treatment differentially affects caveolin-1 (Cav-1) and flotillin-1 (Fl-1) localization in the cell compartment. MDA-MB-231 cells were treated with 10 mmol/L MβCD or vehicle (Control) for 30 minutes and then induced to migrate. Cells were then analyzed by immunofluorescence confocal microscopy for caveolin-1 (red) and flotillin-1 (green) colocalization at either the suprabasal or basal aspect of the cells. Three confocal micrographs containing three to five cells each were analyzed. Following MβCD treatment, flotillin-1 presented a different reorganization between the suprabasal and basal aspects while caveolin-1 was distributed relatively uniformly throughout the cells. This may suggest differential functions of lipid rafts identified by caveolin-1 compared to those identified by flotillin-1.

Pathway Reconstruction

By combining the results shown in Figures 1A and 2C within a logical framework (see *Materials and Methods*), we have been able to generate a self-consistent model for the role of lipid rafts in regulating CD44-mediated cell migration (Figure 8). This model illustrates the natural biophysical order of processes and is also consistent with the interventions of MβCD, DPI, and HA (Figures 4A, 5B, and 6C). Specifically, it illustrates that CD44 is likely to move outside of rafts to interact with threonine-phosphorylated (active) EPM and drive migration. The movement of CD44 outside rafts, which is associated with the cell migratory phenotype, is activated by the addition of HA or scratch wounding, and is inhibited by DPI that cause CD44 to be retained in rafts.

Discussion

CD44 is a highly dynamic molecule involved in many cellular processes, both physiological and pathophysiological. In particular, CD44 and its variants have been described to be altered in many cancers, including breast.[30] However, the involvement of CD44 in breast cancer cell migration (an early requirement for metastasis) is still controversial and incompletely understood. Because CD44 is known to localize in cholesterol- and sphingolipid-enriched regions of the cell membrane known as lipid rafts, our study investigated the involvement of rafts in regulating CD44-dependent breast cancer cell migration.

Although the CD44 standard isoform (CD44s) has been described by some as inhibitory toward cell migration,[31] others have reported it to be directly involved in breast cancer invasion and tumor progression.[30,32] The invasive and metastatic breast cell line MDA-MB-231 mainly expressed CD44 with a molecular weight corresponding to that of CD44s (85 kDa), and thus was a good model to dissect mechanisms regulating CD44s during breast cancer cell migration. Specifically, we were interested in studying CD44 regulation of cell migration via its interaction with the cytoskeleton through the linker protein ezrin. Because CD44 and ezrin interactions have been described to regulate wound healing–induced migration[33] and since the migratory pathways activated during wound repair[34] involve the same signaling cascades activated during normal[35] and tumor cell migration,[36] scratch-wound assays were used as a model to induce migration of MDA-MB-231 cells. Although CD44 and ezrin interactions during cell migration have been widely described,[37–44] to our knowledge, the role of lipid rafts in regulating their interaction during breast cancer cell migration is incompletely understood.

After inducing the migration of confluent MDA-MB-231 cells by scratch wounding, co-immunoprecipitation experiments revealed a net increase in CD44 and ezrin binding. This implied a conformational change in ezrin to release autoinhibitory binding between its N- and C-terminal domains.[45] Such conformational changes of ezrin are needed for its binding with CD44, and can be generated by interactions with lipids (PIP2) or by changes in protein phosphorylation.[46] After induction of cell migration in MDA-MB-231 cells, activation of phosphatidyl-inositol 4-phosphate 5-kinase has been reported to generate an increase in PIP2 concentration in the internal leaflet of the plasma membrane at the cellular migrating edge.[47] Subsequent interactions between PIP2 and ezrin are then thought to induce plasma membrane localization and activation of ezrin.[47,48] To act as a cytoskeletal linker, ezrin has not only to acquire an open conformation but also to be phosphorylated at threonine-567, the binding site for F-actin. Protein kinase C (PKC), which is highly active in MDA-MB-231 cells,[49] may be responsible for this phosphorylation. In support of these findings, we noted a strong increase in the amount of p-EPM bound to CD44 in migrating cells. This may reflect a combination of p-ezrin, p-radixin, and p-moesin, because all three proteins have similar sizes, are expressed in breast cancer cells, and their phospho-forms are recognized by the p-EPM antibody. Interestingly, we also observed co-immunoprecipitation between CD44 and a high molecular weight ezrin band (~ 160 kDa). It is intriguing to speculate that this is a product of PKC phosphorylation.[50] Confocal microscopy studies also confirmed CD44 and ezrin colocalization at the migrating edges of MDA-MB-231 cells.

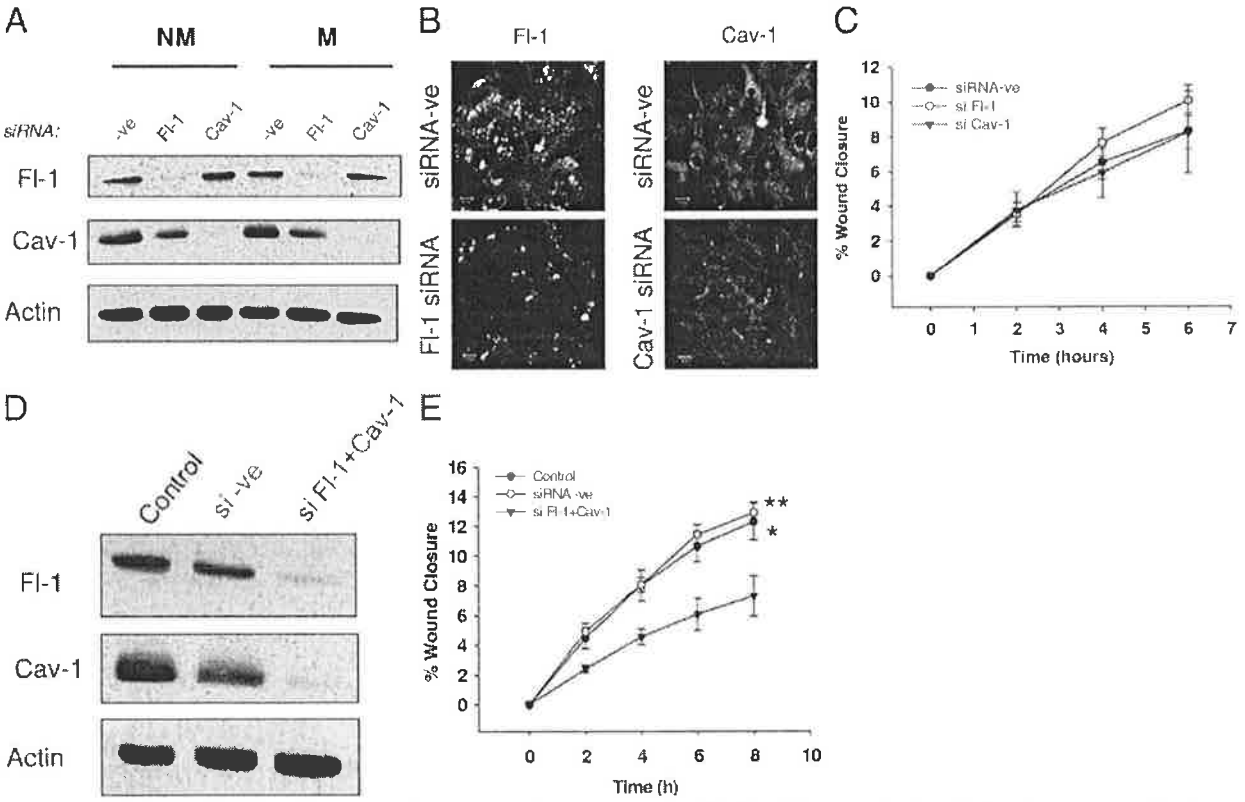

Figure 8. Knockdown of flotillin-1 and caveolin-1 does not alter cell migration in MDA-MB-231. siRNA against flotillin-1 (Fl-1) and/or caveolin-1 (Cav-1) or a universal negative control siRNA (-ve) was used to transiently knock down gene expression in MDA-MB-231 cells for 72 hours before performing migration assays or immunofluorescence analysis. **A:** After 72 hours, the efficiency of transfection was checked by SDS-PAGE and Western blot analysis. Expression of flotillin-1 and caveolin-1 alone was successfully reduced by approximately 90%. **(B)** Decreased expression of Fl-1 and Cav-1 following siRNA knockdown was also confirmed by immunofluorescence confocal microscopy. **C:** Analysis of scratch-wound assays between knockdown conditions (relative to that in cells transfected with the negative control siRNA) did not reveal any significant differences in cell migration. **D:** The efficiency of simultaneous knockdown of flotillin-1 and caveolin-1 after 72 hours from transfection was tested by Western blot analysis of flotillin-1 and caveolin-1 expression. **E:** Analysis of scratch-wound assays of cells double knocked down for flotillin-1 and caveolin-1 revealed significantly less cell migration than in untreated cells or those transfected with the negative control siRNA. $^{*}P = 0.0125$ Control versus Fl-1+Cav-1 knockdown, $^{**}P = 0.0092$ siRNA negative control versus Fl-1+Cav-1 knockdown, linear regression analysis by GraphPad Prism.

with p-ERM mostly localizing at membrane ruffles[59] or in filopodial structures[54] as already reported elsewhere.

Because CD44 has been described to localize to membrane lipid rafts, and lipid rafts have been implicated in regulating cancer migration,[60] we wondered whether rafts could regulate CD44 and ezrin binding by controlling their spatial distribution within cell membranes. Lipid raft extraction from migrating and nonmigrating MDA-MB-231 cells revealed that CD44 mainly localized to flotillin-high lipid raft fractions, although low levels were also detected in flotillin-low nonraft fractions. By contrast, ezrin mainly localized to actin-positive nonraft fractions but was not detected in flotillin-high raft fractions. Pragi et al[16] suggested that nondetection of ezrin in lipid rafts can be due to the low sensitivity of biochemical techniques for the detection of small quantities of ezrin, particularly since rafts already have a very low total protein content. Under our conditions, CD44 and ezrin neither colocalized in, nor co-immunoprecipitated from, lipid raft fractions under either nonmigrating or migrating conditions. However, a small pool of nonraft CD44 recovered under migrating conditions coprecipitated strongly with ezrin, particularly the threonine-phosphorylated (active) form of ERM proteins. It is likely that even a small relative shift of CD44 from raft to nonraft fractions under migratory conditions could permit such an occurrence, and certainly that relative shifts are more important than the absolute presence/absence of CD44 in either raft or nonraft fractions exclusively.

Although the mechanism whereby CD44 is retained in nonraft fractions following the induction of migration is as yet unknown, it is intriguing to speculate that ezrin could sequester CD44 within nonraft fractions after their interaction. Supportive evidence has been drawn from a study in which disruption of the actin cytoskeleton by latrunculin A was found to increase CD44 localization within lipid rafts.[11] Because CD44 interacts with actin via linker proteins such as ezrin, this suggests that actin-binding proteins, including ezrin, may play a major role in the lateral mobility of CD44 outside lipid rafts. However, our preliminary experiments showed that ezrin knockdown did not affect CD44 colocalization with flotillin-1–positive lipid rafts (data not shown).

All together, these findings highlight the dynamic nature of binding interactions between CD44 and ezrin. It has also been described that this binding can be influ-

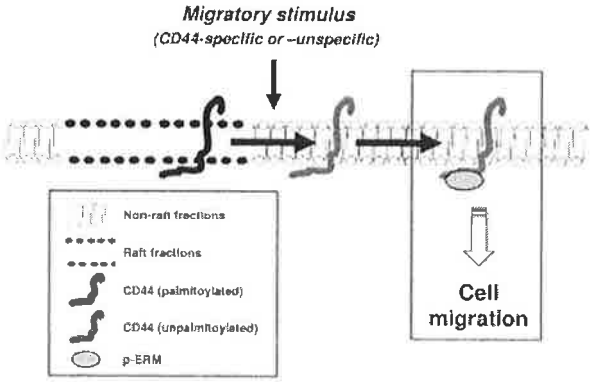

Figure 9. Lipid raft–mediated CD44 and ezrin interaction model. The CD44 cell migration pathway reconstructed using immunoprecipitation experiments and logical modeling. **Horizontal arrows** indicate the resulting flux when transiting from a stationary to migratory cell phenotype. Our model suggests that the transit between a stationary and migratory state is associated with release of CD44 from lipid rafts (possibly via depalmitoylation), whereupon nonraft CD44 can bind phosphorylated (active) ezrin to initiate migration.

enced in a time-dependent manner by CD44 phosphorylation status. MDA-MB-231 cells have been shown to possess high levels of PKC activity,[48] and *in vitro* studies have shown an increased interaction between CD44 and ezrin up to 40 minutes after PKC activation.[9] At approximately 40 minutes, a second phosphorylation event on serine-291 of CD44 reportedly generates conformational changes that decrease CD44 and ezrin affinity.[9] Therefore, we examined CD44 and ezrin interactions after 30 minutes from induction of migration, supposedly before CD44 and ezrin disengage (estimated at 40 minutes after the induction of migration). Results generated using this migration model provided novel information to suggest that the interactions between CD44 and ezrin occur outside lipid rafts. Although we did not directly test CD44-ezrin interactions at later time points, our colocalization data and the results of Legg et al[9] suggest that CD44-ezrin interactions outside lipid rafts most likely occur during the early stages of migration.

Our hypothesis that CD44 and ezrin interact outside lipid raft domains was further supported by experiments in which CD44-specific migration was directly stimulated by exposure to its extracellular matrix ligand HA. This stimulated a significant increase in CD44 localization outside lipid rafts in migrating HA-treated cells compared to the nonmigrating HA-untreated condition. It should also be noted that there are many different types of HA fragments, and it is possible that other fragments could induce a greater translocation of CD44 outside of rafts. It has been described that HA interactions with CD44 are necessary for HA recycling and degradation[49] in tumor cell migration.[53] It is possible that CD44 detection in nonraft fractions after induction of migration could correlate with CD44 internalization into membrane-enclosed vesicles, as has already been described in association with HA degradation. To further support this hypothesis, we found decreased levels of CD44 in single planes of the cell membrane at 120 minutes after induction of migration. In fact, CD44 recycling has already been described as a necessary event in cell migration.[54] Additionally, we observed that in nonmigrating HA-treated cells, CD44 recovery outside lipid rafts was not significantly different from that in other conditions (nonmigrating HA-treated, migrating HA-treated/-untreated). This may suggest that HA treatment in nonmigrating conditions induces changes at the molecular level intermediate between migrating and nonmigrating phenotypes. It is possible that, following HA stimulation in nonmigrating conditions, CD44 can only be partially internalized because contact-inhibited cells cannot properly migrate. This might preclude any further CD44 internalization. Moreover, depending on the size of its particles, HA treatment could cause CD44 clustering, thereby bringing together lipid rafts and increasing CD44 detergent insolubility.[11] This intermediate phenotype may help explain the lack of statistically significant differences between CD44 raft/nonraft segregation in HA-treated versus -untreated nonmigrating cells, or in HA-treated nonmigrating versus migrating cells. Specifically, endocytosis can be a possible mechanism involved in CD44 recycling, and it has been described to be inhibited by MβCD treatments.[52] Therefore, we speculate that enhanced binding between ezrin (total or active) and CD44 after MβCD treatment may be due to a block in the endocytotic pathway inhibiting CD44 and ezrin from disengaging and resulting in an increased interaction between the two. Accordingly, immunofluorescence analysis of CD44 and ezrin after lipid raft disruption confirmed their enhanced localization throughout cell membranes. However, because lipid rafts carry out many important regulatory functions, extensive raft disruption due to MβCD may also interfere with other key cellular functions, including regulation of cell polarity. It should also be noted that MβCD, although widely accepted as a pharmacological disrupter of lipid rafts,[21,23] is nonspecific in this regard. Therefore, our crude evidence of MβCD-induced raft disruption facilitating CD44-ezrin interactions could be better refined, should more selective and specific raft-disruptive reagents become available in the future.

To further test the potential spatial control of lipid rafts over CD44-ezrin interactions, we have begun to explore the possibility of pharmacologically inhibiting the departure of CD44 from rafts using protein palmitoylation inhibitors. CD44 has two conserved cysteine residues that can be palmitoylated[32] a posttranslational modification that increases its hydrophobicity and affinity for lipid raft domains. In turn, lipid raft proteins, such as CD44, can be dynamically depalmitoylated by the action of palmitoyl protein thioesterases,[55] which decrease their affinity for lipid rafts. Moreover, phosphorylation events, such as those described during cell migration, can induce conformational changes that also affect the exposure of the palmitoylation sites and, therefore, regulate protein localization to lipid rafts.[56] Using a combination of DPI to prevent depalmitoylation, we successfully inhibited the release of a pool of CD44 from lipid rafts. The net effect of forced detainment of CD44 within rafts was that CD44-ezrin coprecipitation was practically abolished. This was paralleled by reduced cell migration, supporting our hypothesis that lipid rafts exert a key regulatory influence on

CD44-ezrin interactions and, subsequently, cell migration. This finding also supports the idea that CD44 and ezrin binding is very dynamic and that the relative spatial localization of these two proteins can play an important role in regulating the physiology of binding. However, DPI represent a class of nonselective inhibitors about which little is known, thus the observed functional effects in our exploratory experiments cannot at this time be attributed solely to changes in CD44 palmitoylation status. Because CD44 localization to lipid rafts is due to CD44 palmitoylation on specific cysteines, this represents a logical future strategy to better interrogate the specific contribution of CD44 palmitoylation changes to the functional modulation of cell migration. We speculate that phosphorylation events during cell migration may induce conformational changes in CD44 that mask its palmitoylation sites, decreasing CD44 affinity for lipid rafts. We suggest that this may be a possible mechanism involved in the control of CD44-ezrin relocation outside lipid rafts during breast cancer cell migration. However, further studies are needed to assess this mechanism.

Many different types of lipid rafts have been described to play roles in cell migration. Flotillin-1 and caveolin-1 represent two key markers of different raft populations. Our studies in MDA-MB-231 cells suggest that CD44 predominantly associates with flotillin-positive rather than caveolin-positive rafts. Immunofluorescence analysis also confirmed that caveolin-1 knockdown does not significantly alter CD44 and flotillin-1 colocalization during migration (data not shown), supporting our hypothesis that CD44-dependent cell migration is not under direct regulatory control by caveolin-positive lipid rafts. Accordingly, recent publications describe CD44 as a carrier in non-caveolar, clathrin-independent pathways in mouse embryonic fibroblasts.[54] Interestingly, however, transient knockdown of neither flotillin-1 nor caveolin-1 was sufficient to alter cell migratory characteristics over a short time course in our scratch-wound migration assays relative to a negative control siRNA. Although an increase in migration might have been expected under flotillin knockdown conditions if CD44 was indeed being released from rafts and becoming free to interact with ezrin, it must be remembered that lipid rafts are highly complex structures that regulate the location and function of many cellular proteins. Several such proteins (including key kinases and focal adhesion proteins, including Src and FAK) are known to play key roles in cell migration.[57] Therefore, there are likely to be compensatory mechanisms that act to preserve important cellular functions (such as migration) even in the event of raft loss. Spatial and temporal considerations must also be taken into account, because stable loss of caveolin-1 has been reported to reduce invasive behavior in breast cancer cells over a longer timescale.[58] Accordingly, long-term loss of caveolin-1 has been described to be associated with cell transformation and tumoral growth.[59] Furthermore, potential crosstalk between flotillin-1 and caveolin-1 may also impact cell functional behavior. For example, in intestinal epithelial cells, flotillin-1 down-regulation has been reported to down-regulate caveolin-1 availability by preventing its lysosomal degradation.[60] In fact, scratch-wound assays revealed that cells doubly knocked down for flotillin-1 and caveolin-1 migrated significantly less than control or siRNA negative control cells, further supporting the hypothesis that an organized lipid raft machinery is needed to allow functional cell migration. We speculate that the complete loss of rafts may inflict a global dysregulation on cell migration via the uncoupling of various signaling pathways that depend on raft/nonraft segregation of effector components. Overall, our studies highlight that the regulation of CD44-dependent cell migration by either flotillin-positive or caveolin-positive lipid rafts is complex, and will require very specific experimental approaches in the future to dissect the relative roles of each type of raft population (as well as their crosstalk).

Taken together, our observations have shed novel light on the role of lipid rafts in regulating CD44-mediated cell migration. It is interesting to note that our surface area calculations estimated only <10% of cells to be migrating at any one time, despite our extensive scratch-wounding protocol. This calculation is only a crude physical approximation of the number of migrating cells at 30 minutes after stimulation. On the basis of immunofluorescent observations of flattened cells, we estimated that four to five cells back from each wound edge were likely to be actively migrating. However, it is known that even cells behind the migrating edge are also affected by wounding. Indeed, injured epithelial cells release ATP and different chemotactic factors into culture medium *in vitro*, thereby activating calcium waves that trigger different early responses through activation of A disintegrin and metalloproteases and epidermal growth factor receptors, both of which are involved in the activation of migratory pathways.[29] This suggests that our estimate of only <10% cell migration is very conservative, and could explain why statistically significant differences in submembranous trafficking of CD44 and its interactions with ezrin were detected even at such low levels of migration. Because only small numbers of cells are likely to migrate out of a tumor during early invasion and metastasis, it is intriguing to speculate that our mechanism is biologically relevant to that scenario. However, *in vivo* experimentation would be necessary to better investigate the real relevance to tumor metastasis. Using experimental data to construct a logical framework based on our *in vitro* data, we propose a model (Figure 9) whereby lipid rafts regulate interactions between CD44 with ezrin in its active (phosphorylated) form to orchestrate breast cancer cell migration. Specifically, in the stationary state, CD44 is mostly retained within rafts and unable to interact with phospho-ERM proteins to drive migration. On exposure to a migratory stimulus (such as nonspecific wounding or CD44-specific stimulation with HA), CD44 moves out of rafts, potentially following its depalmitoylation, and is free to interact with activated ERM proteins. This is then associated with the migratory phenotype. We speculate that further exploration of mechanisms to specifically target and modulate CD44 localization to lipid rafts may have value for the long-term development of new anti-migratory breast cancer treatments.

References

1. Sherman L, Sleeman J, Dall P, Hekele A, Moll J, Ponta H, Herrlich P: The CD44 proteins in embryonic development and in cancer. Curr Top Microbiol Immunol 1996, 213 (Pt 1):249–269
2. Lin L, Cheung AW, Chan SO: Chiasmatic neurons in the ventral diencephalon of mouse embryos—changes in arrangement and heterogeneity in surface antigen expression. Brain Res Dev Brain Res 2005, 158:1–12
3. Haynes BF, Telen MJ, Hale LP, Denning SM: CD44—a molecule involved in leukocyte adherence and T-cell activation. Immunol Today 1989, 10:423–428
4. Smadja-Joffe F, Legras S, Girard N, Li Y, Delpech B, Bloget F, Morimoto K, Le Bousse-Kerdiles C, Clay D, Jasmin C, Levesque JP: CD44 and hyaluronan binding by human myeloid cells. Leuk Lymphoma 1996, 21:407–420
5. Wang C, Tammi M, Tammi R: Distribution of hyaluronan and its CD44 receptor in the epithelia of human skin appendages. Histochemistry 1992, 98:105–112
6. Heldin P, Karousou E, Bernert B, Porsch H, Nishitsuka K, Skandalis SS: Importance of hyaluronan-CD44 interactions in inflammation and tumorigenesis. Connect Tissue Res 2008, 49:215–218
7. Weber GF, Ashkar S, Cantor H: Interaction between CD44 and osteopontin as a potential basis for metastasis formation. Proc Assoc Am Physicians 1997, 109:1–9
8. Legg JW, Lewis CA, Parsons M, Ng T, Isacke CM: A novel PKC-regulated mechanism controls CD44 ezrin association and directional cell motility. Nat Cell Biol 2002, 4:399–407
9. Matsui T, Maeda M, Doi Y, Yonemura S, Amano M, Kaibuchi K, Tsukita S, Tsukita S: Rho-kinase phosphorylates COOH-terminal threonines of ezrin/radixin/moesin (ERM) proteins and regulates their head-to-tail association. J Cell Biol 1998, 140:647–657
10. Carter WG, Wayner EA: Characterization of the class III collagen receptor, a phosphorylated, transmembrane glycoprotein expressed in nucleated human cells. J Biol Chem 1988, 263:4193–4201
11. Oliferenko S, Paiha K, Harder T, Gerke V, Schwarzler C, Schwarz H, Beug H, Gunthert U, Huber LA: Analysis of CD44-containing lipid rafts: recruitment of annexin II and stabilization by the actin cytoskeleton. J Cell Biol 1999, 146:843–854
12. Helms JB, Zurzolo C: Lipids as targeting signals: lipid rafts and intracellular trafficking. Traffic 2004, 5:247–254
13. Patra SK: Dissecting lipid raft facilitated cell signaling pathways in cancer. Biochim Biophys Acta 2008, 1785:182–206
14. Orian-Rousseau V: CD44, a therapeutic target for metastasising tumours. Eur J Cancer 2010, 46:1271–1277
15. Lajoie P, Nabi IR: Lipid rafts, caveolae, and their endocytosis. Int Rev Cell Mol Biol 2010, 282:135–163
16. Prag S, Parsons M, Keppler MD, Ameer-Beg SM, Barber P, Hunt J, Beavil AJ, Calvert R, Arpin M, Vojnovic B, Ng T: Activated ezrin promotes cell migration through recruitment of the GEF Dbl to lipid rafts and preferential downstream activation of Cdc42. Mol Biol Cell 2007, 18:2935–2948
17. Hirao M, Sato N, Kondo T, Yonemura S, Monden M, Sasaki T, Takai Y, Tsukita S, Tsukita S: Regulation mechanism of ERM (ezrin/radixin/moesin) protein/plasma membrane association: possible involvement of phosphatidylinositol turnover and Rho-dependent signaling pathway. J Cell Biol 1996, 135:37–51
18. Barret C, Roy C, Montcourrier P, Mangeat P, Niggli V: Mutagenesis of the phosphatidylinositol 4,5-bisphosphate (PIP(2)) binding site in the NH(2)-terminal domain of ezrin correlates with its altered cellular distribution. J Cell Biol 2000, 151:1067–1080
19. Johnson CM, Rodgers W: Spatial segregation of phosphatidylinositol 4,5-bisphosphate (PIP(2)) signaling in immune cell functions. Immunol Endocr Metab Agents Med Chem 2008, 8:349–357
20. Kojic LD, Joshi B, Lajoie P, Le PU, Cox ME, Turbin DA, Wiseman SM, Nabi IR: Raft-dependent endocytosis of autocrine motility factor is phosphatidylinositol 3-kinase-dependent in breast carcinoma cells. J Biol Chem 2007, 282:29305–29313
21. Ortiz-Ferron G, Yerbes R, Eramo A, Lopez-Perez AI, De Maria R, Lopez-Rivas A: Roscovitine sensitizes breast cancer cells to TRAIL-induced apoptosis through a pleiotropic mechanism. Cell Res 2008, 18:664–676
22. Simons K, Toomre D: Lipid rafts and signal transduction. Nat Rev Mol Cell Biol 2000, 1:31–39
23. Awasthi V, Mandal SK, Papanna V, Rao LV, Pendurthi UR: Modulation of tissue factor-factor VIIa signaling by lipid rafts and caveolae. Arterioscler Thromb Vasc Biol 2007, 27:1447–1455
24. Bowie RV, Donatello S, Lyes C, Owens MB, Babina IS, Hudson L, Walsh SV, O'Donoghue DP, Amu S, Barry SP, Fallon PG, Hopkins AM: Lipid rafts are disrupted in mildly-inflamed intestinal microenvironments without overt disruption of the epithelial barrier. Am J Physiol Gastrointest Liver Physiol 2012, 302:G781–G793
25. Nusrat A, Parkos CA, Verkade P, Foley CS, Liang TW, Innis-Whitehouse W, Eastburn KK, Madara JL: Tight junctions are membrane microdomains. J Cell Sci 2000, 113 (Pt 10):1771–1781
26. Kyoda KM, Morohashi M, Onami S, Kitano H: A gene network inference method from continuous-value gene expression data of wild-type and mutants. Genome Inform Ser Workshop Genome Inform 2000, 11:196–204
27. Tsukita S, Oishi K, Sato N, Sagara J, Kawai A, Tsukita S: ERM family members as molecular linkers between the cell surface glycoprotein CD44 and actin-based cytoskeletons. J Cell Biol 1994, 126:391–401
28. Farooqui R, Fenteany G: Multiple rows of cells behind an epithelial wound edge extend cryptic lamellipodia to collectively drive cell-sheet movement. J Cell Sci 2005, 118:51–63
29. Yin J, Xu K, Zhang J, Kumar A, Yu FS: Wound-induced ATP release and EGF receptor activation in epithelial cells. J Cell Sci 2007, 120:815–825
30. Chen Y, Wang D, Guo Z, Zhao J, Wu B, Deng H, Zhou T, Xiang H, Gao F, Yu X, Liao J, Ward T, Xia P, Emenari C, Ding X, Thompson W, Ma K, Zhu J, Aikhionbare F, Dou K, Cheng SY, Yao X: Rho kinase phosphorylation promotes ezrin-mediated metastasis in hepatocellular carcinoma. Cancer Res 2011, 71:1721–1729
31. Milhiet PE, Giocondi MC, Baghdadi O, Ronzon F, Roux B, Le Grimellec C: Spontaneous insertion and partitioning of alkaline phosphatase into model lipid rafts. EMBO Rep 2002, 3:485–490
32. Thankamony SP, Knudson W: Acylation of CD44 and its association with lipid rafts are required for receptor and hyaluronan endocytosis. J Biol Chem 2006, 281:34601–34609
33. Bourguignon LY, Zhu H, Shao L, Chen YW: CD44 interaction with tiam1 promotes Rac1 signaling and hyaluronic acid-mediated breast tumor cell migration. J Biol Chem 2000, 275:1829–1838
34. Bourguignon LY, Zhu H, Zhou B, Diedrich F, Singleton PA, Hung MC: Hyaluronan promotes CD44v3-Vav2 interaction with Grb2-p185(HER2) and induces Rac1 and Ras signaling during ovarian tumor cell migration and growth. J Biol Chem 2001, 276:48679–48692
35. Knudson W, Chow G, Knudson CB: CD44-mediated uptake and degradation of hyaluronan. Matrix Biol 2002, 21:15–23
36. Iida N, Bourguignon LY: New CD44 splice variants associated with human breast cancers. J Cell Physiol 1995, 162:127–133
37. Ilangumaran S, Hoessli DC: Effects of cholesterol depletion by cyclodextrin on the sphingolipid microdomains of the plasma membrane. Biochem J 1998, 335 (Pt 2):433–440
38. Afify A, McNiel MA, Braggin J, Bailey H, Paulino AF: Expression of CD44s, CD44v6, and hyaluronan across the spectrum of normal-hyperplasia-carcinoma in breast. Appl Immunohistochem Mol Morphol 2008, 16:121–127
39. Hill A, McFarlane S, Mulligan K, Gillespie H, Draffin JE, Trimble A, Ouhtit A, Johnston PG, Harkin DP, McCormick D, Waugh DJ: Cortactin underpins CD44-promoted invasion and adhesion of breast cancer cells to bone marrow endothelial cells. Oncogene 2006, 25:6079–6091
40. Jensen PV, Larsson LI: Actin microdomains on endothelial cells: association with CD44, ERM proteins, and signaling molecules during quiescence and wound healing. Histochem Cell Biol 2004, 121:361–369
41. Fenteany G, Janmey PA, Stossel TP: Signaling pathways and cell mechanics involved in wound closure by epithelial cell sheets. Curr Biol 2000, 10:831–838
42. Ridley AJ, Schwartz MA, Burridge K, Firtel RA, Ginsberg MH, Borisy G, Parsons JT, Horwitz AR: Cell migration: integrating signals from front to back. Science 2003, 302:1704–1709
43. Dvorak HF: Tumors: wounds that do not heal. Similarities between tumor stroma generation and wound healing. N Engl J Med 1986, 315:1650–1659

44. Yonemura S, Hirao M, Doi Y, Takahashi N, Kondo T, Tsukita S, Tsukita S: Ezrin/radixin/moesin (ERM) proteins bind to a positively charged amino acid cluster in the juxta-membrane cytoplasmic domain of CD44, CD43, and ICAM-2. J Cell Biol 1998, 140:885–895
45. Jayaraman B, Nicholson LK: Thermodynamic dissection of the Ezrin FERM/CERMAD interface. Biochemistry 2007, 46:12174–12189
46. Fievet BT, Gautreau A, Roy C, Del Maestro L, Mangeat P, Louvard D, Arpin M: Phosphoinositide binding and phosphorylation act sequentially in the activation mechanism of ezrin. J Cell Biol 2004, 164:653–659
47. Yamaguchi H, Yoshida S, Muroi E, Kawamura M, Kouchi Z, Nakamura Y, Sakai R, Fukami K: Phosphatidylinositol 4,5-bisphosphate and PIP5-kinase Ialpha are required for invadopodia formation in human breast cancer cells. Cancer Sci 2010, 101:1632–1638
48. Platet N, Prevostel C, Derocq D, Joubert D, Rochefort H, Garcia M: Breast cancer cell invasiveness: correlation with protein kinase C activity and differential regulation by phorbol ester in estrogen receptor-positive and -negative cells. Int J Cancer 1998, 75:750–756
49. Ng T, Parsons M, Hughes WE, Monypenny J, Zicha D, Gautreau A, Arpin M, Gschmeissner S, Verveer PJ, Bastiaens PI, Parker PJ: Ezrin is a downstream effector of trafficking PKC-integrin complexes involved in the control of cell motility. EMBO J 2001, 20:2723–2741
50. Bretscher A: Rapid phosphorylation and reorganization of ezrin and spectrin accompany morphological changes induced in A-431 cells by epidermal growth factor. J Cell Biol 1989, 108:921–930
51. Nakamura N, Oshiro N, Fukata Y, Amano M, Fukata M, Kuroda S, Matsuura Y, Leung T, Lim L, Kaibuchi K: Phosphorylation of ERM proteins at filopodia induced by Cdc42. Genes Cells 2000, 5:571–581
52. Liu Y, Sun R, Wan W, Wang J, Oppenheim JJ, Chen L, Zhang N: The involvement of lipid rafts in epidermal growth factor-induced chemotaxis of breast cancer cells. Mol Membr Biol 2007, 24:91–101
53. Knudson W: The role of CD44 as a cell surface hyaluronan receptor during tumor invasion of connective tissue. Front Biosci 1998, 3:d604–615
54. Howes MT, Kirkham M, Riches J, Cortese K, Walser PJ, Simpson F, Hill MM, Jones A, Lundmark R, Lindsay MR, Hernandez-Deviez DJ, Hadzic G, McCluskey A, Bashir R, Liu L, Pilch P, McMahon H, Robinson PJ, Hancock JF, Mayor S, Parton RG: Clathrin-independent carriers form a high capacity endocytic sorting system at the leading edge of migrating cells. J Cell Biol 2010, 190:675–691
55. Goswami R, Ahmed M, Kilkus J, Han T, Dawson SA, Dawson G: Differential regulation of ceramide in lipid-rich microdomains (rafts): antagonistic role of palmitoyl:protein thioesterase and neutral sphingomyelinase 2. J Neurosci Res 2005, 81:208–217
56. Salaun C, Greaves J, Chamberlain LH: The intracellular dynamic of protein palmitoylation. J Cell Biol 191:1229–1238
57. Babina I, Donatello S, Nabi I, Hopkins A: Lipid rafts as master regulators of breast cancer cell function. Breast Cancer—Carcinogenesis, Cell Growth and Signalling Pathways. Edited by Gunduz M, Gunduz E, InTech, 2011. *http://dx.doi.org/10.5772/21324*. Published online November 30, 2011
58. Joshi B, Strugnell SS, Goetz JG, Kojic LD, Cox ME, Griffith OL, Chan SK, Jones SJ, Leung SP, Masoudi H, Leung S, Wiseman SM, Nabi IR: Phosphorylated caveolin-1 regulates Rho/ROCK-dependent focal adhesion dynamics and tumor cell migration and invasion. Cancer Res 2008, 68:8210–8220
59. Galbiati F, Volonte D, Engelman JA, Watanabe G, Burk R, Pestell RG, Lisanti MP: Targeted downregulation of caveolin-1 is sufficient to drive cell transformation and hyperactivate the p42/44 MAP kinase cascade. EMBO J 1998, 17:6633–6648
60. Vassilieva EV, Ivanov AI, Nusrat A: Flotillin-1 stabilizes caveolin-1 in intestinal epithelial cells. Biochem Biophys Res Commun 2009, 379:460–465

19

Lipid Rafts as Master Regulators of Breast Cancer Cell Function

Irina S. Babina[1], Simona Donatello[1], Ivan R. Nabi[2] and Ann M. Hopkins[1]
[1]*Royal College of Surgeons in Ireland, Beaumont Hospital, Dublin*
[2]*University of British Columbia, Vancouver*
[1]*Ireland*
[2]*Canada*

1. Introduction

Cancer is a leading cause of death in developed countries, and is on the rise in developing countries due in part to a lack of prophylactic screening and non-universal access to medical care (Jemal et al., 2011). Breast cancer is initiated when breast epithelial cells escape growth arrest and form a proliferating tumour mass. Numerous cellular mechanisms are dysregulated in breast tumour cells, including modified cell fate, altered protein signalling and trafficking, and enhanced cell migratory potential. Although these events are complex and subject to regulation by multiple elements, recent evidence has suggested that specialised cell membrane domains termed lipid rafts are actively involved in each of these processes (Cary & Cooper, 2000; Nabi & Le, 2003; Simons & Toomre, 2000). This chapter will therefore focus on the contribution of lipid rafts to breast cancer initiation and progression under these headings.

Lipid rafts are sub-domains of the cell membrane enriched in cholesterol and glycosphingolipids (Le Moyec et al., 1992; Nohara et al., 1998). These microdomains cluster together proteins involved in the regulation of crucial cellular processes; many of which are altered in cancer cells (Pike, 2003; de Laurentiis et al., 2007). Furthermore, lipid rafts are readily modified by diet and nutrition (Schley et al., 2007; Yaqoob, 2009), and studies have shown that fatty acid supplementation sensitises human mammary tumour cells to the cytotoxic effects of anti-cancer agents *in vitro* and *in vivo* (Germain et al., 1998; Menendez et al., 2005; Colas et al., 2006). This chapter will focus on the potential regulatory functions of lipid rafts as a novel approach towards understanding mechanisms of cancer initiation, progression and cell migration, a key event preceding metastatic progression. Finally it will discuss the potential of lipid rafts as novel therapeutic targets in breast cancer.

2. What are lipid rafts?

The discovery of glycosphingolipid clustering in the Golgi apparatus and at the apical surface of polarised epithelial cells led to the hypothesis of non-random membrane compartmentalisation (Simons & Ikonen, 1997; van Meer et al., 2008). These "compartments" were termed lipid rafts.

The structure and function of lipid raft domains depend on their lipid and protein compositions. An example of this is the sub-population of lipid rafts first identified in endothelial cells as flask-shaped membrane invaginations termed caveolae, or "little caves" (Yamada, 1955), which subsequent characterisation revealed to be enriched in proteins from the caveolin family (Rothberg, K G et al., 1992). Caveolins localise in the cytoplasmic leaflet of the cell membrane, and, together with high concentrations of cholesterol, are responsible for the characteristic curvature of caveolar membranes. Lipid rafts and caveolae have different structural protein markers and different proteins associated with them (Table 1), but their lipid composition and the mechanisms of protein targeting to them are very similar.

	Lipids	Protein Markers	Receptor Proteins	Signalling Proteins	References
Non-caveolar lipid rafts	Cholesterol Glycosphingolipid Sphingomyelin Ganglioside GM1 Ganglioside GM3	Flotillin-1, -2	Fas EGFR HER2 IGF-1R CD44 ER	Ras Src Erk2 Shc	(Nohara et al., 1998; de Laurentiis et al., 2007; Patra, 2008)
Caveolae	Cholesterol Glycosphingolipid Sphingomyelin Ganglioside GM1	Caveolin-1, -2 and -3	Fas EGFR HER2 IGF-1R CD44 ER uPAR MMP-1, -2, -9	Ras Src eNOS PI3 kinase Phospho-lipase C	

Table 1. Lipid and protein contents of caveolae and non-caveolar lipid rafts.

2.1 Lipid composition of membrane rafts

The functional properties of raft sub-populations differ according to subtle variations in the types of lipid and quantities of cholesterol they contain. This has permitted differential detergent extraction of various types of lipid rafts. The cholesterol concentration in detergent-resistant membranes (rafts) is 3-5 times higher than that in total membranes (Brown & Rose, 1992; Pike & Casey, 2002), sphingomyelin represents 10-15% of total lipid content, while glycosphingolipids such as cerebrosides and gangliosides account for a further 10-20% (Brown & Rose, 1992; Prinetti et al., 2000). In contrast, glycerophospholipids (including membrane phospholipids) comprise less than 30% of raft lipids despite accounting for approximately 60% of total membrane lipids (Brown & Rose, 1992; Pike & Casey, 2002). Raft-enriched lipids localise preferentially on the outer leaflet of the cell membrane, unlike glycerophospholipids (Pike, 2003). These observations suggest that lipid rafts are bilayer structures and that a variable composition of the cell membrane leaflets may play a role in recruitment of various proteins into lipid rafts. Accordingly, proteins can be targeted to rafts in many dynamically-regulated ways, including attachment of glycosylphosphatidylinositol (GPI) anchors or via lipid modifications such as prenylation and palmitoylation.

2.2 Protein targeting to lipid rafts

Perhaps the best-characterised system of protein association with lipid rafts is via modification with GPI anchors. The GPI anchor is a conserved oligosaccharide core covalently linked to a lipid moiety embedded in the outer leaflet of the cell membrane through acyl or alkyl chains (Levental et al., 2010). These anchors are added to soluble polypeptides in the lumen of the endoplasmic reticulum (ER), promoting membrane raft affiliation (Brown & Rose, 1992). Partitioning of GPI-anchored proteins into lipid rafts may allow sorting to the apical surface of polarised epithelial cells (Fiedler et al., 1993).

Another way in which proteins are targeted to lipid rafts is through addition of prenyl groups. Two types of prenyl groups, C_{15} farnesyl and C_{20} geranylgeranyl, are added on to C-terminal cysteine-rich domains of cytoplasmic proteins by prenyl transferases (Casey & Seabra, 1996). Although prenylated proteins are reportedly enriched in lipid rafts (Prior & Hancock, 2001; Parmryd et al., 2003), it is thought that the prenyl groups interact with raft-affiliated proteins rather than being directly incorporated into rafts (Magee & Seabra, 2003).

Another lipid post-translational modification, palmitoylation, is dynamically regulated by enzymes (Kang et al., 2008; Wan et al., 2007), and controls raft targeting of certain proteins in physiological and pathophysiological settings. Palmitoylation involves the addition of palmitic acid moieties to integral and peripheral membrane proteins through esterification (Bhatnagar & Gordon, 1997). Membrane-associated palmitoyl acyltransferases (PATs) are the most studied palmitoylation enzymes (Planey & Zacharias, 2009), while the palmitoyl thioesterase family removes palmitate groups (Camp & Hofmann, 1995). Close proximity of protein cysteine residues to the membrane is thought to facilitate palmitoylation by PATs, whereas membrane-distal residues are more likely to be prenylated or N-myristoylated (Bijlmakers & Marsh, 2003). PAT activity has been linked to lipid rafts (Dunphy et al., 2001), with palmitoylated proteins found either at the cell membrane or on intracellular membranes (Lobo et al., 2002; Roth et al., 2002). Palmitoylated proteins are naturally more lipophilic, thus their affinity for lipid rafts is increased. Many proteins are targeted to lipid rafts through palmitoylation, including flotillins, Src family kinases, endothelial nitric oxide synthase and various transmembrane receptors (Ghosh et al., 1998; Gong et al., 2003).

2.2.1 Flotillin-1 and -2 mark non-caveolar lipid rafts

Non-caveolar lipid rafts are associated with expression of the reggie family of proteins, flotillin-1 and flotillin-2 (Figure 1a). Palmitoylation of flotillin-1 is essential for localisation to lipid rafts (Morrow et al., 2002), while two hydrophobic stretches also contribute to its raft affiliation (Liu et al., 2005). On the other hand, flotillin-2 is raft-targeted via both myristoylation and palmitoylation. Flotillins were originally thought to be localised in caveolae (Bickel et al., 1997), however later studies excluded this (Neumann-Giesen et al., 2004; Stuermer et al., 2004). Much remains to be determined about the functionality of flotillins in lipid rafts, in particular, the significance of their highly conserved N-terminal domain (Babuke & Tikkanen, 2007; Tavernarakis et al., 1999).

2.2.2 Caveolins – selective markers for caveolar lipid rafts

Along with glycosphingolipids (Tran et al., 1987) and increased cholesterol (Rothberg, K. G. et al., 1990), caveolae are enriched in the family of 21-24 kDa integral membrane proteins known as caveolins. There are three known caveolins: caveolin-1 (Rothberg, J. M. & Artavanis-Tsakonas, 1992), caveolin-2 (Okamoto et al., 1998) and caveolin-3 (Tang et al., 1996).

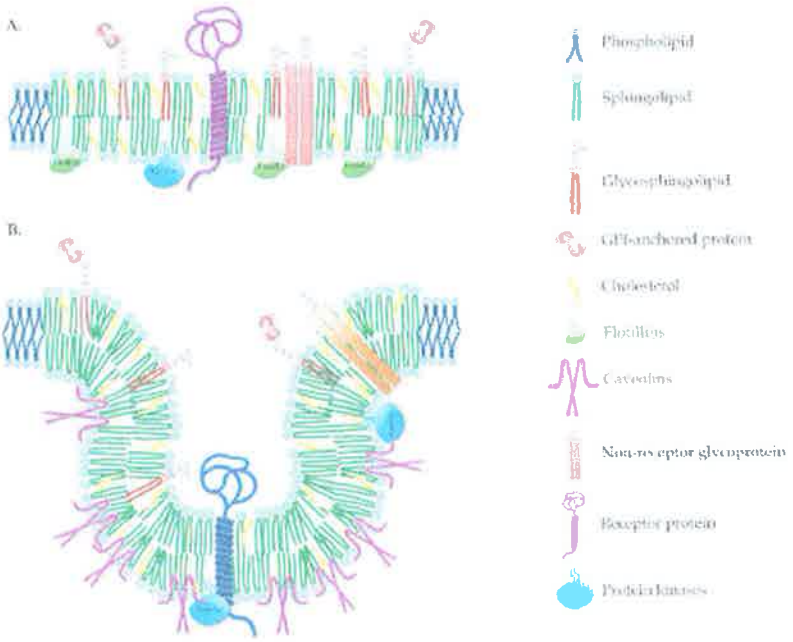

Fig. 1. Lipid and protein components of (A.) non-caveolar lipid rafts and (B.) caveolae.

Caveolins form "omega" structures in the membrane via cytoplasmic localization of both their N- and C-termini (Figure 1b). Aside from palmitoylation, the ability of caveolins to bind sphingolipids (Fra et al., 1995) and cholesterol (Murata et al., 1995) can also explain their high affinity for caveolar lipid rafts. Caveolins -1 and -2 are abundantly expressed in most cell types, including adipocytes, fibroblasts, endothelial and epithelial cells (Fan et al., 1983; Galbiati et al., 2001). Caveolin-3 expression however is restricted to muscle (Rubin et al., 2007). The N-terminal region of caveolin-1 contains a scaffolding domain which aids interactions with various signalling molecules, illustrating the potential importance of caveolin-1 for the signalling functions of caveolar lipid rafts (Everson & Smart, 2006).

2.3 Physiological functions of lipid rafts

Lipid rafts and caveolae are often viewed as organisation centres or signalling platforms, and Table 1 outlines examples of raft-associated proteins which will be discussed in the text. In this chapter, we will concentrate on dynamic raft regulation of a variety of physiological processes, including membrane trafficking, cell polarisation and signal transduction.

2.3.1 Membrane trafficking and cell polarity

Membrane trafficking allows exchange of cellular components between cell sites and cellular organelles. In polarised epithelial cells the trafficking machinery is highly polarised, targeting plasma membrane proteins to separate apical and basolateral domains (Mellman & Nelson, 2008). Following lipid and protein synthesis in the ER, vesicular transfer mediates transport to subsequent or final destinations (Rodriguez-Boulan et al., 2005). The formation and distribution of vesicles requires organised stabilisation of the membrane to allow

deformation and fusion with the target compartment. The most studied mechanism involves coating of the vesicle with clathrin oligomers (Gorelick & Shugrue, 2001), which is thought to be vital in basolateral protein sorting (Deborde et al., 2008; Folsch et al., 2009). Apical trafficking is less understood, but lipid rafts have been proposed to play a decisive role (Schuck & Simons, 2004). Conformational changes in the membrane are proposed to occur via oligomerisation and fusion of many small lipid raft domains (Lipowsky, 1993). Attachment of GPI anchors may also contribute to the polarisation of membrane trafficking (Paladino et al., 2008).

2.3.2 Cell signalling

Lipid raft-mediated trafficking of lipids and proteins facilitates dynamic regulation of cellular signalling cascades. Several frameworks have been suggested to link rafts to signal transduction. The simplest interpretation views lipid rafts as platforms where signalling molecules are co-localised, aiding their structural interactions and influencing downstream signalling (Lingwood et al., 2009). The nature of a signal may be modified by the type of lipid raft the target molecule is localised in and also the primary location of the raft, which in turn enhances the specificity of the signal. Rafts can also control cellular signalling by altering the function of their affiliated proteins. Accumulating evidence suggests that raft-associated proteins behave differently whether localized inside or outside of rafts. Modified signal transduction following lipid raft/caveolar disruption has been reported in the case of several signalling cascades involving Erk (Furuchi & Anderson, 1998), EGFR (Ringerike et al., 2002; Schley et al., 2007), insulin receptor (Parpal et al., 2001), and PDGF receptor (McGuire et al., 1993).

Finally, some lipid rafts are actively involved in endocytosis (reviewed in Lajoie & Nabi, 2010), which promotes internalisation of receptors and signalling molecules. This process may be facilitated by clustering of caveolin or receptor proteins (Paladino et al., 2004). Internalisation of ligands or receptors modifies downstream signal transduction, and is associated with the termination of extracellular ligand-driven signalling events via transient receptor desensitisation.

The ability of lipid rafts to traffic proteins, control cell polarity and alter cell signalling underlies their emerging roles as crucial regulators of cellular processes including cell fate, growth, adhesion and migration. Since all are dysregulated in cancer, it is reasonable to suggest that lipid rafts may modify tumorigenic processes. This will next be addressed.

3. Lipid raft regulation of key processes in breast cancer cells

Alterations in cell fate, growth, adhesion and migration play central roles in the initiation and progression of breast cancer. We next outline how lipid rafts may regulate such processes during the initial stages of cancer development, during tumour growth and during the possible progression to a migratory and metastatic phenotype.

3.1 Apoptosis and regulation of cell fate

Defects in apoptosis allow tumour cells to escape growth-inhibitory signals and to progress through the cell cycle. Two major apoptotic pathways have been described, extrinsic (mediated by activation of death receptors) and intrinsic (mediated by mitochondria). Both may require lipid rafts for successful signal transduction (Li et al., 1998).

Death receptors are located at the cell membrane, and once activated, trigger apoptotic signal transduction. Perhaps the best-characterised death receptor is Fas (CD95 or APO-1), which has been implicated in the apoptotic events that drive physiological remodelling of the mammary gland after breast feeding (Song et al., 2000). Down-regulation of Fas has also been associated with poor prognosis in breast cancer patients (Reimer et al., 2000), and inhibition of Fas activity has been linked to drug resistance (Landowski et al., 1997). Activation of Fas results in receptor aggregation, and recruitment of procaspase-8 to form the death-inducing signalling complex DISC (Peter & Krammer, 2003) (Figure 3a). Recent studies have shown that Fas is translocated into lipid rafts, where apoptotic receptor aggregation takes place (Gajate et al., 2004; Gajate & Mollinedo, 2005). This is the mode of action of a pro-apoptotic drug, edelfosine; with cholesterol depletion being shown to abolish apoptosis (Gajate & Mollinedo, 2001; Gajate & Mollinedo, 2007; Gajate et al., 2009).

Whether rafts could be used as targets to re-trigger Fas-dependent apoptosis in tumour cells is an intriguing concept. A recent study demonstrated that nitric oxide (NO) can reverse apoptotic resistance via increasing Fas S-nitrosylation (Leon et al., 2011). In breast cancer cells that overexpressed wild-type Fas, NO incubation resulted in enhanced recruitment of the receptor into lipid rafts, which in turn sensitized cancer cells to the death-inducing Fas ligand. In fact, DISC formation is impaired in cells expressing nitrosylation (Leon et al., 2011) and palmitoylation (Chakrabandhu et al., 2007) mutants of Fas.

Acquired resistance of breast cancer cells to Fas-induced apoptosis may alternatively result from activation of survival pathways, such as the PI3 kinase pathway. Its engagement leads to activation of the serine-threonine kinase Akt, which negatively regulates apoptosis by inactivating pro-apoptotic proteins such as Bad and caspase-9 (Datta et al., 1999). Lipid raft localisation of Akt has been implicated in facilitating its activation (Hill et al., 2002; Elhyany et al., 2004). Raft disruption has been reported to reduce the sensitivity of normal-like MCF-10a cells to apoptosis, suggesting that tumour cells rely on cholesterol for growth and malignant signalling (Li et al., 2006). Interestingly the cholesterol analogue ginsenoside Rh2 has been shown to reduce lipid raft abundance and increase internalisation, decreasing Akt-dependent survival signalling (Park et al., 2010). It has also been demonstrated that cholesterol depletion induces anoikis-like apoptosis via down-regulation of focal adhesion kinase and hypoxia inducible factor-1 (Lee et al., 2009; Park et al., 2009).

Another apoptotic death receptor is TNF-related apoptosis-inducing ligand (TRAIL) receptor 1 and 2, referred to as DR4 and DR5 respectively (Yang et al., 2010). Studies have demonstrated that translocation of these receptors into lipid rafts after TRAIL engagement is involved in apoptotic signal transduction (Merino et al., 2006; Dumitru et al., 2007; Song et al., 2007). In metastatic MDA-MB-231 cells, for instance, DR4 palmitoylation (Rossin et al., 2009) is crucial not only for its localisation into lipid rafts but also for receptor aggregation, both of which are essential for TRAIL-induced cell death (Merino et al., 2006). Therefore while much remains to be understood about the role of rafts in regulating apoptosis in breast cancer cells, it may offer a novel therapeutic target (see Section 4).

3.2 Growth and metabolism

In conjunction with altered apoptosis, abnormal signalling by growth factor receptors can facilitate breast tumour proliferation and growth. Lipid rafts modulate the signalling functions of several growth factor receptors, including the ErbB (HER) family of receptors.

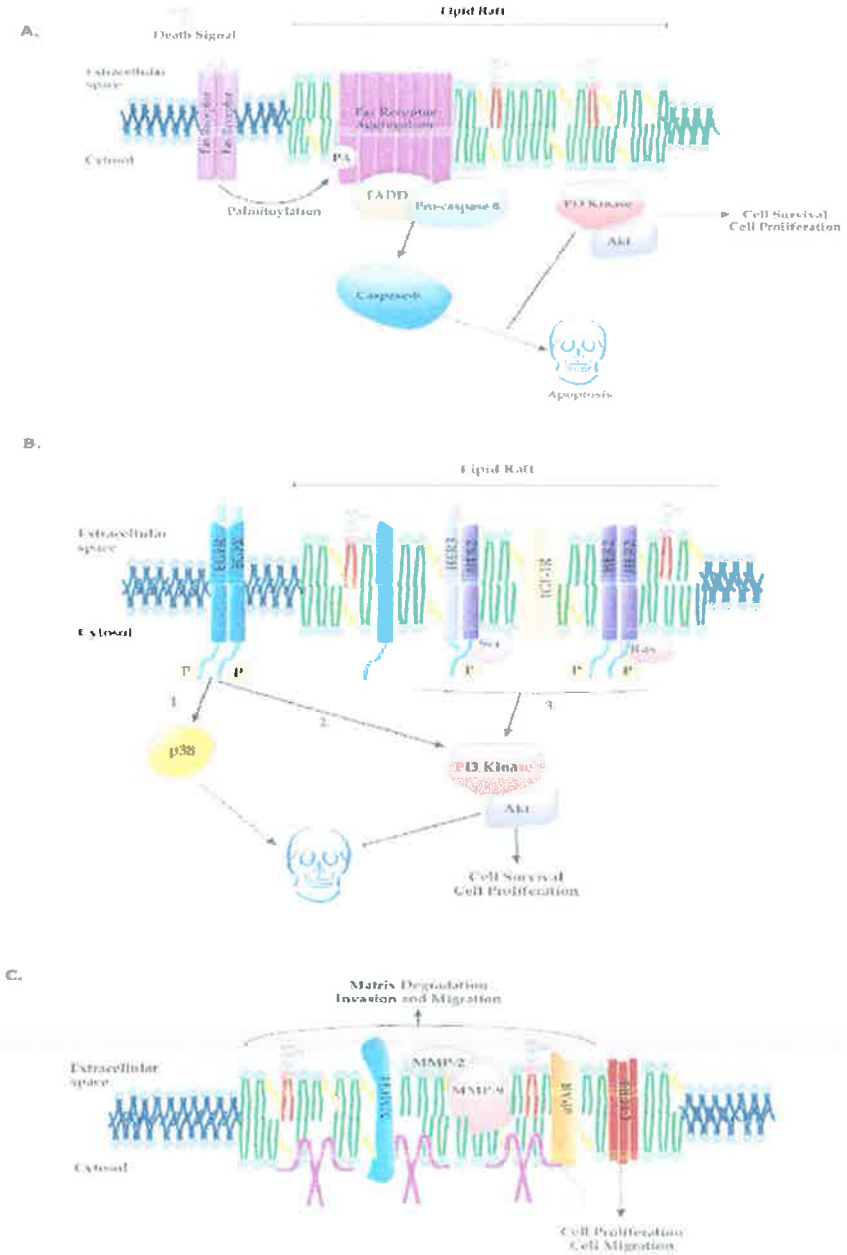

Fig. 2. Lipid raft regulation of breast cancer cell processes. (A.) Apoptotic signals are transduced via lipid rafts. (B.) EGFR signalling may induce apoptosis (1.) or proliferation (2.) outside of lipid rafts. Predominant oncogenic signalling is transduced through rafts (3.). (C.) Rafts cluster many degradation enzymes and proteins crucial for cell migration.

ErbB receptors are often mutated, amplified and/or overexpressed in breast cancer (Troyer & Lee, 2001). In particular, epidermal growth factor receptor, EGFR, and HER2 homo- and heterodimerisations have been described to promote oncogenic proliferation (Barros et al., 2010). Both of these receptors are associated with lipid rafts, and raft modifications can alter their signal transduction (Chen & Resh, 2002; Freeman et al., 2007).

EGFR functionality in particular is largely dependent upon its affiliation with rafts. Upon ligand binding, EGFR translocates out of caveolin-positive raft domains to stimulate downstream signalling (Mineo et al., 1999) and caveolin-1 raft domains negatively regulate EGFR activation (Lajoie et al., 2007). Accordingly, raft disruption via cholesterol depletion reportedly results in EGFR activation (Pike & Casey, 2002; Westover et al., 2003). Although EGFR phosphorylation is associated with oncogenic proliferation, sustained activation of EGFR outside of lipid rafts in fact correlates with increased p38 activation, which is pro-apoptotic. Potential modulations of EGFR activation status by dietary lipids will be discussed in Section 4.

Some studies have examined the activation of downstream targets of EGFR signalling, such as the small GTPase Ras (Rogers et al., 2010), after exposure to fatty acids. Ras associates with lipid rafts via palmitoylation (Calder & Yaqoob, 2007), and is involved in cell survival, growth and proliferation (Downward, 2006). Furthermore, enhanced anti-proliferative effects were seen upon co-treatment with an EGFR inhibitor and DHA (Rogers et al., 2010).

Another member of the ErbB family, HER2, is the favoured dimerisation partner of other ErbB proteins for receptor activation (Tzahar et al., 1996; Park, B. W. et al., 2000). Oncogenic HER2 dimerisation in breast cancer cells takes place in lipid rafts (Nagy et al., 2002), and forced exclusion of HER2 from rafts (via crosslinking of the raft-associated ganglioside GM1) has been shown to decrease HER2 dimerisation and tyrosine phosphorylation (Nagy et al., 2002). Another possible avenue of HER2 signalling regulation by lipid rafts relates to protein trafficking. HER2 is rapidly recycled back to the cell membrane if endocytosed (Worthylake et al., 1999), which maintains its overexpression at the cell membrane of breast cancer cells. Modulation of lipid metabolism may control HER2 overexpression by increasing its endocytosis and preventing redistribution back to the cell membrane (Paris et al., 2010). For instance, phospholipase C (PLC) has been shown to co-localise with HER2 in lipid raft domains of HER2-overexpressing breast cancer cell lines, and PLC antagonism enhances HER2 internalisation and delays its recycling to the cell membrane, reducing breast cancer cell proliferation (Paris et al., 2010). This implies that lipid rafts play a key role in transduction of this oncogenic signal.

Another protein known to localise in lipid rafts with HER2, in addition to EGFR, is the estrogen receptor (ER) (Marquez et al., 2006). Estrogen signalling is linked to lipid rafts, where ER co-localises with ErbB receptors to modulate growth events (Marquez et al., 2006). Both these receptors may be activated by membrane-bound ER (Razandi et al., 2003), resulting in MAP kinase-dependent ER phosphorylation (Pietras, 2003). As these receptors are reportedly lipid raft-affiliated, interference of this union with lipid rafts may prove to be useful in targeting endocrine resistance in breast cancer.

Insulin-like growth factor-1 receptor (IGF-1R) is another receptor tyrosine kinase whose activation leads to proliferation and differentiation via MAP kinase and PI3 kinase/Akt pathways (Adams et al., 2000). IGF-1R activity has been linked to lipid raft affiliation, particularly caveolae. Stable expression of caveolin-1 in MCF7 breast cancer cells, while decreasing cell attachment (Fiucci et al., 2002), results in enhanced matrix-independent

cell survival via upregulation of IGF-1R and subsequent activation of p53 and p21 (Ravid et al., 2005). Caveolin-1 further drives IGF-1R-induced recruitment of β_1-integrin into lipid rafts (Salani et al., 2009), which could in turn regulate the influence of β_1-integrin on cell fate (Li et al., 2005). In fact segregation of IGF-1R in and out of rafts has been shown to dynamically regulate overall signalling potency of the protein (Remacle-Bonnet et al., 2005), which is emerging as a promising pharmaceutical target in breast cancer (Weroha & Haluska, 2008).

Sigma receptors are a novel family of receptors whose physiological and pathophysiological roles are only beginning to emerge. They inhibit proliferation, induce apoptosis and can decrease cell adhesion in mammary carcinoma cell lines (reviewed in Aydar et al., 2004). Sigma receptors were proposed to have the ability to remodel lipid rafts by modulating raft cholesterol levels via cholesterol-binding motifs (Gebreselassie & Bowen, 2004; Takebayashi et al., 2004). Accordingly, raft cholesterol levels are reduced following sigma-1 gene knockdown (Palmer et al., 2007). Sigma-1 receptors also form a complex with β_1-integrin in MDA-MB-231 cells, and their translocation outside rafts decreases breast cancer cell growth and adhesion (Palmer et al., 2007). Because cancer cells have elevated levels of lipid rafts and cholesterol (Li et al., 2006), and because many growth signalling molecules depend on rafts to exert their functions, dietary fat modifications could affect signal transduction in breast cancer cells (as will be further addressed in Section 4).

3.3 Cell migration and metastasis

Cancer progression does not depend solely on increased growth and reduced apoptosis, but also on the ability of tumours to seek out new niches to support their continued survival. Accordingly, cells often activate pathways that reduce adhesion and promote cell migration, increasing the likelihood of the metastatic spread of breast cancer.

Kinases play a significant role in regulating cell adhesion and migration. The Src family of kinases (SFK) integrates signal transduction from many receptor tyrosine kinases, including EGFR, IGF-1R and HER2 (Belsches-Jablonski et al., 2001; Parsons & Parsons, 2004) to multiple downstream targets including PI3-kinase, Ras and focal adhesion kinase (Parsons & Parsons, 2004). SFK activation has been linked to lipid rafts in breast cancer cells (Hitosugi et al., 2007), fuelling speculation that selective targeting of raft-affiliated SFK may offer a more potent therapy than conventional SFK inhibitors such as dasatinib. Src has also been shown to phosphorylate the raft marker flotillin-2 in an EGF-dependent manner, resulting in Src translocation into endosomes and the enhancement of cell spreading (Neumann-Giesen et al., 2007). Conversely, the finding that flotillin-2 knockdown reduces cell spreading further highlights the potential regulatory influence of lipid rafts on cell adhesion and actin dynamics (Neumann-Giesen et al., 2007).

Lipid rafts and caveolin-1 have also been shown to be crucial for the formation of invadopodia, membrane protrusions that penetrate the surrounding matrix through a combination of matrix remodelling and physical force (Buccione et al., 2009). Invadopodia cluster together proteins involved in actin cytoskeleton organisation, signalling, cell-ECM adhesion and membrane remodelling (Gimona et al., 2008). Lipid rafts have been reported to be concentrated at the leading edge of invadopodia in a panel of breast cancer cell lines, and disruption of lipid rafts may suppress invadopodia formation (Yamaguchi et al., 2009). Invasive potential has also been linked with the raft-affiliated proteins caveolin-1 and membrane type 1 matrix metalloproteinase (MMP14) in both breast (Annabi et al., 2001) and

prostate (Wang et al., 2009) cancer cells. In fact caveolin-1 and MMP14 have been shown to co-associate (Labrecque et al., 2004) and to be co-trafficked in invasive breast cancer cell lines (Yamaguchi et al., 2009). Accordingly, a reduction in matrix degradation activity of MMP14 has been reported in MDA-MB-231 cells following disruption of lipid rafts by cholesterol depletion or after knockdown of caveolin-1 in MMP14-overexpressiong MDA-MB-231 cells (Yamaguchi et al., 2009). Together these results highlight that lipid rafts and caveolin-1 are important for invadopodia function in breast cancer cells.

MMP14 is not the only lipid raft-affiliated proteinase implicated in breast cancer progression. Aberrant expression of MMP2 and MMP9, which localize in rafts during cancer cell migration (Patra, 2008), have been associated with high-grade breast cancer (Mira et al., 2004). Downregulation of MMP2 and MMP9 has been shown to decrease tumour cell invasion (Patra, 2008). Similarly, the serine protease urokinase-type plasminogen activator (uPA) and its receptor (uPAR), which have been linked to breast cancer progression and metastasis (Patra, 2008; Sahores et al., 2008), localise to lipid rafts during cancer cell migration (Sahores et al., 2008). A recent study investigating the importance of lipid rafts in regulating uPAR and MMP9 functionality in breast cancer has demonstrated that cholesterol depletion reduces co-localisation of uPAR and MMP9 with lipid rafts and significantly decreases their total protein and mRNA levels (Raghu et al., 2010). Lipid raft disruption in breast cancer cells resulted in reduced amounts of active Src, FAK, Akt and ERK and increased uPAR co-localisation with lysosomal markers, which was reversed after cholesterol repletion (Raghu et al., 2010). This is in agreement with previous observations of differences in MMP9-driven cell migration according to its sub-cellular localisation inside or outside rafts (Mira et al., 2004).

Although controversial, another approach to understanding breast cancer metastasis comes from the observation that disseminated tumour cells have progenitor-like properties, termed "cancer stem cells" (Acconcia et al., 2004). Low expression of CD24, a ligand for P-selectin on cancer and myeloid cells (Aigner et al., 1997), has been proposed as a marker for cancer stem cells, and breast cancer patients with aggressive triple-negative disease reportedly have higher percentages of cancer stem-like cells (May et al., 2011; Reuben et al., 2011). CD24 appears to govern the localization and function of the chemokine receptor CXCR4, which regulates proliferation in primary and metastatic breast cancer (Smith et al., 2004). CXCR4 must localise in lipid rafts for effective signalling (Manes et al., 2001; Wysoczynski et al., 2005), and CD24 reportedly reduces cellular responsiveness to CXCR4 signalling in a metastatic breast cancer cell line by excluding the latter from lipid rafts (Schabath et al., 2006). Thus low CD24 levels in putative cancer stem cells would have a positive effect on CXCR4-driven proliferative signalling, via enhanced raft affiliation of CXCR4. Accordingly, high expression of CD24 has been shown to reduce tumour growth and spread in mice (Schabath et al., 2006). Therefore CXCR4 metastatic potential may be modulated by altering its affiliation with rafts independently of its expression levels.

Another proposed marker for breast cancer stem cells is CD44 (Blick et al., 2010; May et al., 2011), a multi-functional lipid raft-affiliated transmembrane glycoprotein expressed in a variety of tissues (Murai et al., 2011). CD44 is the major receptor for the extracellular matrix component hyaluronan (HA) (Herrera-Gayol & Jothy, 1999); but it can also act as a co-receptor for growth factors (Bourguignon et al., 1997; Orian-Rousseau et al., 2002) and organise the cellular actin cytoskeleton through cytoplasmic linker proteins (Ponta et al., 2003). CD44 abnormalities have been associated with aggressive histological features of

breast cancer (Joensuu et al., 1993; Diaz et al., 2005), and the association of CD44 with MMP9 in breast tumour cells promotes tumour cell migration and invasion (Bourguignon et al., 1998). It is possible that this matrix-degrading association takes place in lipid rafts, where both CD44 and MMP9 localize. Interactions between CD44 and HA also stimulate a variety of events leading to tumour progression, including Rho kinase activation, Ras signalling and others (reviewed in Bourguignon, 2008). Although the exact mechanisms of these events have yet to be clarified, one proposed method involves CD44 interaction with ankyrin within lipid rafts (Singleton & Bourguignon, 2004). Another matrix glucosaminoglycan, osteopontin, can also activate CD44 to promote cell survival and increased endothelial adhesion by recruiting Src and integrins into lipid rafts (Lee et al., 2008).

The influence of CD44 on cancer progression also extends to other growth factor signalling pathways, since it has previously been demonstrated that the growth factor receptor c-Met cannot be activated by its ligand alone, but also requires CD44 co-expression (van der Voort et al., 1999). c-Met, which has been shown to localise in lipid rafts and whose signalling is sensitive to cholesterol depletion (Coleman et al., 2009), is frequently dysregulated in metastatic breast cancer (Gastaldi et al., 2010; Elnagar et al., 2011). It can thus be hypothesised that lipid rafts are required for successful transduction of growth factor-mediated oncogenic signals through formation of functional CD44 complexes.

Taken altogether, several key molecules frequently implicated in breast cancer initiation, growth and migration are regulated by lipid rafts via sequestration, endocytosis or termination of protein interactions. Considering the ongoing need to develop drugs which selectively attack cancer cells while leaving normal cells unaltered, the imbalance in lipid raft composition between tumour and normal cells may suggest rafts as attractive and novel pharmacological targets in the battle against breast cancer.

4. Lipid rafts as novel therapeutic targets in breast cancer

This section will focus on current cancer treatments targeting lipid rafts, the potential importance of lipid raft modulation to overcome mechanisms of drug resistance, and new mechanisms associated with lipid raft physiology that could be targeted by novel drugs. Finally it will discuss the importance of the diet in influencing lipid raft physiology as a potential mechanism to prevent or reduce cancer dissemination.

4.1 Current drug treatments targeting lipid rafts

There is growing interest in the possibility of targeting lipid rafts for cancer treatments due to their role in the regulation of many steps of tumour transformation and progression, such as the apoptotic pathways initiated by FasL and TRAIL. Current treatments targeting lipid rafts are mainly focused on activating these apoptotic pathways in cancer cells. However many classes of drugs routinely used in breast cancer chemotherapy have been shown to exert some of their effects by modulating lipid rafts.

One key example is cisplatin, whose mechanism of action is still incompletely understood, but which has been described to exert some of its actions through modulation of ceramide lipid rafts. In a human colon cancer cell line, cisplatin induced clustering of the Fas receptor in membrane lipid rafts by activating the acid sphingomyelinase (ASMase), which produces ceramide and is responsible for induction of apoptosis. Nystatin, a compound which disrupts lipid rafts, completely reversed this effect (Lacour et al., 2004). It has also been

reported that a combination of cisplatin and an anti-Fas antibody in cells expressing sphingomyelinase induced marked apoptosis of cancer cells (Huang et al., 2010).
Moreover, histone deacetylase inhibitors (HDACi), powerful tumour suppressors for many different solid and hematologic cancers, have also been shown to modulate lipid raft physiology. These compounds act on tumour cells by inducing accumulation of acetylated proteins that can cause growth arrest, apoptosis and ROS-induced cell death (Marks & Xu, 2009). Since normal cells are resistant to these treatments, HDACi have been widely tested in clinical trials alone or in combination with other drugs (Marks & Xu, 2009). Van Oosten and colleagues observed a drastic increase in the expression and localization of TRAIL in lipid rafts after treatment of prostate cancer cells with a HDACi depsipeptide, inducing elevated cell apoptosis (Vanoosten et al., 2005). Similarly, in preclinical mouse breast cancer models the HDACi vorinostat, in combination with administration of monoclonal antibodies against the mouse TRAIL receptor (DR5), induced robust cell apoptosis (Frew et al., 2008).
Likewise, some derivatives of doxorubicin, an anthracycline widely used in breast cancer adjuvant chemotherapy, exercise their actions by activating lipid raft-associated pathways. Aroui and colleagues illustrated that treatment of MDA-MB-231 cells with Dox-CPP, obtained by conjugating doxorubicin to a cell-penetrating peptide, sensitised cells to TRAIL-induced apoptotic pathways by increasing TRAIL clustering and its inclusion in ceramide lipid rafts (Aroui et al., 2009). Lipid raft-mediated activation of TRAIL is also important because it reduces resistance mechanisms associated with doxorubicin resistance.

4.2 Overcoming drug resistance by targeting lipid rafts

One major drawback of current cancer treatment regimens is the development of drug resistance. Two main mechanisms have been described to be involved in this multifactorial process: 1) alterations in tumour cell physiology that cause either insensitivity to drug-induced apoptosis or induction of drug-detoxifying mechanisms; 2) expression of energy-dependent transporters that detect and eject anti-cancer drugs from cells (Wang et al., 2010).
Recent evidence points to the correlation of both mechanisms with lipid raft physiology. Mechanisms of breast cancer resistance to the anti-HER2 therapeutic antibody Herceptin/Trastuzumab may involve compensatory signalling through dimerisation of HER2 with other ErbB family members, cross-talk between HER2 and the IGF-1R pathway, coverage of the antibody binding site by MUC4 overexpression, and constitutive activation of the PI3 kinase/Akt pathways (Nahta & Esteva, 2006). Interestingly, all these events take place in lipid raft compartments and are involved in the activation of alternative oncogenic pathways to overcome the inhibitory effects of cancer treatments. Therefore, treatments altering lipid raft physiology could provide hope in preventing or reducing mechanisms of resistance to specific anti-cancer drugs.
HER2 over-expression in breast cancer cells has also been reported to stimulate fatty acid synthase (FASyn) gene expression (Menendez et al., 2004). FASyn is a major lipogenic enzyme catalyzing the synthesis of long-chain saturated fatty acids, which localize to lipid rafts in epithelial cells. Accordingly, FASyn inhibitors work by altering lipid raft physiology through deregulation of fatty acid synthesis; and have been reported to re-sensitise cells to Trastuzumab, causing growth inhibition and apoptotic cell death. Since these inhibitors also affect EGFR1 localization to lipid rafts, they may also disrupt the cross-talk between HER2 and EGFR which is involved in Trastuzumab resistance (reviewed in Menendez, 2005).
Correspondingly, since ER can localize to lipid rafts through post-translational lipid modifications termed acylations, lipid rafts have been suggested as the possible location of

interactions between ER and growth factor receptors which occur during resistance to endocrine therapy (Acconcia et al., 2004; Weinberg et al., 2005; Arpino et al., 2008). Mutations of ER acylation sites impair the ability of ER to activate transcription and cell proliferation in response to estradiol stimulation (Pietras et al., 2005). It is appealing to speculate that combinations of hormonal therapies and treatments altering ER localization to lipid rafts could prevent cross-talk between ER and EGFR pathways; and may be a future therapeutic strategy to reduce drug resistance arising in hormonal therapy. Furthermore, it has been shown that poor responsiveness of breast cancer cells to treatment with the EGFR inhibitor gefitinib may be due to increased localization of EGFR in lipid raft domains. Treatment of breast cells with lipid raft-disrupting agents (such as lovastatin) induced cellular sensitivity to gefitinib, and abrogated proliferative pathways initiated by Akt phosphorylation (Irwin et al., 2010).

However, along with single drug resistance in breast cancer therapy, the phenomenon of multidrug resistance has also been described (Ogretmen & Hannun, 2001). This occurs when resistance to one drug is accompanied by resistance to drugs whose structures and mechanisms of action may be completely different. Several studies have observed alterations of lipid raft components in multidrug-resistant cells, such as increased caveolin-1 expression, larger numbers of caveolae (Lavie et al., 1998) and elevated membrane cholesterol content (Gayet et al., 2005). Lavie and colleagues suggested that an increased number of caveolae may be more of a cause than an effect of multidrug resistance. In fact, caveolae, being capable of effluxing cholesterol, may be used by cancer cells to efflux lipophilic drugs. Since caveolar efficiency to efflux cholesterol or any cytotoxic drug is very low, they hypothesized that a higher number of caveolae is therefore necessary to compensate for drug cytotoxic effects and efflux them efficiently (Lavie et al., 1998).

Cellular lipid changes are also often accompanied by increased expression of ABC transporters which can localize to lipid rafts (Klappe et al., 2009). One member of this family, BCRP/ABCG2, which was discovered and cloned in breast cancer cells (Doyle et al., 1998), has been recently described to localize to lipid rafts. Interestingly, disruption of lipid rafts using methyl-β-cyclodextrin has been shown to cause a 40% decrease in BCRP activity (Storch et al., 2007); further highlighting the potential value of pharmacological raft targeting as a mechanism of reducing multi-drug resistance.

Overall these examples demonstrate the importance of lipid rafts in clustering oncogenic signalling molecules that are involved in breast cancer resistance to current conventional treatments. It is also evident that treatments aimed at preventing or disrupting the localisation of oncogenic signalling mediators (such as HER2, ER, IGF-1R or ABC transporters) in lipid rafts may prove therapeutically useful in combination with current treatments in order to prevent the development of resistance.

4.3 Novel lipid raft- mediated approaches in breast cancer treatment

Recently, glycomic studies have highlighted an emerging and critical importance of glycans in influencing lipid raft physiology. Therefore potential future cancer treatments may also indirectly target lipid rafts by targeting glycans. For example, in breast cancer cells, gangliosides (such as the ganglioside GM1 or the O-glycosylated protein MUC4) regulate the formation of EGFR growth factor-responsive heterodimer complexes in lipid rafts (Komatsu et al., 2001). Lipid rafts play a fundamental role in providing a microenvironment favouring functional interactions between glycans and HER2 / HER3, which drive tumour

progression (Komatsu et al., 2001; Nagy et al., 2002). Antibodies targeting MUC4 or treatments targeting gangliosides (i.e. ceramide glycosylation inhibitors or ganglioside-targeted vaccines such as NeuGcGM3 and Theratope) may therefore be possible treatments to interfere with ErbB-driven proliferation of breast cancer cells via modulation of lipid raft physiology (Carr et al., 2003; Ibrahim & Murray, 2003; Julien et al., 2009; Mulens et al., 2010). Raft-dependent endocytosis of paclitaxel-conjugated autocrine motility factor is elevated in metastatic breast cancer cells and has been shown to induce tumour regression and promote survival of tumour-bearing mice (Kojic et al., 2008; Kojic et al., 2007). In addition, some new generation treatments have considered the use of nanoparticles to target lipid raft-affiliated proteins involved in tumour progression and invasion. Conjugated nanoparticles present the advantage of selectively targeting cancer cells without affecting the physiology of normal cells. For example, a study in glioma cells using magnetic nanoparticles conjugated to chlorotoxin (which targets MMP2, a protein highly expressed in glioma tumour cells) demonstrated the induction of lipid-raft mediated endocytosis of MMP2 together with Cl^- and K^+ channels (Veiseh et al., 2009), the latter proteins being involved in regulating cell volume during cell invasion. Using this system, a 98% reduction in invasion was observed in nanoparticle-treated cells compared to controls. In the same manner, MMP2 has also been shown to play a role in breast cancer progression and invasion and has been described as a marker for poor prognosis in ER- negative patients (Ma et al., 2009). Therefore, it is conceivable that an approach similar to the one used by Veiseh et al. might be useful as a companion drug strategy for breast cancer chemotherapy.

4.4 Lipid rafts and diet in cancer progression

Cancer cells generally possess higher levels of saturated fatty acids and cholesterol than normal cells (Li et al., 2006). Emerging evidence thus suggests the potential of diet to influence raft composition and the role of rafts in cancer pathophysiology (section 3.2).

Several studies have shown that polyunsaturated fatty acids (PUFAs) may have anti-carcinogenic properties (Sauer et al., 2007). The mechanism by which PUFAs work is still incompletely understood, but two mechanisms have been proposed. The first suggests that PUFAs affect the palmitoylation status of lipid raft proteins (Webb et al., 2000); while the second model suggests that PUFAs, having a low affinity for cholesterol due to their bulky structure, reduce raft cholesterol levels and cause displacement of raft proteins (Stulnig et al., 2001). In fact, it has been described that *in vivo* PUFA supplementation affects lipid raft composition by depleting up to 50% of cholesterol and by altering lipid raft/caveolar protein composition. In comparison to chemical disruption of lipid rafts (e.g. with methyl-β-cyclodextrin and nystatin), PUFA treatment is very selective and depletes only membrane cholesterol without affecting other cellular sources of cholesterol (Ma et al., 2004).

It has also been shown that PUFAs such as EPA and DHA inhibit protein palmitoylation of selected T cell lipid raft proteins (such as Fyn) similarly to the chemical compound 2-bromopalmitate (Webb et al., 2000). Interestingly, in MDA-MB-231 breast cancer cells, PUFAs have been shown to decrease cell proliferation and induce apoptotic cell death probably by decreasing Akt/NFκB signal transduction (Schley et al., 2005). Furthermore, PUFA treatment has been shown to increase EPA and DHA concentrations in lipid rafts, with a corresponding decrease of sphingomyelin, cholesterol and diacylglycerol (Schley et al., 2007). In particular, PUFAs reduce sphingomyelin levels by inducing its hydrolysis to ceramide, which (as discussed) activates pro-apoptotic pathways (Schley et al., 2005).

Section 3 discussed how lipid raft disruption negatively modulates EGFR localization and signalling, and, similarly, PUFAs have been shown to exert pro-apoptotic properties by reducing EGFR localization within lipid rafts, thus inducing a sustained activation of EGFR and p38 phosphorylation in breast cancer cells (Schley et al., 2007). In the same way, (-)-epigallocatechin-3-gallate (EGCG), the active compound contained in green tea, can alter lipid raft domain composition. EGCG has been described to prevent EGF interactions with its receptor, to prevent EGFR dimerisation and to inhibit its localisation within rafts. This would promote pro-apoptotic signalling via p38. Altogether, EGFR translocation alters its activation status and may have anti-cancer effects (Patra et al., 2008). EGCG also exerts further anti-cancer activity by suppressing proliferation and enhancing apoptosis by interfering with lipid raft remodelling (Patra et al., 2008). Indeed, EGCG has been described to block the laminin-1 receptor, a raft-affiliated protein (Tachibana et al., 2004) whose activation is connected with a kinase/phosphatase cascade involved in tumour progression (Patra et al., 2008). Interestingly, EGCG also seems to play a role in modulating multidrug resistance. In fact it has been described that EGCG causes a dose-dependent increase in apoptosis in Trastuzumab- (Eddy et al., 2007), Tamoxifen- and multidrug-resistant breast cancer cells (Farabegoli et al., 2010).

Taken together, we have summarized putative anti-tumour mechanisms involving interference with lipid rafts, and highlighted the importance of rafts as targets for cancer therapy. Development of drugs directed to specific raft components could facilitate widespread use of these treatments; while dietary modification alone could influence tumorigenic behaviour through modulation of lipid raft composition. Overall we suggest that lipid rafts play a key role both in the prevention and treatment of breast cancer, and are confident that further studies in this area will prove highly fruitful in the future.

5. References

Acconcia, F, Ascenzi, P, Fabozzi, G, Visca, P & Marino, M (2004). S-palmitoylation modulates human estrogen receptor-alpha functions. *Biochem Biophys Res Commun*, Vol. 316, No. 3, (2004), pp 878-83

Adams, TE, Epa, VC, Garrett, TP & Ward, CW (2000). Structure and function of the type 1 insulin-like growth factor receptor. *Cell Mol Life Sci*, Vol. 57, No. 7, (2000), pp 1050-93

Aigner, S, Sthoeger, ZM, Fogel, M, Weber, E, Zarn, J et al. (1997). CD24, a mucin-type glycoprotein, is a ligand for P-selectin on human tumor cells. *Blood*, Vol. 89, No. 9, (1997), pp 3385-95

Annabi, B, Lachambre, M, Bousquet-Gagnon, N, Page, M, Gingras, D et al. (2001). Localization of membrane-type 1 matrix metalloproteinase in caveolae membrane domains. *Biochem J*, Vol. 353, No. Pt 3, (2001), pp 547-53

Aroui, S, Brahim, S, Hamelin, J, De Waard, M, Breard, J et al. (2009). Conjugation of doxorubicin to cell penetrating peptides sensitizes human breast MDA-MB 231 cancer cells to endogenous TRAIL-induced apoptosis. *Apoptosis*, Vol. 14, No. 11, (2009), pp 1352-65

Arpino, G, Wiechmann, L, Osborne, CK & Schiff, R (2008). Crosstalk between the estrogen receptor and the HER tyrosine kinase receptor family: molecular mechanism and clinical implications for endocrine therapy resistance. *Endocr Rev*, Vol. 29, No. 2, (2008), pp 217-33

Aydar, E., Palmer, C.P. & Djamgoz, M.B. (2004). Sigma receptors and cancer: possible involvement of ion channels. *Cancer Res*, Vol. 64, No. 15, (2004), pp 5029-35

Babuke, T. & Tikkanen, R. (2007). Dissecting the molecular function of reggie/flotillin proteins. *Eur J Cell Biol*, Vol. 86, No. 9, (2007), pp 525-32

Barros, F.F., Powe, D.G., Ellis, I.O. & Green, A.R. (2010). Understanding the HER family in breast cancer: interaction with ligands, dimerization and treatments. *Histopathology*, Vol. 56, No. 5, (2010), pp 560-72

Belsches-Jablonski, A.P., Biscardi, J.S., Peavy, D.R., Tice, D.A., Romney, D.A. et al. (2001). Src family kinases and HER2 interactions in human breast cancer cell growth and survival. *Oncogene*, Vol. 20, No. 12, (2001), pp 1465-75

Bhatnagar, R.S. & Gordon, J.I. (1997). Understanding covalent modifications of proteins by lipids: where cell biology and biophysics mingle. *Trends Cell Biol*, Vol. 7, No. 1, (1997), pp 14-20

Bickel, P.E., Scherer, P.E., Schnitzer, J.E., Oh, P., Lisanti, M.P. et al. (1997). Flotillin and epidermal surface antigen define a new family of caveolae-associated integral membrane proteins. *J Biol Chem*, Vol. 272, No. 21, (1997), pp 13793-802

Bijlmakers, M.J. & Marsh, M. (2003). The on-off story of protein palmitoylation. *Trends Cell Biol*, Vol. 13, No. 1, (2003), pp 32-42

Blick, T., Hugo, H., Widodo, E., Waltham, M., Pinto, C. et al. (2010). Epithelial mesenchymal transition traits in human breast cancer cell lines parallel the CD44(hi/)CD24 (lo/-) stem cell phenotype in human breast cancer. *J Mammary Gland Biol Neoplasia*, Vol. 15, No. 2, (2010), pp 235-52

Bourguignon, L.Y. (2008). Hyaluronan-mediated CD44 activation of RhoGTPase signaling and cytoskeleton function promotes tumor progression. *Semin Cancer Biol*, Vol. 18, No. 4, (2008), pp 251-9

Bourguignon, L.Y., Zhu, D. & Zhu, H. (1998). CD44 isoform-cytoskeleton interaction in oncogenic signaling and tumor progression. *Front Biosci*, Vol. 3, No. (1998), pp d637-49

Bourguignon, L.Y., Zhu, H., Chu, A., Iida, N., Zhang, L. et al. (1997). Interaction between the adhesion receptor, CD44, and the oncogene product, p185HER2, promotes human ovarian tumor cell activation. *J Biol Chem*, Vol. 272, No. 44, (1997), pp 27913-8

Brown, D.A. & Rose, J.K. (1992). Sorting of GPI-anchored proteins to glycolipid-enriched membrane subdomains during transport to the apical cell surface. *Cell*, Vol. 68, No. 3, (1992), pp 533-44

Buccione, R., Caldieri, G. & Ayala, I. (2009). Invadopodia: specialized tumor cell structures for the focal degradation of the extracellular matrix. *Cancer Metastasis Rev*, Vol. 28, No. 1-2, (2009), pp 137-49

Calder, P.C. & Yaqoob, P. (2007). Lipid rafts--composition, characterization, and controversies. *J Nutr*, Vol. 137, No. 3, (2007), pp 545-7

Camp, L.A. & Hofmann, S.L. (1993). Purification and properties of a palmitoyl-protein thioesterase from bovine brain with activity toward palmitoylated H-Ras as substrate. *Methods Enzymol*, Vol. 250, No. (1995), pp 536-47

Carr, A., Rodriguez, E., Arange Mdel, C., Camacho, R., Osorio, M. et al. (2003). Immunotherapy of advanced breast cancer with a heterophilic ganglioside (NeuGcGM3) cancer vaccine. *J Clin Oncol*, Vol. 21, No. 6, (2003), pp 1015-21

Cary, L.A. & Cooper, J.A. (2000). Molecular switches in lipid rafts. *Nature*, Vol. 404, No. 6781, (2000), pp 945, 947

Casey, P.J. & Seabra, M.C. (1996). Protein prenyltransferases. *J Biol Chem*, Vol. 271, No. 10, (1996), pp 5289-92

Chakrabandhu, K., Herincs, Z., Huault, S., Dost, B., Peng, L. et al. (2007). Palmitoylation is required for efficient Fas cell death signaling. *EMBO J*, Vol. 26, No. 1, (2007), pp 209-20

Chen, X. & Resh, M.D. (2002). Cholesterol depletion from the plasma membrane triggers ligand-independent activation of the epidermal growth factor receptor. *J Biol Chem*, Vol. 277, No. 51, (2002), pp 49631-7

Colas, S., Maheo, K., Denis, F., Goupille, C., Heinard, C. et al. (2006). Sensitization by dietary docosahexaenoic acid of rat mammary carcinoma to anthracycline: a role for tumor vascularization. *Clin Cancer Res*, Vol. 12, No. 19, (2006), pp 5879-86

Coleman, D.T., Bigelow, R. & Cardelli, J.A. (2009). Inhibition of fatty acid synthase by luteolin post-transcriptionally down-regulates c-Met expression independent of proteosomal/lysosomal degradation. *Mol Cancer Ther*, Vol. 8, No. 1, (2009), pp 214-24

Datta, S.R., Brunet, A. & Greenberg, M.E. (1999). Cellular survival: a play in three Akts. *Genes Dev*, Vol. 13, No. 22, (1999), pp 2905-27

de Laurentiis, A., Donovan, L. & Arcaro, A. (2007). Lipid rafts and caveolae in signaling by growth factor receptors. *Open Biochem J*, Vol. 1, No. (2007), pp 12-32

Deborde, S., Perret, E., Gravotta, D., Deora, A., Salvarezza, S. et al. (2008). Clathrin is a key regulator of basolateral polarity. *Nature*, Vol. 452, No. 7188, (2008), pp 719-23

Diaz, L.K., Zhou, X., Wright, E.T., Cristofanilli, M., Smith, T. et al. (2005). CD44 expression is associated with increased survival in node-negative invasive breast carcinoma. *Clin Cancer Res*, Vol. 11, No. 9, (2005), pp 3309-14

Downward, J. (2006). Signal transduction. Prelude to an anniversary for the RAS oncogene. *Science*, Vol. 314, No. 5798, (2006), pp 433-4

Doyle, L.A., Yang, W., Abruzzo, L.V., Krogmann, T., Gao, Y. et al. (1998). A multidrug resistance transporter from human MCF-7 breast cancer cells. *Proc Natl Acad Sci U S A*, Vol. 95, No. 26, (1998), pp 15665-70

Dumitru, C.A., Carpinteiro, A., Trarbach, T., Hengge, U.R. & Gulbins, E. (2007). Doxorubicin enhances TRAIL-induced cell death via ceramide-enriched membrane platforms. *Apoptosis*, Vol. 12, No. 8, (2007), pp 1533-41

Dunphy, J.T., Greentree, W.K. & Linder, M.E. (2001). Enrichment of G-protein palmitoyltransferase activity in low density membranes: in vitro reconstitution of Galphai to these domains requires palmitoyltransferase activity. *J Biol Chem*, Vol. 276, No. 46, (2001), pp 43300-4

Eddy, S.F., Kane, S.E. & Sonenshein, G.E. (2007). Trastuzumab-resistant HER2-driven breast cancer cells are sensitive to epigallocatechin-3 gallate. *Cancer Res*, Vol. 67, No. 19, (2007), pp 9018-23

Elhyany, S., Azaz-Kutnik, E., Tsory, S., Muller, T., Fedida, S. et al. (2004). The integrity of cholesterol enriched microdomains is essential for the constitutive high activity of protein kinase B in tumour cells. *Biochem Soc Trans*, Vol. 32, No. Pt 5, (2004), pp 837-9

Elnagar, A.Y., Sylvester, P.W. & El Sayed, K.A. (2011). (-)-Oleocanthal as a c-Met Inhibitor for the Control of Metastatic Breast and Prostate Cancers. *Planta Med*, Vol. No. (2011), 1439-0221

Everson, W.V. & Smart, E.J. (2006). *Caveolin and its Role in Intracellular Chaperone Complexes* (edition), Wiley-VCH Verlag GmbH & Co. KGaA, 9783527608072,

Fan, J.Y., Carpentier, J.L., van Obberghen, E., Grunfeld, C., Gorden, P. et al. (1983). Morphological changes of the 3T3-L1 fibroblast plasma membrane upon differentiation to the adipocyte form. *J Cell Sci*, Vol. 61, No. (1983), pp 219-30

Farabegoli, F., Papi, A., Bartolini, G., Ostan, R. & Orlandi, M. (2010). (-)-Epigallocatechin-3-gallate down-regulates Pg-P and BCRP in a tamoxifen resistant MCF-7 cell line. *Phytomedicine*, Vol. 17, No. 5, (2010), pp 356-62

Fiedler, K., Kobayashi, T., Kurzchalia, T.V. & Simons, K. (1993). Glycosphingolipid-enriched, detergent-insoluble complexes in protein sorting in epithelial cells. *Biochemistry*, Vol. 32, No. 25, (1993), pp 6365-73

Fiucci, G., Ravid, D., Reich, R. & Liscovitch, M. (2002). Caveolin-1 inhibits anchorage-independent growth, anoikis and invasiveness in MCF-7 human breast cancer cells. *Oncogene*, Vol. 21, No. 15, (2002), pp 2365-75

Folsch, H., Mattila, P.E. & Weisz, O.A. (2009). Taking the scenic route: biosynthetic traffic to the plasma membrane in polarized epithelial cells. *Traffic*, Vol. 10, No. 6, (2009), pp 972-81

Fra, A.M., Williamson, E., Simons, K. & Parton, R.G. (1995). De novo formation of caveolae in lymphocytes by expression of VIP21-caveolin. *Proc Natl Acad Sci U S A*, Vol. 92, No. 19, (1995), pp 8655-9

Freeman, M.R., Cinar, B., Kim, J., Mukhopadhyay, N.K., Di Vizio, D. et al. (2007). Transit of hormonal and EGF receptor-dependent signals through cholesterol-rich membranes. *Steroids*, Vol. 72, No. 2, (2007), pp 210-7

Frew, A.J., Lindemann, R.K., Martin, B.P., Clarke, C.J., Sharkey, J. et al. (2008). Combination therapy of established cancer using a histone deacetylase inhibitor and a TRAIL receptor agonist. *Proc Natl Acad Sci U S A*, Vol. 105, No. 32, (2008), pp 11317-22

Furuchi, T. & Anderson, R.G. (1998). Cholesterol depletion of caveolae causes hyperactivation of extracellular signal-related kinase (ERK). *J Biol Chem*, Vol. 273, No. 33, (1998), pp 21099-104

Gajate, C., Del Canto-Janez, E., Acuna, A.U., Amat-Guerri, F., Geijo, E. et al. (2004). Intracellular triggering of Fas aggregation and recruitment of apoptotic molecules into Fas-enriched rafts in selective tumor cell apoptosis. *J Exp Med*, Vol. 200, No. 3, (2004), pp 353-65

Gajate, C., Gonzalez-Camacho, F. & Mollinedo, F. (2009). Lipid raft connection between extrinsic and intrinsic apoptotic pathways. *Biochem Biophys Res Commun*, Vol. 380, No. 4, (2009), pp 780-4

Gajate, C. & Mollinedo, F. (2001). The antitumor ether lipid ET-18-OCH(3) induces apoptosis through translocation and capping of Fas/CD95 into membrane rafts in human leukemic cells. *Blood*, Vol. 98, No. 13, (2001), pp 3860-3

Gajate, C. & Mollinedo, F. (2005). Cytoskeleton-mediated death receptor and ligand concentration in lipid rafts forms apoptosis-promoting clusters in cancer chemotherapy. *J Biol Chem*, Vol. 280, No. 12, (2005), pp 11641-7

Gajate, C. & Mollinedo, F. (2007). Edelfosine and perifosine induce selective apoptosis in multiple myeloma by recruitment of death receptors and downstream signaling molecules into lipid rafts. *Blood*, Vol. 109, No. 2, (2007), pp 711-9

Galbiati, F., Engelman, J.A., Volonte, D., Zhang, X.L., Minetti, C. et al. (2001). Caveolin-3 null mice show a loss of caveolae, changes in the microdomain distribution of the dystrophin-glycoprotein complex, and t-tubule abnormalities. *J Biol Chem*, Vol. 276, No. 24, (2001), pp 21425-33

Gastaldi, S., Comoglio, P.M. & Trusolino, L. (2010). The Met oncogene and basal-like breast cancer: another culprit to watch out for? *Breast Cancer Res*, Vol. 12, No. 4, (2010), pp 208

Gayet, L., Dayan, G., Barakat, S., Labialle, S., Michaud, M. et al. (2005). Control of P-glycoprotein activity by membrane cholesterol amounts and their relation to multidrug resistance in human CEM leukemia cells. *Biochemistry*, Vol. 44, No. 11, (2005), pp 4499-509

Gebreselassie, D. & Bowen, W.D. (2004). Sigma-2 receptors are specifically localized to lipid rafts in rat liver membranes. *Eur J Pharmacol*, Vol. 493, No. 1-3, (2004), pp 19-28

Germain, E., Chajes, V., Cognault, S., Lhuillery, C. & Bougnoux, P. (1998). Enhancement of doxorubicin cytotoxicity by polyunsaturated fatty acids in the human breast tumor cell line MDA-MB-231: relationship to lipid peroxidation. *Int J Cancer*, Vol. 75, No. 4, (1998), pp 578-83

Ghosh, R.N., Mallet, W.G., Soe, T.T., McGraw, T.E. & Maxfield, F.R. (1998). An endocytosed TGN38 chimeric protein is delivered to the TGN after trafficking through the endocytic recycling compartment in CHO cells. *J Cell Biol*, Vol. 142, No. 4, (1998), pp 923-36

Gimona, M., Buccione, R., Courtneidge, S.A. & Linder, S. (2008). Assembly and biological role of podosomes and invadopodia. *Curr Opin Cell Biol*, Vol. 20, No. 2, (2008), pp 235-41

Gong, M., Wilson, M., Kelly, T., Su, W., Diessman, J. et al. (2003). HDL-associated estradiol stimulates endothelial NO synthase and vasodilation in an SR-BI-dependent manner. *J Cardiovasc Pharmacol Ther*, Vol. 8, No. 1, (2003), pp 43-52

Gorelick, F.S. & Shugrue, C. (2001). Exiting the endoplasmic reticulum. *Mol Cell Endocrinol*, Vol. 177, No. 1-2, (2001), pp 13-5

Herrera-Gayol, A. & Jothy, S. (1999). Adhesion proteins in the biology of breast cancer: contribution of CD44. *Exp Mol Pathol*, Vol. 66, No. 2, (1999), pp 119-56

Hill, M.M., Feng, J. & Hemmings, B.A. (2002). Identification of a plasma membrane Raft-associated PKB Ser473 kinase activity that is distinct from ILK and PDK1. *Curr Biol*, Vol. 12, No. 14, (2002), pp 1251-5

Hitosugi, T., Sato, M., Sasaki, K. & Umezawa, Y. (2007). Lipid raft specific knockdown of SRC family kinase activity inhibits cell adhesion and cell cycle progression of breast cancer cells. *Cancer Res*, Vol. 67, No. 17, (2007), pp 8139-48

Huang, C.R., Jin, Z.X., Dong, L., Tong, M., Yue, S. et al. (2010). Cisplatin augments FAS-mediated apoptosis through lipid rafts. *Anticancer Res*, Vol. 30, No. 6, (2010), pp 2065-71

Ibrahim, N.K. & Murray, J.L. (2003). Clinical development of the 5Tu-KLH vaccine [Theratope]. *Clin Breast Cancer*, Vol. 3 Suppl 4, No. (2003), pp S139-43

Irwin, ME, Mueller, KL, Bohin, N, Ge, Y & Boerner, JL (2010). Lipid raft localization of EGFR alters the response of cancer cells to the EGFR tyrosine kinase inhibitor gefitinib. *J Cell Physiol*, Vol. No. (2010), 1097-4652.

Jemal, A, Bray, F, Center, MM, Ferlay, J, Ward, E et al. (2011). Global cancer statistics. *CA Cancer J Clin*, Vol. 61, No. 2, (2011), pp 69-90.

Joensuu, H, Klemi, PJ, Toikkanen, S & Jalkanen, S (1993). Glycoprotein CD44 expression and its association with survival in breast cancer. *Am J Pathol*, Vol. 143, No. 3, (1993), pp 867-74.

Julien, S, Picco, G, Sewell, R, Vercoutter-Edouart, AS, Tarp, M et al. (2009). Sialyl-Tn vaccine induces antibody-mediated tumour protection in a relevant murine model. *Br J Cancer*, Vol. 100, No. 11, (2009), pp 1746-54.

Kang, R, Wan, J, Arstikaitis, P, Takahashi, H, Huang, K et al. (2008). Neural palmitoyl-proteomics reveals dynamic synaptic palmitoylation. *Nature*, Vol. 456, No. 7224, (2008), pp 904-9.

Klappe, K, Hummel, I, Hoekstra, D & Kok, JW (2009). Lipid dependence of ABC transporter localization and function. *Chem Phys Lipids*, Vol. 161, No. 2, (2009), pp 57-61.

Komatsu, M, Jepsen, S, Arango, ME, Carothers Carraway, CA & Carraway, KL (2001). Muc4/sialomucin complex, an intramembrane modulator of ErbB2/HER2/Neu, potentiates primary tumor growth and suppresses apoptosis in a xenotransplanted tumor. *Oncogene*, Vol. 20, No. 4, (2001), pp 461-70.

Labrecque, L, Nyalendo, C, Langlois, S, Durocher, Y, Roghi, C et al. (2004). Src-mediated tyrosine phosphorylation of caveolin-1 induces its association with membrane type 1 matrix metalloproteinase. *J Biol Chem*, Vol. 279, No. 50, (2004), pp 52132-40.

Lacour, S, Hammann, A, Grazide, S, Lagadic-Gossmann, D, Athias, A et al. (2001). Cisplatin-induced CD95 redistribution into membrane lipid rafts of HT29 human colon cancer cells. *Cancer Res*, Vol. 64, No. 10, (2004), pp 3593-8.

Lajoie, P & Nabi, IR (2010). Lipid rafts, caveolae, and their endocytosis. *Int Rev Cell Mol Biol*, Vol. 282, No. (2010), pp 135-63.

Lajoie, P, Partridge, EA, Guay, G, S., N, Goetz, JG et al. (2007). Plasma membrane domain organization regulates EGFR signaling in tumor cells. *J Cell Biol*, Vol. 179, No. 2, (2007), pp 341-56.

Landowski, TH, Gleason-Guzman, MC & Dalton, WS (1997). Selection for drug resistance results in resistance to Fas-mediated apoptosis. *Blood*, Vol. 89, No. 6, (1997), pp 1854-61.

Lavie, Y, Fiucci, G & Liscovitch, M (1998). Up-regulation of caveolae and caveolar constituents in multidrug-resistant cancer cells. *J Biol Chem*, Vol. 273, No. 49, (1998), pp 32380-3.

Le Moyec, L, Tatoud, R, Eugene, M, Gauville, C, Primot, I et al. (1992). Cell and membrane lipid analysis by proton magnetic resonance spectroscopy in five breast cancer cell lines. *Br J Cancer*, Vol. 66, No. 4, (1992), pp 623-8.

Lee, IL, Wang, MJ, Sudhir, PR & Chen, JY (2008). CD44 engagement promotes matrix-derived survival through the CD44 SRC integrin axis in lipid rafts. *Mol Cell Biol*, Vol. 28, No. 18, (2008), pp 5710-23.

Lee, SH, Koo, KH, Park, JW, Kim, HJ, Yo, SK et al. (2009). HIF-1 is induced via EGFR activation and mediates resistance to anoikis-like cell death under lipid

rafts/caveolae-disrupting stress. *Carcinogenesis*, Vol. 30, No. 12, (2009), pp 1997-2001.

Leon, L, Subramaniam, S, Canvard, O, Plenchette-Colas, S, Paul, C et al. (2011). S-Nitrosylation of the Death Receptor Fas Promotes Fas Ligand-Mediated Apoptosis in Cancer Cells. *Gastroenterology*, Vol. No. (2011), 1528-0012.

Levental, I, Grzybek, M & Simons, K (2010). Greasing their way: lipid modifications determine protein association with membrane rafts. *Biochemistry*, Vol. 49, No. 30, (2010), pp 6305-16.

Li, H, Zhu, H, Xu, CJ & Yuan, J (1998). Cleavage of BID by caspase 8 mediates the mitochondrial damage in the Fas pathway of apoptosis. *Cell*, Vol. 94, No. 4, (1998), pp 491-501.

Li, N, Zhang, Y, Naylor, MJ, Schatzmann, F, Maurer, F et al. (2005). Beta1 integrins regulate mammary gland proliferation and maintain the integrity of mammary alveoli. *EMBO J*, Vol. 24, No. 11, (2005), pp 1942-53.

Li, YC, Park, MJ, Ye, SK, Kim, CW & Kim, YN (2006). Elevated levels of cholesterol-rich lipid rafts in cancer cells are correlated with apoptosis sensitivity induced by cholesterol-depleting agents. *Am J Pathol*, Vol. 168, No. 4, (2006), pp 1107-18.

Lingwood, D, Kaiser, HJ, Levental, I & Simons, K (2009). Lipid rafts as functional heterogeneity in cell membranes. *Biochem Soc Trans*, Vol. 37, No. Pt 5, (2009), pp 955-60.

Lipowsky, R (1993). Domain-induced budding of fluid membranes. *Biophys J*, Vol. 64, No. 4, (1993), pp 1133-8.

Liu, J, Deyoung, SM, Zhang, M, Dold, LH & Saltiel, AR (2005). The stomatin/prohibitin/flotillin/HflK/C domain of flotillin-1 contains distinct sequences that direct plasma membrane localization and protein interactions in 3T3-L1 adipocytes. *J Biol Chem*, Vol. 280, No. 16, (2005), pp 16125-34.

Lobo, S, Greentree, WK, Linder, ME & Deschenes, RJ (2002). Identification of a Ras palmitoyltransferase in Saccharomyces cerevisiae. *J Biol Chem*, Vol. 277, No. 43, (2002), pp 41268-73.

Ma, DW, Seo, J, Switzer, KC, Fan, YY, McMurray, DN et al. (2004). n-3 PUFA and membrane microdomains: a new frontier in bioactive lipid research. *J Nutr Biochem*, Vol. 15, No. 11, (2004), pp 700-6.

Ma, XJ, Dahiya, S, Richardson, E, Erlander, M & Sgroi, DC (2009). Gene expression profiling of the tumor microenvironment during breast cancer progression. *Breast Cancer Res*, Vol. 11, No. 1, (2009), pp R7, 1465-542X.

Magee, AI & Seabra, MC (2003). Are prenyl groups on proteins sticky fingers or greasy handles? *Biochem J*, Vol. 376, No. Pt 2, (2003), pp e3-4.

Manes, S, Lacalle, RA, Gomez-Mouton, C, del Real, G, Mira, E et al. (2001). Membrane raft microdomains in chemokine receptor function. *Semin Immunol*, Vol. 13, No. 2, (2001), pp 147-57.

Marks, PA & Xu, WS (2009). Histone deacetylase inhibitors: Potential in cancer therapy. *J Cell Biochem*, Vol. 107, No. 4, (2009), pp 600-8.

Marquez, DC, Chen, HW, Curran, EM, Welshons, WV & Pietras, RJ (2006). Estrogen receptors in membrane lipid rafts and signal transduction in breast cancer. *Mol Cell Endocrinol*, Vol. 246, No. 1-2, (2006), pp 91-100.

May, CD, Sphyris, N, Evans, KW, Werden, SJ, Guo, W et al. (2011). Epithelial-mesenchymal transition and cancer stem cells: a dangerously dynamic duo in breast cancer progression. *Breast Cancer Res*, Vol. 13, No. 1, (2011), pp 202.

McGuire, TF, Corey, SJ & Sebti, SM (1993). Lovastatin inhibits platelet-derived growth factor (PDGF) stimulation of phosphatidylinositol 3-kinase activity as well as association of p85 subunit to tyrosine-phosphorylated PDGF receptor. *J Biol Chem*, Vol. 268, No. 30, (1993), pp 22237-30.

Mellman, I & Nelson, WJ (2008). Coordinated protein sorting, targeting and distribution in polarized cells. *Nat Rev Mol Cell Biol*, Vol. 9, No. 11, (2008), pp 833-45.

Menendez, JA, Lupu, R & Colomer, R (2005). Exogenous supplementation with omega-3 polyunsaturated fatty acid docosahexaenoic acid (DHA; 22:6n-3) synergistically enhances taxane cytotoxicity and downregulates Her-2/neu (c-erbB-2) oncogene expression in human breast cancer cells. *Eur J Cancer Prev*, Vol. 14, No. 3, (2005), pp 263-70.

Menendez, JA, Vellon, L, Mehmi, I, Oza, BP, Ropero, S et al. (2004). Inhibition of fatty acid synthase (FAS) suppresses HER2/neu (erbB-2) oncogene overexpression in cancer cells. *Proc Natl Acad Sci U S A*, Vol. 101, No. 29, (2004), pp 10715-20.

Merino, D, Lalaoui, N, Morizot, A, Schneider, P, Solary, E et al. (2006). Differential inhibition of TRAIL-mediated DR5-DISC formation by decoy receptors 1 and 2. *Mol Cell Biol*, Vol. 26, No. 19, (2006), pp 7046-55.

Mineo, C, Gill, GN & Anderson, RG (1999). Regulated migration of epidermal growth factor receptor from caveolae. *J Biol Chem*, Vol. 274, No. 43, (1999), pp 30636-43.

Mira, E, Lacalle, RA, Buesa, JM, de Buitrago, GG, Jimenez-Baranda, S et al. (2004). Secreted MMP9 promotes angiogenesis more efficiently than constitutive active MMP9 bound to the tumor cell surface. *J Cell Sci*, Vol. 117, No. Pt 9, (2004), pp 1847-57.

Morrow, IC, Rea, S, Martin, S, Prior, IA, Prohaska, R et al. (2002). Flotillin-1/reggie-2 traffics to surface raft domains via a novel golgi-independent pathway. Identification of a novel membrane targeting domain and a role for palmitoylation. *J Biol Chem*, Vol. 277, No. 50, (2002), pp 48834-41.

Mulens, V, de la Torre, A, Marinello, P, Rodriguez, R, Cardoso, J et al. (2010). Immunogenicity and safety of a NeuGcGM3 based cancer vaccine: Results from a controlled study in metastatic breast cancer patients. *Hum Vaccin*, Vol. 6, No. 9, (2010), 1554-8619.

Murai, T, Maruyama, Y, Mio, K, Nishiyama, H, Suga, M et al. (2011). Low cholesterol triggers membrane microdomain-dependent CD44 shedding and suppresses tumor cell migration. *J Biol Chem*, Vol. 286, No. 3, (2011), pp 1999-2007.

Murata, M, Peranen, J, Schreiner, R, Wieland, F, Kurzchalia, TV et al. (1995). VIP21/caveolin is a cholesterol-binding protein. *Proc Natl Acad Sci U S A*, Vol. 92, No. 22, (1995), pp 10339-43.

Nabi, IR & Le, PU (2003). Caveolae/raft-dependent endocytosis. *J Cell Biol*, Vol. 161, No. 4, (2003), pp 673-7.

Nagy, P, Vereb, G, Sebestyen, Z, Horvath, G, Lockett, SJ et al. (2002). Lipid rafts and the local density of ErbB proteins influence the biological role of homo- and heteroassociations of ErbB2. *J Cell Sci*, Vol. 115, No. Pt 22, (2002), pp 4251-62.

Nahta, R & Esteva, FJ (2006). HER2 therapy: molecular mechanisms of trastuzumab resistance. *Breast Cancer Res*, Vol. 8, No. 6, (2006), pp 215, 1465-542X.

Neumann-Giesen, C, Falkenbach, B, Beicht, P, Claasen, S, Luers, G et al. (2004). Membrane and raft association of reggie-1/flotillin-2: role of myristoylation, palmitoylation and oligomerization and induction of filopodia by overexpression. *Biochem J*, Vol. 378, No. Pt 2, (2004), pp 509-18.

Neumann-Giesen, C, Fernow, I, Amaddii, M & Tikkanen, R (2007). Role of EGF-induced tyrosine phosphorylation of reggie-1/flotillin-2 in cell spreading and signaling to the actin cytoskeleton. *J Cell Sci*, Vol. 120, No. Pt 3, (2007), pp 395-406.

Nohara, K, Wang, F & Spiegel, S (1998). Glycosphingolipid composition of MDA-MB-231 and MCF-7 human breast cancer cell lines. *Breast Cancer Res Treat*, Vol. 48, No. 2, (1998), pp 149-57.

Ogretmen, B & Hannun, YA (2001). Updates on functions of ceramide in chemotherapy-induced cell death and in multidrug resistance. *Drug Resist Updat*, Vol. 4, No. 6, (2001), pp 366-77.

Okamoto, T, Schlegel, A, Scherer, PE & Lisanti, MP (1998). Caveolins, a family of scaffolding proteins for organizing "preassembled signaling complexes" at the plasma membrane. *J Biol Chem*, Vol. 273, No. 10, (1998), pp 5419-22.

Orian-Rousseau, V, Chen, L, Sleeman, JP, Herrlich, P & Ponta, H (2002). CD44 is required for two consecutive steps in HGF/c-Met signaling. *Genes Dev*, Vol. 16, No. 23, (2002), pp 3074-86.

Paladino, S, Lebreton, S, Tivodar, S, Campana, V, Tempre, R et al. (2008). Different GPI-attachment signals affect the oligomerisation of GPI-anchored proteins and their apical sorting. *J Cell Sci*, Vol. 121, No. Pt 24, (2008), pp 4001-7.

Paladino, S, Sarnataro, D, Pillich, R, Tivodar, S, Nitsch, L et al. (2004). Protein oligomerization modulates raft partitioning and apical sorting of GPI-anchored proteins. *J Cell Biol*, Vol. 167, No. 4, (2004), pp 699-709.

Palmer, CP, Mahen, R, Schnell, E, Djanigoz, MB & Aydar, E (2007). Sigma-1 receptors bind cholesterol and remodel lipid rafts in breast cancer cell lines. *Cancer Res*, Vol. 67, No. 23, (2007), pp 11166-75.

Paris, I, Cecchetti, S, Spadaro, F, Abalsamo, L, Lugini, L et al. (2010). Inhibition of phosphatidylcholine-specific phospholipase C downregulates HER2 overexpression on plasma membrane of breast cancer cells. *Breast Cancer Res*, Vol. 12, No. 3, (2010), pp R27, 1465-542X.

Park, BW, Zhang, HT, Wu, C, Berezov, A, Zhang, X et al. (2000). Rationally designed anti-HER2/neu peptide mimetic disables P185HER2/neu tyrosine kinases in vitro and in vivo. *Nat Biotechnol*, Vol. 18, No. 2, (2000), pp 194-8.

Park, EK, Lee, EJ, Lee, SH, Koo, KH, Sung, JY et al. (2010). Induction of apoptosis by the ginsenoside Rk2 by internalization of lipid rafts and caveolae and inactivation of Akt. *Br J Pharmacol*, Vol. 160, No. 5, (2010), pp 1212-23.

Park, EK, Park, MJ, Lee, SH, Li, YC, Kim, J et al. (2009). Cholesterol depletion induces anoikis-like apoptosis via FAK down-regulation and caveolae internalization. *J Pathol*, Vol. 218, No. 3, (2009), pp 337-49.

Parmryd, I, Adler, J, Patel, R & Magee, AI (2003). Imaging metabolism of phosphatidylinositol 4,5-bisphosphate in T-cell GM1-enriched domains containing Ras proteins. *Exp Cell Res*, Vol. 285, No. 1, (2003), pp 27-36.

Parpal, S, Karlsson, M, Thorn, H & Stralfors, P (2001). Cholesterol depletion disrupts caveolae and insulin receptor signaling for metabolic control via insulin receptor

substrate-1, but not for mitogen-activated protein kinase control. *J Biol Chem*, Vol. 276, No. 13, (2001), pp 9670-8
Parsons, SJ & Parsons, JT (2004). Src family kinases, key regulators of signal transduction. *Oncogene*, Vol. 23, No. 48, (2004), pp 7906-9
Patra, SK (2008). Dissecting lipid raft facilitated cell signaling pathways in cancer. *Biochim Biophys Acta*, Vol. 1785, No. 2, (2008), pp 182-206
Patra, SK, Rizzi, F, Silva, A, Rugina, DO & Bettuzzi, S (2008). Molecular targets of (-)-epigallocatechin-3-gallate (EGCG): specificity and interaction with membrane lipid rafts. *J Physiol Pharmacol*, Vol. 59 Suppl 9, No. (2008), pp 217-35
Peter, ME & Krammer, PH (2003). The CD95(APO-1/Fas) DISC and beyond. *Cell Death Differ*, Vol. 10, No. 1, (2003), pp 26-35
Pietras, RJ (2003). Interactions between estrogen and growth factor receptors in human breast cancers and the tumor-associated vasculature. *Breast J*, Vol. 9, No. 5, (2003), pp 361-73
Pietras, RJ, Marquez, DC, Chen, HW, Tsai, E, Weinberg, O et al. (2005). Estrogen and growth factor receptor interactions in human breast and non-small cell lung cancer cells. *Steroids*, Vol. 70, No. 5-7, (2005), pp 372-81
Pike, LJ (2003). Lipid rafts: bringing order to chaos. *J Lipid Res*, Vol. 44, No. 4, (2003), pp 655-67
Pike, LJ & Casey, L (2002). Cholesterol levels modulate EGF receptor-mediated signaling by altering receptor function and trafficking. *Biochemistry*, Vol. 41, No. 32, (2002), pp 10315-22
Planey, SL & Zacharias, DA (2009). Palmitoyl acyltransferases, their substrates, and novel assays to connect them (Review). *Mol Membr Biol*, Vol. 26, No. 1, (2009), pp 11-31
Ponta, H, Sherman, L & Herrlich, PA (2003). CD44: from adhesion molecules to signalling regulators. *Nat Rev Mol Cell Biol*, Vol. 4, No. 1, (2003), pp 33-45
Prinetti, A, Chigorno, V, Tettamanti, G & Sonnino, S (2000). Sphingolipid-enriched membrane domains from rat cerebellar granule cells differentiated in culture. A compositional study. *J Biol Chem*, Vol. 275, No. 16, (2000), pp 11658-65
Prior, IA & Hancock, JF (2001). Compartmentalization of Ras proteins. *J Cell Sci*, Vol. 114, No. Pt 9, (2001), pp 1603-8
Raghu, H, Sodadasu, PK, Malla, RR, Gondi, CS, Estes, N et al. (2010). Localization of uPAR and MMP-9 in lipid rafts is critical for migration, invasion and angiogenesis in human breast cancer cells. *BMC Cancer*, Vol. 10, No. (2010), pp 647, 1471-2407
Ravid, D, Maor, S, Werner, H & Liscovitch, M (2005). Caveolin-1 inhibits cell detachment-induced p53 activation and anoikis by upregulation of insulin-like growth factor-I receptors and signaling. *Oncogene*, Vol. 24, No. 8, (2005), pp 1338-47
Razandi, M, Pedram, A, Park, ST & Levin, ER (2003). Proximal events in signaling by plasma membrane estrogen receptors. *J Biol Chem*, Vol. 278, No. 4, (2003), pp 2701-12
Reimer, T, Herrmann, C, Kocean, D, Richter, D, Gerber, B et al. (2000). FasL:Fas ratio--a prognostic factor in breast carcinomas. *Cancer Res*, Vol. 60, No. 4, (2000), pp 822-5
Remacle Bonnet, M, Garrouste, F, Baillat, G, Andre, F, Marvaldi, J et al. (2005). Membrane rafts segregate pro- from anti-apoptotic insulin-like growth factor-I receptor signaling in colon carcinoma cells stimulated by members of the tumor necrosis factor superfamily. *Am J Pathol*, Vol. 167, No. 3, (2005), pp 761-73

Reuben, JM, Lee, BN, Gao, H, Cohen, EN, Mego, M et al. (2011). Primary breast cancer patients with high risk clinicopathologic features have high percentages of bone marrow epithelial cells with ALDH activity and CD44(+)CD24(lo) cancer stem cell phenotype. *Eur J Cancer*, Vol. No. (2011), 1879-0852
Ringerike, T, Blystad, FD, Levy, FO, Madshus, IH & Stang, E (2002). Cholesterol is important in control of EGF receptor kinase activity but EGF receptors are not concentrated in caveolae. *J Cell Sci*, Vol. 115, No. Pt 6, (2002), pp 1331-40
Rodriguez-Boulan, E, Kreitzer, G & Musch, A (2005). Organization of vesicular trafficking in epithelia. *Nat Rev Mol Cell Biol*, Vol. 6, No. 3, (2005), pp 233-47
Rogers, KR, Kikawa, KD, Mouradian, M, Hernandez, K, McKinnon, KM et al. (2010). Docosahexaenoic acid alters epidermal growth factor receptor-related signaling by disrupting its lipid raft association. *Carcinogenesis*, Vol. 31, No. 9, (2010), pp 1523-30
Rossin, A, Derouet, M, Abdel-Sater, F & Hueber, AO (2009). Palmitoylation of the TRAIL receptor DR4 confers an efficient TRAIL-induced cell death signalling. *Biochem J*, Vol. 419, No. 1, (2009), pp 165-92
Roth, AF, Feng, Y, Chen, L & Davis, NG (2002). The yeast DHHC cysteine-rich domain protein Akr1p is a palmitoyl transferase. *J Cell Biol*, Vol. 159, No. 1, (2002), pp 23-8
Rothberg, JM & Artavanis-Tsakonas, S (1992). Modularity of the slit protein. Characterization of a conserved carboxy-terminal sequence in secreted proteins and a motif implicated in extracellular protein interactions. *J Mol Biol*, Vol. 227, No. 2, (1992), pp 367-70
Rothberg, KG, Heuser, JE, Donzell, WC, Ying, Y-S, Glenney, JR et al. (1992). Caveolin, a protein component of caveolae membrane coats. *Cell*, Vol. 68, No. (1992), pp 673-682
Rothberg, KG, Ying, YS, Kolhouse, JF, Kamen, BA & Anderson, RG (1990). The glycophospholipid-linked folate receptor internalizes folate without entering the clathrin-coated pit endocytic pathway. *J Cell Biol*, Vol. 110, No. 3, (1990), pp 637-49
Rubin, J, Schwartz, Z, Boyan, BD, Fan, X, Case, N et al. (2007). Caveolin-1 knockout mice have increased bone size and stiffness. *J Bone Miner Res*, Vol. 22, No. 9, (2007), pp 1408-18
Sahores, M, Prinetti, A, Chiabrando, G, Blasi, F & Sonnino, S (2005). uPA binding increases UPAR localization to lipid rafts and modifies the receptor microdomain composition. *Biochim Biophys Acta*, Vol. 1778, No. 1, (2008), pp 250-9
Salani, B, Briatore, L, Contini, P, Passalacqua, M, Melloni, E et al. (2009). IGF-I induced rapid recruitment of integrin beta1 to lipid rafts is Caveolin-1 dependent. *Biochem Biophys Res Commun*, Vol. 380, No. 3, (2009), pp 499-92
Sauer, LA, Blask, DE & Dauchy, RT (2007). Dietary factors and growth and metabolism in experimental tumors. *J Nutr Biochem*, Vol. 18, No. 10, (2007), pp 637-49
Schabath, H, Runz, S, Joumaa, S & Altevogt, P (2006). CD24 affects CXCR4 function in pre-B lymphocytes and breast carcinoma cells. *J Cell Sci*, Vol. 119, No. Pt 2, (2006), pp 314-25
Schley, PD, Brindley, DN & Field, CJ (2007). (n-3) PUFA alter raft lipid composition and decrease epidermal growth factor receptor levels in lipid rafts of human breast cancer cells. *J Nutr*, Vol. 137, No. 3, (2007), pp 548-53

Schley, PD, Jijon, HB, Robinson, LE & Field, CJ (2003). Mechanisms of omega-3 fatty acid-induced growth inhibition in MDA-MB-231 human breast cancer cells. *Breast Cancer Res Treat*, Vol. 82, No. 2, (2003), pp 187-95
Schuck, S & Simons, K (2004). Polarized sorting in epithelial cells: raft clustering and the biogenesis of the apical membrane. *J Cell Sci*, Vol. 117, No. Pt 25, (2004), pp 5955-64
Simons, K & Ikonen, E (1997). Functional rafts in cell membranes. *Nature*, Vol. 387, No. 6633, (1997), pp 569-72
Simons, K & Toomre, D (2000). Lipid rafts and signal transduction. *Nat Rev Mol Cell Biol*, Vol. 1, No. 1, (2000), pp 31-9
Singleton, PA & Bourguignon, LY (2004). CD44 interaction with ankyrin and IP3 receptor in lipid rafts promotes hyaluronan-mediated Ca2+ signaling leading to nitric oxide production and endothelial cell adhesion and proliferation. *Exp Cell Res*, Vol. 295, No. 1, (2004), pp 102-18
Smith, MC, Luker, KE, Garbow, JR, Prior, JL, Jackson, E et al. (2004). CXCR4 regulates growth of both primary and metastatic breast cancer. *Cancer Res*, Vol. 64, No. 23, (2004), pp 8604-12
Song, J, Sapi, E, Brown, W, Nilsen, I, Tartaro, K et al. (2000). Roles of Fas and Fas ligand during mammary gland remodeling. *J Clin Invest*, Vol. 106, No. 10, (2000), pp 1209-20
Song, IH, Tse, MC, Bellail, A, Phuphanich, S, Khuri, F et al. (2007). Lipid rafts and nonrafts mediate tumor necrosis factor related apoptosis-inducing ligand induced apoptotic and nonapoptotic signals in non small cell lung carcinoma cells. *Cancer Res*, Vol. 67, No. 14, (2007), pp 6946-55
Storch, CH, Ehehalt, R, Haefeli, WE & Weiss, J (2007). Localization of the human breast cancer resistance protein (BCRP/ABCG2) in lipid rafts/caveolae and modulation of its activity by cholesterol in vitro. *J Pharmacol Exp Ther*, Vol. 323, No. 1, (2007), pp 257-64
Stuermer, CA, Langhorst, MF, Wiechers, MF, Legler, DF, Von Hanwehr, SH et al. (2004). PrPc capping in T cells promotes its association with the lipid raft proteins reggie-1 and reggie-2 and leads to signal transduction. *FASEB J*, Vol. 18, No. 14, (2004), pp 1731-3
Stubbs, EM, Huber, J, Leitinger, N, Imre, EM, Angelisova, P et al. (2001). Polyunsaturated eicosapentaenoic acid displaces proteins from membrane rafts by altering raft lipid composition. *J Biol Chem*, Vol. 276, No. 40, (2001), pp 37335-40
Tachibana, H, Koga, K, Fujimura, Y & Yamada, K (2004). A receptor for green tea polyphenol EGCG. *Nat Struct Mol Biol*, Vol. 11, No. 4, (2001), pp 380-1
Takebayashi, M, Hayashi, T & Su, TP (2004). Sigma-1 receptors potentiate epidermal growth factor signaling towards neuritogenesis in PC12 cells: potential relation to lipid raft reconstitution. *Synapse*, Vol. 53, No. 2, (2004), pp 90-103
Tang, Z, Scherer, PE, Okamoto, T, Song, K, Chu, C et al. (1996). Molecular cloning of caveolin-3, a novel member of the caveolin gene family expressed predominantly in muscle. *J Biol Chem*, Vol. 271, No. 4, (1996), pp 2255-61
Tavernarakis, N, Driscoll, M & Kyrpides, NC (1999). The SPFH domain: implicated in regulating targeted protein turnover in stomatins and other membrane-associated proteins. *Trends Biochem Sci*, Vol. 24, No. 11, (1999), pp 425-7

Trau, D, Carpentier, JL, Sawano, F, Gorden, P & Orci, L (1987). Ligands internalized through coated or noncoated invaginations follow a common intracellular pathway. *Proc Natl Acad Sci U S A*, Vol. 84, No. 23, (1987), pp 7957-61
Troyer, KL & Lee, DC (2001). Regulation of mouse mammary gland development and tumorigenesis by the ERBB signaling network. *J Mammary Gland Biol Neoplasia*, Vol. 6, No. 1, (2001), pp 7-21
Tzahar, E, Waterman, H, Chen, X, Levkowitz, G, Karunagaran, D et al. (1996). A hierarchical network of interreceptor interactions determines signal transduction by Neu differentiation factor/neuregulin and epidermal growth factor. *Mol Cell Biol*, Vol. 16, No. 10, (1996), pp 5276-87
van der Voort, R, Taher, TE, Wielenga, VJ, Spaargaren, M, Prevo, R et al. (1999). Heparan sulfate-modified CD44 promotes hepatocyte growth factor/scatter factor-induced signal transduction through the receptor tyrosine kinase c-Met. *J Biol Chem*, Vol. 274, No. 10, (1999), pp 6499-506
van Meer, G, Voelker, DR & Feigenson, GW (2008). Membrane lipids: where they are and how they behave. *Nat Rev Mol Cell Biol*, Vol. 9, No. 2, (2008), pp 112-24
Vanoosten, RL, Moore, JM, Ludwig, AT & Griffith, TS (2005). Depsipeptide (FR901228) enhances the cytotoxic activity of TRAIL by redistributing TRAIL receptor to membrane lipid rafts. *Mol Ther*, Vol. 11, No. 4, (2005), pp 542-52
Veiseh, O, Gunn, JW, Kievit, FM, Sun, C, Fang, C et al. (2009). Inhibition of tumor-cell invasion with chlorotoxin-bound superparamagnetic nanoparticles. *Small*, Vol. 5, No. 2, (2009), pp 256-64
Wan, J, Roth, AF, Bailey, AO & Davis, NG (2007). Palmitoylated proteins: purification and identification. *Nat Protoc*, Vol. 2, No. 7, (2007), pp 1573-84
Wang, B, Rosano, JM, Cheheltani, R, Achary, MP & Kiani, MF (2010). Towards a targeted multi-drug delivery approach to improve therapeutic efficacy in breast cancer. *Expert Opin Drug Deliv*, Vol. 7, No. 10, (2010), pp 1159-73
Wang, X, Wilson, MJ, Slaton, JW, Sinha, AA, Ewing, SL et al. (2009). Increased aggressiveness of human prostate PC-3 tumor cells expressing cell surface localized membrane type-1 matrix metalloproteinase (MT1-MMP). *J Androl*, Vol. 30, No. 3, (2009), pp 259-74
Webb, Y, Hermida-Matsumoto, L & Resh, MD (2000). Inhibition of protein palmitoylation, raft localization, and T cell signaling by 2-bromopalmitate and polyunsaturated fatty acids. *J Biol Chem*, Vol. 275, No. 1, (2000), pp 261-70
Weinberg, OK, Marquez-Garban, DC & Pietras, RJ (2005). New approaches to reverse resistance to hormonal therapy in human breast cancer. *Drug Resist Updat*, Vol. 8, No. 4, (2005), pp 219-33
Wersha, SJ & Haluska, P (2008). IGF-1 receptor inhibitors in clinical trials--early lessons. *J Mammary Gland Biol Neoplasia*, Vol. 13, No. 4, (2008), pp 471-83
Westover, EJ, Covey, DF, Brockman, HL, Brown, RE & Pike, LJ (2003). Cholesterol depletion results in site-specific increases in epidermal growth factor receptor phosphorylation due to membrane level effects. Studies with cholesterol enantiomers. *J Biol Chem*, Vol. 278, No. 51, (2003), pp 51125-33
Worthylake, R, Opresko, LK & Wiley, HS (1999). ErbB-2 amplification inhibits down-regulation and induces constitutive activation of both ErbB-2 and epidermal growth factor receptors. *J Biol Chem*, Vol. 274, No. 13, (1999), pp 8865-74

Wysoczynski, M., Reca, R., Ratajczak, J., Kucia, M., Shirvaikar, N. et al. (2005). Incorporation of CXCR4 into membrane lipid rafts primes homing-related responses of hematopoietic stem/progenitor cells to an SDF-1 gradient. *Blood*, Vol. 105, No. 1, (2005), pp. 40-8

Yamada, E. (1955). The fine structure of the renal glomerulus of the mouse. *J Biophys Biochem Cytol*, Vol. 1, No. 6, (1955), pp. 551-66

Yamaguchi, H., Takeo, Y., Yoshida, S., Kouchi, Z., Nakamura, Y. et al. (2009). Lipid rafts and caveolin-1 are required for invadopodia formation and extracellular matrix degradation by human breast cancer cells. *Cancer Res.*, Vol. 69, No. 22, (2009), pp. 8594-602

Yang, A., Wilson, NS & Ashkenazi, A. (2010). Proapoptotic DR4 and DR5 signaling in cancer cells: toward clinical translation. *Curr Opin Cell Biol*, Vol. 22, No. 6, (2010), pp. 837-44

Yaqoob, P. (2009). The nutritional significance of lipid rafts. *Annu Rev Nutr*, Vol. 29, No. (2009), pp. 257-82

Breast Cancer - Carcinogenesis, Cell Growth and Signalling Pathways
Edited by Prof. Mehmet Gunduz

ISBN 978-953-307-714-7
Hard cover, 732 pages
Publisher InTech
Published online 30, November, 2011
Published in print edition November, 2011

Cancer is the leading cause of death in most countries and its consequences result in huge economic, social and psychological burden. Breast cancer is the most frequently diagnosed cancer type and the leading cause of cancer death among females. In this book, we discussed various aspects of breast cancer carcinogenesis from clinics to its hormone-based as well as genetic-based etiologies for this deadly cancer. We hope that this book will contribute to the development of novel diagnostic as well as therapeutic approaches.

INTECH

InTech Europe
University Campus STeP Ri
Slavka Krautzeka 83/A
51000 Rijeka, Croatia
Phone: +385 (51) 770 447
Fax: +385 (51) 686 166
www.intechopen.com

InTech China
Unit 405, Office Block, Hotel Equatorial Shanghai
No.65, Yan An Road (West), Shanghai, 200040, China
中国上海市延安西路65号上海国际贵都大饭店办公楼405单元
Phone: +86-21-62489820
Fax: +86-21-62489821

Lipid rafts are disrupted in mildly inflamed intestinal microenvironments without overt disruption of the epithelial barrier

Rachel V. Bowie, Simona Donatello, Clíona Lyes, Mark B. Owens, Irina S. Babina, Lance Hudson, Shaun V. Walsh, Diarmuid P. O'Donoghue, Sylvie Amu, Sean P. Barry, Padraic G. Fallon and Ann M. Hopkins

Am J Physiol Gastrointest Liver Physiol 302:G781-G793, 2012. First published 12 January 2012; doi: 10.1152/ajpgi.00002.2011

Am J Physiol Gastrointest Liver Physiol 302: G781–G793, 2012.
First published January 12, 2012; doi:10.1152/ajpgi.00002.2011.

Lipid rafts are disrupted in mildly inflamed intestinal microenvironments without overt disruption of the epithelial barrier

Rachel V. Bowie,[1]* Simona Donatello,[1]* Cliona Lyes,[1]* Mark B. Owens,[1] Irina S. Babina,[1] Lance Hudson,[1] Shaun V. Walsh,[2] Diarmuid P. O'Donoghue,[3] Sylvie Amu,[4] Sean P. Barry,[4] Padraic G. Fallon,[4] and Ann M. Hopkins[1]

[1]*Department of Surgery, Royal College of Surgeons in Ireland;* [2]*Department of Pathology, Ninewells Hospital, Dundee, Scotland;* [3]*Centre for Colorectal Disease, St. Vincent's University Hospital, Dublin; and* [4]*Institute of Molecular Medicine, St. James's Hospital, Trinity College Dublin, Ireland.*

Submitted 7 January 2011; accepted in final form 10 January 2012

Bowie RV, Donatello S, Lyes C, Owens MB, Babina IS, Hudson L, Walsh SV, O'Donoghue DP, Amu S, Barry SP, Fallon PG, Hopkins AM. Lipid rafts are disrupted in mildly inflamed intestinal microenvironments without overt disruption of the epithelial barrier. *Am J Physiol Gastrointest Liver Physiol* 302: G781–G793, 2012. First published January 12, 2012; doi:10.1152/ajpgi.00002.2011.—Intestinal epithelial barrier disruption is a feature of inflammatory bowel disease (IBD), but whether barrier disruption precedes or merely accompanies inflammation remains controversial. Tight junction (TJ) adhesion complexes control epithelial barrier integrity. Since some TJ proteins reside in cholesterol-enriched regions of the cell membrane termed lipid rafts, we sought to elucidate the relationship between rafts and intestinal epithelial barrier function. Lipid rafts were isolated from Caco-2 intestinal epithelial cells primed with the proinflammatory cytokine interferon-γ (IFN-γ) or treated with methyl-β-cyclodextrin as a positive control for raft disruption. Rafts were also isolated from the ileal mucosa of mice in which colitis had been induced in conjunction with in vivo intestinal permeability measurements, and lastly from intestinal biopsies of ulcerative colitis (UC) patients with predominantly mild or quiescent disease. Raft distribution was analyzed by measuring activity of the raft-associated enzyme alkaline phosphatase and by performing Western blot analysis for flotillin-1. Epithelial barrier integrity was estimated by measuring transepithelial resistance in cytokine-treated cells or in vivo permeability to fluorescent dextran in colitic mice. Raft and nonraft fractions were analyzed by Western blotting for the TJ proteins occludin and zonula occludens-1 (ZO-1). Our results revealed that lipid rafts were disrupted in IFN-γ-treated cells, in the ileum of mice with subclinical colitis, and in UC patients with quiescent inflammation. This was not associated with a clear pattern of occludin or ZO-1 relocalization from raft to nonraft fractions. Significantly, a time-course study in colitic mice revealed that disruption of lipid rafts preceded the onset of increased intestinal permeability. Our data suggest for the first time that lipid raft disruption occurs early in the inflammatory cascade in murine and human colitis and, we speculate, may contribute to subsequent disruption of epithelial barrier function.

epithelium; barrier function; tight junction; colitis; adhesion

THE INTESTINAL EPITHELIAL barrier separates the contents of the gut lumen from the interstitium. Barrier function is maintained via protein-protein interactions between neighboring cells at adhesion sites called tight junctions (TJs). The dynamic intercellular seal formed by TJs creates a polarized semipermeable barrier across which the traffic of nutrients and antigenic particles is tightly regulated (31, 33). Accordingly, the integrity of the intestinal epithelial barrier is a crucial determinant of mucosal homeostasis (39), and impaired epithelial barrier function has been implicated in mucosal inflammatory disorders including Crohn's disease and ulcerative colitis (UC) (35, 48).

It remains controversial whether epithelial barrier dysfunction is a primary cause or merely a consequence of inflammatory bowel disease (IBD). In vivo patient evidence has argued both for (15, 17, 34) and against (41, 54) a role for altered intestinal permeability in the etiology of IBD. Recent work in mouse models has echoed the conflict, with reports that permeability alterations precede the onset of colitis in IL-10 knockout mice (29, 47), whereas loss of barrier function alone is insufficient to induce murine colitis in mice constitutively overexpressing myosin light chain kinase in the intestinal epithelium (52). Intermodel variability serves to illustrate the complexity of the problem and to highlight that much remains to be understood about the regulation of epithelial adhesion complexes and barrier function during intestinal inflammation.

Some key TJ proteins reside in subdomains of the plasma membrane known as detergent-resistant membranes or lipid rafts (42). Lipid rafts are unique biophysical entities enriched in glycosphingolipids, cholesterol, and sphingomyelin, giving them a "liquid-ordered" state resulting from tighter packing of these lipids relative to the "liquid-disordered" state of phospholipids in the bulk plasma membrane (4, 13). Raft localization of some TJ proteins involves cholesterol-mediated stabilization within the membrane (20). Accordingly, interference with cellular cholesterol levels can profoundly impact TJ assembly and the establishment of barrier function (11, 21, 25–27).

However, little is known about the potential regulatory influence of lipid rafts on epithelial adhesion and barrier function under inflammatory conditions. Displacement of the TJ protein junction adhesion molecule-A from raft fractions has been noted in intestinal epithelial cells exposed to a combination of the proinflammatory cytokines IFN-γ and TNF-α (6), and the same cytokines have been shown to alter the lipid composition of membrane microdomains (22). Therefore our study investigated the relationship between raft integrity, barrier function, and an inflammatory microenvironment using three complementary models: intestinal epithelial cells primed with a proinflammatory barrier-disrupting cytokine, mouse models of colitis, and human intestinal IBD biopsies. We focused on experimental conditions best described as early inflammatory or primed for inflammation, to dissect events that might precede epithelial barrier disruption rather than accom-

* R. V. Bowie, S. Donatello, and C. Lyes contributed equally to this work.
Address for reprint requests and other correspondence: A. Hopkins, Dept. of Surgery, Royal College of Surgeons in Ireland, RCSI Education & Research Centre, Beaumont Hospital, Dublin 9, Ireland (e-mail: annhopkins@rcsi.ie).

Table 1. *Profiles of biopsy patients in pilot study*

Patient	Sex	Age	Biopsy Histopathology
Control 1	Female	61	Normal
Control 2	Female	46	Normal
Control 3	Female	63	Normal
UC 1	Female	26	Quiescent UC, normal biopsy
UC 2	Female	67	Quiescent UC, normal biopsy
UC 3	Female	58	Mild inflammation

UC, ulcerative colitis.

pany it. This study reports for the first time that lipid raft disruption is a feature of all three inflammatory microenvironments and provides novel evidence that raft disruption precedes the loss of barrier function in colitic mice. Given that rafts are sensitive to alterations in lipid balance (22) and that dietary modulation of lipid balance reportedly influences the course of human IBD (55), this may merit further investigation into the role of lipid rafts in modifying early-stage inflammatory events associated with IBD.

MATERIALS AND METHODS

Cell culture and treatments. Caco-2 cells were obtained from ATCC and maintained in DMEM plus Glutamax, containing 4,500 mg/l D-glucose (Invitrogen, Paisley, UK) supplemented with 10% (vol/vol) fetal bovine serum (Lonza, Basel, Switzerland), 1% (vol/vol) MEM nonessential amino acids (Invitrogen), 100 U/ml penicillin, and 100 μg/ml streptomycin (Invitrogen). Cultures were subcultured with 0.05% trypsin-EDTA (Invitrogen) and grown either on 0.33 cm^2 polyester Transwell filters (0.4 μm pores, Costar) or on 10-cm dishes. Once filters reached a high stable transepithelial resistance (measured using an EndOhm-6; World Precision Instruments), they were treated for 7 days with the anti-inflammatory cytokine interleukin-10 (IL-10, 10 ng/ml; R&D Systems) or for 5 days with the proinflammatory cytokine interferon-γ (IFN-γ, 150 U/ml; R&D Systems). In combination experiments, cells were incubated with IFN-γ and IL-10 for 5 days following 2 days of pretreatment with IL-10. Control cells were treated with vehicle alone (sterile water/0.1% bovine serum albumin; Sigma). As a positive control for lipid raft disruption, some filters were treated bilaterally for 30 min with 10 mM methyl-β-cyclodextrin (MβCD, Sigma) and some dishes were treated for 3 h with 3 mM MβCD.

Preparation of intestinal mucosal lysates from colitic mice. Ileal tissues were excised from two separate mouse models of colitis in parallel with ileal from age- and sex-matched control animals. In the first model, 8- to 10-wk-old C57/BL6 mice were treated for 3 days with 2% dextran sulfate salts (DSS; MP Biomedicals, OH) in drinking water to initiate colitis (10, 50). In complementary experiments, mice were treated with DSS for either 0, 3, or 5 days and assessed in parallel for intestinal permeability (see *Mouse intestinal in vivo permeability assay*) or lipid raft status. The second model used 10- to 12-wk-old Balb/c mice genetically engineered to lack the IL-10 gene, in which colitis spontaneously develops from 10 to 12 wk (10, 19). The ileum was opened along the mesenteric border and irrigated in ice-cold HBSS/10 mM HEPES to remove the luminal contents. Tissues were washed and agitated for 5 min in Ca^{2+}-free isolation buffer (30 mM EDTA, 52 mM NaCl, 5 mM KCl, 10 mM HEPES, 2 mM DTT, and 60 mM HCl, pH 7.1) (24), then minced and agitated for 2 × 10 min in isolation buffer at 4°C. Released cells were collected by centrifugation at 100 *g* for 10 min at 4°C. Mucosal isolates from DSS mice were resuspended in HBSS/10 mM HEPES containing 1% Triton X-100 and a protease inhibitor cocktail for lipid raft isolation. The nonionic detergent Triton X-100 was used in preference to stronger ionic detergents on the basis of the definition of lipid rafts as insoluble in cold nonionic detergents (38). Mucosal isolates from IL-10 knockout animals were resuspended in 500 mM sodium carbonate (pH 11) containing a protease inhibitor cocktail for detergent-free lipid raft isolation. In all cases, two ileа from each group were pooled per raft preparation. All animal experiments were performed in compliance with regulations issued by the Irish Department of Health and Children and were approved by the Trinity College BioResources ethical review board.

Mouse intestinal in vivo permeability assay. In vivo intestinal permeability to fluoresceinated dextran was assessed essentially as described (53). Briefly, mice exposed to 2% DSS for either 0, 3, or 5 days (2 per condition, $n = 3$ experiments) were orally gavaged with 0.6 mg/g body wt of fluorescein isothiocyanate (FITC)-labeled dextran (4 kDa; TdB Consultancy, Uppsala, Sweden). After 3.5 h the mice were euthanized and exsanguinated by cardiac puncture. Plasma FITC levels were subsequently determined by fluorometry.

Isolation of intestinal mucosal homogenates from human patient biopsies. In a pilot study, superficial mucosal biopsies were obtained from six patients attending a gastroenterology outpatients clinic: three controls and three UC patients (Table 1). Specimens were obtained with informed consent after full ethical approval had been granted by the Ethics and Medical Research Committee of St. Vincent's University Hospital, Dublin, Ireland. Control samples were obtained from healthy patients undergoing colonoscopy screening for cancer. Areas were sampled on the basis of macroscopically visible inflammation or the macroscopic appearance of healthy, normal tissue. Histopathological reports were later used to report the official diagnosis. Biopsies were immersed in ~2.5 ml ice-cold HBSS/HEPES containing 1% Triton X-100 and a protease inhibitor cocktail and mechanically disaggregated on ice with 35 strokes of a Dounce homogenizer followed by 15 passes through a 26-gauge needle. Lysates were rotated for 30 min at 4°C before being mixed with 60% sucrose for lipid raft preparation as described in *Lipid raft isolation from Caco-2 cells and DSS mouse mucosal lysates*.

We subsequently extended the study by obtaining mucosal biopsy specimens from 17 patients using the same methods and under the same ethical approval as above. Patient demographics are reported in Table 2 and in brief amounted to 5 control patients and 12 UC patients (of which 7 had inactive disease, 3 had active disease, and a further 2 had active disease but were biopsied in a macroscopically uninvolved area distal from the disease). Biopsies were transported, homogenized, rotated, and mixed with 60% sucrose exactly as above, but a slightly different procedure was used for isolation of lipid rafts as described below.

Table 2. *Profiles of biopsy patients in secondary study*

Patient	Sex	Age	Biopsy Histopathology
Control 1	Male	36	Normal
Control 2	Female	67	Normal
Control 3	Female	42	Normal
Control 4	Male	86	Normal
Control 5	Female	51	Normal
UC 1	Female	48	Inactive disease
UC 2	Male	47	Inactive disease
UC 3	Female	49	Inactive disease
UC 4	Male	57	Inactive disease
UC 5	Male	27	Inactive disease
UC 6	Female	71	Inactive disease
UC 7	Female	48	Inactive disease
UC 8	Female	83	Active disease
UC 9	Female	53	Active disease
UC 10	Male	48	Mildly active disease
UC 11	Female	55	Active disease, but uninvolved region sampled
UC 12	Male	29	Active disease, but uninvolved region sampled

Lipid raft isolation from Caco-2 cells and DSS mouse mucosal lysates. Isopycnic sucrose density gradient fractionation was used to isolate lipid rafts as described (42). Briefly, confluent Caco-2 cells (2 × 10 cm^2 petri dishes/condition) or mucosal lysate preparations from DSS and control animals were washed × 3 in ice-cold HBSS-10 mM HEPES and dounced × 20 in HBSS HEPES 1% Triton X-100 containing a protease inhibitor cocktail. Then 2 ml lysate was combined with 2 ml 60% (wt/vol) sucrose and transferred to a 12.5-ml ultraclear ultracentrifuge tube (Beckman Coulter, Galway, Ireland). This was overlaid with a linear 30–5% sucrose gradient and ultracentrifuged for 19 h (39,000 rpm, 4°C) in a Beckman Optima L-100K ultracentrifuge (SW41 rotor). Gradients were fractionated by use of a model 2110 Fraction Collector (Bio-Rad, Hemel Hempstead, UK), ensuring that any cloudy bands were collected in a single fraction. Pellets were solubilized in 500 μl 0.5% SDS (Sigma).

Detergent-free lipid raft isolation from mucosal lysates of IL-10 knockout mice. Mucosal lysates from IL-10 knockout mice or age- and sex matched wild type mice were resuspended in 500 mM sodium carbonate (pH 11) containing a protease inhibitor cocktail, dounced and triturated 20 times, and rotated at 4°C for 20 min. Lysates were mixed with an equivalent volume of 90% sucrose (in 250 mM sodium carbonate pH 11), and 740 μl were placed at the bottom of a microultracentrifuge tube. The 490 μl volumes of 30, 20, and 5% sucrose (all prepared in 250 mM sodium carbonate pH 11) were sequentially layered on top and tubes were ultracentrifuged for 19 h (52,000 rpm, 4°C) in a Sorvall M120EX microultracentrifuge (RP55S rotor). Six equal volume fractions were removed, and the pellet was resuspended in the same volume of 0.5% SDS before being analyzed as described in *Analysis of Lipid raft gradient fractions*.

Lipid raft isolation from human mucosal homogenates. For our pilot study, human mucosal homogenates were combined with equivalent volumes of 60% sucrose (prepared in HBSS/10 mM HEPES), of which 740 μl was placed at the bottom of a microultracentrifuge tube and layered sequentially with 490 μl of 30% sucrose, 20% sucrose, and finally 5% sucrose. Gradients were ultracentrifuged in a Sorvall M120EX microultracentrifuge and fractionated into six equal fractions plus an SDS-solubilized pellet.

For the larger population of 17 patient samples, full size continuous sucrose gradients of 12 ml volume were poured exactly as described for the Caco-2 and DSS preparations and centrifuged as described in a Beckman SW41 rotor before being fractionated into 12 equal volume fractions and analyzed as above.

Analysis of lipid raft gradient fractions. Sucrose density was read in 2 μl volumes of all fractions via a hand held refractometer (Bellingham-Stanley). Raft-enriched fractions were identified on the basis of a peak in activity of the raft-associated enzyme alkaline phosphatase. Briefly, 20 μl fractions were incubated with *p* nitrophenyl phosphate substrate (SigmaFast, Sigma) at 37°C for at least 1 h. Yellow coloration, indicative of alkaline phosphatase activity, was quantitated at 405 nm on a Wallac Victor^2 1420 plate reader (Perkin Elmer). Protein concentrations in each fraction were determined by the bicinchoninic acid method (Pierce), relative to a standard curve of bovine serum albumin.

Electrophoresis and Western blotting. Representative raft and nonraft fractions from sucrose gradients were subjected to SDS-polyacrylamide gel electrophoresis, transferred to nitrocellulose membranes under constant voltage and Western blotted as described (16) for the lipid raft marker flotillin-1 and the TJ proteins occludin and zonula occludens 1 (ZO-1). Equivalent protein concentrations (5–40 μg) were run for human gradients, and equivalent volumes were run for gradients from cytokine-treated cells and mouse samples. Antibodies were obtained from BD Biosciences (flotillin-1 mouse IgG), Invitrogen (occludin and ZO-1 rabbit IgGs), and Sigma (horseradish peroxidase-conjugated goat anti-mouse or goat anti-rabbit IgG secondaries). Signals were detected by enhanced chemiluminescence using Western Lightning (Perkin-Elmer) and Kodak film.

Immunofluorescence confocal microscopy. Caco-2 cells grown to confluence on permeable supports (as described above) were treated for 2 h with 10 mM MβCD or vehicle (sterile water), then fixed in paraformaldehyde (3.7%; 10 min) and permeabilized with Triton X-100 (0.5%; 30 min). Cells were blocked in goat serum (5%; 1 h) and stained for F-actin and the nuclei with Alexa Fluor-488 phalloidin (0.3 U/ml; 1 h) followed by DAPI (1 μg/ml; 10 min). Filters were mounted in *p*-phenylenediamine hydrochloride-PBS-glycerol (0.01:1:1 vol/vol/vol) antifade reagent and examined on a Zeiss LSM 510-Meta confocal microscope.

Statistical analysis. Quantitative data are expressed as means ± SE, with *n* numbers and internal replicates indicated in the figure legends. Statistical analysis was done by two-sample equal-variance Student's *t*-tests, with significance assumed at $P < 0.05$.

RESULTS

Mild reductions in intestinal epithelial cell barrier function are accompanied by lipid raft disruption. Epithelial barrier function was evaluated by the measurement of transepithelial electrical resistance (TER) in confluent, polarized Caco-2 intestinal epithelial cells that had been exposed to combinations of the proinflammatory cytokine IFN-γ (to disrupt barrier function) and the anti-inflammatory cytokine IL-10 as a control reagent that should not damage barrier function. As shown in Fig. 1*A*, TER of control (vehicle-treated) cells at *day 7* was ~100% of the *day 0* value. Similarly, IL-10 treatment for 7 days did not alter baseline TER values. However, exposure to IFN-γ for 5 days caused a subtle but statistically significant reduction in TER, to 70 ± 10% of baseline values. Transepithelial permeation of the paracellular marker fluoresceinated dextran (3,000 Da) was also increased in IFN-γ-treated cells relative to controls (data not shown). Cells that had been preexposed to IL-10 for 2 days followed by 5 days of coexposure to IL-10 and IFN-γ also showed reductions in TER that were comparable with those induced by IFN-γ alone (to 66 ± 10% of baseline values by *day 7*). In contrast, treatment of Caco-2 cells with the lipid raft disrupting agent MβCD for just 30 min virtually abrogated TER. The dramatic compromise in intestinal epithelial barrier function induced by MβCD could not be accounted for by necrotic cell death (as estimated by MTT assay), since the viability of Caco-2 cells treated with 10 mM MβCD was >97% even after 3-h exposure (Supplemental Fig. S3*A*). There was also no evidence of death by apoptosis secondary to MβCD treatment, as confirmed by the absence of cleaved caspase-3 staining in Caco-2 cells treated for 30 min with 10 mM MβCD, relative to a positive control of etoposide (200 μM for 24 h; Supplemental Fig. S3*B*). However, cellular polarity was disrupted by MβCD treatment, with evidence of multilayering in *xz* confocal micrographs of treated relative to control cells (Fig. 1*A*, *inset*).

Since barrier function is regulated by membrane proteins in the TJ, some of which have been shown to affiliate with lipid rafts (42), we next tested whether the mild reductions in barrier function featured disruption of membrane lipid rafts. Isopycnic density gradient centrifugation was used to isolate lipid rafts from Caco-2 monolayers treated with the cytokine combinations described above, or with 3 mM MβCD to induce raft disruption. Figure 1*B* represents the profiles of fractions isolated from sucrose gradients: the *left* panel shows an equivalent (predictable) increase in sucrose density with increasing fraction number across all gradients. Similarly, the protein concentration across all gradients was similar (*middle*), being very

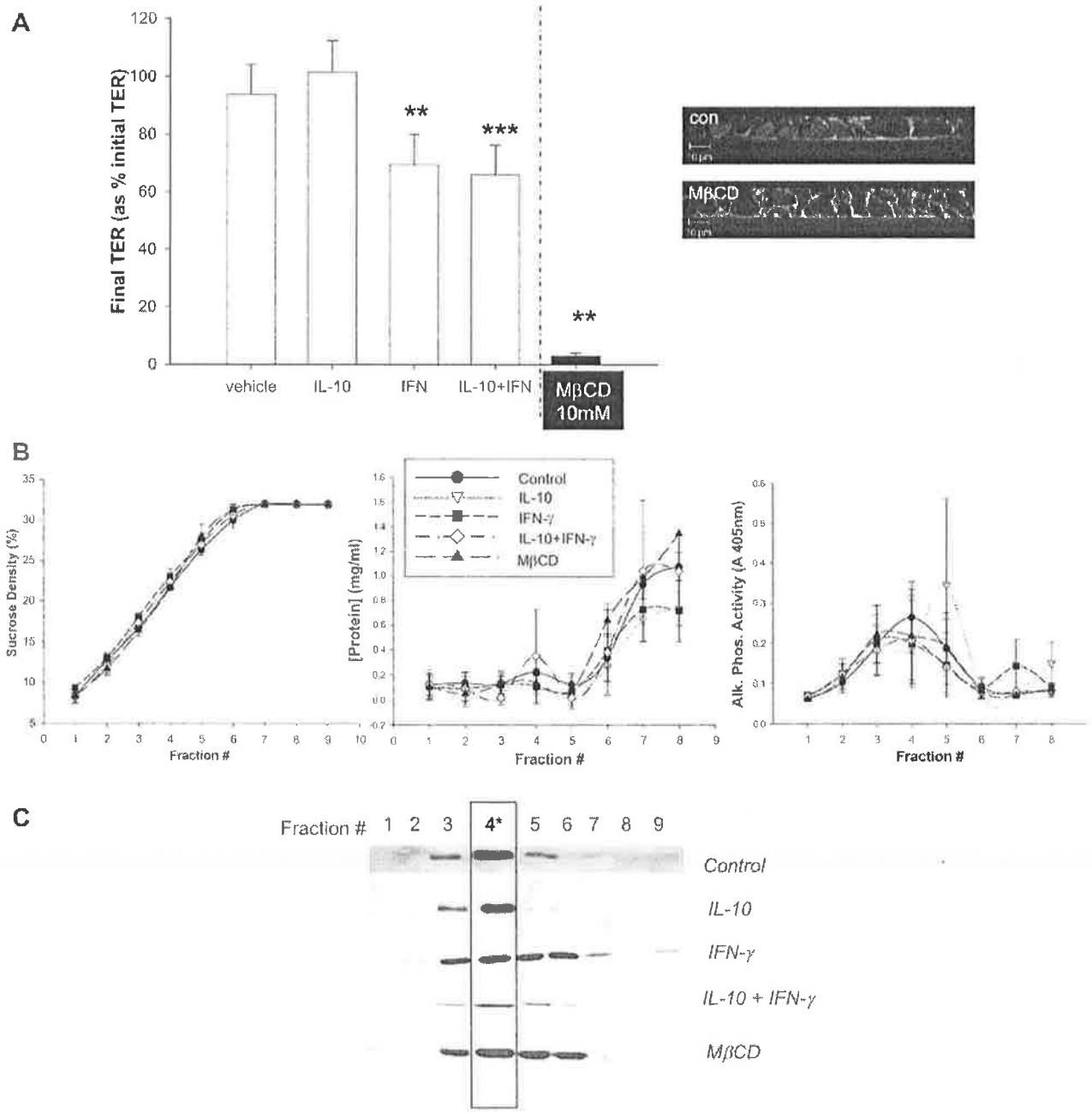

Fig. 1. Lipid rafts are disrupted in Caco-2 intestinal epithelial monolayers primed with the proinflammatory cytokine interferon-γ (IFN-γ). *A*: filter-grown confluent Caco-2 intestinal epithelial monolayers were exposed bilaterally to interleukin-10 (IL-10; 10 ng/ml; 7 days) ± IFN-γ (150 U/ml; *days 3–7*) or vehicle, and posttreatment transepithelial electrical resistances (TER) expressed as % of pretreatment values. Both IFN-γ and IL-10+IFN-γ significantly reduced Caco-2 TER, but to a lesser extent than the lipid raft-disrupting reagent methyl-β-cyclodextrin (MβCD; 10 mM; 30 min). The graph represents means ± SE of 4 independent experiments, with ≥2 filters/experiment (**$P < 0.01$; ***$P < 0.001$). *Inset*: in x-z confocal micrographs of cells treated with MβCD (10 mM; 2 h) vs. vehicle control (con), it was seen that MβCD treatment disrupted cell polarity. *B*: confluent Caco-2 cells on 10-cm tissue culture dishes were exposed to IL-10 (10 ng/ml; 7 days) ± IFN-γ (150 U/ml; *days 2–7*) or vehicle. Lipid rafts were isolated by sucrose density gradient fractionation, and fractions analyzed for sucrose density, protein concentration and activity of the raft marker enzyme alkaline phosphatase. Alkaline phosphatase (Alk. Phos.) activity was enriched in a single fraction from control preparations, whereas in IFN-γ- or MβCD-treated preparations it was spread across 2–3 fractions with approximately equal intensity. Graphs represent means ± SE of 3 independent experiments. *C*: gradient fractions as above were blotted for the lipid raft marker protein flotillin-1. Flotillin-1 was strongly enriched in a single fraction from control cells, but spread equally across several fractions in cells treated with IFN-γ ± IL-10 or MβCD. *Lipid raft fractions compared with control gradients.

dilute in earlier fractions and most concentrated in the higher fraction numbers (≥30% sucrose density).

Alkaline phosphatase activity (Fig. 1*B*, *right*) was used as an indicator of the presence of rafts, due to the enrichment of this membrane enzyme in lipid rafts (38). A single peak of alkaline phosphatase activity was observed in *fraction 4* of control samples (and *fraction 5* of IL-10-treated samples), suggesting that rafts were strongly enriched in a single fraction (~22–26% sucrose). In contrast, gradients isolated from cells treated with IFN-γ (alone or in combination with IL-10) showed equivalent alkaline phosphatase activity across multiple fractions, not peaking in a single one. A similarly broad distribution was observed in MβCD-treated cells, suggesting that both treatments disrupted lipid rafts and prevented their predominant recovery from a single gradient fraction. To further test this, equivalent volumes of sequential gradient fractions were probed by Western blotting for the lipid raft marker flotillin-1 (Fig. 1*C*). Although protein concentrations in the lower fractions (*fractions 1–5*) were negligible compared with those in the higher fractions (*fractions 6–9*), flotillin-1 was strongly enriched in a single fraction (*fraction 4*) in both control and IL-10 gradients. In contrast, flotillin-1 was equally spread across *fractions 3–6* in gradients from IFN-γ-treated cells and MβCD-treated cells. Lack of flotillin-1 enrichment in a single fraction of either cytokine-treated and MβCD-treated cells suggested similar levels of raft disruption, although only MβCD treatment caused a significant depletion of cholesterol from Caco-2 cells whereas IFN-γ treatment did not (data not shown).

Since the disruption of Caco-2 barrier function obtained with IFN-γ was relatively modest, we also exposed filter-grown Caco-2 cells to concentrations of IFN-γ ranging from 50 to 1,000 U/ml. As shown in Supplemental Fig. S1*A*, IFN-γ evoked concentration-dependent reductions in TER, which after 5 days exposure were statistically different from controls at concentrations ≥150 U/ml (the concentration used in our studies). A time-dependent component to TER reductions induced by IFN-γ was also evident (Supplemental Fig. S1*B*). Specifically, whereas TER of control filters and those treated with the lowest concentration of IFN-γ (50 U/ml) remained stable or increased over 7 days, TER of filters treated with IFN-γ concentrations ≥150 U/ml gradually decreased after 3 days' exposure and plateaued at 5–7 days.

To begin interrogating potential links between IFN-induced reductions in barrier function and lipid raft status, in a proof-of-principle experiment we performed isopycnic density gradient fractionation on Caco-2 cells treated for 7 days with each of the indicated concentrations of IFN-γ. As shown in Supplemental Fig. S2*A*, the profiles of fractions isolated from each condition were relatively similar in terms of sucrose density (*left*), protein concentrations (*middle*), and alkaline phosphatase intensity (*right*). However, densitometric quantification of expression of the lipid raft marker flotillin-1 in each of the gradient fractions (represented per unit protein concentration; Supplemental Fig. S2*B*) revealed flotillin expression to be highest in raft *fraction 5* of control conditions, with less flotillin expression in the same fraction of all IFN-treated conditions. Another difference was that flotillin expression dropped very sharply in *fraction 6* of controls but remained in two adjacent fractions of all IFN-treated conditions (suggesting a potential dispersal of rafts). Finally, analysis of occludin expression in equivalent volume fractions (Supplemental Fig. S2*C*) revealed enriched recovery in *fraction 5* of control conditions (in light of the very low protein concentration in this sample) and also high levels recovered at the highest sucrose densities at the bottom of the gradient. Strikingly, occludin was recovered additionally in *fractions 3* and *4* of all IFN-treated gradients (corresponding to a very low sucrose density of only 11–18% at which occludin is never normally recovered). This provides suggestive evidence of raft dispersal or disruption in a concentration-independent fashion in response to IFN-γ treatment even at concentrations before barrier disruption is evident.

Lipid rafts are disrupted in two mouse models of colitis even without histological evidence of inflammation. Having demonstrated that lipid raft disruption was associated with mild epithelial barrier dysfunction in intestinal epithelial cells primed with the proinflammatory cytokine IFN-γ, we next wanted to determine whether lipid raft disruption was associated with in vivo intestinal inflammation. We first utilized a DSS mouse model of colitis, in which mice were exposed to 2% DSS for 3 days. Lipid rafts could not be successfully isolated from the colon (data not shown) even at this early stage when the DSS-treated mice had not yet developed overt colitis-like symptoms [as assessed via a disease activity index score involving weight loss, presence of diarrhea, and blood in feces (50)]. Therefore we harvested the ilea for lipid raft isolation, because, although the ileum of DSS mice traditionally is histologically uninflamed, it is nonetheless within an inflammatory microenvironment in the intestine as a whole. As shown in Fig. 2*A*, hematoxylin- and eosin-stained sections taken through the proximal, mid, and distal ileum and examined by a histopathologist (S. V. Walsh) confirmed no histological differences between 3-day DSS-treated and control mice. In particular, no evidence of cryptitis, crypt abscess, ulceration or excess chronic inflammatory cells was seen in the DSS animals. Villi remained tall and slender, mitotic cells were confined to the basal compartment of the crypts, and there was no change in Paneth cell or goblet cell numbers.

Epithelial lysates harvested from control and DSS mice ilea were then subjected to sucrose density gradient fractionation, whereupon characterization of the gradient fractions revealed similar sucrose density and protein concentration profiles between treatment groups (Fig. 2*B*, *left* and *middle*, respectively). The only exception was that protein concentration dropped off in the higher sucrose density fractions of DSS samples relative to controls.

When lipid raft recovery was analyzed in DSS relative to control gradients, a peak of alkaline phosphatase activity was observed in a single fraction of control preparations (Fig. 2*B*, *right*), suggesting a high density of rafts harvested from control preparations. Alkaline phosphatase activity did not peak in a single fraction of IFN-γ- or MβCD-treated preparations but was recorded at approximately equivalent levels across two to three fractions. When equivalent fraction volumes were immunoblotted for flotillin-1, enrichment of the raft marker in a single fraction of control gradients was observed (Fig. 2*C*). It is interesting to note that the raft-enriched fraction, *fraction 4*, had a total protein content of approximately four- to fivefold less than that of *fractions 8* and *9*, which contained no detectable flotillin-1. In contrast to control gradients, flotillin-1 expression in DSS gradients was not enriched in a single fraction

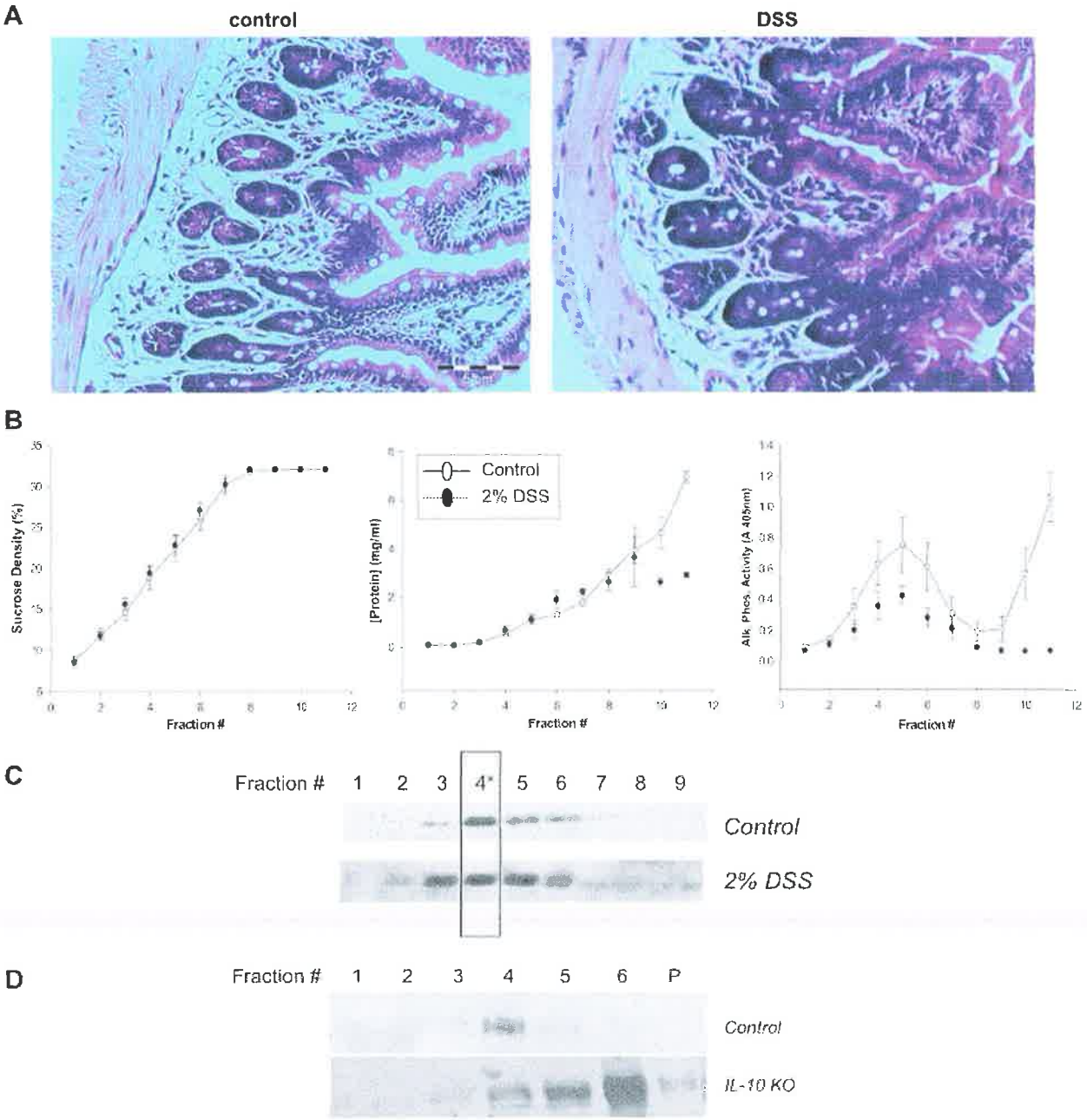

Fig. 2. Small intestinal lipid rafts are disrupted in mucosal preparations from mice with mild colitis. *A*: hematoxylin/eosin-stained small intestinal mucosal sections of C57/BL6 mice exposed for 3 days to 2% dextran sulfate salts (DSS) or control mice. No evidence of inflammation was observed in DSS sections relative to controls. *B*: lipid rafts were isolated from the ileal mucosa of C57/BL6 mice exposed for 3 days to 2% DSS or control mice, and gradient fractions were analyzed for sucrose density, protein concentration, and activity of the raft marker enzyme alkaline phosphatase. Peak alkaline phosphatase activity was reduced in fractions from DSS mice. Graphs represent means ± SE of 5 independent gradients (2 mice per gradient). *C*: gradient fractions as above were blotted for the lipid raft marker protein flotillin-1. The distribution of flotillin-1 was broader in DSS-treated mice fractions relative to controls. *, Lipid raft fraction. *D*: lipid rafts were isolated from the ileal mucosa of IL-10 knockout mice and wild-type controls by using a detergent-free method of sucrose density gradient fractionation. Equivalent volumes of gradient fractions were electrophoretically separated and blotted for flotillin-1. A broader distribution of flotillin-1 was observed in IL-10 knockout gradients relative to controls. P, pellet.

but rather recovered at equivalent band densities across multiple fractions. This suggested a disruption of lipid rafts rather than a global increase in flotillin-1 expression levels, since total flotillin-1 levels in control and DSS lysates were similar to each other (data not shown).

To exclude the possibility that lipid raft disruption in the uninflamed ileal of DSS mice was artifactual, we utilized a second mouse model and an alternative lipid raft isolation strategy. Lipid rafts were isolated from the ileal of mice genetically deficient in IL-10, in which mild low-grade inflammation

had developed in the colon. Ileal inflammation in these animals is possible but rare, and in our animals no ileal inflammation was observed at a histological level (data not shown). When detergent-free lipid raft gradients were prepared and analyzed by Western blotting, we detected strong enrichment of flotillin-1 in a single fraction of control gradients (Fig. 2*D*). In contrast, flotillin-1 bands were dispersed among several gradient fractions prepared from IL-10 knockout mice, being enriched in high sucrose density fractions (>32%) rather than the 22–26% sucrose density fractions in which rafts are characteristically found. Taken together with our previous observations, this supported the hypothesis that lipid raft disruption occurs even in uninflamed/uninvolved areas of the intestine within an inflammatory intestinal microenvironment.

To better interrogate the temporal relationship between loss of barrier function and putative lipid raft disruption, we performed a time course of 2% DSS treatments in C57/Bl6 mice and examined in vivo permeability in parallel with lipid raft status. As shown in Fig. 3*A*, intestinal permeability to the paracellular tracer FITC-dextran (4 kDa) was low in animals treated for either 0 or 3 days with DSS. This indicates no significant loss of intestinal epithelial barrier function by 3 days, the time frame used for the experiments described above. In contrast, mice exposed to the same concentration of FITC-dextran for 5 days showed significant loss of barrier function, with over fivefold more tracer detected in plasma ($P < 0.001$; $n = 3$ experiments).

When lipid raft gradients were poured from ileal epithelial preparations of mice treated for 0, 3 or 5 days with DSS, the sucrose density profiles and protein concentrations were quite similar between all conditions (data not shown). However, subtle differences were observed in the profile of alkaline phosphatase activity across fractions from different gradient conditions (Fig. 3*B*). Enzyme activity peaked on average in a single fraction (*fraction 6*; corresponding to 22.3 ± 1.7% sucrose density) in control/0 days DSS animals. In contrast, enzyme activity in 3-day DSS preparations was slightly lower and did not peak in a single fraction. Instead relatively equivalent levels of enzyme activity were observed across *fractions 4–6*, corresponding to 17.4 ± 1.1 up to 24.5 ± 0.8% sucrose. This suggested mild disruption or dispersal of lipid rafts (consistent with our data in Fig. 2), and it is interesting to note that lipid rafts are never usually recovered below 20% sucrose. Finally, two abnormally high peaks of alkaline phosphatase intensity were observed in *fractions 5* and *6* of gradients prepared from animals treated for 5 days with DSS, corresponding to 21.3 ± 0.3 and 24.5 ± 0.2% sucrose. When gradients were blotted for the lipid raft marker flotillin-1 (representative blots shown in Fig. 3*C*), there was generally enrichment of flotillin-1 in one to two fractions of control (0 days DSS) preparations, whereas the profile was broader in both 3- and 5-day DSS preparations. No particular differences could be seen between the broadened profiles of 3- and 5-day preparations, suggesting that any raft disruption had already occurred by the early time point and did not worsen over time.

UC patient intestinal biopsies display evidence of lipid raft disruption. To translate the preceding results into the context of human inflammation, we undertook a pilot study to analyze lipid raft status in a small group of UC patients with mild or quiescent inflammation relative to control patients with no history of IBD. As shown in Fig. 4*A* (*left*), there was no difference between the sucrose densities in gradient fractions from either control or UC patients (*UC 3* and *control 3* shown; see Table 1). Protein concentration profiles too were broadly similar (Fig. 4*A*, *middle*), although slightly less protein was

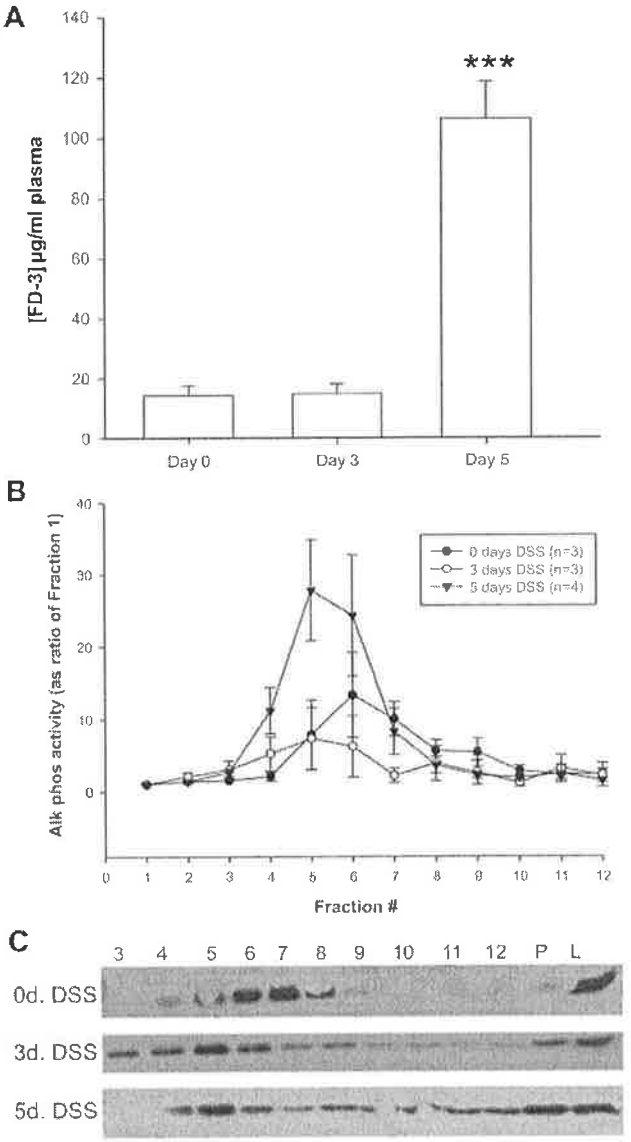

Fig. 3. Lipid raft disruption precedes loss of barrier function in mucosal preparations from mice with colitis. *A*: in vivo intestinal permeability to FITC-dextran (molecular mass 4 kDa) was assessed in C57/Bl6 mice treated for 0, 3, or 5 days with 2% DSS ($n = 3$ experiments, duplicate mice per condition). Permeability was low following 0 or 3 days exposure to DSS but increased significantly (~5-fold) by 5 days (***$P < 0.001$ by 2-tailed unpaired Student's *t*-test). *B*: isopycnic sucrose density gradients were poured from ileal lysates of mice treated as above, and all 12 fractions were analyzed for activity of the lipid raft marker enzyme alkaline phosphatase. Pooled results indicate a single peak in activity in *fraction 6* of control [0-day (0d.) DSS] samples, corresponding to the lipid raft fraction. The peak was lower and more evenly distributed across 3 fractions in the 3-day (3d.) DSS group, and abnormally high in the 5-day (5d.) DSS group. *C*: representative immunoblots for the lipid raft marker flotillin-1 in equivalent volumes of gradient fractions showed enrichment in *fractions 6* and *7* of control preparations and a more diffuse distribution across the fractions in 3-day or 5-day DSS preparations. L, lysate.

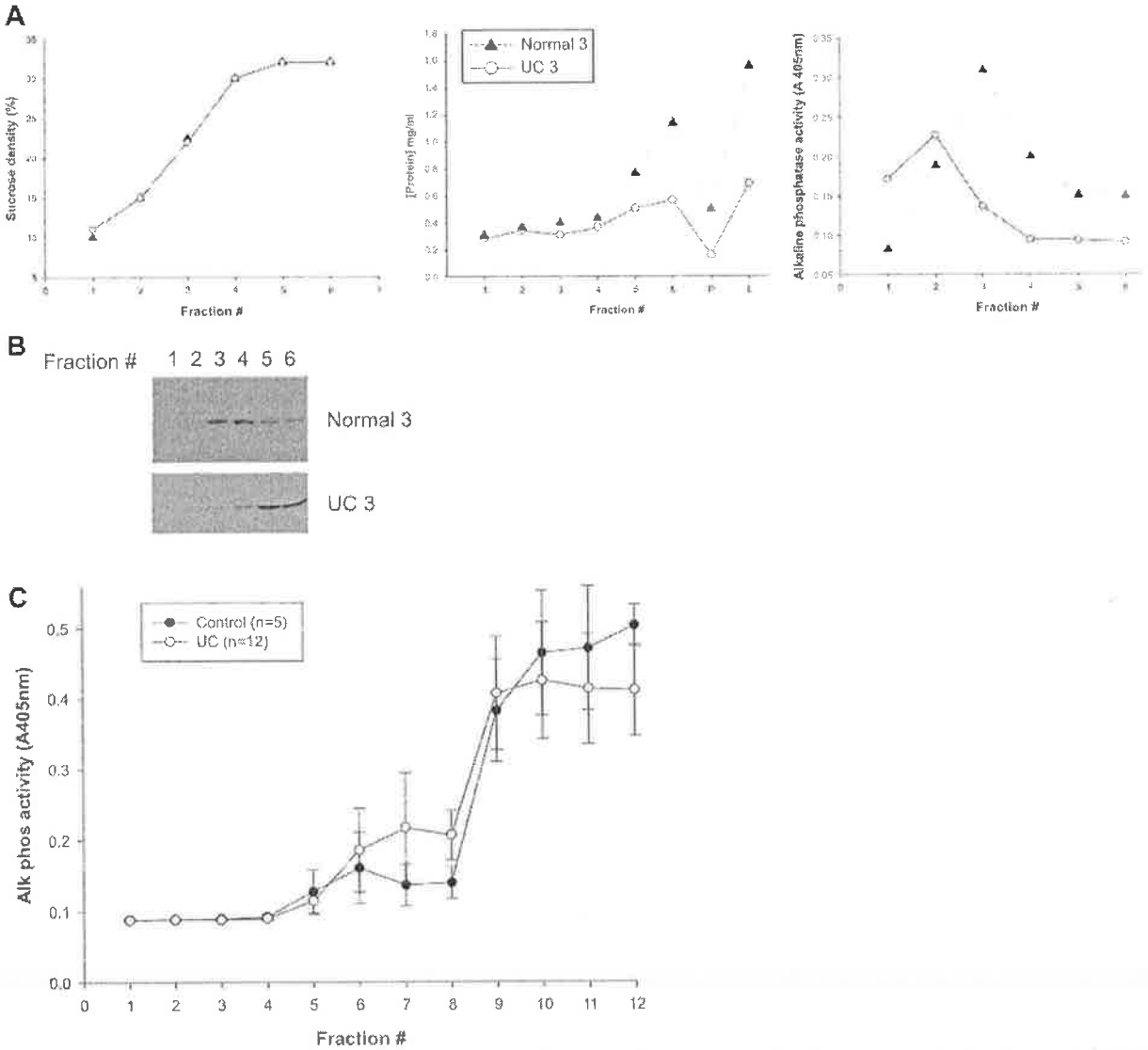

Fig. 4. Lipid rafts are disrupted in human biopsy homogenates from ulcerative colitis (UC) patients. *A*: lipid rafts were isolated by density gradient fractionation from intestinal biopsy homogenates of a control patient (*control 3*) and a patient with mild ulcerative colitis (*UC 3*). Gradient fractions were analyzed for sucrose density, protein concentration and activity of the lipid raft marker enzyme alkaline phosphatase. Peak fraction intensity for alkaline phosphatase activity was reduced and shifted to a lower fraction in the UC sample relative to control. *B*: equivalent concentrations of gradient fractions (5 μg/lane control; 10 μg/lane UC) were electrophoretically separated and Western blotted for the raft marker flotillin-1. Enrichment of flotillin-1 was observed in lipid raft-associated fractions (*3* and *4*) from the control gradient, but only in fractions at the bottom of the gradient prepared from UC homogenates (*fractions 5* and *6*). *C*: in a separate study involving 17 patients (5 controls and 12 UC), we prepared sucrose density gradients and compared alkaline phosphatase activity levels between fractions from the different conditions. Enzyme activity peaked in *fraction 6* of control samples and then declined in the following fractions before increasing again in the protein-rich fractions at the bottom of the gradient (*fractions 9–12*). In contrast, enzyme activity was similar in *fractions 6–8* of UC samples and did not decline before reaching the bottom of the gradient.

recovered from the higher gradient fractions of UC vs. control tissues. This was echoed by a lower protein concentration in mucosal homogenates from UC vs. control samples and may reflect mucosal denudation in patients with prior inflammation.

When alkaline phosphatase enzyme activity assays were performed to identify the gradient fractions putatively containing lipid rafts (Fig. 4*A*, *right*), interesting differences between control and UC samples were observed. Specifically, a high peak of activity was observed in *fraction 3* (~23% sucrose) of the representative control sample, whereas a peak of lower intensity was observed in *fraction 2* (~15% sucrose) of the representative UC sample. Analysis of equivalent protein concentrations (5 μg/lane) in control fractions by SDS-PAGE and Western blot analysis (Fig. 4*B*) revealed enrichment of the raft marker flotillin-1 in the predicted raft fraction, *fraction 3*, along with *fraction 4*. In contrast, equivalent protein concentrations electrophoretically separated from the UC gradient (10 μg/lane) detected flotillin-1 only at the bottom of the gradient, at >32% sucrose density in *fractions 5* and *6*. Consistent with our previous results, this indicated a possible disruption of lipid

rafts in even uninflamed/uninvolved regions within an inflammatory microenvironment.

In a larger study, we also used density gradient fractionation to isolate lipid rafts from 17 patient biopsy samples (Table 2). Five and 12 samples represented, respectively, control and UC conditions, with only 2 of the 12 UC samples having active inflammation. Analysis of the 12-fraction gradients for sucrose density profiles, as expected, revealed no differences between control and UC conditions (data not shown). Similarly, there were no real differences between the protein content profiles of control vs. UC gradients (data not shown). Alkaline phosphatase activity profiles of control gradients (pooled in Fig. 4C) revealed a single small peak in enzyme activity in *fraction 6*, corresponding to 22.5 ± 0.3% sucrose, the density at which lipid rafts are normally recovered. As expected, there was also a predictable rise in alkaline phosphatase activity toward the bottom of the gradient (*fractions 9–12*), reflecting the much higher protein concentrations in later fractions. In contrast, pooled samples from UC gradients did not show a single peak of alkaline phosphatase activity in *fraction 6*. Instead there was a small and approximately equivalent peak in enzyme activity across *fractions 6–8* (23.50 up to 30.7 ± 0.1% sucrose), suggesting lipid raft disruption or dispersal. As with control samples, alkaline phosphatase activity was also high in the high-protein *fractions 9–12* at the bottom of the gradient.

Because of exceedingly low protein concentrations in individual fractions, the lipid raft marker flotillin-1 could not consistently be detected by immunoblotting even after acetone precipitations were carried out to concentrate the volumes (data not shown). However, on the basis of extensive experience that flotillin-1 expression is typically highest in the middle fractions (21–25% sucrose), showing a peak of alkaline phosphatase activity, we think it likely that flotillin-1 expression would be highest in a single fraction of control samples (*fraction 6*) but more diffusely spread out across *fractions 6–8*, reflecting disrupted lipid rafts within UC gradients.

Affiliation of TJ proteins with lipid rafts is mildly perturbed during early inflammation. Having presented evidence of lipid raft disruption in cells, mouse tissues, and human biopsy samples under pre-/early-inflammatory conditions featuring only minor (if any) disruptions in barrier function, we wanted to test whether this reflected altered affiliations between candidate TJ proteins and lipid rafts. Accordingly, raft vs. nonraft fractions from cytokine-treated Caco-2 cells were Western blotted for the raft-associated TJ protein occludin (Fig. 5*A*). Occludin was strongly enriched in raft fractions (*fractions 4* and *5*) relative to nonraft fractions (*fractions 10* and *12*) in control monolayers. Lysate levels of occludin were reduced in all cytokine-treated conditions, and there was a small increase in the levels of occludin recovered in nonraft fractions from IFN-γ- or IL-10-treated cells in parallel with reductions in occludin recovery from raft fractions.

When equivalent protein concentrations of raft vs. nonraft fractions from mouse gradients were blotted for occludin (Fig. 5*B*, *top*), we observed occludin enrichment in raft fractions from control animals. Mucosal lysate levels of occludin were substantially reduced in DSS-treated animals, and occludin was not detected in raft or nonraft subcellular fractions. This is unlikely to reflect a global loss of protein in DSS samples since no histological sloughing of the epithelium was observed (Fig. 1*A*), total protein profiles were similar (Fig. 1*B*), and overall flotillin-1 expression was not altered even by 5-day DSS treatment (Supplemental Fig. S4). Fractions were also blotted for the raft-associated TJ protein, ZO-1. As shown (Fig. 5*B*, *bottom*), ZO-1 levels were slightly reduced in mucosal lysates of DSS relative to control animals. On a subcellular level, ZO-1 was recovered predominantly in the raft fractions of both control and DSS animals.

Lastly, the profile of occludin expression in raft vs. nonraft fractions was determined in gradients isolated from human

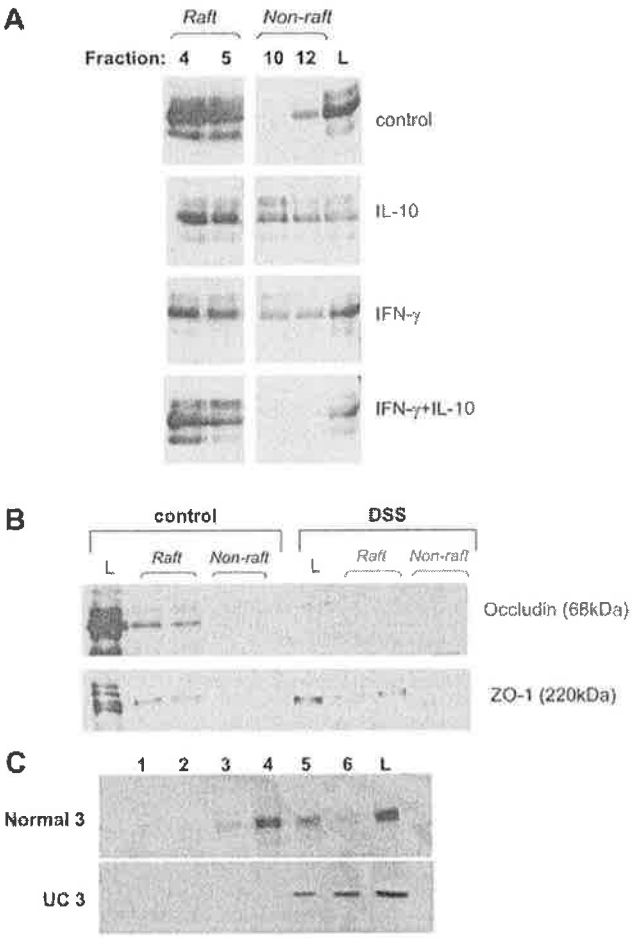

Fig. 5. TJ protein expression is reduced in cell and tissue models of early inflammation. *A*: Caco-2 cells were treated for 7 days with IL-10 (10 ng/ml) ± IFN-γ (150 U/ml; final 5 days) or vehicle and subjected to sucrose density gradient fractionation. Equivalent protein concentrations of fractions and whole cell lysate (L) were Western blotted for occludin. Occludin was recovered predominantly in raft fractions of control cells and at high levels in lysates. Occludin levels dropped in lysates and raft fractions following all cytokine treatments. *B*: rafts were isolated from the ileal mucosa of C57/Bl6 mice exposed for 3 days to 2% DSS or vehicle control, and equivalent protein concentrations in raft fractions, nonraft fractions, and mucosal lysates were blotted for occludin and zonula occludens-1 (ZO-1). Both proteins were strongly expressed in control lysates and raft fractions. Occludin was barely detected in lysate or fractions from DSS mice, whereas ZO-1 was reduced in both lysate and raft fractions. *C*: rafts were isolated from human mucosal biopsies and equivalent protein concentrations of sucrose gradient fractions blotted for occludin. Occludin was enriched in *fraction 4* (corresponding to rafts) from the normal mucosa, whereas its expression was reduced and shifted into higher sucrose density fractions in the patient with quiescent UC.

intestinal biopsy homogenates (Fig. 5*C*). Data from *UC 3* and *control 3* are represented here (for patient details see Table 1). Because of the global reduction in protein expression previously noted in UC relative to control samples (Fig. 4*B*), 10 and 5 μg/lane were loaded in, respectively, UC and control gradients. As shown in the representative control sample in Fig. 5*C*, occludin was predominantly recovered in raft-associated *fractions 3* and *4*. In contrast, occludin was only recovered in nonraft fractions prepared from a UC patient with mild inflammation (*fractions 5* and *6*). Overall levels of occludin protein were also reduced in the UC sample.

DISCUSSION

An intact intestinal epithelial barrier is essential for homeostasis. Loss of barrier function can result in self-amplifying cycles of immune activation, facilitating uncontrolled transepithelial passage of antigens (9). Epithelial disruption has been linked to inflammation in intestinal disorders including IBD. TJ proteins, key regulators of barrier function, have been associated with cholesterol-enriched membrane domains termed lipid rafts (20, 42). Thus the aim of this study was to investigate links between rafts and barrier dysfunction in pre-/early-inflammatory microenvironments without overt inflammation by using a cell line, two mouse colitis models, and human IBD biopsies.

In accordance with published data (11, 21, 25–27), the raft-disrupting agent MβCD impeded both formation (data not shown) and maintenance of epithelial barrier function. Exposure of Caco-2 intestinal epithelial cells to MβCD induced rapid reductions in TER paralleled by enhanced paracellular permeability (data not shown). To simulate inflammation, cells were treated with the proinflammatory cytokine IFN-γ, which induces barrier leakiness (1, 28, 36, 58). Under our conditions, IFN-γ provoked mild barrier function reductions compared with those induced by MβCD. Barrier function was unaltered by the control cytokine IL-10, nor could the reported anti-inflammatory properties of IL-10 protect against the barrier-disruptive effects of IFN-γ.

We questioned whether mild barrier compromise induced by IFN-γ was associated with disruption of lipid rafts, since several barrier-regulatory TJ proteins reside in rafts. Rafts were separated from Caco-2 lysates on the basis of a characteristically low buoyant density after ultracentrifugation on sucrose gradients. Immunoblotting for the raft marker flotillin-1 revealed a broader distribution in IFN-γ or MβCD gradients relative to controls, consistent with raft dispersal. Raft disruption in response to IFN-γ or MβCD was further supported by a wider distribution of alkaline phosphatase enzyme activity across several gradient fractions, relative to control samples where an activity peak was detected in a single fraction (~22–26% sucrose). However, since TER reductions were much greater with MβCD than IFN-γ (despite similarities in raft disruption), this may imply a complex relationship between raft disruption and barrier disruption. Treatment of T84 intestinal epithelial cells with IFN-γ and TNF-α has been shown to alter the lipid composition of lipid rafts in conjunction with loss of barrier function (22). Thus it is possible that the fundamental organization of rafts is impacted in inflammatory microenvironments, which in turn could influence the localization of key membrane proteins and the execution of their biological functions (adhesion/signaling).

Cells primed with proinflammatory cytokines lack the complexity of in vivo models. IFN-γ is a key contributor to inflammation in murine models of colitis, particularly in the DSS model to which IFN-γ-null animals are resistant (18). Thus we examined the link between rafts and barrier integrity in mice primed for intestinal inflammation by low doses of DSS. The DSS model reliably reproduces several features of UC (44), and under our conditions small intestinal involvement was histologically undetectable. Although we could not isolate colonic lipid rafts in our system because of very low yields of colonic epithelial cells (even from as many as 4 mice pooled per condition), we found that even ileal lipid rafts were disrupted, evidenced by broadened flotillin-1 distribution and reductions in peak alkaline phosphatase activity in DSS animals. Interestingly, alkaline phosphatase may itself play a direct role in inflammation, with reduced expression in response to IL-1β and TNF-α (30) and evidence of a rise in alkaline phosphatase activity during resolution of DSS colitis induced by lipid mediators (7). Further exploration of this phenomenon along a temporal scale revealed an interesting divergence between loss of barrier function and putative disruption of lipid rafts. Specifically, although in vivo intestinal permeability to a paracellular tracer was, respectively, very low and significantly higher following 3 and 5 days exposure to DSS, subtle changes in the biochemical and protein distribution profiles within lipid raft gradients suggested equivalent levels of lipid raft disruption or dispersal under both conditions. This supports the hypothesis that lipid raft disruptions precede the loss of epithelial barrier function.

We also used IL-10 knockout mice with mild colonic inflammation to further interrogate whether lipid raft disruption is associated with inflammatory microenvironments even in uninflamed/uninvolved intestinal regions. Conventionally housed IL-10 knockout mice spontaneously develop colitis and exhibit increased small intestinal permeability prior to the onset of inflammation (2, 29). Although our mice had no ileal inflammation, again we observed ileal raft disruption in the intestinal inflammatory microenvironment. An alternative raft isolation strategy (49) was used to exclude artifacts, since methods vary subtly via extraction of cholesterol or specific lipids/proteins (5, 49, 51). Detergent methods may induce membrane reorganization and raft coalescence whereas nondetergent methods preserve membrane structure (45). The consistency with which we observed raft disruption (across mouse models and across raft isolation procedures) supports our conviction that raft disruption is a real feature of inflammatory microenvironments. This was supported in biopsies of UC patients with mild or quiescent inflammation, in which flotillin-1 distribution was broadened and alkaline phosphatase activity reduced or shifted relative to that in control biopsies from patients undergoing cancer colonoscopy screening. Although no control model is ideal given the complexities of human subjects, the use of tissue from cancer screening patients still offers a better comparison than tissue from patients with non-IBD intestinal disease.

Further exploration of a larger number of patient samples revealed the trend toward a more diffuse pattern of activity for the lipid raft marker enzyme alkaline phosphatase in gradient fractions from UC patients ($n = 12$), relative to control patient

fractions in which alkaline phosphatase activity peaked in a single fraction of 22.5 ± 0.7% sucrose (n = 5 patients). Because of the heterogeneity of our patient population and a relatively limited number of samples (<20; which necessitated pooling UC active, UC inactive, and UC active/uninvolved cases together), it was not possible to detect statistically significant variation by using our methods. Nor was it possible to meaningfully detect proteins of interest such as flotillin-1, occludin, or ZO-1 in multiple samples per category (because of low protein concentrations even after acetone precipitation for fraction volume concentration). Nonetheless, we feel that trends from our collective data utilizing cells, mice, and humans suggest that subtle disruptions in lipid rafts occur early on in an environment primed for inflammation and/or barrier disruption.

In the context both of human ulcerative colitis and DSS murine colitis, it is particularly intriguing to speculate why lipid rafts might be disrupted in ileal tissue, which is classically considered to be uninvolved in the inflammatory process. Whether this is inconsequential or reflects a propensity to later develop inflammation/barrier disruption cannot be inferred from our study. However, it is interesting to note that ileal involvement in human ulcerative colitis (distinct from that in Crohn's disease) has been reported in 6–17% of patients, most commonly involving the terminal ileum in phenomena known as backwash ileitis or retrograde ileitis (12, 14). Therefore we feel that a full investigation of the cellular mechanisms of lipid raft disruption in inflammatory microenvironments (despite histological evidence of "normality" or a functional epithelial barrier) deserve consideration for their potential contribution to later inflammation. It would also be particularly interesting to determine whether lipid raft disruption accompanies or precedes the intestinal leakiness that is characteristic of healthy next-degree relatives of IBD patients (15, 17).

Finally, we asked whether key TJ proteins were displaced from rafts in uninflamed regions (considering both histologically normal and barrier-intact properties) within inflammatory microenvironments. However, we did not find consistent evidence of this in cells or tissues. Reduced occludin expression was more commonly observed in inflammatory microenvironments, although it is possible that other TJ proteins (e.g., nonraft-enriched claudins) could compensate for its loss in the epithelial barrier. IFN-γ has been shown to decrease occludin expression, possibly via phosphatidylinositol 3-kinase and NF-κB cross talk (3). Although it was surprising to note that the anti-inflammatory cytokine IL-10 also reduced the total protein expression of occludin in Caco-2 cells, it has previously been shown that IL-10 is a significant soluble factor released from lamina propria lymphocytes that is capable of reducing the barrier function of cocultured intestinal epithelial cells (46).

Taken together, these findings illustrate the fact that the relationship between TJ protein loss or gain and inflammation is complex. In fact, enhanced claudin expression has been associated with IBD and colitis-associated carcinoma (37, 56). It is likely that any alterations in TJ protein expression disturb adhesion signaling and barrier function. Since none of our models was overtly "inflamed," it may be that any extra-raft translocation of TJ proteins happens later on. Still, associations between TJ translocation out of rafts and loss of barrier function remain controversial, even in studies using similar cytokine combinations (6, 22). ZO-1 and occludin displacement outside rafts has been linked to profound barrier loss after *Clostridium difficile* intoxication (43). It will be interesting to test whether spatial reorganization of TJ proteins within epithelial membranes is temporally regulated during IBD inflammatory progression.

The possibility that TJ protein displacement from rafts might impair protein-protein interactions and contribute to dysregulated cell-cell adhesion is an interesting one. Dietary modifications that alter TJs have already been described (40), and it is intriguing to speculate that modifications that modulate membrane lipid content could regulate the onset or severity of inflammation via this mechanism. Polyunsaturated fatty acids (n-3 PUFA) enhance intestinal epithelial barrier function (57) and reportedly relocalize occludin and ZO-1 to lipid raft fractions (23). In vivo, n-3 PUFA supplementation has been shown to attenuate inflammation or promote remission in both murine (8, 32) and human (55) IBD.

In conclusion, our study has shown for the first time (to our knowledge) that disruption of intestinal epithelial lipid rafts is a feature of early-inflammatory or primed inflammatory conditions in cells, in mouse models of colitis, and in quiescent human IBD even in the absence of visible inflammation or significant epithelial barrier disruption. Evidence of lipid raft disruption even in the absence of overt damage to the epithelial barrier suggests that this may constitute an early signal in the inflammatory cascade that culminates in IBD.

GRANTS

The authors are grateful for funding from the Health Research Board of Ireland (RP/2006/95, HRA/2009/49 to A. M. Hopkins) and Science Foundation Ireland (07/IN.1/B902 to P. G. Fallon). The confocal microscope was funded through the National Biophotonics and Imaging Platform, Ireland, and by the Irish Government's Programme for Research in Third Level Institutions, Cycle 4, Ireland's EU Structural Funds Programmes 2007–2013.

DISCLOSURES

No conflicts of interest, financial or otherwise, are declared by the author(s).

REFERENCES

1. **Adams RB, Planchon SM, Roche JK.** IFN-gamma modulation of epithelial barrier function. Time course, reversibility, and site of cytokine binding. *J Immunol* 150: 2356–2363, 1993.
2. **Arrieta MC, Madsen K, Doyle J, Meddings J.** Reducing small intestinal permeability attenuates colitis in the IL10 gene-deficient mouse. *Gut* 58: 41–48, 2009.
3. **Boivin MA, Roy PK, Bradley A, Kennedy JC, Rihani T, Ma TY.** Mechanism of interferon-gamma-induced increase in T84 intestinal epithelial tight junction. *J Interferon Cytokine Res* 29: 45–54, 2009.
4. **Brown DA, London E.** Functions of lipid rafts in biological membranes. *Annu Rev Cell Dev Biol* 14: 111–136, 1998.
5. **Brown DA, Rose JK.** Sorting of GPI-anchored proteins to glycolipid-enriched membrane subdomains during transport to the apical cell surface. *Cell* 68: 533–544, 1992.
6. **Bruewer M, Luegering A, Kucharzik T, Parkos CA, Madara JL, Hopkins AM, Nusrat A.** Proinflammatory cytokines disrupt epithelial barrier function by apoptosis-independent mechanisms. *J Immunol* 171: 6164–6172, 2003.
7. **Campbell EL, MacManus CF, Kominsky DJ, Keely S, Glover LE, Bowers BE, Scully M, Bruyninckx WJ, Colgan SP.** Resolvin E1-induced intestinal alkaline phosphatase promotes resolution of inflammation through LPS detoxification. *Proc Natl Acad Sci USA* 107: 14298–14303.
8. **Camuesco D, Galvez J, Nieto A, Comalada M, Rodriguez-Cabezas ME, Concha A, Xaus J, Zarzuelo A.** Dietary olive oil supplemented with fish oil, rich in EPA and DHA (n-3) polyunsaturated fatty acids, attenuates

colonic inflammation in rats with DSS-induced colitis. *J Nutr* 135: 687–694, 2005.
9. **Clayburgh DR, Shen L, Turner JR.** A porous defense: the leaky epithelial barrier in intestinal disease. *Lab Invest* 84: 282–291, 2004.
10. **Feighery LM, Smith P, O'Mahony L, Fallon PG, Brayden DJ.** Effects of Lactobacillus salivarius 433118 on intestinal inflammation, immunity status and in vitro colon function in two mouse models of inflammatory bowel disease. *Dig Dis Sci* 53: 2495–2506, 2008.
11. **Francis SA, Kelly JM, McCormack J, Rogers RA, Lai J, Schneeberger EE, Lynch RD.** Rapid reduction of MDCK cell cholesterol by methyl-beta-cyclodextrin alters steady state transepithelial electrical resistance. *Eur J Cell Biol* 78: 473–484, 1999.
12. **Goldstein N, Dulai M.** Contemporary morphologic definition of backwash ileitis in ulcerative colitis and features that distinguish it from Crohn disease. *Am J Clin Pathol* 126: 365–376, 2006.
13. **Harder T, Simons K.** Caveolae, DIGs, and the dynamics of sphingolipid-cholesterol microdomains. *Curr Opin Cell Biol* 9: 534–542, 1997.
14. **Haskell H, Andrews CW Jr, Reddy SI, Dendrinos K, Farraye FA, Stucchi AF, Becker JM, Odze RD.** Pathologic features and clinical significance of "backwash" ileitis in ulcerative colitis. *Am J Surg Pathol* 29: 1472–1481, 2005.
15. **Hollander D, Vadheim CM, Brettholz E, Petersen GM, Delahunty T, Rotter JI.** Increased intestinal permeability in patients with Crohn's disease and their relatives. A possible etiologic factor. *Ann Intern Med* 105: 883–885, 1986.
16. **Hopkins AM, Walsh SV, Verkade P, Boquet P, Nusrat A.** Constitutive activation of Rho proteins by CNF-1 influences tight junction structure and epithelial barrier function. *J Cell Sci* 116: 725–742, 2003.
17. **Irvine EJ, Marshall JK.** Increased intestinal permeability precedes the onset of Crohn's disease in a subject with familial risk. *Gastroenterology* 119: 1740–1744, 2000.
18. **Ito R, Shin-Ya M, Kishida T, Urano A, Takada R, Sakagami J, Imanishi J, Kita M, Ueda Y, Iwakura Y, Kataoka K, Okanoue T, Mazda O.** Interferon-gamma is causatively involved in experimental inflammatory bowel disease in mice. *Clin Exp Immunol* 146: 330–338, 2006.
19. **Kuhn R, Lohler J, Rennick D, Rajewsky K, Muller W.** Interleukin-10-deficient mice develop chronic enterocolitis. *Cell* 75: 263–274, 1993.
20. **Lambert D, O'Neill CA, Padfield PJ.** Depletion of Caco-2 cell cholesterol disrupts barrier function by altering the detergent solubility and distribution of specific tight-junction proteins. *Biochem J* 387: 553–560, 2005.
21. **Lambert D, O'Neill CA, Padfield PJ.** Methyl-beta-cyclodextrin increases permeability of Caco-2 cell monolayers by displacing specific claudins from cholesterol rich domains associated with tight junctions. *Cell Physiol Biochem* 20: 495–506, 2007.
22. **Li Q, Zhang Q, Wang M, Zhao S, Ma J, Luo N, Li N, Li Y, Xu G, Li J.** Interferon-gamma and tumor necrosis factor-alpha disrupt epithelial barrier function by altering lipid composition in membrane microdomains of tight junction. *Clin Immunol* 126: 67–80, 2008.
23. **Li Q, Zhang Q, Wang M, Zhao S, Xu G, Li J.** n-3 polyunsaturated fatty acids prevent disruption of epithelial barrier function induced by proinflammatory cytokines. *Mol Immunol* 45: 1356–1365, 2008.
24. **Lu L, Khan S, Lencer W, Walker WA.** Endocytosis of cholera toxin by human enterocytes is developmentally regulated. *Am J Physiol Gastrointest Liver Physiol* 289: G332–G341, 2005.
25. **Lynch RD, Francis SA, McCarthy KM, Casas E, Thiele C, Schneeberger EE.** Cholesterol depletion alters detergent-specific solubility profiles of selected tight junction proteins and the phosphorylation of occludin. *Exp Cell Res* 313: 2597–2610, 2007.
26. **Lynch RD, Tkachuk-Ross LJ, McCormack JM, McCarthy KM, Rogers RA, Schneeberger EE.** Basolateral but not apical application of protease results in a rapid rise of transepithelial electrical resistance and formation of aberrant tight junction strands in MDCK cells. *Eur J Cell Biol* 66: 257–267, 1995.
27. **Lynch RD, Tkachuk LJ, Ji X, Rabito CA, Schneeberger EE.** Depleting cell cholesterol alters calcium-induced assembly of tight junctions by monolayers of MDCK cells. *Eur J Cell Biol* 60: 21–30, 1993.
28. **Madara JL, Stafford J.** Interferon-gamma directly affects barrier function of cultured intestinal epithelial monolayers. *J Clin Invest* 83: 724–727, 1989.
29. **Madsen KL, Malfair D, Gray D, Doyle JS, Jewell LD, Fedorak RN.** Interleukin-10 gene-deficient mice develop a primary intestinal permeability defect in response to enteric microflora. *Inflamm Bowel Dis* 5: 262–270, 1999.
30. **Malo MS, Biswas S, Abedrapo MA, Yeh L, Chen A, Hodin RA.** The pro-inflammatory cytokines, IL-1beta and TNF-alpha, inhibit intestinal alkaline phosphatase gene expression. *DNA Cell Biol* 25: 684–695, 2006.
31. **Marchiando AM, Graham WV, Turner JR.** Epithelial barriers in homeostasis and disease. *Annu Rev Pathol* 5: 119–144.
32. **Matsunaga H, Hokari R, Kurihara C, Okada Y, Takebayashi K, Okudaira K, Watanabe C, Komoto S, Nakamura M, Tsuzuki Y, Kawaguchi A, Nagao S, Miura S.** Omega-3 polyunsaturated fatty acids ameliorate the severity of ileitis in the senescence accelerated mice (SAMP1/Yit mice model. *Clin Exp Immunol* 158: 325–333, 2009.
33. **Matter K, Baldu MS.** Signalling to and from tight junctions. *Nat Rev Mol Cell Biol* 4: 225–236, 2003.
34. **May GR, Sutherland LR, Meddings JB.** Is small intestinal permeability really increased in relatives of patients with Crohn's disease? *Gastroenterology* 104: 1627–1632, 1993.
35. **McGuckin MA, Eri R, Simms LA, Florin TH, Radford-Smith G.** Intestinal barrier dysfunction in inflammatory bowel diseases. *Inflamm Bowel Dis* 15: 100–113, 2009.
36. **McKay DM, Singh PK.** Superantigen activation of immune cells evokes epithelial (T84) transport and barrier abnormalities via IFN-gamma and TNF alpha: inhibition of increased permeability, but not diminished secretory responses by TGF-beta2. *J Immunol* 159: 2382–2390, 1997.
37. **Mees ST, Mennigen R, Spieker T, Rijcken E, Senninger N, Haier J, Bruewer M.** Expression of tight and adherens junction proteins in ulcerative colitis associated colorectal carcinoma: upregulation of claudin-1, claudin-3, claudin-4, and beta-catenin. *Int J Colorectal Dis* 24: 361–368, 2009.
38. **Melkonian KA, Chu T, Tortorella LB, Brown DA.** Characterization of proteins in detergent-resistant membrane complexes from Madin-Darby canine kidney epithelial cells. *Biochemistry* 34: 16161–16170, 1995.
39. **Mullin JM, Agostino N, Rendon-Huerta E, Thornton JJ.** Keynote review: epithelial and endothelial barriers in human disease. *Drug Discov Today* 10: 395–408, 2005.
40. **Mullin JM, Skrovanek SM, Valenzano MC.** Modification of tight junction structure and permeability by nutritional means. *Ann NY Acad Sci* 1165: 99–112, 2009.
41. **Munkholm P, Langholz E, Hollander D, Thornberg K, Orholm M, Katz KD, Binder V.** Intestinal permeability in patients with Crohn's disease and ulcerative colitis and their first degree relatives. *Gut* 35: 68–72, 1994.
42. **Nusrat A, Parkos CA, Verkade P, Foley CS, Liang TW, Innis-Whitehouse W, Eastburn KK, Madara JL.** Tight junctions are membrane microdomains. *J Cell Sci* 113: 1771–1781, 2000.
43. **Nusrat A, von Eichel-Streiber C, Turner JR, Verkade P, Madara JL, Parkos CA.** Clostridium difficile toxins disrupt epithelial barrier function by altering membrane microdomain localization of tight junction proteins. *Infect Immun* 69: 1329–1336, 2001.
44. **Okayasu I, Hatakeyama S, Yamada M, Ohkusa T, Inagaki Y, Nakaya R.** A novel method in the induction of reliable experimental acute and chronic ulcerative colitis in mice. *Gastroenterology* 98: 694–702, 1990.
45. **Pike LJ.** Lipid rafts: bringing order to chaos. *J Lipid Res* 44: 655–667, 2003.
46. **Planchon S, Fiocchi C, Takafuji V, Roche JK.** Transforming growth factor-beta1 preserves epithelial barrier function: identification of receptors, biochemical intermediates, and cytokine antagonists. *J Cell Physiol* 181: 55–66, 1999.
47. **Resta-Lenert S, Smitham J, Barrett KE.** Epithelial dysfunction associated with the development of colitis in conventionally housed mdr1a$^{-/-}$ mice. *Am J Physiol Gastrointest Liver Physiol* 289: G153–G162, 2005.
48. **Schmitz H, Barmeyer C, Fromm M, Runkel N, Foss HD, Bentzel CJ, Riecken EO, Schulzke JD.** Altered tight junction structure contributes to the impaired epithelial barrier function in ulcerative colitis. *Gastroenterology* 116: 301–309, 1999.
49. **Smart EJ, Ying YS, Mineo C, Anderson RG.** A detergent-free method for purifying caveolae membrane from tissue culture cells. *Proc Natl Acad Sci USA* 92: 10104–10108, 1995.
50. **Smith P, Mangan NE, Walsh CM, Fallon RE, McKenzie AN, van Rooijen N, Fallon PG.** Infection with a helminth parasite prevents experimental colitis via a macrophage-mediated mechanism. *J Immunol* 178: 4557–4566, 2007.
51. **Song KS, Li S, Okamoto T, Quilliam LA, Sargiacomo M, Lisanti MP.** Co-purification and direct interaction of Ras with caveolin, an integral

membrane protein of caveolae microdomains. Detergent-free purification of caveolae microdomains. *J Biol Chem* 271: 9690–9697, 1996.

52. **Su L, Shen L, Clayburgh DR, Nalle SC, Sullivan EA, Meddings JB, Abraham C, Turner JR.** Targeted epithelial tight junction dysfunction causes immune activation and contributes to development of experimental colitis. *Gastroenterology* 136: 551–563, 2009.
53. **Tambuwala MM, Cummins EP, Lenihan CR, Kiss J, Stauch M, Scholz CC, Fraisl P, Lasitschka F, Mollenbauer M, Saunders SP, Maxwell PH, Carmeliet P, Fallon PG, Schneider M, Taylor CT.** Loss of prolyl hydroxylase-1 protects against colitis through reduced epithelial cell apoptosis and increased barrier function. *Gastroenterology* 139: 2093–2101.
54. **Teahon K, Smethurst P, Levi AJ, Menzies IS, Bjarnason I.** Intestinal permeability in patients with Crohn's disease and their first degree relatives. *Gut* 33: 320–323, 1992.
55. **Uchiyama K, Nakamura M, Odahara S, Koido S, Katahira K, Shiraishi H, Ohkusa T, Fujise K, Tajiri H.** N-3 polyunsaturated fatty acid diet therapy for patients with inflammatory bowel disease. *Inflamm Bowel Dis* 16: 1696–1707, 2010.
56. **Weber CR, Nalle SC, Tretiakova M, Rubin DT, Turner JR.** Claudin-1 and claudin-2 expression is elevated in inflammatory bowel disease and may contribute to early neoplastic transformation. *Lab Invest* 88: 1110–1120, 2008.
57. **Willemsen LE, Koetsier MA, Balvers M, Beermann C, Stahl B, van Tol EA.** Polyunsaturated fatty acids support epithelial barrier integrity and reduce IL-4 mediated permeability in vitro. *Eur J Nutr* 47: 183–191, 2008.
58. **Youakim A, Ahdieh M.** Interferon-γ decreases barrier function in T84 cells by reducing ZO-1 levels and disrupting apical actin. *Am J Physiol Gastrointest Liver Physiol* 276: G1279–G1288, 1999.